

CASE FILE  
COPY

**SPACE SHUTTLE  
AUXILIARY PROPULSION SYSTEM  
DESIGN STUDY**

**PHASE C AND E REPORT  
STORABLE PROPELLANTS  
RCS/OMS/APU INTEGRATION STUDY**

***MCDONNELL DOUGLAS ASTRONAUTICS COMPANY - EAST***



COPY NO. 125

---

**SPACE SHUTTLE  
AUXILIARY PROPULSION SYSTEM  
DESIGN STUDY  
PHASE C AND E REPORT  
STORABLE PROPELLANTS  
RCS/OMS/APU INTEGRATION STUDY**

---

**29 DECEMBER 1972**

**REPORT MDC E0708**

Prepared by: D.D. Anglim  
A.E. Bruns  
D.C. Perryman  
D.L. Wieland

Approved by: P.J. Kelly  
Study Manager

Contract No. NAS9-12013

**MCDONNELL DOUGLAS AERONAUTICS COMPANY - EAST**

*Saint Louis, Missouri 63166 (314) 232-0232*

**MCDONNELL DOUGLAS**  
  
**CORPORATION**

**ABSTRACT**

This report describes Phases C and E of the "Space Shuttle Auxiliary Propulsion System Design Study", Contract NAS 9-12013. The objective of this study was to fully define the competing Auxiliary Propulsion concepts and to compare them on the basis of selection criteria such as weight, reliability and technology requirements. Propulsion systems using both cryogenic oxygen/hydrogen and earth storable propellants were considered. The main thrust of the cryogenic effort was focused on the detailed design and operating analysis for gaseous, oxygen/hydrogen Reaction Control Systems (RCS). The effort described in this report broadened the study by evaluating the potential of both monopropellant and bipropellant earth storable reaction control systems. The fundamental concepts evaluated in this phase were:

1. Monopropellant and bipropellant systems installed integrally within the vehicle
2. Monopropellant and bipropellant systems installed modularly in nose and wing tip pods
3. Monopropellant and bipropellant systems installed modularly in nose and fuselage pods.

Numerous design variations within these three concepts were evaluated. This report provides the results of system design analysis and compares various means of implementing each of the concepts. The final comparisons of alternate systems indicate the following:

1. Considerations of safety and ease of maintenance eliminate integral systems from contention.
2. No significant weight difference exists between systems employing modular wing tip pods and analogous modular fuselage pod systems.
3. The weight penalty for a modularized monopropellant RCS relative to a modularized bipropellant RCS is on the order of 2500 lbm.
4. The weight penalty for a modularized bipropellant RCS used for all maneuvers relative to a modularized bipropellant RCS coupled with a dedicated OMS is approximately 600 lbm.

TABLE OF CONTENTS

<u>SECTION</u>	<u>PAGE</u>
1. INTRODUCTION . . . . .	1-1
2. STUDY APPROACH . . . . .	2-1
3. REQUIREMENTS AND CONSTRAINTS . . . . .	3-1
4. SYSTEM ANALYSIS . . . . .	4-1
4.1 Preliminary System Design Points . . . . .	4-1
4.2 Systems Description . . . . .	4-3
4.3 System Implementation . . . . .	4-12
4.4 Design Point Weights and Sensitivities . . . . .	4-36
4.5 Fuselage Mounted Modular RCS-OMS Options . . . . .	4-60
4.6 Instrumentation Requirements . . . . .	4-73
4.7 Reliability Estimates . . . . .	4-77
4.8 Ground Support Operations and Maintenance Operations . . . . .	4-78
4.9 Integrated Versus Modular Systems . . . . .	4-93
5. SUMMARY . . . . .	5-1
6. REFERENCES . . . . .	6-1
Appendix A COMPONENT MODELS . . . . .	A-1
A1 Monopropellant Thruster . . . . .	A-1
A2 Plug Nozzle Thruster . . . . .	A-1
A3 Bipropellant Thruster . . . . .	A-7
A4 Bipropellant OMS Engine . . . . .	A-12
A5 Propellant Valves . . . . .	A-12
A6 Auxiliary Power Unit Components . . . . .	A-12
Appendix B PRELIMINARY SYSTEM ANALYSIS . . . . .	B-1
B1 Preliminary Requirements . . . . .	B-1
B2 Preliminary System Descriptions . . . . .	B-10
B3 Preliminary Analysis . . . . .	B-15
B4 APU Preliminary Analysis . . . . .	B-33
Appendix C REENTRY EFFECTS ON THRUSTER LOCATION AND NOZZLE CONFIGURATION . . . . .	C-1
C1 Thruster Location . . . . .	C-1
C2 Nozzle Configuration . . . . .	C-1
Appendix D ALTERNATE PRESSURIZATION CONCEPTS . . . . .	D-1
D1 Regulated Helium . . . . .	D-1
D2 Hydrazine Decomposition . . . . .	D-1

TABLE OF CONTENTS (CONTINUED)

<u>SECTION</u>	<u>PAGE</u>
D3 Pump Fed . . . . .	D-13
D4 Volatile Liquids . . . . .	D-21
Appendix E TANKAGE AND PROPELLANT ACQUISITION . . . . .	E-1
E1 Bladders . . . . .	E-5
E2 Bellows . . . . .	E-9
E3 Pistons . . . . .	E-15
E4 Surface Tension . . . . .	E-18
E5 Failure Detection . . . . .	E-22
E6 Composite Tank Materials . . . . .	E-27
E7 Compatibility . . . . .	E-31
E8 Fracture Mechanics . . . . .	E-36
Appendix F THERMAL CONTROL . . . . .	F-1
F1 Environments . . . . .	F-1
F2 Thruster Thermal Control . . . . .	F-3
F3 Wing Tip Module Thermal Control . . . . .	F-7
F4 Fuselage Mounted RCS/OMS Module Thermal Response . . . . .	F-36
F5 APU Thermal Control . . . . .	F-41
Appendix G PROPELLANT UTILIZATION . . . . .	G-1
G1 Vehicle Center of Gravity . . . . .	G-1
G2 Pod Thrust Tolerance and IMU . . . . .	G-8
G3 Specific Impulse Tolerance . . . . .	G-11
G4 Mixture Ratio Tolerance . . . . .	G-11
G5 Loading Accuracy . . . . .	G-13
G6 Failure Mode Conditions . . . . .	G-13
G7 Propellant Loading Margins . . . . .	G-16
Appendix H REUSE . . . . .	H-1
H1 Related Systems Experience . . . . .	H-1
H2 Rheopexy . . . . .	H-27

List of Pages

Title Page

- ii through iv
- 1-1 through 1-3
- 2-1 through 2-5
- 3-1 through 3-7
- 4-1 through 4-95
- 5-1 through 5-7
- 6-1
- A-1 through A-24
- B-1 through B-53
- C-1 through C-11
- D-1 through D-30
- E-1 through E-59
- F-1 through F-44
- G-1 through G-18
- H-1 through H-28

## 1. INTRODUCTION

To provide the technology base necessary for design of the Space Shuttle, NASA has sponsored a number of technology programs related to Auxiliary Propulsion Systems (APS). Among such programs has been a series of design studies intended to provide the system design data necessary for selection of preferred system concepts, and to delineate requirements for complementing component design and test programs. The first of these system study programs considered a broad spectrum of system concepts but, because of high vehicle impulse requirements coupled with safety, reuse, and logistics considerations, only cryogenic oxygen and hydrogen were considered as a propellant combination. Additionally, unknowns in thruster pulse mode ignition and concern over the distribution of cryogenic liquids served to eliminate liquid-liquid feed systems from the list of candidate concepts. Therefore, only systems which delivered propellants to the thrusters in a gaseous state were considered for the Reaction Control System (RCS). The results of these initial studies, reported in References A through D, indicated that among the many options for design of a gaseous oxygen/hydrogen system, an approach using heat exchangers to thermally condition the propellants and turbopumps to provide system operating pressure would best satisfy requirements for a fully reusable Space Shuttle. These studies focused attention on this general system type but did not examine in depth several viable approaches for turbopump system design and control. To fill this need, NASA contracted with McDonnell Douglas Astronautics Company-East (MDAC-E) in July 1971 for additional study of Space Shuttle Auxiliary Propulsion Systems. This contract (NAS 9-12013) titled "Space Shuttle Auxiliary Propulsion System Design Study", was under the technical direction of Mr. Darrell Kendrick, Propulsion and Power Division, Manned Spacecraft Center, Houston, Texas.

As originally defined, this design study was a five phase program considering only oxygen and hydrogen propellants. Reference E provides an Executive Summary of program results, and Reference F describes in detail the program plan for each of the five program phases listed below:

1. Phase A-Requirements Definition
2. Phase B-Candidate RCS Concept Comparisons
3. Phase C-RCS/OMS Integration
4. Phase D-Special RCS Studies
5. Phase E-System Dynamic Performance Analysis

Phase A defined all design and operating requirements for the APS. The results of this phase (which are documented in Reference G) showed that requirements for the booster and orbiter stages were sufficiently similar to allow concentration of all design effort on the orbiter stage as the results obtained would be applicable to fly-back-type booster stages. In Phase B, very detailed design and control analyses for the three most attractive gaseous oxygen/hydrogen RCS concepts were conducted. Reference H documents the Phase B results. Phase C was aimed at defining the potential for integration of the RCS with the Orbit Maneuvering System (OMS). As defined by the original contract, only oxygen and hydrogen were considered in this phase. However, vehicle studies which were concurrent with this design effort showed that smaller Shuttle orbiters with external, expendable main engine tankage would provide a more cost effective vehicle approach. This change in vehicle design resulted in a significant reduction in APS requirements. This, coupled with a companion Shuttle program decision to allow scheduled system refurbishment, allowed consideration of systems using earth storable propellants for auxiliary propulsion. Thus, in November 1971, NASA issued a contract change order that extended the scope of Phase C to include earth storable monopropellant and bipropellant systems and redirected Phase E to provide final performance analyses on storable propellant systems. Reference I provides documentation of the Phase C oxygen/hydrogen effort, and this report documents the results of both Phase C and E effort on earth storable propellant systems. In addition to the oxygen/hydrogen effort in Phases B and C, the study included an exploratory effort (Phase D) to evaluate two alternatives to gaseous oxygen/hydrogen turbopump RCS. Reference J documents the results of the Phase D studies.

In Phase C, RCS/OMS/APU storable propellant integration options were evaluated to determine the proper compromise between performance and operating requirements. Both monopropellant (hydrazine) and bipropellant (nitrogen tetroxide/monomethylhydrazine) concepts were considered. Preliminary baseline designs, reflecting various levels of system integration, served as reference points for detailed design and installation studies, and for concurrent studies of APU implementation and advanced pressurization and tankage concepts. Phase E consisted of a final performance analysis of the systems selected by NASA. In this phase, the system designs and performance were updated, and system reuse, maintenance, safety, and operational criteria were established.

The report documents the work performed and serves as a final definition of the Phase C and E effort on earth storables. The report body provides a description of the study approach followed by a discussion of the RCS requirements and constraints that are pertinent to system design and performance. Analysis necessary to trace concept evolution is documented. Finally, the candidate systems are compared on the basis of selected criteria. Substantiating technical detail is included as warranted in the attached appendices.



## 2. STUDY APPROACH

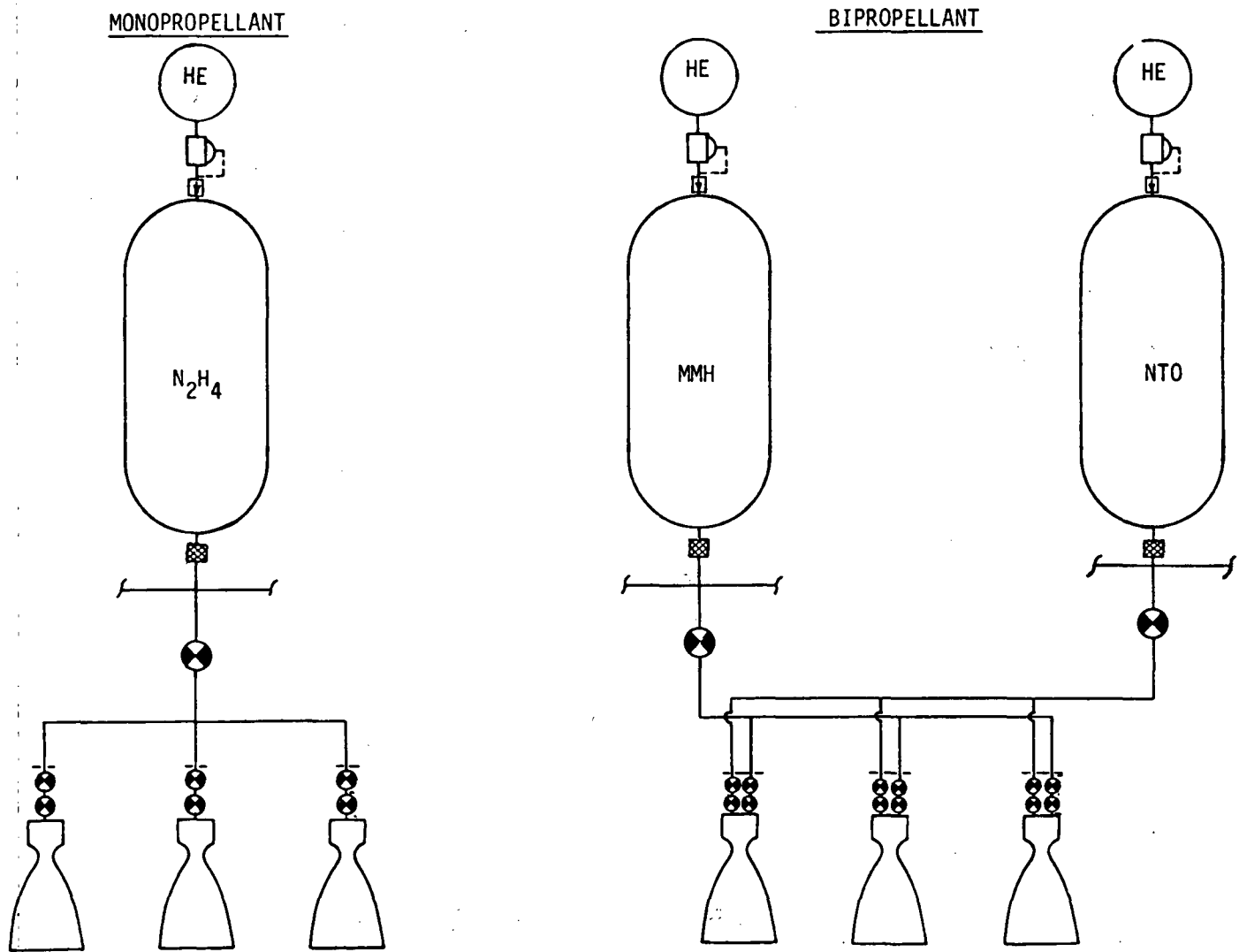
The basic earth storable Reaction Control Systems are shown schematically in Figure 2-1 for both monopropellant and bipropellant configurations. During system operation, liquid propellants are supplied at high pressure to the thrusters. Propellant tank pressures are maintained by regulated gaseous helium, and propellant acquisition is accomplished through the use of surface tension screens. Component redundancy is consistent with a fail-safe, fail-safe philosophy.

The Phase C and E earth storable study was conducted for the purpose of providing design data sufficient to allow resolution of the following options:

1. Choice of propellants
2. Method of installation (modular vs integral)
3. Degree of OMS-RCS integration
4. Degree of APU integration

To fulfill these objectives, the effort was divided into two phases, entitled RCS/OMS/APU Integration Study (Phase C), and System Performance Analysis (Phase E). Figure 2-2 delineates the specific tasks performed in these two phases. Initially, vehicle auxiliary propulsion system requirements were defined consistent with the maneuvering and attitude control requirements of the earth storable propellant orbiter. Vehicle configuration drawings were developed to aid in defining potential locations for RCS installation. Based on these studies, three general arrangements, shown in Figure 2-3, were identified as feasible. Component assembly models specifically suited to the requirements of storable propellant systems were developed for synthesis. Applying the data generated in these tasks, preliminary system analyses established operating design points and weight sensitivities to system parameters. Systems which were unattractive from the standpoint of weight were eliminated, and six concepts were selected for design trade studies. For these systems, alternative pressurization and propellant expulsion approaches were evaluated. The implications of reuse were considered and component requirements and systems implementation adjusted accordingly. Additionally, the effects of component tolerances, C. G. location variances, and propellant loading accuracies were assessed to define propellant margin requirements. This data served as a basis for the Phase E System Performance Analysis.

# EARTH STORABLE RCS STUDY CONCEPTS

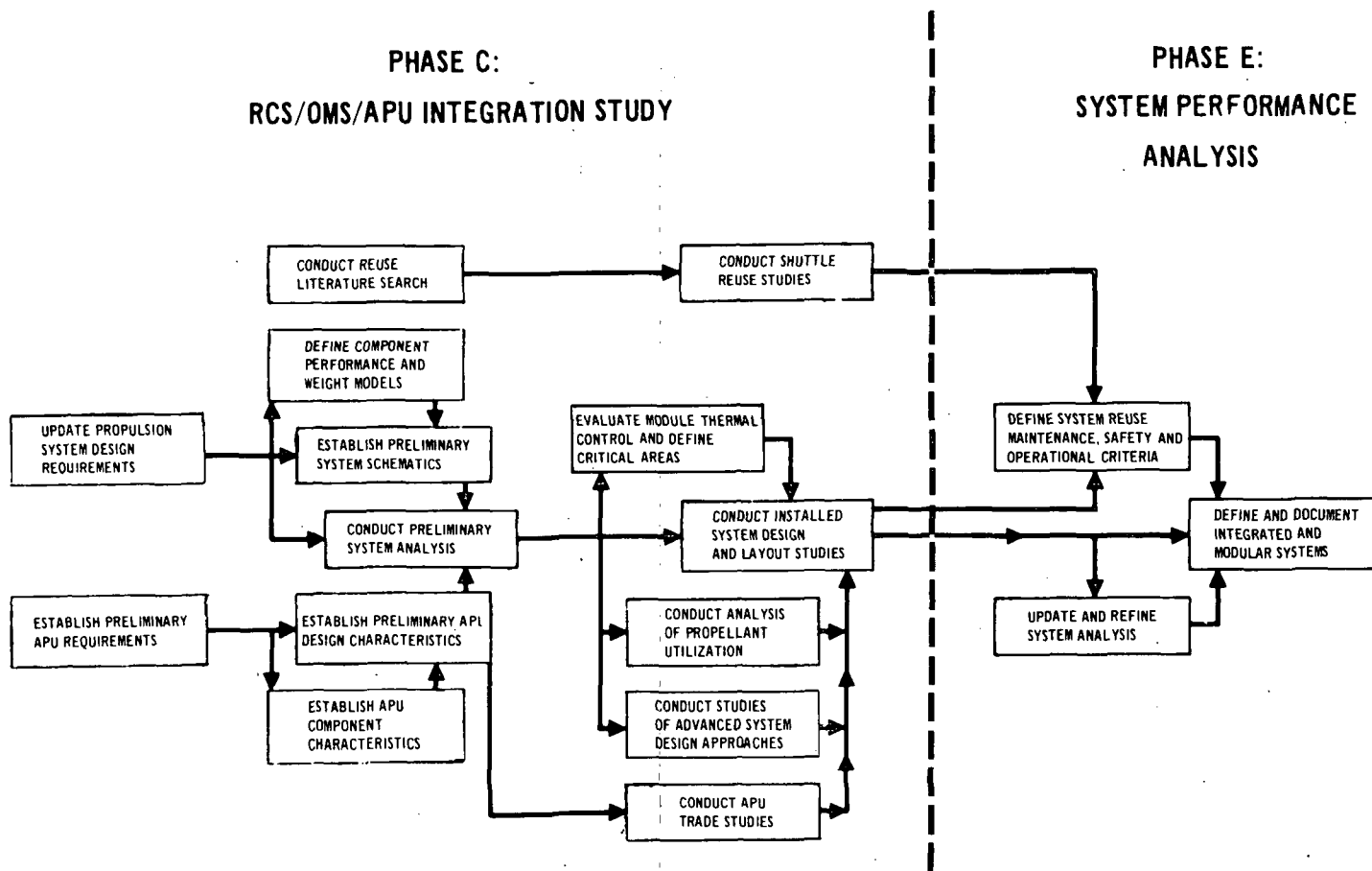


APS-780

2-2

Figure 2-1

# TASK FLOW CHART - PHASES C AND E

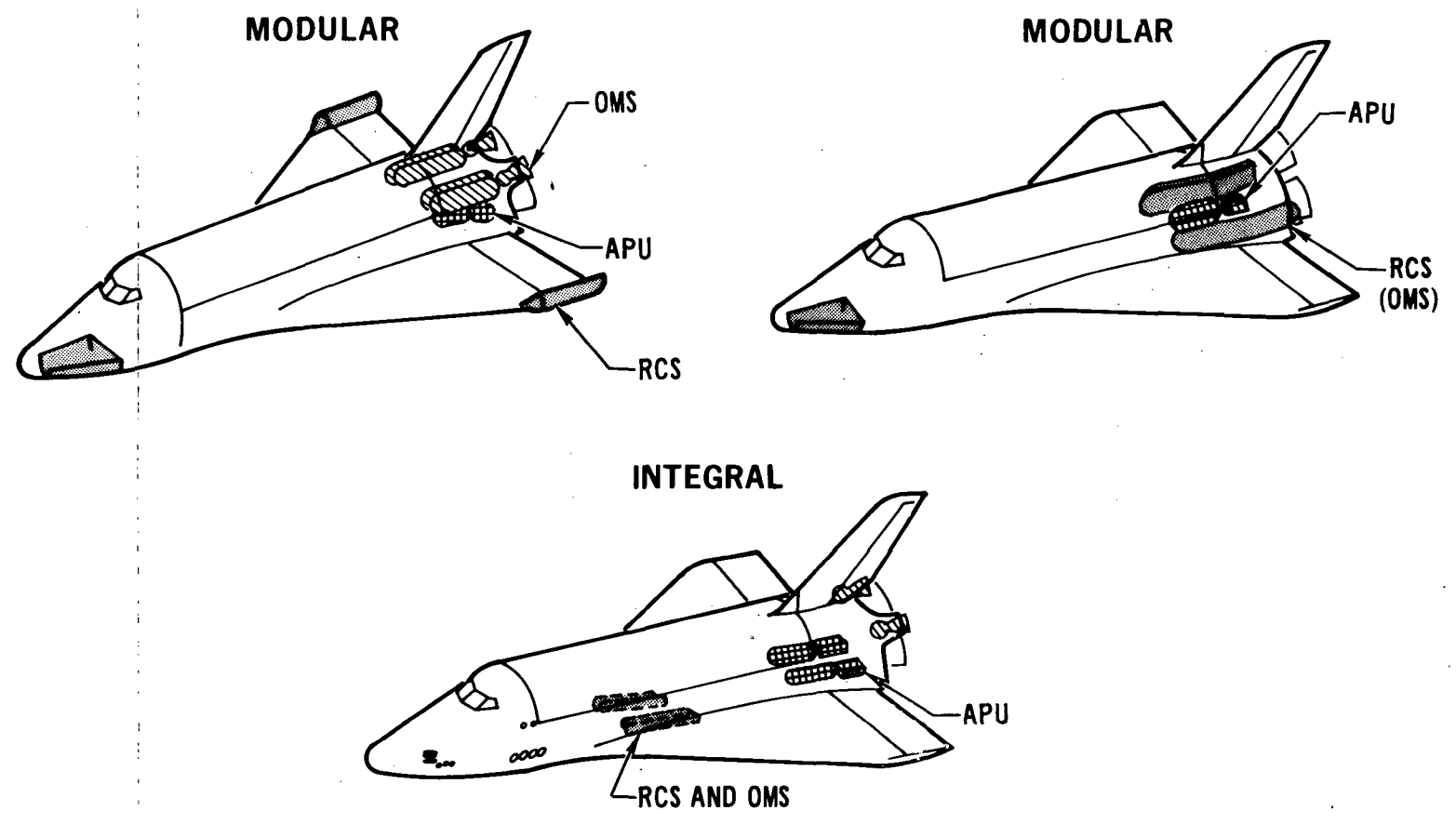


2-3

Figure 2-2

APS-101

# CANDIDATE VEHICLE INSTALLATIONS



2-4

Figure 2-3

11-222

In Phase E the results of the Phase C installed system studies were used to refine the analysis. Component models were updated, and the effects of propellant utilization were included. System design optimizations were performed and the following data generated for each of the candidate systems:

1. System schematic
2. Detailed weight breakdown
3. Weight sensitivities to design parameters
4. Weight sensitivities to configuration modifications.

Safety and maintenance guidelines were established. Finally these factors were combined, and candidate systems were compared on the basis of weight, technology, safety, ease of maintenance, and reusability forecasts.

Pertinent vehicle and system requirements applicable to this study are defined in the following section, and results from the tasks delineated in Figure 2-2 are summarized in Section 4.

### 3. REQUIREMENTS AND CONSTRAINTS

The baseline orbiter configuration used for the storable propellant RCS studies is shown in Figure 3-1 with the basic vehicle parameters and requirements. In this configuration, the main engine propellant tanks are expendable and external to the vehicle. This results in an orbiter considerably smaller than the baseline vehicle used in the oxygen/hydrogen studies.

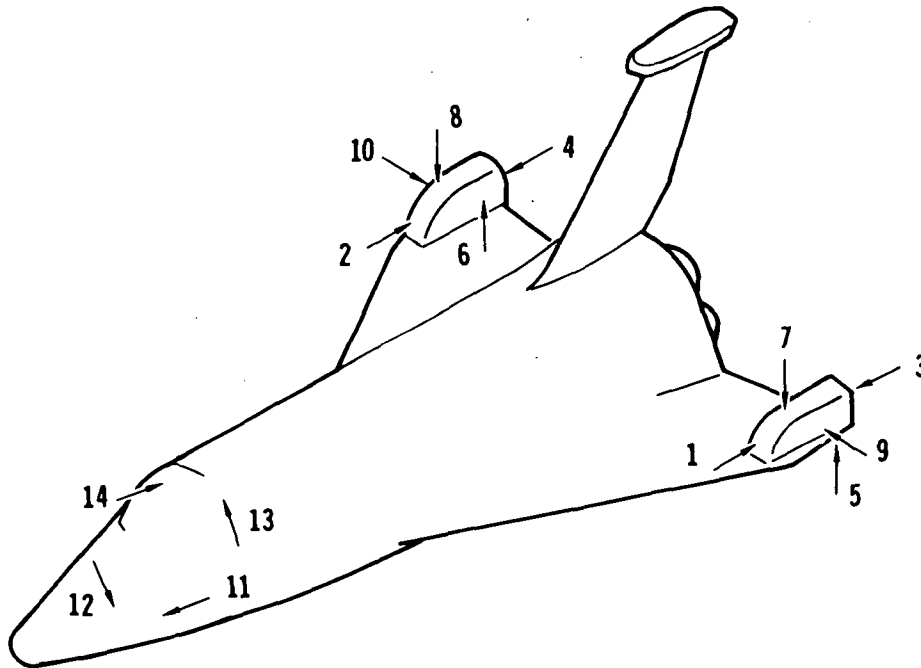
The vehicle requirements which have a major impact on the RCS are engine thrust, number of engines, total system thrust, total impulse, and total impulse expenditure histories. The approach taken to define these requirements was as follows: using the baseline vehicle configuration, the number of RCS engines and their thrust level was varied to satisfy the vehicle control and maneuvering acceleration requirements. Then, using a 20 millisecond equivalent (square wave) pulse for limit cycle control, total impulse expenditures were determined for attitude control during the three baseline missions.

The three baseline missions, defined in the "Space Shuttle Vehicle Description and Requirements Document" (included in Reference G), are (1) an easterly launch mission, which is intended primarily for delivering and retrieving payloads in a 100 nautical mile (nmi) circular orbit; (2) a south polar mission in which the orbiter is launched into an injection orbit of 50 by 100 nmi and circularized at apogee using the orbital maneuvering propulsion system; and (3) a resupply mission to provide logistic support for a space station/space base in a 270 nmi orbit. The easterly mission is designated the design mission, while the south polar and resupply missions are designated reference missions.

Several general requirements which applied to the RCS/OMS design included minimal maintenance with ease of removal and replacement and a minimum service life of 100 mission cycles over a 10-year period with cost effective refurbishment. Mission duration requirements are 7 days of self-sustaining operation and a 30 day capability with consumables supplied from the payload bay. In addition, failure criteria required that fail-safe conditions be achieved after the failure of any two components, not including structure, such as lines, tanks, and fittings.

Figure 3-2 provides a summary of the basic guidelines and requirements involved in the study. As indicated by the figure, the OMS has a minimum

# BASELINE ORBITER FOR STORABLE APS STUDIES



WEIGHT (INSERTION) (LBM)	265,000
PAYLOAD (LBM)	65,000
LENGTH (FT)	112.5
NUMBER OF THRUSTERS	40
THRUSTER THRUST (LB)	600
TOTAL IMPULSE (LB-SEC)	$1.832 \times 10^6$

11-71A

3-2

Figure 3-1

vehicle acceleration requirement of 0.02g and must have the capability of providing at least six engine burns per flight. The maximum incremental vehicle velocity required by the OMS is 1000 ft/sec. All maneuvers involving a change in vehicle velocity of less than 20 ft/sec are performed by the RCS.

The impulse requirements of the baseline orbiter, which weighs 265,000 lbm, are categorized by maneuvers for the Integral RCS, Modular RCS, and Modular RCS (OMS) in Figure 3-3. These requirements are based on the use of pure couples for all on-orbit maneuvers.

A detailed breakdown of the orbiter attitude control acceleration requirements is shown in Figure 3-4. The maximum RCS acceleration requirement occurs during reentry in which a yaw angular acceleration of  $1.5 \text{ deg/sec}^2$  is required.

The hydraulic and electrical power requirements of the orbiter are listed in Figure 3-5. The 230 HP hydraulic requirement is needed for the operation of items such as rudder, elevons, brakes, landing gear, etc. The minimum electrical requirement of 15 KW is required to power the recirculation pumps and main engine during ascent and to power avionics during entry.

The requirements discussed herein are final requirements, and in some cases, represent revisions to initial requirements. A discussion of the requirements used in the preliminary analysis may be found in Appendix B.



## SUMMARY OF GUIDELINES AND REQUIREMENTS

### GUIDELINES

- o STUDY (SYSTEMS) RCS, OMS AND APU  
(PROPELLANTS) MONOPROPELLANT HYDRAZINE, BIPROPELLANT NTO/MMH  
(TANKAGE) INTEGRAL AND MODULAR  
(PRESSURIZATION) REGULATED HELIUM, HYDRAZINE DECOMP., VOLATILE LIQUIDS, PUMP FEED
- o VEHICLE INSERTION WEIGHT = 265,000 LBM
- o MISSIONS EASTERLY, 100 N.M. x 28.5°  
SOUTH POLAR, 100 N.M. x 90°  
RESUPPLY, 270 N.M. x 55°

### REQUIREMENTS

- o RCS IMPULSE =  $1.832 \times 10^6$  LB-SEC  
ACCELERATION =  $0.5 - 0.8 \text{ }^\circ/\text{SEC}^2$ ;  $0.2-0.4 \text{ FT}/\text{SEC}^2$  (ON-ORBIT)  
 $1.5^\circ/\text{SEC}^2$  BANK ACCEL. (ENTRY)
- o OMS  $\Delta V = 1000 \text{ FT}/\text{SEC}$   
NO. BURNS = 6  
ACCELERATION =  $0.02g$  (MIN)
- o APU POWER = 230 HP (HYDRAULIC); 15 KW (ELECTRIC)  
ENERGY = 150 HP-HR

## IMPULSE REQUIREMENTS

	IMPULSE REQUIREMENT, LB-SEC				
	INTEGRAL RCS	MODULAR RCS		MODULAR RCS (OMS)	
		NOSE POD	EACH WING POD	NOSE POD	EACH FUSELAGE POD
ON ORBIT TRANSLATIONS	1,133,470	136,995	498,845	119,500	4,449,674 (OMS = 3,915,924) (RCS = 533,750)
ATTITUDE MANEUVERS	167,321	26,320	64,225	69,000	52,250
ON ORBIT LIMIT CYCLE	35,315	6,420	24,830	20,575	15,222
RCS DISTURBANCE	48,260	21,445	26,540	25,675	30,470
REENTRY - YAW	333,712	302,330		302,330	
- ROLL	123,000		14,430		47,000
- PITCH	58,600		40,280		39,500
		493,510	669,150	537,080	4,634,116
<b>TOTAL</b>	<b>1,899,678</b>	<b>1,831,810</b>		<b>9,805,313</b>	

MCDONNELL DOUGLAS ASTRONAUTICS COMPANY - EAST

3-5

Figure 3-3

ORBITER ACCELERATION REQUIREMENTS

MISSION PHASE		ON-ORBIT			RE-ENTRY		
		-X (FWD)	+X (AFT)	+Y, Z (UP/DOWN/LATERAL)	-X (FWD)	+X (AFT)	+Y, Z (UP/DOWN/LATERAL)
TRANSLATION ACCELERATION  FT/SEC <sup>2</sup>	DESIGN	0.4	0.2	0.2	N/R*		
	SAFE	0.6OMS 0.2	0.1	0.1			
ANGULAR ACCELERATION  DEG/SEC <sup>2</sup>	DESIGN	PITCH	YAW	ROLL	PITCH	YAW	ROLL
		0.8	0.8	0.8	0.8	1.5	1.2
	SAFE	0.5	0.5	0.5	0.5	1.0	0.8

\* NO REQUIREMENT

APS-222

3-6

Figure 3-4

# ORBITER APU POWER REQUIREMENTS

E243-21

HYDRAULIC (MINIMUM VEHICLE REQUIREMENT = 230 HP)

- RUDDER
- ELEVONS
- SPEED BRAKES
- CARGO DOOR
- LANDING GEAR
- STEERING
- BRAKES

ELECTRIC (MINIMUM VEHICLE REQUIREMENT = 15 KW)

- ORBITER ELECTRICAL POWER DURING ASCENT AND ENTRY
  - ASCENT - RECIRCULATION PUMPS
  - MAIN ENGINES
- ENTRY - AVIONICS

3-7

Figure 3-5

#### 4.0 SYSTEM ANALYSIS

During the storable propellant portion of the auxiliary propulsion system study, various APU/RCS/OMS systems were considered to evaluate their relative system performance, weight, complexity, flexibility, and vehicle interface characteristics. Concepts considered included various levels of APU/RCS/OMS integration. Both modular concepts and concepts installed integrally within the vehicle were evaluated. Propellant candidates were monopropellant hydrazine and hypergolic bipropellants (NTO/MMH). Preliminary system analyses were conducted to establish nominal design points and establish system sizing data. These baseline design points then served as references for detailed design and installation studies and for concurrent studies of APU implementation, propellant utilization, and advanced pressurization and tankage concepts. Based on the results from the system installation studies and a system reuse study conducted in parallel, the various concepts were compared on the basis of safety in flight and ground operations, ease of maintenance, reusability forecasts, and complexity of flight and ground operations. The baseline systems were then updated and refined to incorporate installed system considerations, revisions to the component models, and revisions resulting from advanced technology studies. System analyses were then repeated to establish the design points and thus define final system weights, volumes, and component requirements.

While this study was in progress, North American Rockwell (NR) was awarded the Space Shuttle prime contract. The NR Shuttle configuration employs a dedicated bipropellant OMS and a monopropellant RCS installed in fuselage and nose modules. In order to keep the study germane, therefore, additional evaluation of fuselage module RCS and OMS concepts was performed. Both common and dedicated tankage and engines were considered. System design points, sensitivities, and weights were defined for comparison with the baseline systems.

4.1 Preliminary System Design Points - In Phase C, preliminary system sizing analyses were conducted for each of the APU/RCS/OMS integration options. The resulting design points are summarized in Figure 4-1. Component models employed in the preliminary analysis together with applicable requirements, system schematics and descriptions are reported in Appendix B. The design points and the supplementary analyses of Appendix B provided the basic data

E243-97

## OPTIMAL DESIGN PARAMETERS

◦ HELIUM PRESSURIZATION

		MIXTURE RATIO	CHAMBER PRESSURE	EXPANSION RATIO
M O N O P R O P E L L A N T	APU		500	
	RCS		150	40-50
	OMS		110 <sup>(1)</sup>	45 <sup>(1)</sup>
	RCS(OMS)		100	60
	APU+RCS		200	55
	APU+RCS+OMS		110	40 (RCS) 45 (OMS)
	APU+RCS(OMS)		100	60
B I P R O P E L L A N T	RCS	1.535	175	40
	OMS	1.745	125 <sup>(1)</sup>	60 <sup>(1)</sup>
	RCS(OMS)	1.584	100	60
	RCS+OMS	1.545 (RCS) 1.745 (OMS)	125	40 (RCS) 60 (OMS)

(1) BASED ON NOZZLE EXIT DIAMETER CONSTRAINT = 33 IN. (MAX)

4-2

Figure 4-1

necessary for detailed design and installation studies. The use of monopropellant hydrazine for the OMS and all maneuver RCS functions introduced unacceptably high weight penalties and was thus discontinued in order to concentrate effort on the more viable concepts. The concurrent studies of APU implementation, advanced pressurization and tankage concepts, and propellant utilization are reported in Appendices B, D, E and G respectively. From these studies, design concepts were updated and systems were selected for final performance analyses, and system reuse, maintenance, safety, and operational criteria established. Based on the weight comparisons of the candidate configurations discussed in Appendix B, six systems were selected for the Phase E system performance analysis.

4.2 Systems Description - The six systems selected for Phase E study are listed below.

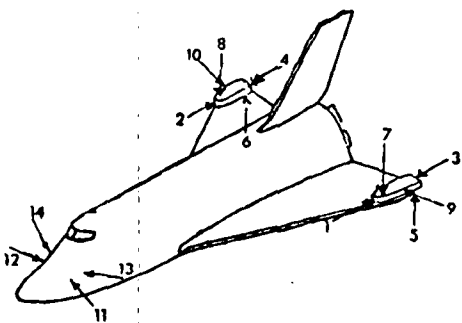
1. Modularized monopropellant RCS
2. Modularized bipropellant RCS
3. Modularized bipropellant RCS performing all maneuvers
4. Integral bipropellant RCS sharing common tankage with the OMS
5. Integral monopropellant RCS sharing common tankage with the APU
6. Modularized monopropellant APU

These configurations are all derivatives of the three basic vehicle installation concepts which evolved during the preliminary effort. The three concepts, which were depicted in Figure 2-3, are a reference Modular RCS which has a nose pod and two wing tip pods housing RCS thrusters that are completely separate from the two dedicated OMS engines, a Modular RCS(OMS) having a nose pod and two fuselage-mounted side pods containing RCS thrusters also capable of performing OMS maneuvers, and an Integral RCS, wherein centrally located tankage supplies the non-modularized thrusters.

Figure 4-2 defines the RCS thruster locations for these three concepts. Thruster locations have been chosen to maximize control moments, consistent with vehicle and thermal (reentry heating) constraints. Thruster requirements are dictated by a fail safe/fail safe redundancy criteria. The additional X translation thrusters on the Fuselage Module configuration preclude the requirement for a separate OMS engine.

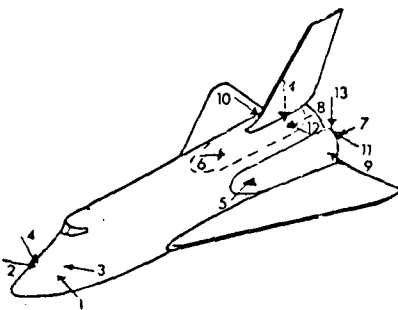
## RCS THRUSTER INSTALLATIONS

WING TIP MODULES



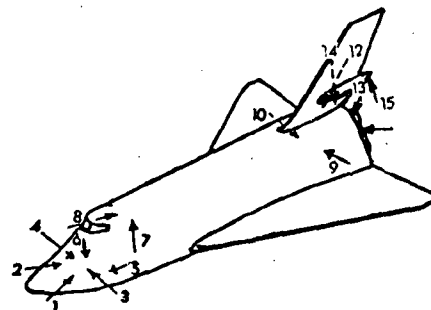
LOCATION	FUNCTION	NO. <sup>(1)</sup>
1	y*, X	3
2	y*, X	3
3	y*, X	3
4	y*, X	3
5	p, r, Z	3
6	p, r, Z	3
7	p, r, Z	4
8	p, r, Z	4
9	Y	2
10	Y	2
11	p, y, Y, Z	2
12	p, y, Y, Z	2
13	p, y, Y, Z	3
14	p, y, Y, Z	3
TOTAL		40

FUSELAGE MODULES



LOCATION	FUNCTION	NO. <sup>(1)</sup>
1	p, y, Y, Z	3
2	p, y, Y, Z	3
3	p, y, Y, Z	3
4	p, y, Y, Z	3
5	X	2
6	X	2
7	X	6
8	X	6
9	y*, Y	3
10	y*, Y	3
11	p, r, Z	4
12	p, r, Z	4
13	p, r, Z	3
14	p, r, Z	3
TOTAL		48

INTEGRATED



LOCATION	FUNCTION	NO. <sup>(1)</sup>
1	X	2
2	X	2
3	X	3
4	y, Y	3
5	v, Y	3
6	p, r, Z	2
7	p, r, Z	2
8	p, r, Z	2
9	v, Y	3
10	y, Y	3
11	X	3
12	X	3
13	p, Z	2
14	p, Z	2
15	p, Z	3
TOTAL		37

NOTE: p - pitch, y - yaw, r - roll  
 X - fore/aft translation  
 Y - left/right translation  
 Z - up/down translation  
 \* - on orbit only

(1) NUMBER OF 600 LBF THRUSTERS.



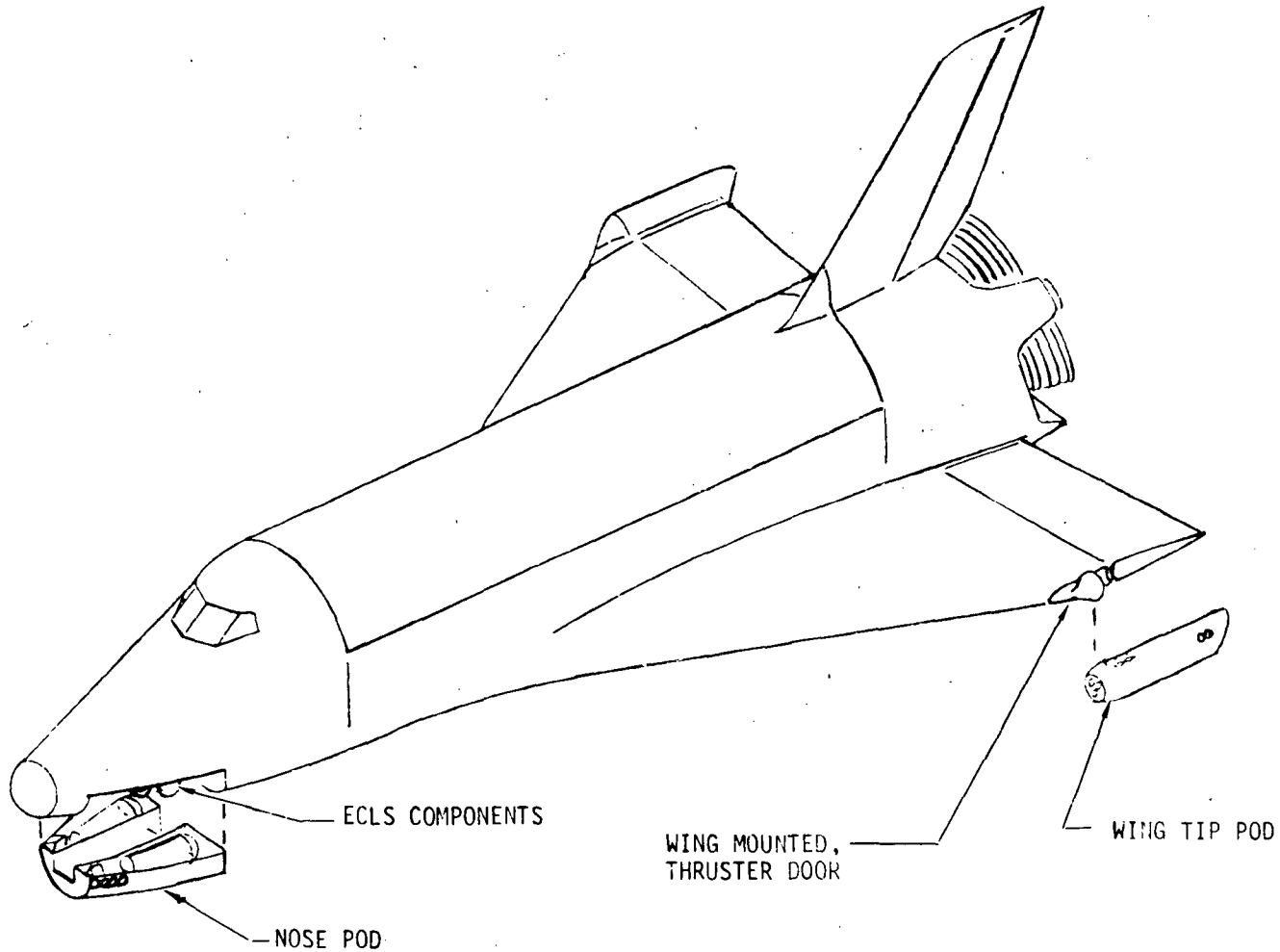
The Modular RCS pod installation concept is illustrated in Figure 4-3. In this baseline design, the two wing tip pods and nose pod are used for all on-orbit RCS functions. Reentry yaw is provided entirely by the nose pod. The forward-firing thrusters of the wing tip pods are protected against the high reentry heating rates and heat loads by thermal protection doors. As shown, the doors and door hydraulic actuation mechanisms are attached to the wing, thus facilitating pod installation and removal by eliminating the need for a hydraulic interface between the pod and wing. A more detailed view of the thermal protection door design is shown in Figure 4-4 which shows the reference wing pod installation for a helium pressurized monopropellant system. In this design concept, only the forward-firing thrusters require thermal protection because all of the other thrusters are shielded from direct stagnation heating at reentry angles of attack up to  $34^\circ$ . (Reentry heating of the forward module thrusters is cause for some concern; additional testing is required to fully assess the implications of aeroheating on thruster integrity. Appendix C elaborates on this topic, and discusses some alternate thruster configurations which could be employed to minimize entry heating.) Figure 4-5 presents a typical wing pod installation of a cluster of three thrusters. The thrusters are truss-mounted to the surrounding support structure in this installation arrangement. The basic wing pod installation features of the bipropellant and monopropellant systems differ very little. A typical bipropellant wing pod is illustrated in Figure 4-6 and its associated nose pod installation is depicted in Figure 4-7. The thrusters in the nose pod are canted to provide, in conjunction with the wing tip thrusters, up-down and left-right translational maneuvers.

In an effort to eliminate the need for thermal protection doors, alternate wing pod configurations were considered. Such an alternate design is featured in Figure 4-8. The design has the advantage of a more forward pod center-of-gravity in addition to the elimination of thermal protection doors. Its disadvantages are increased thrust cosine losses and exhaust scrubbing of pod and wing structure.

Figure 4-9 illustrates the general arrangement and pod installation of the Modular RCS(OMS) configuration. In this concept, RCS thrusters are used to perform all maneuvers, thereby eliminating the need for a dedicated OMS engine. The nose pod arrangement for this design is similar to the nose installation for the reference case (Figure 4-7) with two fuel and two oxidizer tanks clustered around the Environmental Control and Life Support Bay in the lower front section

# REFERENCE (DESIGN) RCS POD INSTALLATION

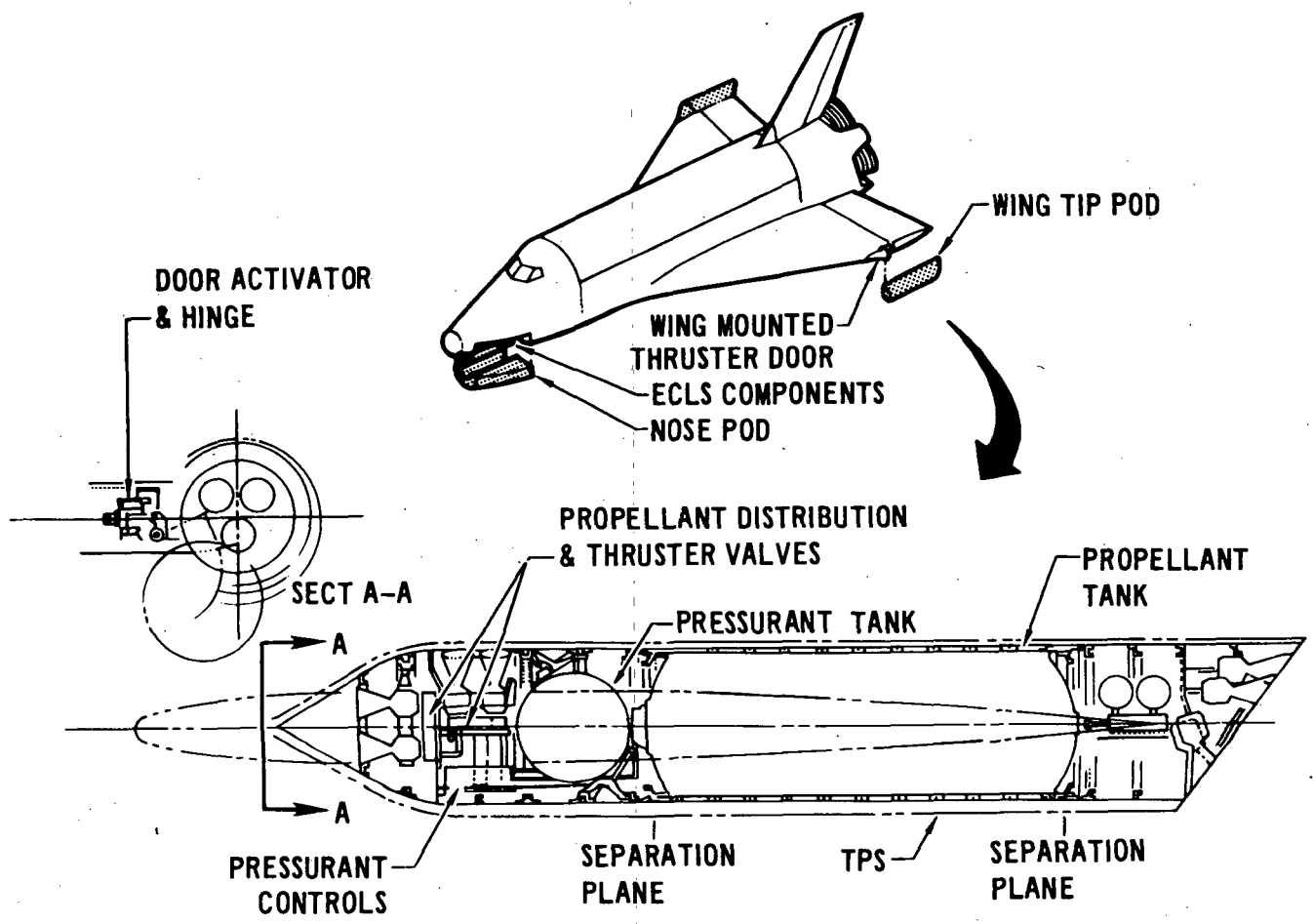
E243-134



4-6

Figure 4-3

# WING TIP RCS POD INSTALLATION



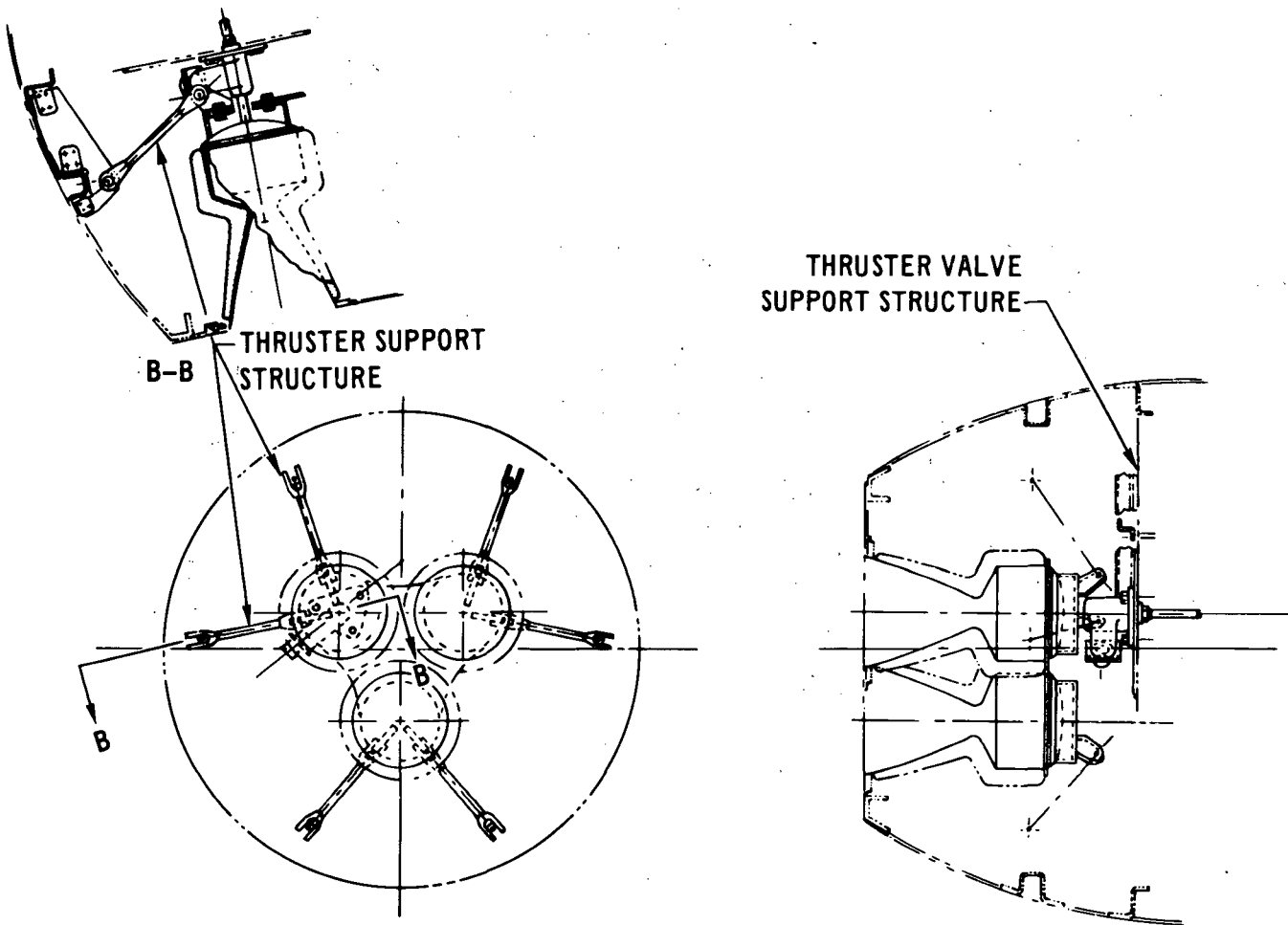
4-7

MCDONNELL DOUGLAS AERONAUTICS COMPANY - EAST

Figure 4-4

11-224

# TYPICAL THRUSTER INSTALLATION

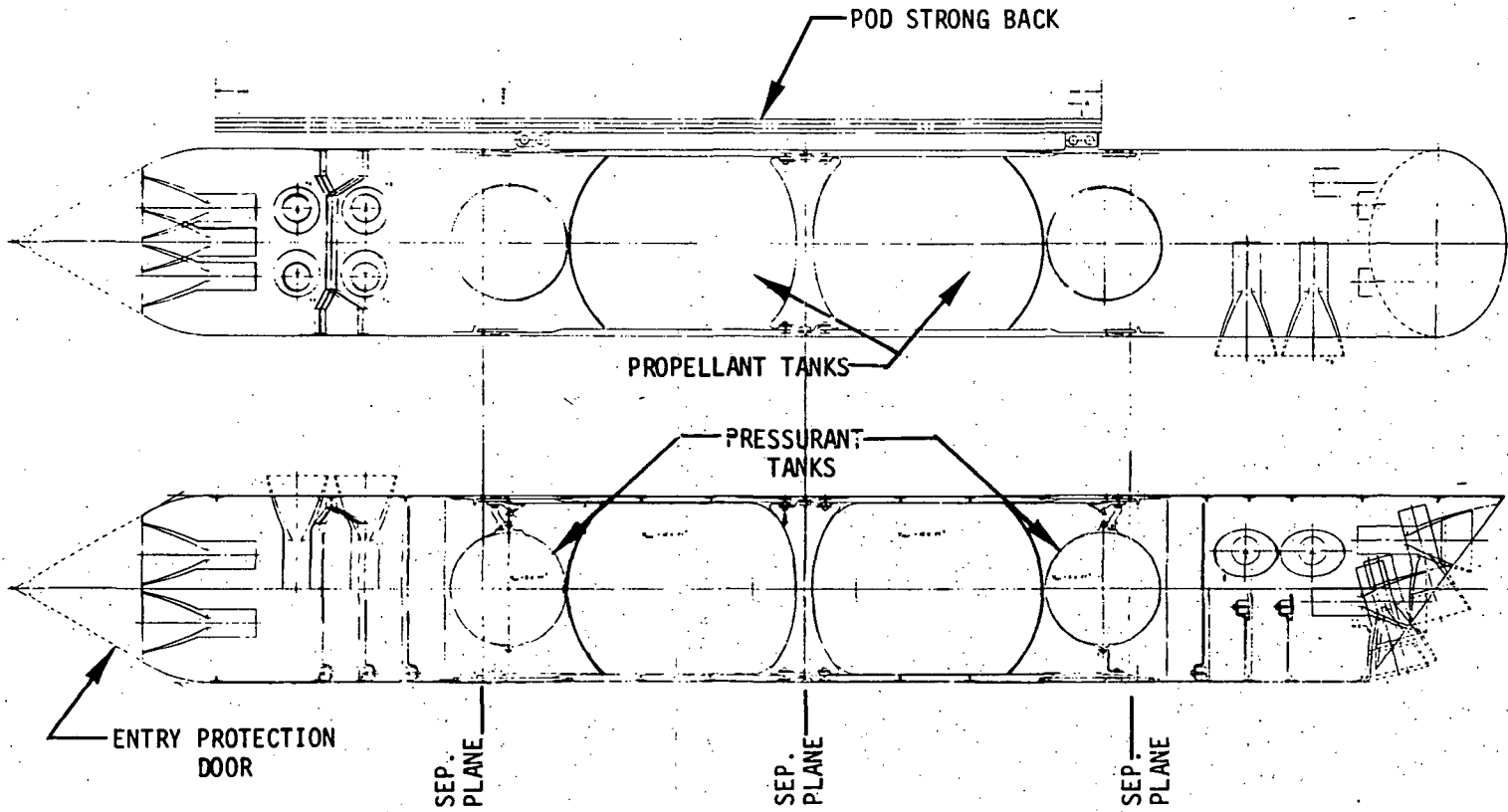


4-8

Figure 4-5

APS-310

# BIPROPELLANT RCS WING POD INSTALLATION

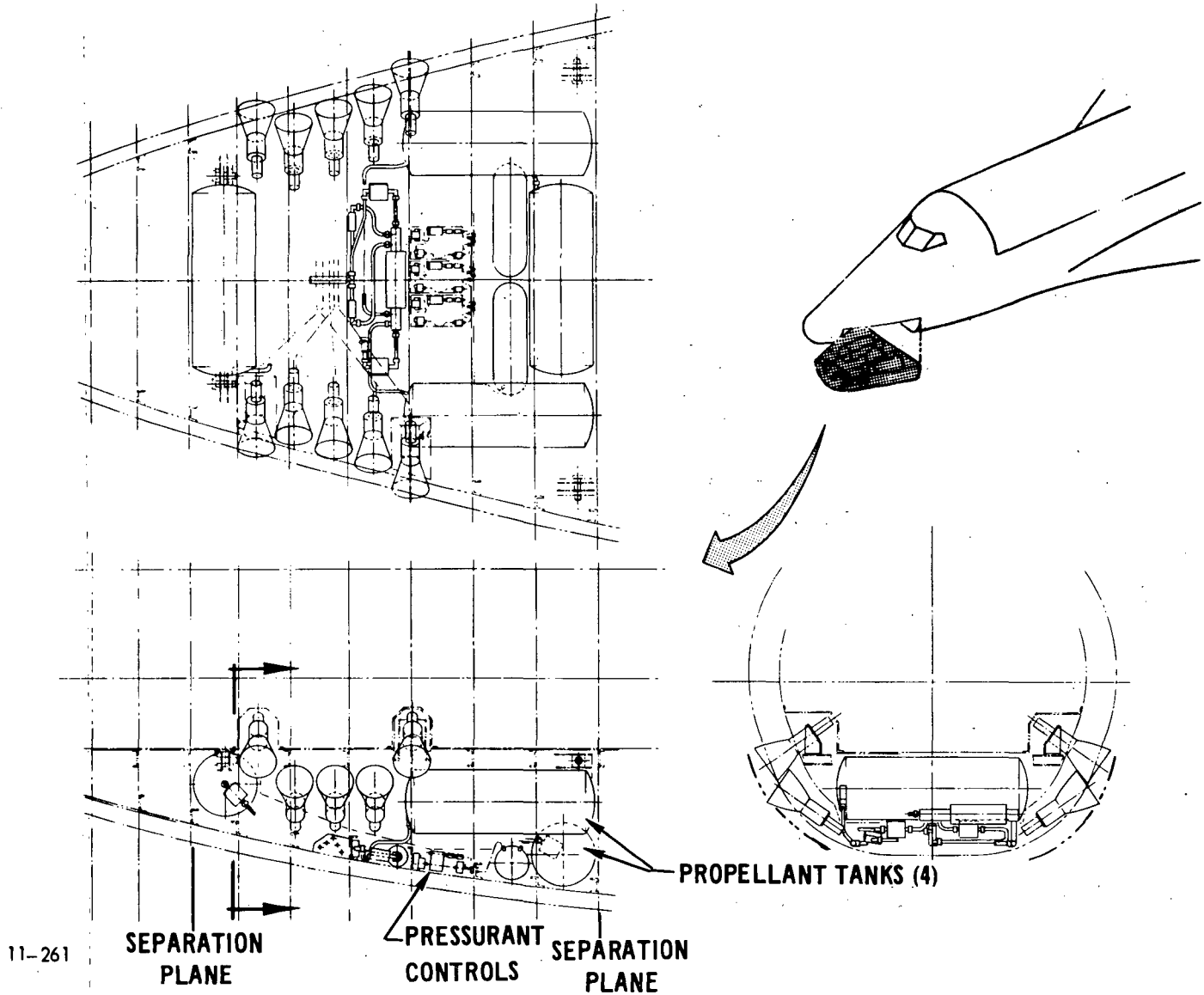


4-9

APS-248

Figure 4-6

# NOSE RCS POD INSTALLATION

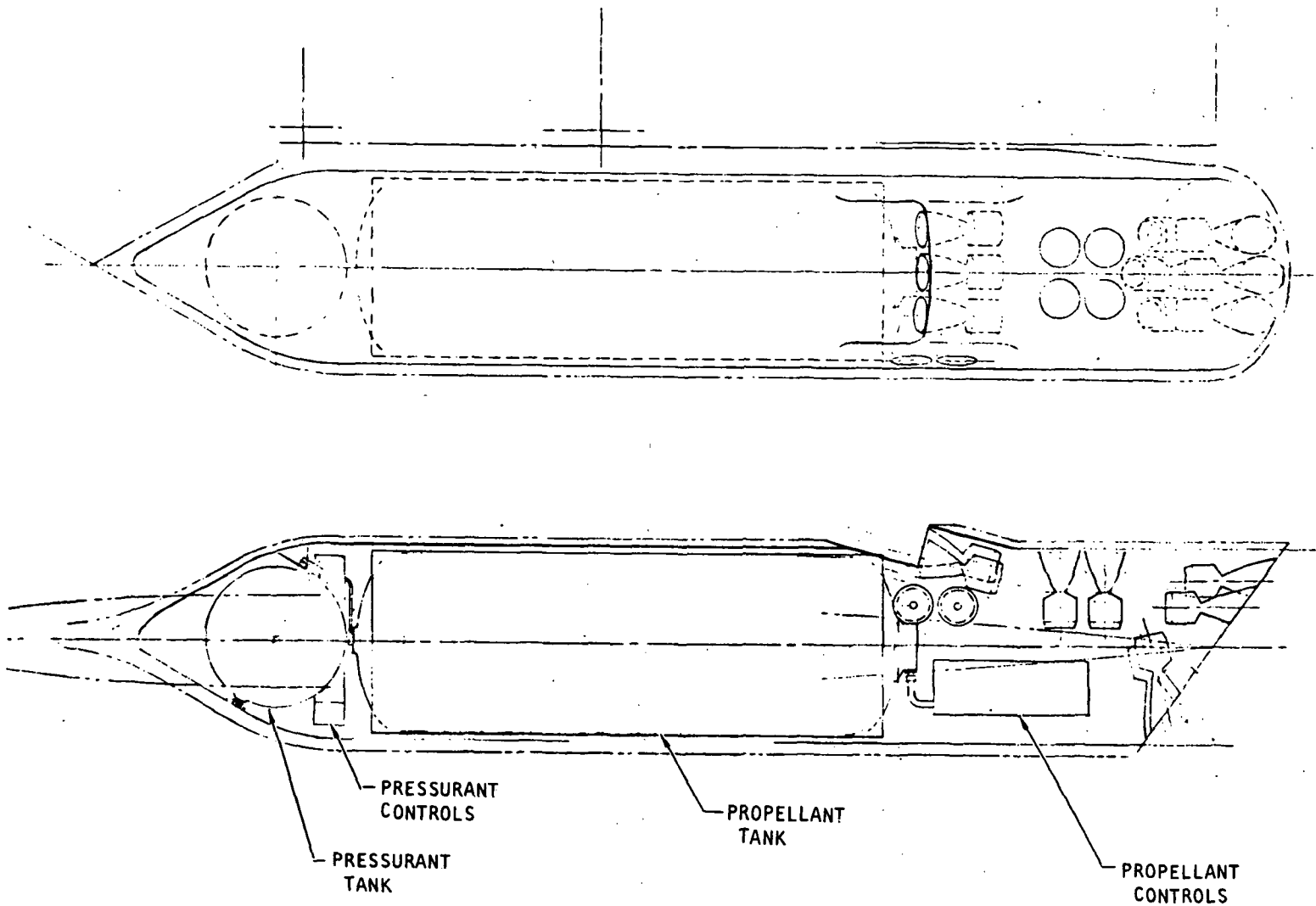


4-10

Figure 4-7

E243-201

# ALTERNATE WING TIP POD CONFIGURATION



4-11

Figure 4-8

of the vehicle nose. The RCS(OMS) side pods are illustrated in greater detail in Figure 4-10. One of the principle design features of the fuselage-mounted side pods is that they are shielded by the wings during reentry. The pod location and shape are tailored to preclude any interference with the payload bay door. Landing center-of-gravity problems are minimized in the Modular RCS (OMS) by extending the side pods forward of the aft payload bulkhead and by placing the oxidizer tanks in the most forward portions of the pods.

Figures 4-11 and 4-12 depict the installation for the Integrated RCS/OMS. As illustrated, the entire system is installed integrally within the vehicle. The design incorporates thirty-seven 600 lbf RCS engines and two 6000 lbf OMS engines which are served by common tankage. The two fuel and two oxidizer tanks are mounted directly below the payload bay to minimize axial center-of-gravity changes and to preclude the need for a propellant dump during launch aborts. Vertical center-of-gravity travel is accommodated by gimbaling the OMS engines.

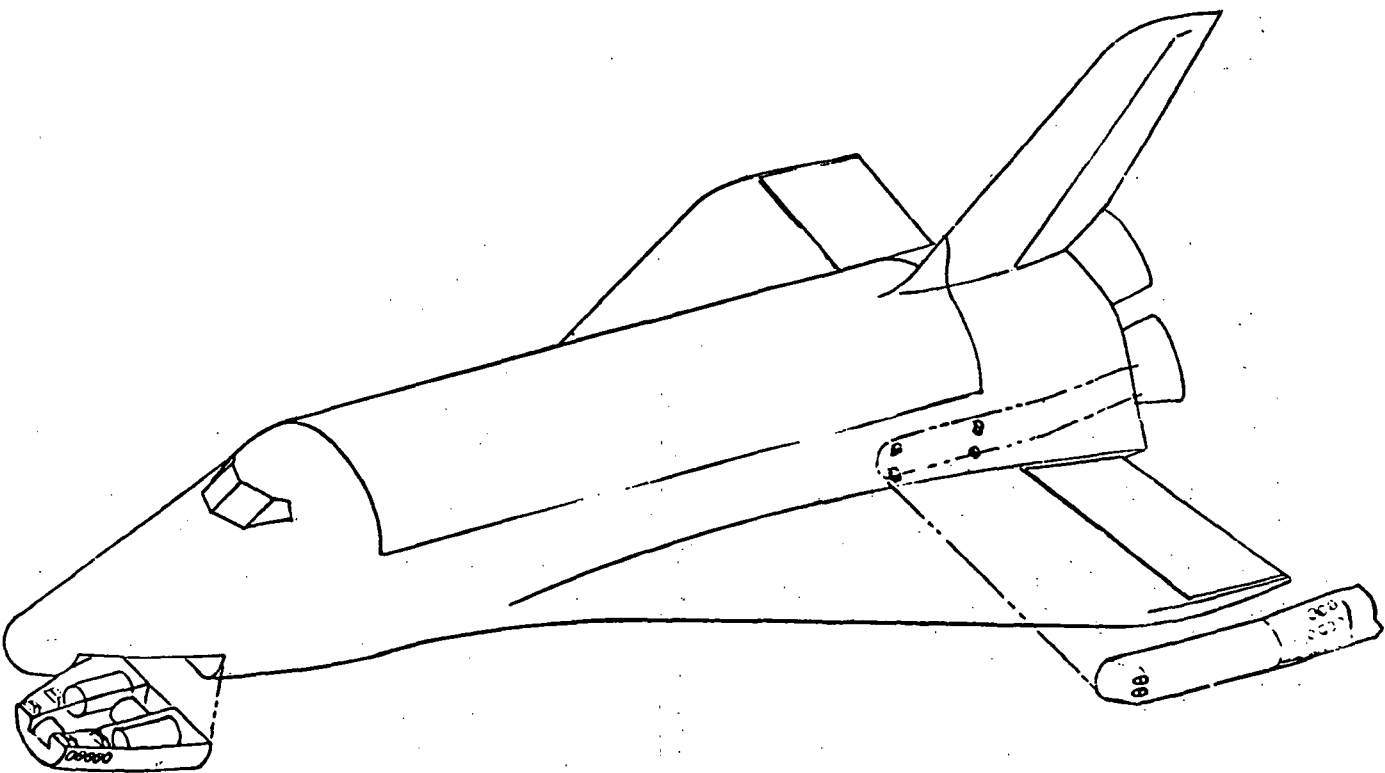
The installation and layout of the Modular APU system is shown in Figure 4-13. The Modular APU installation is basically the same in all three of the candidate vehicle concepts. The design includes two monopropellant tanks and four APU's. In normal operation, two of the APU's are active, one is idle and one dormant. The propellant tanks employ non-redundant surface tension devices to provide positive expulsion. Two tanks are provided to preclude interruption of propellant flow in the event of a propellant acquisition failure.

When the RCS and APU are integrated, four APU's with the same active, active, idle, dormant operation as in the Modular APU are used. However, when integrated, the propellant is supplied to the APU's and RCS thrusters through a common tankage located below the payload bay. In addition, APU propellant pressure is raised from tank pressure to a higher chamber pressure by an APU-driven boost pump. As in the other systems, non-redundant surface tension expulsion devices are employed in the Integrated RCS/APU.

4.3 System Implementation - The general implementation approach of the candidate configurations is relatively uniform. All systems incorporate helium pressurization, titanium tankage with surface tension propellant expulsion, and either film cooled bipropellant thrusters or catalytic monopropellant thrusters. These design configurations have evolved based on the preliminary



# BIPROPELLANT RCS(OMS) POD INSTALLATION

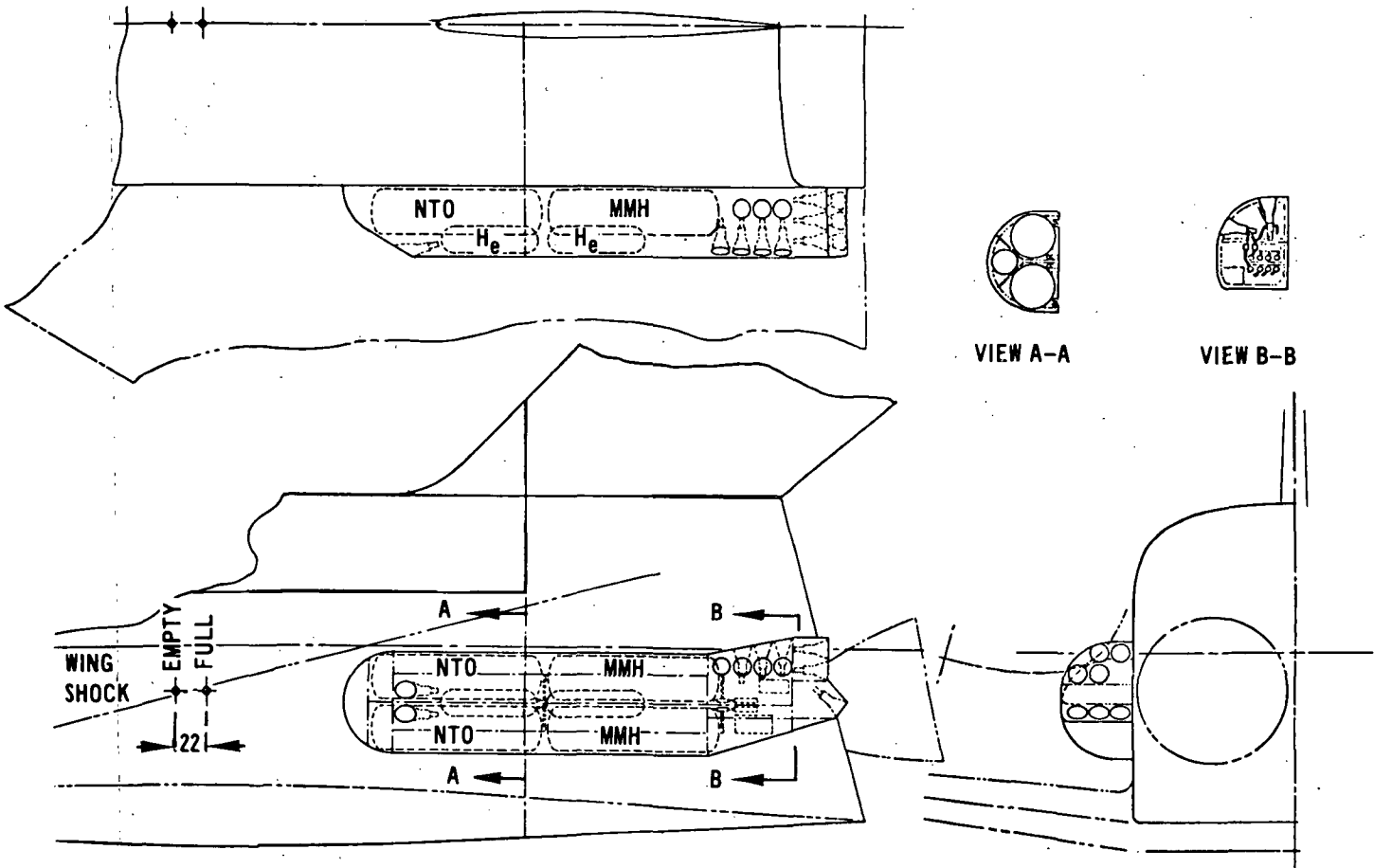


4-13

APS-395

Figure 4-9

# MODULARIZED RCS (OMS) SIDE PODS

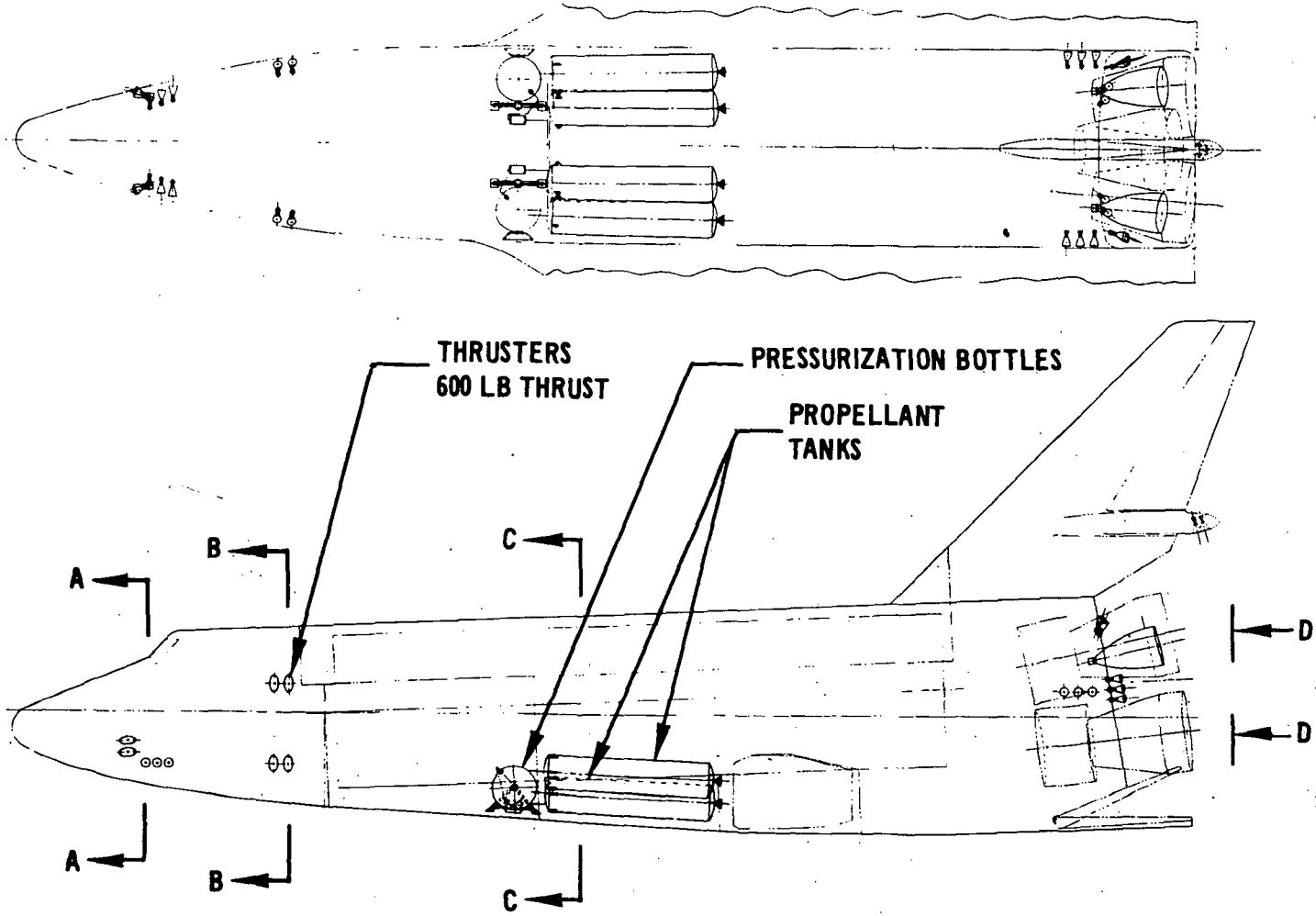


4-14

Figure 4-10

11-223

# INTEGRATED RCS AND OMS INSTALLATION

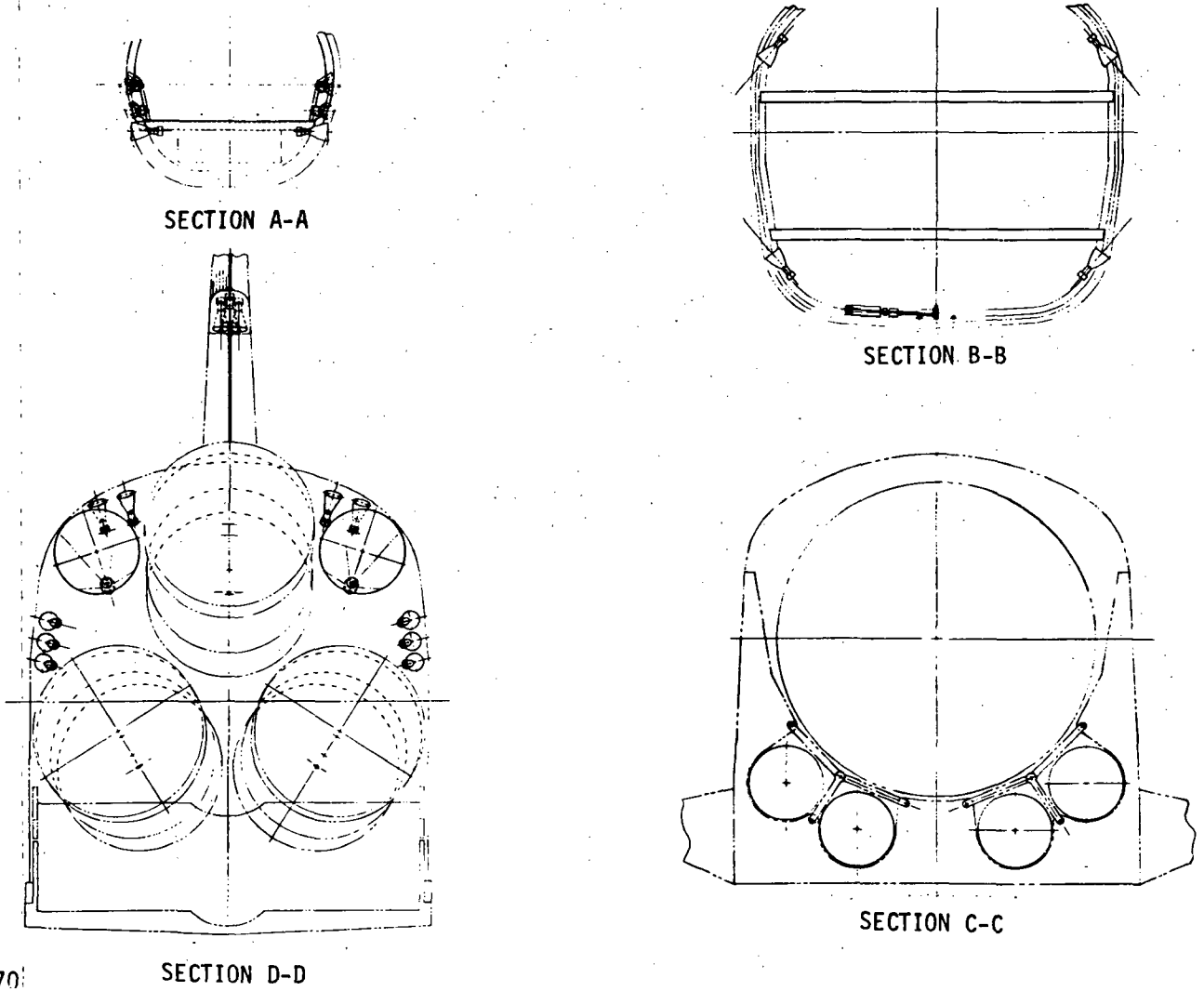


APS-102

4-15

Figure 4-11

# INTEGRATED RCS AND OMS INSTALLATION

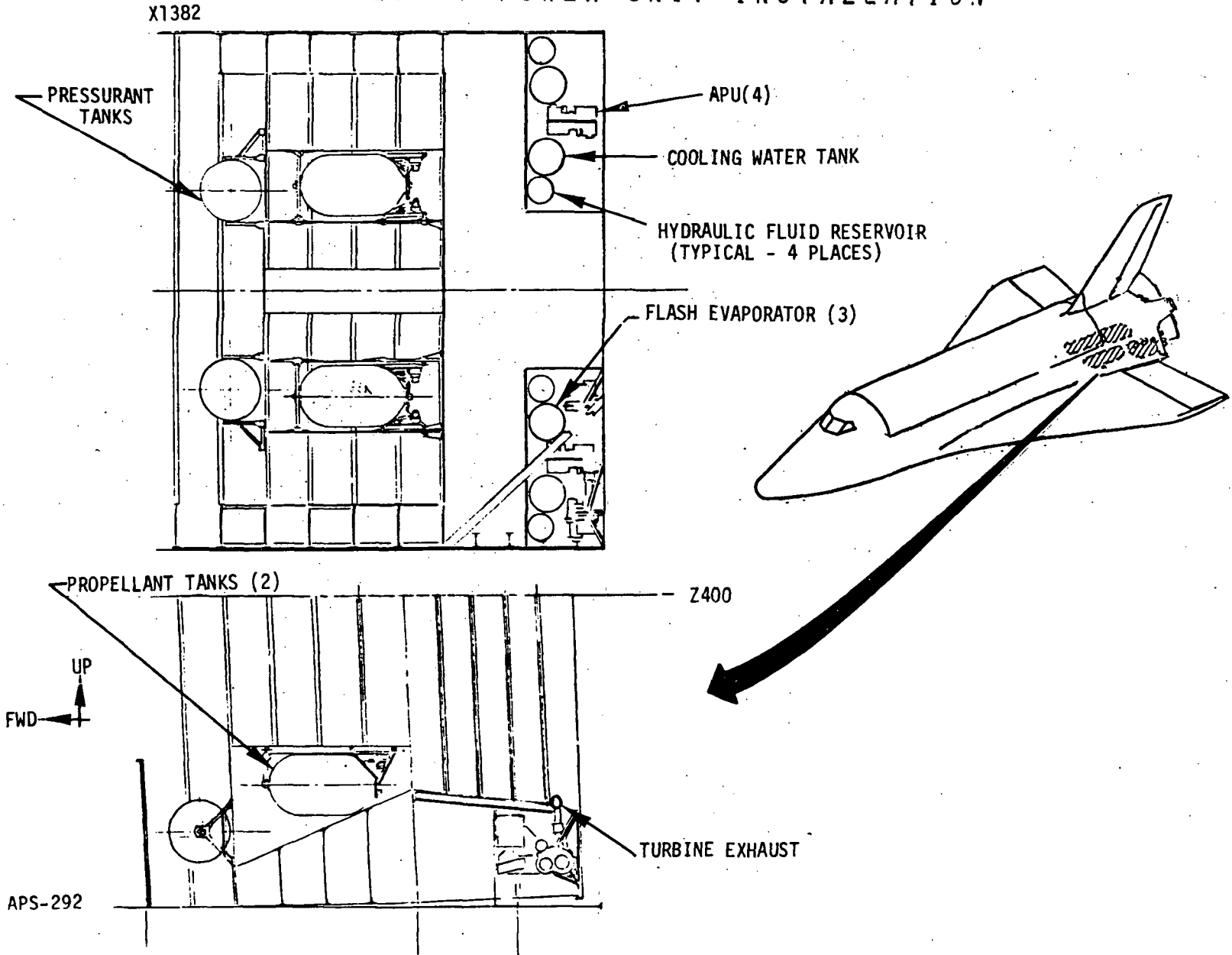


APS-270

4-16

Figure 4-12

# AUXILIARY POWER UNIT INSTALLATION



4-17

Figure 4-13

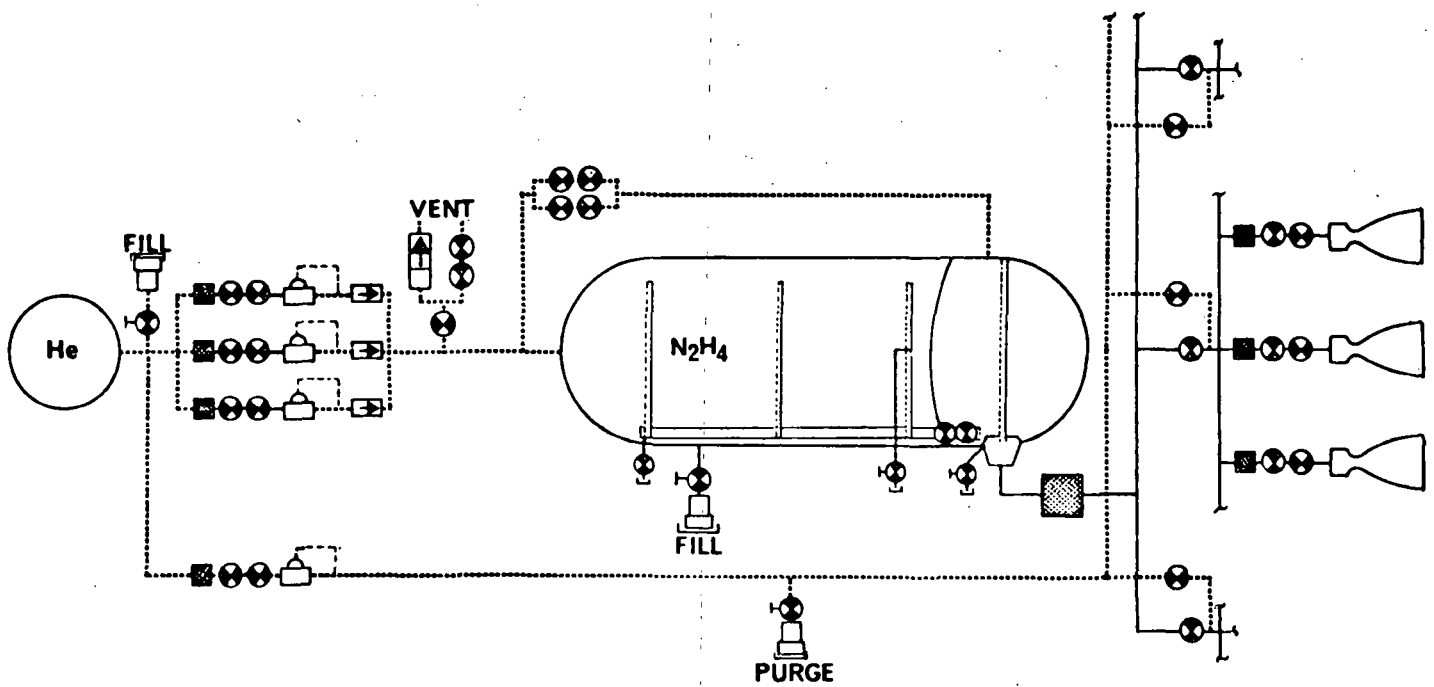
(Phase C) studies and the alternate configurations analyses. Comparisons of regulated helium pressurization with more advanced pressurization concepts are discussed in Appendix D. Titanium tankage with surface tension propellant acquisition was baselined as the result of the analyses presented in Appendix E.

Figure 4-14 presents the modular monopropellant RCS schematic. Propellant tank operating pressure is maintained by the use of pressure regulators, and regulation redundancy is provided by utilizing three parallel regulator branches. On-orbit propellant acquisition is accomplished by cylindrical surface tension screens. Because reentry accelerations will cause screen breakdown, a false bottom is incorporated in the tanks to isolate sufficient propellant in the lower compartment for entry maneuvers. Thrusters are grouped in sets of two or three, and in the event of a malfunction, can be isolated either individually or in groups. Upon completion of the mission, a helium purge downstream of the thruster isolation valves is accomplished using residual pressurant. The schematic for the modular bipropellant RCS and modular bipropellant RCS(OMS) (shown in Figure 4-15) is similar, reflecting only those changes associated with dual propellants. Equality in propellant tank pressure is accomplished by the pressure equalizing valve located downstream of the oxidizer helium regulator. The integrated bipropellant RCS/OMS schematic is shown in Figure 4-16. The two OMS engines, which share common tankage with the RCS, distinguish this configuration from the preceding bipropellant concepts. The modular APU schematic (Figure 4-17) details the gas generator and turbo power units, as well as the hydraulic and coolant loops. The integrated monopropellant RCS/APU schematic is illustrated in Figure 4-18. Here a turbine-driven boost pump is used to supply hydrazine at high pressure to the gas generator.

Figure 4-19 summarizes design conditions for the alternate configurations, and Figure 4-20 presents the specific design data used in the systems sizing analysis discussed in Section 4.4. Heating and thermal protection requirements are discussed in Appendix F.

Pressure budget optimizations were performed for the six Phase E Systems. These optimizations used the pressure drop-sensitive valve weight models described in Appendix A and the relationships defined in Figure 4-21. For a constant thruster chamber pressure, this optimization is a tradeoff between pressurization system weight plus propellant tank weight, and propellant valve weight. This tradeoff and the resulting optimum total pressure drop for the monopropellant RCS is illustrated in Figure 4-22. For the OMS

# MODULAR RCS-N<sub>2</sub>H<sub>4</sub>

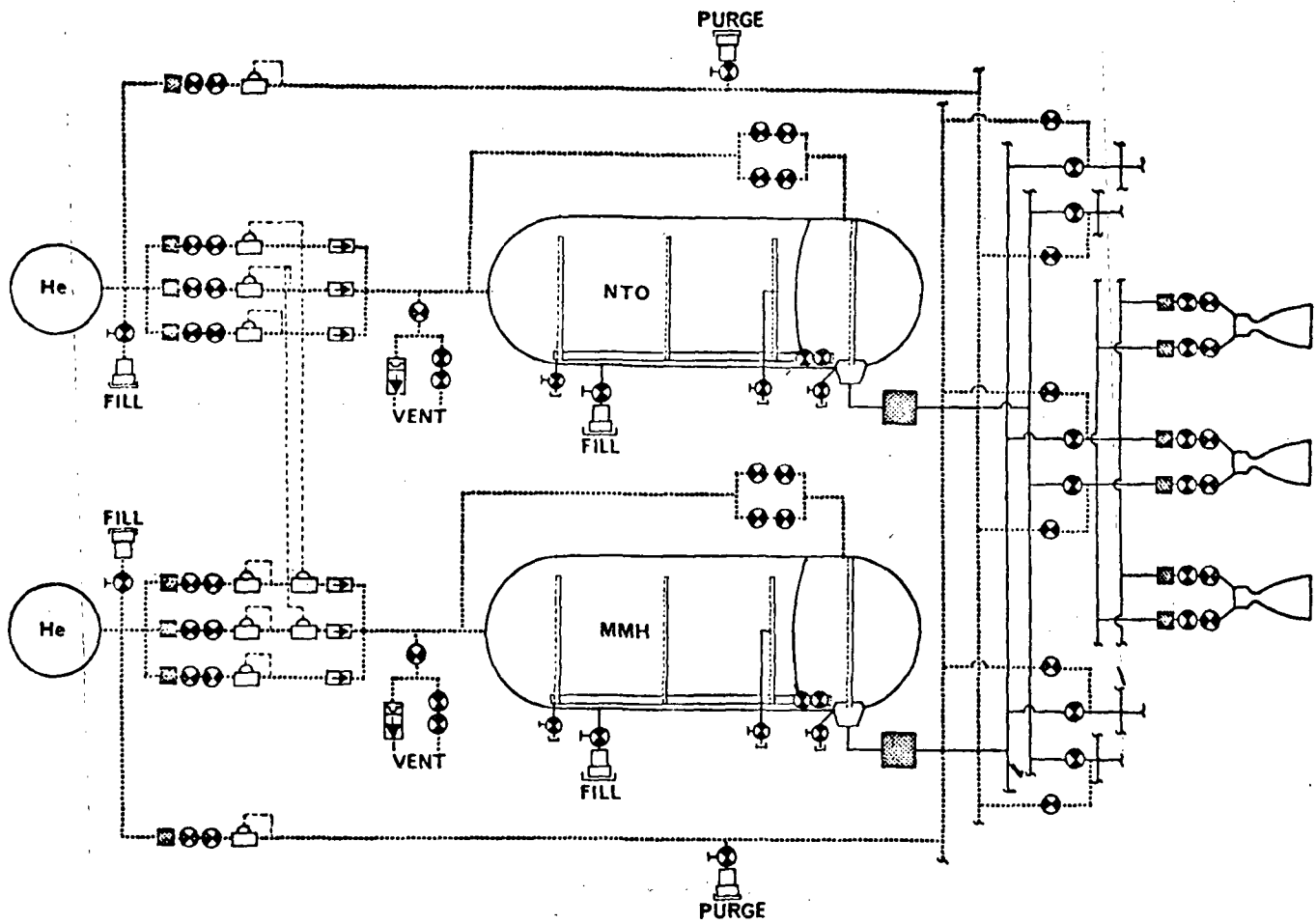


APS-150A

4-19

Figure 4-14

# MODULAR RCS - NTO/MMH MODULAR RCS (OMS) - NTO/MMH



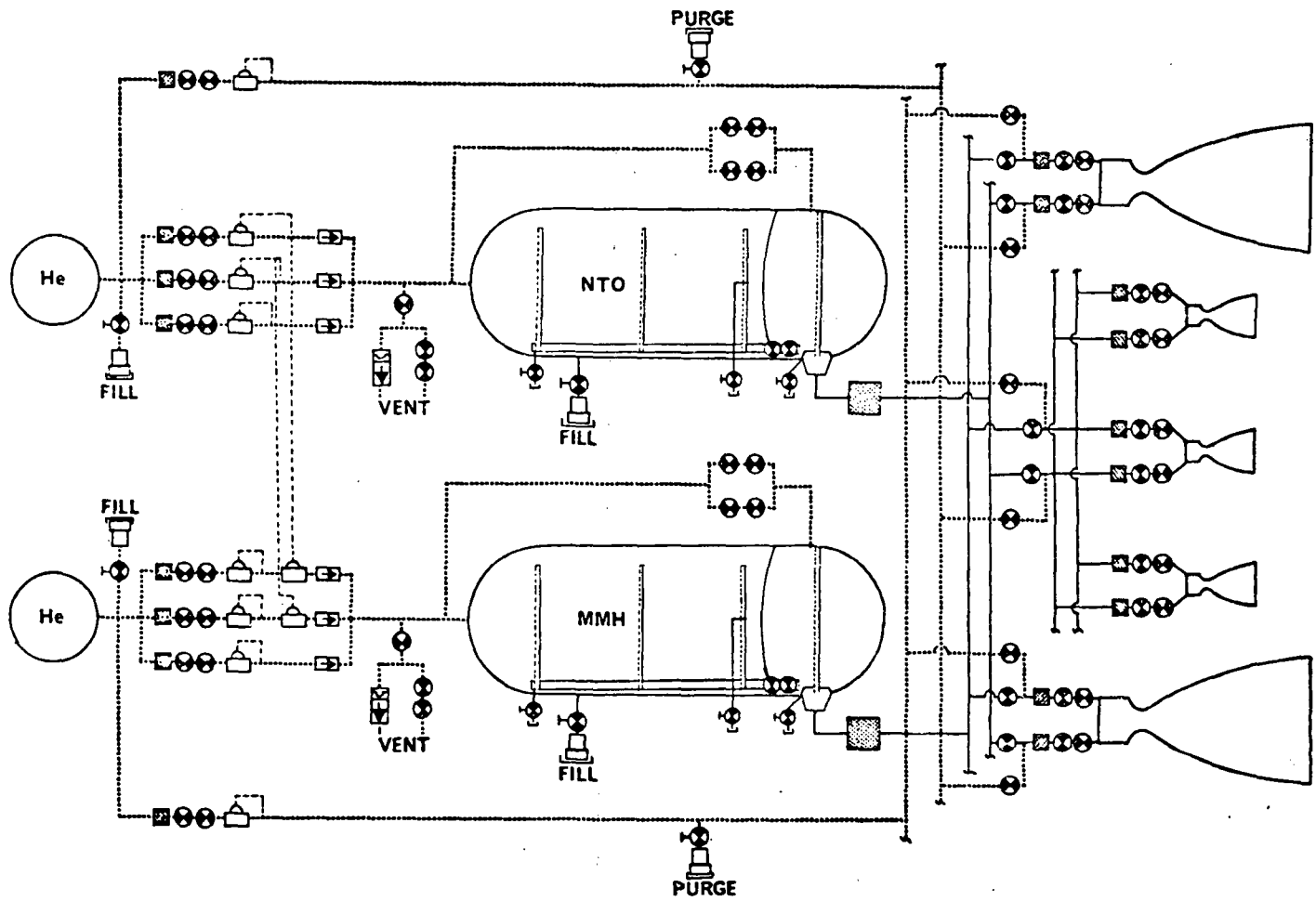
APS-137A

4-20

Figure 4-15



# INTEGRATED RCS/OMS - NTO/MMH

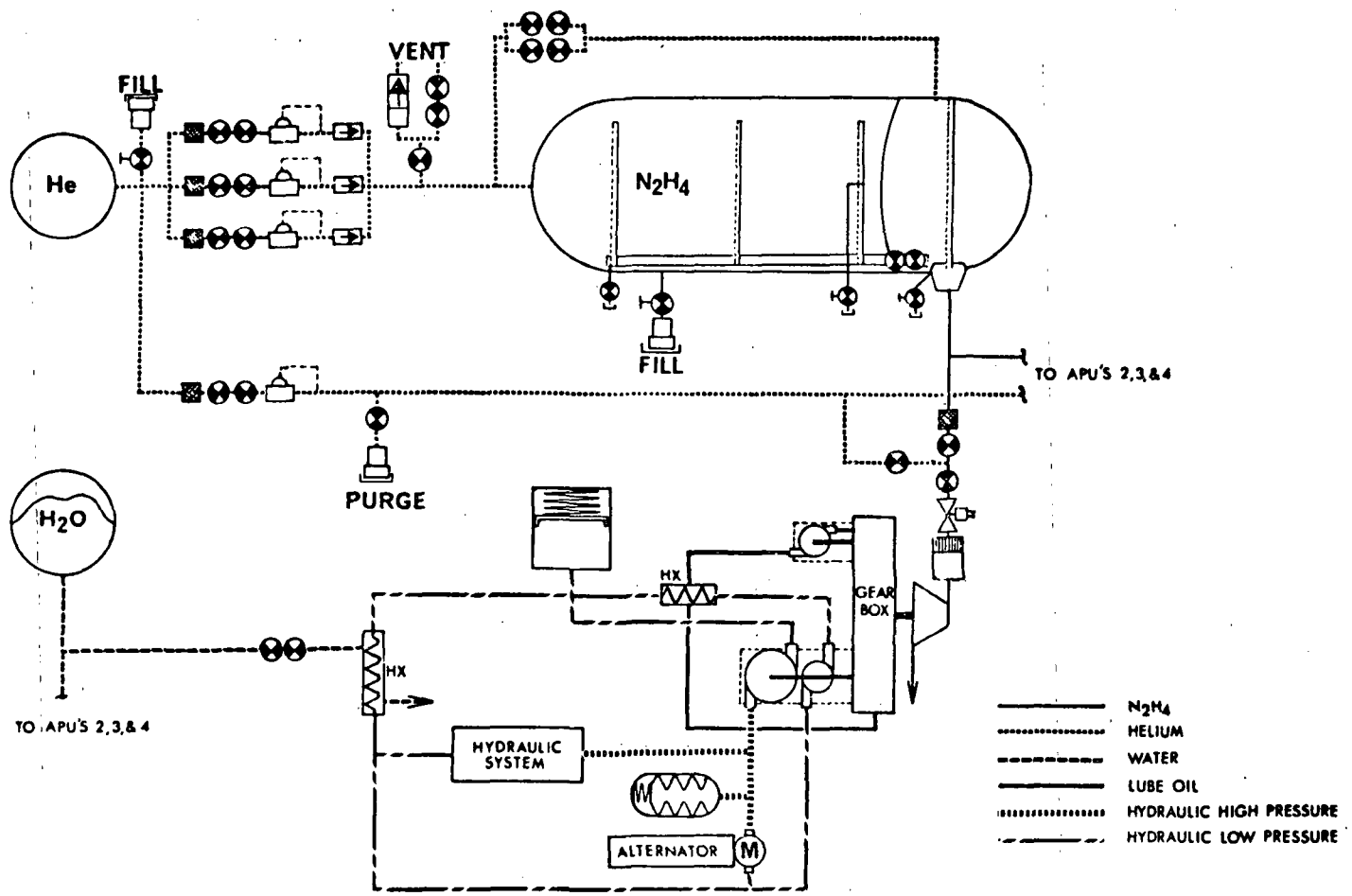


APS-136A

4-21

Figure 4-16

### MODULAR APU - N<sub>2</sub>H<sub>4</sub>

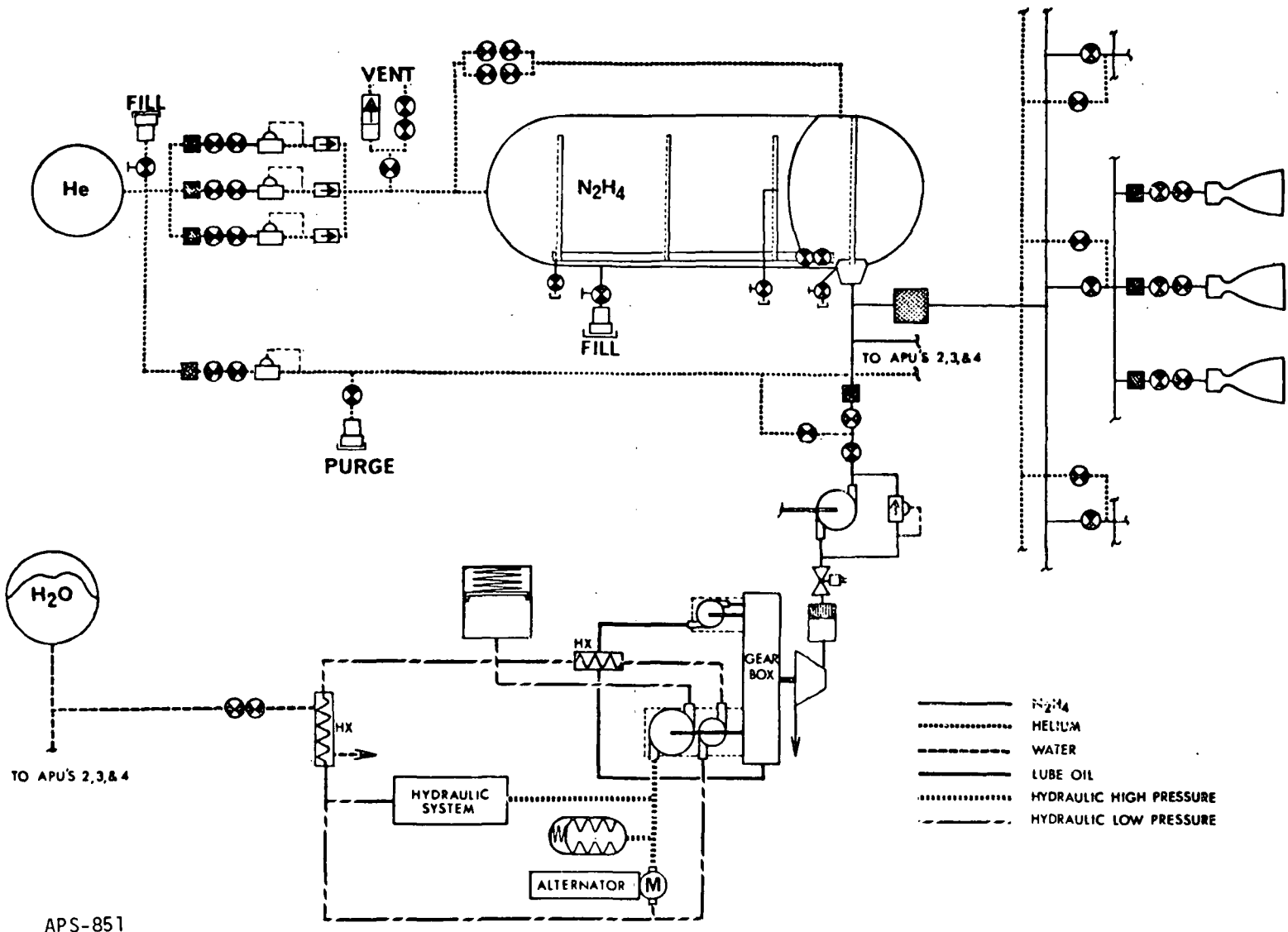


APS-138A

4-22

Figure 4-17

# INTEGRATED RCS/APU - N<sub>2</sub>H<sub>4</sub>



APS-851

4-23

Figure 4-18

## PHASE E SYSTEM STUDIES

MODULAR RCS	- N <sub>2</sub> H <sub>4</sub>	WING AND NOSE MODULES UTILIZING HELIUM PRESSURIZATION; TITANIUM TANKAGE; SURFACE TENSION PROPELLANT EXPULSION; CONVENTIONAL NOZZLE THRUSTERS; ELECTRIC HEATER/HEAT PIPE THERMAL CONTROL; NO PROPELLANT INTERCONNECTS BETWEEN MODULES
	- NTO/MMH	WING AND NOSE MODULES CONTAINING HELIUM PRESSURIZATION; ULLAGE PRESSURE EQUALIZATION; TITANIUM TANKAGE; SURFACE TENSION PROPELLANT EXPULSION; FILM-COOLED THRUSTERS; ELECTRIC HEATER THERMAL CONTROL; NO INTRA-MODULE INTERCONNECTS
MODULAR RCS (OMS)	- NTO/MMH	BIPROPELLANT FUSELAGE AND NOSE MODULES CONTAINING HELIUM PRESSURIZATION; ULLAGE PRESSURE EQUALIZATION; TITANIUM TANKAGE; SURFACE TENSION PROPELLANT EXPULSION; FILM-COOLED THRUSTERS; ELECTRIC HEATER THERMAL CONTROL; NO INTRA-MODULE INTERCONNECTS
INTEGRATED RCS/OMS	- NTO/MMH	BIPROPELLANT SYSTEM WITH COMMON, INTEGRATED TANKAGE; HELIUM PRESSURIZATION; ULLAGE PRESSURE EQUALIZATION; TITANIUM TANKS; SURFACE TENSION PROPELLANT EXPULSION; FILM-COOLED RCS THRUSTERS; REGEN-COOLED OMS ENGINES (2); ELECTRIC HEATER THERMAL CONTROL
INTEGRATED RCS/APU	- N <sub>2</sub> H <sub>4</sub>	MONOPROPELLANT SYSTEM WITH COMMON, INTEGRATED, TITANIUM TANKAGE; HELIUM PRESSURIZATION/APU BOOST PUMP; SURFACE TENSION PROPELLANT EXPULSION; CONVENTIONAL NOZZLE THRUSTERS; WATER-COOLED APU; ELECTRIC HEATER/HEAT PIPE THRUSTER THERMAL CONTROL
MODULAR APU	- N <sub>2</sub> H <sub>4</sub>	MONOPROPELLANT SYSTEM WITH ACTIVE-ACTIVE-IDLE-DORMANT REDUNDANCY; MANIFOLDED TITANIUM TANKAGE; HELIUM PRESSURIZATION; SURFACE TENSION PROPELLANT EXPULSION; THERMAL BED GAS GENERATOR; MODULATED, WATER-COOLED HYDRAULIC SYSTEM, CONDUCTIVE-COOLED ALTERNATORS

11-314A

4-24

Figure 4-19

# SYSTEM DESCRIPTIONS

SYSTEM CHARACTERISTICS			DESIGN CONDITIONS*										
SYSTEM	PROPEL- LANTS	CONFIG- URATION	NO. OF ENGINES			NO. OF ENGINES VALVES		NO. OF ISOLATION VALVES	NO. OF TANKS	TANK DIAMETER	THRUSTER HEATING (KW-HR)	PROPELLANT HEATING (KW-HR/LBM)	THERMAL PROTECTION (LBM/FT <sup>2</sup> )
			ACS	± X	OMS	RCS	OMS						
RCS	N <sub>2</sub> H <sub>4</sub>	MODULAR	10/9/9	0/6/6	0	20/30/30	0	6/7/7	4/1/1	19/32/32	62	1.4 x 10 <sup>-3</sup>	2.34
RCS	N <sub>2</sub> O <sub>4</sub> MMH	MODULAR	10/9/9	0/6/6	0	40/60/60	0	12/14/14	4/2/2	19/32/32	36	4.05 x 10 <sup>-3</sup>	2.34
RCS(OMS)	N <sub>2</sub> O <sub>4</sub> MMH	MODULAR	12/10/10	0/8/8	0	48/72/72	0	10/12/12	4/4/4	19/30/30	44	1.08 x 10 <sup>-3</sup>	1.65
RCS/OMS	N <sub>2</sub> O <sub>4</sub> MMH	INTEGRATED	27	10	2	148	4/4	36	4	40	34	4.83 x 10 <sup>-4</sup>	0
RCS/APU	N <sub>2</sub> H <sub>4</sub>	INTEGRATED	27	10	0	74	0	18	2	40	62	1.42 x 10 <sup>-3</sup>	0
APU	N <sub>2</sub> H <sub>4</sub>	MODULAR	0	0	0	0	0	0	2	19	0.5**	0	0

\*FORWARD MODULE /AFT MODULE /AFT MODULE  
\*\*POWER REQD. FOR THERMAL BED GAS GENERATOR

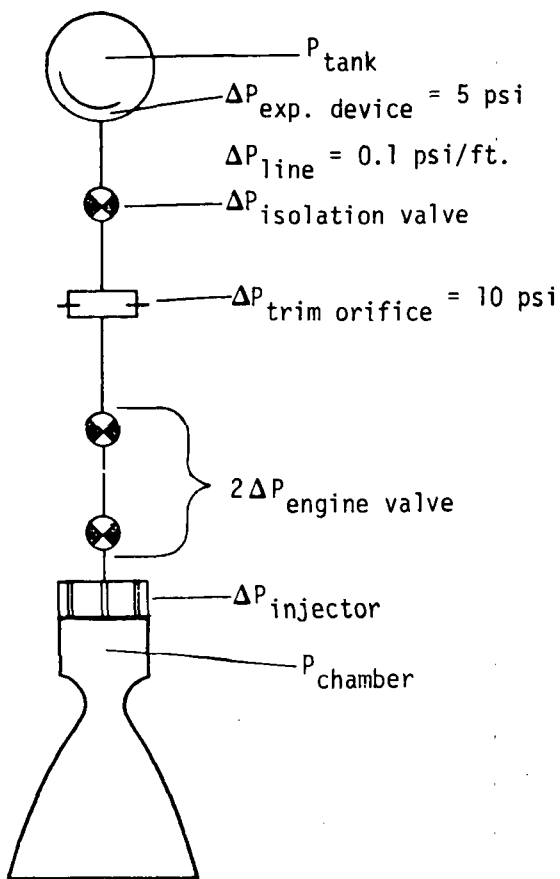
systems (modular RCS(OMS) and integrated RCS/OMS), the high valve weights corresponding to low pressure drop valves are balanced by the weight savings in pressurization systems and large volume propellant tanks at lower operating pressures resulting in system optima of 100 lbf/in.<sup>2</sup> pressure drop. For the separate RCS, where the smaller volume propellant tanks and pressurization systems weight savings are not as sensitive to tank pressure decreases, the optima occurs at a total pressure drop of 150 lbf/in.<sup>2</sup>. Figures 4-23 through 4-27 define the design pressure budgets, flowrates, and line diameters for the six systems evaluated in Phase E.

Line and component joining techniques were evaluated to provide a broader basis for systems comparison. A summary of line and component joining techniques is presented in Figure 4-28. The candidate techniques include swaged, brazed and welded joints and separable rigid and flex connectors. The swaged and welded joints are limited to permanent connections whereas brazed joints and separable connections can also be used where occasional part replacement is necessary. Since no heat affected zone is developed in the critical fatigue area at the joint, swaged designs avoid the weight penalty associated with the use of heavier wall thickness over the entire tube length to allow for the local strength reduction resulting from welding or brazing. Brazed connections were used on both Gemini and Apollo. These connections proved to be very reliable, leak-free and strong. The major disadvantage of brazed connections is the large number of brazing heads required for different fittings and tube sizes. Welding produces reliable, leak-free joints, without introduction of dissimilar metals as in brazing. Experience with welded joints, though favorable, is not extensive. The biggest disadvantage with welded joints is strength degradation in the heat affected area of the tube.

The state-of-the-art on separable connectors has not advanced significantly in the past few years. Recent testing and evaluation of separable connectors at MDAC have shown that Resistoflex Dynatube fittings will provide a lightweight, reliable system. Where relative movement occurs between joined parts, separable flex couplings such as the Gamah and Wiggins couplings may be required. They allow for 0.25 in. axial and  $\pm 4^\circ$  angular movement.

Although the Resistoflex, Gamah and Wiggins connectors are marked improvements over the flared and flareless types using a variety of sleeves, ferrules, seals, washers, etc., presently available separable connector technology does not guarantee a leak-proof joint. Figure 4-29 summarizes the recommended line joining methods for use on the Shuttle RCS. As shown in Figure 4-29, swaged

# SYSTEM PRESSURE DROP OPTIMIZATION GROUND RULES



$$\begin{aligned} \Delta P_{\text{total}} &= P_{\text{tank}} - P_{\text{chamber}} \\ &= \Delta P_{\text{injector}} + 2 \Delta P_{\text{engine valve}} + \Delta P_{\text{trim orifice}} \\ &\quad + \Delta P_{\text{expulsion device}} + \Delta P_{\text{line}} + \Delta P_{\text{isolation valve}} \end{aligned}$$

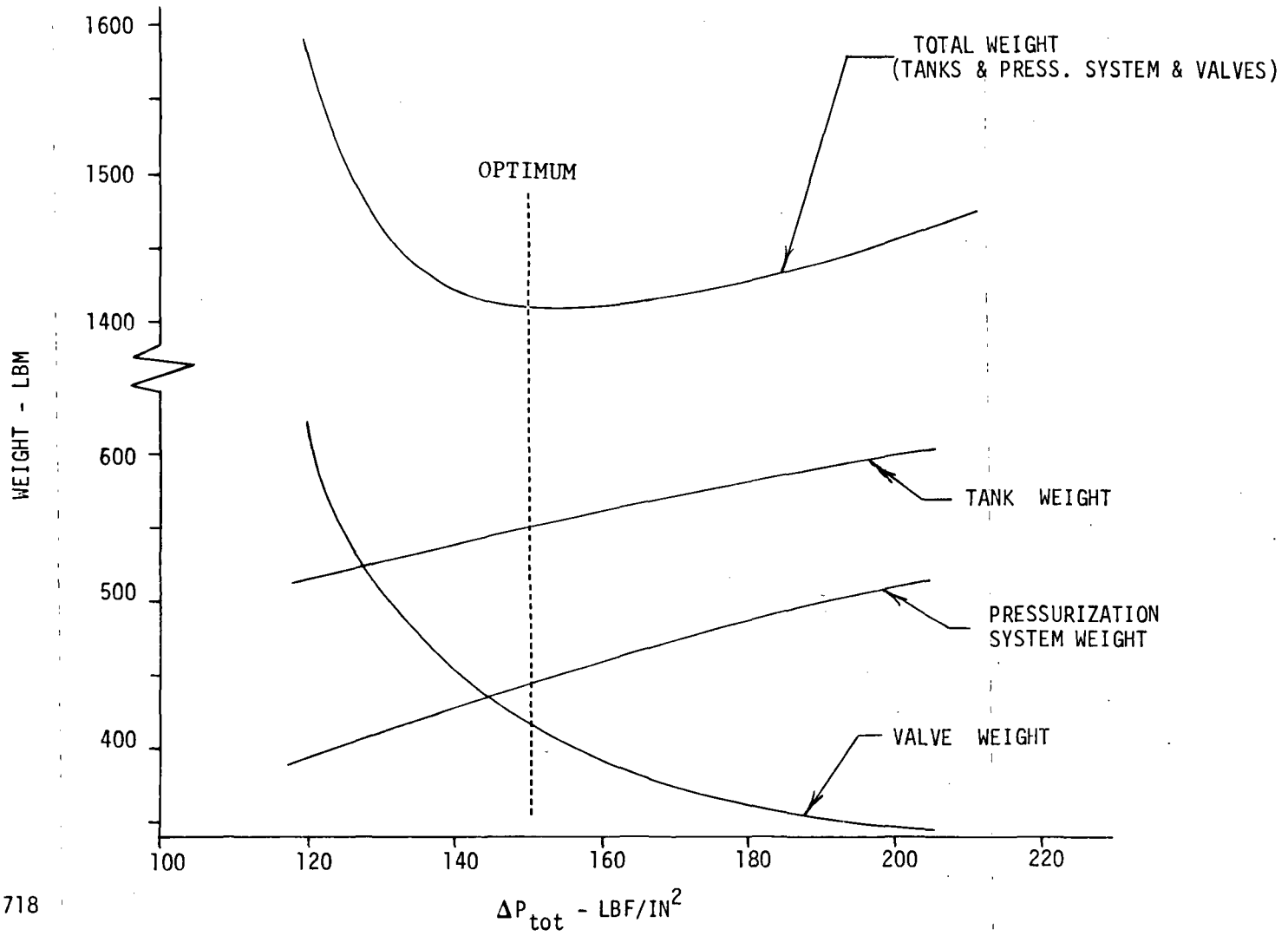
$$\Delta P_{\text{isolation valve}} = (.667) \Delta P_{\text{engine valve}}$$

$$\Delta P_{\text{injector}} = (K) P_{\text{chamber}}$$

Mono RCS;  $K = 0.4$   
 Biprop RCS;  $K = 0.35$   
 RCS(OMS);  $K = 0.3$

# SYSTEM PRESSURE DROP OPTIMIZATION

MONOPROPELLANT RCS



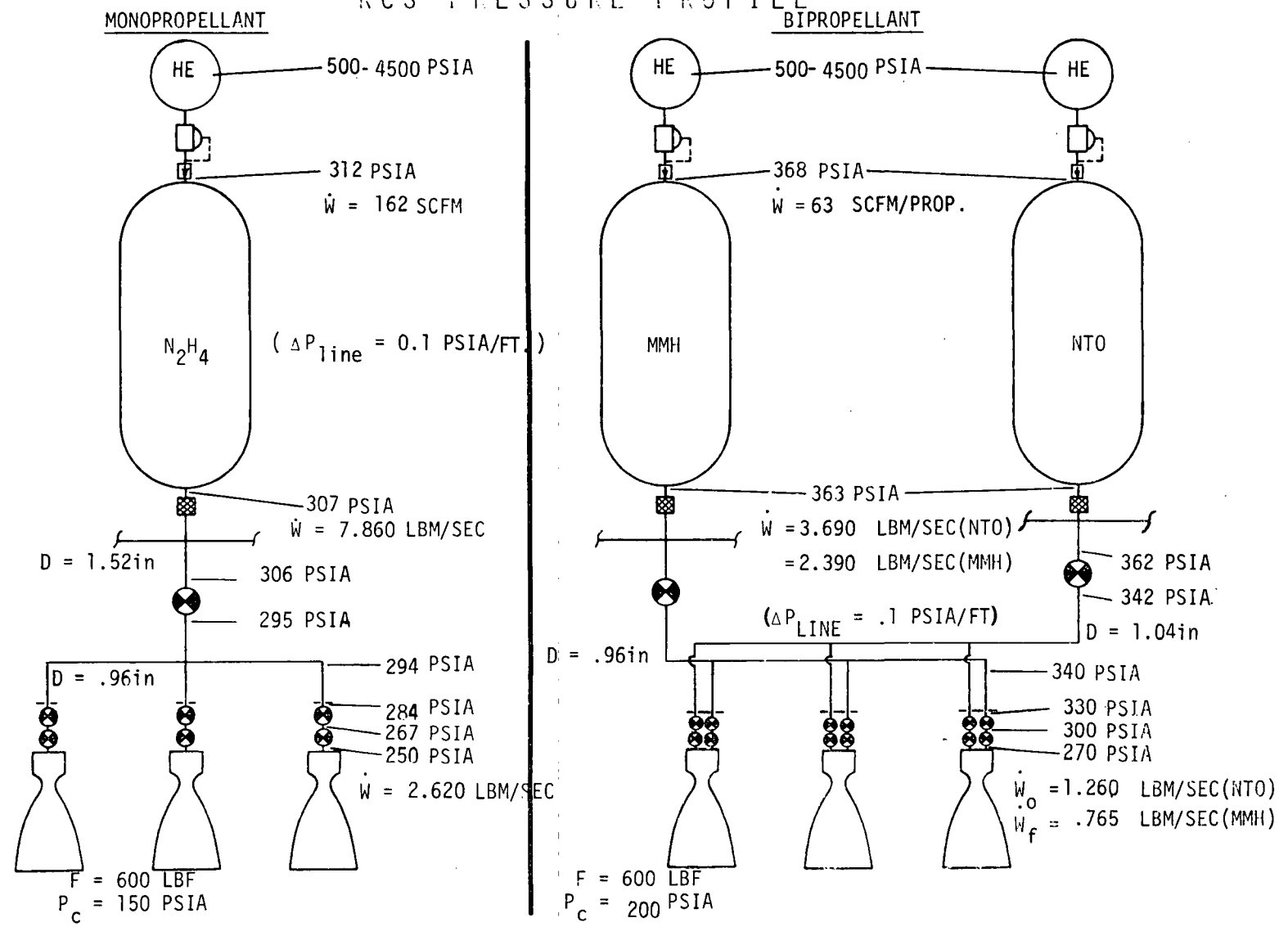
APS-718

4-28

Figure 4-22



### RCS PRESSURE PROFILE



APS-313 A NOTE: REDUNDANT COMPONENTS OMITTED FOR CLARITY

MCDONNELL DOUGLAS ASTRONAUTICS COMPANY - EAST

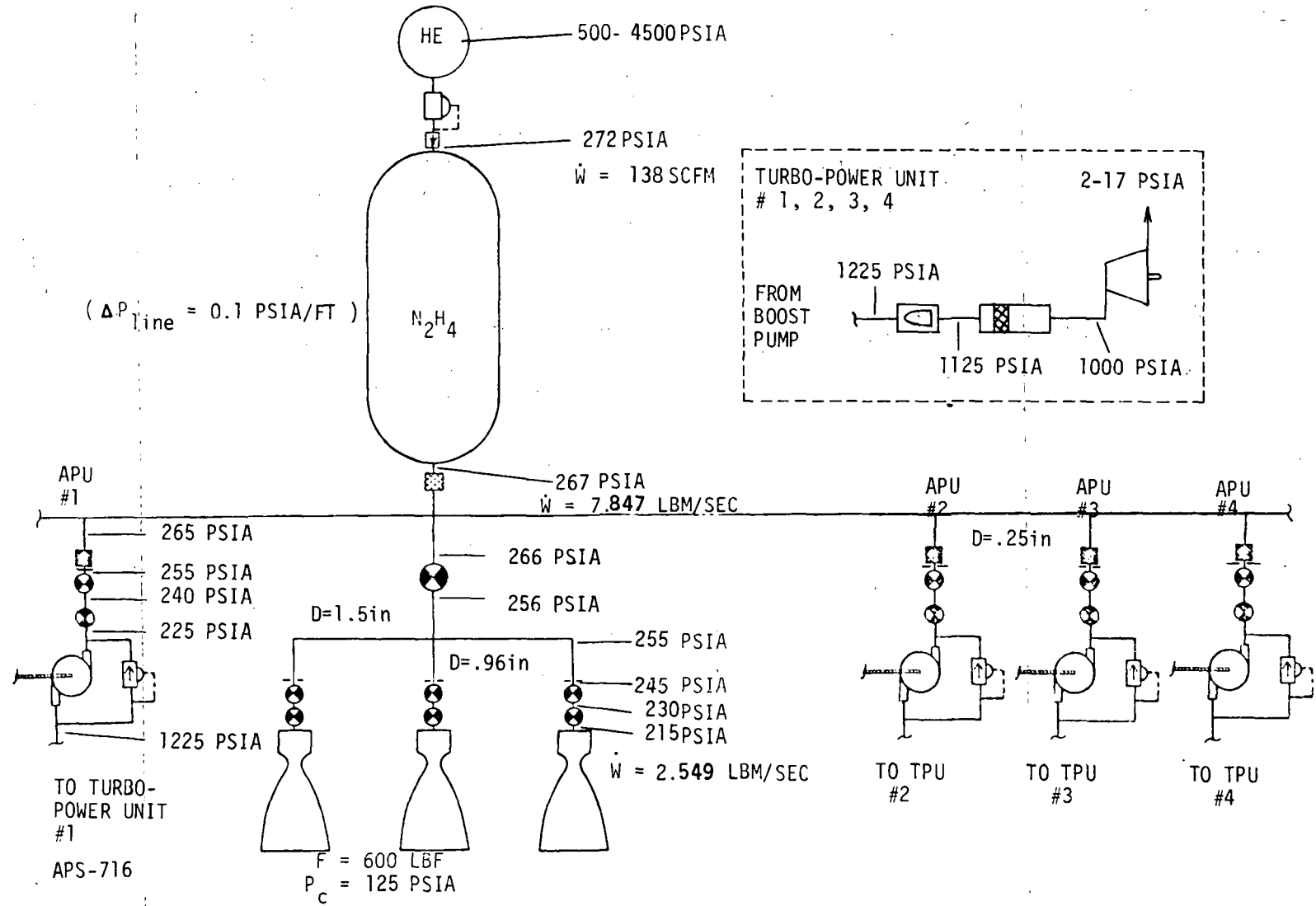
4-29

Figure 4-23





# INTEGRATED RCS/APU PRESSURE PROFILE

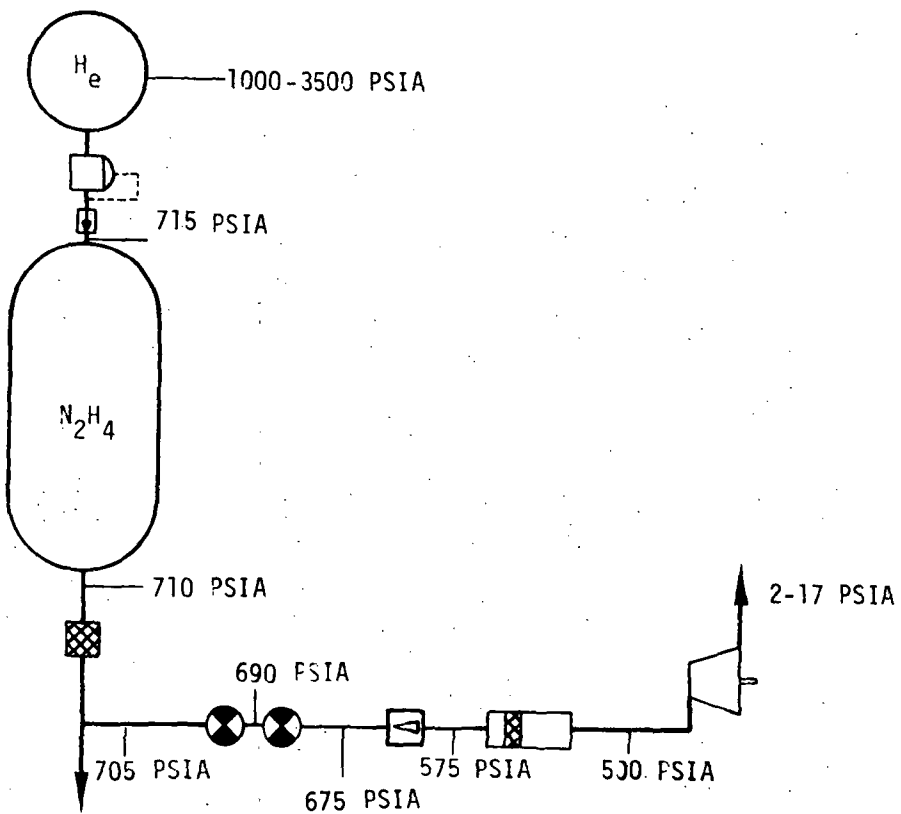


MCDONNELL DOUGLAS AERONAUTICS COMPANY - EAST

4-32

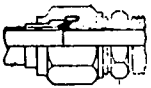



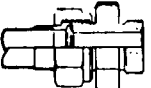

Figure 4-26

### APU PRESSURE PROFILE



APS-314

## SUMMARY CANDIDATE CONNECTORS

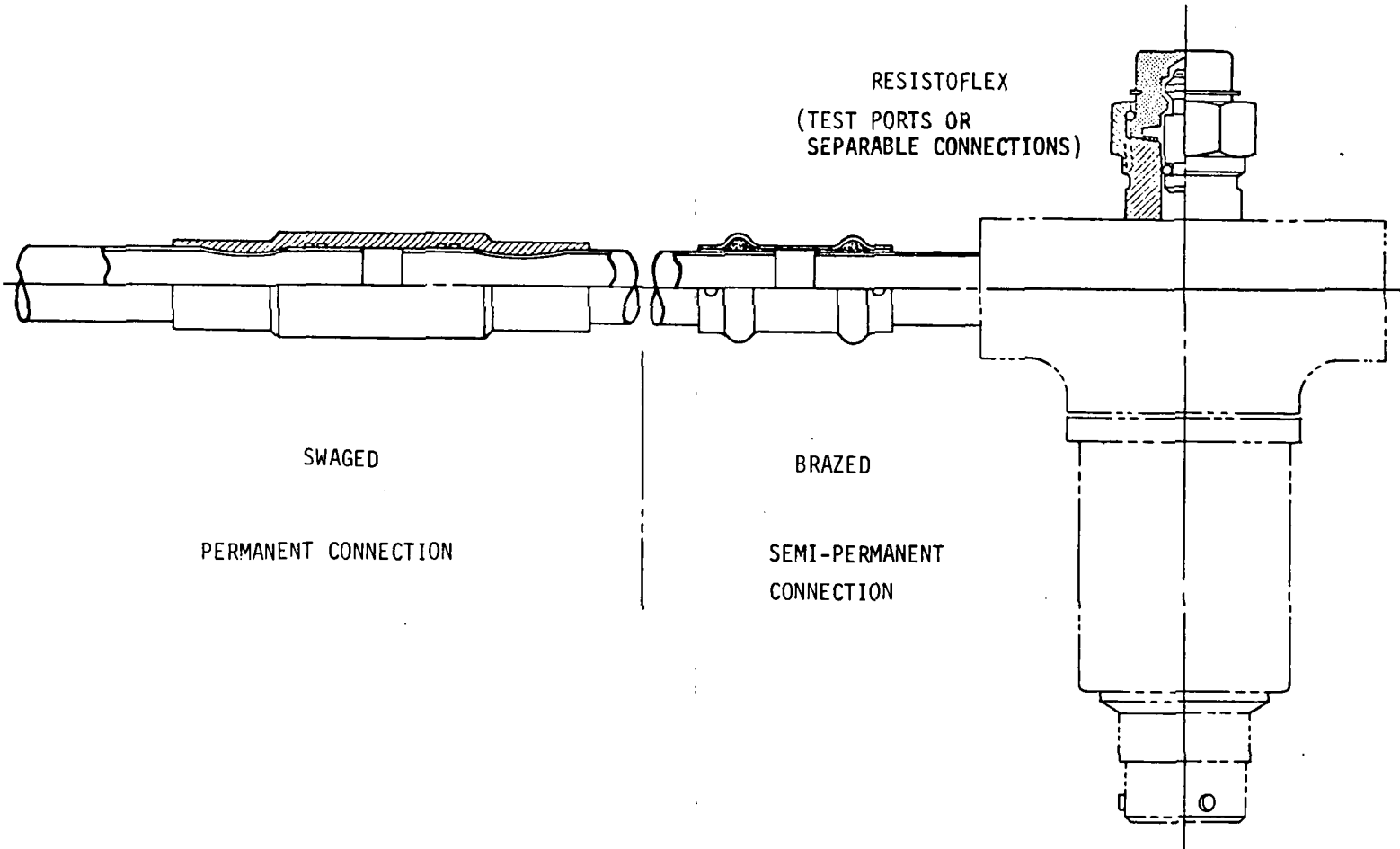
		RELATIVE WEIGHT	COST (\$)	TYPE PERM/SEP	ALLOWABLE MISALIGNMENT	MATERIAL	ASSEMBLE IN PLACE	LEAKAGE CAPABILITY	REQUIRED ASSEMBLY TOOLS
AN(MS) STANDARD		1.0	12.50	SEP.	+2°	AL. ALY. CRES	YES	10 <sup>-6</sup> SCC/ SEC. HELIUM	5
BRAZED		0.2	31.25	SEMI- PERM	±1° -2	CRES	LIMITED	10 <sup>-6</sup> SCC/ SEC HELIUM	5
MECHANICAL SWAGE		0.2	26.50	PERM.	+1° -2	AL. ALY CRES TI.	LIMITED	NO DATA	6
WELDED		0.8	11.25	PERM.	+1° -2	AL. ALY CRES TI.	LIMITED	10 <sup>-6</sup> SSC/ SEC HELIUM	4
RESISTOFLEX "DYNATUBE"		0.9	26.25	SEP.	+1°	CRES TI.	YES	NO DATA	4
"GAMA"		0.5	26.25	SEP.	+4°	AL. ALY	YES	NO DATA	4

11-324

4-34

Figure 4-28

# RECOMMENDED LINE JOINING METHODS



4-35

APS-390

Figure 4-29

and brazed connections are the preferred approaches for all permanent and semi-permanent connections, respectively for the RCS. Where separable connectors are unavoidable, such as for capping system test ports and for interface connections (e.g., intra-module propellant interconnects), the Resistoflex Dynatube fitting is the recommended approach.

4.4 Design Point Weights and Sensitivities - The preliminary system designs of Phase B were the references against which the component and sub-assembly design investigations of Appendices A, D, and E were conducted. The results of these investigations were included in the system models, along with the effects of component and environmental tolerances in establishing propellant margins. Figure 4-30 summarizes the Phase C to Phase E transitions in systems implementation. The resulting final (Phase E) system design point summaries are presented in Figure 4-31. Included are system descriptions, optimal design parameters, and system weights. In order to provide a common ground for weight comparison, a total propulsion system weight comprised of the applicable RCS, APU, and OMS weight is also shown. The evaluation of a dedicated OMS was not a part of this study. However, in order to properly compare the alternate concepts, a generic OMS was necessary. The OMS weight was derived from the Orbit Maneuvering System Trade Studies (Contract NAS 9-12755). A brief design summary of this configuration is presented in Figure 4-32.

Two methods of maximizing the RCS(OMS) thruster performance have been implemented in this analysis:

1. Use of statistically separated thrusters for the -X function
2. Reduced thruster life.

Figure 4-33 presents the system weight sensitivity to thruster performance for the RCS(OMS) configuration. Although the system weight is relatively insensitive to RCS performance (21 lbm/sec), improvements in the -X translational performance result in significant weight savings - 103 lbm per second of specific impulse increase. To take advantage of this potential weight savings, a statistical procedure for selecting high performance thrusters was used. In this method, illustrated in Figure 4-34, thruster performance data from injector tests and/or thruster flight acceptance tests is used to identify the higher performing injectors. The average increase in selected thruster performance relative to the shipset nominal value is dependent upon the ratio



## IMPLEMENTATION REVISIONS (PHASE C TO PHASE E)

- o VEHICLE WEIGHT INCREASE FROM 230,000 LBM TO 265,000 LBM
- o UPDATED RCS TOTAL IMPULSE - (1.97 M FUSELAGE MTD, 1.82 M WING TIP MTD)
  - ALL ENTRY YAW PROPELLANT IN NOSE
  - PURE COUPLES FOR ON-ORBIT LIMIT CYCLE
  - REVISED CROSS-COUPLING IMPULSE LOSSES
- o UPDATED BI-PROPELLANT THRUSTER PERFORMANCE
- o INCREASE IN MONO-PROPELLANT THRUSTER WEIGHTS
- o ADDITION OF THRUSTER MOUNTING STRUCTURE WEIGHT
- o UPDATED TANKAGE WEIGHT MODELS
- o REVISED VALVE MODELS
- o UPDATED MODULE STRUCTURE WEIGHTS
- o PROPELLANT MARGIN ACCOUNTING INCLUDED

APS-850

4-37

Figure 4-30

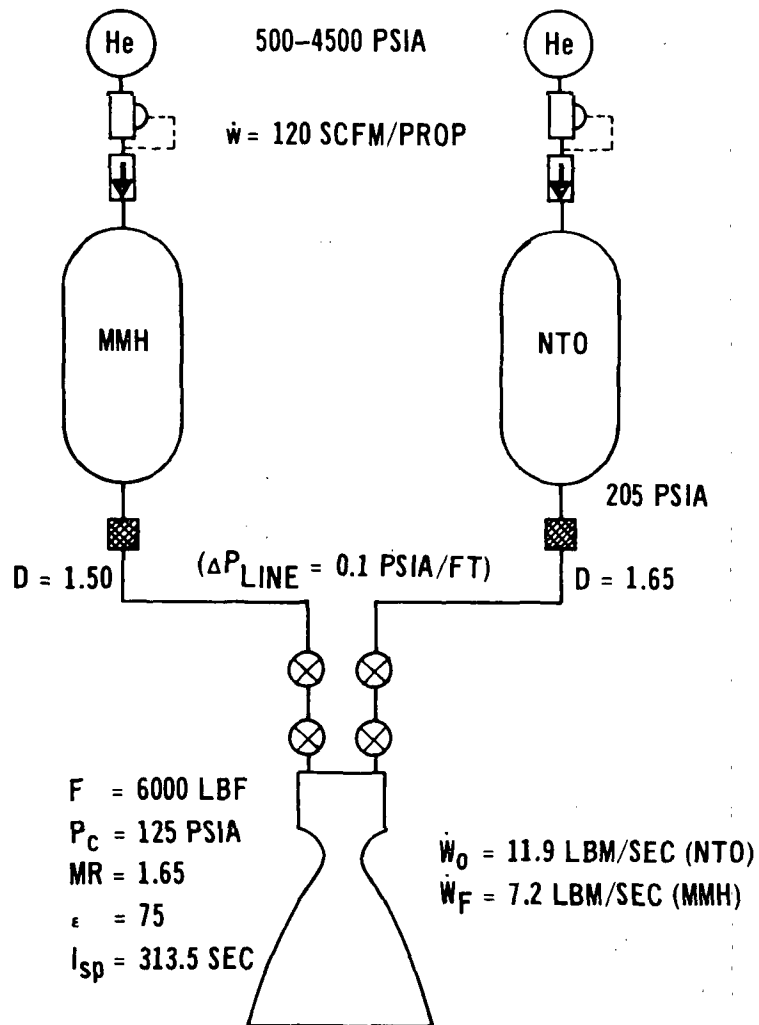
## DESIGN POINT SUMMARIES

SYSTEM	DESIGN SUMMARY	OPTIMAL DESIGN PARAMETERS							
		RCS IMPULSE	F	P <sub>TANK</sub>	P <sub>C</sub>	ε	MR	I <sub>sp</sub>	WEIGHT
MODULAR RCS (MONOPROPELLANT)	WING AND NOSE MODULES HELIUM PRESSURIZATION TITANIUM TANKAGE SURFACE TENSION POSITIVE EXPULSION CONVENTIONAL NOZZLE THRUSTERS	1,831,810	600	312	150	20 (ATT CONT) 20 (: X)	-	228.8 (ATT CONT) 228.8 (: X)	12,889 (12,889 - RCS) ( 3,295 - APU) <u>(28,790 - OMS)*</u> 44,974
MODULAR RCS (BIPROPELLANT)	WING AND NOSE MODULES HELIUM PRESSURIZATION TITANIUM TANKAGE SURFACE TENSION POSITIVE EXPULSION FILM COOLED THRUSTERS	1,831,810	600	368	200	40 (ATT CONT) 40 (: X)	1.65	296.1 (ATT CONT) 296.1 (: X)	10,133 (10,133 - RCS) ( 3,295 - APU) <u>(28,790 - OMS)*</u> 42,218
MODULAR RCS RCS (OMS) (BIPROPELLANT)	FUSELAGE AND NOSE MODULES HELIUM PRESSURIZATION TITANIUM TANKAGE SURFACE TENSION POSITIVE EXPULSION FILM COOLED THRUSTERS	1,973,464 (RCS) 7,831,849 (OMS)	600	250	150	60 (ATT CONT) 80 (: X)	1.65	299.1 (ATT CONT) 306.2 (-X)	40,155 (40,155 - RCS (OMS)) ( 3,295 - APU) <u>43,410</u>
INTEGRATED RCS,OMS (BIPROPELLANT)	COMMON TANKAGE LOCATED BELOW PAYLOAD BAY HELIUM PRESSURIZATION TITANIUM TANKAGE SURFACE TENSION POSITIVE EXPULSION FILM COOLED THRUSTERS	1,899,678 (RCS) 7,841,338 (OMS)	600	250	150 (RCS) 150 (OMS)	60 (ATT CONT) 60 (: X)	1.65	299.1 (ATT CONT) 299.1 ( X) 315.9 (OMS)	37,360 (37,360 - RCS/OMS) ( 3,295 - APU) <u>40,655</u>
INTEGRATED RCS/APU (MONOPROPELLANT)	COMMON TANKAGE LOCATED BELOW PAYLOAD BAY HELIUM PRESSURIZATION (RCS) BOOST PUMP PRESSURIZATION (APU) SURFACE TENSION POSITIVE EXPULSION CONVENTIONAL NOZZLE THRUSTERS ACTIVE, ACTIVE, IDLE, DORMANT APU REDUNDANCY WATER COOLED APU	1,899,678	600	272	125 (RCS) 1000 (APU)	40 (ATT CONT) 40 (: X)	-	235.4 (ATT CONT) 235.4 (: X)	14,586 (14,586 - RCS APU) (28,790 - OMS)* <u>43,376</u>
MODULAR APU (MONOPROPELLANT)	AFT FUSELAGE MODULES HELIUM PRESSURIZATION TITANIUM TANKAGE SURFACE TENSION POSITIVE EXPULSION ACTIVE, ACTIVE, IDLE, DORMANT APU REDUNDANCY WATER COOLED APU	-	-	766	500	-	-	-	3,295

\* OMS SPECIFIC IMPULSE = 313 SEC

11-246 C

# "BOGEY" STORABLE PROPELLANT OMS DESCRIPTION



11-371A

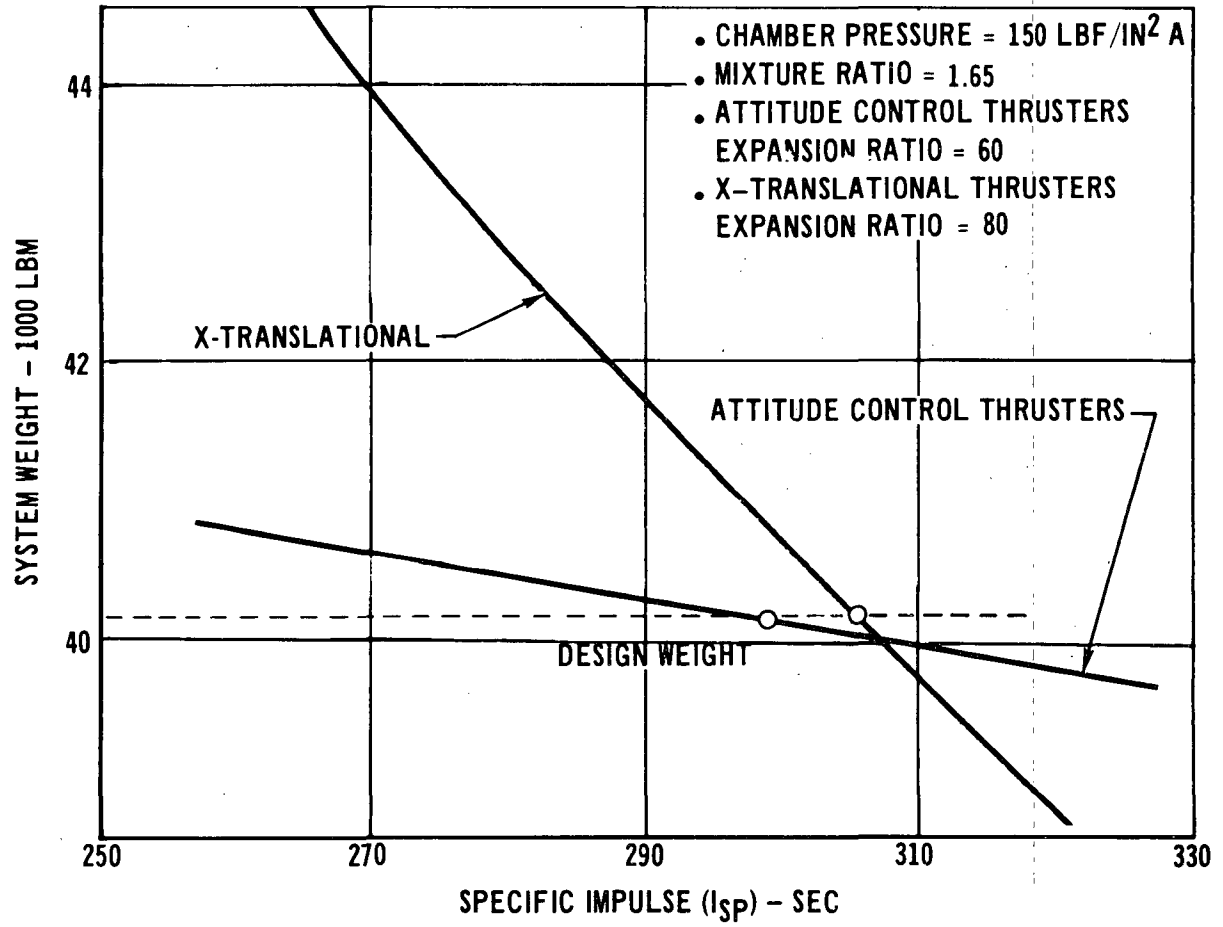
$I = 3,920,670 \text{ LB-SEC/MODULE}$

## WEIGHT/MODULE\*

IMPULSE PROPELLANT	12,506
TRAPPED	25
TANK RESIDUALS	125
MARGINS	146
PROPELLANT TANKS	332
PRESSURANT	33
REGULATORS AND CONTROLS	48
PRESSURANT TANKS	308
LINES AND VALVES	112
ENGINE ASSEMBLY	182
STRUCTURE	417
ACTUATORS AND PNEUMATICS	26
INSTALLATION	135
	14,395 LBM
<b>TOTAL SYSTEM WEIGHT</b>	<b>28,790 LBM</b>

\*INCLUDES COMPONENT REDUNDANCY

# EFFECT OF SPECIFIC IMPULSE ON MODULAR RCS (OMS) SYSTEM WEIGHT



4-40

MCDONNELL DOUGLAS ASTRONAUTICS COMPANY - EAST

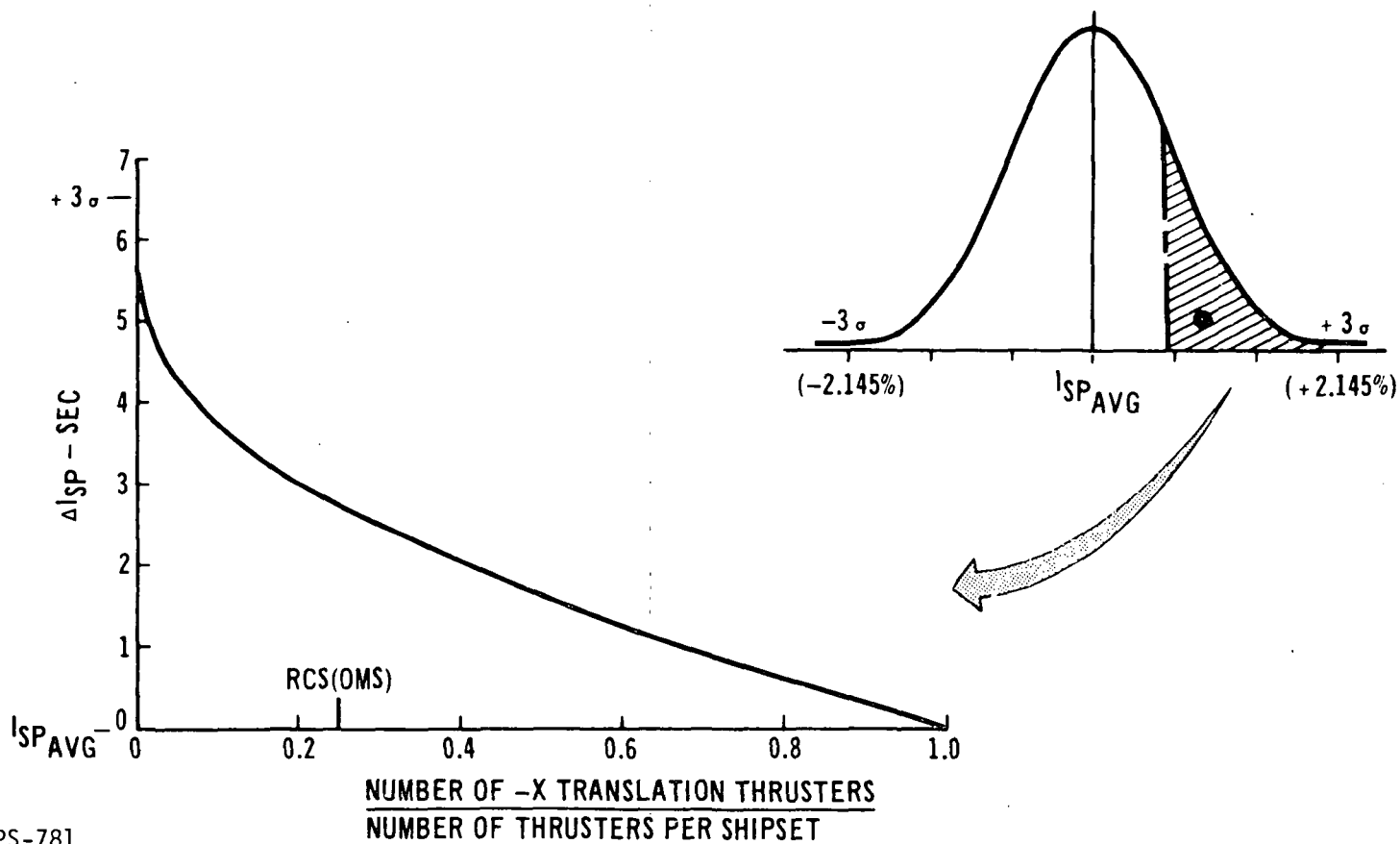
Figure 4-33

11-290 A

# PERFORMANCE SCREENING OF RCS (OMS) THRUSTERS

APPROACH: THRUSTER PERFORMANCE DATA FROM INJECTOR TESTS AND/OR THRUSTER FLIGHT ACCEPTANCE TESTS WILL BE USED TO SCREEN HIGH-PERFORMANCE THRUSTER S/N'S FOR THE AXIAL TRANSLATION FUNCTIONS

MARQUARDT R4D PERFORMANCE DISTRIBUTION  
434 THRUSTER SAMPLES



APS-781

4-41

Figure 4-34

of the number of -X thrusters required to the number of thrusters per shipset. For the RCS(OMS), where 12 out of 48 thrusters are required, the average performance gain is three seconds. Concurrent with the -X thruster performance gain is a one second performance degradation in the remaining 36 thrusters of the shipset. This procedure results in an overall weight reduction of 288 lbm (309-21).

The second method of improving thruster performance is to design for a shorter service life. Since the primary life constraint is the number of thruster cold starts, thruster replacement rates are established by the RCS thrusters. Data presented in Appendix B indicates that a one second performance gain would result in a thruster replacement every 50 missions.

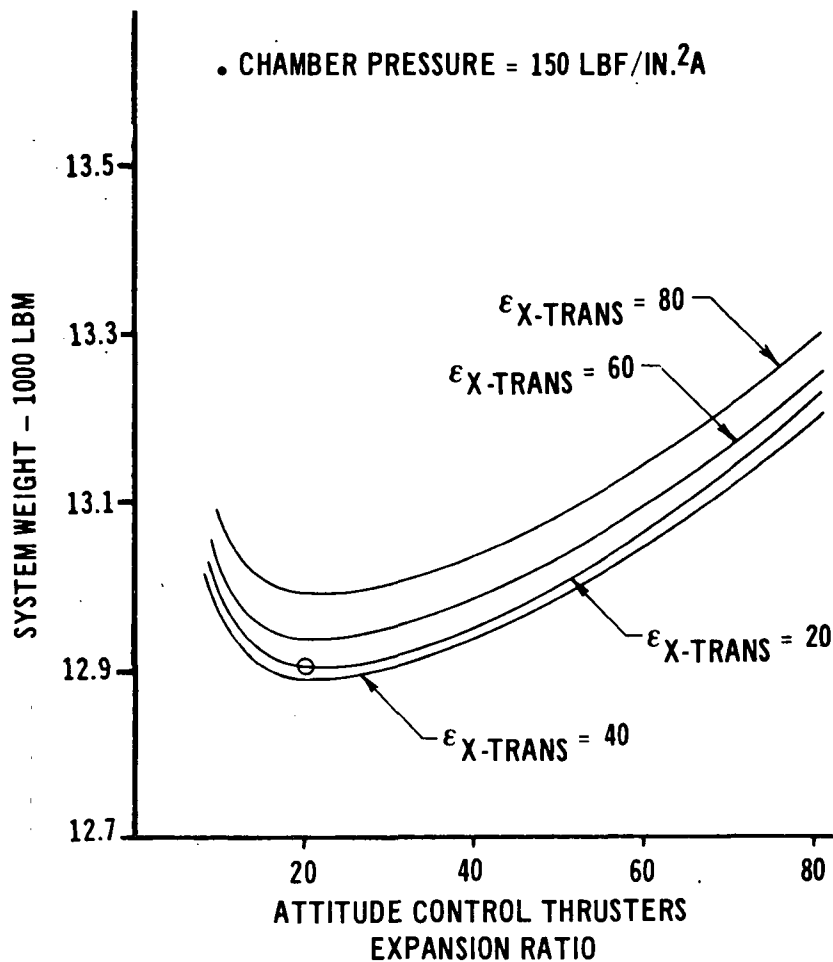
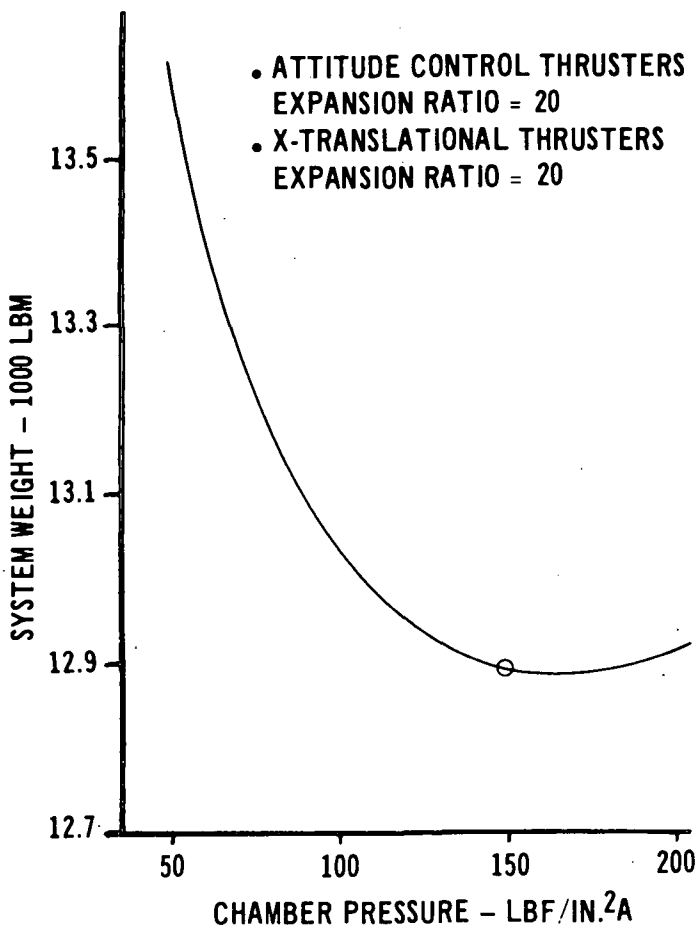
The implementation of these two modifications on the modular RCS (OMS) thruster results in an -X translational thruster specific impulse of 306.2, or four seconds greater than the nominal performance presented in Appendix A. This value is listed in Figure 4-31 and was used for the RCS (OMS) sizing analysis.

The optimal design points were determined by generating system weight sensitivities to chamber pressure, expansion ratio, and mixture ratio (for bipropellant systems), as shown in Figures 4-35 through 4-40. As shown, the expansion ratios of the X translational thrusters have been optimized as an independent parameter. This results in a significant weight savings for the RCS (OMS); the savings realized by the remaining systems are minimal and would not warrant the use of a different expansion ratio. Pod structure and thermal protection weight drives the optimum modular RCS design points to low expansion ratio and high chamber pressure (both favoring smaller thrusters and therefore smaller pods). Detailed design point weight breakdowns are presented in Figures 4-41 and 4-42.

When comparing system weights, it is necessary to differentiate between system expendables weight, which has a 1:1 tradeoff with payload, and system inert weight, which reduces payload by 1.4 lb for each pound increase. Thus, the proper method of comparing systems is on the basis of payload penalty. Comparisons on the basis of payload magnify the weight penalty associated with modularized system concepts. Figure 4-43 presents the relative payload weights. The incorporation of the modular APU into the remaining systems yields five RCS-OMS-APU configurations for evaluation. Comparison of the candidate configurations reveals the following:

# SYSTEM WEIGHT SENSITIVITIES

## MODULAR RCS $N_2H_4$



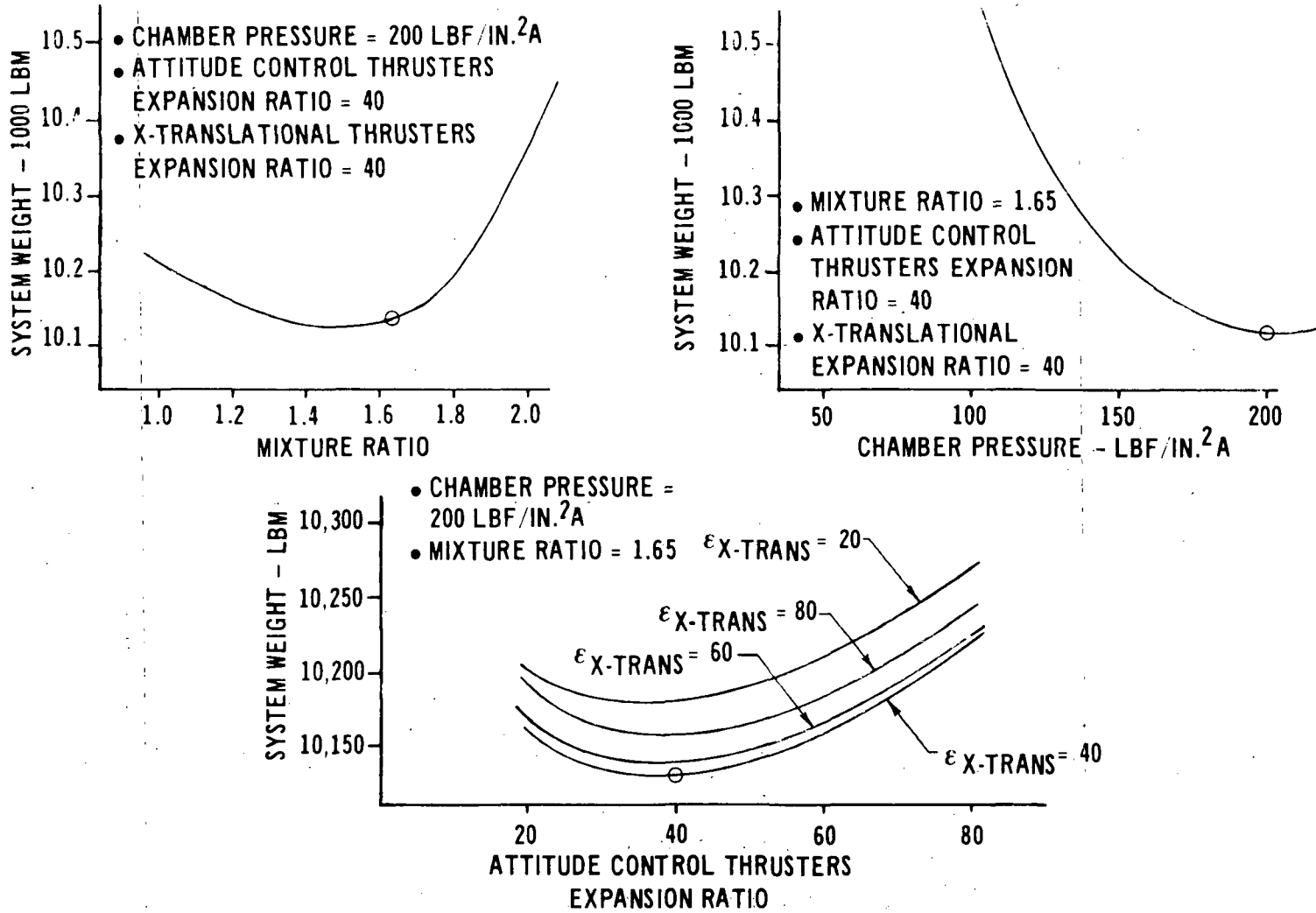
APS-110A

4-43

Figure 4-35

# SYSTEM WEIGHT SENSITIVITIES

## MODULAR RCS - NTO/MMH



4-44

MCDONNELL DOUGLAS AERONAUTICS COMPANY - EAST

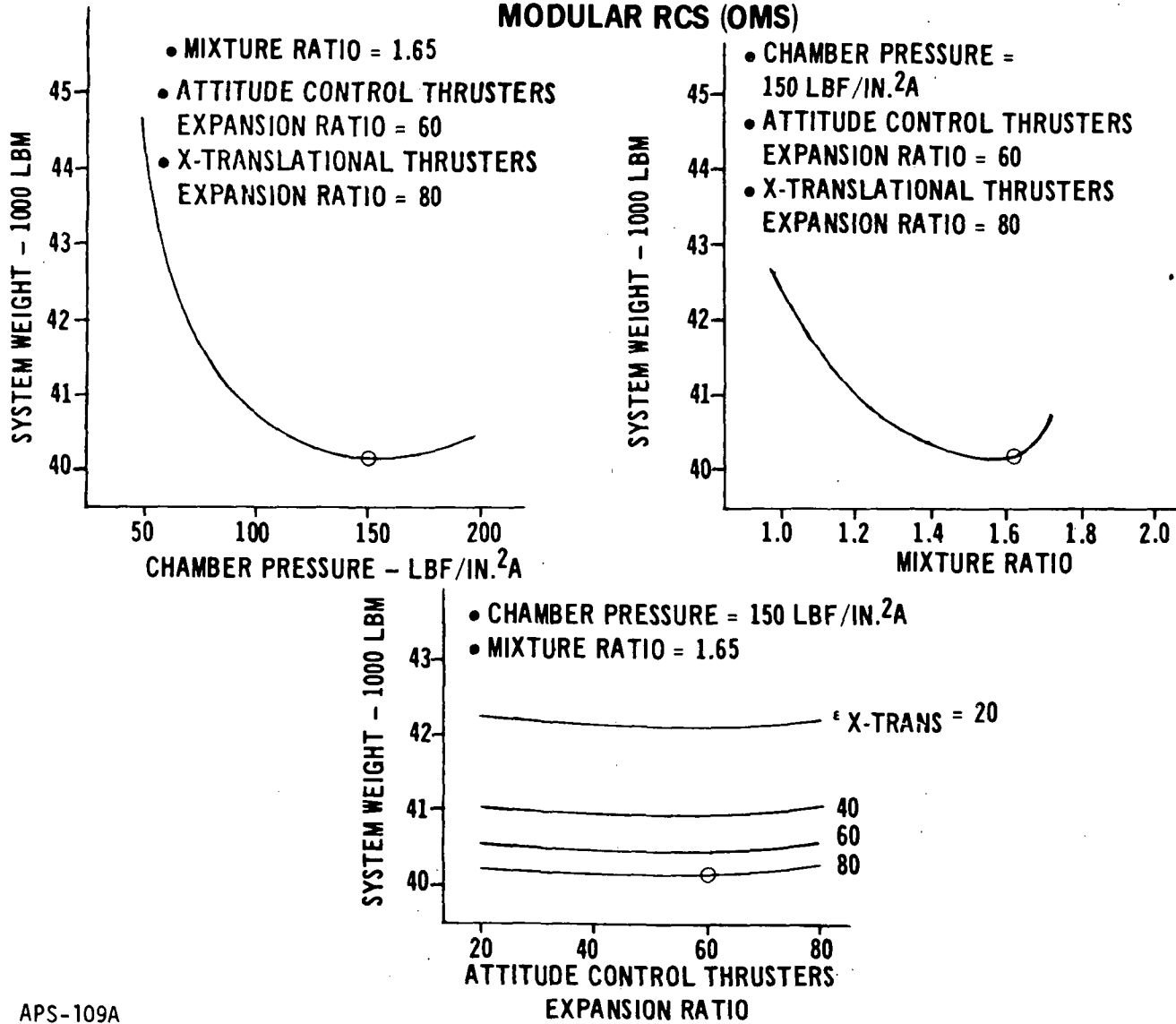
Figure 4-36

APS-107A



# SYSTEM WEIGHT SENSITIVITIES

## MODULAR RCS (OMS)

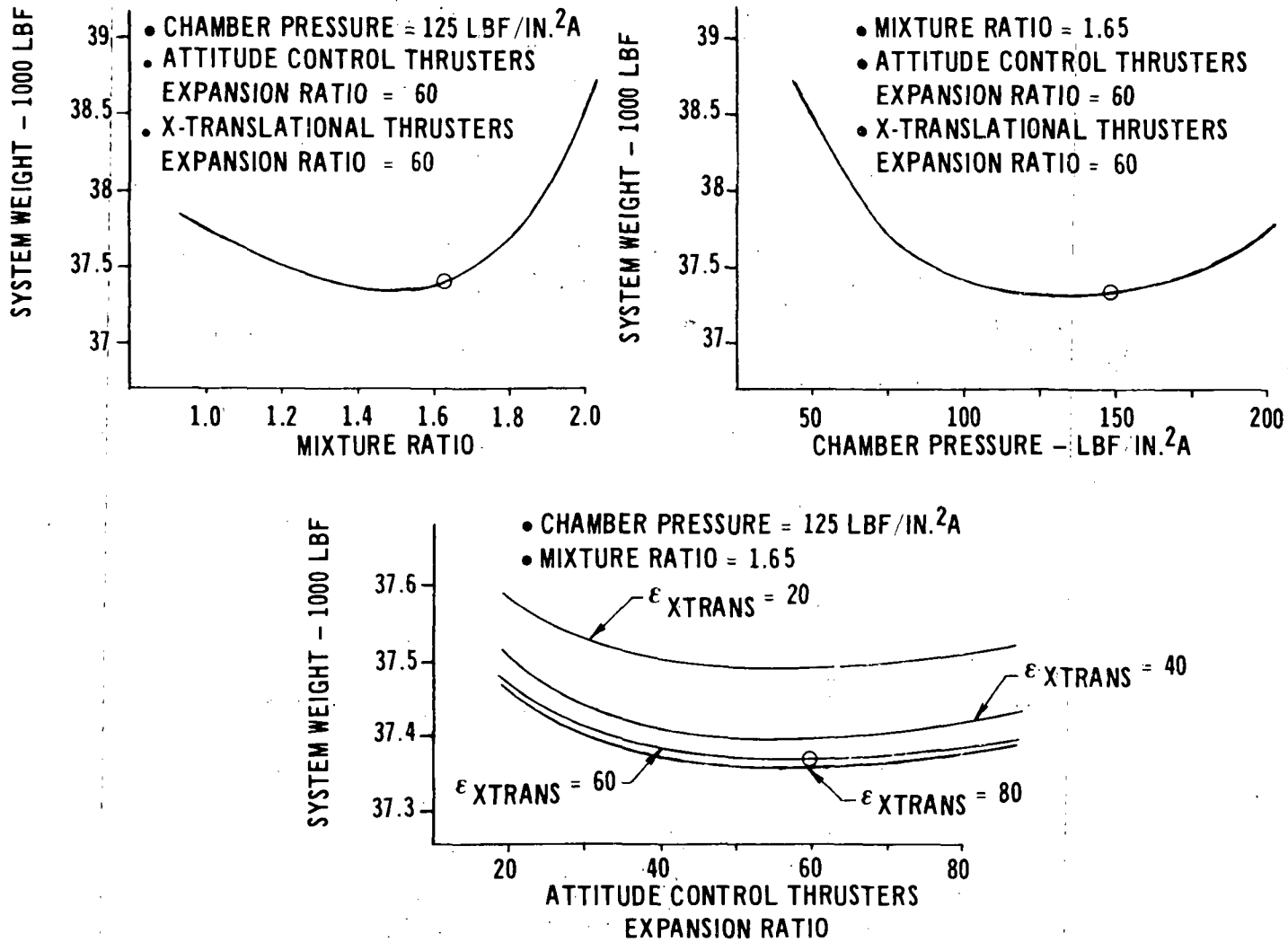


APS-109A

4-45

Figure 4-37

## SYSTEM WEIGHT SENSITIVITIES INTEGRATED RCS/OMS NTO/MMH



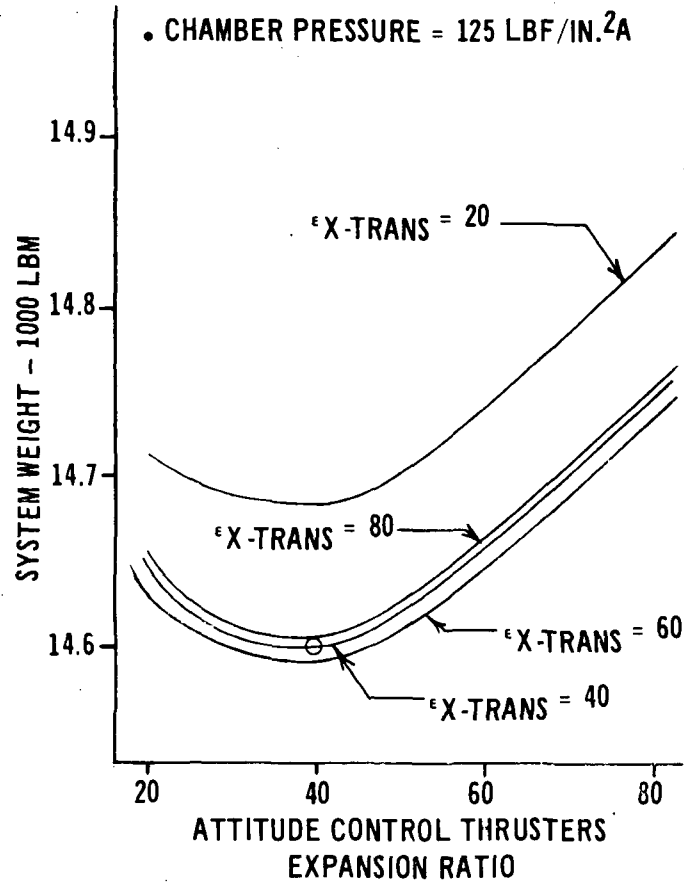
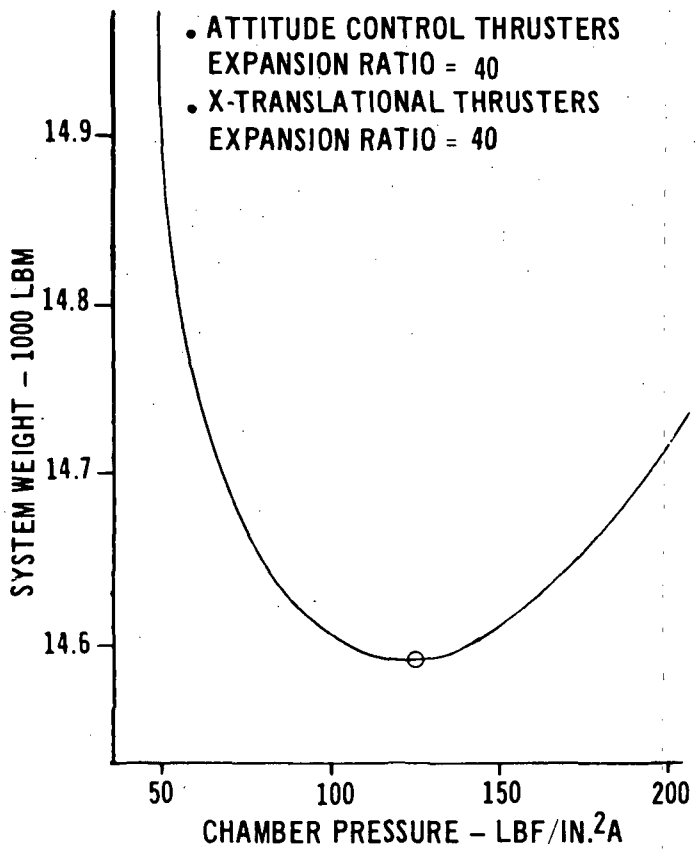
4-46

Figure 4-38

APS-146A

# SYSTEM WEIGHT SENSITIVITIES

## INTEGRATED RCS/APU $N_2H_4$

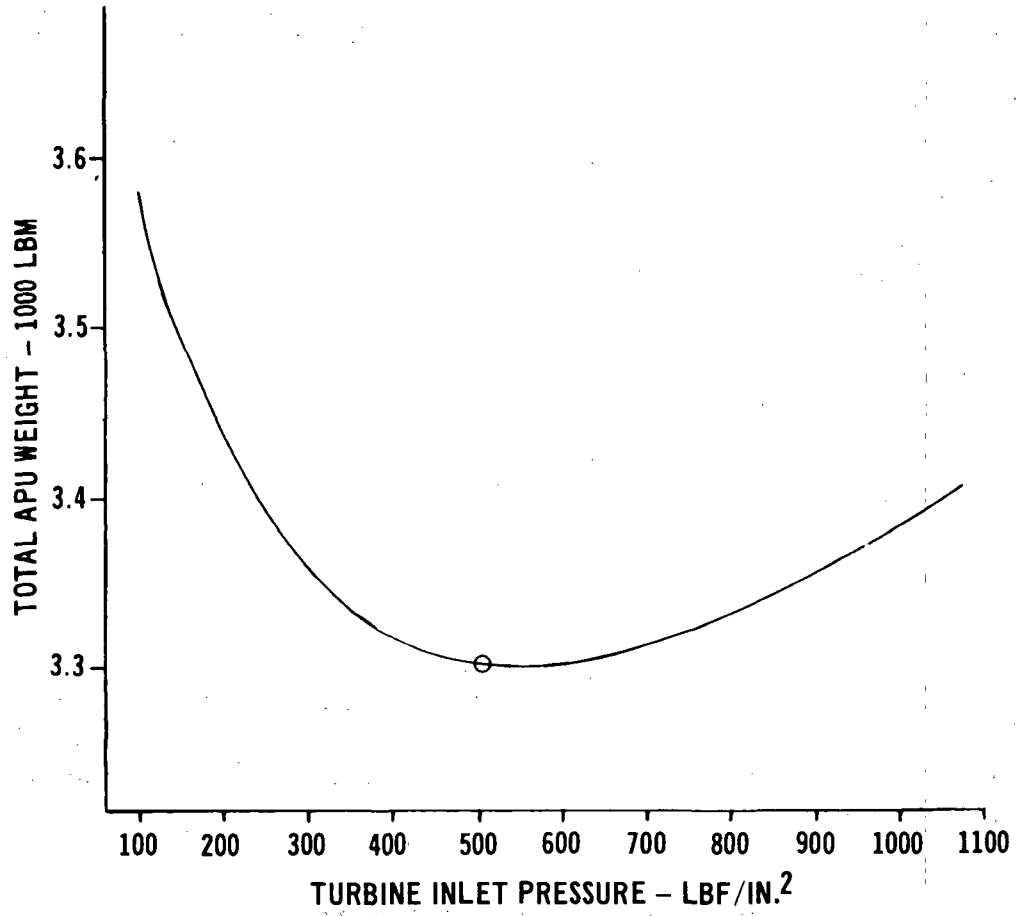


APS-125A

4-47

Figure 4-39

# SYSTEM WEIGHT SENSITIVITY MODULAR APU $N_2H_4$



APS-111A

4-48

Figure 4-40

### SYSTEM WEIGHTS

	MODULAR RCS N <sub>2</sub> H <sub>4</sub>	MODULAR RCS NTO/MMH	MODULAR RCS (OMS) NTO/MMH	INTEGRATED RCS/OMS NTO/MMH
<b>PRESSURIZATION</b>				
TANKS	366	375	1,184	888
REGULATORS AND CONTROLS	67	59	64	31
PRESSURANT	36	30	98	93
<b>PROPELLANT SYSTEM</b>				
TANKS	472	492	1,274	1,134
PROPELLANT				
USABLE - RCS	8,300	6,491	6,899	6,598
USABLE - OMS			25,582	24,822
TRAPPED	113	94	102	218
TANK RESIDUALS	166	130	654	628
MARGINS	81	85	587	320
<b>DISTRIBUTION SYSTEM</b>				
LINES, VALVES AND FILTERS	359	408	506	561
<b>THRUSTER ASSEMBLIES (RCS)</b>	991	480	794	614
<b>OME ASSEMBLIES</b>				364
<b>THERMAL CONTROL</b>				
HEATERS AND HEAT PIPES	223	9	13	13
POWER	256	241	227	139
<b>POD STRUCTURE</b>				
STRUCTURE	633	551	1,709	937
THERMAL PROTECTION	826	688	422	
<b>TOTAL</b>	<b>12,889</b>	<b>10,133</b>	<b>40,115</b>	<b>37,360</b>

APS-778

## SYSTEM WEIGHTS

	INTEGRATED RCS/APU N <sub>2</sub> H <sub>4</sub>	MODULAR APU N <sub>2</sub> H <sub>4</sub>
PRESSURIZATION		
TANKS	340	121
REGULATORS AND CONTROLS	37	19
PRESSURANT	35	13
BOOST PUMPS	25	—
PROPELLANT SYSTEM		
TANKS	576	167
PROPELLANT		
USABLE - RCS	8,336	—
USABLE - APU	1,190	1,216
TRAPPED	120	
TANK RESIDUAL	190	
MARGINS	114	49
DISTRIBUTION SYSTEM		
LINES, VALVES AND FILTERS	346	30
POWER CONVERSION		
GAS GENERATORS	34	29
TURBINES AND GEAR BOXES	256	243
VENT LINES	198	205
PUMPS	109	109
ALTERNATORS	132	132
ALTERNATOR DRIVE SYSTEMS	88	88
THRUSTER ASSEMBLIES	1,007	—
THERMAL CONTROL		
HEATERS AND HEAT PIPES	216	4
APU HEAT EXCHANGERS	200	200
APU COOLANT AND TANKAGE	346	346
ELECTRICAL POWER	258	129
STRUCTURE	433	195
TOTAL	14,586	3,295

APS-779

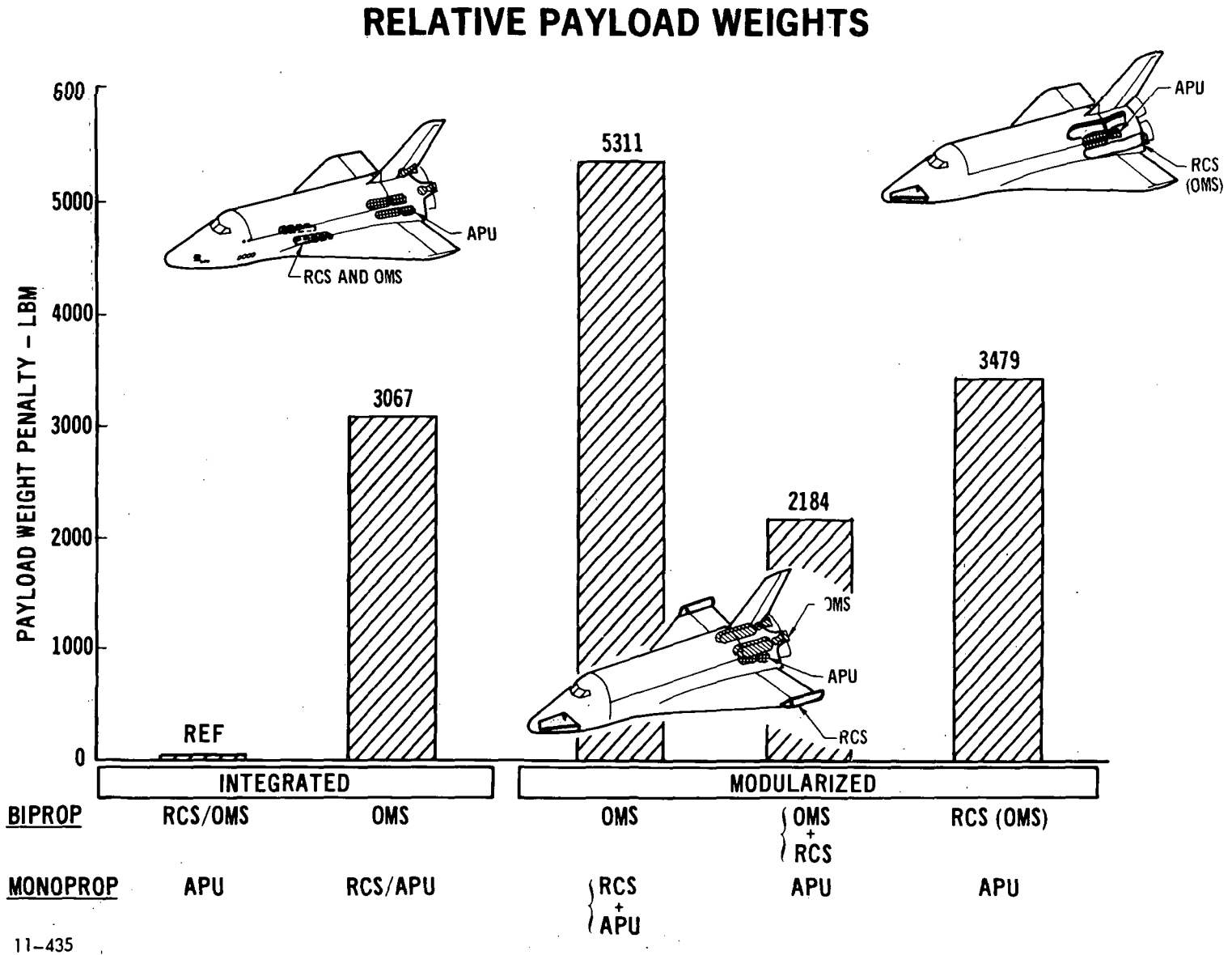
- 1) The lightest systems approach is realized with an integral, bipropellant RCS/OMS and a modular monopropellant APU.
- 2) The payload penalty for modularizing the bipropellant RCS and OMS is 2184 lbm.
- 3) The modularized, bipropellant RCS(OMS) is almost 1300 lbm heavier (on a payload basis) than the combined weight of a modularized RCS and modularized OMS.
- 4) The modularized, monopropellant RCS has a reduced payload of 3130 lbm when compared with the modularized bipropellant RCS system.

Each configuration is the result of an individual optimization; tankage and thruster locations have been separately established, and design points defined consistent with the particular requirements of each system. These final comparisons are therefore considered to be realistic evaluations of the alternate configurations.

As discussed in Section 1, the objective of this study is to develop design and programmatic data for competitive reaction control systems in sufficient detail that a selection can later be made between the various concepts. In keeping with this objective, the concluding effort on this topic was an assessment of selected configuration changes on the design point weights. Changes in pressurization concept, type of tank expulsion, tank material, thruster type, and thruster thermal control are shown in Figures 4-44 through 4-49. Weight savings are possible in the area of pressurization, with the largest savings available for the high impulse configurations (modular RCS(OMS) and integrated RCS/OMS). In general, the pump fed pressurization concept described in Appendix D offers the largest savings; however, its adoption results in increased system complexity. By contrast, the savings afforded by composite pressurant tanks reflect no decrease in system reliability. Additionally, they generally provide a leakage failure mode rather than fracture as discussed in Appendix E. The weight penalties associated with system redundancy are also presented to allow evaluation of the weight penalty associated with the fail safe/fail safe redundancy philosophy. Figure 4-50 compares redundant and non-redundant configurations for the monopropellant modular RCS. The weight savings shown represent the elimination of all components except those necessary for completion of a failure free mission.

4-52

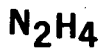
Figure 4-43



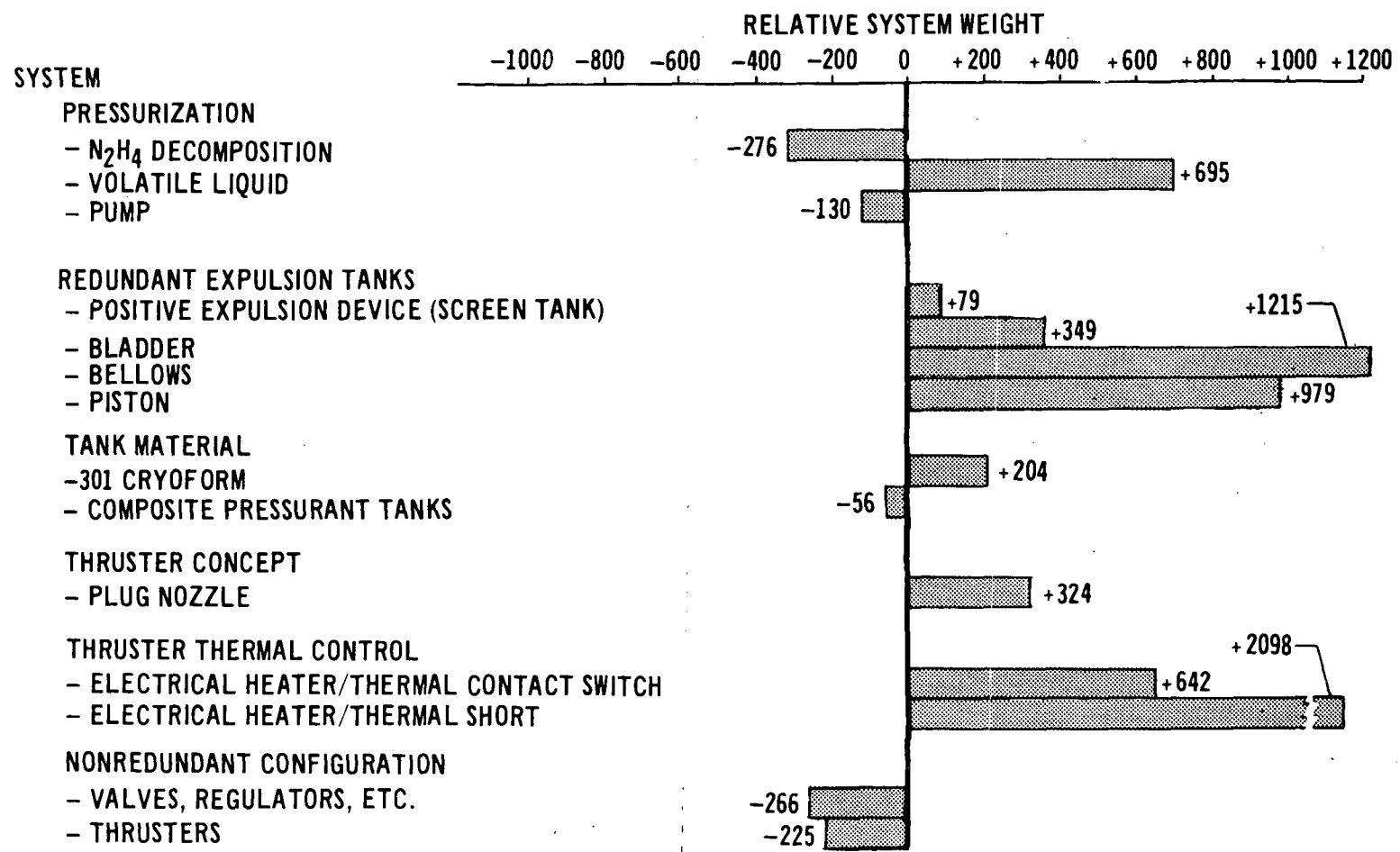
11-435



# WEIGHT RELATIVE TO BASELINE MODULAR RCS



BASELINE SYSTEM: TWO WING TIP AND ONE NOSE-MOUNTED MODULES CONTAINING A TOTAL OF FORTY 600 LBF CONVENTIONAL NOZZLE THRUSTERS, HELIUM PRESSURIZATION, TITANIUM TANKS, AND SURFACE TENSION POSITIVE EXPULSION



REFERENCE WEIGHT = 12,889 LBM

APS-153A

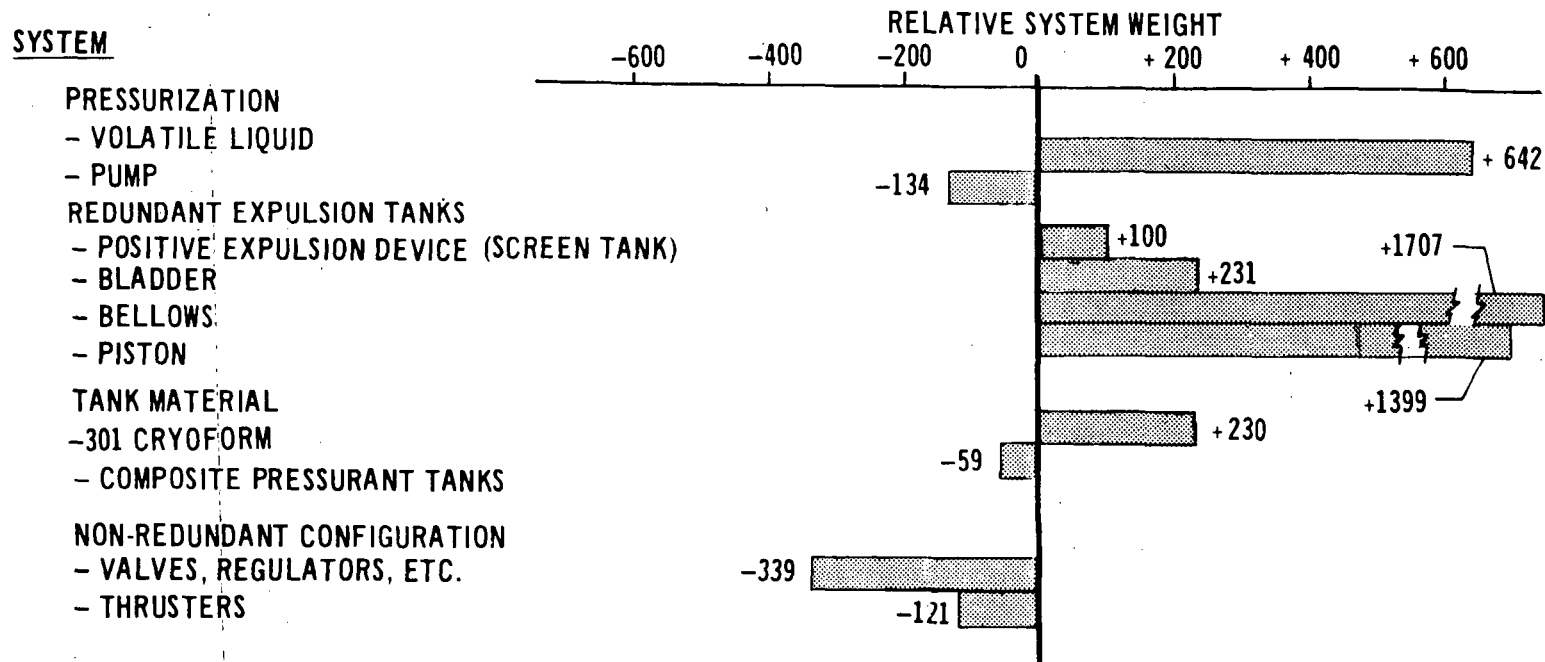
MCDONNELL DOUGLAS AERONAUTICS COMPANY - EAST

4-53

Figure 4-44

## WEIGHT RELATIVE TO BASELINE MODULAR RCS (N<sub>2</sub>O<sub>4</sub>/MMH)

BASELINE SYSTEM: TWO WING TIP AND ONE NOSE-MOUNTED MODULES CONTAINING A TOTAL OF FORTY 600 LBF FILM COOLED THRUSTERS, HELIUM PRESSURIZATION, TITANIUM TANKS, AND SURFACE TENSION POSITIVE EXPULSION.



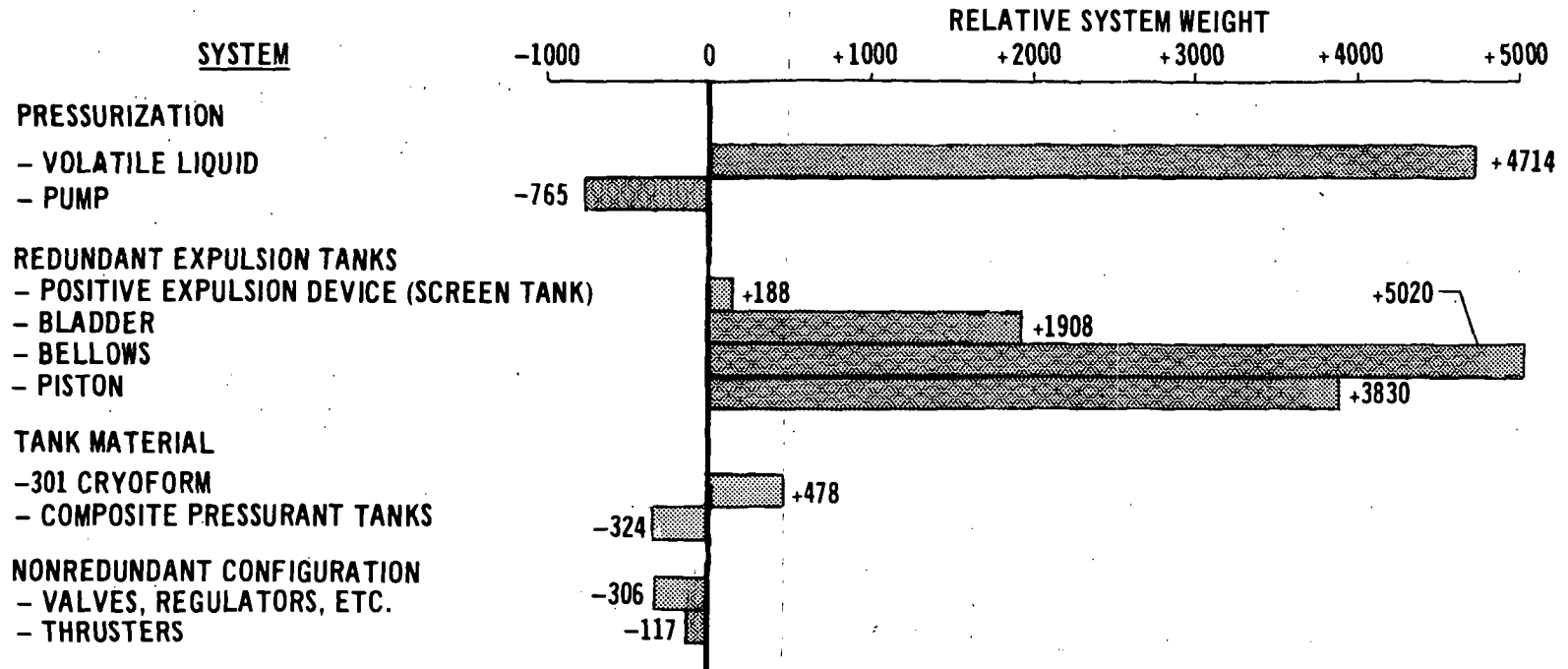
REFERENCE WEIGHT = 10,133 LBM

APS-108A

# WEIGHT RELATIVE TO BASELINE MODULAR RCS (OMS)

(N<sub>2</sub>O<sub>4</sub>/MMH)

BASELINE SYSTEM: TWO FUSELAGE AND ONE NOSE-MOUNTED MODULES CONTAINING A TOTAL OF FORTY-EIGHT 600 LBF FILM COOLED THRUSTERS, HELIUM PRESSURIZATION, TITANIUM TANKS, AND SURFACE TENSION POSITIVE EXPULSION



REFERENCE WEIGHT = 40,155 LBM

MCDONNELL DOUGLAS ASTRONAUTICS COMPANY - EAST

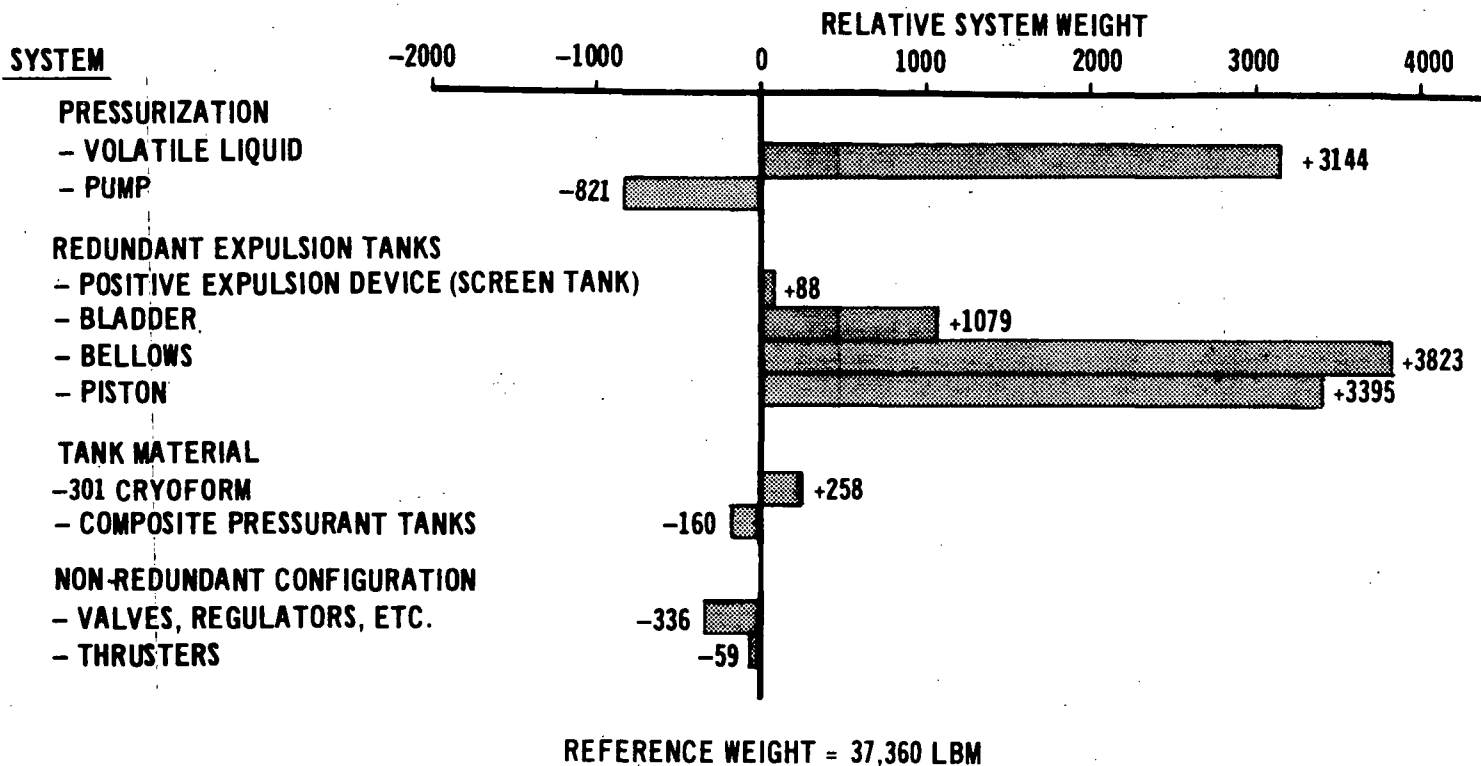
4-55

Figure 4-46

APS-132A

## WEIGHT RELATIVE TO BASELINE INTEGRATED RCS/OMS (N<sub>2</sub>O<sub>4</sub>/MMH)

BASELINE SYSTEM: INTERNAL INSTALLATION UTILIZING A TOTAL OF THIRTY-SEVEN 600 LBF  
FILM COOLED THRUSTERS, HELIUM PRESSURIZATION, TITANIUM TANKS,  
AND SURFACE TENSION POSITIVE EXPULSION.

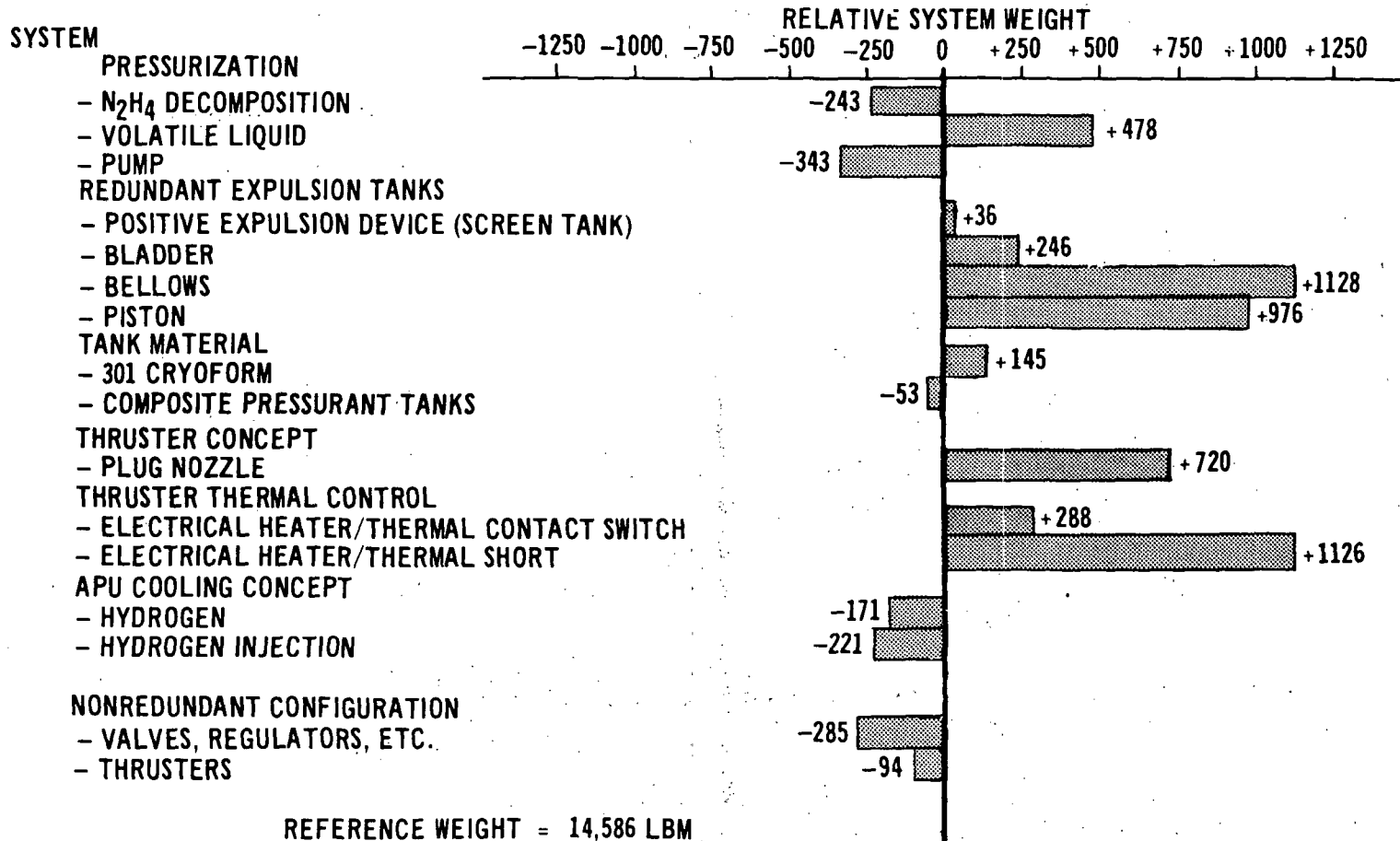


APS-106A

# WEIGHT RELATIVE TO BASELINE INTEGRATED RCS/APU

$N_2H_4$

BASELINE SYSTEM: INTERNAL INSTALLATION UTILIZING A TOTAL OF THIRTY-SEVEN 600 LBF FILM COOLED THRUSTERS, HELIUM PRESSURIZATION, TITANIUM TANKS, SURFACE TENSION POSITIVE EXPULSION, AND WATER COOLED APU



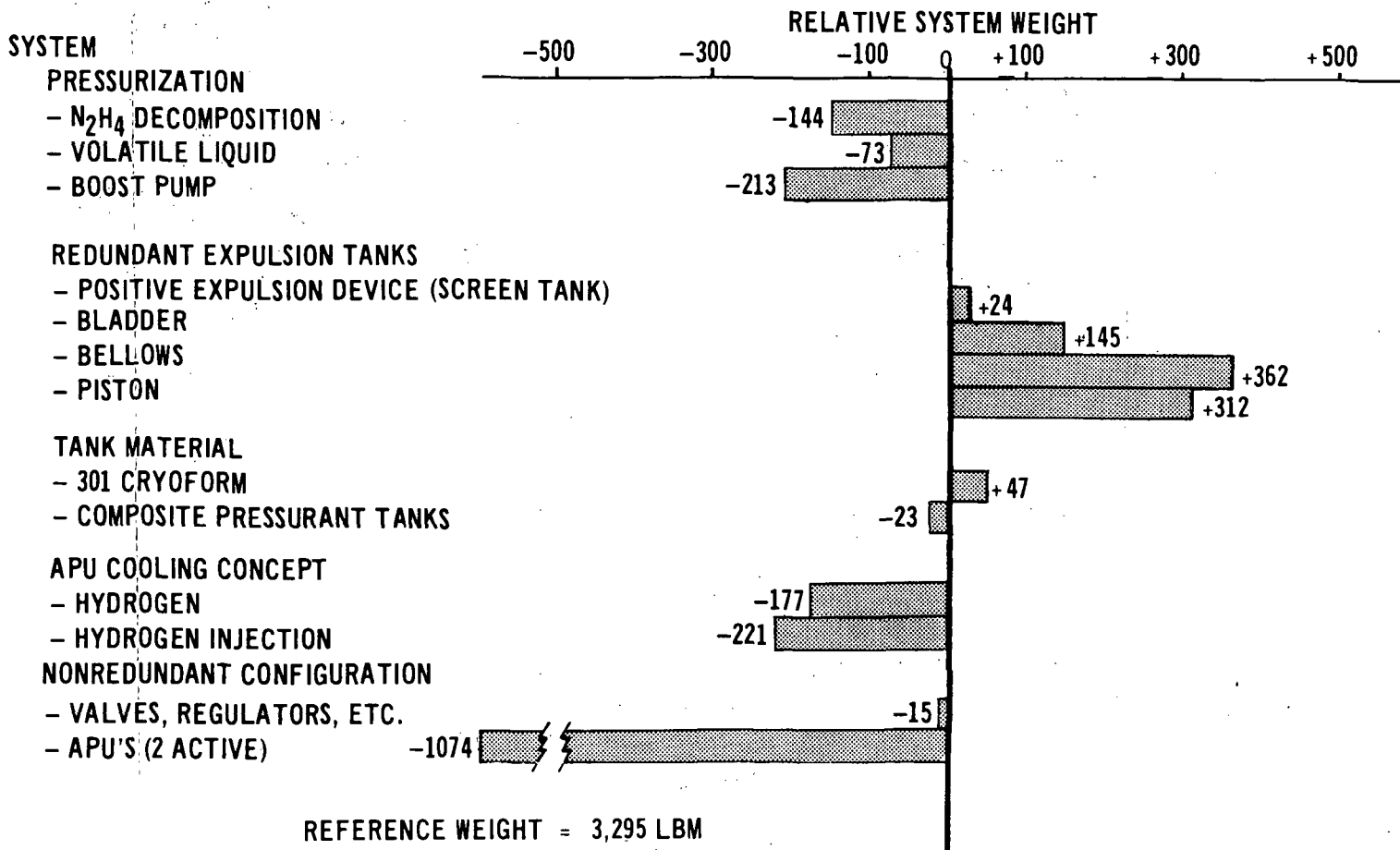
REFERENCE WEIGHT = 14,586 LBM

APS-154A

# WEIGHT RELATIVE TO BASELINE MODULAR APU



BASELINE SYSTEM: FOUR APU UNITS OPERATED IN ACTIVE, ACTIVE, IDLE, DORMANT MODE, HELIUM PRESSURIZATION, TITANIUM TANKS, SURFACE TENSION POSITIVE EXPULSION, AND WATER COOLING

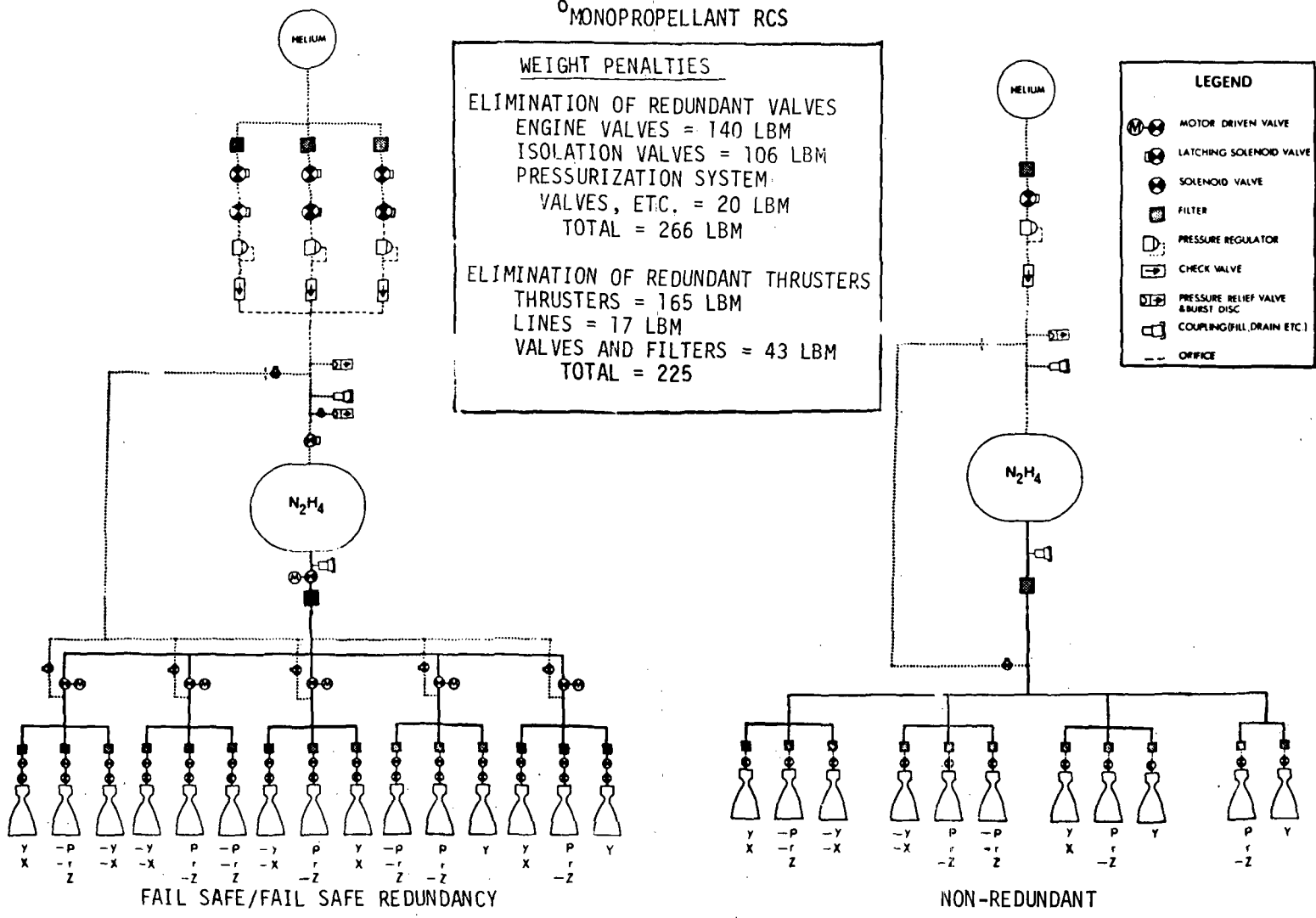


APS-112A

4-58

Figure 4-49

# REDUNDANCY WEIGHT PENALTY MONOPROPELLANT RCS



APS-405 A

4-59

Figure 4-50

4.5 Fuselage Mounted Modular RCS-OMS Options - As originally defined, Phase E was to be a final performance analysis of the six systems described above. However, prior to the completion of this evaluation, North American Rockwell (NR) was awarded the Space Shuttle prime contract by NASA. The NR Shuttle configuration employs a dedicated bipropellant OMS and a monopropellant RCS installed in fuselage and nose modules. The RCS utilizes 40 thrusters of 1000 lbf each. Common size propellant and pressurant tanks are used in the nose and fuselage modules. In order to keep this study germane, additional analysis was performed to allow further study of fuselage module options.

A variety of alternate configurations can be housed in fuselage modules; originally, this study evaluated only a bipropellant RCS performing all maneuvers. The additional fuselage module study, therefore, focused on four variations:

1. The use of 1000 lbf thrusters for the RCS (OMS)
2. The use of an OMS (instead of an all maneuver RCS)
3. Comparison of common versus dedicated tankage
4. Consideration of a monopropellant as well as the bipropellant RCS.

The last three variations are interdependent and thus are considered simultaneously.

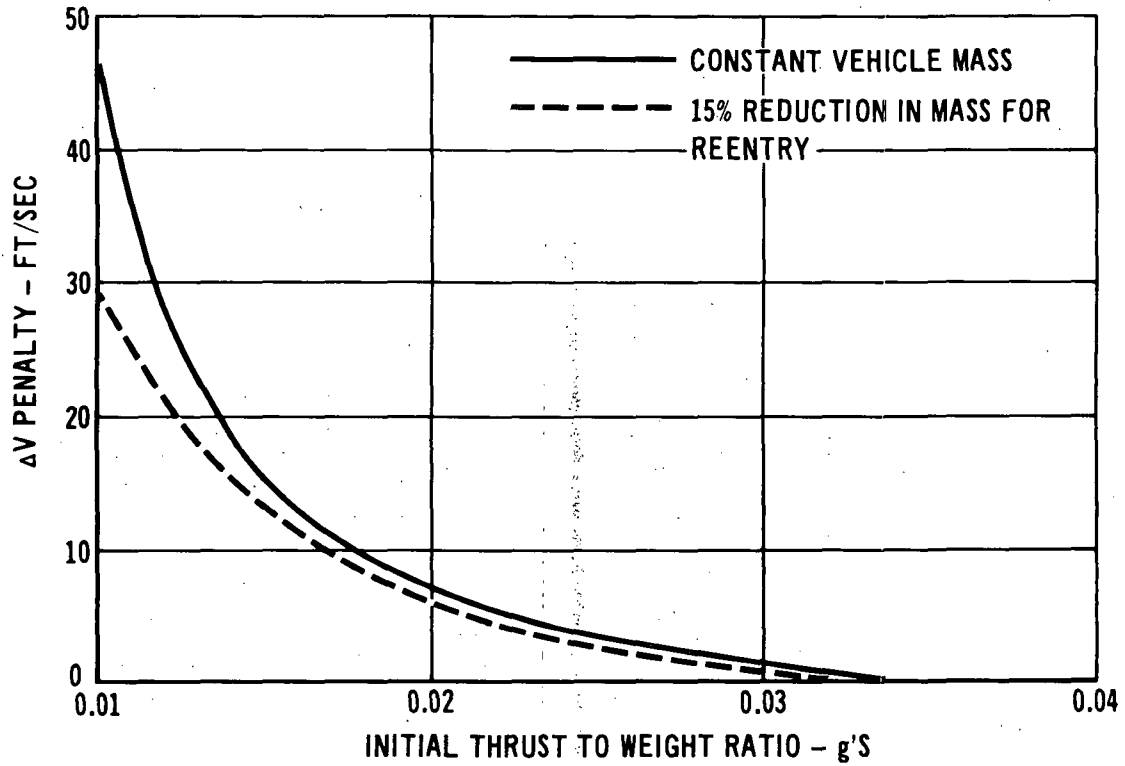
The RCS (OMS) analysis presented in Section 4.4 utilized six -X translational thrusters per module. However, the implications of OMS  $\Delta V$  acceleration exchanges were not considered. Figure 4-51 depicts this exchange, showing thrust to vehicle weight ratio and energy losses sustained during the orbit transfer, circularization and deorbit maneuvers. These losses arise because of the non-optimum thrust vector associated with longer burn times (as opposed to instantaneously imparted impulse).

Comparison of 600 and 1000 lbf -X translation thruster configurations should include the constraint of equal total base area. Within this constraint, the number of thrusters and their expansion ratios can be varied to achieve the optimum design. Figures 4-52 and 4-53 present system weight for varying expansion ratios and numbers of 600 and 1000 lbf thrusters for fixed circular base diameters of 30 and 50 in. The  $\Delta V$  losses shown correspond to a double failure condition, wherein two engines per module are inactive; i.e., worst condition of two -X thruster failures in one pod and two thrusters shut down in the other pod to avoid disturbance torques. The number of axial



# ORBITAL $\Delta V$ PENALTY

ORBIT TRANSFER + CIRCULARIZATION + DEORBIT



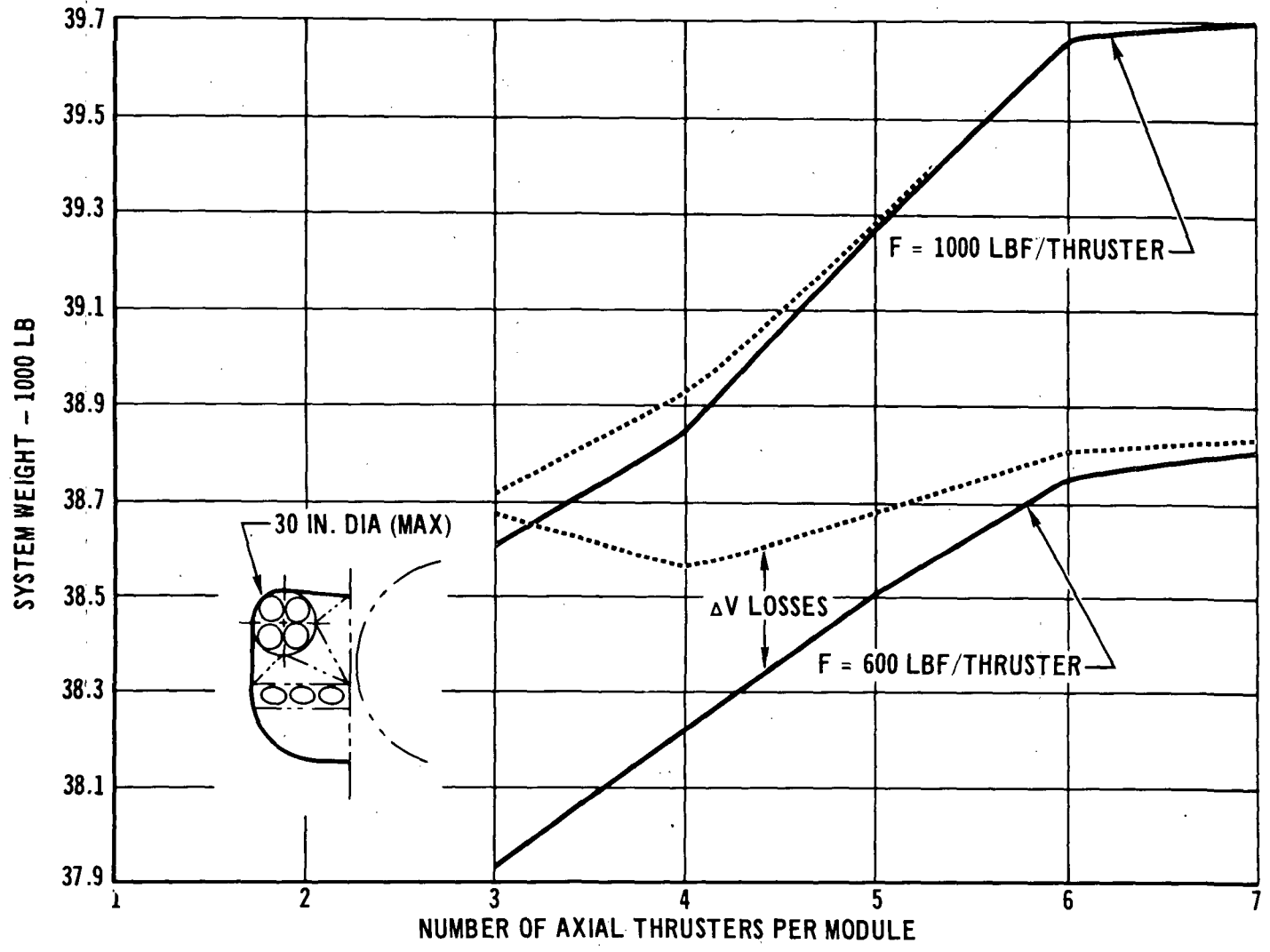
4-61

Figure 4-51

11-274

# THRUSTER INSTALLATIONS EFFECTS

## 30 INCH ENVELOPE CONSTRAINT



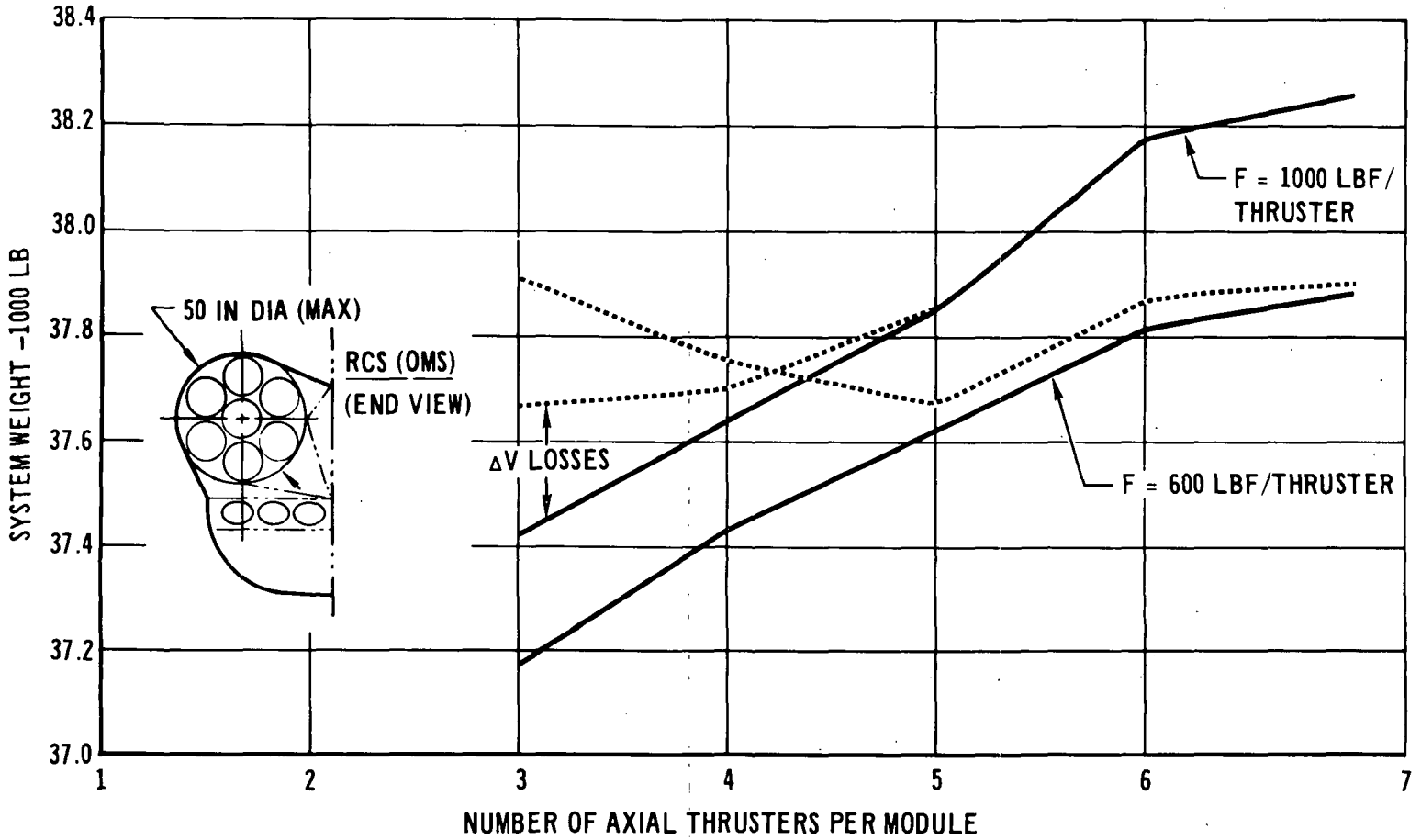
4-62

Figure 4-52

APS-147

# THRUSTER INSTALLATION EFFECTS

## FIFTY INCH ENVELOPE CONSTRAINT



APS-149

4-63

Figure 4-53

engines per module determines the expansion ratio used and in turn the performance of each engine. The performance gains associated with fewer thrusters becomes less significant for large envelopes.

When the RCS is used for the -X translation function, gimbals are unattractive and, as detailed in Appendix G, CG tracking in pitch is achieved by off-logic - shutting down either the upper or lower firing pair of thrusters from both modules. (Yaw control is achieved with RCS thrusters.) Since the use of off-logic pitch control requires the pulsing of up to two thrusters per pod, six 600 lbf thrusters per pod is considered to be a logical design. It should be noted that the weight comparison between 600 and 1000 lbf thrusters is not entirely valid, since the 1000 lbf thrusters MIB was not increased over that used for the 600 lbf thrusters. Based on these considerations, the RCS(OMS) design point of six 600 lbf -X translation thrusters per pod was maintained.

The remaining effort was devoted to the comparison of the following five alternate fuselage configuration options.

1. Dedicated OMS, common RCS-OMS tankage
2. Common RCS-OMS thrusters, common tankage (the RCS(OMS) of Phase E)
3. Dedicated OMS, dedicated tankage (bipropellant RCS)
4. Common RCS-OMS thrusters, dedicated tankage
5. Dedicated OMS, dedicated tankage (monopropellant RCS)

Figure 4-54 delineates the design points for these systems. The design points for these alternate fuselage configurations were established by analogy to the Phase E systems. The first, third and fifth concepts utilize dedicated OMS engines. Differences between the first and third concepts arise from the tankage configuration employed. Common tankage contains RCS and OMS propellants jointly, whereas dedicated tankage provides separate tankage for the two functions. The use of dedicated tankage for the OMS function profits from the fact that full-tank surface tension acquisition is no longer required for the large tanks, since settling forces can be used to orient the propellant at a small screen trap. Figure 4-55 illustrates the arrangement of a typical pod utilizing dedicated tankage. In the fifth concept, a monopropellant RCS replaces the bipropellant RCS of concept three. The second concept is identical to the RCS(OMS) configuration of Section 4.4. In the fourth concept, this configuration is modified by the use of dedicated tankage.

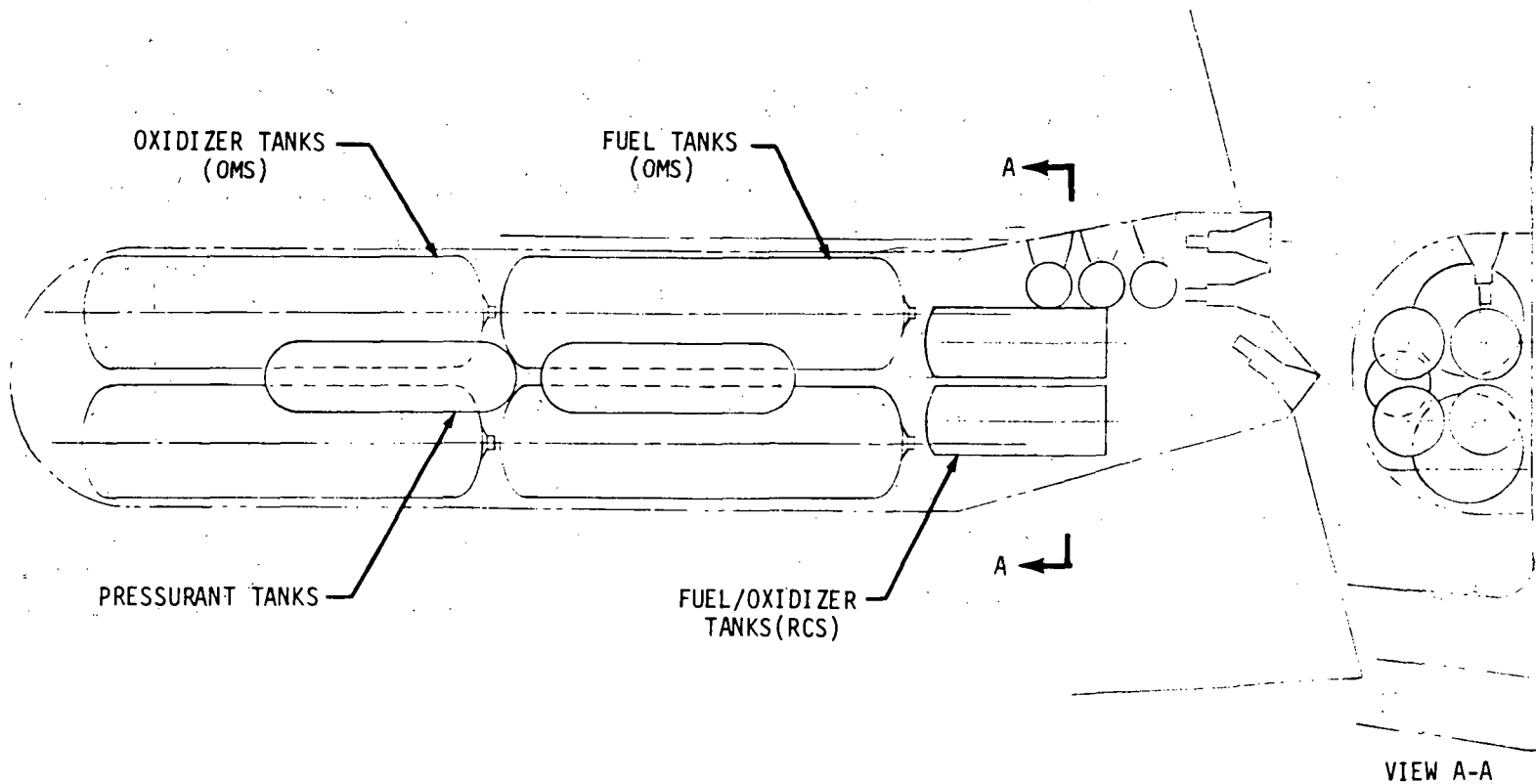
# DESIGN POINT SUMMARY

POD DESIGN CHARACTERISTICS				SYSTEM DESIGN POINTS													
RCS/OMS TANKAGE	PROPELLANTS		RCS/OMS ENGINES	THRUST		CHAMBER PRESSURE		TANK PRESSURE		EXPANSION RATIO			MIXTURE RATIO		SPECIFIC IMPULSE		
	RCS	OMS		RCS	OMS	RCS	OMS	RCS	OMS	RCS	+X RCS	OMS	RCS	OMS	RCS <sup>(1)</sup>	X RCS	OMS
COMMON	N <sub>2</sub> O <sub>4</sub> /MMH	N <sub>2</sub> O <sub>4</sub> /MMH	DEDICATED	600	6000	150	150	249	249	60	60	90	1.65	1.65	299.1	299.1	315.9
COMMON	N <sub>2</sub> O <sub>4</sub> /MMH	N <sub>2</sub> O <sub>4</sub> /MMH	COMMON	600	600	150	150	249	249	60	90	-	1.65	1.65	299.1	306.2	-
DEDICATED	N <sub>2</sub> O <sub>4</sub> /MMH	N <sub>2</sub> O <sub>4</sub> /MMH	DEDICATED	600	6000	175	125	285	205	60	60	75	1.65	1.65	299.3	299.3	313.5
DEDICATED	N <sub>2</sub> O <sub>4</sub> /MMH	N <sub>2</sub> O <sub>4</sub> /MMH	COMMON	600	600	150	150	249	249	60	90	-	1.65	1.65	299.1	306.2	-
DEDICATED	N <sub>2</sub> H <sub>4</sub>	N <sub>2</sub> O <sub>4</sub> /MMH	DEDICATED	600	6000	125	125	235	205	40	40	75	-	1.65	235.3	235.3	313.5

(1) USE 76% I<sub>SP</sub> (SS) FOR PULSING

11-340

# FUSELAGE MODULE DEDICATED TANKAGE



4-66

Figure 4-55

APS-220

Figures 4-56 and 4-57 summarize the principal design details used in the analysis. Propellant margin requirements were defined, as discussed in Appendix G, based on the use of series burns for dedicated OMS engines, and hybrid control for the RCS(OMS) concepts. Those configurations which employ dedicated tankage utilize a single RCS tank design for both the nose and fuselage modules. Figure 4-58 presents a detailed weight breakdown for the alternate concepts. A comparison of relative payload penalties for the five concepts is presented in Figure 4-59. This figure reflects a 1:1 trade-off between system expendable weight and payload decrease, and a 1:1.4 trade-off between system inert weight and payload decrease. Comparison of these systems reveals the following:

1. Minimum vehicle weight is provided by the concept employing a dedicated OMS and dedicated tankage.
2. A 2700 lbm payload penalty is associated with the use of a monopropellant RCS, as opposed to a bipropellant RCS.
3. The use of RCS thrusters for all maneuvers results in a 750 lb payload penalty, referenced to the minimum weight system.
4. Dedicated tankage is the preferred choice for the RCS (OMS) configuration, since weight differences are minimal.

The final comparison of interest concerns the dedicated tankage concept described above, and the bipropellant modular RCS concept of Section 4.4. Figure 4-60 presents a weight comparison for the two systems. As shown, the wing module configuration is approximately 300 lbm lighter. This difference is minimal, and therefore definition of the more attractive concept must certainly consider additional parameters, such as maintainability. For example, component accessibility during maintenance operations would be impaired for wing tip modules because of their total enclosure; by contrast fuselage modules would offer more favorable accessibility. In the sections that follow, the alternate configurations are evaluated with regard to operational, maintenance, and safety considerations. Specifically, effort was devoted to the following areas:

1. Instrumentation requirements
2. Reliability estimates
3. Ground support and maintenance requirements
4. Comparison of integral and modular systems.

# SYSTEM DESCRIPTION

POD DESIGN CHARACTERISTICS				DESIGN CONDITIONS														
RCS/OMS	PROPELLANTS		RCS/OMS	NO. OF ENGINES			NO. OF TANKS		TANK MTL		EXPULSION DEVICE		ULLAGE*	TANK DIAMETER		PRESSURIZATION (GHe)		EXPUL REDUND
TANKAGE	RCS	OMS	ENGINES	RCS	±RCS	OMS	RCS	OMS	RCS	OMS	RCS	OMS	(PERCENT)	RCS	OMS	RCS	OMS	
COMMON	N <sub>2</sub> O <sub>4</sub> /MMH	N <sub>2</sub> O <sub>4</sub> /MMH	DEDICATED	10/10/10	0/5/5	2	4/4/4	4/4/4	Ti	6Al-4V f	SURFACE TENSION	SURFACE TENSION	4/5	19(N)	30	SEPARATE	SEPARATE	NO
COMMON			COMMON	10/10/10	0/8/8	0	4/4/4	4/4/4	Ti	6Al-4V r	SURFACE TENSION	SURFACE TENSION	4/5	19(N)	30	SEPARATE	SEPARATE	
DEDICATED			DEDICATED	10/10/10	0/5/5	2	4/4/4 (COMMON TANK SIZE) NOSE & FUSE-LAGE	0/4/4	Ti	6Al-4V	SURFACE TENSION	SURFACE TENSION	4/5	19	30	SEPARATE	COMMON	
DEDICATED			COMMON	10/10/10	0/8/8	0	4/4/4	0/4/4	Ti	6Al-4V	SURFACE TENSION	SURFACE TENSION	4/5	19	30	SEPARATE	COMMON	
DEDICATED	N <sub>2</sub> H <sub>4</sub>		DEDICATED	10/10/10	0/5/5	2	4/5/5 COMMON TANK NOSE & FUSE-LAGE	0/4/4	Ti	6Al-4V	BLADDER	SURFACE TENSION	4/5	19	30	-	COMMON	

\*FUEL/OXIDIZER

11-341 A

4-68

Figure 4-56



### SYSTEMS DESCRIPTION (Continued)

POD DESIGN CHARACTERISTICS				DESIGN CONDITIONS										
RCS/OMS TANKAGE	PROPELLANTS		RCS/OMS ENGINES	NO. OF ENGINE VALVES			NO. OF ISOLATION VALVES			NO. OF OMS INTERCONNECT VALVES	HEAT PIPES & HEATERS (LBM)	THRUSTER HEATING (KW-HR)	PROPELLANT HEATING (KW-HR/LBM)	TPS (LBM/FT <sup>2</sup> )
	RCS	OMS		RCS	X RCS	OMS	RCS	X RCS	OMS					
COMMON	N <sub>2</sub> O <sub>4</sub> /MMH	N <sub>2</sub> O <sub>4</sub> /MMH	DEDICATED	40,60,60	-	16	10,10,10	-	8	8	13	40	1.08 x 10 <sup>-3</sup>	1.65
COMMON	↓	↓	COMMON	40,72,72	-	-	10,12,12	-	-	-	↓	44	↓	↓
DEDICATED	↓	↓	DEDICATED	40,60,60	-	16	10,10,10	-	8	8	↓	40	↓	↓
DEDICATED	↓	↓	COMMON	40,40,40	0,32,32	-	10,8,8	0,6,6	-	-	↓	44	↓	↓
DEDICATED	N <sub>2</sub> H <sub>4</sub>	↓	DEDICATED	20,30,30	-	16	5,5,5	-	8	8	233	74	↓	↓

4-69

Figure 4-57

APS-155

## WEIGHT BREAKDOWN SUMMARY

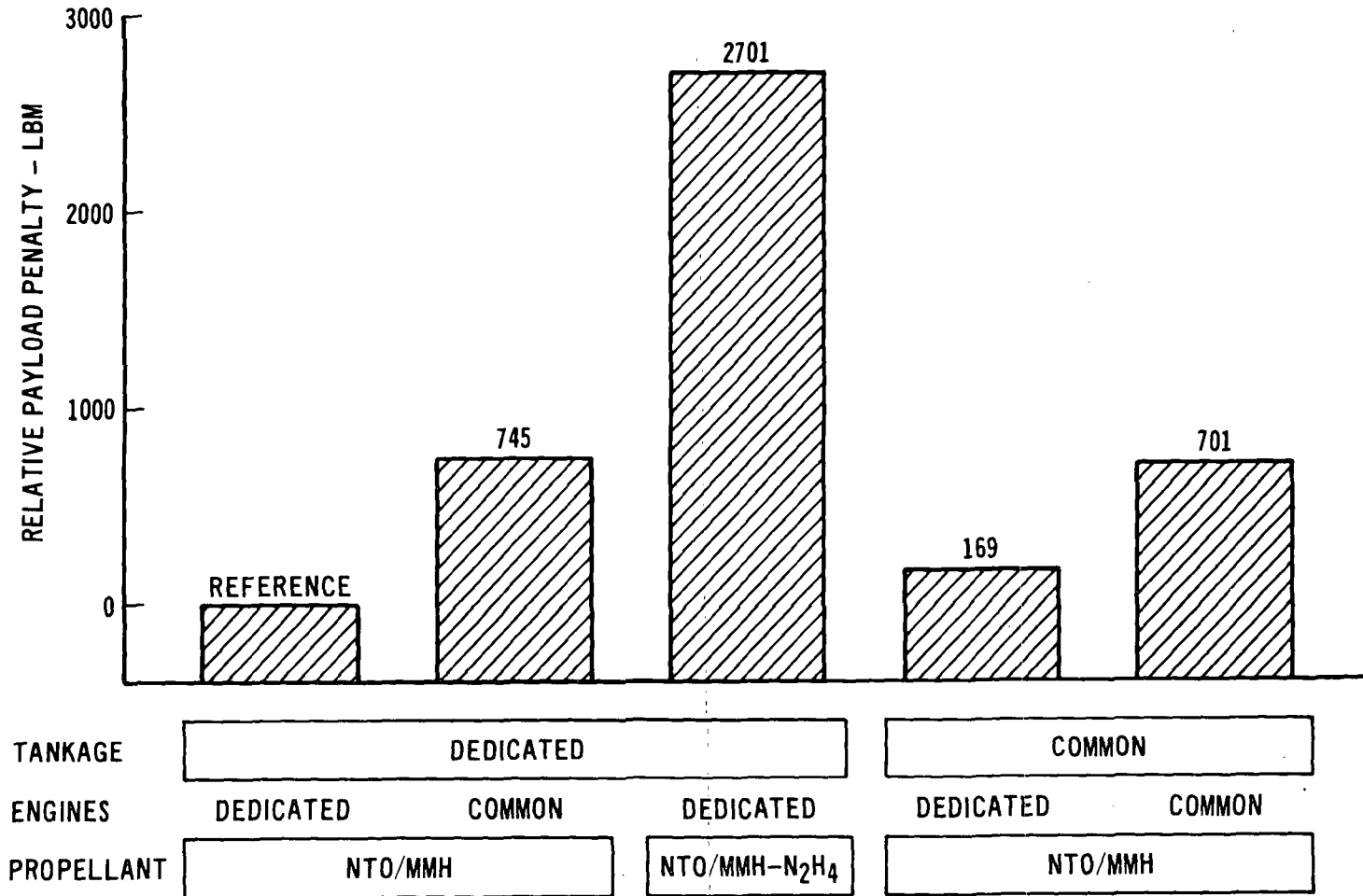
	COMMON TANKAGE		DEDICATED TANKAGE		
	DEDICATED RCS/OMS ENGINES	COMMON RCS/OMS ENGINES	DEDICATED RCS/OMS ENGINES	COMMON RCS/OMS ENGINES	DEDICATED RCS/OMS ENGINES (MONOPROPELLANT RCS)
<b>PRESSURIZATION</b>					
TANKS	1,142	1,172	1,026	1,179	1,014
REGULATORS AND CONTROLS	64	64	116	64	82
PRESSURANT	94	97	85	97	86
<b>PROPELLANT SYSTEM</b>					
TANKS	1,286	1,274	1,362	1,478	1,196
PROPELLANT					
USABLE-RCS	6,927	6,899	6,922	6,899	8,805
USABLE-OMS	24,822	25,582	25,012	25,582	25,012
TRAPPED TANK & LINE	122	102	122	102	127
TANK RESIDUAL	640	654	386	386	425
MARGINS-OMS			292	380	292
MARGINS-RCS	365	587	78	247	53
<b>DISTRIBUTION SYSTEM</b>					
LINES, VALVES AND FILTERS	714	506	714	506	696
<b>THRUSTERS</b>					
RCS	668	794	601	794	1,113
OMS	364	-	364	-	364
<b>THERMAL CONTROL</b>					
HEATERS & HEAT PIPES	13	13	13	13	233
POWER	225	227	227	226	282
<b>POD STRUCTURE</b>					
STRUCTURE	1,658	1,709	1,715	1,759	1,705
THERMAL PROTECTION	414	422	416	422	435
<b>TOTAL</b>	<b>39,519</b>	<b>40,102</b>	<b>39,451</b>	<b>40,134</b>	<b>41,920</b>

11-330 B

4-70

Figure 4-58

## COMPARATIVE PAYLOAD PENALTIES FOR CANDIDATE TANK/ENGINE SYSTEMS



4-71

Figure 4-59

## RCS SYSTEM WEIGHT COMPARISON

- WING TIP POD VS FUSELAGE PODS
- BIROPELLANT SYSTEM
- 600 LBF THRUST

	WING TIP MODULES	FUSELAGE MODULES
<b>OPTIMUM DESIGN PARAMETERS</b>		
CHAMBER PRESSURE	200	175
EXPANSION RATIO	40	60
MIXTURE RATIO	1.6	1.6
<b>WEIGHTS</b>		
<b>PRESSURIZATION</b>		
TANK	375	275
REGULATORS AND CONTROLS	59	64
PRESSURANT	30	26
<b>PROPELLANT SYSTEM</b>		
TANKS	492	474
PROPELLANT	6,800	7,235
<b>DISTRIBUTION SYSTEM</b>		
LINES, VALVES AND FILTERS	408	412
THRUSTERS	480	601
<b>THERMAL CONTROL</b>		
HEATERS AND HEAT PIPES	9	13
POWER	241	165
<b>POD STRUCTURE</b>		
STRUCTURE	551*	905
THERMAL PROTECTION	688*	230*
<b>TOTAL</b>	<b>10,133 LBM</b>	<b>10,400 LBM</b>

\*NET WEIGHT (ALLOWANCES MADE FOR ELIMINATION OF WING TIP FAIRINGS/FUSELAGE TPS)

11-370B

The objective was to determine what advantages or disadvantages are associated with various classes of systems, thereby allowing general comparisons to be made, e.g., monopropellant vs bipropellant, integral vs modular.

4.6 Instrumentation Requirements - Information on systems operation is needed for the purposes of propellant gauging and identifying faulty components. Four major system failure modes have been investigated; namely valve failure, pressurant regulator failure, helium leakage, and thermal conditioning system failures. Additionally, data pertaining to filter  $\Delta P$  and, in the case of monopropellant systems, catalyst bed  $\Delta P$  are required to define maintenance requirements. Minimum RCS instrumentation requirements have been established consistent with these goals. Parallel redundant sensors are used for the detection of critical malfunctions; however, through the use of logical comparisons between data sources, instrumentation redundancy has been minimized. Figure 4-61 delineates the system failure modes and resulting minimum instrumentation requirements for the monopropellant RCS, and Figure 4-62 presents an instrumented schematic. Although this schematic pertains specifically to a modular monopropellant RCS, it applies generally to all the systems under study.

Propellant quantity determination is accomplished based on pressure and temperature data of the helium in the propellant and pressurant tanks, i.e., helium mass inventory. The use of this method on Gemini demonstrated that an accuracy of  $\pm 3$  percent could be easily achieved. An analysis of the RCS indicates that an accuracy of  $\pm 2.7$  percent is realistic (Figure 4-63), based on component tolerances compiled during the oxygen/hydrogen studies (Reference H). As can be seen, reduction of this error could be accomplished most readily by refinement of the helium tank instrumentation.

Discrete valve position indicators are included on critical valves, and are used to identify inadvertent operation or failure to operate. Valve leakage, however, remains a difficult problem to isolate. On monopropellant systems, thruster valve leakage can be identified by the resulting thruster temperature anomalies, although if the leakage is slight, the heat input would only serve to minimize the thruster heater on-time. On bipropellant systems, leakage determination is even more difficult. Oxidizer evaporation could conceivably result in a pressure variation, although it would be slight. Profuse leakage would result in disturbance torques which could be detected; minor leakage could feasibly be detected only during regular ground maintenance operations.

## RCS INSTRUMENTATION MONOPROPELLANT N<sub>2</sub>H<sub>4</sub>

SYSTEM FAILURE MODES	SYSTEM INSTRUMENTATION								INSTRUMENTATION REDUNDANCY  SENSOR REDUNDANCY REQUIRED ONLY FOR CATASTROPIC FAILURE MODES AND PROPELLANT QUANTITY MEASUREMENT
	He TANK PRESSURANT	He TANK TEMPERATURE	PROPELLANT TANK PRESSURE	PROPELLANT TANK TEMPERATURE	VALVE POSITION	FILTER PRESSURE	THRUSTER INJECTOR TEMPERATURE	THRUSTER CHAMBER PRESSURE	
SYSTEM He LEAKAGE	✓								
REGULATOR LEAKAGE/ IMPROPER OPERATION			✓						
HIGH FILTER ΔP						✓			
ISOLATION VALVE FAILS TO ACTUATE					✓				
THRUSTER VALVE LEAKS/FAILS OPEN					✓		✓	✓	
THRUSTER VALVE FAILS CLOSED					✓				
INADVERTENT VALVE ACTUATION					✓				
HIGH CATALYST BED ΔP								✓	
THRUSTER INSTABILITY								✓	
HEAT PIPE FAILS							✓		
SYSTEM STATUS									
PROPELLANT QUANTITY	✓	✓	✓	✓					
PROPELLANT TANK PRESSURE			✓						
PROPELLANT TANK TEMPERATURE				✓					
HELIUM TANK PRESSURE	✓								
NO. SENSORS	8	8	12	12	68	3	80	40	= 231 (TOTAL)

11-244 A

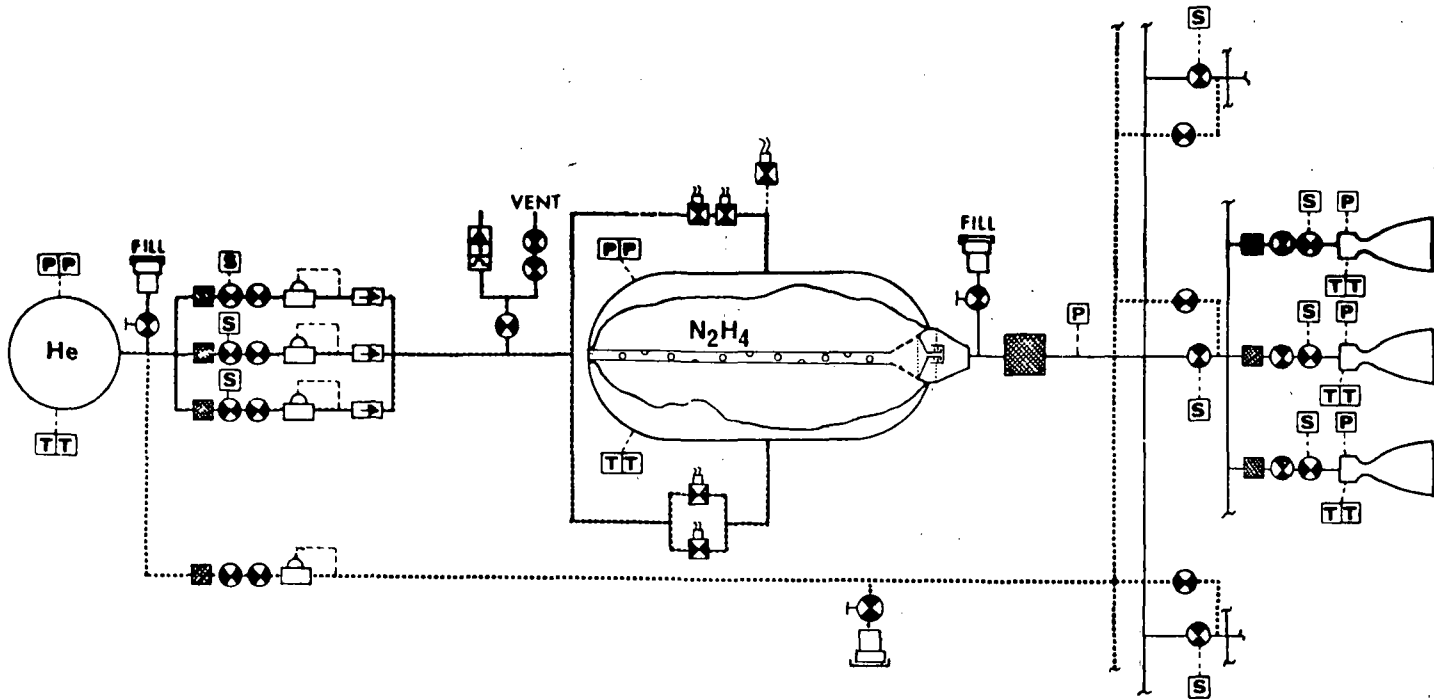
4-74

Figure 4-61

# INSTRUMENTED SYSTEM SCHEMATIC

o MODULAR RCS (MONOPROPELLANT)

- SENSORS**
- T** TEMPERATURE
  - P** PRESSURE
  - S** VALVE POSITION

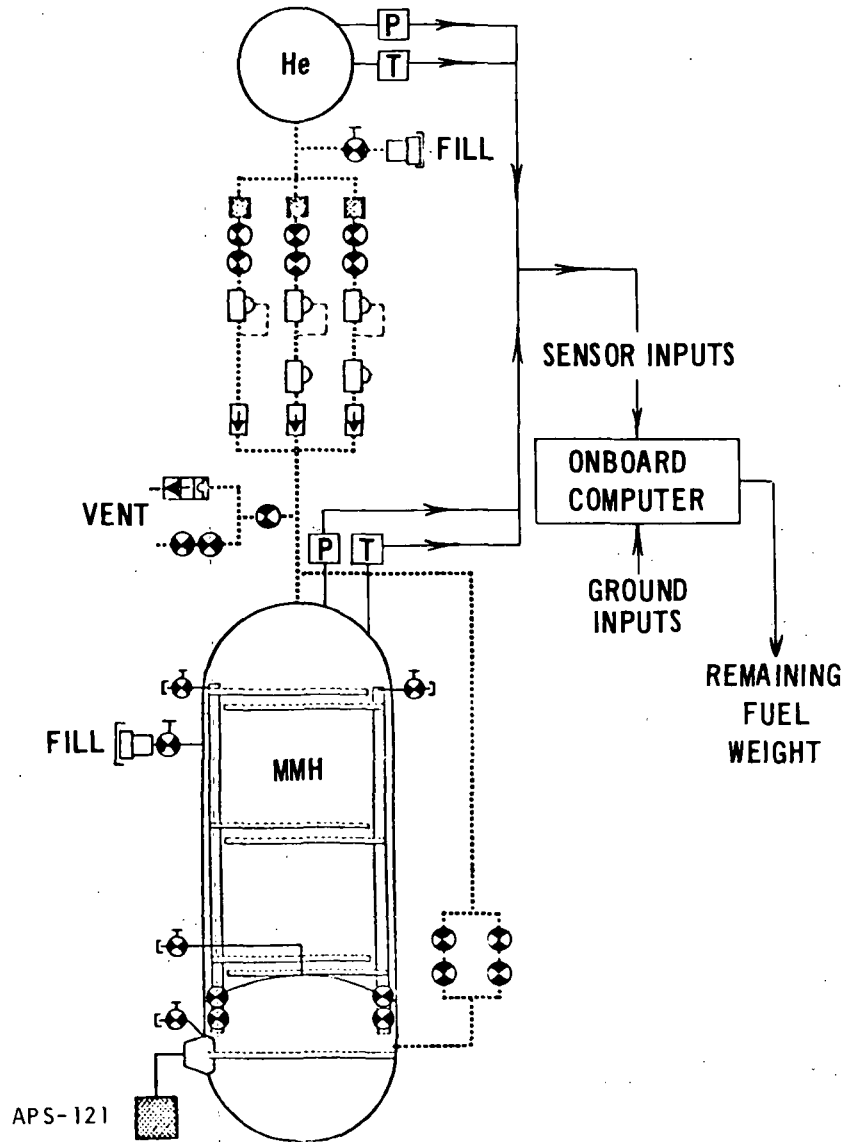


APS-139

4-75

Figure 4-62

## PROPELLANT QUANTITY DETERMINATION



POTENTIAL ERRORS IN DETERMINING REMAINING FUEL WEIGHT WITH TANK 25% FULL			
ERROR SOURCE	TOLERANCE (PERCENT)	CONTRIBUTION TO TOTAL ERROR (PERCENT)	
TEMPERATURE HELIUM (INITIAL)	1	23.8	
TEMPERATURE HELIUM (FINAL)		7.6	
TEMPERATURE ULLAGE (INITIAL)		0.1	
TEMPERATURE ULLAGE (FINAL)		8.1	
PRESSURE HELIUM (INITIAL)		23.4	
PRESSURE HELIUM (FINAL)		7.6	
PRESSURE ULLAGE (INITIAL)		0.1	
PRESSURE ULLAGE (FINAL)		8.0	
TANK VOLUME HELIUM		0.5	7.0
TOTAL INITIAL FUEL WEIGHT		1	13.7
SOLUBILITY	-	0.6	
<b>TOTAL ERROR = 2.7% OF TOTAL FUEL WEIGHT</b>			

4-76

Figure 4-63



The critical failure mode for the pressurant regulator is failed-full-open. Parallel redundant propellant tank pressure transducers serve to sense an overpressure condition and closure of the regulator backup valves is called for in the event of a malfunction signal from either of the sensors.

Loss of the pressurant supply through leakage is also considered to be a critical failure mode. However, no attractive method is available for direct monitoring of pressurant system integrity. Consequently, helium leakage will be detected through a comparison between the propellant expenditures based on the PVT method discussed above, and an approximation made by summing propellant valve on times at nominal flow rates. A significant discrepancy will indicate either a propellant or pressurant leak. Corrective action would then be based on the estimated leakage rate, and on whether or not the leakage source could be isolated.

A monopropellant system heat pipe failure represents the most critical thermal conditioning failure since at elevated temperatures, explosive decomposition of hydrazine can occur under certain malfunction conditions. Parallel redundant temperature sensors located on each thrust chamber are used to identify a temperature out of the acceptable range.

Comparisons between various outputs will be utilized to indicate additional anomalies. For example, the source of excessive pressure drops can be isolated by a comparison of pressure measurements at the tank, the main line, and the thrust chamber.

The instrumentation requirements discussed above are considered to be minimum values. As indicated in Figure 4-61, a total of 231 sensors are required for the modular monopropellant RCS. The corresponding bipropellant system would require a total of 318 sensors.

4.7 Reliability Estimates - Reliability estimates were desired to allow further comparison of monopropellant and bipropellant systems. Additionally, this data was necessary during evaluation of maintenance requirements since these are affected by the anticipated failure frequency. Reliability estimates were developed for the modular monopropellant RCS and the modular bipropellant RCS. The following criteria were established to provide a basis for reliability analyses.

1. Structure, such as tanks, lines, fittings, and static seals were assumed to have a reliability of 1.0
2. Thrusters will not fail in a catastrophic mode as long as propellants are supplied at an acceptable pressure and mixture ratio
3. A "NORMALLY CLOSED" shutoff valve will not fail open prior to first flight operational cycle and internal leakage will be of a magnitude which will not degrade system operation
4. A "NORMALLY OPEN" shutoff valve will not fail closed prior to first flight operational cycle
5. Liquid propellant storage tanks will not normally require venting
6. The subsystem will be considered operational up to the point at which one additional failure jeopardizes safe mission completion
7. Component external leakage can be virtually eliminated by special attention to component design details. Redundancy for this failure mode will not be considered in this study.

Based on data for previously flown propulsion systems, component failure rates were established and failure probabilities determined for both monopropellant and bipropellant systems to allow definition of component replacement rates. In Figure 4-64, failure rates are listed by component for both the active (operating) and the passive (nonoperating) condition. Each item includes two estimates, representing low (50%) and high (90%) confidence level limits. Figures 4-65 and 4-66 present, for a monopropellant and a bipropellant system respectively, the probabilities of at least one failure per mission.

4.8 Ground Support Operations and Maintenance Operations - Propellant handling considerations have a considerable influence on earth storable system designs. Due to the toxicity, corrosiveness and, in the case of the bipropellant, hypergolic nature of the propellants, safety considerations dictate that only those personnel directly involved in RCS servicing be allowed in the proximity of the system during these operations. For a system that is installed integrally within the vehicle, this constraint would force vehicle maintenance operations to be conducted serially, and would extend the vehicle turnaround time by approximately two days. To meet the Shuttle objective of a two week turnaround, attention has focused on the use of removable, self-contained

## COMPONENT FAILURE RATES

COMPONENT TYPE	OPERATING		NONOPERATING	
	LOW x 10 <sup>6</sup>	HIGH x 10 <sup>6</sup>	LOW x 10 <sup>6</sup>	HIGH x 10 <sup>6</sup>
BURST DISK	10.0/UNIT	100.0/UNIT	0.01/HR	0.10/HR
DISCONNECT	18.0/CYCLE	42.0/CYCLE	0.05/HR	0.50/HR
FILTER, HELIUM	51.5/HR FLOW	93.6/HR FLOW	0.01/HR	0.10/HR
FILTER, PROPELLANT	515.0/HR FLOW	936.0/HR FLOW	0.10/HR	1.0/HR
HEATER	0.7/HR	1.7/HR	-	-
REGULATOR, PRESSURE	7.5/HR	15.0/HR	0.10/HR	1.0/HR
SENSOR, CHAMBER PRESSURE	1700/HR BURN	6600/HR BURN	0.01/HR	0.10/HR
SENSOR, INJECTOR TEMPERATURE	150/HR BURN	640/HR BURN	0.01/HR	0.10/HR
SENSOR, PRESSURE	1.7/HR	6.6/HR	0.01/HR	0.10/HR
SENSOR, TEMPERATURE	1.5/HR	6.4/HR	0.01/HR	0.10/HR
SENSOR, PROPELLANT QUALITY	2.7/HR	6.6/HR	0.01/HR	0.10/HR
TANK, PRESSURANT	5/CY + 0.036/HR	50/CY + 0.36/HR	-	-
TANK, PROPELLANT, BELLOWS	100/CY + 1.8/HR	1000/CY + 18.0/HR	-	-
TANK, PROPELLANT, BLADDER	100/CY + 3.6/HR	1000/CY + 36.0/HR	-	-
THERMOSTAT	0.6/HR	1.9/HR	0.01/HR	0.10/HR
THRUSTER, MONOPROPELLANT	10.0/SEC BURN	100.0/SEC BURN	-	-
THRUSTER, BIPOPELLANT	2.0/CYCLE	20.0/CYCLE	-	-
VALVE, CHECK	9.0/CYCLE	21.0/CYCLE	0.05/HR	0.50/HR
VALVE, MANUAL	2.4/CYCLE	4.0/CYCLE	0.05/HR	0.50/HR
VALVE, PYROTECHNIC	10.0/UNIT	100.0/UNIT	0.01/HR	0.10/HR
VALVE, RELIEF	5.3/CYCLE	9.0/CYCLE	0.05/HR	0.50/HR
VALVE, SOLENOID	4.8/CYCLE	8.0/CYCLE	0.10/HR	1.0/HR

4-79

Figure 4-64

APS-122

## MONOPROPELLANT SYSTEM FAILURE PROBABILITY

COMPONENT TYPE	NUMBER IN SYSTEM	COMBINED MISSION DUTY CYCLE		FAILURE RATE/MISSION ( $\lambda t + \lambda C$ )	
		OPERATING	NON-OPERATING	LOW	HIGH
				FAILURE RATE	FAILURE RATE
BURST DISK	3	-	2,628 HR	0.000056	0.000563
DISCONNECT, HELIUM	6	12 CYCLES	5,256 HR	0.000479	0.003132
DISCONNECT, FUEL	3	6 CYCLES	2,628 HR	0.000239	0.001566
FILTER, HELIUM	12	0.65 HR (FLOW)	10,512 HR	0.000138	0.001112
FILTER, FUEL	46	8.0 HR (FLOW)	40,288 HR	0.008149	0.047776
HEATER, THRUSTER	40	8000 HR	27,040 HR	0.005600	0.013600
REGULATOR, PRESSURE	12	600 HR	9,912 HR	0.005491	0.018912
SENSOR, CHAMBER PRESSURE	40	0.78 HR (BURN) + 8000 HR	27,040 HR	0.015196	0.060652
SENSOR, INJECTOR TEMP	80	1.56 HR (BURN) + 16,000 HR	54,080 HR	0.024774	0.108806
SENSOR, TANK PRESSURE	20	3600 HR	12,168 HR	0.006241	0.024976
SENSOR, TANK TEMP	20	3600 HR	12,168 HR	0.005521	0.024256
SENSOR, FILTER $\Delta P$	3	1200 HR	4,056 HR	0.002080	0.008325
TANK, HELIUM	4	4 CY + 800 HR	2,704 HR	0.000049	0.000488
TANK, FUEL, BLADDER	6	6 CY + 1200 HR	4,056 HR	0.004920	0.049200
THERMOSTAT, THRUSTER	40	8000 HR	27,040 HR	0.005070	0.017904
THRUSTER, MONOPROPELLANT	40	2800 SEC	35,040 HR	0.028000	0.280000
VALVE, CHECK	9	530 CYCLES	7,884 HR	0.005164	0.015072
VALVE, MANUAL	9	18 CYCLES	7,884 HR	0.000437	0.004014
VALVE, PYROTECHNIC	30	-	26,280 HR	0.000563	0.005628
VALVE, RELIEF	3	6 CYCLES	2,628 HR	0.000163	0.001368
VALVE, SOLENOID	111	222 CYCLES	97,236 HR	0.010789	0.099012
VALVE, THRUSTER	40	14,700 CYCLES	35,040 HR	0.074064	0.152640
TOTAL FAILURE RATE/MISSION $\Sigma(\lambda t + \lambda C) = 0.209744$					0.955653
PROBABILITY OF AT LEAST ONE FAILURE = $1 - e^{-\Sigma(\lambda t + \lambda C)} = 0.289$					0.615

11-267 A

4-80

Figure 4-65

## BIPROPELLANT SYSTEM FAILURE PROBABILITY

COMPONENT TYPE	NUMBER IN SYSTEM	COMBINED MISSION DUTY CYCLE		FAILURE RATE/MISSION ( $\lambda t + \lambda C$ )	
		OPERATING	NONOPERATING	LOW FAILURE RATE	HIGH FAILURE RATE
BURST DISK	6	-	5.256 HR	0.000112	0.001126
DISCONNECT, HELIUM	12	24 CYCLES	10.512 HR	0.000958	0.006264
DISCONNECT, PROPELLANT	6	12 CYCLES	5.256 HR	0.000479	0.003132
FILTER, HELIUM	24	1.3 HR (FLOW)	21.024 HR	0.000276	0.002224
FILTER, PROPELLANT	88	15 HR (FLOW)	77.073 HR	0.015432	0.091113
HEATER, THRUSTER	80	16,000 HR	54.080 HR	0.011200	0.037824
REGULATOR, PRESSURE	30	1,800 HR	24,480 HR	0.015948	0.051480
SENSOR, CHAMBER PRESSURE	40	0.78 HR (BURN) + 8,000 HR	27.040 HR	0.015196	0.060652
SENSOR, INJECTOR TEMPERATURE	80	1.56 HR (BURN) + 16,000 HR	54.080 HR	0.024774	0.108806
SENSOR, TANK PRESSURE	28	5,600 HR	18,928 HR	0.009709	0.038853
SENSOR, TANK TEMPERATURE	28	5,600 HR	18,928	0.008589	0.037733
SENSOR, FILTER $\Delta P$	6	1,600 HR	5,408 HR	0.002774	0.011101
TANK HELIUM	6	6 CY + 1200 HR	4,056 HR	0.000073	0.000730
TANK, PROPELLANT, BELLOWS	8	8 CY + 1600 HR	5,408 HR	0.003680	0.036800
THERMOSTAT, THRUSTER	80	16,000 HR	54,080 HR	0.010140	0.035808
THRUSTER, BIPROPELLANT	40	14,700 CYCLES	35,040 HR	0.029400	0.294000
VALVE, CHECK	18	1,060 CYCLES	15,768 HR	0.010328	0.030144
VALVE, MANUAL	18	36 CYCLES	15,768 HR	0.000874	0.008028
VALVE, PYROTECHNIC	40	-	35,040 HR	0.000750	0.007508
VALVE, RELIEF	6	12 CYCLES	5,256 HR	0.000326	0.002736
VALVE, SOLENOID	222	444 CYCLES	194,472 HR	0.021578	0.198024
VALVE, THRUSTER	80	29,400 CYCLES	70,080 HR	0.148128	0.305280
TOTAL FAILURE RATE, MISSION, $\Sigma(\lambda t + \lambda C) = 0.339472$				1.391568	
PROBABILITY OF AT LEAST ONE FAILURE = $1 - e^{-\Sigma(\lambda t + \lambda C)} = 0.298$				0.752	

APS-128 A

4-81

Figure 4-66

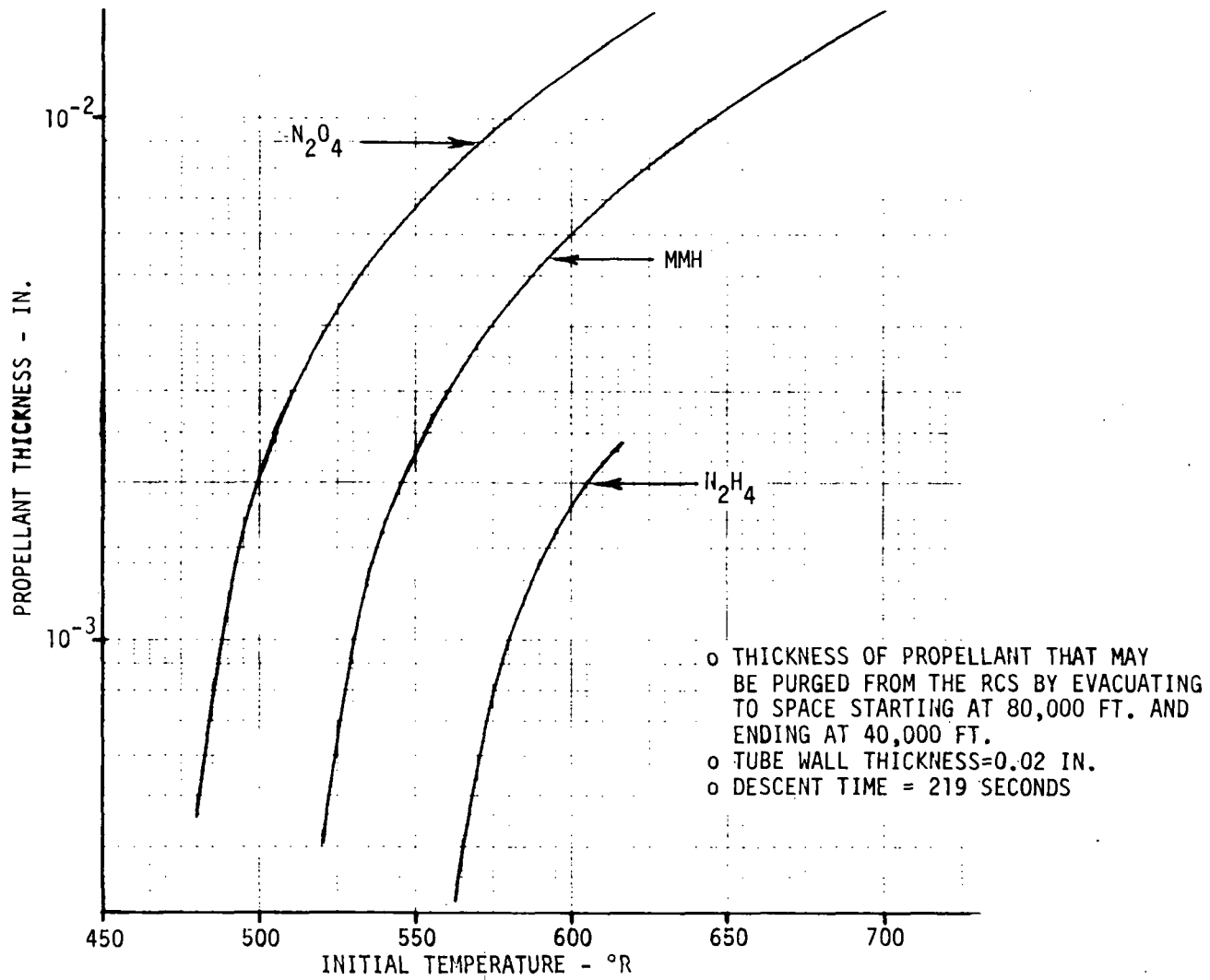
modules. The modules will be removed from the vehicle after landing and taken to a remote facility suitable for safe maintenance and filling operations. Vehicle maintenance could then proceed without elaborate precautions.

The following discussion defines the anticipated maintenance procedures, assuming a modularized propulsion system. Three topics have been identified; namely inflight checkout, safing, and servicing and maintenance.

4.8.1 Inflight Checkout - System repair requirements will be established by onboard instrumentation during flight. Checkout will occur shortly before the deorbit burn and will consist of firing opposing thruster groups to a short preprogrammed firing sequence. Analog pressure and temperature data plus bilevel valve position indicator data will be recorded on onboard tapes. During maintenance operations, the tapes will be removed and analyzed to identify those components requiring replacement. Differences in inflight checkout requirements between monopropellant and bipropellant systems are minimal, resulting only from the somewhat higher instrumentation requirements associated with bipropellant systems.

4.8.2 Safing - The major portion of the system will remain "wet" but it is considered necessary to purge dry the thruster assemblies for safety and reuse. System safing will begin during reentry, following vehicle transition to airplane mode of flight. At this time, propellant isolation valves will be closed and the thruster assemblies purged with residual helium pressurant. A slow steady purge at 15 psig is considered to be a more effective means of removing line propellant residuals than a rapid purge followed by vacuum dry. This conclusion is based on calculations performed to determine the extent of vacuum drying from the nominal deactivation altitude of 80,000 ft down to 40,000 ft for  $N_2O_4$ , MMH and  $N_2H_4$ . The data show that only a negligible quantity of propellant can be removed through vacuum evaporation (including flash and nucleate boiling). During the 219 second vacuum dry interval, wall temperatures drop rapidly to the saturation temperature during the first few seconds and then stabilize for the remainder of the time. At an initial temperature of 560°F, propellant film thicknesses of only 0.0077 in. ( $N_2O_4$ ), 0.0029 in. (MMH), and 0.002 in. ( $N_2H_4$ ) can be evaporated from the walls of the propellant lines as shown in Figure 4-67. The vacuum evaporation phenomena in other components of the propellant distribution system will depend on the component mass and exposed surface area but, even with greater heat capacities, sonic flow conditions are quickly established, restricting evaporation rates to very low values.

### VACUUM DRYING EFFECTIVENESS



APS-782

4-83

Figure 4-67

Figure 4-68 summarizes the ground safing and servicing requirements. After vehicle landing and cooldown, system depressurization will be verified and a nitrogen purge of the thrusters will be performed to assure that all propellants have been cleared. System power will then be removed and thruster throat plugs will be installed.

4.8.3 Servicing and Maintenance - Propulsion modules will be removed to a remote facility for servicing. Normal servicing will include such operations as testing valve driver circuits and the heater system and performing leak checks. The tanks and control components will be maintained wet to the maximum extent possible. Gravity fill procedures will be employed, and propellant quantities determined by weight (modules removed) or by overfilling and metering off the required ullage volume (modules installed). As discussed in Appendix H, the use of molecular sieves during fill operations is recommended to remove soluble iron from  $N_2O_4$  propellant and thereby limit the potential for rheopexy. This precaution should eliminate the need for propellant temperature conditioning during fill operations.

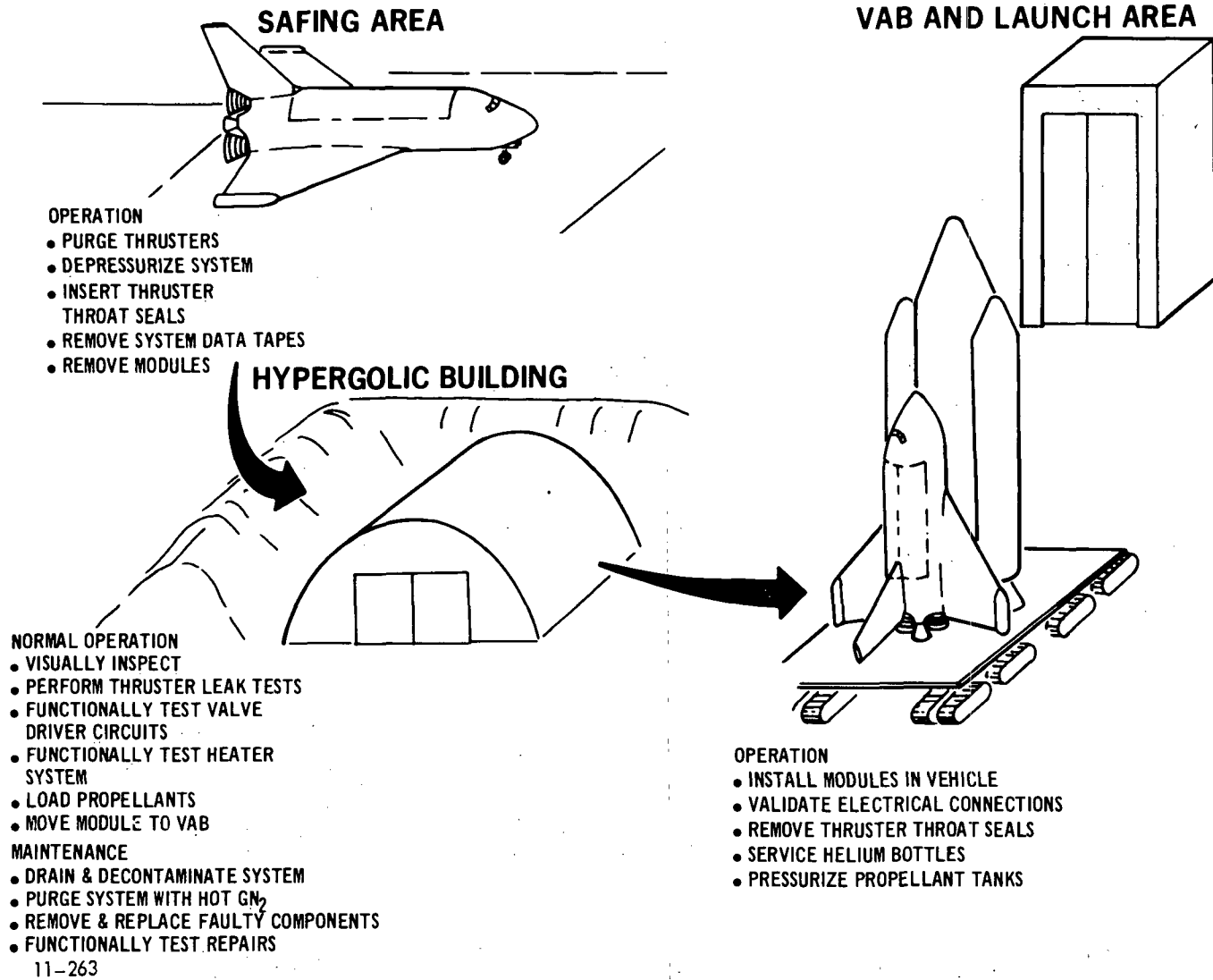
It is estimated that monopropellant thruster catalyst beds, containing Shell 405 spontaneous catalyst, will require replacement every 5 to 10 flights. Due to this anticipated high repair frequency, interest has been focused on monopropellant thruster maintenance.

Two thruster installation concepts were considered as means of simplifying thruster maintenance. In the first concept (Figure 4-69), the thruster and thruster valve are separately mounted to support structure; gland seals between the two components permit the thruster to be removed without disturbing the valve(s) or necessitating system drain and decontamination. The series thruster valves provide adequate protection to ground personnel from the toxic propellant. Once removed, the entire unit would be transferred to the supplying facility for servicing. Catalyst pack replacement would be accomplished by cutting open the thrust chamber body, replacing the bed, and rewelding the chamber. Flight acceptance tests would be performed at the same facility.

An alternate approach, readily adaptable to plug nozzle thrusters has also been configured to minimize maintenance effort. As shown in Figure 4-70, the catalyst retainer assembly is removable as a unit. A press fit between the catalyst retainer assembly and the radial outflow injector is needed to preclude the presence of voids between the injector and catalyst. In this



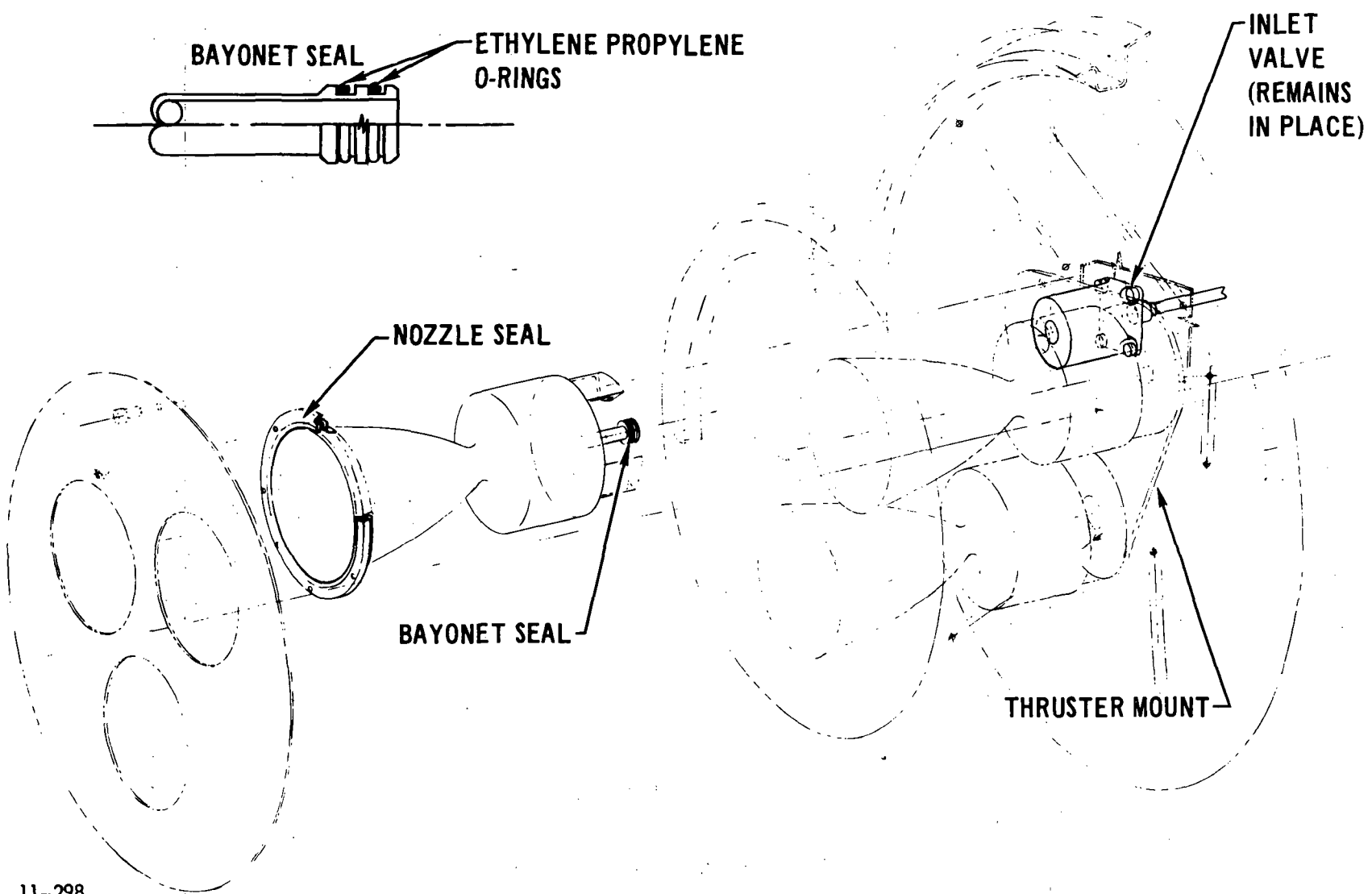
# GSE REQUIREMENTS



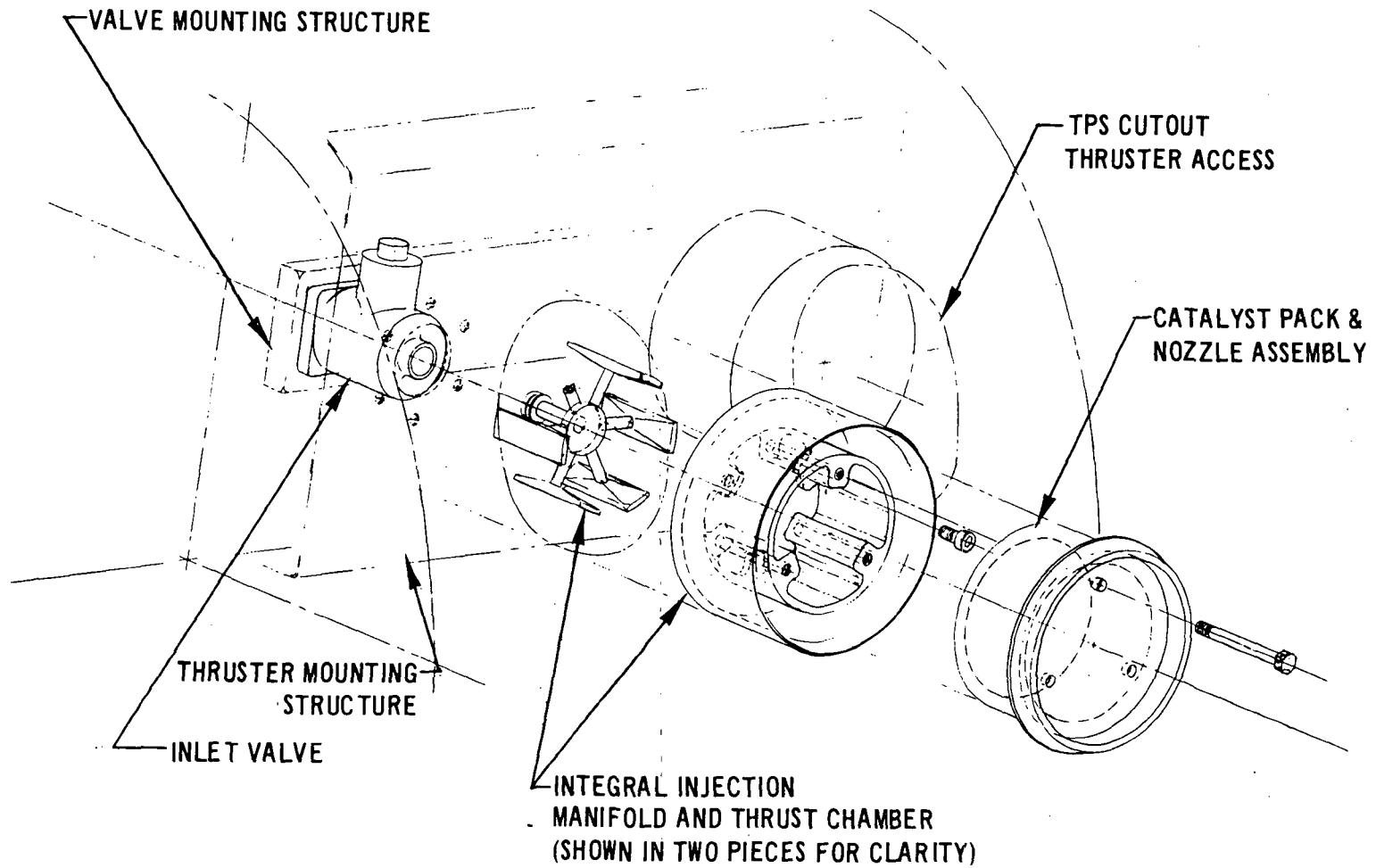
4-85

Figure 4-68

# MONOPROPELLANT THRUSTER INSTALLATION



# PLUG NOZZLE THRUSTER INSTALLATION



4-87

Figure 4-70

APS-123

case, catalyst replacement can proceed at the vendors facility, and integrity of the restored unit verified in a work horse chamber. Removal of the thrust chamber, and access to the first thruster valve, is facilitated by a removable plug closure and gland seals between the thruster and thruster valve.

Component failure data from previously flown spacecraft has been compiled, and are presented in Appendix H. Analysis of this data indicates the following:

1. The most prevalent failure mode is leakage.
2. The primary cause of failure is contamination.
3. The major type of contamination is particulate - both metallic and nonmetallic.
4. The components most susceptible to contamination are the pressurant check valves and the propellant valves.

Several conclusions can be derived from this data. Particular emphasis must be placed on the cleanliness of parts, facilities, and environment during the manufacturing and testing operations. Facilities, and particularly ground support equipment must be carefully controlled and maintained, and all fluids introduced into the vehicle must be adequately filtered. Handling procedures must be devised which will prevent the generation of contamination. Cleaning and flushing procedures must be instituted to remove contaminants produced during component manufacturing, so that the vehicle is clean when assembled. Test methods must provide for complete removal of all test fluids and provide a clean vehicle when testing is complete.

Maintenance operations will be performed based on inflight checkout intelligence data. Failure probability analyses (Section 4.7) show that the required system repair frequency will be high. As shown in Figure 4-71 estimates vary from a propellant system failure every 1 to 3 flights for a bipropellant RCS and a propellant system failure every 1 to 5 flights for a monopropellant RCS. These numbers illustrate the importance of component accessibility in reducing maintenance downtime. However, for most components, the time to physically replace the component is small when compared to the time required to safe the system so component removal and replacement can take place. Past propulsion system experience indicates that system reliability and reusability would be benefited by maintaining the propellant feed system in a wetted condition. Flush and clean operations can expose the system to moisture, solvents, and atmospheric constituents which react with the propellants to form acids or salts. Unless these agents can be completely removed, the final state of the system

## MEAN TIME BETWEEN COMPONENT FAILURE MODULAR RCS

SUBSYSTEM ASSEMBLY	MONOPROPELLANT MISSIONS	BIPROPELLANT MISSIONS
TOTAL RCS	1.0 → 4.7	0.7 → 2.9
TOTAL RCS LESS INSTRUMENTATION	1.4 → 6.6	0.9 → 3.7
RCS INSTRUMENTATION	4.1 → 16.5	3.5 → 14.3
PRESSURIZATION COMPONENTS	10.4 → 57.3	5.0 → 25.3
PROPELLANT STORAGE AND CONTROL	6.5 → 52.0	4.1 → 31.8
PROPELLANT TANKS & FILL VALVES	19.1 → 187.0	23.4 → 224.0
THRUSTER ASSEMBLIES	2.1 → 8.8	1.4 → 5.0

4-89

Figure 4-71

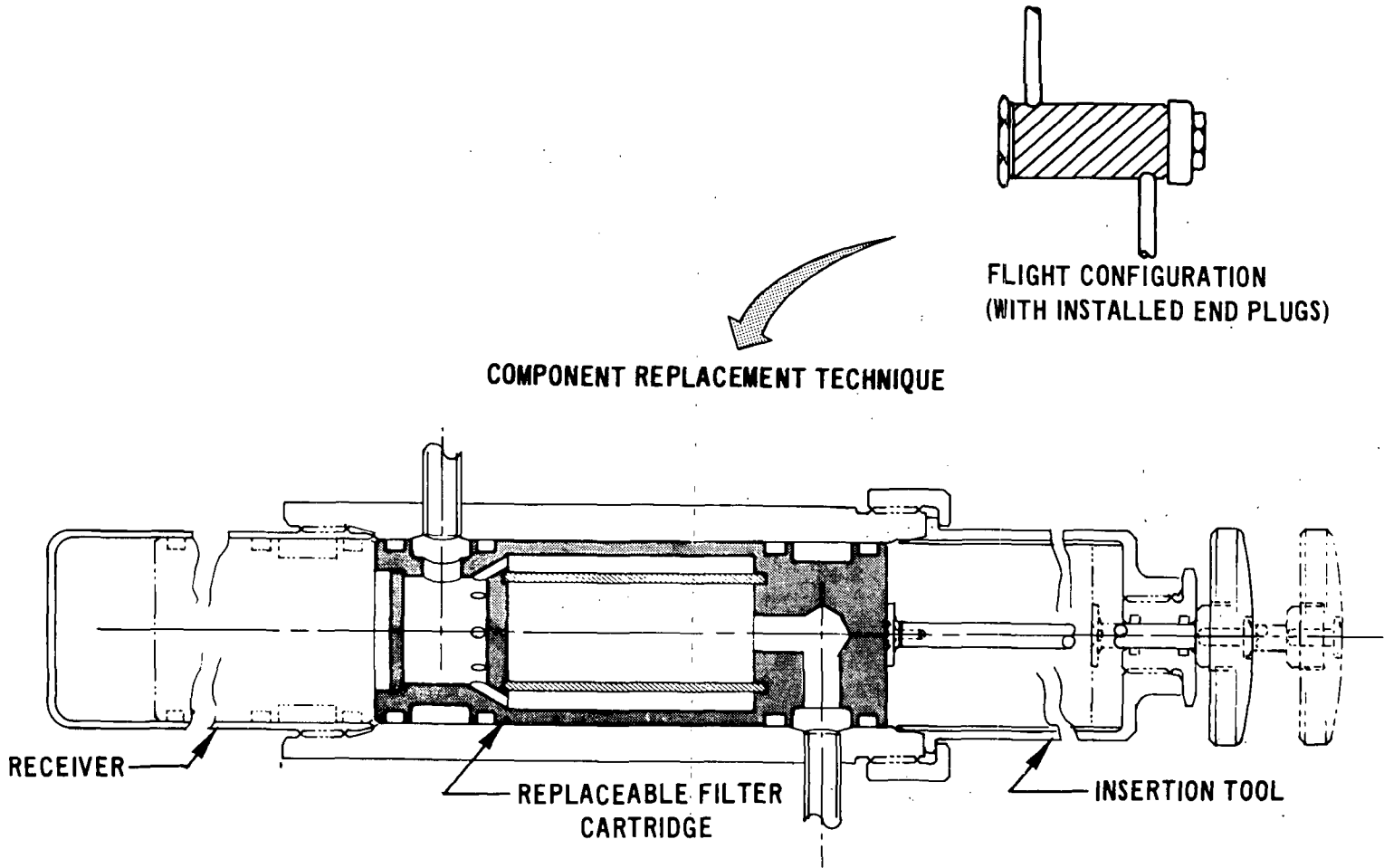
11-265

might be worse than it was at the start. Consequently, the wet system concept is attractive, but if flush and clean operations are to be minimized, other means must be provided to assure that the safety of maintenance personnel and other vehicle equipment is safeguarded during component replacement and removal. One attractive approach relies on a replaceable cartridge-type component packaging technique. Figure 4-72 shows a conceptual design for the replacement of a propellant filter. The filter cartridge is packaged in a cylindrical housing containing end plugs. Gland seals on the cartridge provide assurance that the system seal will not be broken with the end plugs removed. To replace the cartridge, the system is depressurized and the end plugs are removed. In place of the end plugs are threaded a receiver on one end of the housing and an ejector tool on the other. The replacement cartridge is contained within the ejector tool and is inserted into the housing by the plunger action of the tool which simultaneously displaces the old cartridge into the receiver. The tool and receiver are then removed and the end plugs replaced, completing the repair. The displaced cartridge seals against the receiver to preclude the escape of propellant during disposal. Similarity in housing design and seal configuration can be utilized in the design of other components to minimize development effort. Figure 4-73 shows a conceptual design for a cartridge-type propellant shutoff valve.

The use of this approach for propellant system filters and shutoff valves would reduce the probability of a failure requiring system flushing operations to a minimum of 19 missions for a bipropellant RCS and 23 missions for a monopropellant RCS. Conventional components would be used in the pressurant system, and replacement of these components would require only gas purging precautions.

The replacement of propellant system components other than thrusters, filters and shutoff valves would require either complete or partial system draining and flushing to remove residual propellants from the system in order to assure a safe working environment for maintenance personnel. Methods proposed for past programs have included heated  $\text{GN}_2$  purge, vacuum drying, steam cleaning, volatile neutralization, serial dilution, neutralizing solution, tri-flush, and the single-flush method used for the Gemini and Apollo programs. Of these, the single-flush method and a variation of that method appear to be the most promising approaches for decontamination of the shuttle RCS when necessary. A review of available solvents (Appendix E) has identified

# REPLACEABLE COMPONENT EJECTION CONCEPT

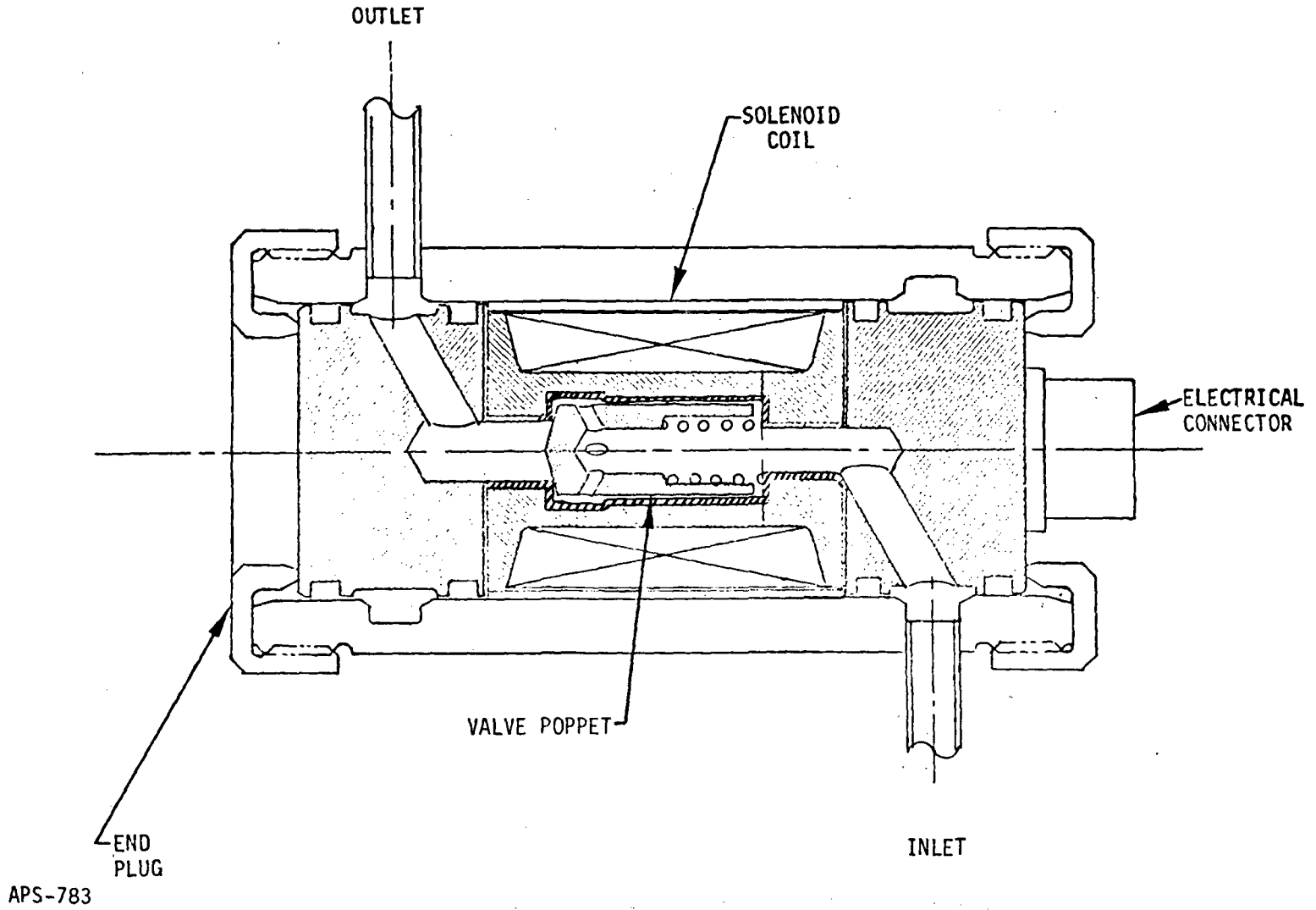


4-91

Figure 4-72

11-240

# CARTRIDGE-TYPE PROPELLANT SHUTOFF VALVE



4-92

Figure 4-73



Isopropanol and Freon TF as the most attractive solvents for fuel and oxidizer systems, respectively.

The single-flush method utilizes a volatile liquid solvent in a single stage flushing operation, followed by a  $\text{GN}_2$  purge to facilitate drying. The Dow Chemical Company recommended a variation to this approach for decontaminating Apollo propulsion subsystems (Reference K). Although this approach was not adopted for Apollo, its advantages make it attractive for consideration. The solvent is introduced into the contaminated system in its vapor phase; the solvent then condenses on the system internal surfaces. The flowing film of condensed solvent vapor is effective in removing solid as well as liquid contaminants, while the non-condensed vapors sweep out the fumes. Since the rate of release of contaminants from elastomers is temperature dependent, the higher temperatures associated with vapor phase cleaning serve to quicken the cleaning procedure. Pressure pulsing during vapor-phase cleaning to create turbulence can be employed to further facilitate the operation.

4.9 Integral Versus Modular Systems - One of the objectives of the Phase C and E Studies was to compare candidate systems on the basis of weight as well as on operational characteristics and technology considerations.

Figure 4-74 summarizes the relative merits of integral and modular systems. In addition to lower system weights, integral systems offer advantages in the areas of thermal control requirements, effect on aerodynamics, and severity of dynamic environment. Modular configurations benefit primarily from safety and maintenance considerations.

The safety advantages featured in modular systems result primarily from the isolation of the propellants from the vehicle. This isolation would limit the effects of leakage to just the RCS modules. In addition, since servicing operations would be performed at a dedicated facility, a catastrophic failure during maintenance would have no effect on the vehicle and would involve only a limited number of personnel.

Both vehicle turnaround and maintenance are enhanced by modularization because the entire pod could be replaced in the event of major maintenance requirements. Additionally, RCS maintenance could be performed concurrently with vehicle maintenance unlike integral systems in which RCS vehicle maintenance must be performed consecutively, potentially causing delays in vehicle turnaround.

## MODULAR VS INTEGRAL COMPARISON

	MODULAR	INTEGRAL
WEIGHT	MONOPROPELLANT - 44,974 (RCS - 12,889, OMS - 28,790, APU - 3,295) BIPROPELLANT - 42,218 (RCS - 10,133, OMS - 28,790, APU 3,295)	MONOPROPELLANT - 43,376 (RCS/APU - 14,586, OMS 28,790) BIPROPELLANT - 40,655 (RCS/OMS - 37,360, APU - 3,295)
MAINTENANCE	POD REMOVAL AFTER LANDING DEDICATED FACILITY FOR POD SERVICING COMPONENT ACCESSIBILITY INCORPORATED IN MODULE DESIGN	RCS SERVICED BY PROPELLANT CARTS COMPONENT ACCESSIBILITY COMPROMISED BY VEHICLE DESIGN
VEHICLE TURNAROUND	RCS MAINTENANCE PERFORMED CONCURRENTLY WITH VEHICLE MAINTENANCE ENTIRE POD COULD BE REPLACED IN THE EVENT OF MAJOR MAINTENANCE REQUIREMENTS	RCS-VEHICLE MAINTENANCE PERFORMED CONSECUTIVELY RCS MAINTENANCE COULD CAUSE DELAYS IN VEHICLE TURNAROUND
SAFETY	ON ORBIT - EFFECTS OF LEAKAGE LIMITED TO RCS MODULES SERVICING OPERATIONS - <ul style="list-style-type: none"> <li>PERFORMED AT DEDICATED FACILITY</li> <li>ONLY INVOLVED PERSONNEL IN PROXIMITY</li> <li>CATASTROPHIC FAILURE HAS NO EFFECT ON VEHICLE</li> </ul>	ON ORBIT - COMPONENT EXTERNAL LEAKAGE COULD AFFECT OTHER SYSTEMS SERVICING OPERATIONS - <ul style="list-style-type: none"> <li>PERFORMED AT VEHICLE SERVICING AREA</li> <li>LARGE NUMBER OF PERSONNEL IN PROXIMITY OF LOADED RCS</li> <li>VEHICLE DAMAGE LIKELY IN THE EVENT OF CATASTROPHIC FAILURE</li> </ul>
THERMAL CONTROL	UNCONTROLLED TEMPERATURE RANGE - 100°F TO + 165°F POD TPS - NOSE - SLA - 561, CYLINDRICAL SURFACE - MDAC-RSI (AVERAGE UNIT WT 2.34 LBM/FT <sup>2</sup> ) THRUSTER HEATERS - 10 WATTS/THRUSTER (MONOPROPELLANT) 5.4 WATTS/THRUSTER (BIPROPELLANT) HEAT PIPES (MONOPROPELLANT) - WATER/COPPER CONNECTED TO ECLS TANK HEATERS - 153 WATTS (MONOPROPELLANT) 140 WATTS (BIPROPELLANT) HEAT SOAKBACK AFTER TOUCHDOWN - 350°F (MAXIMUM) APU HYDRAULIC OIL COOLING - WATER FLASH EVAPORATOR, ON-OFF CONTROL	UNCONTROLLED TEMPERATURE RANGE - 0°F TO + 150°F TPS - NONE REQUIRED THRUSTER HEATERS - 10 WATTS/THRUSTER (MONOPROPELLANT) 5.4 WATTS/THRUSTER (BIPROPELLANT) HEAT PIPES (MONOPROPELLANT) - WATER/COPPER TANK HEATERS - 160 WATTS (MONOPROPELLANT) 135 WATTS (BIPROPELLANT) HEAT SOAKBACK AFTER TOUCHDOWN - 350°F (MAXIMUM) APU HYDRAULIC OIL COOLING - WATER FLASH EVAPORATOR, ON-OFF CONTROL
SEVERITY OF DYNAMIC ENVIRONMENTS AFFECT ON AERODYNAMICS	UNSTEADY FLOW ON WING MAY INDUCE WING/POD RESPONSE THAT COULD RESULT IN FLUTTER  EFFECTS MINIMIZED BY - <ul style="list-style-type: none"> <li>KEEPING PODS ON TOP SIDE OF WING (HYPERSONIC STABILITY)</li> <li>MINIMIZING POD FRONTAL AREA (DRAG)</li> </ul> TAPERING OF ELEVONS IS REQUIRED TO PROVIDE SUFFICIENT WING STRUCTURE FOR POD SUPPORT	EFFECT ON TANKS MINIMAL DUE TO LOCATION (IN CLOSE PROXIMITY TO VEHICLE CG)  NO DIRECT AFFECT
DEVELOPMENT CONSIDERATIONS	EFFECT OF OTHER SYSTEMS ON TEST REQUIREMENTS IS MINIMAL ACCURATE ENVIRONMENTAL SIMULATION DURING FULL SYSTEM TESTING IS FEASIBLE	TEST REQUIREMENTS AFFECTED BY ADJACENT SYSTEMS COMPLETE ENVIRONMENTAL SIMULATION DURING TESTING NOT PRACTICAL
GROWTH CAPABILITY	MODULE MOLD LINES CAN BE REVISED TO ACCOMMODATE FUTURE UPDATED REQUIREMENTS WITHOUT AFFECTING BASIC VEHICLE DESIGN	RCS UPDATING LIMITED BY VEHICLE ENVELOPE CONSTRAINTS

4-94

Figure 4-74

The only significant advantage afforded by integral systems is weight. Although weight minimization is an attractive goal, the maintenance complications associated with integral systems are unacceptable on a reusable vehicle. Consequently, only modular systems can be seriously considered for use on shuttle.

## 5. SUMMARY AND CONCLUSIONS

During this study, viable earth storable RCS configurations were identified and compared on the basis of weight, technology, safety in flight, ease of maintenance, and reusability forecasts. Three basic concepts were defined: a modular concept utilizing wing and nose modules, a modular concept utilizing fuselage and nose modules, and a non-modular concept wherein the RCS was integral within the vehicle. For each concept, alternate configurations were defined by specifying the propellants (monopropellant or bipropellant) and either common or dedicated tankage and RCS thrusters/OMS engines.

Integral systems suffer, relative to modular systems, in four areas:

1. Safety
2. Ease of Maintenance
3. Development Flexibility
4. Growth Capability

Although attractive from a weight standpoint, the above considerations are sufficient to eliminate integral systems from contention.

Figure 5-1 summarizes the relative advantages of wing and fuselage modular systems. No clearcut preference is evident; weights are comparable, and no significant technology concerns impact either concept. However, the wing modules do complicate wing design, and the forward firing thruster protection doors are unattractive. These considerations, coupled with the benefits associated with the design and development of a consolidated propulsion system make the fuselage module concept somewhat more attractive.

Within a fuselage module concept, three viable configurations remain: a dedicated OMS coupled with either a monopropellant or a bipropellant RCS, and a bipropellant RCS for all maneuvers. For each system dedicated tankage is more attractive relative to common tankage due to development ease. Based on the study criteria the dedicated OMS - bipropellant RCS is the most attractive concept. However, cost considerations, not included in this study, could alter this position. The monopropellant RCS suffers a significant weight penalty, but potentially offers reduced development effort and maintenance requirements. Cost trades between reduced development costs but increased operational costs (due to the payload penalty) are necessary to define the monopropellant RCS potential. The RCS(OMS) is quite weight competitive with the dedicated RCS-OMS configuration and, additionally would be less costly since it

## WING-TIP VS FUSELAGE POD COMPARISON

### BIPROPELLANT N<sub>2</sub>O<sub>4</sub>/MMH

	WING TIP POD	FUSELAGE POD
<b>WEIGHT</b>	10,133 LBM	10,400 LBM
<b>CONTROL</b>	IMPULSE REQUIREMENTS MINIMIZED BY LARGE MOMENT ARMS. (FINE CONTROL MORE DIFFICULT TO ACHIEVE). THRUSTER LOCATIONS MINIMIZE CROSS-COUPLING	BIAS DISTURBANCE TORQUES (YAW) RESULT IN UNEQUAL PROPELLANT EXPENDITURE BETWEEN PODS FOR ON-ORBIT CONTROL
<b>SAFETY/ MAINTENANCE</b>	POD LOCATIONS FACILITATE REMOVAL/INSTALLATION OPERATIONS. COMPONENT ACCESSIBILITY MORE DIFFICULT (PODS REMOVED) BECAUSE OF TOTAL ENCLOSURE - MORE ACCESS DOORS	POD ACCESS DIFFICULT BECAUSE OF POD LOCATION OVER THE WING. COMPONENTS EASILY ACCESSIBLE WITH PODS REMOVED
<b>THERMAL CONTROL</b>	UNCONTROLLED TEMPERATURE RANGE - 110°F TO +165°F. MDAC-RSI AVERAGE UNIT WEIGHT = 2.34 LBM/FT <sup>2</sup> THRUSTER HEATERS - 5.4 WATTS/THRUSTER TANK HEATERS - 140 WATTS DOORS REQUIRED OVER FWD-FACING THRUSTERS	UNCONTROLLED TEMPERATURE RANGE -120°F TO +115°F. MDAC-RSI AVERAGE UNIT WEIGHT = 1.65 LBF/FT <sup>2</sup> THRUSTER HEATERS - 5.4 WATTS/THRUSTER TANK HEATERS - 50 WATTS
<b>AFFECT ON AERODYNAMICS</b>	EFFECTS MINIMIZED BY • KEEPING PODS ON TOP SIDE OF WING (HYPERSONIC STABILITY) • MINIMIZING POD FRONTAL AREA (DRAG) TAPERING OF ELEVONS IS REQUIRED TO PROVIDE SUFFICIENT WING STRUCTURE FOR POD SUPPORT	EFFECTS MINIMIZED BY • MINIMIZING POD FRONTAL AREA (DRAG) • POD BOATTAIL (BASE DRAG)  MINIMAL JI EFFECTS ON CONTROL SURFACES DUE TO AFT LOCATION OF CONTROL THRUSTERS
<b>SEVERITY OF DYNAMIC ENVIRONMENTS</b>	UNSTEADY FLOW ON WING MAY INDUCE WING/POD RESPONSE THAT COULD RESULT IN FLUTTER HIGH ACCELERATION AND PROPELLANT SLOSH LOADS LIKELY BECAUSE OF RCS LOCATION (REMOTE FROM VEHICLE CG)	MINIMAL EFFECT ON TANKAGE DUE TO CLOSE PROXIMITY TO VEHICLE ROLL AXIS

MCDONNELL DOUGLAS ASTRONAUTICS COMPANY - EAST

5-2

Figure 5-1

11-375 B

deletes the costs associated with OMS engine development. This concept suffers in comparison to the dedicated RCS-OMS configuration solely on the basis of its reduced flexibility to future increases in translational thrust requirements, e.g., potential future high thrust requirements for ascent abort.

Several conclusions regarding reuse are applicable regardless of the configuration chosen. The successful implementation of a multi-mission vehicle will require thorough consideration of reusability throughout system design, including the establishment of thermal control requirements consistent with reusability, and in the definition of servicing, safing and maintenance operating procedures. The safety and reuse criteria identified in this study have been so categorized, and are summarized in Figures 5-2 through 5-5. Reuse considerations necessitate added care in the selection of component types and arrangement to minimize the generation and effects of contaminants on system operation.

## **SAFETY AND REUSE CRITERIA (DESIGN)**

- PROVIDE SYSTEM ACCESS WITH VEHICLE IN EITHER HORIZONTAL OR VERTICAL (LAUNCH) ATTITUDE
- EMPLOY INTERLOCKS OR OTHER SAFEGUARDS ON MANUAL VALVES TO ASSURE VALVES ARE IN FLIGHT POSITION PRIOR TO LIFT-OFF
- USE SEPARATE PRESSURANT SUPPLIES FOR FUEL AND OXIDIZER
- DESIGN FOR FAIL-SAFE, FAIL-SAFE REDUNDANCY OR BACK-UP CAPABILITY ON ALL ACTIVE COMPONENTS
- USE COMPOSITE (OVER WRAP) PRESSURANT TANKS TO ASSURE TANK FAILURE IS BY LEAKAGE RATHER THAN FRACTURE
- EMPLOY FLEXIBLE PROOF TEST FACTORS ON PRESSURE VESSELS, ADJUSTING FOR TANK MATERIAL, ENVIRONMENT, HOOP LOADS AND REQUIRED LIFE. PROOF TEST WITH LIQUID NITROGEN TO REDUCE REQUIRED PROOF PRESSURE LEVELS AND/OR TO VERIFY GREATER CYCLE LIFE FOR GIVEN DESIGN SAFETY FACTOR
- USE MATERIALS THAT ARE COMPATIBLE WITH PROPELLANTS AND RESIDUES FORMED BY PROPELLANT REACTION WITH THIRD AGENTS, I.E., H<sub>2</sub>O, CO<sub>2</sub>, SOLVENTS, ETC
- PROVIDE REPLACEABLE COMPONENT CARTRIDGES FOR HIGH FAILURE RATE ITEMS
- USE PLUG NOZZLE DESIGN OR BREAKABLE SEALS BETWEEN MONOPROPELLANT THRUSTER AND THRUSTER VALVES TO FACILITATE CATALYST REPLACEMENT

5-4

Figure 5-2

11-241

## SAFETY AND REUSE CRITERIA (Continued)

### (THERMAL CONTROL)

• THERMALLY CONTROL TO FOLLOWING TEMPERATURE CONSTRAINTS:

		(°F)	
N <sub>2</sub> H <sub>4</sub> THRUSTER	CATALYST	≥ 150	(CATALYST LIFE)
	INJECTOR	≤ 500	(DETONATION POTENTIAL)
	VALVE	≤ 200	(SEAT LIFE)
N <sub>2</sub> O <sub>4</sub> /MMH THRUSTER	INJECTOR	≥ 70	(IGNITION PRESSURE SPIKING)
	VALVE	≤ 200	(SEAT LIFE)
PROPELLANTS	N <sub>2</sub> H <sub>4</sub>	≥ 50	(FREEZING)
	N <sub>2</sub> O <sub>4</sub> /MMH	≥ 40	(IGNITION PRESSURE SPIKING/ N <sub>2</sub> O <sub>4</sub> FREEZING)

11-242

5-5

Figure 5-3



## SAFETY AND REUSE CRITERIA (Continued) (SERVICING)

- UTILIZE MOLECULAR SIEVES TO REMOVE SOLUBLE IRON FROM  $N_2O_4$  PROPELLANT DURING FILL OPERATIONS (MINIMIZE RHEOPEXY POTENTIAL)
- EMPLOY GRAVITY FILL PROCEDURES FOR PROPELLANT SERVICING
- AVOID BACKFILL THROUGH SCREEN SURFACE TENSION TANKS TO AVOID SCREEN LOADING IN UNSUPPORTED DIRECTION
- AVOID PROPELLANT TEMPERATURE CONDITIONING DURING FILL. VERIFY PROPELLANT LOAD BY COMPLETELY FILLING TANKS AND OFF-LOADING ULLAGE

11-282

5-6

Figure 5-4

## SAFETY AND REUSE CRITERIA (Continued)

### (SAFING AND MAINTENANCE)

- PERFORM POST-DEACTIVATION FLIGHT PURGE OF THRUSTER ASSEMBLIES
- DEPRESSURIZE SYSTEM FOR GROUND SERVICING AND/OR POD TRANSPORT
- INSERT THRUSTER THROAT SEALS AFTER LANDING
- MAINTAIN WET TANK AND CONTROL COMPONENTS TO MAXIMUM PRACTICAL EXTENT. WHEN NECESSARY, FLUSH SYSTEM WITH VAPORIZED SOLVENTS (FREON TF-NT0; ISOPROPANOL - MMH,  $N_2H_4$ ) FOLLOWED BY HOT  $GN_2$  PURGE. PULSATE FLOW OF GASIFIED SOLVENTS TO SCAVENGE PROPELLANT VAPORS).
- PROVIDE CLOSED-VENT SYSTEM FOR PROPELLANT DUMP
- AVOID AIR DRY OF EPT RUBBER EXPULSION BLADDERS

11-243 A

5-7

Figure 5-5

6. REFERENCES

- A. Kendall, A. S., McKee, H. B., and Orton, G. F., "Space Shuttle Low Pressure Auxiliary Propulsion Subsystem Definition - Subtask A Report", McDonnell Douglas Report No. MDC E0303, 29 January 1971.
- B. Green, W. M., and Patten, T. C., "Space Shuttle Low Pressure Auxiliary Propulsion Subsystem Definition - Subtask B Report", McDonnell Douglas Report No. MDC E0302, 29 January 1971.
- C. Anglim, D. D., Baumann, T. L., and Ebbesmeyer, L. H., "Space Shuttle High Pressure Auxiliary Propulsion Subsystem Definition Study - Subtask A Report", McDonnell Douglas Report No. MDC E0299, 12 February 1971.
- D. Gaines, R. D., Goldford, A. I., and Kaemming, T. A., "Space Shuttle High Pressure Auxiliary Propulsion Subsystem Definition Study - Subtask B Report", McDonnell Douglas Report No. MDC E0298, 12 February 1971.
- E. Kelly, P. J., "Space Shuttle Auxiliary Propulsion System Design Study - Executive Summary", McDonnell Douglas Report No. MDC E0674, 29 December 1972.
- F. Kelly, P. J., "Space Shuttle Auxiliary Propulsion System Design Study - Program Plan", McDonnell Douglas Report No. MDC E0436, 15 July 1971, revised 6 December 1971.
- G. Orton, G. F. and Schweickert, T. F., "Space Shuttle Auxiliary Propulsion System Design Study - Phase A Requirements Definition", McDonnell Douglas Report No. MDC E0603, 15 February 1972.
- H. Orton, G. F. and Schweickert, T. F., "Space Shuttle Auxiliary Propulsion System Design Study - Phase B Report, Candidate RCS Concept Comparisons", McDonnell Douglas Report No. MDC E0567, 15 February 1972.
- I. Bruns, A. E. and Regnier, W. W., "Space Shuttle Auxiliary Propulsion System Design Study - Phase C Report, Oxygen-Hydrogen RCS/OMS Integration Study", McDonnell Douglas Report No. MDC E0523, 15 June 1972.
- J. Baumann, T. L., Patten T. C., and McKee, H. B., "Space Shuttle Auxiliary Propulsion System Design Study - Phase D Report, Oxygen-Hydrogen Special RCS Studies", McDonnell Douglas Report No. MDC E0615, 15 June 1972.
- K. Smith, H. G., Williams, J. C., and Mattson, G. C., "Study to Determine an Improved Method for Apollo Propellant System Decontamination and Propellant Tank Drying", Dow Chemical Co. Report 4605-F, November 1966.

APPENDIX A

COMPONENT MODELS

Component weight and performance models were necessary to perform valid trade studies and to allow accurate system weight and performance comparisons. Models used for the preliminary analysis are discussed in Appendix B while the following paragraphs summarize the final component models for storable propellant systems.

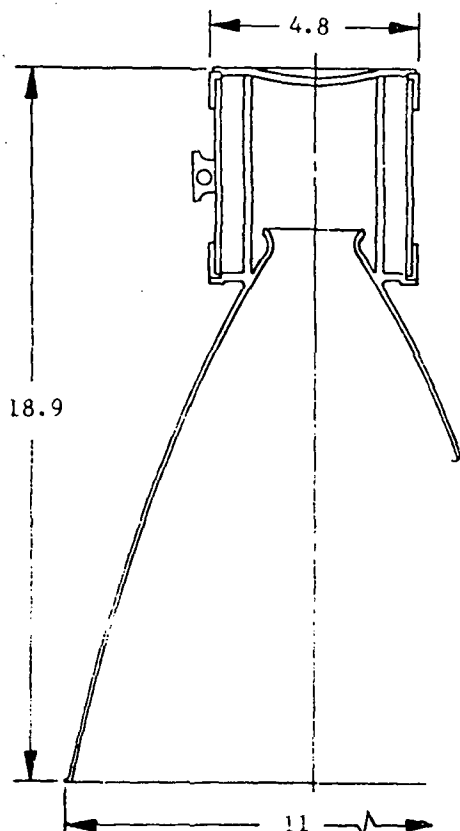
A1 Monopropellant Thruster - The analytical model for the monopropellant thruster was defined by the Aerojet Liquid Rocket Company (ALRC). The model incorporates a radial-inflow platelet injector, a modularized catalyst bed, and a submerged DeLaval thin-wall nozzle. A schematic drawing of the monopropellant thruster assembly with the associated pressure budget, performance, and weights is shown in Figure A-1. Design thrust is 600 lbf at a chamber pressure of 150 lbf-in.<sup>2</sup>. Parametric weight and performance data are presented as functions of thrust level, chamber pressure, and expansion ratio in Figures A-2 and A-3.

The injector, fabricated from 304L stainless steel, supplies fuel to the catalyst bed at low velocities. The Shell 405 catalyst granules are retained by two layers of screen and a cylindrical, perforated tube retainer. The entire replaceable catalyst cartridge is contained within a compartment which provides lateral and columnar support to the catalyst granules. All parts of the catalyst cartridge as well as the DeLaval nozzle are fabricated from Hastelloy B.

A2 Plug Nozzle Monopropellant Thruster - The weight and performance characteristics of a fully truncated plug nozzle monopropellant thruster were developed for use in systems analyses. Performance and envelope parameters, defined in Figure A-4, were based on data presented in Reference A-1. The design incorporates partial internal expansion, thereby permitting a somewhat higher area ratio in a fixed diameter envelope. The weight model was developed around a Rocket Research Corporation fixed point design at 400 lbf thrust, and is presented in Figure A-5. The motivating factor in the consideration of plug nozzle thrusters is the reduced reentry heating (compared to bell nozzle thrusters) due to the minimal plug nozzle exit gap. The superposition of nozzle exit gap on these curves illustrates how gap size decreases with increasing chamber pressure and overall nozzle expansion ratio.

600 LBF MONOPROPELLANT  
THRUSTER ASSEMBLY

E243-124-A



PRESSURES (PSIA)

266	VALVE INLET
250	INJECTOR INLET
190	UPSTREAM BED
150	CHAMBER

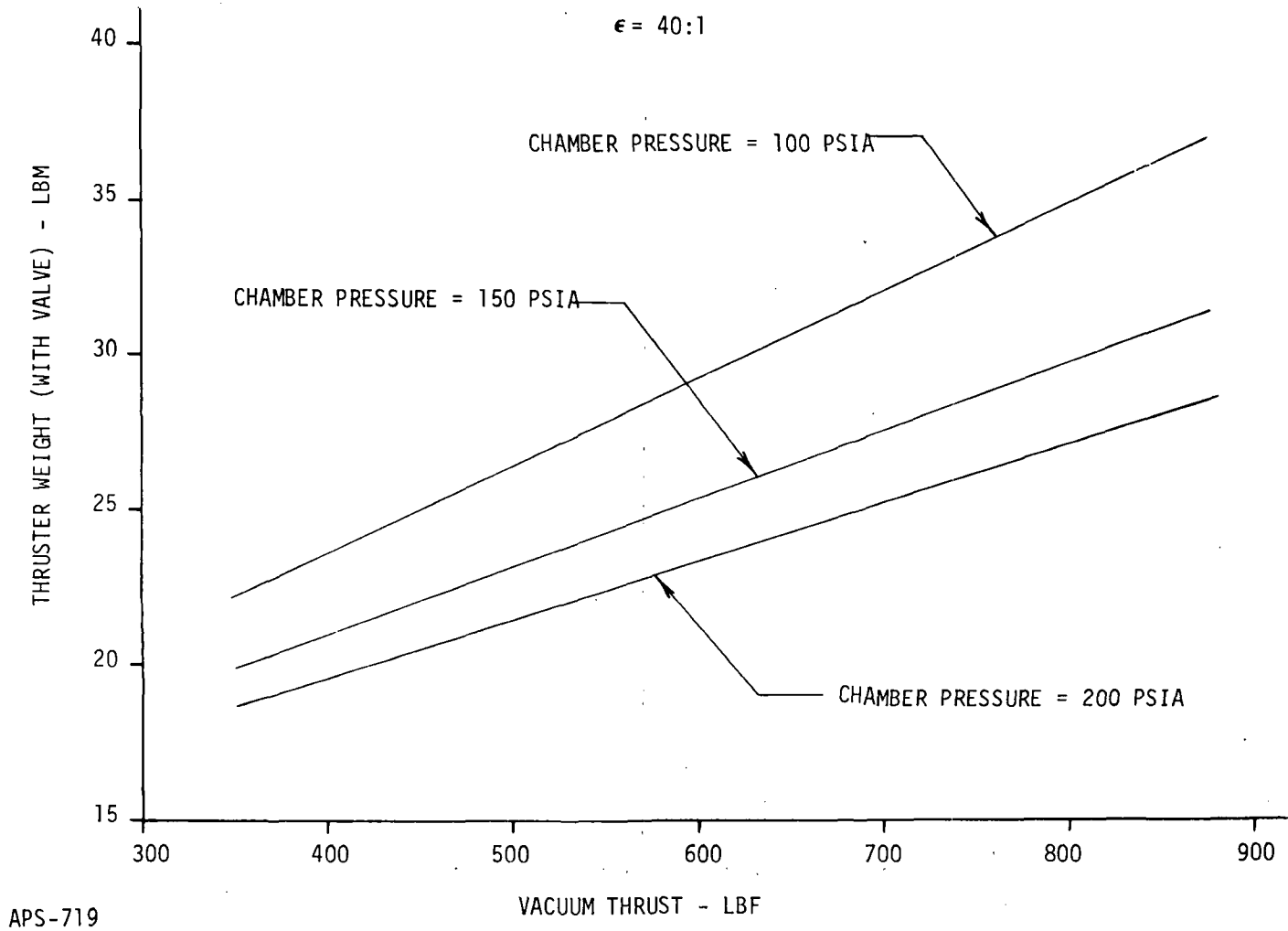
PERFORMANCE ( $\epsilon = 40:1$ )

239.7	SPECIFIC IMPULSE, SEC
1.78	THRUST COEFFICIENT
4250	CHARACTERISTIC VEL. FT/SEC

WEIGHT (LB)

18.8	INJECTOR, CHAMBER & NOZZLE
2.7	CATALYST
3.6	VALVE
<hr/> 25.1	TOTAL

# HYDRAZINE MONOPROPELLANT THRUSTER WEIGHT

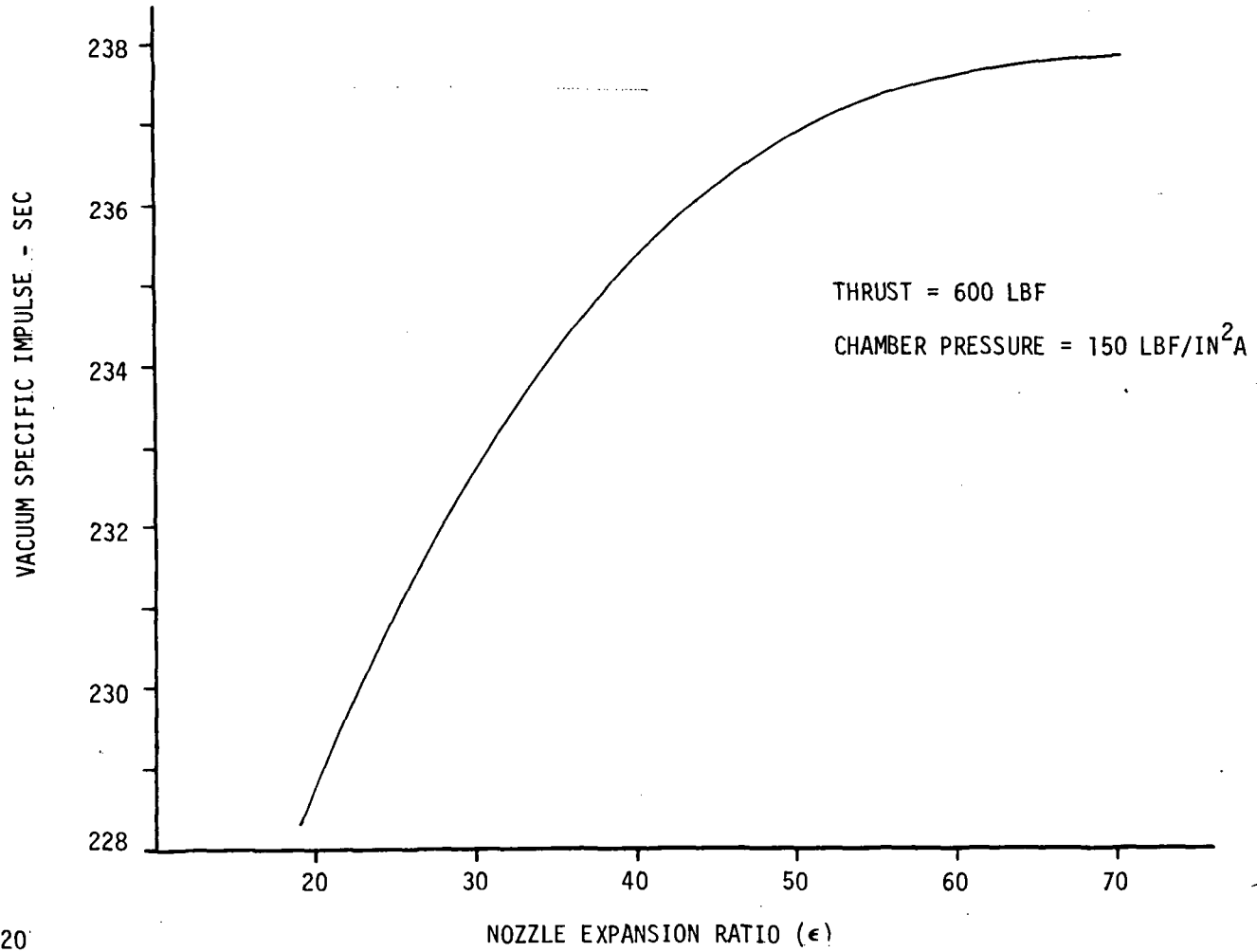


A-3

Figure A-2

APS-719

# HYDRAZINE MONOPROPELLANT THRUSTER SPECIFIC IMPULSE



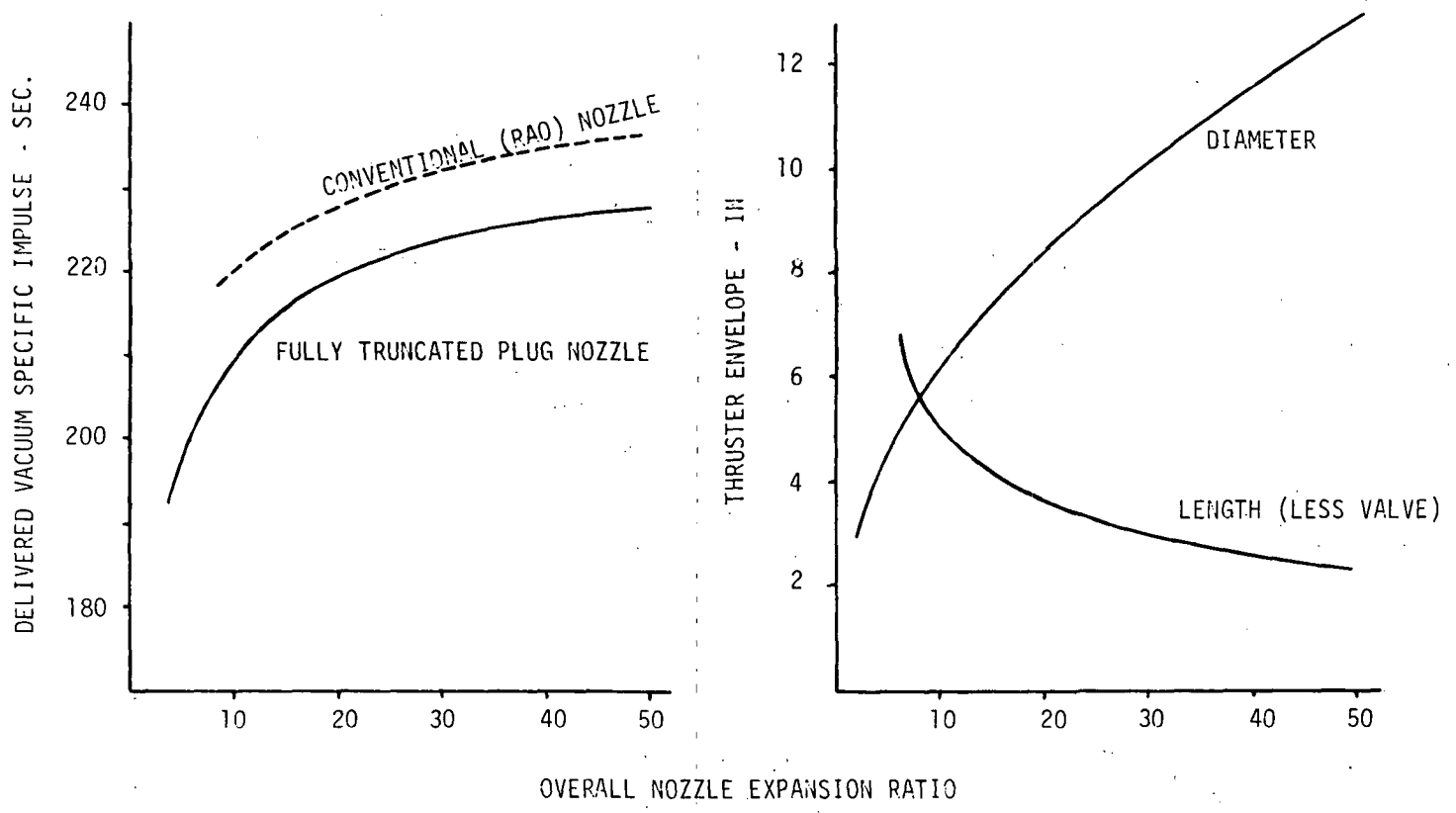
APS-720

A-4

Figure A-3

# PERFORMANCE AND ENVELOPE OF MONOPROPELLANT THRUSTER WITH TRUNCATED PLUG NOZZLE

F = 600 LBF  
P = 150 PSIA



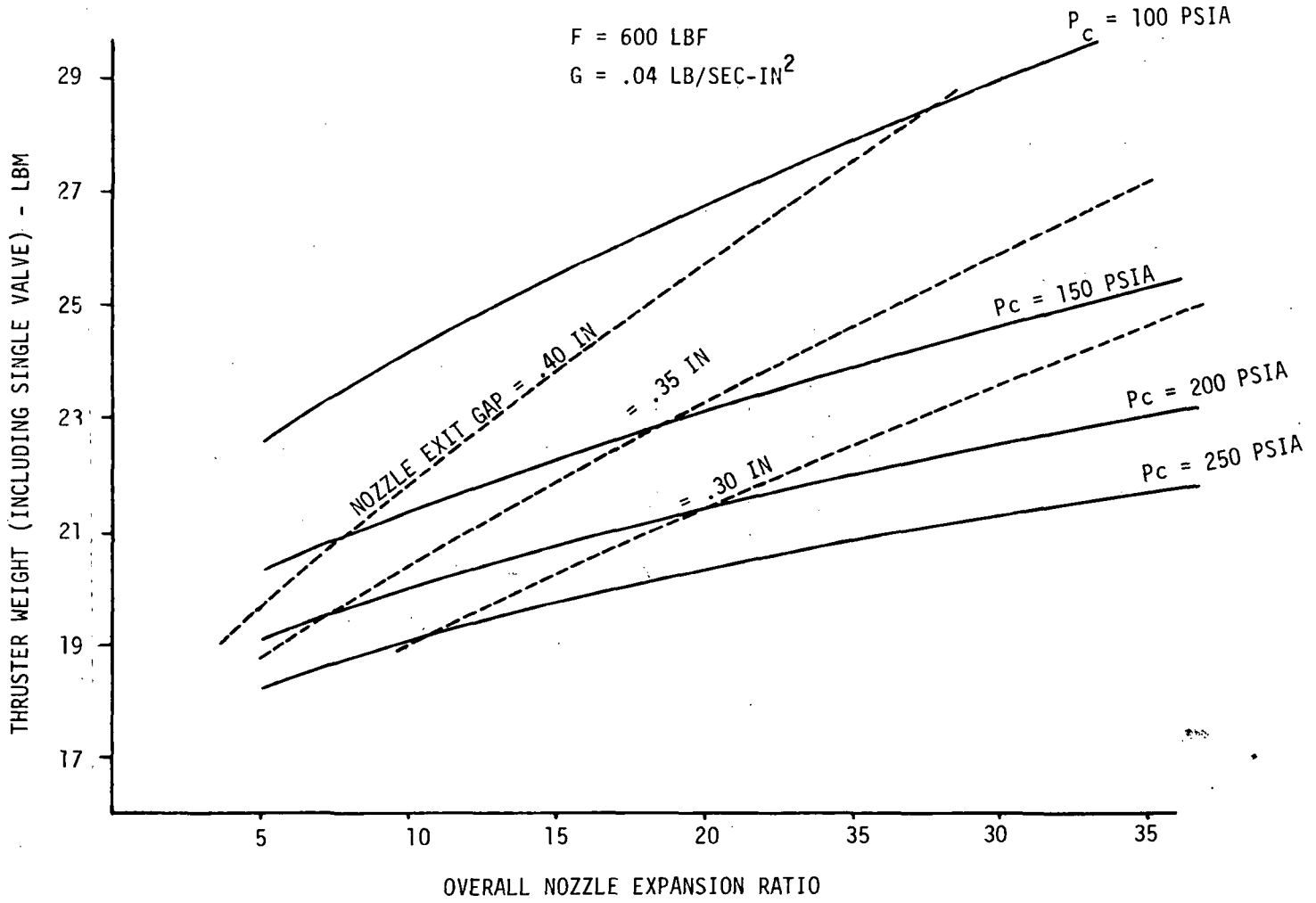
APS-294

A-5

Figure A-4



# WEIGHT OF MONOPROPELLANT THRUSTER WITH FULLY TRUNCATED PLUG NOZZLE



A-6

Figure A-5

APS-295

A3 Bipropellant Thruster - A fuel film cooled bipropellant thruster model was developed for the Phase C and E RCS study. Parametric weight, performance and envelope data were developed by the Aerojet Liquid Rocket Company under subcontract to MDAC-E. A thruster schematic, along with the performance, weight, envelope and pressure budget are presented in Figure A-6. The baseline thruster for these studies consists of a stainless steel parallel platelet injector and an integral thrust chamber and nozzle of silicide coated columbium. Figure A-7 presents thruster weight for thrust levels of 600 and 1000 lbf over a range of expansion ratios and chamber pressures, and Figure A-8 defines thruster performance sensitivities to chamber pressure, expansion ratio, and thrust level.

The following table delineates thruster performance losses for the design point.

BIPROPELLANT THRUSTER PERFORMANCE LOSSES	
F = 600 LBF	
$P_c = 200$ PSIA	
$\epsilon = 40:1$	
MR= 1.65	
THEORETICAL VACUUM SPECIFIC IMPULSE (SEC.)	329.8
CHEMICAL NON-EQUILIBRIUM LOSSES (SEC.)	-4.2
NON-AXIAL EXIT FLOW LOSSES (SEC.)	-5.0
BOUNDARY LAYER LOSSES (SEC.)	-6.2
FILM COOLANT LOSSES (SEC.)	-8.1
ENERGY RELEASE LOSSES (SEC.)	-10.2
DELIVERED SPECIFIC IMPULSE (SEC.)	296.1

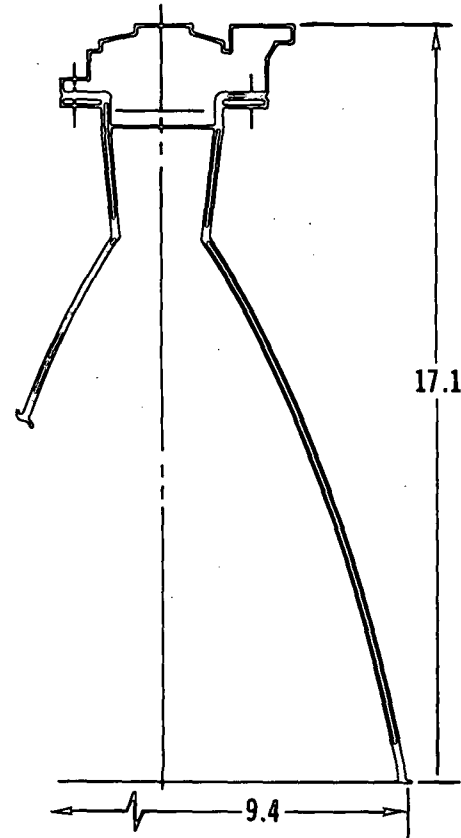
This data is based on a nominal wall temperature of 2200°F, and corresponds to 22% fuel film cooling. The effect of percent fuel film cooling on thruster core mixture ratio and maximum thruster wall temperature is presented in Figure A-9. As can be seen, performance can be improved by decreasing the film cooling losses. However, this results in an increase in wall temperature and therefore a decrease in service life. A 2200°F wall temperature corresponds to a 100 mission life for the RCS function; the primary life constraint is the number of thruster cold starts. For the -X (OMS) function, the relation between thruster wall temperature and thruster mission

# 600 LBF RCS THRUSTER ASSEMBLY

<u>PRESSURES (PSIA)</u>	
VALVE INLET	300
INJECTOR INLET	270
UPSTREAM BED	-
CHAMBER	200

<u>PERFORMANCE (<math>\epsilon = 40:1</math>)</u>	
SPECIFIC IMPULSE, SEC	296.1
THRUST COEFFICIENT	1.77
CHARACTERISTIC VELOCITY, FT/SEC	5390

<u>WEIGHT (LB)</u>	
INJECTOR	3.6
CHAMBER AND NOZZLE	3.5
VALVE	4.4
<b>TOTAL</b>	<b>11.5</b>

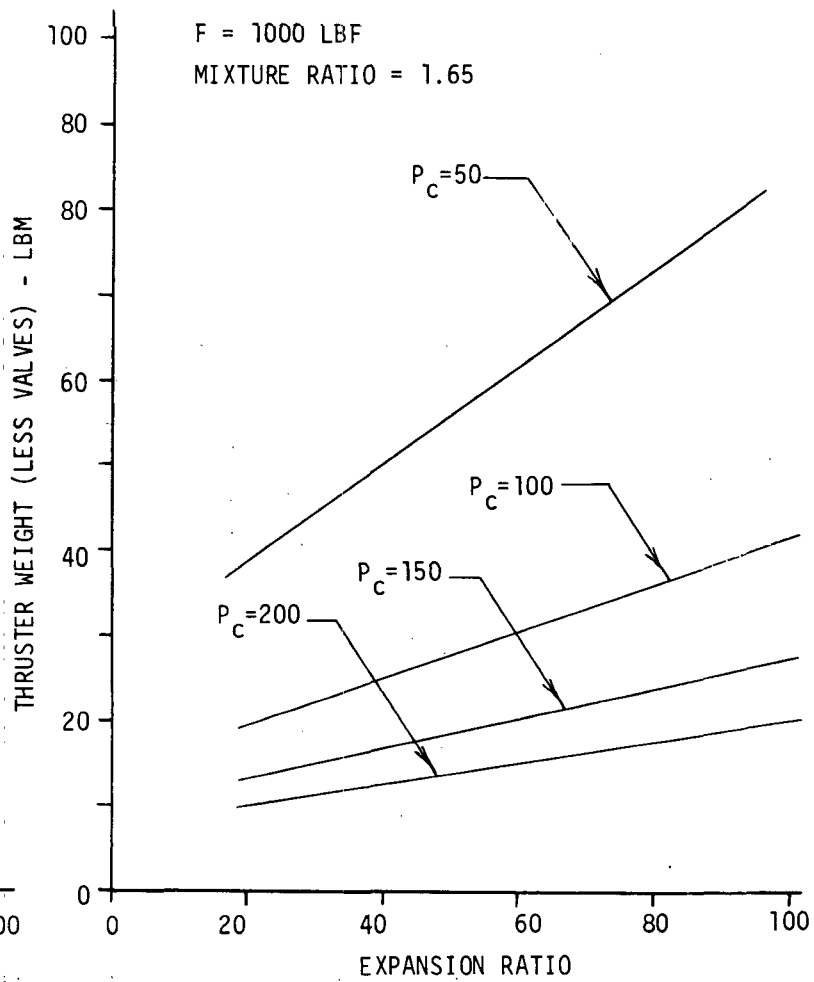
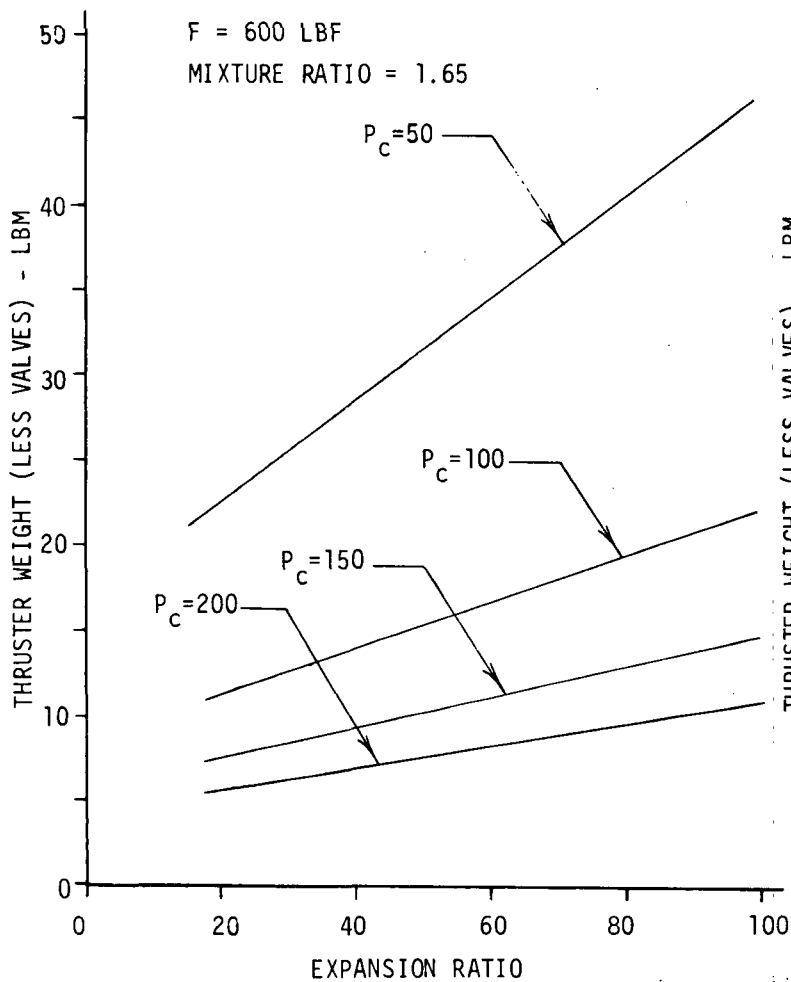


APS-858

A-8

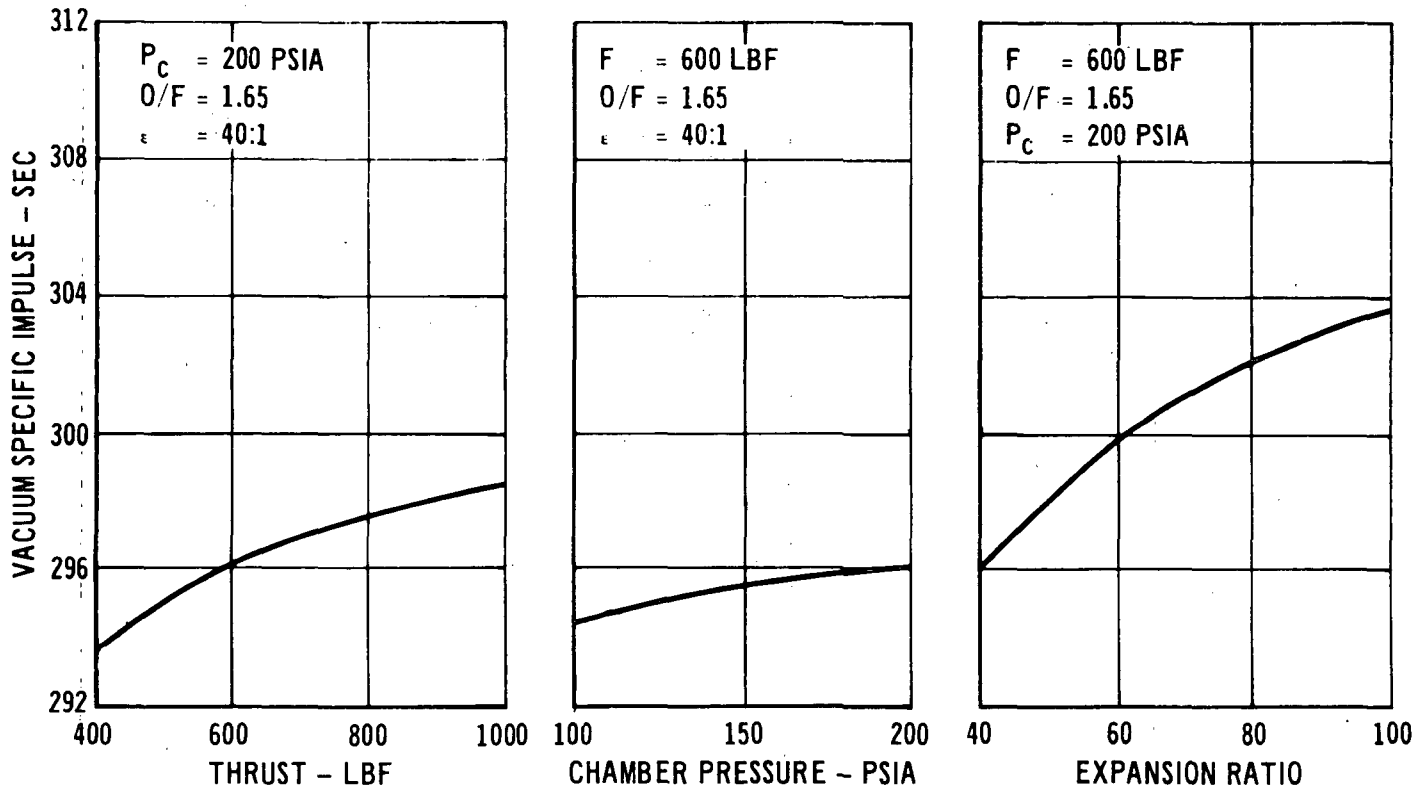
Figure A-6

# BIPROPELLANT THRUSTER WEIGHT CHARACTERISTICS (ALRC DATA)



APS-722

# BIPROPELLANT RCS THRUSTER PERFORMANCE



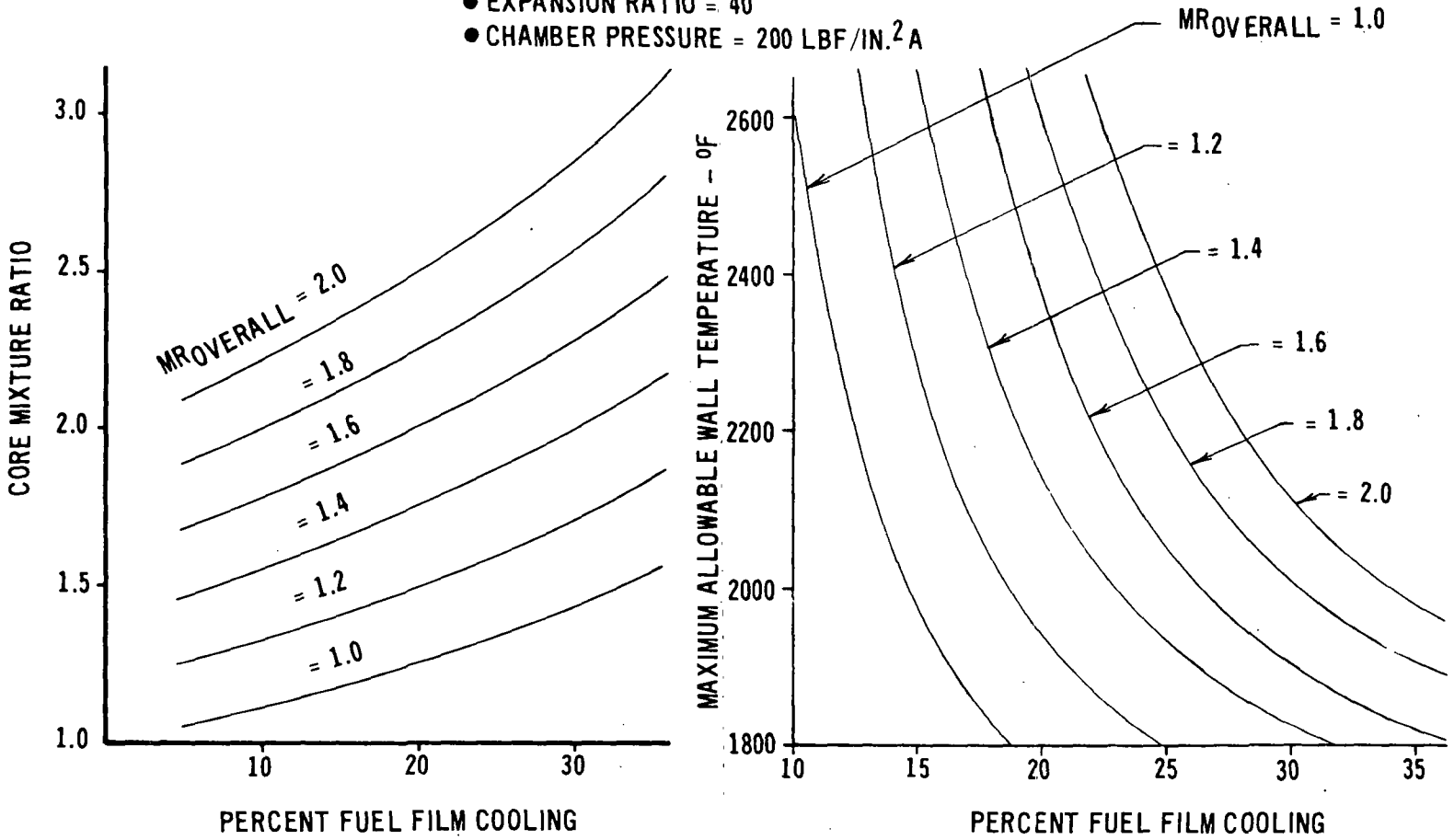
A-10

Figure A-8

APS-795

# FILM COOLING SENSITIVITIES

- THRUST = 600 LBF
- EXPANSION RATIO = 40
- CHAMBER PRESSURE = 200 LBF/IN.<sup>2</sup>A



life is shown in Figure A-10 for both the radiation can and insulated installation concepts. The variance in mission life between these concepts is due to differences in the temperature margins used for stress calculations. For the insulated thruster, a margin of 200°F is used, whereas the radiation-can reduces temperature nonuniformities and allows a margin of 110°F. Figure A-11 summarizes the relation between thruster performance and service life assuming a radiation-can installation. At the design value of 2200°F, a service life of 50 hours is predicted which is well in excess of the 100 mission life requirement.

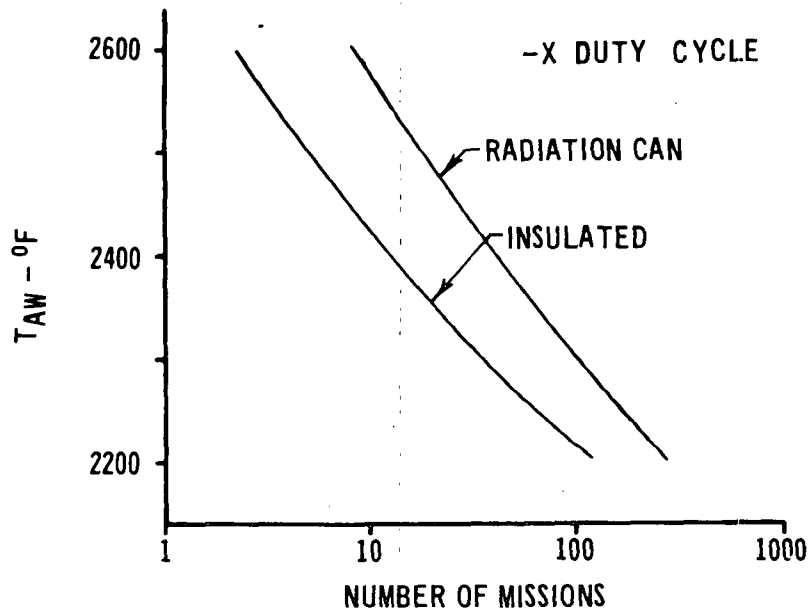
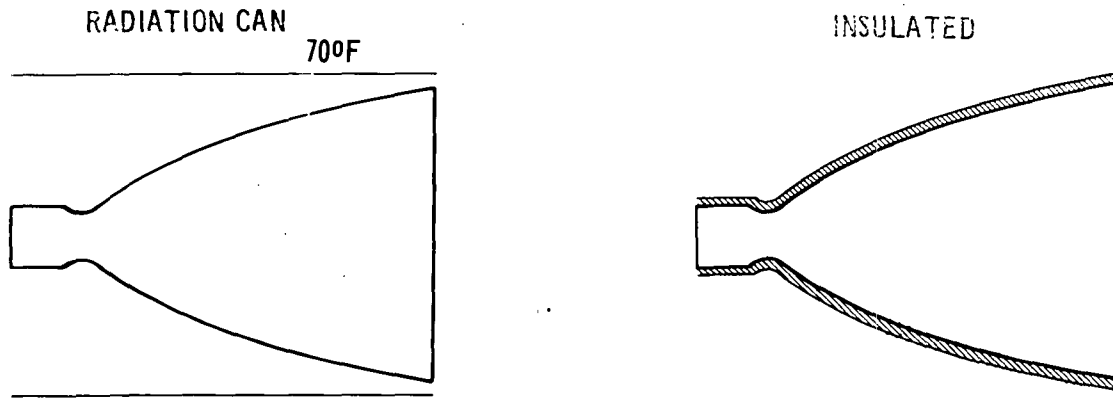
A4 Bipropellant OMS Engine - A parametric model was also developed by ALRC for a bipropellant OMS engine. The configuration of this engine and its design point are shown in Figure A-12. Regenerative cooling was selected for the OMS engine. OMS engine weight and performance characteristics are presented in Figure A-13.

A5 Propellant Valves - Empirical propellant valve weight models have been developed by MDAC-E from data obtained from numerous valve manufacturing companies. Both solenoid actuated engine valves and pneumatically actuated isolation valves have been modeled, and are presented in Figure A-14 for a range of line diameters and valve pressure drops. These weights are independent of the propellant used.

A6 Auxiliary Power Unit Components - The auxiliary power unit consists of a turbine, reactor, hydraulic pump, and alternator. Component weight and performance models for these components have been developed and are described below.

A6.1 APU Turbine - The APU incorporates a two stage, axial flow impulse turbine with pressure compounded staging for power generation. The analytical model is an adaptation of the one discussed in Reference H. The design speed is 70,000 RPM. Additional effort was directed toward the determination of the optimum operating temperature in the APU environment. Waspalloy and Udimet 700 were considered as candidate materials for the turbine disks as a result of their high strength properties at elevated temperatures. Temperature-strength properties for these materials are shown in Figure A-15. A constant-stress turbine disk was assumed, and typical strength margins applied to compute allowable pitch line blade speed as a function of turbine disk temperature. Turbine adiabatic wall temperatures were calculated, based on a temperature recovery

# CORRELATION BETWEEN THRUSTER INSTALLATION AND MISSION LIFE



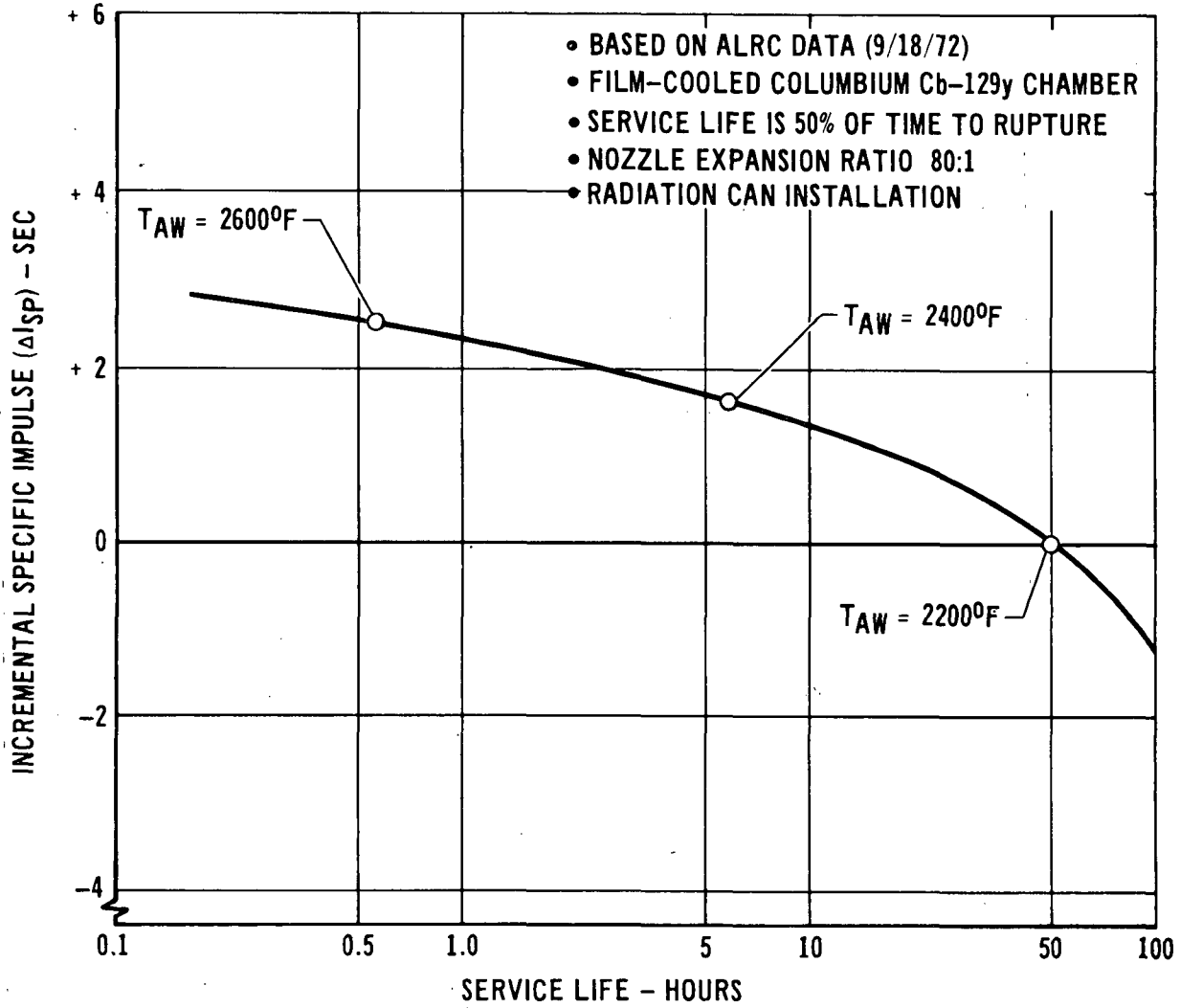
A-13

Figure A-10

APS-116



### THRUSTER PERFORMANCE VS SERVICE LIFE

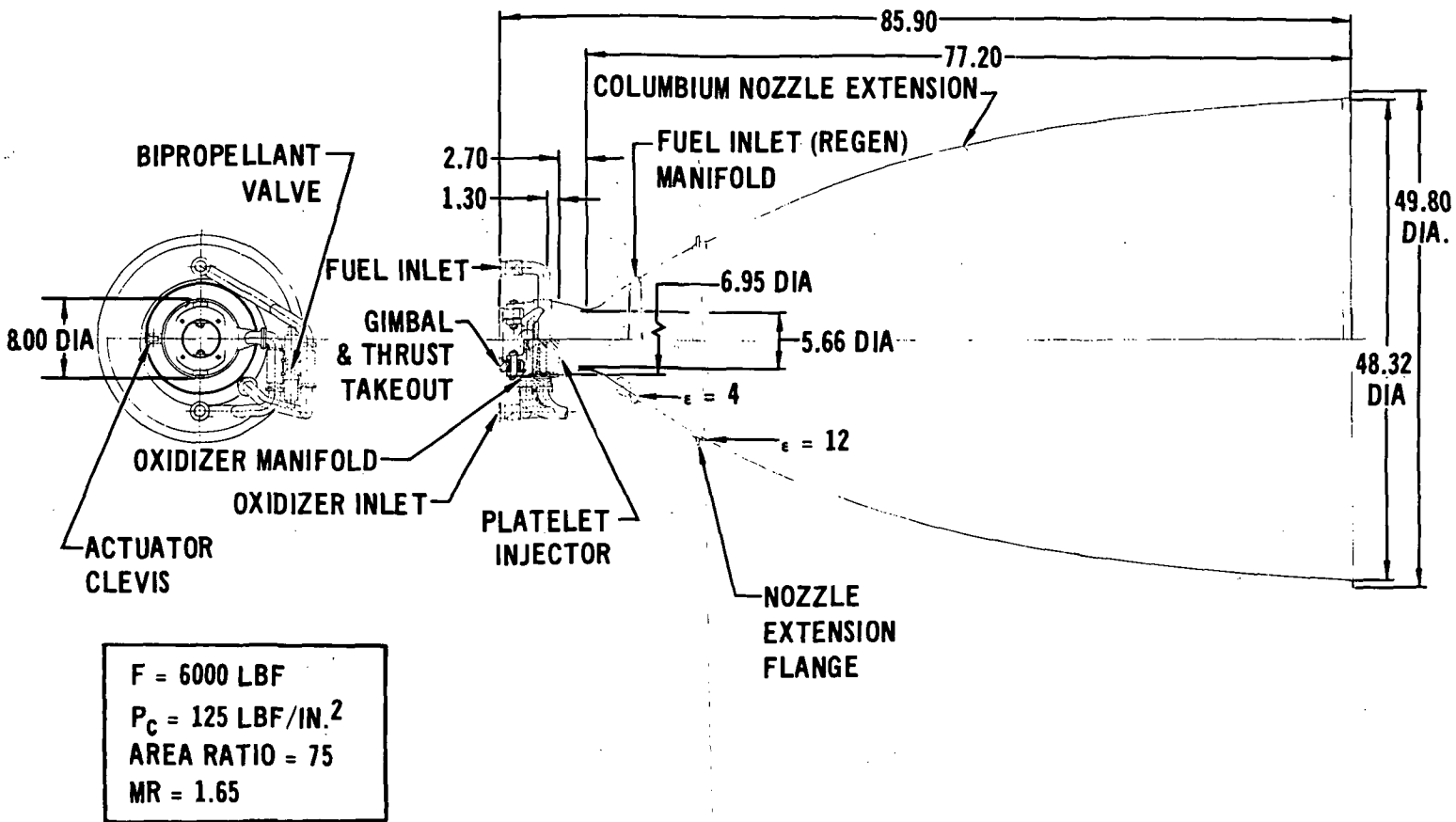


11-292 C

A-14

Figure A-11

# OMS BIROPELLANT ENGINE CONFIGURATION



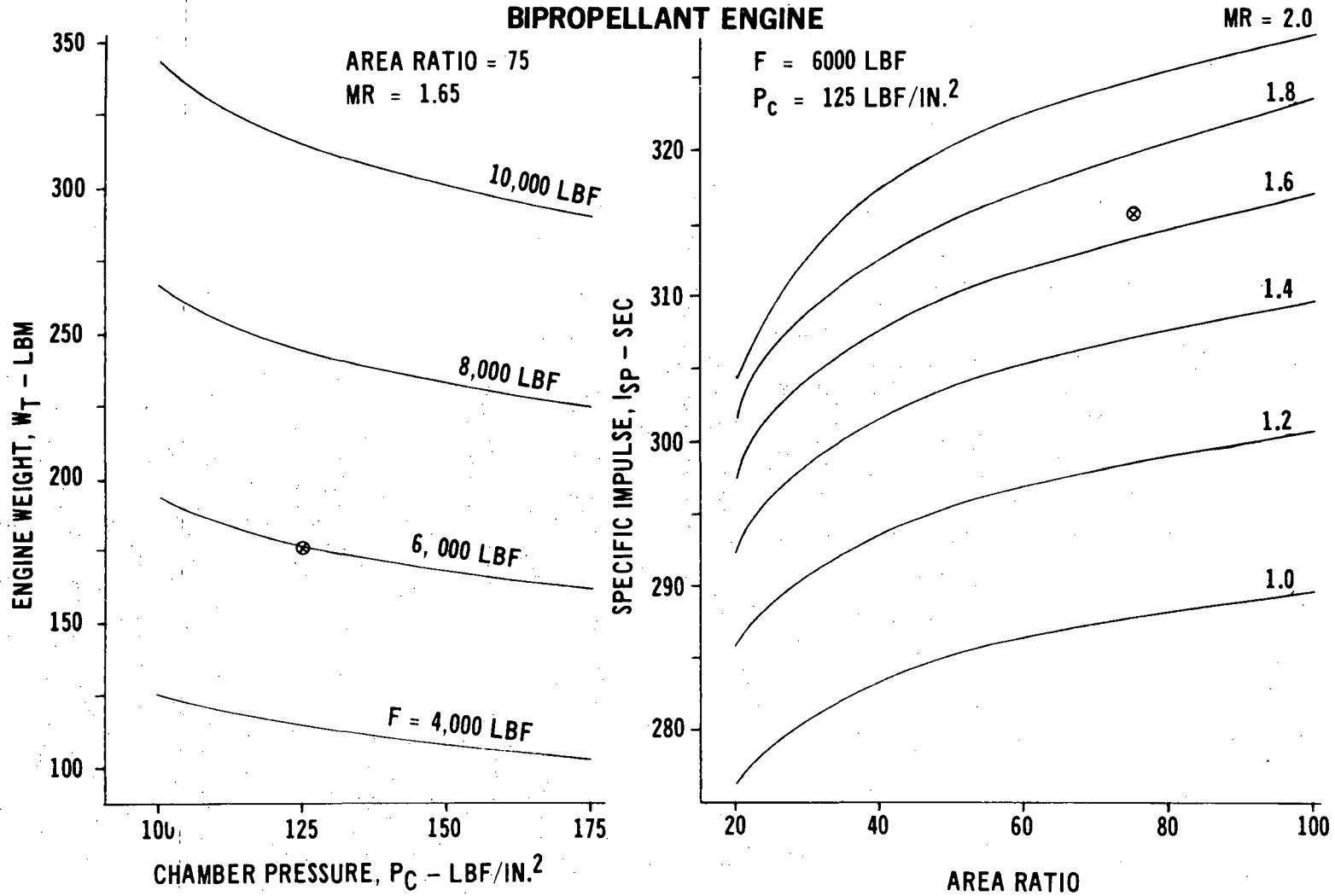
APS-104A

A-15

Figure A-12

# OMS ENGINE WEIGHT AND PERFORMANCE CHARACTERISTICS

## BIPROPELLANT ENGINE



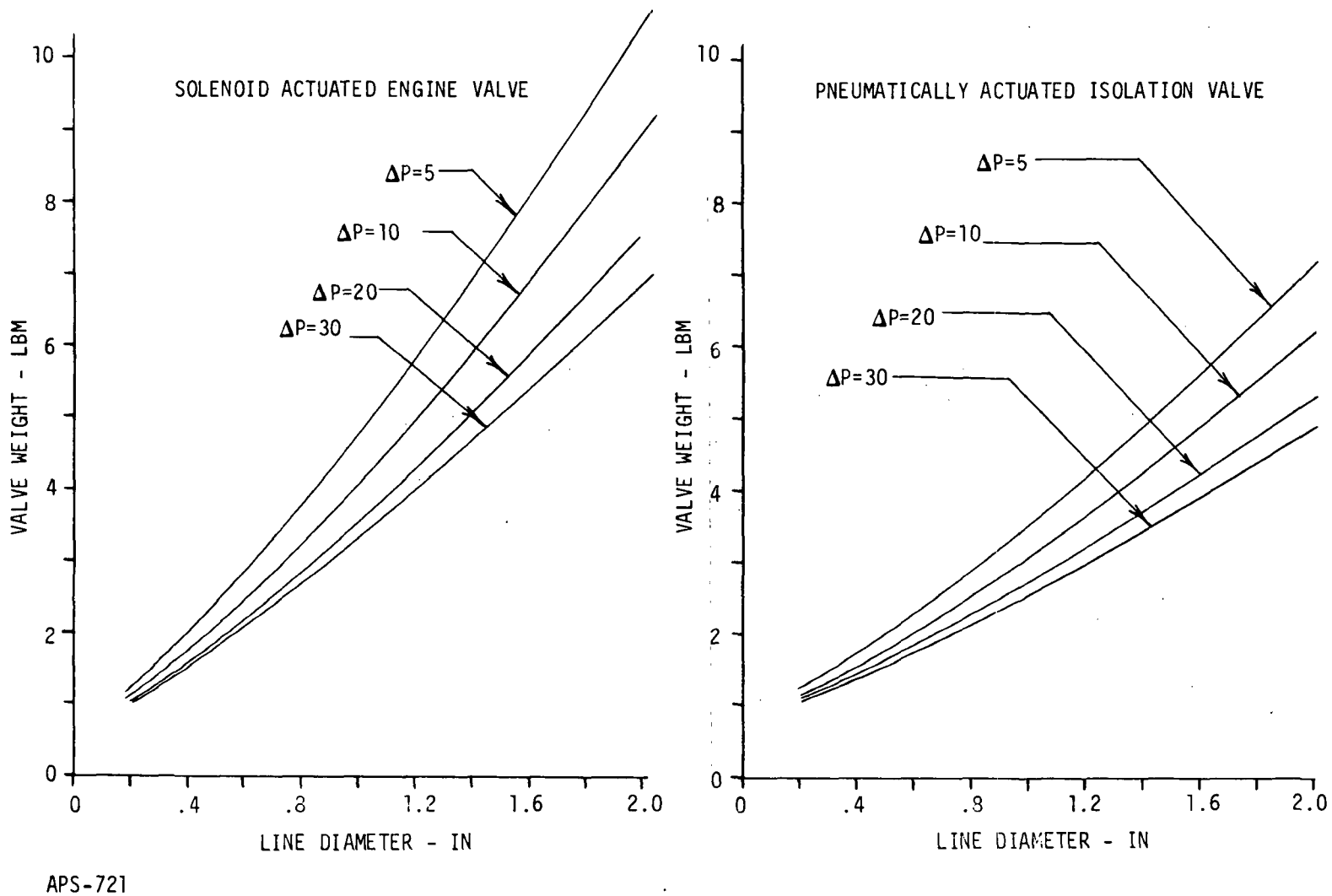
MCDONNELL DOUGLAS AERONAUTICS COMPANY - EAST

A-16

Figure A-13

APS-105A

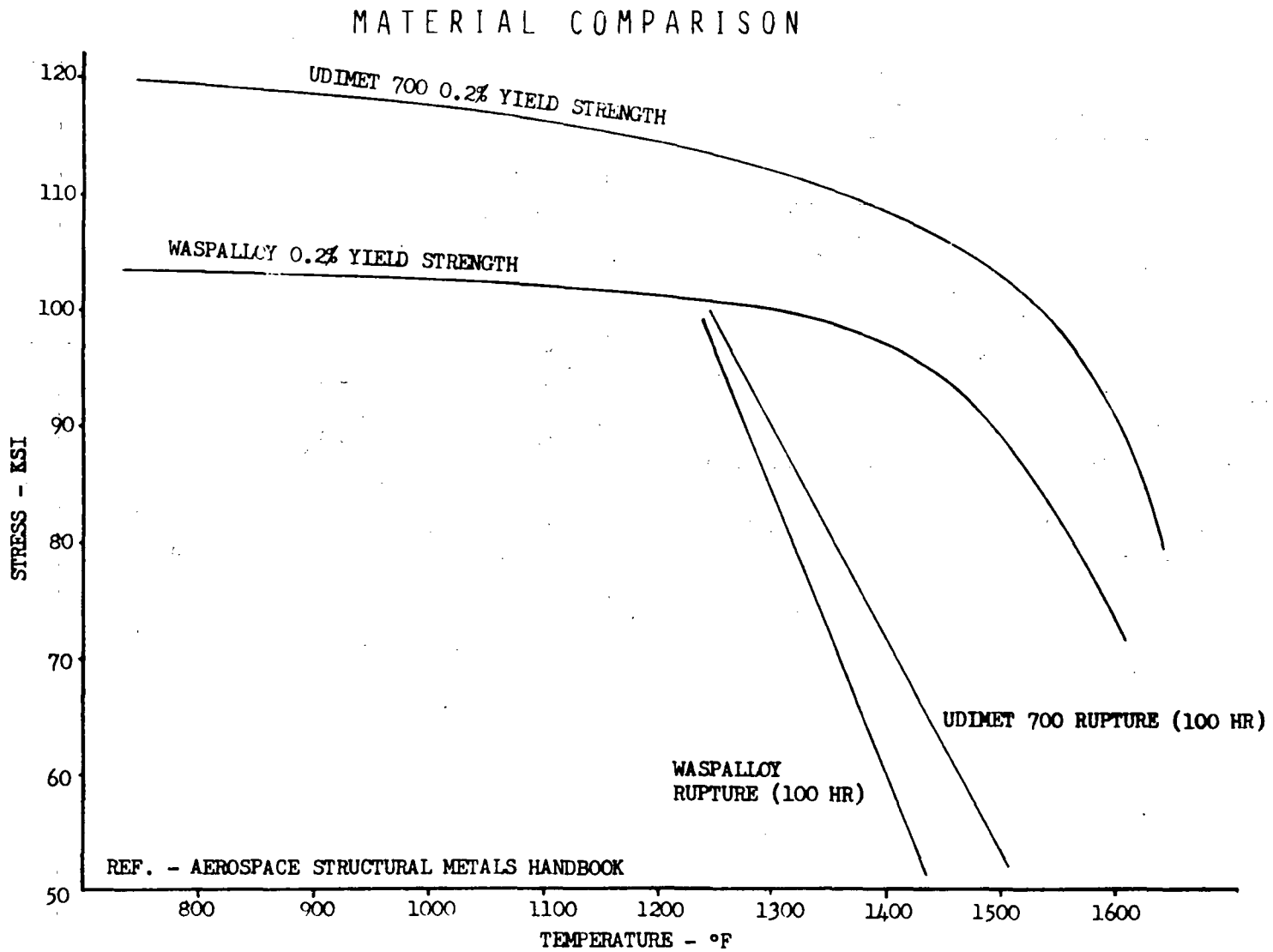
### PROPELLANT VALVE WEIGHT MODELS



A-17

Figure A-14

APS-721



MCDONNELL DOUGLAS AERONAUTICS COMPANY - EAST

A-18

Figure A-15

APS-784

factor of 0.85. The resultant relationship is shown in Figure A-16 for Udimet 700. The parameter of blade speed/nozzle velocity is commonly used to express the performance of a turbine stage, as shown in Figure A-17a. By replotting this curve (Figure A-17b) and then superimposing the blade velocity-temperature constraint of Figure A-17b, it can be seen that turbine efficiency must fall off sharply with increasing temperature. Thus, although ideal turbine output increases with increasing temperature (Figure A-17c), actual performance optimizes at approximately 1600°F. The pitch line velocity corresponding to this temperature is 1600 ft/sec, as shown in Figure A-16.

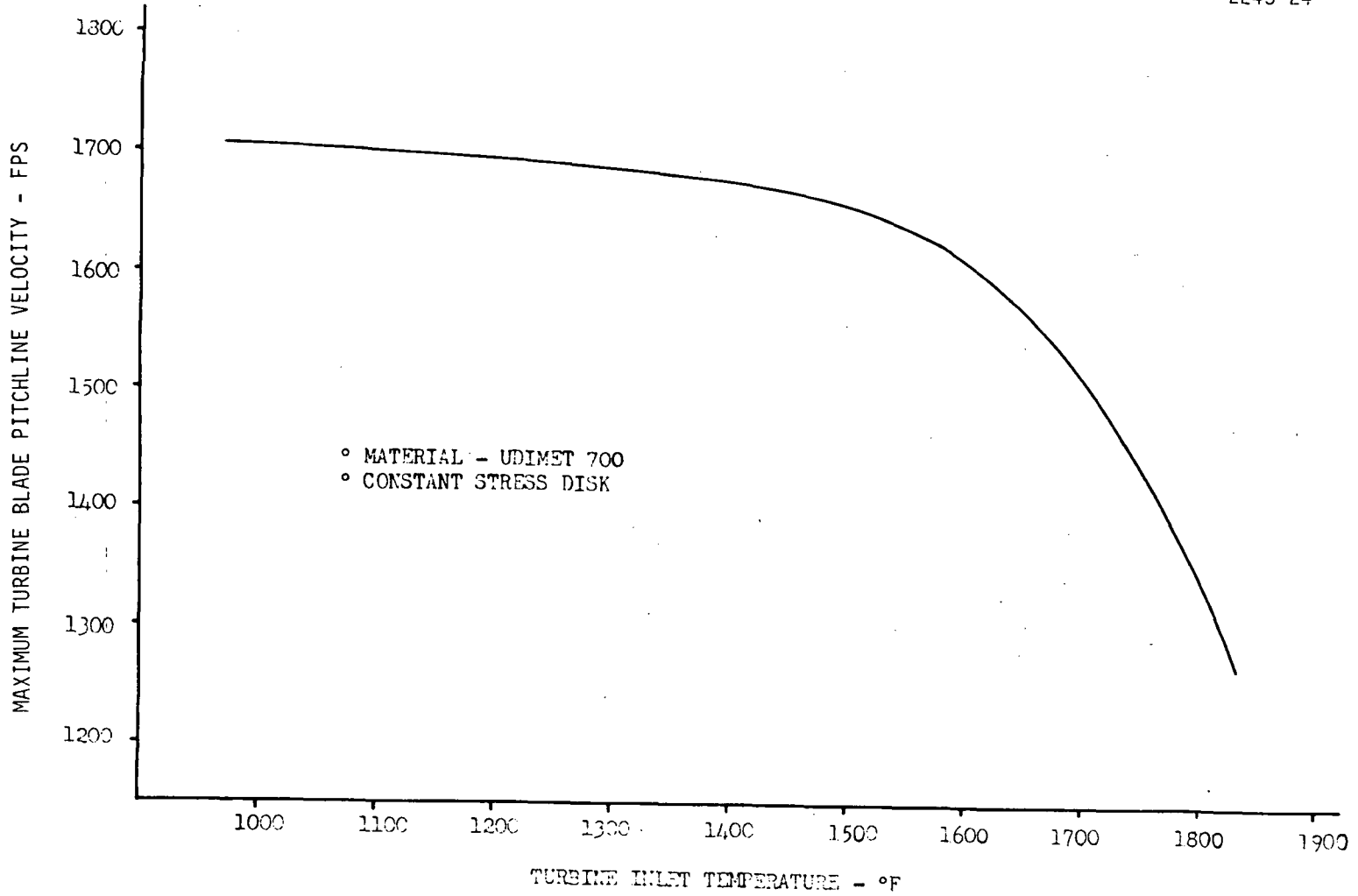
A6.2 APU Reactor - A thermal bed reactor was chosen for use with the APU in preference to a catalytic reactor for the following reasons:

1. Minimal maintenance requirements
2. Relative insensitivity of decomposition temperature to variations in turbine power level. Electrical power requirements have been defined to be 1000 watts corresponding to a start time of 15 minutes.

A6.3 APU Pump, Alternator and Power Transmission - Weight models for the APU components are lumped in the fixed weight summary presented in Figure A-18. The hydraulic pump is a variable displacement axial-piston pump. Design speed (6000 RPM), weight, and efficiency are based on existing aerospace hydraulic pumps. APU electrical power output is generated by a conduction cooled DC alternator driven by a hydraulic motor operating at a speed of 8000 RPM. Figure A-19 defines the component efficiencies used in this study.

E243-24

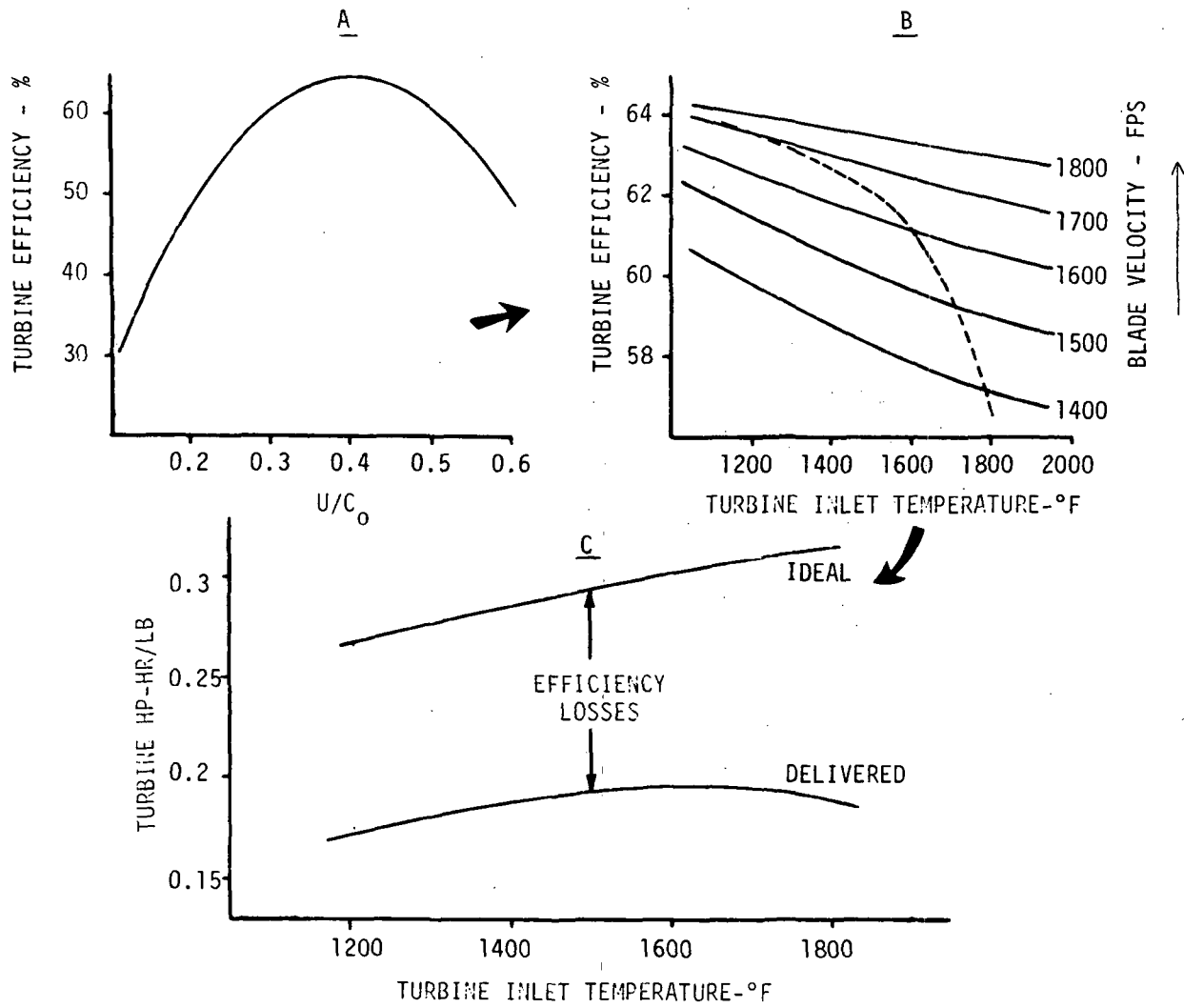
# TURBINE BLADE SPEED CONSTRAINT



A-20

Figure A-16

# TURBINE GAS TEMPERATURE-BLADE VELOCITY TRADE-OFF

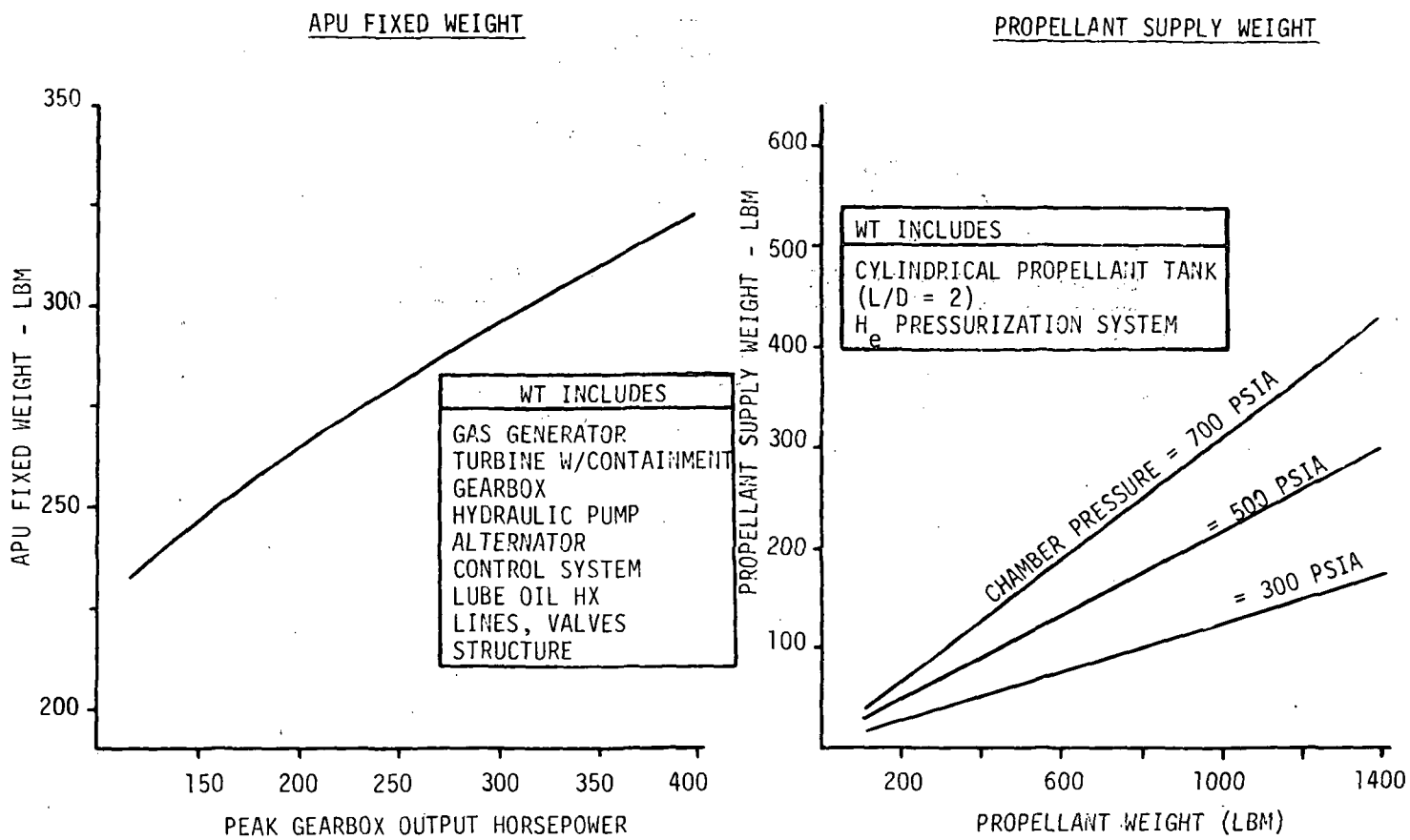


A-21

Figure A-17



APU WEIGHT DETERMINATION

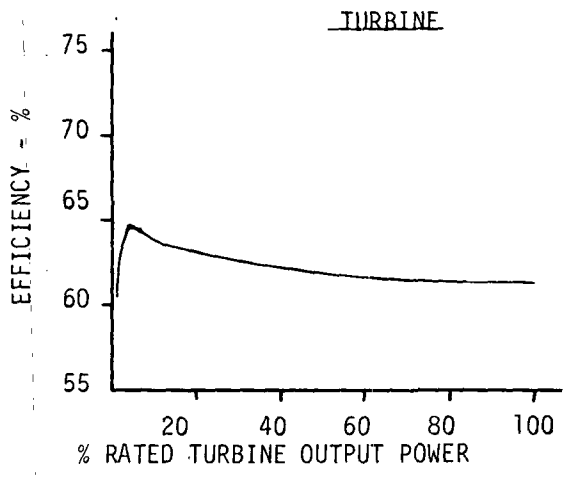
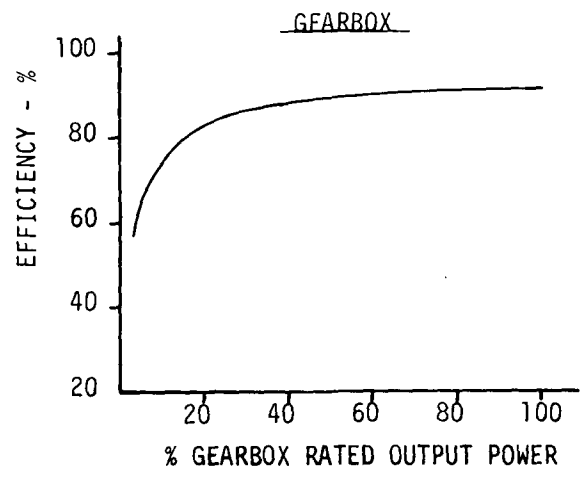
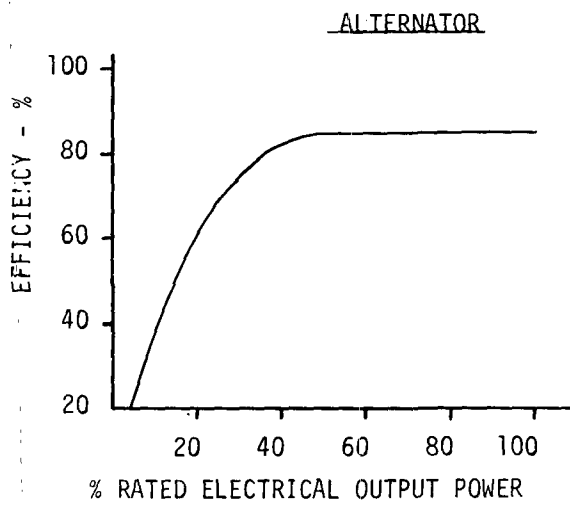
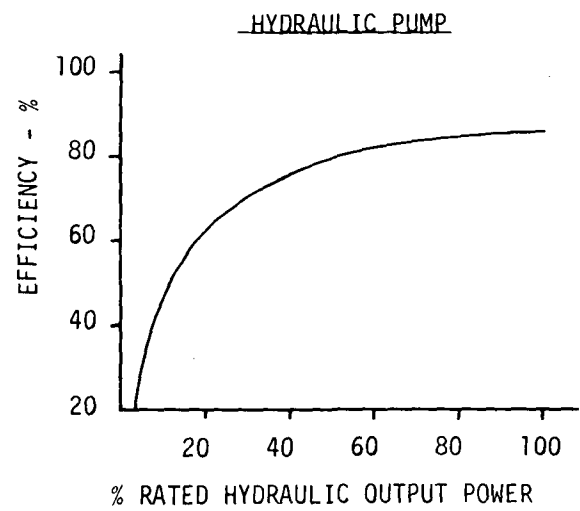


A-22

Figure A-18

E243-150

# APU COMPONENT EFFICIENCIES



A-23

Figure A-19

**REFERENCE**

- A-1 Wasko, R. A., "Performance of Annular Plug and Expansion-Deflection Nozzles Including External Flow Effects at Transonic Mach Numbers", NASA TND-4462, April 1968.

APPENDIX B  
PRELIMINARY SYSTEM ANALYSIS

The Phase C storable propellant system design points reported in Section 4.1 were based on the system design and analyses reported in this appendix. Identified are those studies and trades performed to obtain RCS/OMS/APU system weights as a function of the principal design parameters including expansion ratio, chamber pressure, and mixture ratio. Concepts considered included various levels of RCS/OMS/APU integration. Both modular concepts, and concepts installed integrally within the vehicle were evaluated. Propellant candidates were monopropellant hydrazine and hypergolic bipropellants (NTO/MMH). The preliminary system analysis was performed for two vehicle sizes; a minimum technology orbiter (MSC-040A) and a higher performance orbiter (Mark II).

This appendix documents, for the preliminary RCS/OMS/APU concepts, the requirements, system descriptions and schematics, component performance and weight models, and system analysis. Those requirements and component models which differ from the final requirements (Section 3) and the final component models (Appendix A) are discussed herein.

The analyses was performed using a Modular Storable Propulsion Sizing computer program (MSP). This program provides a computerized capability for calculating weight, geometry, and performance of a space vehicle stage using storable propellants. The components to be sized are assembled from a library of analytical models provided in the program. Program inputs permit definition of system and component operating requirements as well as component hardware descriptions.

B1 Preliminary Requirements - The system requirements and vehicle interface criteria used in the preliminary earth storable system analysis are defined herein for the RCS and OMS as well as the APU. The NAS 9-12013 APS study originally considered only fully reusable hydrogen/oxygen propulsion systems. However, due to the high development costs associated with a fully reusable vehicle, alternate, partially reusable, vehicle designs evolved resulting in reduced system requirements. Consequently, the APS study was expanded to include earth storable propellants and APU concepts. The requirements for the earth storable propellant studies are summarized and compared to the original cryogenic propellant requirements in Figure B-1. A complete

description of the original requirements as used in the Phase B, C (oxygen/hydrogen), and D studies may be found in Reference G.

B1.1 RCS and OMS Requirements - The orbiter vehicles considered in this study differed from the fully reusable vehicles in that they contain no main engine (boost) inboard tankage. Instead, the main engine tanks are attached to the underside of the vehicle and are jettisoned after orbit insertion. The general orbiter configuration is shown in Figure B-2. Two versions of this configuration were used in the preliminary system analysis; a minimum technology orbiter (MSC-040A) and a higher performance orbiter (Mark II). Overall size and general equipment arrangement were common to both configurations but they differed in weight and inertia. The orbiter mass properties are presented in Figure B-3.

Three baseline missions are defined for the study program: (1) an easterly launch mission, intended for delivering and retrieving payloads in a 100 nmi circular orbit, (2) a south polar mission consisting of launching the orbiter into an injection orbit of 50 x 100 nmi and circularizing at apogee utilizing the OMS, and (3) a resupply mission intended to provide logistic support for a space station/space base in a 270 nmi orbit. The easterly launch mission was designated as the design mission while the south polar and resupply missions were designated reference missions.

The on-orbit translational maneuver requirements were defined by NASA to consist of a total-X axis velocity increment ( $\Delta V$ ) of 1000 ft/sec and a multiaxis  $\Delta V$  of 130 ft/sec. Additionally, with add-on propellant tankage mounted in the payload bay, increases of 1000 ft/sec (-X) were a design requirement. The basic propulsion and power requirements are delineated in Figures B-4 and B-5. In summary, the RCS must provide on-orbit angular accelerations of 0.5 - 0.8 deg/sec<sup>2</sup>, on-orbit translation accelerations of 0.2 - 0.4 ft/sec<sup>2</sup>, and reentry bank accelerations of 1.5 deg/sec<sup>2</sup>; while the OMS must provide the 1000 ft/sec, -X axis, velocity increment. The OMS translational acceleration requirement is 0.6 ft/sec<sup>2</sup> which dictates the OMS minimum thrust level.

B1.2 APU Requirements - The APU hydraulic and electrical power profiles were defined for the easterly launch, design mission, based upon the mission timeline and anticipated aerodynamic loading. These power profiles are tabulated in Figure B-6 for the ascent and descent mission phases. The total duration of the various operations within each phase is also presented. No attempt was made to define the actual sequence of operations. The projected

REVISED REQUIREMENTS FOR  
EARTH STORABLE PROPELLANT STUDIES

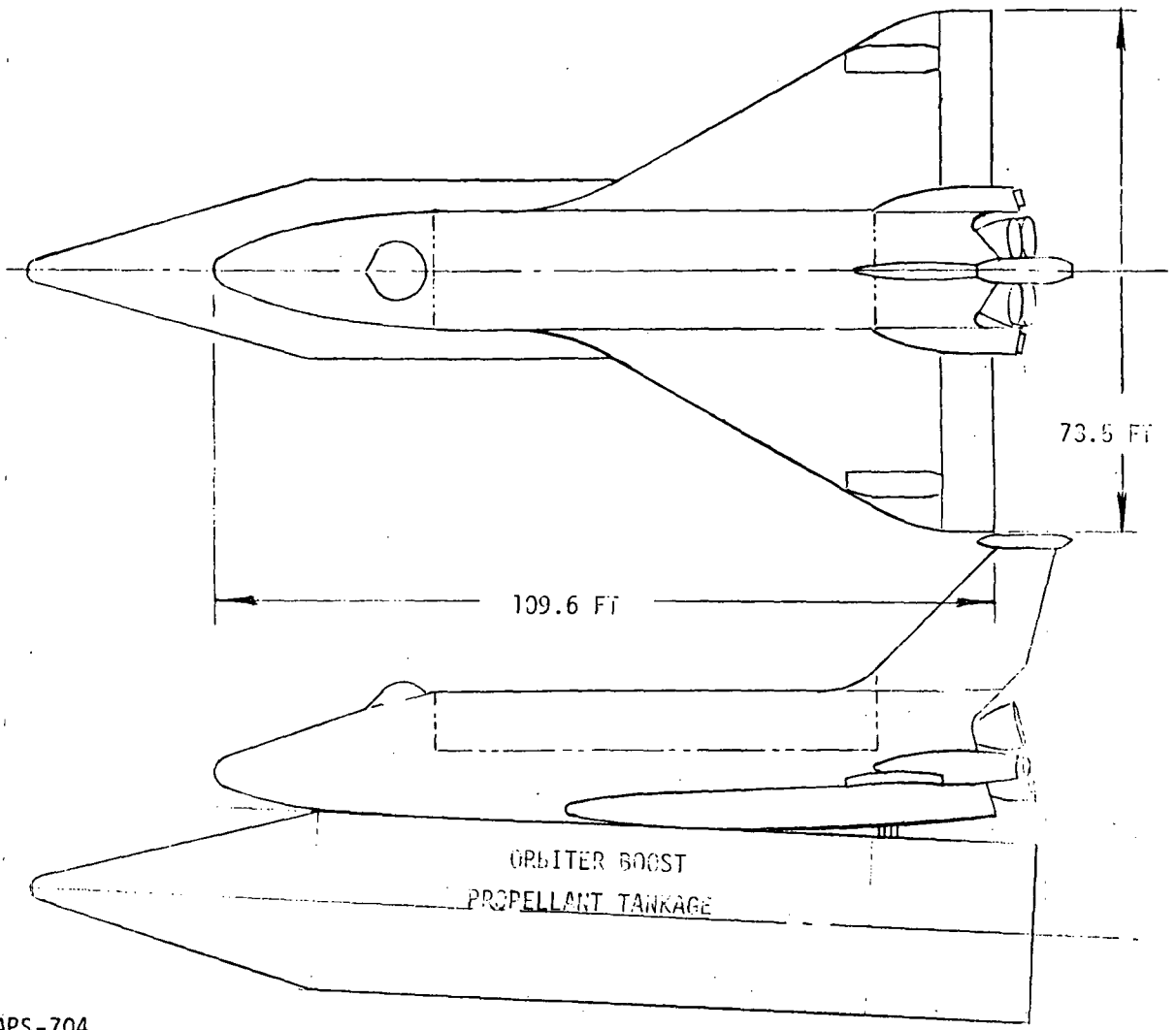
	<u>O<sub>2</sub>/H<sub>2</sub> STUDIES</u>	<u>EARTH STORABLE STUDIES</u>
<u>VEHICLE</u>	FULLY REUSABLE	PARTIALLY REUSABLE (EXPEND- ABLE BOOST PROPELLANT TANKS)
<u>SYSTEM STUDIES</u>	RCS AND OMS	RCS, OMS, AND APU
<u>REDUNDANCY CRITERIA</u>	FAIL-OPERATIONAL, FAIL-SAFE	FAIL-SAFE, FAIL-SAFE
<u>SYSTEMS OPERATION</u>		
- OMS	ASCENT ABORT; ON-ORBIT $\Delta V$ TANKAGE FOR 2000 FT/SEC	ON-ORBIT $\Delta V$ TANKAGE FOR 1000 FT/SEC (ADD-ON TANKS IN P/L BAY)
- RCS	3 AXIS ATTITUDE CONTROL; VERNIER $\Delta V$ (130 FT/SEC)	3 AXIS ATTITUDE CONTROL; VERNIER $\Delta V$ (130 FT/SEC)
- APU	NO STUDY REQUIREMENT	ASCENT AND REENTRY HYDRAULIC/ELECTRICAL POWER (56 HP-HR)

B-3

Figure B-1

APS-286

GENERAL ORBITER CONFIGURATION



APS-704

B-4

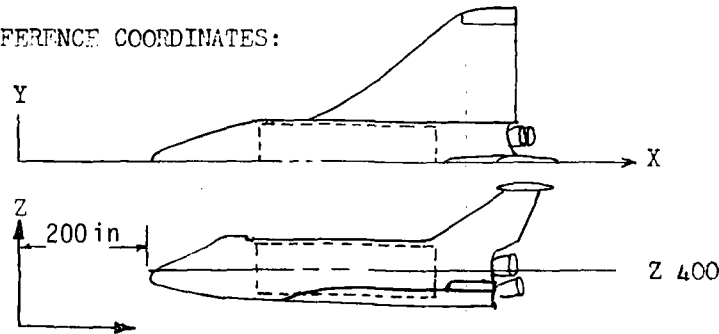
Figure B-2

E243-49

VEHICLE MASS PROPERTIES

	MSC-040A			MARK II		
WEIGHT (LB)						
- INSERTION	156,800			230,800		
- ON ORBIT	155,400			226,000		
- RETRO	144,750			194,000		
- REENTRY	141,150			178,100		
	X	Y	Z	X	Y	Z
CENTER OF GRAVITY (IN) <sup>(1)</sup>						
- INSERTION	1080	0	362	1105	0	375
- ON ORBIT	1078	0	362	1098	0	375
- RETRO	1069	0	360	1090	0	375
- REENTRY	1051	0	360	1067	0	375
	PITCH	YAW	ROLL	PITCH	YAW	ROLL
INERTIA (SLUG - FT <sup>2</sup> x 10 <sup>3</sup> )						
- INSERTION	4650	4540	566	6015	6134	1021
- ON ORBIT	4630	4500	565	5965	6354	1018
- RETRO	4340	4200	560	5451	5716	832
- REENTRY	4190	4050	560	5113	5313	828

(1) REFERENCE COORDINATES:





E243-47

PROPULSION/POWER REQUIREMENTS

ORBIT MANEUVERING SYSTEM

TRANSLATIONAL  $\Delta V$  (6 BURNS) 1000 FT/SEC

REACTION CONTROL SYSTEM

ON-ORBIT MANEUVERS 130 FT/SEC

ATTITUDE MANEUVERS (0.5 DEG/SEC RATE) 17 MAN./AXIS

LIMIT CYCLE 4 HRS @  $\pm 0.5$  DEG  
6 DAYS 15 HRS @  $\pm 5$  DEG

RCS DISTURBANCE (CROSS-COUPLING)  $CD^{(1)}$

RE-ENTRY - YAW  $11.56 \times 10^6$  ft-lb-sec

ROLL  $0.80 \times 10^6$  ft-lb-sec

PITCH  $1.59 \times 10^6$  ft-lb-sec

AUXILIARY POWER UNIT

HYDRAULIC (230 HP) 45.4 HP-HR

ELECTRICAL (15 KW) 10.9 HP-HR

(1) CONFIGURATION DEPENDENT

E243-48 B

ORBITER ACCELERATION REQUIREMENTS

MISSION PHASE		ON-ORBIT			RE-ENTRY		
		-X (FWD)	+X (AFT)	+Y, Z (UP/DOWN/LATERAL)	-X (FWD)	+X (AFT)	+Y, Z (UP/DOWN/LATERAL)
TRANSLATION ACCELERATION  FT/SEC <sup>2</sup>	DESIGN	0.4	0.2	0.2	N/R*		
	SAFE	0.2	0.1	0.1			
ANGULAR ACCELERATION  DEG/SEC <sup>2</sup>	DESIGN	PITCH	YAW	ROLL	PITCH	YAW	ROLL
		0.8	0.8	0.8	0.8	1.5	1.2
	SAFE	0.5	0.5	0.5	0.5	1.0	0.8

\* NO REQUIREMENT

## ORBITER APU POWER PROFILE

<u>MISSION PHASE</u>	<u>VEHICLE HYDRAULIC POWER REQUIREMENTS (HP)</u>	<u>VEHICLE ELECTRIC POWER REQUIREMENTS (HP)</u>	<u>DURATION (SEC)</u>	<u>AVERAGE BACK PRESSURE (PSIA)</u>
PRE-LAUNCH				
MISC. CHECKOUT	48	42	30	17
ELEVON	216	42	10	17
RUDDER	54	42	10	17
SPEED BRAKE	74	42	10	17
LANDING GEAR	74	42	10	17
GROUND IDLE	20	42	110	17
BOOST & COAST				
IDLE	20	42	45	13
IDLE	20	42	35	7.5
IDLE	20	42	52	3.5
IDLE	20	42	88	2.0
INSERTION				
TVC	84	20	78	2.0
TVC	62	20	112	2.0
IDLE	20	20	10	2.0
POST INJECTION				
IDLE	20	20	60	2.0
PRE-RETROGRADE				
MISC. CHECKOUT	48	32	30	2.0
ELEVON	216	32	10	2.0
RUDDER	54	32	10	2.0
SPEED BRAKE	74	32	10	2.0
IDLE	20	32	120	2.0

APS-702

B-8

Figure B-6

ORBITER APC POWER PROFILE (CONTINUED)

<u>MISSION PHASE</u>	<u>VEHICLE HYDRAULIC POWER REQUIREMENTS (HP)</u>	<u>VEHICLE ELECTRIC POWER REQUIREMENTS (HP)</u>	<u>DURATION (SEC)</u>	<u>AVERAGE BACK PRESSURE (PSIA)</u>
REENTRY				
ELEVON	216	32	20	2.0
ELEVON, RUDDER	136	32	100	2.0
ELEVON	62	32	300	2.0
RUDDER	54	32	10	2.0
IDLE	20	32	270	2.0
TERMINAL CORRECTION				
IDLE	20	32	1200	2.0
ELEVON	114	32	80	2.0
ELEVON	216	32	40	2.0
ELEVON, RUDDER	62	32	200	2.0
IDLE	20	32	150	2.0
RUDDER	54	32	100	2.2
RUDDER	32	32	200	2.9
IDLE	20	32	210	5.9
APPROACH AND FLARE				
GEAR DOWN	74	32	10	9.0
FLIGHT CONTROLS	200	32	20	11.0
FLIGHT CONTROLS	216	32	10	12.0
FLIGHT CONTROLS	56	32	60	15.0
FLIGHT CONTROLS	54	32	10	17.0
TOUCHDOWN				
FLIGHT CONTROLS	216	32	2	17.0
BRAKES, STEERING, ETC.	48	32	8	17.0
POST LAND				
MISC.	40	32	30	17.0
IDLE	20	32	30	17.0

APS-703

B-9

Figure B-6 (Continued)

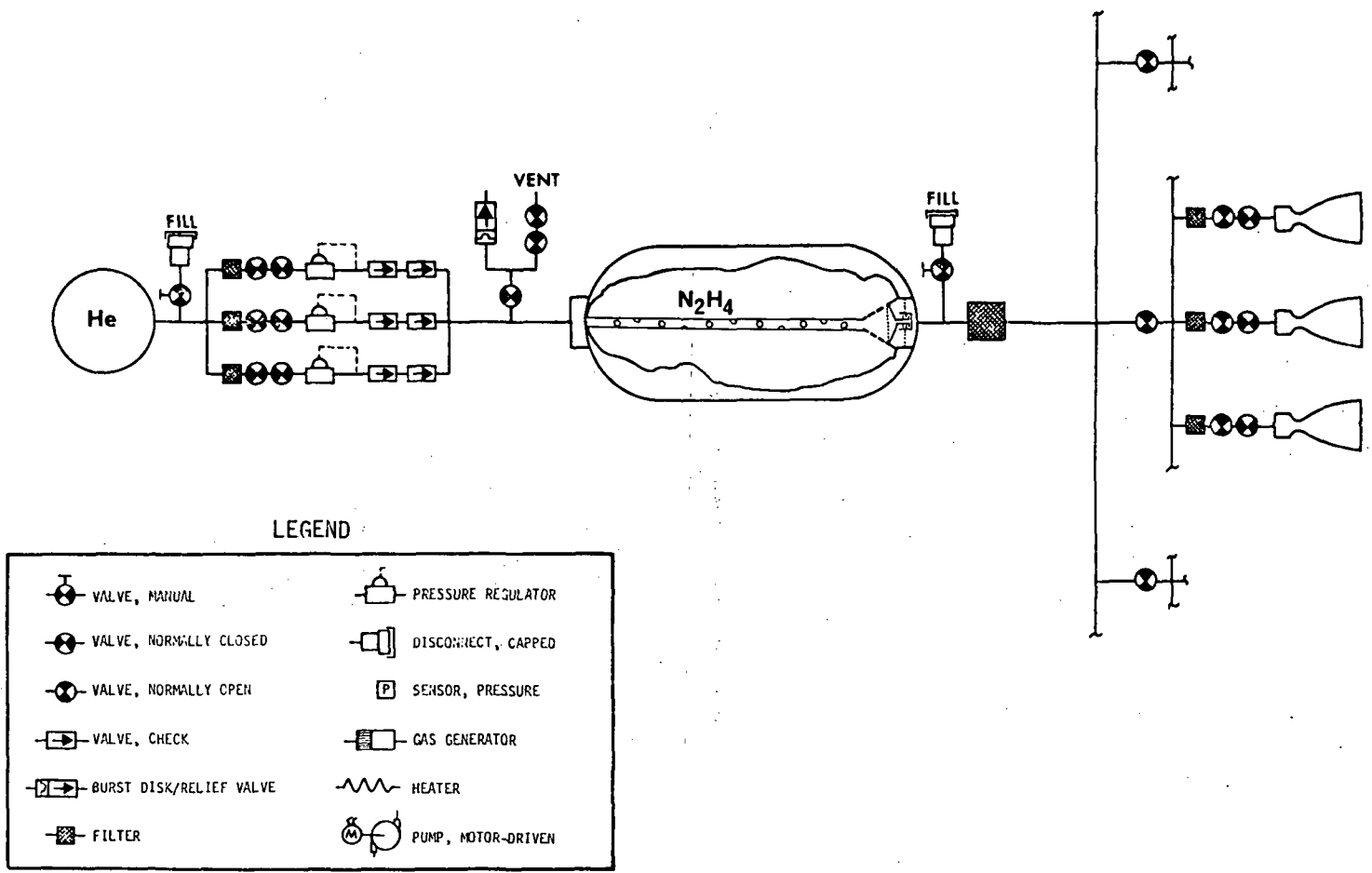
durations of APU operation may be summarized as follows: ascent-11 min., descent-54 min., and a prelaunch operation of 15 min. using ground supplied propellant. Possible horizontal or ferry flight operation requires another 150 min. of APU operation. No consideration was given in this preliminary analysis to the APU requirements for thrust vector control during boost and/or orbiter ferry. The total APU energy output requirements are summarized in Figure B-4.

B2 Preliminary System Descriptions - Preliminary system schematics were prepared for both monopropellant hydrazine and bipropellant RCS and OMS concepts and a hydrazine APU concept. The functional schematics were based on shuttle fail safe /fail safe failure criteria and a tentative assessment of the system installation. The schematics, together with preliminary component characteristic models, describe the systems used in this preliminary analysis to define nominal design points.

B2.1 Monopropellant and Bipropellant RCS and OMS - The monopropellant and bipropellant schematics for the RCS are shown in Figures B-7 and B-8 respectively. These schematics are also applicable for the OMS. As shown, helium pressurization was assumed for both the RCS and OMS. For the bipropellant, a separate pressure regulation assembly was employed for the oxidizer and fuel, since past failure analyses have indicated that, with a common pressurant supply, there is a propensity for propellant vapors to diffuse upstream and react within the pressurization system. Positive expulsion of the hydrazine propellant is accomplished with rubber bladders. Bipropellant expulsion for the RCS is achieved with metal bellows. In the separate OMS, propellants were positioned by RCS settling maneuvers prior to each burn, while the integrated system approaches used surface tension acquisition devices. The tank material was 6Al-4V Titanium in all cases.

Two RCS thruster assemblies were considered for the study, one a radial flow monopropellant hydrazine thruster and the other a film cooled bipropellant thruster. The bipropellant design employed a hyperthin injector and a fuel film cooled, columbium thrust chamber. Preliminary design conditions were 600 lb thrust, 40:1 expansion ratio, and 150 and 200 lbf/in.<sup>2</sup> chamber pressure for the monopropellant and bipropellant designs respectively. To provide equal volume tanks, the bipropellant design mixture ratio was 1.6:1. Both thrusters employed RAO contoured nozzles. Thruster design, performance, and weight are summarized in Figure B-9. Performance in both the steady state and pulsing modes is shown as a function of expansion ratio in Figure B-10.

BASIC MONOPROPELLANT RCS SCHEMATIC



LEGEND

	VALVE, MANUAL		PRESSURE REGULATOR
	VALVE, NORMALLY CLOSED		DISCONNECT, CAPPED
	VALVE, NORMALLY OPEN		SENSOR, PRESSURE
	VALVE, CHECK		GAS GENERATOR
	BURST DISK/RELIEF VALVE		HEATER
	FILTER		PUMP, MOTOR-DRIVEN

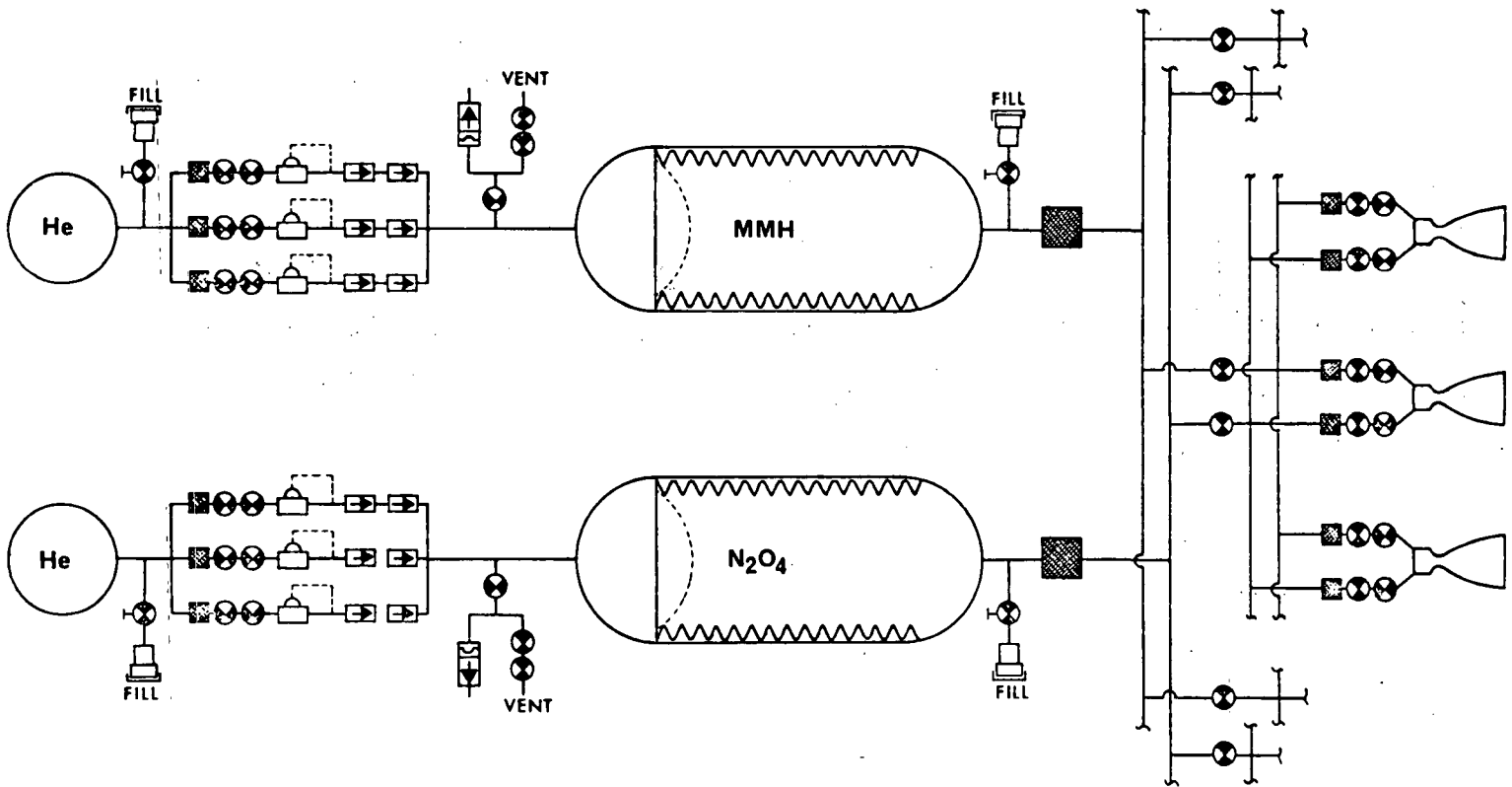
APS-281

B-11

Figure B-7

E243-52

# BASIC BIROPELLANT RCS SCHEMATIC



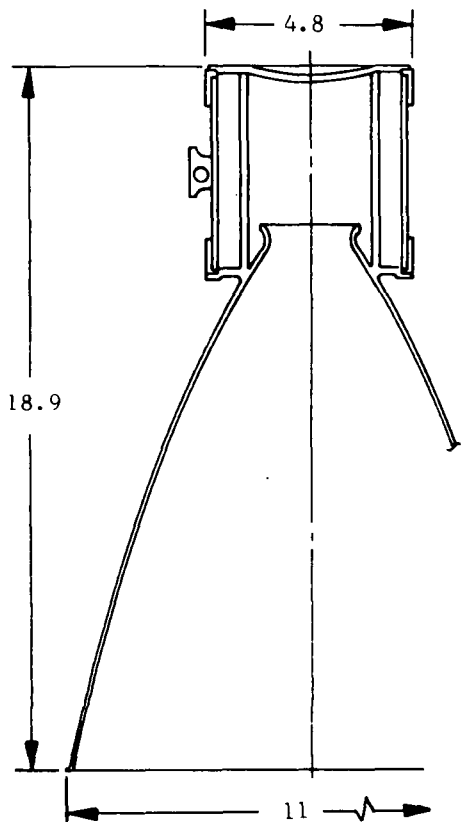
B-12

Figure B-8

# 600 LBF RCS THRUSTER ASSEMBLIES AEROJET LIQUID ROCKET COMPANY

E243-124

## MONOPROPELLANT

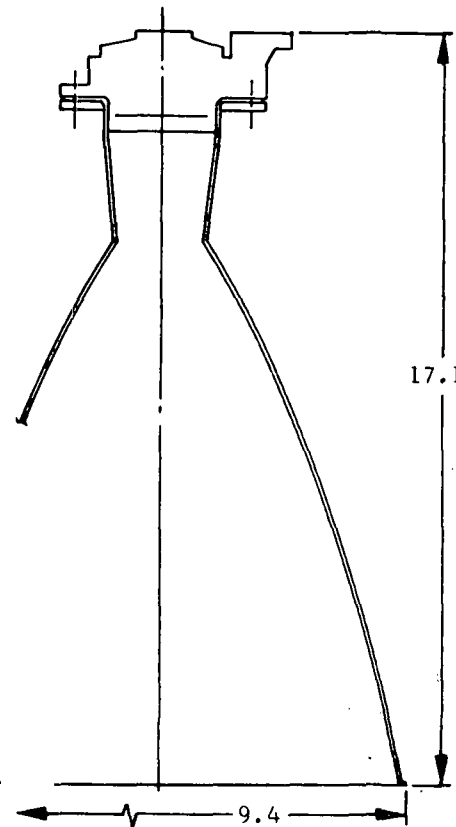


PRESSURES (PSIA)	
304	VALVE INLET
274	INJECTOR INLET
190	UPSTREAM BED
150	CHAMBER

PERFORMANCE ( $\epsilon = 40:1$ )	
239.7	SPECIFIC IMPULSE, SEC
1.78	THRUST COEFFICIENT
4343	CHARACTERISTIC VEL. FT/SEC

WEIGHT, LB	
-	INJECTOR
10.1	CHAMBER & NOZZLE
2.7	CATALYST & SUPPORT
2.0	VALVE
14.8	TOTAL

## BIPROPELLANT



B-13

Figure B-9

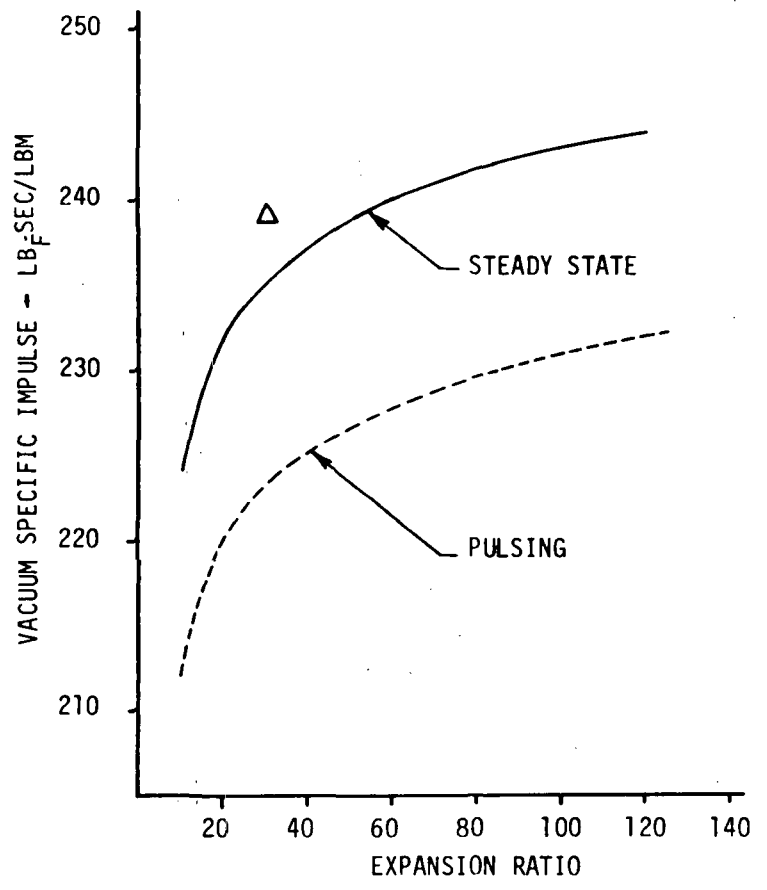


# THRUSTER PERFORMANCE

o PRELIMINARY SYSTEM DEFINITION STUDIES

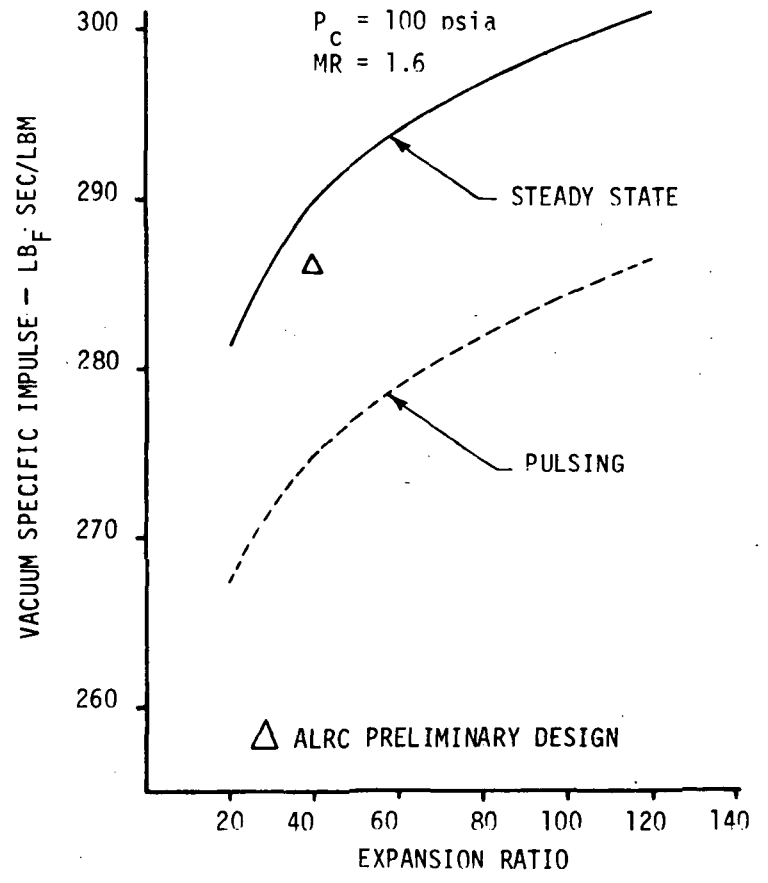
E243-98

MONOPROPELLANT  $N_2H_4$



BIPROPELLANT  $N_2O_4/MMH$

$P_c = 100$  psia  
 $MR = 1.6$



B-14

Figure B-10

Thruster weights are shown parametrically as a function of thrust and chamber pressure in Figure B-11. In addition, the bipropellant thruster performance and weight dependence on overall mixture ratio is illustrated in Figure B-12.

B2.2 Monopropellant APU - The preliminary monopropellant APU system is schematically shown in Figure B-13. A regulated helium subsystem is used to pressurize the rubber bladder, positive expulsion tank. The hydrazine gas generator utilized a thermal reactor for increased life capability. At the design flowrate, the ammonia dissociation is 65 percent, resulting in a maximum turbine inlet temperature of 2060°R. A two stage, axial impulse turbine drives a hydraulic pump, an oil cooled, constant speed drive alternator, and a lubrication pump. The hydraulic pump is a variable displacement, axial piston pump. The APU component performance and weight models are fully described in Appendix A.

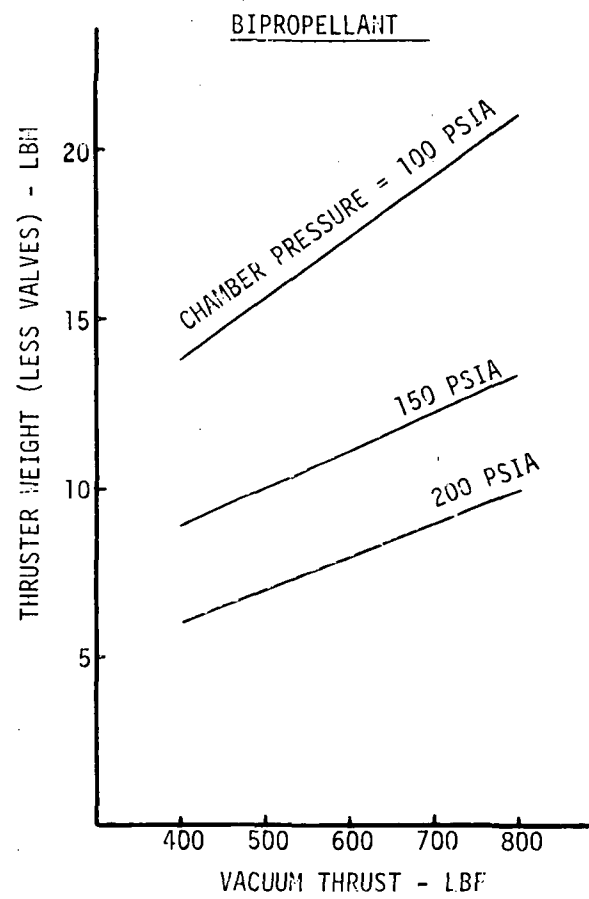
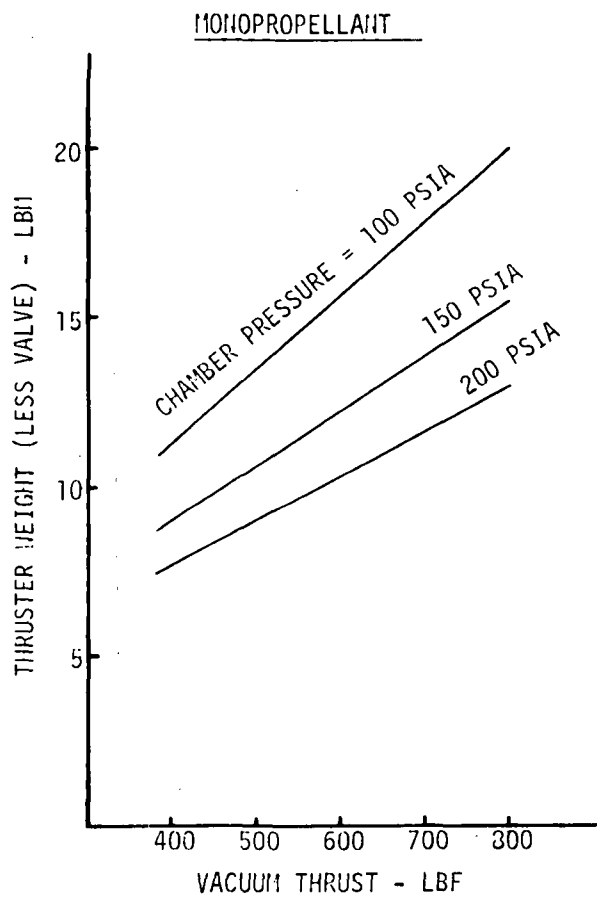
B3 Preliminary Analysis - Nominal system design points were defined and preliminary system sizing data established for bipropellant and hydrazine, RCS and OMS concepts, coupled with a hydrazine APU. Additionally, integrated RCS/APU and RCS/OMS/APU design points and sizing data were defined. Vehicle effects were included in the analysis in order to properly weigh system vehicle interactions. Study of the RCS/OMS impulse allocation covered the full range of using the RCS only for attitude control and vernier translation maneuvers to an RCS used for all on-orbit maneuvers. The study matrix is shown in Figure B-14. Only stored gas pressurization was considered in this preliminary study. A complete discussion of the pressurization trade study is given in Appendix D.

B3.1 Configuration Definition - Configuration details and vehicle interface characteristics for both integral and modular systems were defined for the RCS. Specifically, potential component locations were defined and a comparison made of alternate RCS thruster number and location. The orbiter general equipment arrangement was found to be fairly compact and thus restrictive on the number of potential locations for major APS components/modules within the vehicle. Figure B-15 shows the locations and volumes available for this purpose. Also studied was the placement of external propulsion modules (pods). These modules were located to produce minimal effect on vehicle aerodynamic characteristics, and, preferably, in a region where they are shielded during reentry heating (Figure B-16). Using Figures B-15

E243-158

# THRUSTER WEIGHTS

$\epsilon = 40:1$

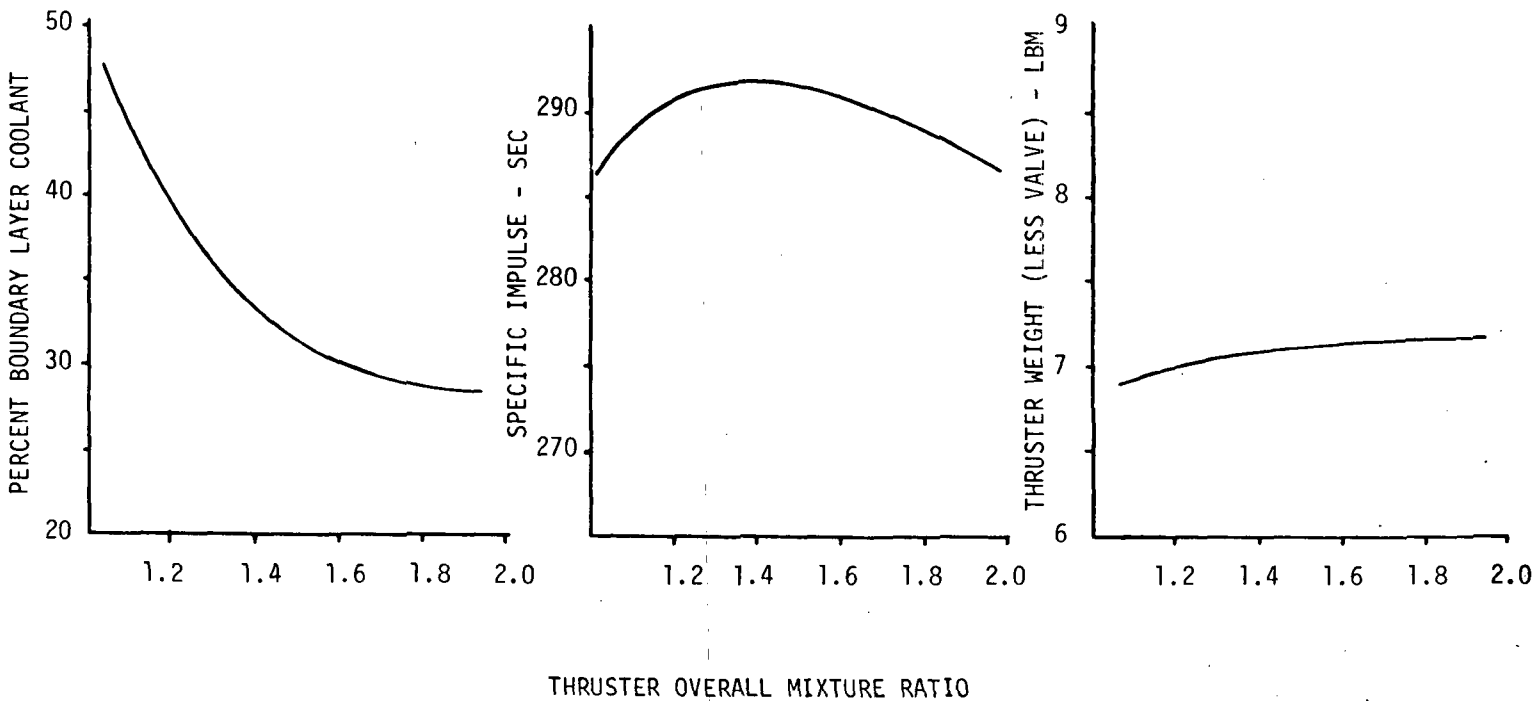


B-16

Figure B-11

# BIPROPELLANT THRUSTER WEIGHT AND PERFORMANCE CHARACTERISTICS

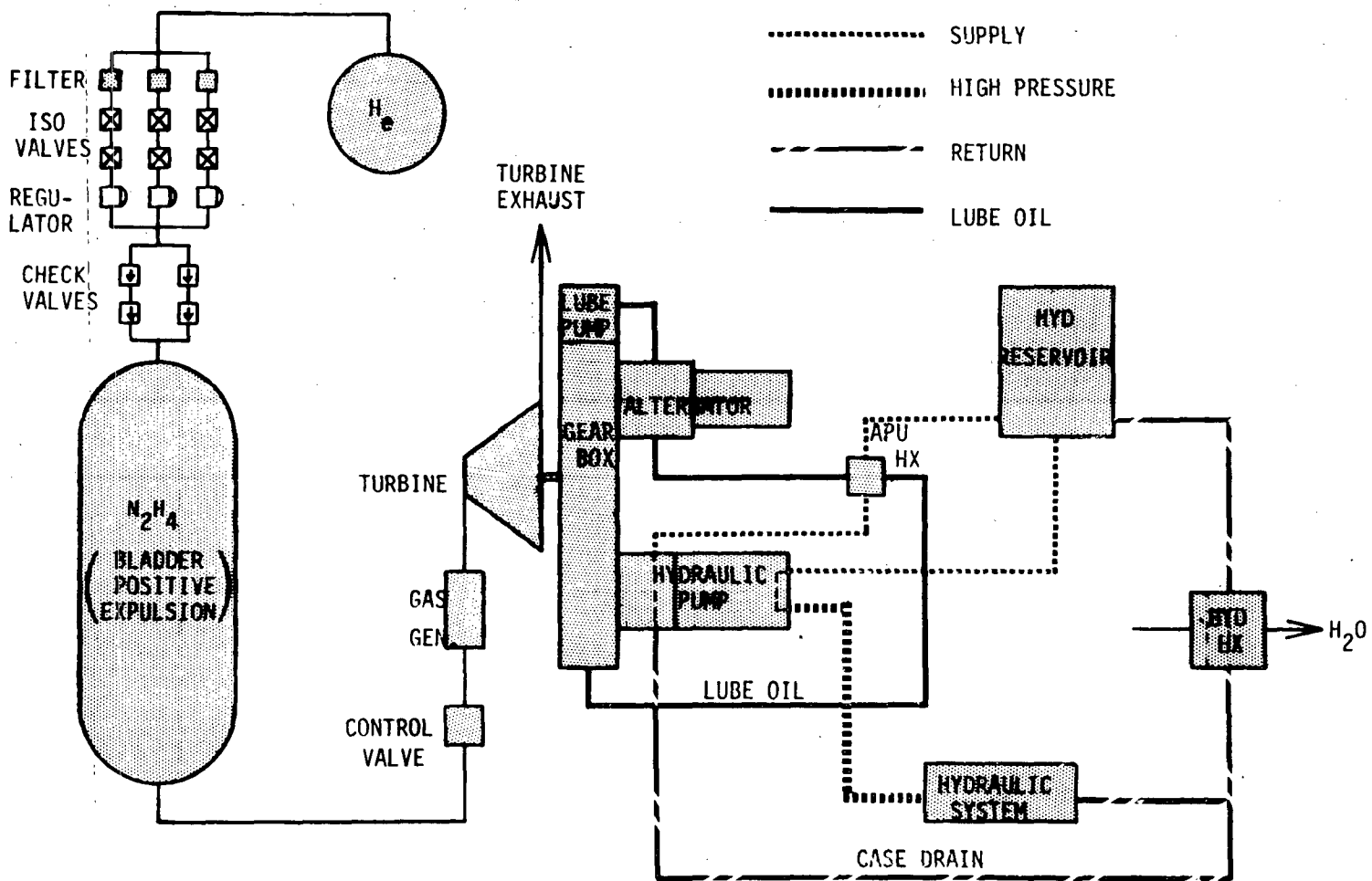
- o THRUST = 600 LBF
- o CHAMBER PRESSURE = 200 PSIA
- o EXPANSION RATIO = 40:1



THRUSTER DESIGN FOR 100 MISSION CAPABILITY

APS-705

REFERENCE APU SCHEMATIC



B-18

Figure B-13

APS-785

CANDIDATE RCS/OMS/APU INTEGRATION CONCEPTS E243-50

CONCEPT	SYSTEM	PROPELLANTS		TANKAGE OPTIONS	PRESSURIZATION OPTIONS
		HYDRAZINE	HYPERGOLIC BIPROPELLANTS		
1	APU	X		INTEGRATED SEPARATE REFILLABLE MODULES (APU & RCS)	HELIUM VOLATILE LIQUID HYDRAZINE DECOMPOSITION PUMPED
	RCS	X			
	OMS	X			
2	APU	X		INTEGRATED SEPARATE REFILLABLE MODULES (APU & RCS)	HELIUM VOLATILE LIQUID HYDRAZINE DECOMPOSITION PUMPED
	RCS OMS	X			
3	APU	X		SEPARATE	HELIUM VOLATILE LIQUID HYDRAZINE DECOMPOSITION PUMPED
	RCS OMS		X	SEPARATE REFILLABLE MODULES (RCS)	HELIUM VOLATILE LIQUID PUMPED
4	APU	X		SEPARATE	HELIUM VOLATILE LIQUID HYDRAZINE DECOMPOSITION PUMPED
	RCS OMS		X	INTEGRATED SEPARATE REFILLABLE MODULES (RCS)	HELIUM VOLATILE LIQUID PUMPED
5	APU RCS	X		INTEGRATED SEPARATE REFILLABLE MODULES (APU & RCS)	HELIUM VOLATILE LIQUID HYDRAZINE DECOMPOSITION
	OMS		X	SEPARATE	HELIUM PUMPED

(OMS) RCS PERFORMS OMS MANEUVERS

and B-16 as installation guidelines, several RCS thruster arrangements were examined. These are shown in Figure B-17, which also tabulates the thruster locations, thruster functions, and direction cosine angles of the applied thrust vectors.

Each configuration represents a compromise in the number of thrusters and/or modules, the number of thruster heat shield penetrations, the amount of cross-coupling, the magnitude of thrust cosine losses and available control moment arms. Figure B-18 gives the number of thrusters required for each configuration at thrust levels of 400, 600 and 800 lb. Also shown are the total impulse requirements and system weights for the integral and modular approaches at 600 lb thrust. It is noteworthy that the lowest total impulse and system weight is obtained with an integral system (Configuration E), whereas the modularized systems (Configurations A and B) result in the lowest number of thrusters.

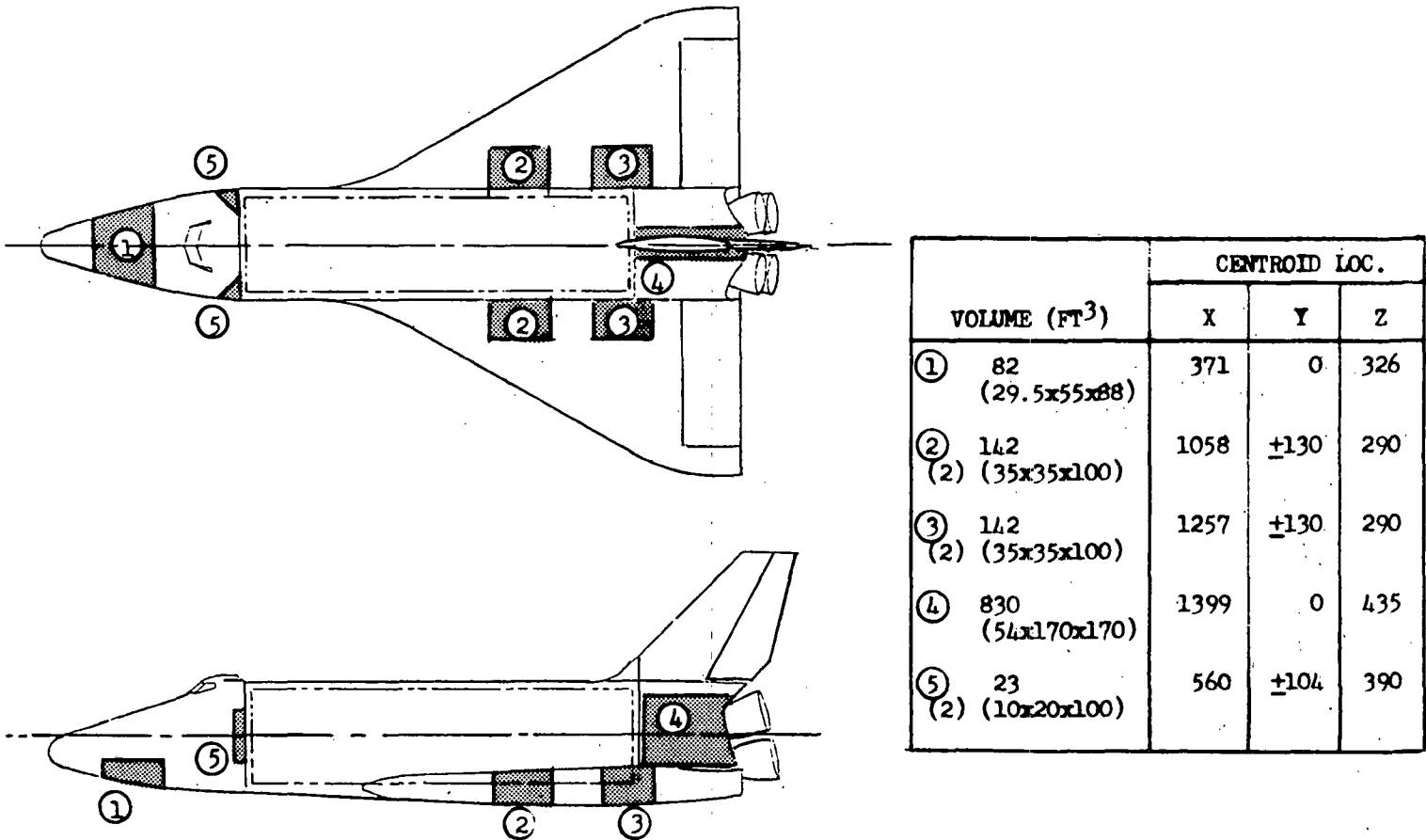
The modular system weights of Figure B-18 do not include structural and thermal protection system (TPS) weights. The impact of the module system on vehicle structural weight is graphically shown in Figure B-19. Also presented is the TPS and structural weight model. Inclusion of these weights revises the module system weights of Figure B-18 as shown in Figure B-20. This chart summarizes the system weight for the MSC-040A and Mark II vehicles for candidate monopropellant RCS configurations. The tail mounted configurations (A and B) now become the heaviest, due to structural effects.

The configurations for subsequent system sensitivities and design point definition were selected, based primarily on weight considerations. These were: Configuration D for modularized APU and RCS concepts, Configuration E for integrated and separate tankage concepts, and Configuration F for the RCS all maneuver case. In addition, the RCS thrust level was fixed at 600 lbf per thruster.

B3.2 System Optimization and Nominal Design Points - Optimization of candidate RCS/APU and RCS/OMS/APU integration options was conducted to define nominal system design points and to establish preliminary system sizing data. The separate, integrated, and modularized concepts of Figure B-14 were evaluated using the appropriate installation of Configurations D, E, or F to include and assess system-vehicle interactions. The study was performed using

E243-57

AVAILABLE INTERNAL VOLUMES



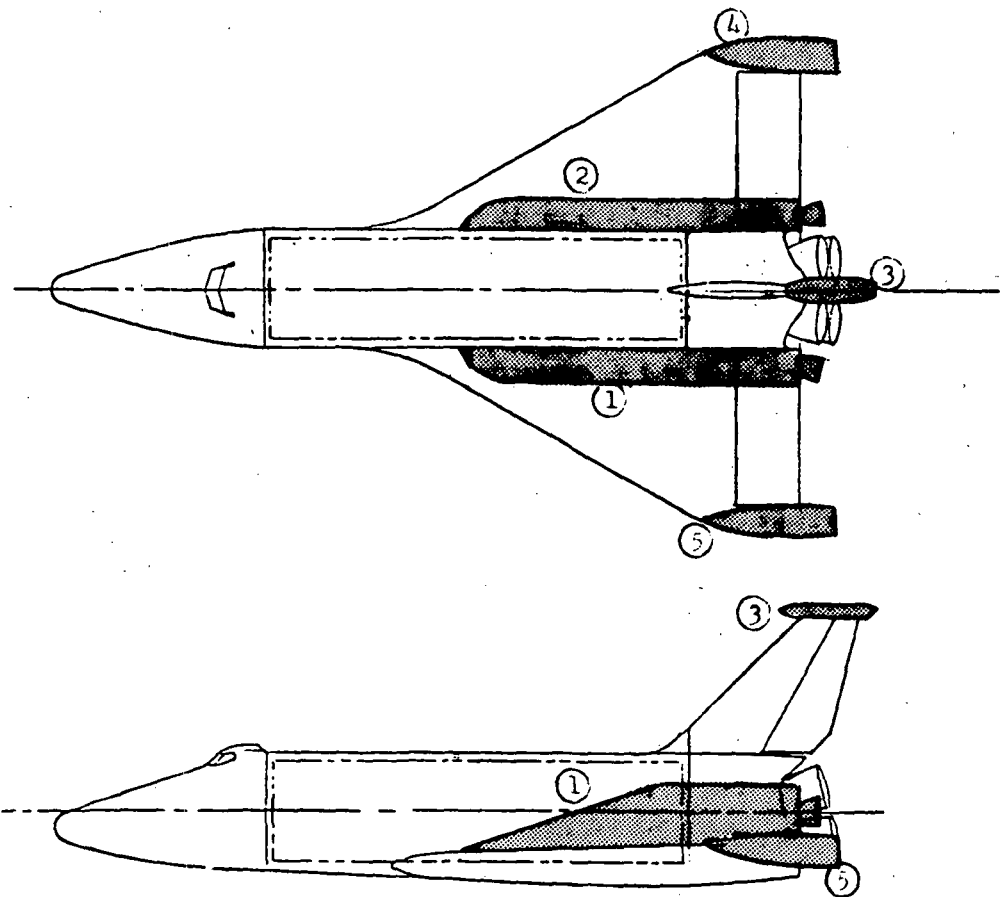
B-21

Figure B-15



E243-56

POTENTIAL EXTERNAL TANKAGE LOCATIONS



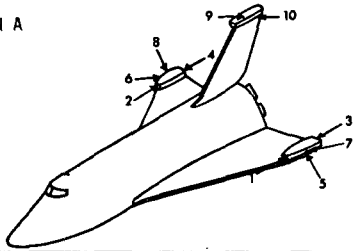
LOCATION	CENTROID		
	X	Y	Z
①	1334	-130	370
②	1334	+130	370
③	1555	0	800
④	1445	+415	340
⑤	1445	-415	340

B-22

Figure B-16

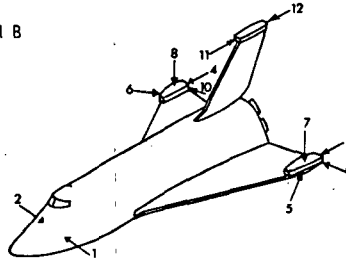
# CANDIDATE ORBITER THRUSTER ARRANGEMENTS

CONFIGURATION A



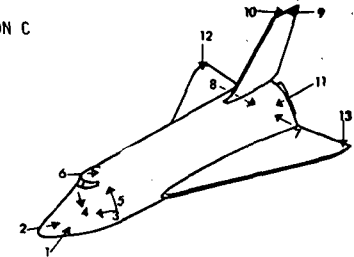
THRUSTER LOCATION	FUNCTION (1)	COORDINATES (2)			COSINE ANGLES		
		X	Y	Z	$\alpha_{XX}$	$\alpha_{YY}$	$\alpha_{ZZ}$
1	Y,X	1358	-415	360	1.0	0	0
2	Y,X	1358	415	360	1.0	0	0
3	Y,X	1515	-415	344	-1.0	0	0
4	Y,X	1515	415	344	-1.0	0	0
5	P,r,Y,Z	1450	-441	352	0	0.6	0.8
6	P,r,Y,Z	1450	441	352	0	-0.6	0.8
7	P,r,Y,Z	1450	-441	352	0	0.6	-0.8
8	P,r,Y,Z	1450	441	352	0	-0.6	-0.8
9	P	1600	0	790	0.625	0	-0.786
10	P	1620	0	782	-0.625	0	0.786

CONFIGURATION B



THRUSTER LOCATION	FUNCTION (1)	COORDINATES (2)			COSINE ANGLES		
		X	Y	Z	$\alpha_{XX}$	$\alpha_{YY}$	$\alpha_{ZZ}$
1	Y,I	371	-76	340	0	1.0	0
2	Y,I	371	76	340	0	-1.0	0
3	Y,X	1515	-415	372	-1.0	0	0
4	Y,X	1515	415	372	-1.0	0	0
5	Y,X	1384	-435	372	0.80	0.60	0
6	Y,X	1384	435	372	0.80	-0.60	0
7	P,r,Z	1450	-415	388	0	0	-1.0
8	P,r,Z	1450	415	388	0	0	-1.0
9	P,r,Z	1515	-415	345	-0.707	0	-0.707
10	P,r,Z	1515	415	345	0.707	0	-0.707
11	P	1470	0	800	1.0	0	0
12	P	1636	0	800	-1.0	0	0

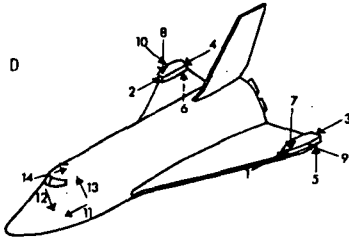
CONFIGURATION C



THRUSTER LOCATION	FUNCTION (1)	COORDINATES (2)			COSINE ANGLES		
		X	Y	Z	$\alpha_{XX}$	$\alpha_{YY}$	$\alpha_{ZZ}$
1	X	340	-65	340	0.942	0.344	0
2	X	340	65	340	0.942	-0.344	0
3	P,r,Y,Z*	565	-100	332	0	0.644	-0.766
4	P,r,Y,Z*	565	100	332	0	-0.644	-0.766
5	P,r,Y,Z*	565	-105	440	0	0.644	0.766
6	P,r,Y,Z*	565	105	440	0	-0.644	0.766
7	Y,I	1400	-105	375	0	1.0	0
8	Y,I	1400	105	375	0	-1.0	0
9	P	1620	0	782	-0.625	0	0.786
10	P	1540	0	800	0.625	0	-0.786
11	X	1490	0	375	-1.0	0	0
12	r	1450	415	388	0	0	-1.0
13	r	1450	-415	388	0	0	-1.0

\*ALSO ON-ORBIT ROLL

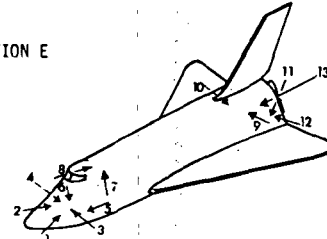
CONFIGURATION D



THRUSTER LOCATION	FUNCTION (1)	COORDINATES (2)			COSINE ANGLES		
		X	Y	Z	$\alpha_{XX}$	$\alpha_{YY}$	$\alpha_{ZZ}$
1	Y,X	1358	-415	360	1.0	0	0
2	Y,X	1358	415	360	1.0	0	0
3	Y,X	1515	-415	344	-1.0	0	0
4	Y,X	1515	415	344	-1.0	0	0
5	P,r,Z	1495	-415	292	0	0	1.0
6	P,r,Z	1495	415	292	0	0	1.0
7	P,r,Z	1335	-415	350	0	0	-1.0
8	P,r,Z	1335	415	350	0	0	-1.0
9	Y	1495	440	352	0	1.0	0
10	Y	1495	440	352	0	-1.0	0
11	Y,Z*	565	-100	332	0	0.766	-0.644
12	Y,Z*	565	100	332	0	-0.766	-0.644
13	Y,Z*	565	-105	440	0	0.766	0.644
14	Y,Z*	565	105	440	0	-0.766	0.644

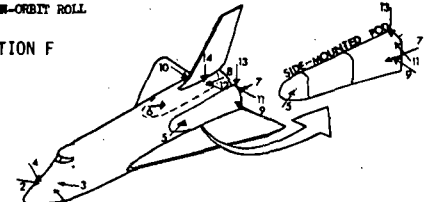
\*ALSO ON-ORBIT ROLL

CONFIGURATION E



THRUSTER LOCATION	FUNCTION (1)	COORDINATES (2)			COSINE ANGLES		
		X	Y	Z	$\alpha_{XX}$	$\alpha_{YY}$	$\alpha_{ZZ}$
1	X	340	-65	340	0.942	0.344	0
2	X	340	65	340	0.942	-0.344	0
3	Y	371	-76	340	0	1.0	0
4	Y	371	76	340	0	-1.0	0
5	P,r,Y,Z	565	-100	332	0	0.644	-0.766
6	P,r,Y,Z	565	100	332	0	-0.644	-0.766
7	P,r,Y,Z	565	-105	440	0	0.644	0.766
8	P,r,Y,Z	565	105	440	0	-0.644	0.766
9	Y,I	1400	-105	375	0	1.0	0
10	Y,I	1400	105	375	0	-1.0	0
11	P,Z	1500	0	300	-0.342	0	-0.94
12	P,Z	1500	0	300	-0.342	0	0.94
13	X	1490	0	375	-1.0	0	0

CONFIGURATION F



THRUSTER LOCATION	FUNCTION (1)	COORDINATES (2)			COSINE ANGLES		
		X	Y	Z	$\alpha_{XX}$	$\alpha_{YY}$	$\alpha_{ZZ}$
1	Y,I,Z	371	-76	325	0	0.766	0.644
2	Y,I,Z	371	76	325	0	-0.766	0.644
3	Y,I,Z	371	-76	340	0	0.766	-0.644
4	Y,I,Z	371	76	340	0	-0.766	-0.644
5	X	1345	-140	400	0.965	0.259	0
6	X	1345	140	400	0.965	-0.259	0
7	X	1480	-153	400	-0.950	0.308	0
8	X	1480	153	400	-0.950	-0.308	0
9	Y,I	1470	-160	400	0.342	0.940	0
10	Y,I	1470	160	400	0.342	-0.940	0
11	P,r,Z	1470	-153	425	-0.60	0	0.80
12	P,r,Z	1470	153	425	-0.60	0	0.80
13	P,r,Z	1470	133	430	0	0	-1.0
14	P,r,Z	1470	133	430	0	0	-1.0

NOTES: (1) p-pitch, y - yaw, r - roll, X - fore/aft translation, Y - left/right translation, Z - up/down translation

(2) Ref. Figure 22 for coordinate system.

APS-786

B-23

Figure B-17

# THRUSTER ARRANGEMENT

## COMPARISON MATRIX

CONFIG. NO.	VEHICLE	NUMBER OF THRUSTERS			APPLICABLE TANKAGE CONCEPTS(1)	HEAT SHIELD PENETRATION	TOTAL IMPULSE(2) ( $\bar{M}$ LB-SEC)	SYSTEM WEIGHT, LB(3)		REMARKS
		F = 400 LB	F = 600 LB	F = 800 LB				INTEGRATED	MODULAR	
A	MSC-040A	38	30	26	I,M	NO	1.354	7365	8024	<ul style="list-style-type: none"> <li>o SIGNIFICANT CROSS-COUPLING BETWEEN Y, Z TRANSLATION AND PITCH/YAW THRUSTERS</li> <li>o DOORS MAY BE REQUIRED ON FORWARD FIRING WING POD THRUSTERS</li> </ul>
	MARK II	46	34	30				9133	9827	
B	MSC-040A	42	30	26	I,M	NO	1.316	7174	7997	<ul style="list-style-type: none"> <li>o FORWARD THRUSTERS USED FOR <math>\pm</math>Y TRANSLATION AND REENTRY YAW MANEUVERS ONLY</li> <li>o SIGNIFICANT ROLL-PITCH AND Z TRANSLATION-PITCH CROSS COUPLING</li> </ul>
	MARK II	50	36	30				8973	9693	
C	MSC-040A	43	36	31	I	NO	1.371	7604	--	<ul style="list-style-type: none"> <li>o FUSELAGE MOUNTED THRUSTERS (STA. 565) USED FOR ON-ORBIT ROLL CONTROL</li> <li>o MINIMAL CROSS-COUPLING</li> <li>o SMALL EFFECTIVE MOMENT ARM FOR RE-ENTRY YAW</li> </ul>
	MARK II	53	39	32				9329	--	
D	MSC-040A	42	34	32	I,M	YES	1.343	7416	7975	<ul style="list-style-type: none"> <li>o TRANSLATION THRUSTERS NO. 9-14 CAN BE USED FOR BACK-UP PITCH AND YAW</li> </ul>
	MARK II	50	42	34				9254	9848	
E	MSC-040A	35	32	27	I	NO	1.250	6911	--	<ul style="list-style-type: none"> <li>o INTEGRATED APPROACH HANDICAPS SYSTEM DESERVICING AND MAINTENANCE OPERATIONS</li> </ul>
	MARK II	47	35	32				8599	--	
F	MSC-040A	44	36	30	M	NO	1.298	--	8085	<ul style="list-style-type: none"> <li>o INTEGRAL RCS/OMS SIDE PODS</li> </ul>
	MARK II	56	42	36				--	9913	

(1) I - INTEGRATED, M - MODULAR

(2) ENGINE THRUST = 600 LB<sub>F</sub> (NO ALLOWANCE FOR OMS  $\Delta$ V DISTURBANCE)

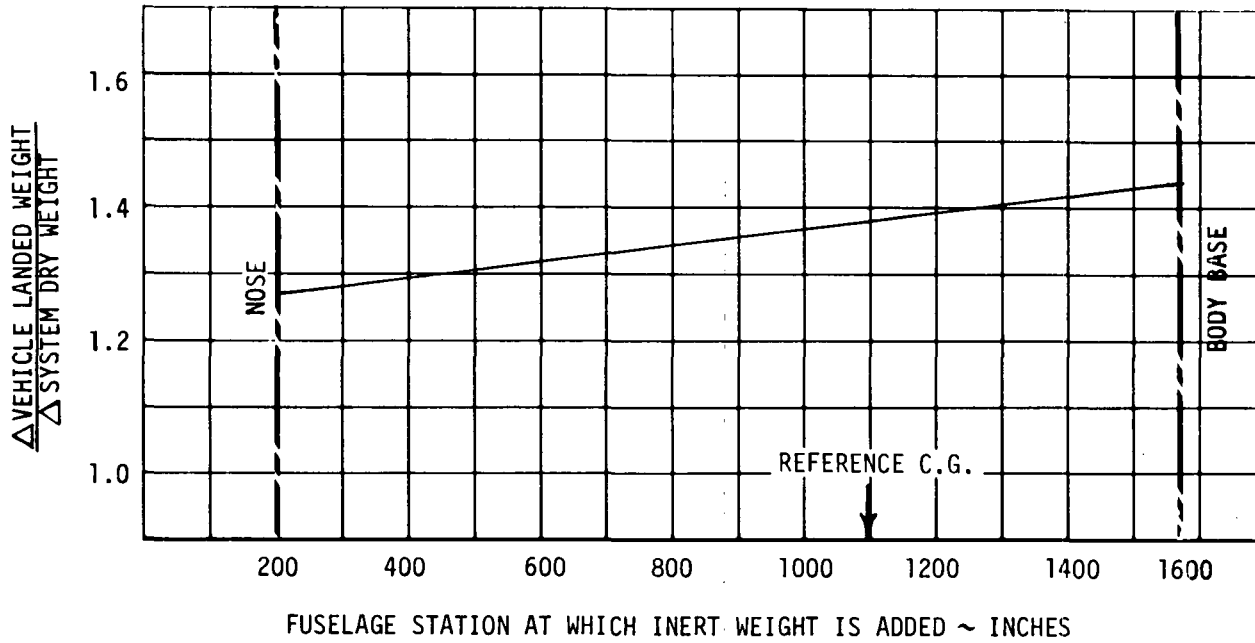
(3) MONOPROPELLANT HYDRAZINE SYSTEM, ENGINE THRUST = 600 LB<sub>F</sub>,  
MODULAR WEIGHT INCLUDES STRUCTURAL MODIFICATIONS

APS-793

# IMPACT OF SYSTEM ON VEHICLE STRUCTURAL WEIGHT

E243-132A

o MARK II VEHICLE



B-25

## POD WEIGHT (MODULAR CONCEPTS)

$$\text{WT}_{\text{POD}} \text{ (LBM)} = \bar{W} \times (\text{POD SURFACE AREA}) + \left[ 3 \times (\text{POD CROSS-SECTIONAL AREA}) \times (.05) \times (.101) \times (1.28) \right] + 38$$

UNIT WEIGHT OF SKIN/TPS  
 3.31 RCS  
 2.96 RCS (OMS)

NO. WEBS/RINGS

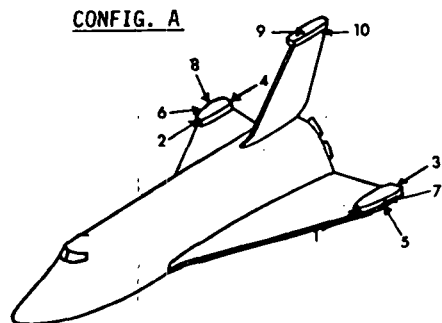
EQUIV. MAT'L THICKNESS  
 ALUMINUM DENSITY  
 ATTACHMENTS  
 MISC.

Figure B-19

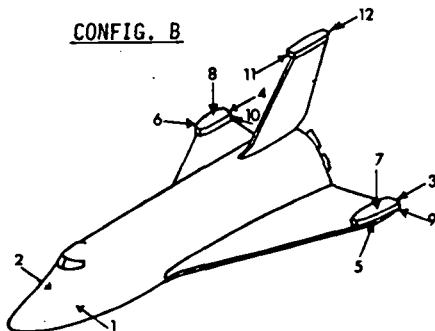
# CANDIDATE RCS THRUSTER LOCATIONS

E243-54A

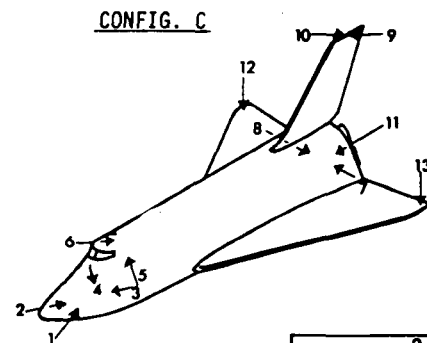
- 600 LBF THRUSTERS
- MONOPROPELLANT



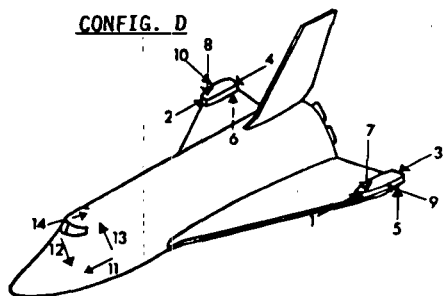
VEH.	NO.	WEIGHT <sup>2</sup>	
		INT.	MOD.
MSC 040	30	7365	8604
MARK II	34	9133	10506



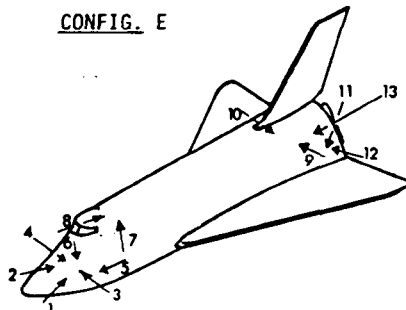
VEH.	NO.	WEIGHT <sup>2</sup>	
		INT.	MOD.
MSC 040	30	7174	8483
MARK II	36	8973	10317



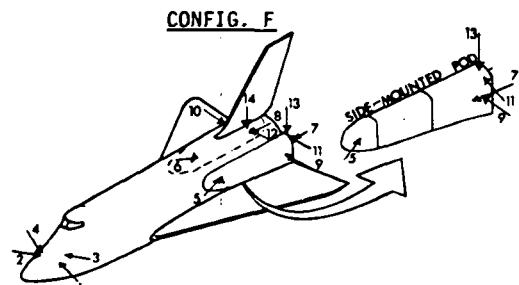
VEH.	NO.	WEIGHT <sup>2</sup>	
		INT.	MOD.
MSC 040	36	7604	-
MARK II	39	9329	-



VEH.	NO.	WEIGHT <sup>2</sup>	
		INT.	MOD.
MSC 040	34	7416	8365
MARK II	42	9254	10348



VEH.	NO.	WEIGHT <sup>2</sup>	
		INT.	MOD.
MSC 040	32	6911	-
MARK II	35	8599	-



VEH.	NO.	WEIGHT <sup>2</sup>	
		INT.	MOD.
MSC 040	36	-	8367
MARK II	42	-	10313

1. NUMBER OF THRUSTERS, 2. TOTAL RCS SYSTEM WEIGHT FOR INTEGRATED AND MODULAR CONCEPTS.

the MSP computer program. Parametric system weight data was generated as a function of the principal design parameters; RCS expansion ratios of 20 to 60, chamber pressures of 50 to 250 lbf/in.<sup>2</sup>, and bipropellant mixture ratios of 1.2 to 1.8. Individual RCS and OMS engine thrust levels were fixed at 600 and 3500 lbf respectively and the OMS engine expansion ratio was held constant at 60:1 (bipropellant) and 40:1 (monopropellant), as these were established as optimal for a maximum exit diameter of 33 inches. Total RCS and OMS impulse requirements are tabulated in Figure B-21 for the MSC-040A orbiter and in Figure B-22 for the Mark II vehicle.

The results, i.e., preliminary design points and weights, are contained in Figures B-23 and B-24. The optimal propellant storage tank pressure has been included with the optimal chamber pressure and expansion ratio. In addition, weights are presented for the individual RCS, OMS, or APU as well as total weights. Pertinent system weight differentials are summarized in Figure B-25 for the Mark II vehicle. This bar graph shows the increment in combined system weights when referenced to a bipropellant RCS and OMS (integral tankage) and a separate, monopropellant APU. The figure reflects the weight penalties associated with (1) monopropellant OMS or monopropellant all maneuver RCS concepts, (2) monopropellant RCS versus bipropellant RCS, and (3) modular tankage. As can be seen from the results, the use of monopropellant for high total impulse functions introduces large weight penalties. For instance, the use of monopropellant hydrazine for the OMS function introduces system penalties on the order of 7000 to 8000 lbm; this was considered to be unacceptably high, and in conversations with the NASA Contract Technical Monitor it was agreed that the study of monopropellant OMS and monopropellant RCS for all maneuvers would be discontinued in order to emphasize effort on the more viable concepts.

B3.3 Vehicle Payload Impact - The input of the system integration options on vehicle payload weight was defined using the data reported in Paragraph B3.4. Here, it was necessary to differentiate between system propellant weight, which has a 1:1 tradeoff with payload, and system inert weight, which reduces payload by 1.4 lbm for each 1 lbm increase. Thus, comparisons on the basis of payload magnifies the weight penalty associated with modularized system concepts (high inert weight) and reduces the weight differential between monopropellant hydrazine and hypergolic bipropellant systems. The

# MSC-040A IMPULSE REQUIREMENTS

o PRELIMINARY ANALYSIS

	IMPULSE REQUIREMENT, LB-SEC		
	MODULAR RCS CONFIGURATION D	INTEGRATED CONFIGURATION E	MODULAR RCS (OMS) CONFIGURATION F
<u>RCS</u>			
ON ORBIT TRANSLATIONS	693,000	680,000	5,522,000
ATTITUDE MANEUVERS	92,400	89,400	97,500
ON ORBIT LIMIT CYCLE	88,500	65,900	32,500
RCS DISTURBANCE	55,100	13,900	63,300
REENTRY - YAW	334,000	270,000	326,000
- ROLL	23,100	84,200	75,500
- PITCH	56,700	46,800	51,000
SUBTOTAL	1,342,800	1,250,200	6,167,800
<u>OMS</u>			
-X ΔV TRANSLATION	4,870,000	4,870,000	--
TOTAL	6,212,800	6,120,200	6,167,800

APS-853

# MARK II IMPULSE REQUIREMENTS

o PRELIMINARY ANALYSIS

	IMPULSE REQUIREMENT, LB-SEC		
	MODULAR RCS CONFIGURATION D	INTEGRATED CONFIGURATION E	MODULAR RCS (OMS) CONFIGURATION F
<u>RCS</u>			
ON ORBIT TRANSLATIONS	1,020,000	1,001,000	8,133,000
ATTITUDE MANEUVERS	127,000	128,000	138,500
ON ORBIT LIMIT CYCLE	52,100	45,700	20,300
RCS DISTURBANCE	80,300	20,200	92,200
REENTRY - YAW	334,000	270,000	326,000
- ROLL	23,100	84,200	75,500
- PITCH	56,700	46,800	51,000
SUBTOTAL	1,693,200	1,595,900	8,836,300
<u>OMS</u>			
-X ΔV TRANSLATION	7,170,000	7,170,000	--
TOTAL	8,863,200	8,765,900	8,836,300

APS-852

B-29

Figure B-22



PRELIMINARY RCS/OMS/APU DESIGN POINTS

o MSC040 VEHICLE

E243-194

SYSTEM (1) (TANKAGE)	PROPEL- LANT	PRESSURIZ- ATION	INSTAL. CONFIG. (2)	OPTIMAL DESIGN PARAMETERS			WEIGHT	
				P <sub>TANK</sub>	P <sub>c</sub>	ε	SYSTEM	TOTAL
APU+RCS+ OMS (I)	N <sub>2</sub> H <sub>4</sub>	HELIUM	E	447	110	40(RCS) 45(OMS)		31344
APU(S) RCS(S) OMS(S)	N <sub>2</sub> H <sub>4</sub> N <sub>2</sub> H <sub>4</sub> N <sub>2</sub> H <sub>4</sub>	HELIUM HELIUM HELIUM	E	287 221	500 150 110	40 45	2290 6930 22451	31671
APU(S) RCS(H) OMS(S)	N <sub>2</sub> H <sub>4</sub> N <sub>2</sub> H <sub>4</sub> N <sub>2</sub> H <sub>4</sub>	HELIUM HELIUM HELIUM	D	281 221	500 150 110	40 45	2290 8223 22451	32964
APU+RCS(OMS) (I)	N <sub>2</sub> H <sub>4</sub>	HELIUM	E	207	100	60		21605
APU(S) RCS(OMS)(S)	N <sub>2</sub> H <sub>4</sub> N <sub>2</sub> H <sub>4</sub>	HELIUM HELIUM	E	207	500 100	60	2290 24002	31292
APU+RCS(OMS) (H)	N <sub>2</sub> H <sub>4</sub>	HELIUM	F	201	100	60		34253
APU(S) RCS(OMS)(S)	N <sub>2</sub> H <sub>4</sub> NTO/MMH	HELIUM HELIUM	E	161	500 100	60	2290 23630	25920
APU(S) RCS(OMS)(M)	N <sub>2</sub> H <sub>4</sub> NTO/MMH	HELIUM HELIUM	F	160	500 100	60	2290 25550	27840
APU(S) RCS+OMS(I)	N <sub>2</sub> H <sub>4</sub> NTO/MMH	HELIUM HELIUM	E	341	500 125	40(RCS) 60(OMS)	2290 23459	25749
APU(S) RCS(S) OMS(S)	N <sub>2</sub> H <sub>4</sub> NTO/MMH NTO/MMH	HELIUM HELIUM HELIUM	E	281 191	500 175 125	40 60	2290 5959 17908	26157
APU(S) RCS(H) OMS(S)	N <sub>2</sub> H <sub>4</sub> NTO/MMH NTO/MMH	HELIUM HELIUM HELIUM	D	232 191	500 175 125	40 60	2290 7187 17908	27385
APU+RCS(I) OMS(S)	N <sub>2</sub> H <sub>4</sub> NTO/MMH	HELIUM HELIUM	E	367 191	200 125	55	2277 17908	27185
APU(S) RCS(S) OMS(S)	N <sub>2</sub> H <sub>4</sub> N <sub>2</sub> H <sub>4</sub> NTO/MMH	HELIUM HELIUM HELIUM	E	287 191	500 150 125		2290 6930 17908	27128
APU(S) RCS(S) OMS(S)	N <sub>2</sub> H <sub>4</sub> N <sub>2</sub> H <sub>4</sub> NTO/MMH	HELIUM HELIUM HELIUM	D	281 191	500 150 125	40 60	2290 8233 17908	28431

(OMS) RCS PERFORMS OMS MANEUVERS

- 1 (S) SEPARATE TANKAGE
- (M) MODULAR CONCEPT
- (I) INTEGRATED TANKAGE

2 REFERENCE (H), TASK 3.7

E243-195

PRELIMINARY RCS/OMS/APU DESIGN POINTS  
o MARK II VEHICLE

SYSTEM (1) (TANKAGE)	PROPEL- LANT	PRESSURIZ- ATION	INSTAL. (2) CONFIG.	OPTIMAL DESIGN PARAMETERS			WEIGHT	
				P <sub>TANK</sub>	P <sub>C</sub>	c	SYSTEM	TOTAL
APU+RCS+ OMS(I)	N <sub>2</sub> H <sub>4</sub>	HELIUM	E	447	110	40 (RCS) 45 (OMS)		43421
APU(S) RCS(S) OMS(S)	N <sub>2</sub> H <sub>4</sub> N <sub>2</sub> H <sub>4</sub> N <sub>2</sub> H <sub>4</sub>	HELIUM HELIUM HELIUM	E	287 221	500 150 110	40 45	2290 8619 32819	43728
APU(S) RCS(M) OMS(S)	N <sub>2</sub> H <sub>4</sub> N <sub>2</sub> H <sub>4</sub> N <sub>2</sub> H <sub>4</sub>	HELIUM HELIUM HELIUM	D	281 221	500 150 110	40 45	2290 10318 32819	45427
APU+RCS (OMS) (I)	N <sub>2</sub> H <sub>4</sub>	HELIUM	E	207	100	60		43742
APU(S) RCS(OMS)(S)	N <sub>2</sub> H <sub>4</sub> N <sub>2</sub> H <sub>4</sub>	HELIUM HELIUM	E	207	500 100	60	2290 41060	43350
APU+RCS (OMS) (M)	N <sub>2</sub> H <sub>4</sub>	HELIUM	F	201	100	60		47160
APU(S) RCS(OMS)(S)	N <sub>2</sub> H <sub>4</sub> N <sub>2</sub> O/MMH	HELIUM HELIUM	E	161	500 100	60	2290 33340	35630
APU(S) RCS(OMS)(M)	N <sub>2</sub> H <sub>4</sub> N <sub>2</sub> O/MMH	HELIUM HELIUM	F	160	500 100	60	2290 35846	38136
APU(S) RCS+OMS(I)	N <sub>2</sub> H <sub>4</sub> N <sub>2</sub> O/MMH	HELIUM HELIUM	E	341	500 125	40 (RCS) 60 (OMS)	2290 33049	35339
APU(S) RCS(S) OMS(S)	N <sub>2</sub> H <sub>4</sub> N <sub>2</sub> O/MMH N <sub>2</sub> O/MMH	HELIUM HELIUM HELIUM	E	281 191	500 175 125	40 60	2290 7365 26021	35676
APU(S) RCS(M) OMS(S)	N <sub>2</sub> H <sub>4</sub> N <sub>2</sub> O/MMH N <sub>2</sub> O/MMH	HELIUM HELIUM HELIUM	D	232 191	500 175 125	40 60	2290 8916 26021	37227
APU+RCS(I) OMS(S)	N <sub>2</sub> H <sub>4</sub> N <sub>2</sub> O/MMH	HELIUM HELIUM	E	367 191	200 125	55 60	10980 26021	37001
APU(S) RCS(S) OMS(S)	N <sub>2</sub> H <sub>4</sub> N <sub>2</sub> H <sub>4</sub> N <sub>2</sub> O/MMH	HELIUM HELIUM HELIUM	E	287 191	500 150 125	40 60	2290 8619 26021	36930
APU(S) RCS(M) OMS(S)	N <sub>2</sub> H <sub>4</sub> N <sub>2</sub> H <sub>4</sub> N <sub>2</sub> O/MMH	HELIUM HELIUM HELIUM	D	281 191	500 150 125	40 60	2290 10318 26021	38629

(OMS) RCS PERFORMS OMS MANEUVERS

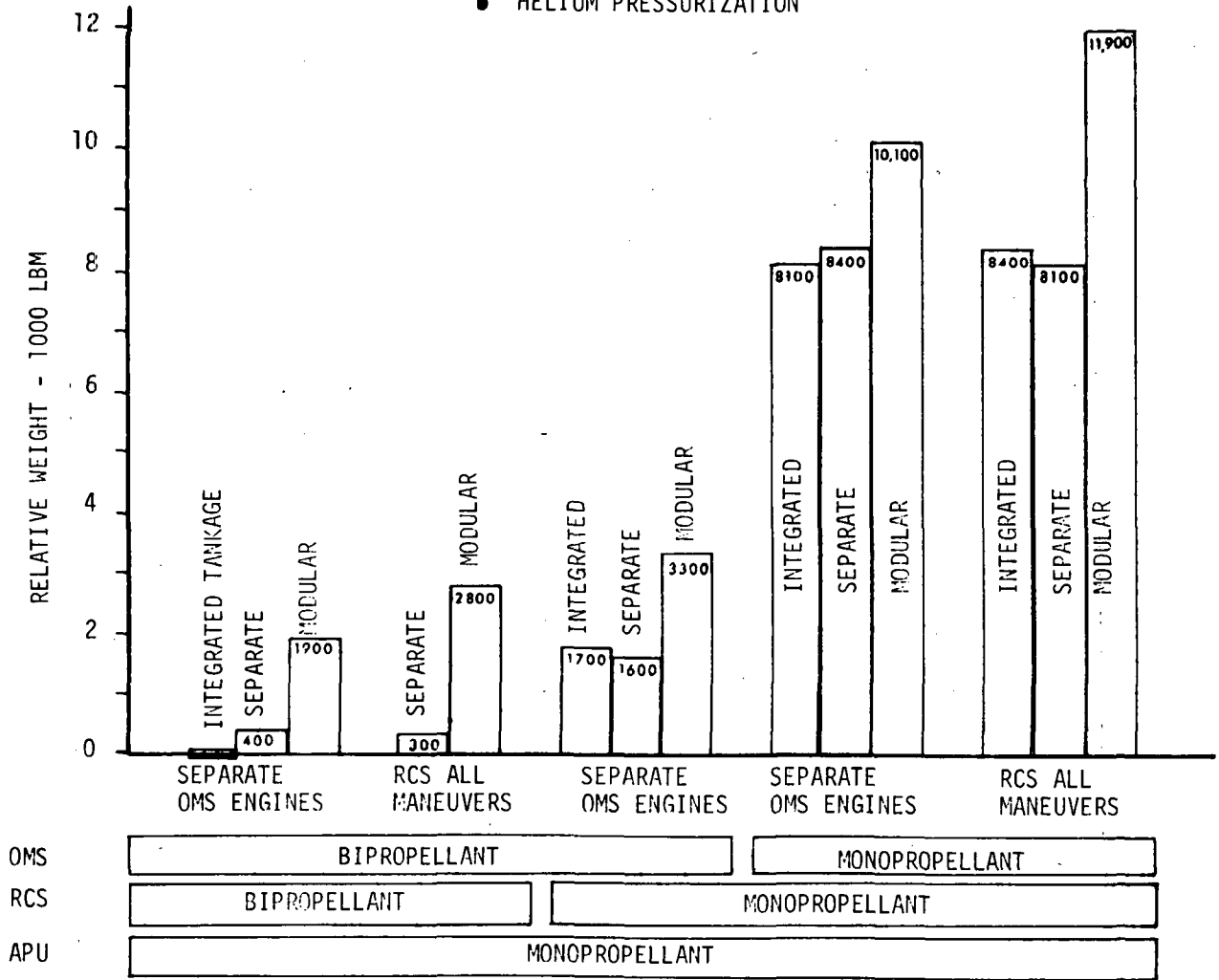
- 1 (S) SEPARATE TANKAGE
- (M) MODULAR CONCEPT
- (I) INTEGRATED TANKAGE

2 REFERENCE (H), TASK 3.7

E243-196

### APU/RCS/OMS WEIGHT COMPARISON

- STORABLE PROPELLANTS
- MARK II VEHICLE
- HELIUM PRESSURIZATION



B-32

Figure B-25

results are shown in Figures B-26 (monopropellant) and B-27 (mixed propellant concepts) for the Mark II vehicle and helium pressurization. The referenced system is a bipropellant all maneuver RCS and a monopropellant APU using separate tankage. The results may be summarized as follows:

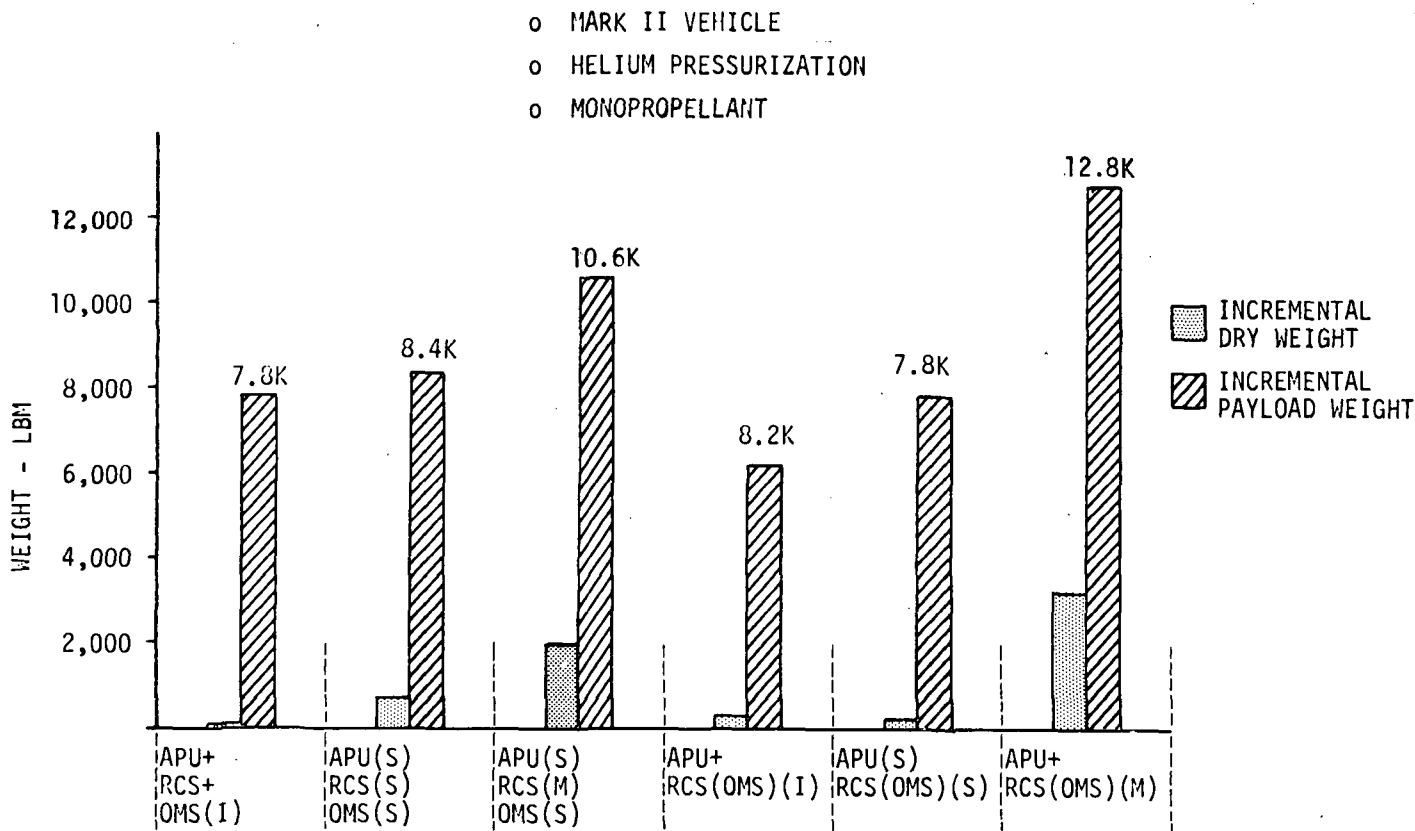
1. The payload penalty for modularization of the RCS is approximately 2000 lbm (bipropellant) or 2200 lbm (monopropellant) when compared to equivalent separate systems with centrally-located tankage.
2. The payload penalty for modularization of the RCS for all on-orbit maneuvers is 3300 lbm (bipropellant) or 4600 lbm (monopropellant) when compared to equivalent, integral systems with centrally located tankage.
3. The payload penalty for a monopropellant RCS is 1200 and 1400 lbm respectively, when compared to a bipropellant system on a centrally located basis or a modularized basis.
4. The payload penalty for a monopropellant RCS for all on-orbit maneuvers is 7800 lbm when compared to an equivalent bipropellant system.
5. The payload increments are additive, e.g., a modularized monopropellant OMS is 3600 lbm (2200 + 1400) heavier than an equivalent integral bipropellant system or a modularized bipropellant RCS is 800 lbm (2000 - 1200) heavier than an integral monopropellant RCS.

B4 APU Preliminary Analysis - Preliminary APU design characteristics were established using the vehicle operational requirements defined in Section B1.2 and the APU component characteristics discussed in Appendix A. Effort has been devoted to design point optimization, configuration definition, and alternate thermal control concept evaluation as discussed below.

B4.1 APU Initial Analysis - The APU power profile includes operation over a range of turbine power settings and at sea level as well as on orbit ambient pressures. One of the first tasks, therefore, was to determine the optimum chamber pressure over the wide range of operating conditions. Figure B-28 presents the effect of chamber pressure on specific propellant consumption for sea level operation. The significant performance increases associated with high chamber pressures suggest the possibility of a pump fed system, with propellant pressure increased from a low tank pressure to a higher chamber pressure by an APU-driven boost pump. Figure B-29 presents APU specific

# INCREMENTAL PAYLOAD WEIGHT RCS/APU/OMS INTEGRATION OPTIONS

E243-93A



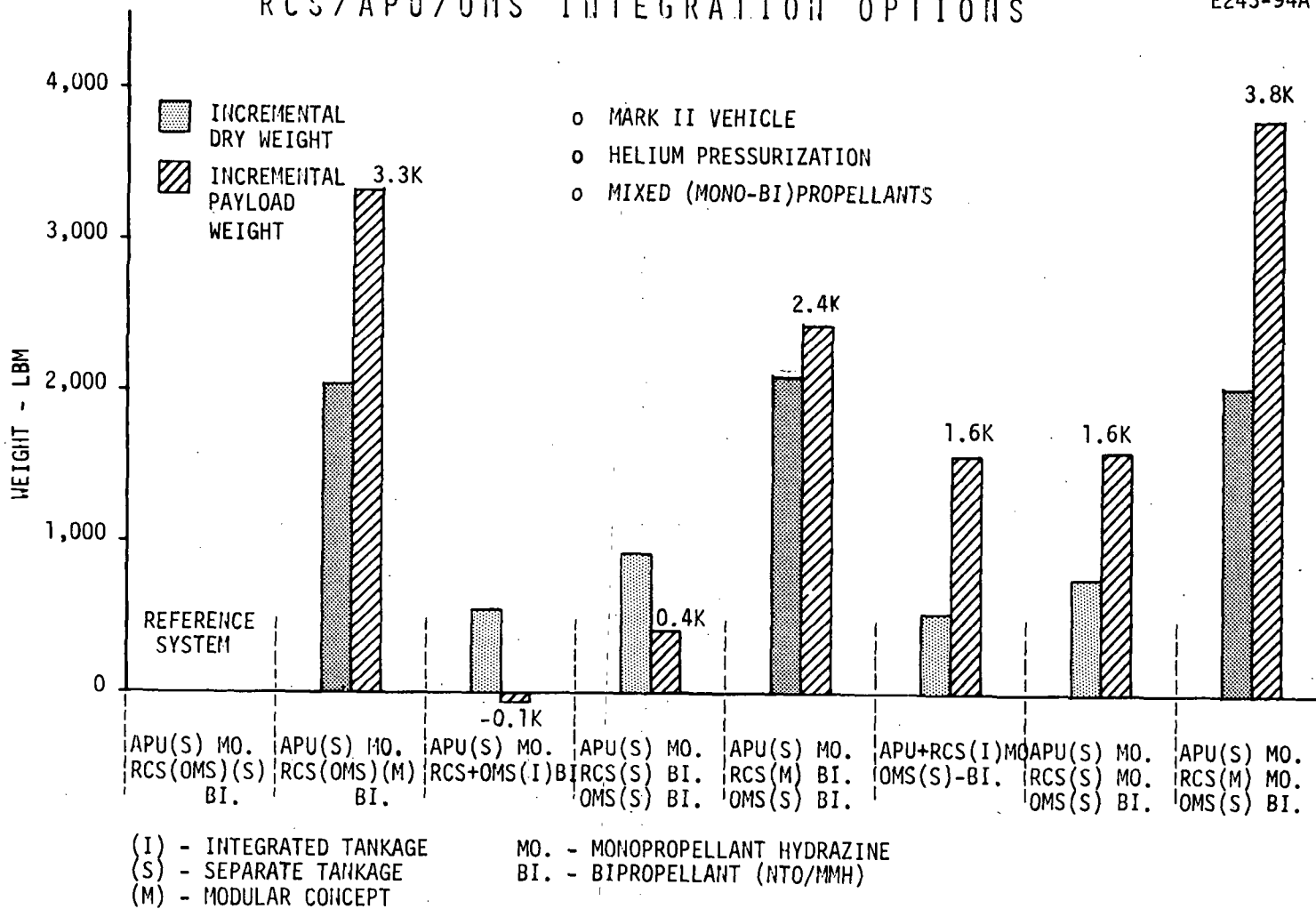
TANKAGE  
 (I) - INTEGRATED TANKAGE  
 (S) - SEPARATE TANKAGE  
 (M) - MODULAR CONCEPT

B-34

Figure B-26

# INCREMENTAL PAYLOAD WEIGHT RCS/APU/OMS INTEGRATION OPTIONS

E243-94A

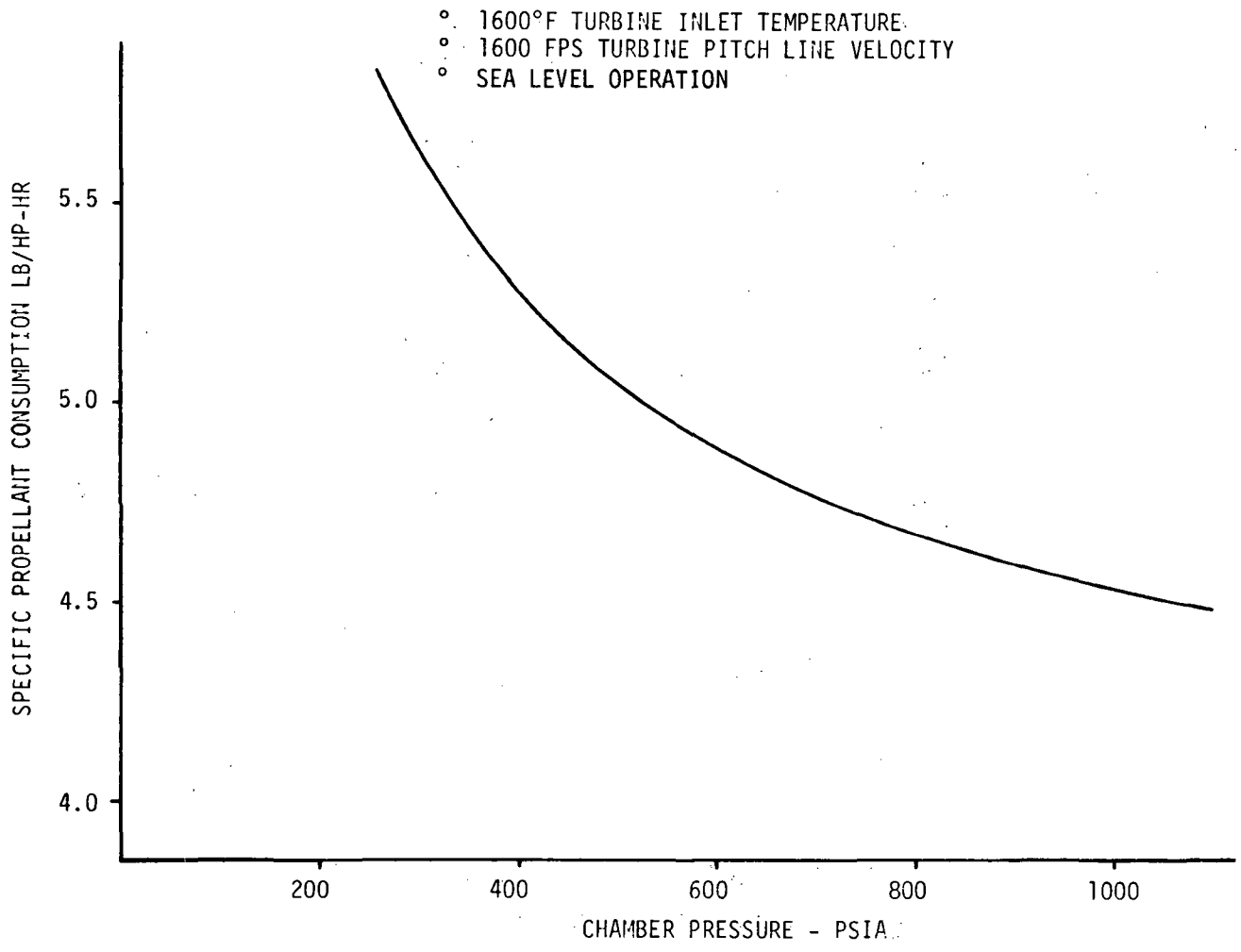


B-35

Figure B-27

E243-25

# EFFECT OF CHAMBER PRESSURE ON APU PERFORMANCE



B-36

Figure B-28

propellant consumption over the range of power settings and at the extremes of altitude. As expected, a performance advantage is associated with the pump fed system operating at high chamber pressure. This performance data corresponds to operation at the respective optimums shown in Figure B-30. As shown, the pump fed system offers weight savings of up to 200 lbm in relation to the 500 lbf/in<sup>2</sup> regulated helium pressurized system.

B4.2 APU Implementation Trade Studies - APU implementation options were evaluated and the most attractive option selected for final system studies. Multiple APU's are required to satisfy redundancy requirements and various configurations, as defined below, consisting of three or four APU's, each coupled to an independent hydraulic system, were considered.

ALTERNATE APU CONFIGURATIONS

CONFIGURATION	NUMBER OF APU'S	MAXIMUM HYD. HP PER APU
A	4	115
B	4	115
C	4	115
D	3	230
E	3	230

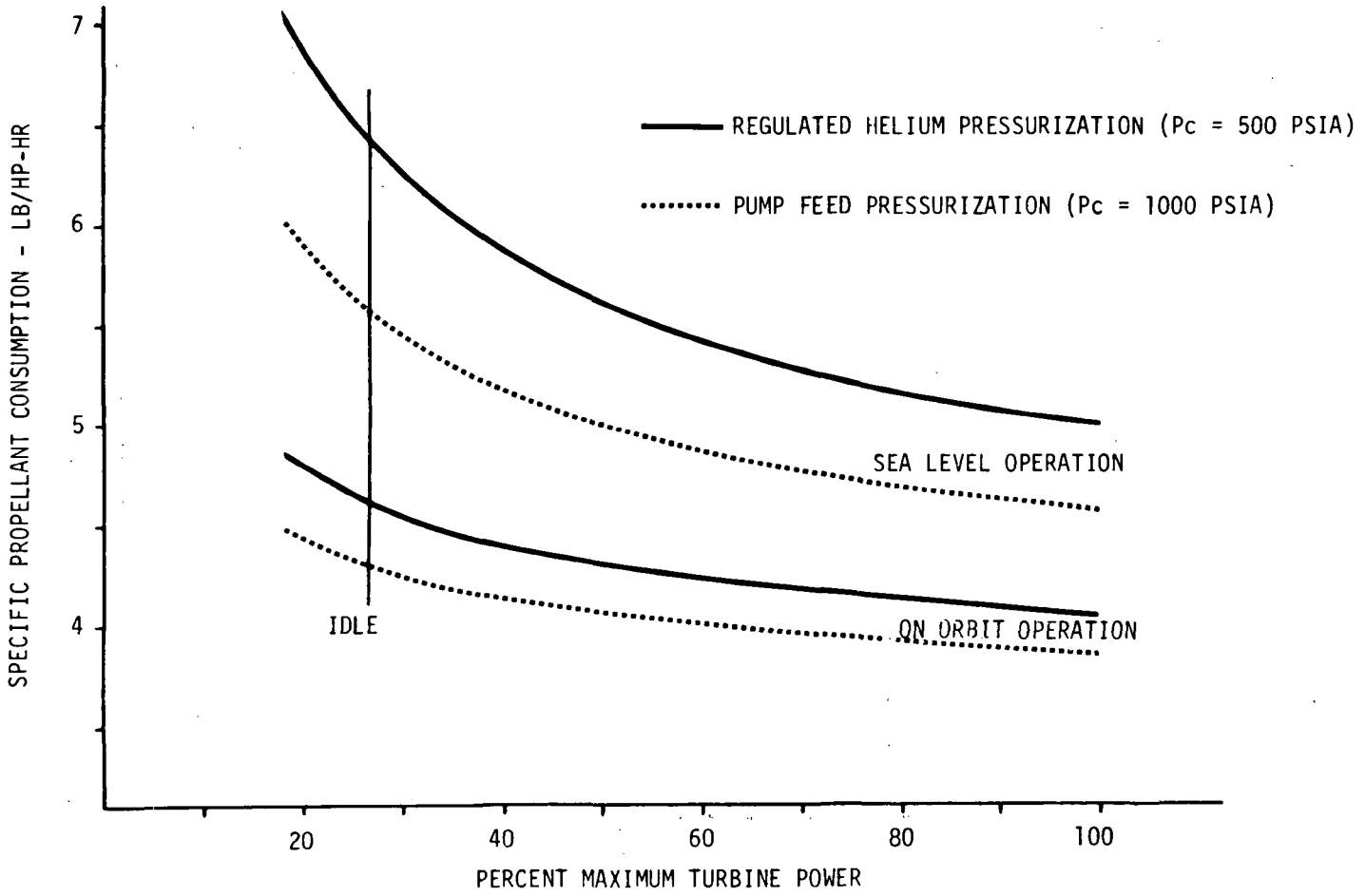
Configurations A through C consist of four APU's, each capable of producing 115 hydraulic horsepower and 15 KW electrical power. As shown in Figure B-31, all four APU's of Configuration A operate such that each unit produces 1/2 of the vehicle power requirements as defined by the power profile. The failure of either one or two units has no effect on the remaining units. Configuration B satisfies the vehicle power requirements by having two units follow the power profile, while the remaining two units are at idle. In the event of a failure, one of the idling units is brought to active status. In Configuration C, all four APU's are active, but unlike Configuration A, each unit produces only 1/4 of the vehicle power requirements as defined by the power profile. The failure of one unit causes each of the remaining three units to assume 1/3 of the power requirements. It can be seen in Figure B-31 that after the second failure, Configurations A through C all operate in a similar fashion; that is, two units active, each producing 1/2 of the vehicle power requirements. Configurations D and E consist of three APU's, each capable of producing 230 hydraulic horsepower and 15 KW electrical power.



E243-30

### PERFORMANCE COMPARISON

TURBINE INLET TEMPERATURE = 1600°F  
TURBINE BLADE PITCH LINE VELOCITY = 1600 FPS



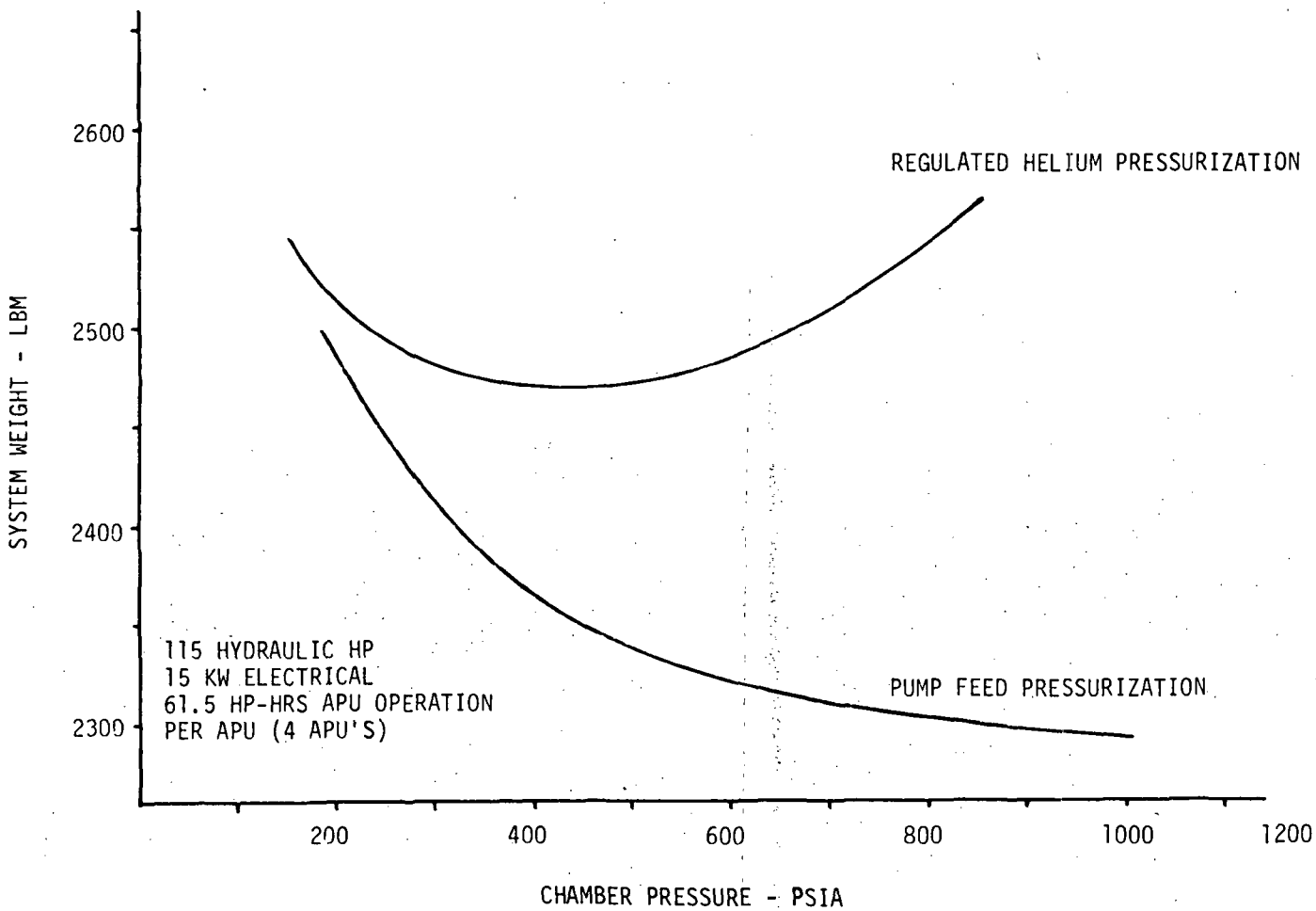
B-38

MC DONNELL DOUGLAS ASTRONAUTICS COMPANY - EAST

Figure B-29

# CHAMBER PRESSURE OPTIMIZATION

E243-40A



B-39

Figure B-30

# COMPARISON OF ALTERNATE CONFIGURATION OPERATION MODES

E243-27

CONF.	NORMAL MODE				FIRST FAILURE				SECOND FAILURE							
A ①	ACTIVE (115)	ACTIVE (115)	ACTIVE (115)	ACTIVE (115)	②	460	⊗	ACTIVE (115)	ACTIVE (115)	ACTIVE (115)	345	⊗	⊗	ACTIVE (115)	ACTIVE (115)	230
B	ACTIVE (115)	ACTIVE (115)	IDLE	IDLE	230	⊗	ACTIVE (115)	ACTIVE (115)	IDLE	230	⊗	⊗	ACTIVE (115)	ACTIVE (115)	230	
C	ACTIVE (58)	ACTIVE (58)	ACTIVE (58)	ACTIVE (58)	230	⊗	ACTIVE (77)	ACTIVE (77)	ACTIVE (77)	230	⊗	⊗	ACTIVE (115)	ACTIVE (115)	230	
D	ACTIVE (230)	IDLE	IDLE	230	⊗	ACTIVE (230)	IDLE	230	⊗	⊗	ACTIVE (230)	230	230			
E	ACTIVE (77)	ACTIVE (77)	ACTIVE (77)	230	⊗	ACTIVE (115)	ACTIVE (115)	230	⊗	⊗	ACTIVE (230)	230	230			

① SINGLE UNIT PEAK HYDRAULIC POWER OUTPUT (HP)  
 ② SYSTEM PEAK HYDRAULIC POWER OUTPUT (HP)

B-40

Figure B-31

As shown in Figure B-31, the implementation options are similar to those already discussed.

The candidate configurations were analyzed to determine weight and performance characteristics. Figure B-32 presents a summary of these results. Although the units which run at idle or reduced power level have a higher specific propellant consumption, significant reductions in system weight are achieved by these configurations because their total energy output is held to a minimum. An alternate approach to Configurations B and D is to operate only one of the back-up units in an idle mode, keeping the other back-up unit dormant. In the event of a failure, the idle unit is activated and the dormant unit is brought to idle status. This scheme provided an incremental weight savings of 330 lbm on Configuration B and 460 lbm on Configuration D.

Configuration C and the alternate Configuration B were selected for in-depth evaluation and are summarized in Figure B-33 as to design, operation, and weight. The system weights of Configuration C and B (Mod) are 2206 and 1976 lbm, respectively.

These weights are based on the use of constant speed drives (CSD) between the gearboxes and alternators to minimize variations in alternator frequency drift and frequency drift rates. However, analysis of the CSD characteristics reveals that although it would be capable of nulling the steady state frequency variations, it would be unable to cope with the extremely high frequency drift rates (app. 1500 HZ/Sec) caused by sudden changes in hydraulic loads. To alleviate this problem, the APU concept shown in Figure B-13 was revised by driving the alternator with a dedicated hydraulic motor. Figure B-34 presents the revised APU schematic. In this configuration, the hydraulic motor and alternator are directly coupled, operating at a design speed of 800 RPM. To desensitize the alternator to hydraulic load transients, a small hydraulic accumulator is incorporated in the alternator hydraulic line. These changes result in system weight growths of 138 lbm and 113 lbm for Configurations C and B (Mod.), respectively. The weight penalties are justified on the basis of reduced APU development risk and improved electrical power quality.

The two configurations were then compared on the basis of mission energy effects. Figure B-35 presents the weight sensitivities to APU power level and power usage. As shown, Configuration B (Mod.) remains the lightest and this approach was used for subsequent studies.

SUMMARY OF IMPLEMENTATION OPTIONS

E243-16A

CONFIGURATION	TOTAL HP-HRS OF TURBINE OPERATION	AVERAGE SPECIFIC PROPELLANT CONSUMPTION (LB/HP-HRS)	TOTAL PROPELLANT WEIGHT (LBM)*	TOTAL FIXED WEIGHT (LBM)	TOTAL PROP SUPPLY SYSTEM WEIGHT (LBM)	TOTAL SYSTEM WEIGHT (LBM)
A	246	4.81	1230	1012	231	2473
B	211	4.89	1088	1012	206	2306
C	193	4.95	1004	1012	190	2206
D	249	4.97	1301	840	245	2386
E	233	4.96	1214	840	230	2284

\* INCLUDES 5% CONTINGENCY  
CHAMBER PRESSURE = 500 PSIA

B-42

Figure B-32

## SUMMARY OF ALTERNATE IMPLEMENTATION OPTIONS

	CONFIGURATION C	CONFIGURATION B(MOD.)
NUMBER OF APU'S IN CONFIGURATION	4	4
PUMP HYDRAULIC HORSEPOWER PER APU	144	144
ALTERNATOR KVA PER APU	15	15 (3 of 4)
TURBINE HORSEPOWER PER APU	180	180
APU #1 STATUS (MAXIMUM HYD. HP)	ACTIVE (72)	ACTIVE (144)
APU #2 STATUS (MAXIMUM HYD. HP)	ACTIVE (72)	ACTIVE (144)
APU #3 STATUS (MAXIMUM HYD. HP)	ACTIVE (72)	IDLE
APU #4 STATUS (MAXIMUM HYD. HP)	ACTIVE (72)	DORMANT
TOTAL HP-HRS OF TURBINE OPERATION	224.8	190.1
AVERAGE SPECIFIC PROPELLANT CONSUMPTION (LB/HP-HR)	5.04	4.94
TOTAL PROPELLANT WEIGHT (LBM)	1131	940
TOTAL FIXED WEIGHT (LBM)	1010	985
TOTAL PROPELLANT SUPPLY WEIGHT (LBM)	216	178
TOTAL APU SYSTEM WEIGHT (LBM)	2206	1976

MCDONNELL DOUGLAS AERONAUTICS COMPANY - EAST

B-43

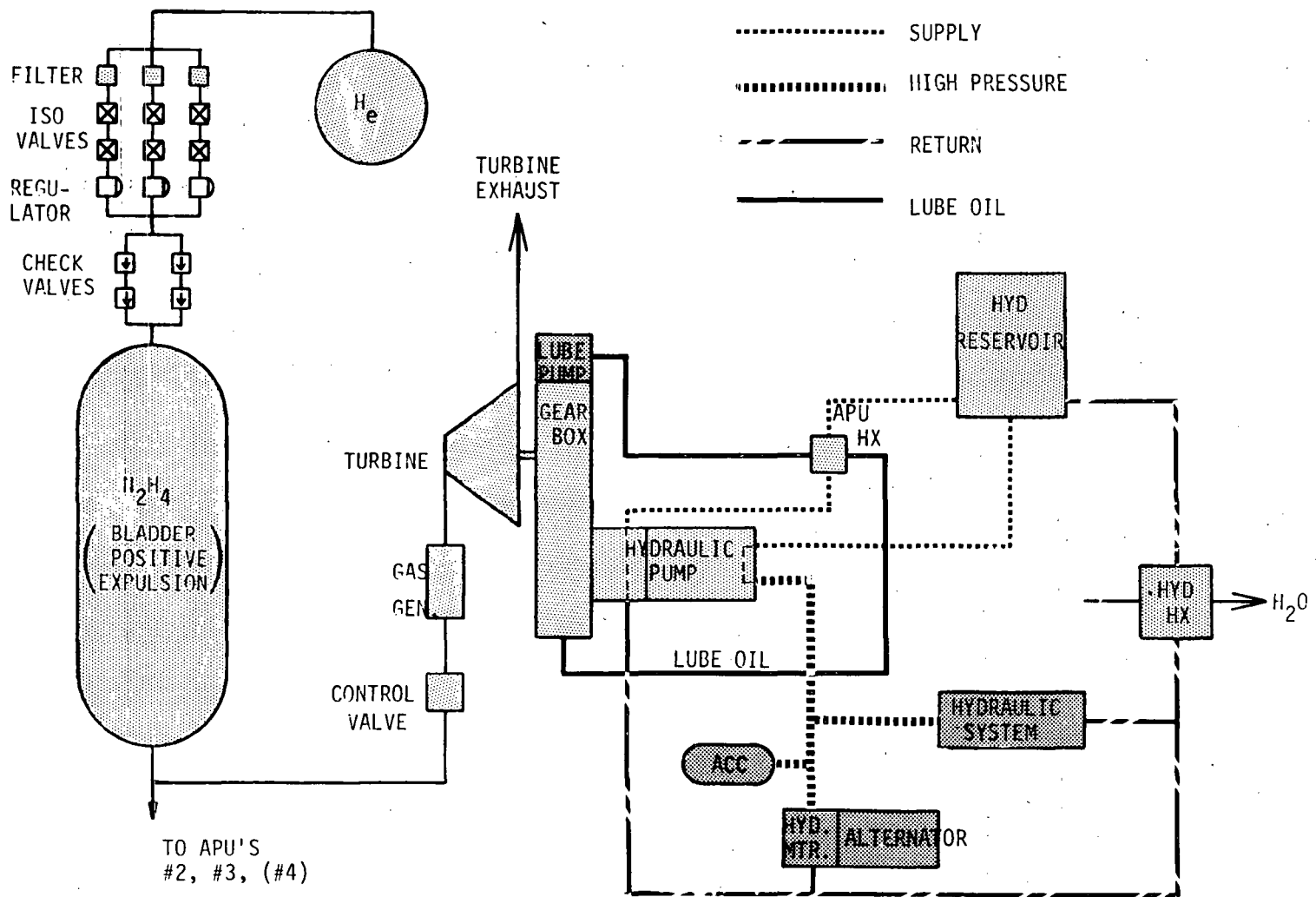
Figure B-33

APS-322 A

APS STUDY  
Phase C and E Report

MDC E0708  
29 December 1972

### BASELINE APU SCHEMATIC



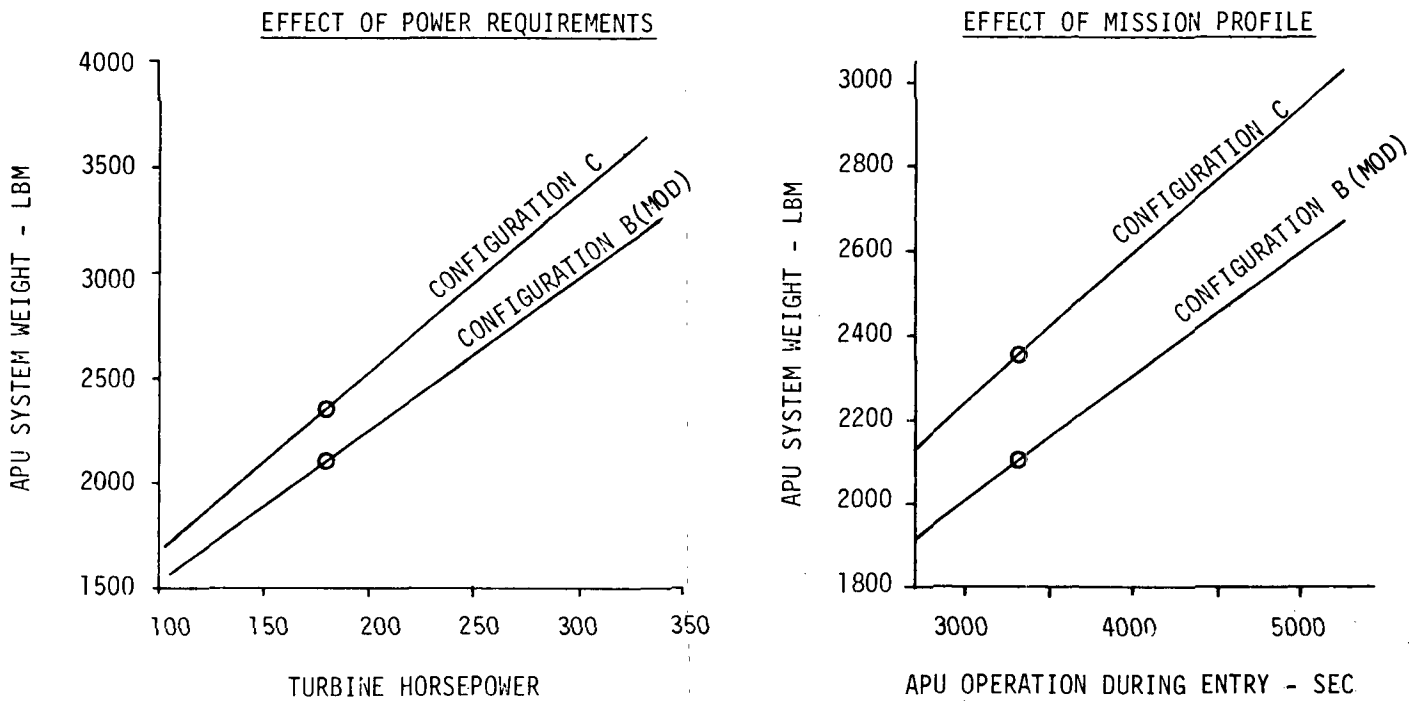
TO APU'S  
#2, #3, (#4)

APS-304

B-44

Figure B-34

# MISSION ENERGY EFFECTS



APS-340 A

B-45

Figure B-35



B4.3 APU Thermal Control Analysis - Two alternate APU thermal conditioning systems were evaluated and are shown in Figure B-36. Hydrogen offers a greater heat capacity than water. Additionally, since the heat transfer is limited primarily by the thermal resistance of the heat exchanger walls, a larger (and heavier) exchanger is required for the water than for the lower temperature liquid hydrogen. Another advantage in using hydrogen is that it also serves as a supplemental fluid for turbine drive whereas the water is vented directly overboard as it exits from the heat exchanger. Use of water to augment the turbine flow is not possible because of the low water pressures required to keep its saturation temperature below the maximum hydraulic fluid temperature. For efficient cooling, water must be used subcritically and undergo a phase change. However, the water coolant system is simpler and requires fewer controls than the hydrogen system.

In both concepts, a small lube oil/hydraulic fluid heat exchanger is used to condition the lube oil. The hydraulic fluid heat capacity is sufficient to absorb heating loads during ascent without exceeding the maximum temperature (275°F). Coolant requirements are thus completely determined by the temperature levels at the start of reentry and the heat loads during reentry.

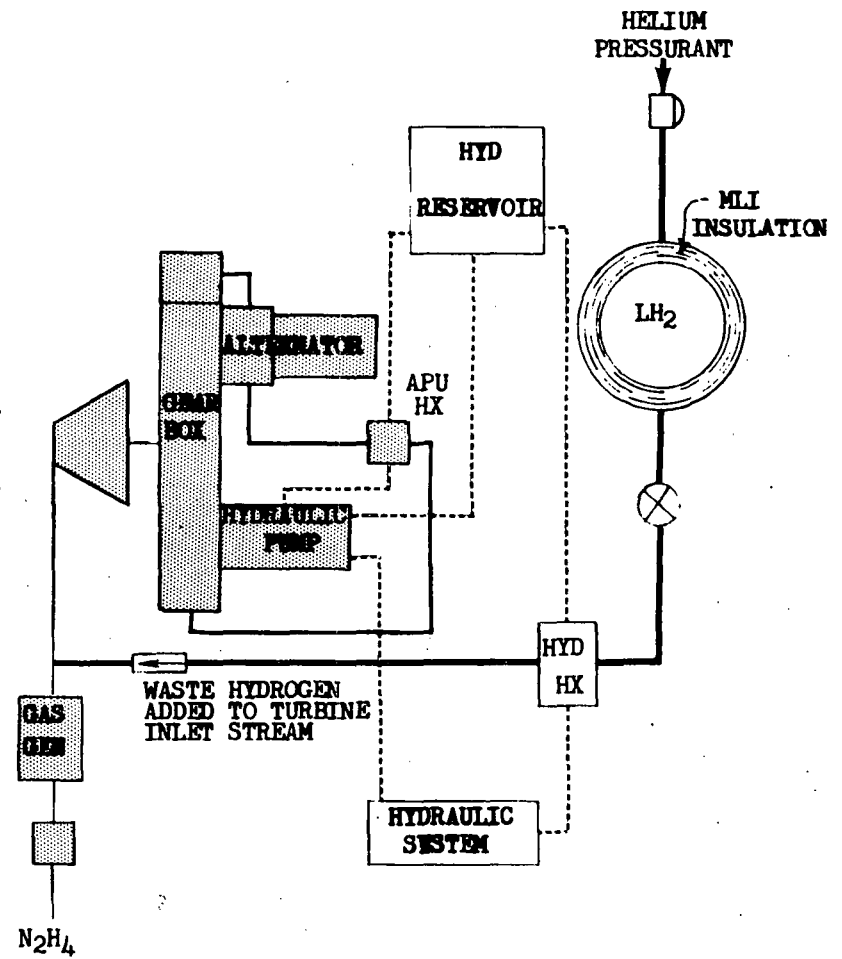
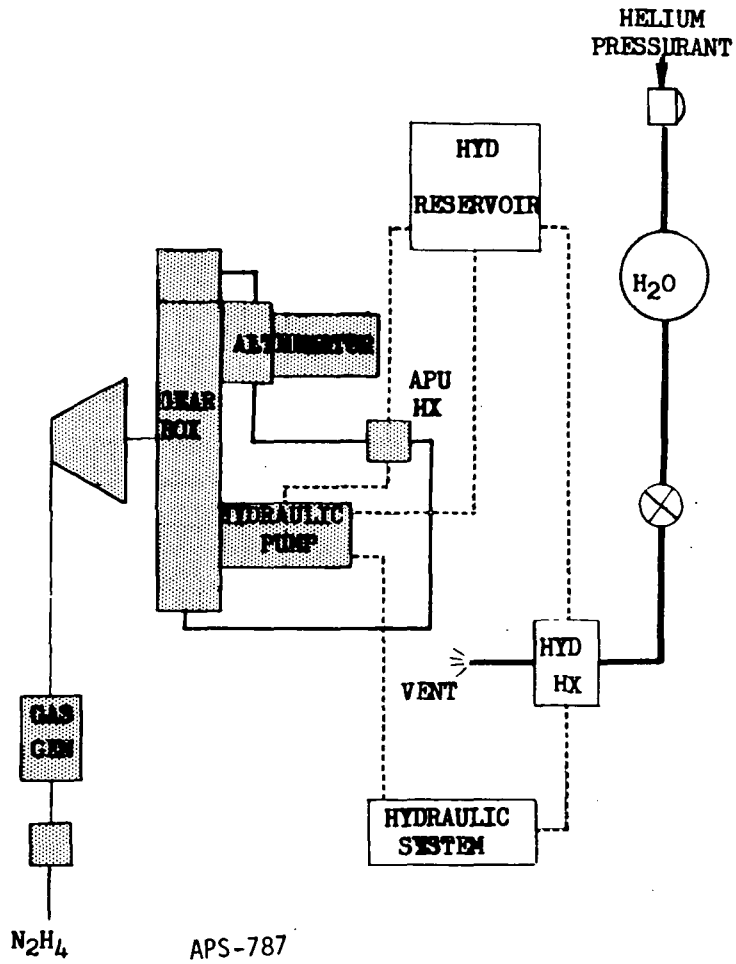
Typical designs for heat exchangers with water or hydrogen as the coolant fluid are shown schematically in Figure B-37. The contrasting design concepts are dictated by the critical pressures of the two alternate coolant fluids. Water must be used subcritically and undergo a phase change for maximum efficiency. For the design shown, water sprays uniformly over the heat exchanger surface, evaporating as single droplets. The hydrogen cooler is a simple coaxial counterflow heat exchanger which operates supercritically. A primary design consideration is the prevention of excessive localized cooling of the hydraulic fluid. Heat exchanger weights are 40 lbm and 11.1 lbm for the water and hydrogen coolants, respectively.

Figure B-38 presents the effect of hydrogen injection on specific propellant consumption. As shown, a performance increase is realized even at low mixture ratios. The effect of hydrogen injection on turbine inlet temperature and flow rate is shown in Figure B-39. Although the turbine inlet temperature decreases substantially, the turbine must still be designed for an inlet temperature of 2060°R, since hydraulic fluid cooling is required only during entry.

# ALTERNATE APU THERMAL CONDITIONING SYSTEMS

## WATER COOLING SYSTEM

## HYDROGEN COOLING SYSTEM

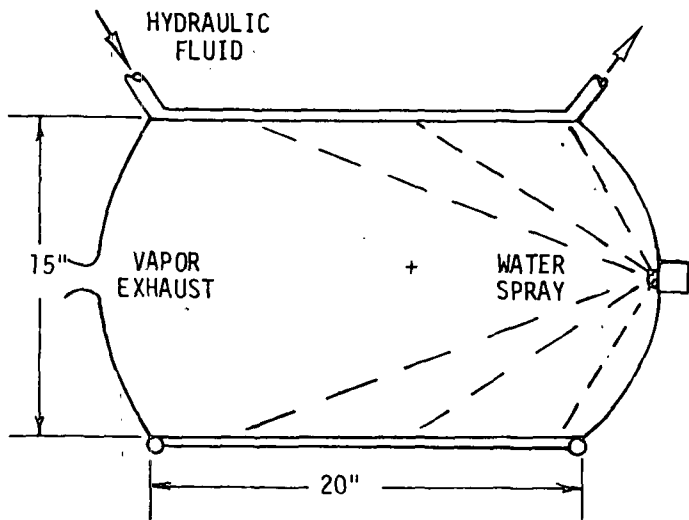


B-47

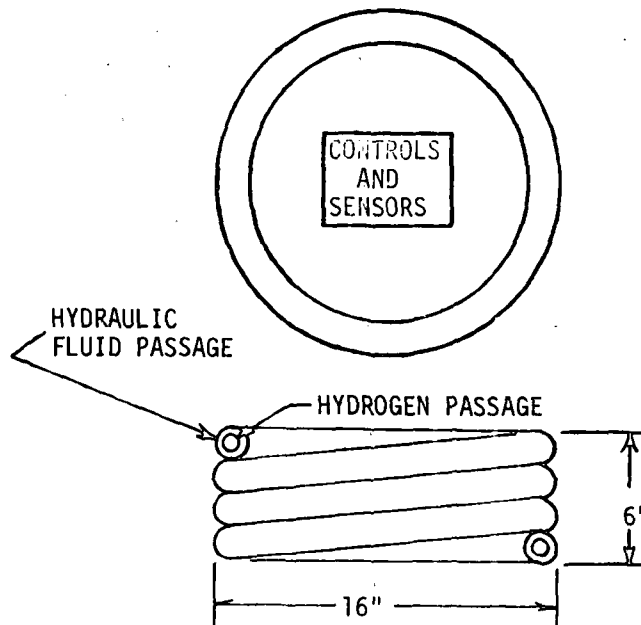
Figure B-36

# HEAT EXCHANGER COMPARISON

## HYDRAULIC EVAPORATOR



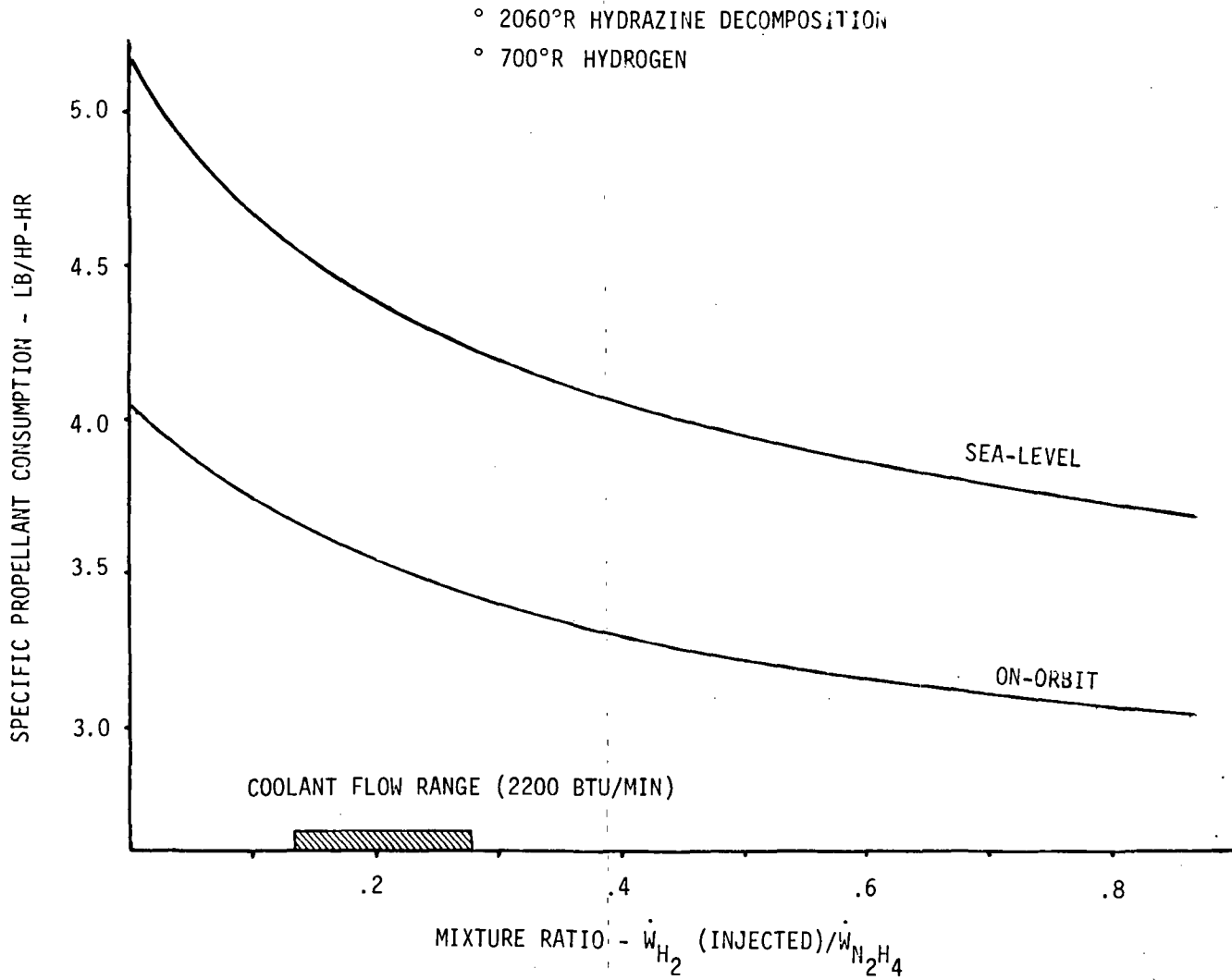
## SUPERCRITICAL HYDROGEN COAXIAL HEAT EXCHANGER



PARAMETER	H <sub>2</sub> O EVAPORATOR	HYDROGEN HX
NOMINAL COOLANT INLET TEMPERATURE	100°F	40°R
NOMINAL COOLANT INLET/CHAMBER PRESSURE	25 PSIA	300 PSIA
COOLANT FLOW RATE FOR 2200 BTU/MIN	2.015 LBM/MIN	0.89 LBM/MIN
NOMINAL EXIT/CHAMBER TEMP.	240°F	240°F
HEAT EXCHANGER WT. (DRY/WET)	40/49 LBM	11.1/21.0 LBM

APS-338

# EFFECT OF HYDROGEN INJECTION ON PERFORMANCE

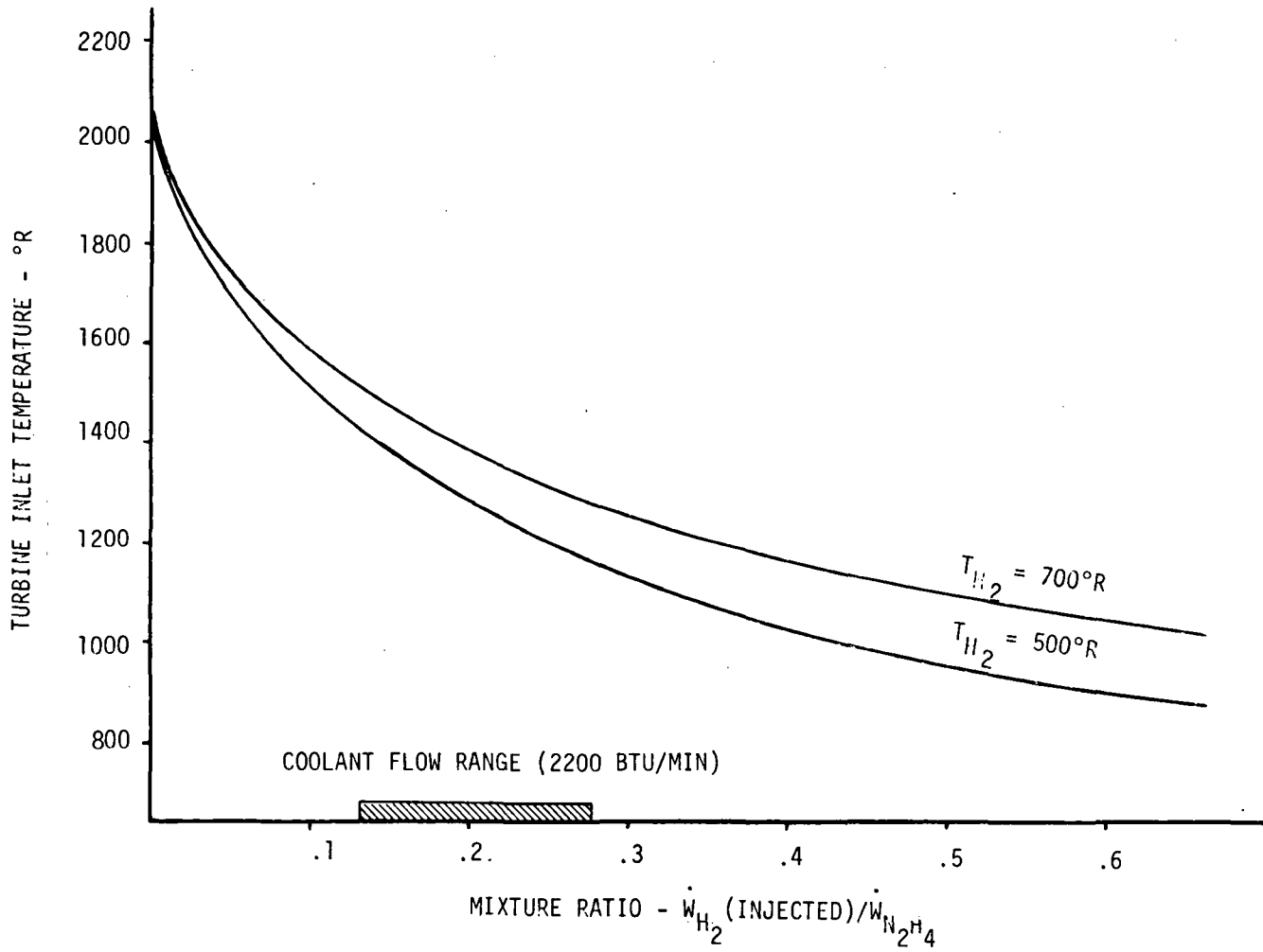


APS-337

B-49

Figure B-38

### EFFECT OF HYDROGEN INJECTION ON TURBINE INLET TEMPERATURE



APS-320

B-50

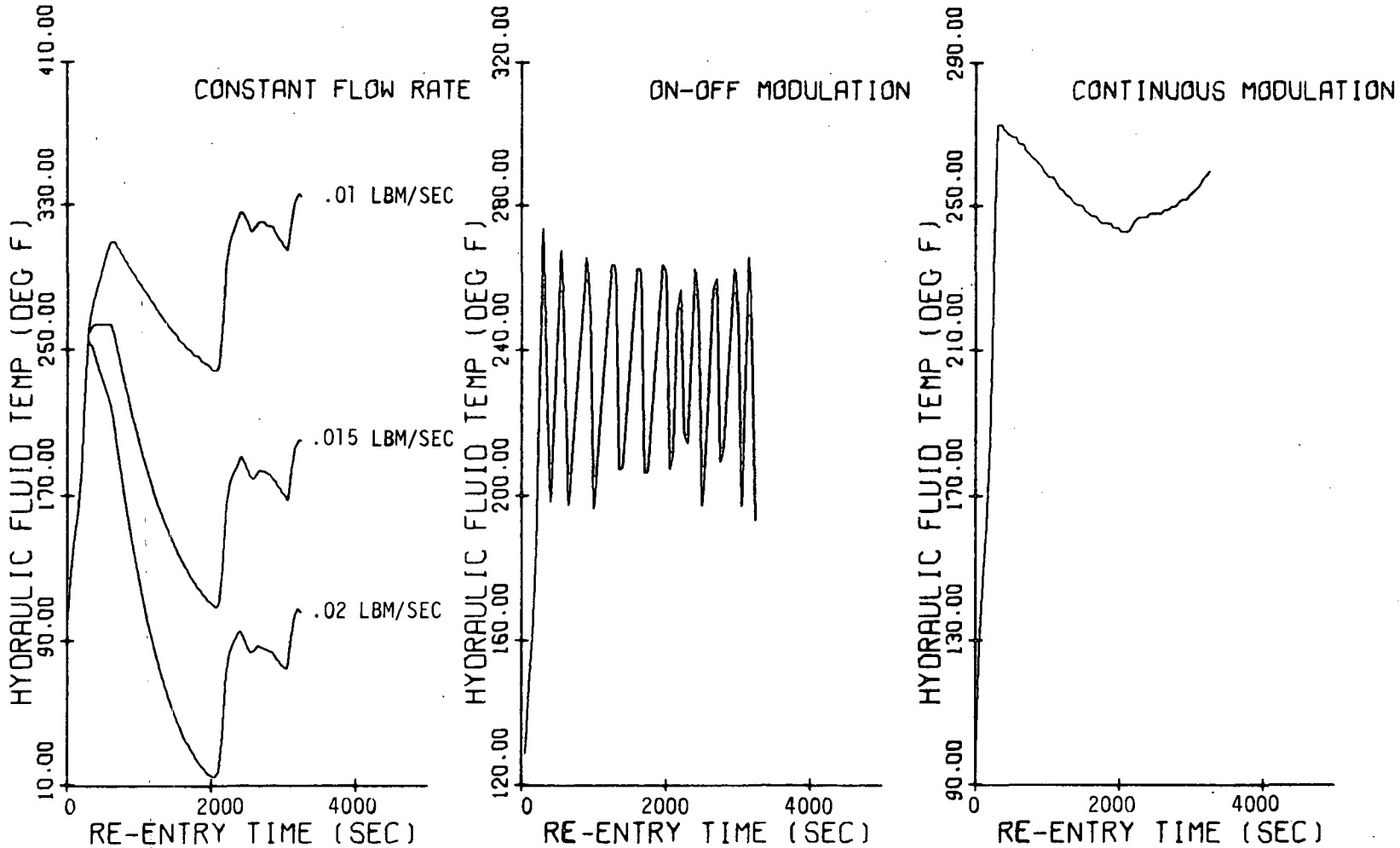
Figure B-39

Another factor which must be considered in the selection of the APU coolant is the complexity of the temperature control concept. Three control concepts were examined for the hydrogen coolant. The differences between them are illustrated by the hydraulic fluid temperature profiles shown in Figure B-40. The constant flowrate concept; the simplest of the three to implement, is not responsive to the heating level that must be absorbed. On-off modulation provides closer temperature control but results in intermittent injection of hydrogen into the turbine, making turbine speed control much more difficult. Continuous modulation provides tight temperature control and injection of the hydrogen into the turbine is in direct proportion to turbine power, a desirable feature.

These approaches are compared with similar coolant control approaches using water in Figure B-41. For the baseline system (two active, one standby, and one dormant APU), the nominal coolant requirements are 70 lbm and 167 lbm for hydrogen and water respectively. The weight of the hydrogen coolant loop, including liquid hydrogen tank and pressurization system, heat exchanger and associated controls is 335 lbm. However, a savings of 130 lbm in hydrazine and associated tankage results in an equivalent total weight of 205 lbm using hydrogen as the coolant. The coolant requirements for the water flash evaporator are significantly higher than for hydrogen. However, the water tankage and pressurization assemblies are much lighter. For the baseline system, the water, tank and pressurization assemblies, flash evaporator and associated controls have a total weight of 307 lbm.

The net weight differential of 102 lbm was considered to be too small to warrant the greater complexity and development risk associated with hydrogen storage and turbine injection. Thus the water coolant loop was selected as the preferred approach for the final system Phase E studies. Also influencing this decision was the high probability that waste water will be available from either the ECLS or fuel cells, negating any weight advantage shown for hydrogen cooling.

# LH2 COOLED HYDRAULIC FLUID TEMP HISTORY



APS-321

B-52

Figure B-40

APU COOLANT REQUIREMENTS

APU STATUS	TIME HX TURNS-ON (SEC)	TEMP. HYDRAULIC FLUID FOR TURN ON/OFF (°F)	MODE	COOLANT MASS FLOW RATE (LB/SEC)	COOLANT REQUIRED/APU (LB)	TOTAL COOLANT REQUIRED (LB)
HYDROGEN HEAT EXCHANGER						
ACTIVE	950	270	CONSTANT FLOW RATE	.015	34.95	} 70*
ACTIVE	950	270/200	ON-OFF	.05	33.50	
ACTIVE	1000	275	MODULATED	0-.04	27.00	
STAND-BY	2200	275	MODULATED	0-.04	8.38	
WATER FLASH EVAPORATOR						
ACTIVE	1000	275/270	ON-OFF	.05	63.00	} 167*
ACTIVE	1000	275	MODULATED	0-.096	64.79	
STAND-BY	2200	275	MODULATED	0-.032	21.00	

\* INCLUDES 10% CONTINGENCY



APPENDIX C

REENTRY EFFECTS ON THRUSTER LOCATION AND NOZZLE CONFIGURATION

Aerodynamic heating during reentry dictates a number of design selections including RCS thruster location and possibly thruster configuration selection. Vehicle heat shield penetrations by the thrusters create potential hot spots during entry and can result in excessive erosion of the thermal protection system (TPS) or overheating of the thrusters. The problem is most acute for the nose-mounted thrusters since the forward moldline contours offer very little reentry shielding. These thrusters are used to provide reentry yaw control and therefore protective nozzle covers cannot be used. Plug nozzle thrusters were considered as a means of circumventing the heating effects. The weight penalty associated with an RCS employing plug nozzle thrusters was defined and compared to a conventional nozzle system.

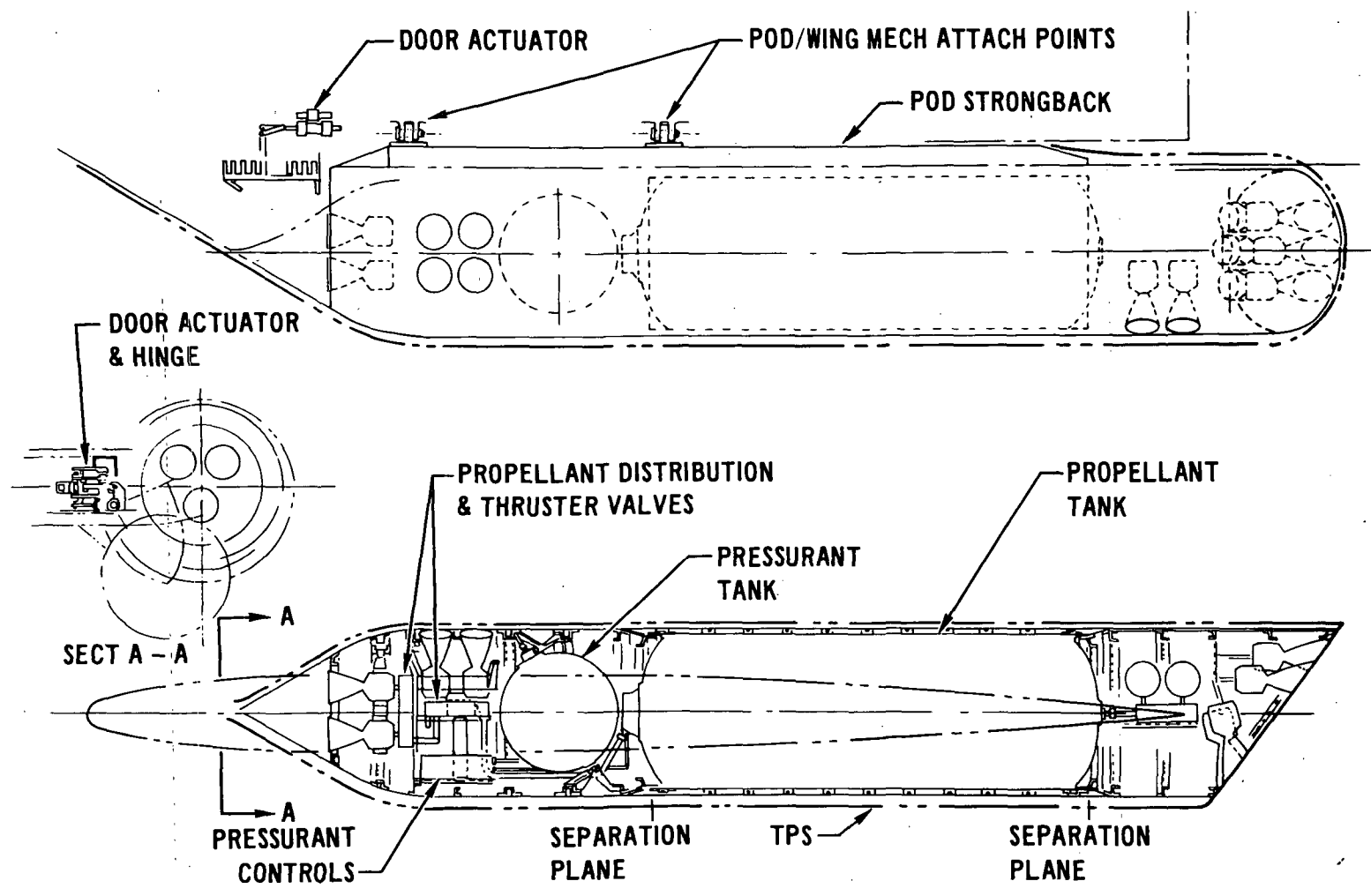
C1 Thruster Location - Limitations on nozzle temperatures make it desirable to place thrusters located in wing tip or fuselage pods in regions with minimum free stream flow impingement, either directly or indirectly, after flow expansion into the vehicle base region. Based on Reference C1, the turning angle for the flow has been conservatively identified as equal to the angle of attack ( $\alpha$ ) plus 20 degrees ( $\alpha + 20^\circ$ ). Thus for an assumed nominal entry angle of 34 deg, no thruster components should extend into a 54 deg section as measured from the horizontal with the apex located at the module lower rear corner. All thrusters in the aft regions of the wing tip and fuselage mounted pods have been placed using this criteria.

For forward firing thrusters, shielding cannot be achieved. Accordingly, these thrusters are protected by an ablative nose cap (shown in Figure C-1) which opens in space to permit unhindered thruster operation. These thrusters are used only for -X translation and are therefore not required during entry.

The thrusters mounted in the vehicle nose do fire during entry. Therefore, protective doors are unacceptable. The shape of the main fuselage similarly precludes the application of wake shielding to protect the thrusters. A typical forward thruster location is shown in Figure C-2 superimposed on a peak surface temperature map.

C2 Nozzle Configuration - Reentry heating rates are intensified in the vicinity of the forward mounted thrusters because of the flow separation,

# WING TIP RCS POD INSTALLATION

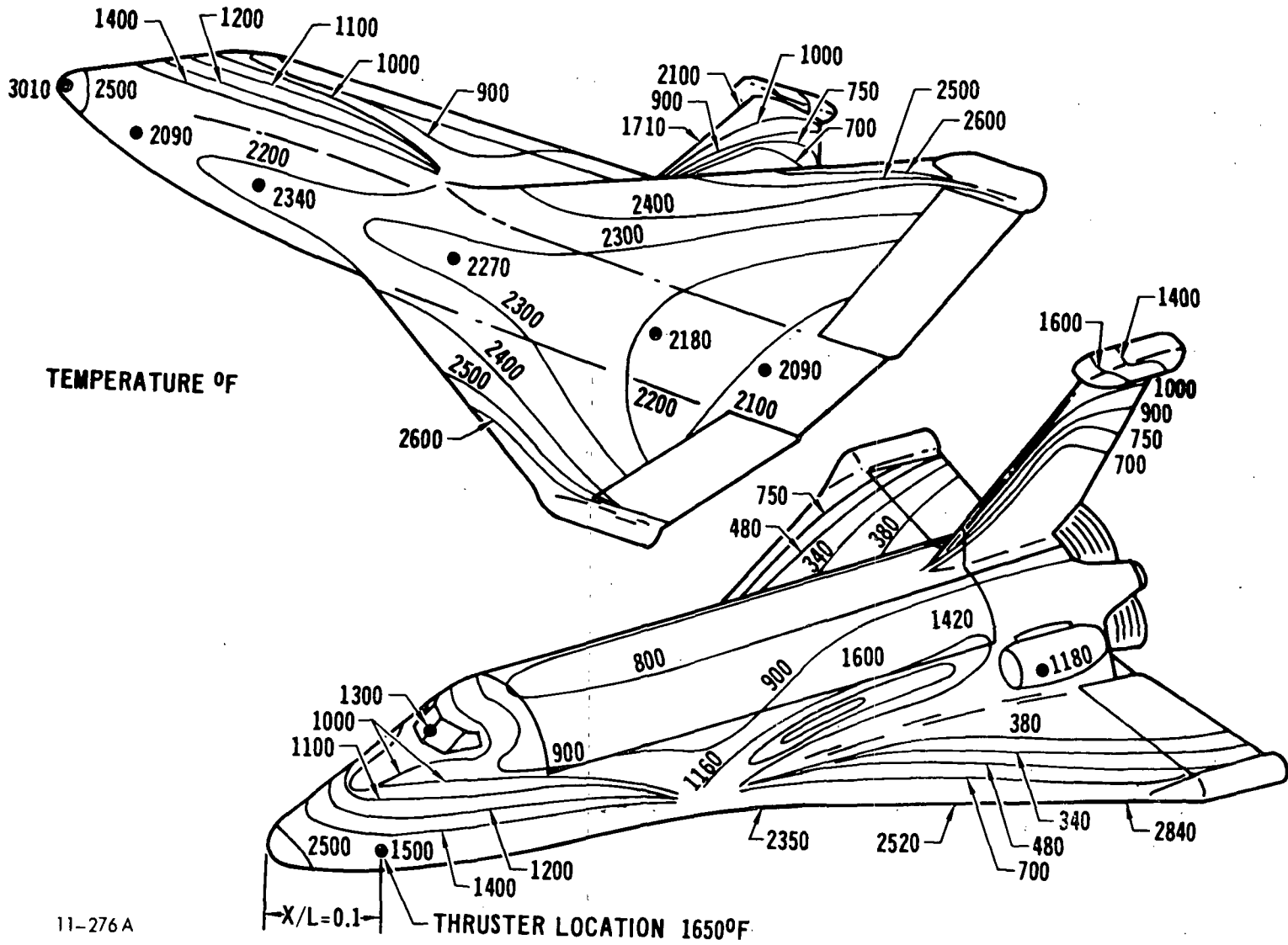


MCDONNELL DOUGLAS ASTRONAUTICS COMPANY - EAST

C-2

Figure C-1

# BASELINE ENTRY ISOTHERMS



C-3

Figure C-2

impingement, and reattachment in the nozzle. A detailed evaluation of the heating in the vicinity of the thrusters was beyond the scope of the current study and available experimental data was limited. However, order of magnitude effects and comparative differences were defined for plug and conventional bell type nozzles.

The principal characteristic lengths affecting heating are the gap width W, gap depth D, and the boundary layer displacement thickness  $\delta^*$ . In the limit of vanishing gap size, the heating rate approaches that for flow without any thrusters; i.e., gap temperatures approach the surface temperatures of Figure C-2. For gap dimensions ranging from  $0.1 \delta^*$  to  $1.0 \delta^*$ , the increased heating on the downstream lip will be approximately double the local heating rate. For gaps large compared to  $\delta^*$ , increased heating associated with direct impingement on the forward facing part of the gap will approach the local free stream stagnation conditions.

A greatly simplified model for nominal heating variations was based on correlations in References C2 thru C5 and is shown in Figure C-3. The displacement thickness for an experimental point from Reference C6 was computed using a simplified formula from Reference C7, evaluated for a free stream unit Reynolds number of  $8.6 \times 10^5/\text{ft}$ .

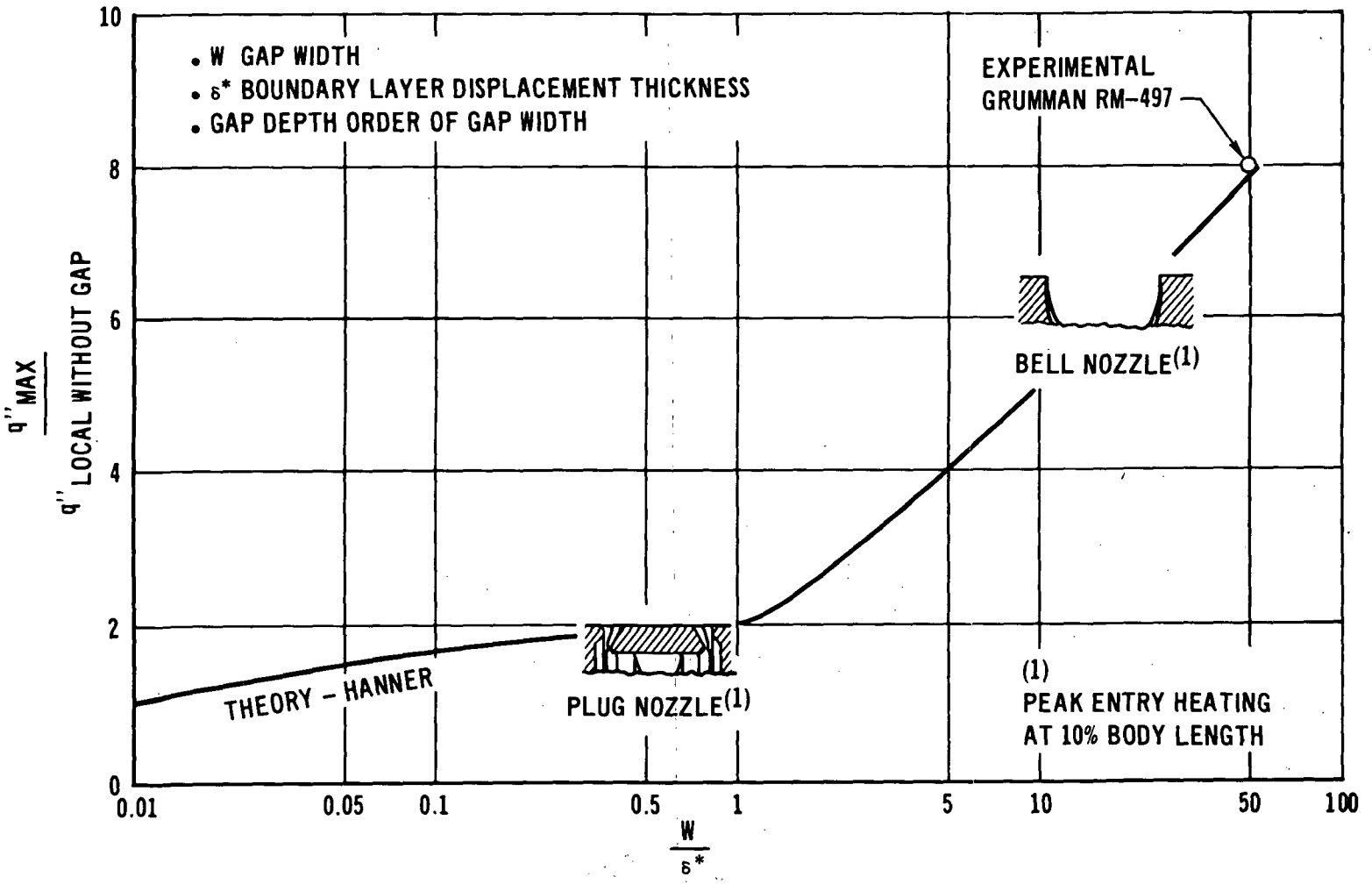
$$\delta^* = 1.73 \sqrt{\frac{X}{V_\infty x / 2}}$$

As shown in Figure C-3, there is general agreement between the experimental point and an extrapolation of the theory for the ratio of gap width to displacement thickness much greater than one ( $w/\delta^* \gg 1$ ).

A comparison of the nominal displacement thickness and associated heating using Figure C-3 is shown as a function of time for a typical entry in Figure C-4. Nominal nozzle sizes as shown in Figure C-5 illustrate the importance of entry heating in thruster selection. Entry maximum heating profiles for both nozzles are compared in Figure C-4 to the nominal entry heating rate for the lower fuselage position and in the absence of gaps. These calculations indicate that local temperatures may be more than  $600^\circ\text{F}$  higher for the bell nozzle than for a plug nozzle.

Experimental data reported in Reference C8 indicates even more severe heating effects accompany interference of an operating thruster. These data

### NOMINAL HEATING DEPENDENCE ON GAP SIZE

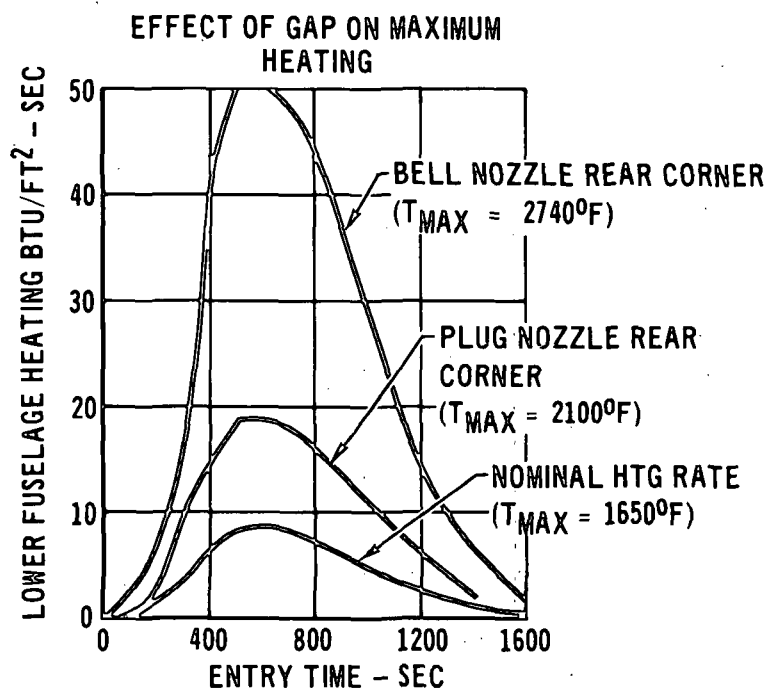
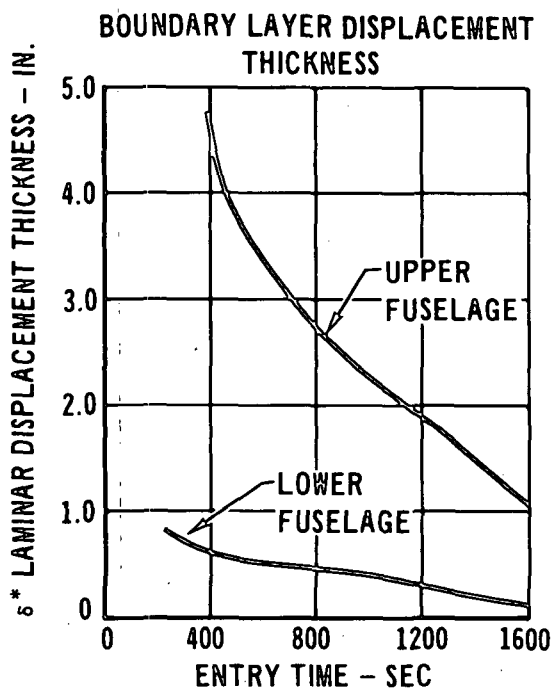


11-285

C-5

Figure C-3

# PLUG NOZZLE HEATING



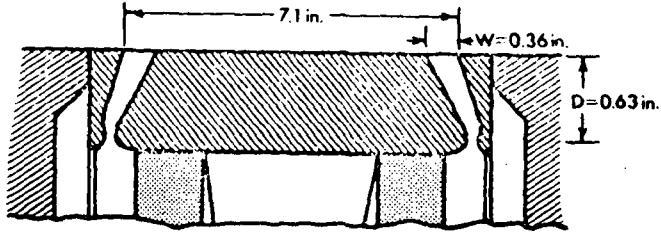
C-6

Figure C-4

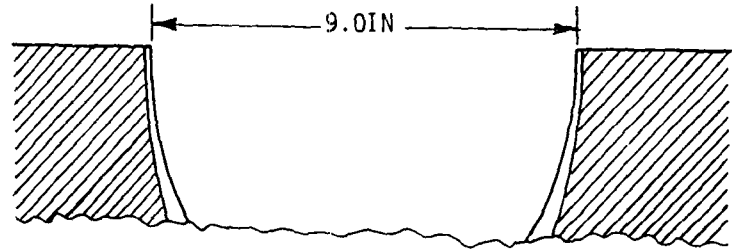
11-266

# COMPARISON OF PLUG NOZZLE/BELL NOZZLE "GAP" SIZE

- o EXPANSION RATIO
- BELL NOZZLE 40/1
- PLUGGED NOZZLE 20/1



PLUG NOZZLE SCHEMATIC



BELL NOZZLE SCHEMATIC

APS-406

C-7

Figure C-5

obtained from a test program conducted at AEDC show heating rates 10 - 40 times local nominal heating in the recirculation region upstream of the thruster.

Additional experimental testing will be required to validate the aero-heating implications on the plug nozzle versus bell nozzle decision. In view of these implications, various performance analyses were performed to evaluate the plug nozzle thrusters.

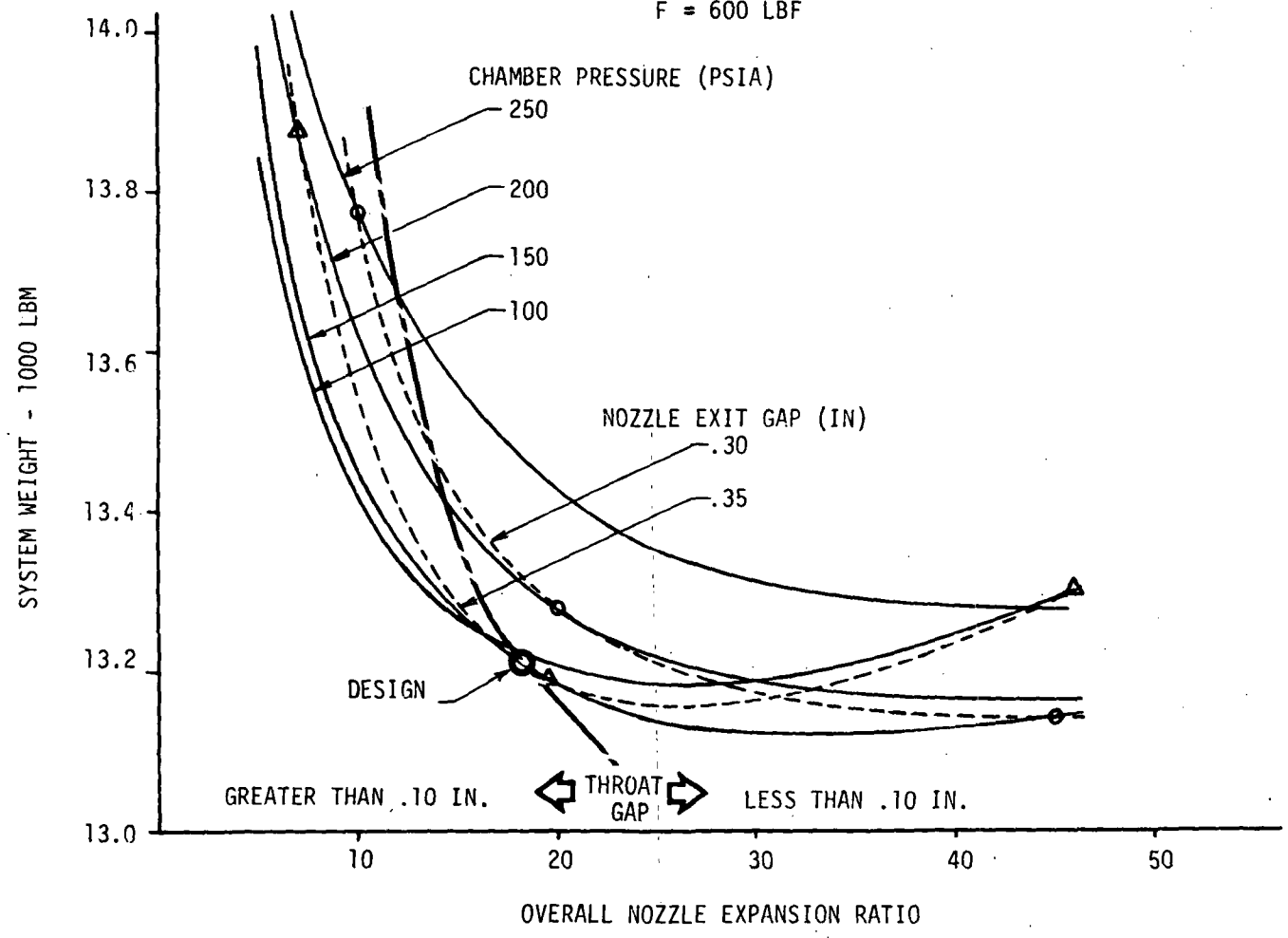
Design point optimization sensitivities for plug nozzle thrusters are shown in Figure C-6. These data reflect thruster performance characteristics as defined in Appendix A. Fabrication considerations require the nozzle throat size to be at least 0.10 inches, a locus which has been superimposed on the parametric curves. This throat size constraint limits the expansion ratio to a value of about 20.

A comparison between a plug nozzle thruster ( $P_c = 150 \text{ lbf/in.}^2$ ) configuration satisfying the above design constraints and a system employing conventional bell nozzle thrusters is made in Figure C-7. The figure shows that plug nozzle thrusters incur a system weight penalty of 324 lbm for the forward mounted, reference configuration. However, if the gap aero-heating near the vehicle nose should prove so severe that the installation of bell nozzle thrusters mounted in the forward fuselage proved to be untenable, a configuration comprised of wing and tail pods could be employed. For this configuration, the plug nozzle thrusters would provide a 572 lbm weight advantage compared to conventional thrusters.



# DESIGN POINT OPTIMIZATION FULLY TRUNCATED PLUG NOZZLE THRUSTERS

F = 600 LBF



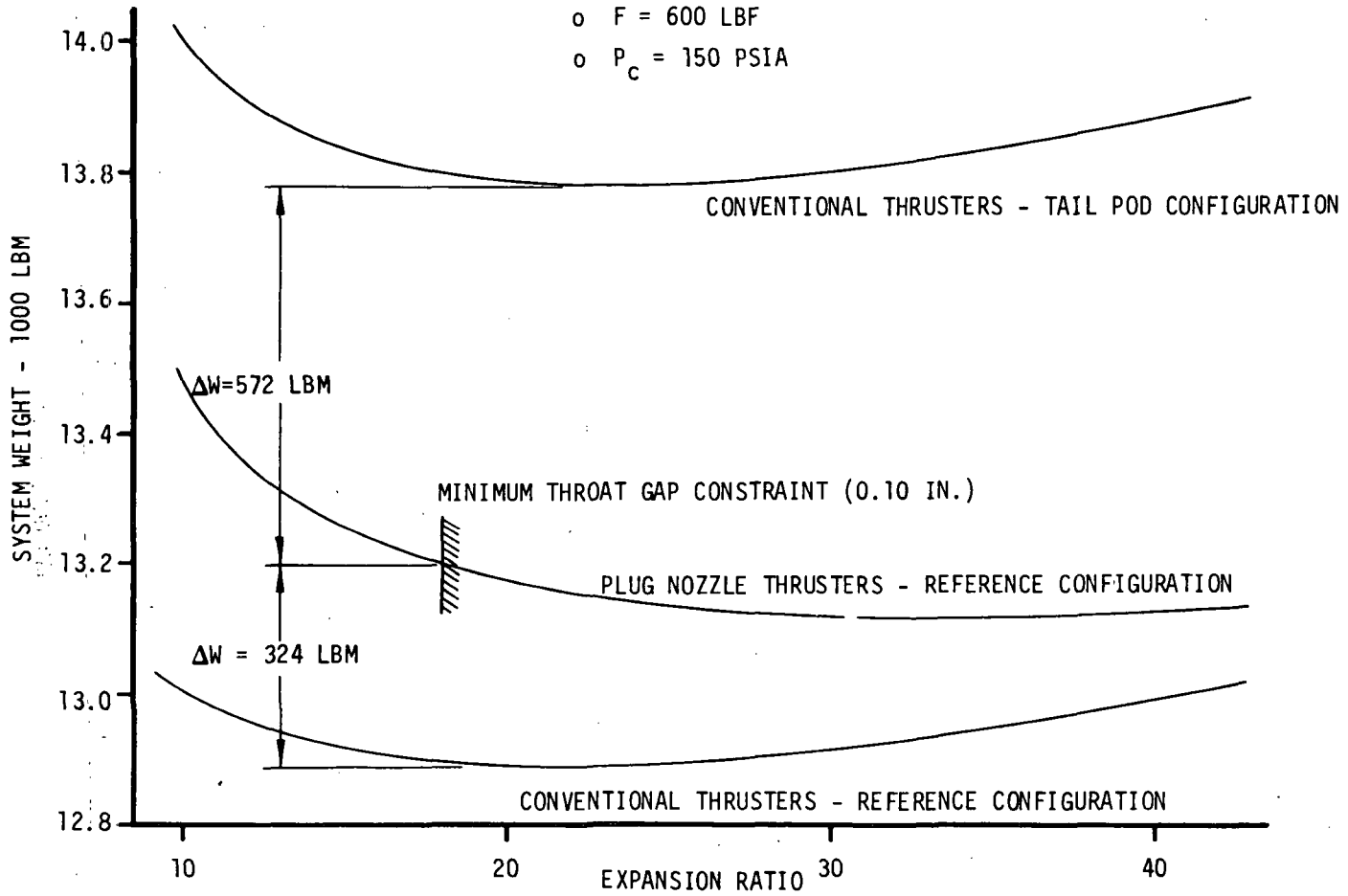
C-9

Figure C-6

APS-275

ALTERNATE CONFIGURATION SYSTEM WEIGHT COMPARISON

- o MODULAR RCS ( $N_2H_4$ )
- o  $F = 600$  LBF
- o  $P_c = 150$  PSIA



APS-820

C-10

Figure C-7

REFERENCES

- C-1 Staylor, W. F., and Goldberg, T. J., "Afterbody Pressure on Two Dimensional Boattailed Bodies Having Turbulent Boundary Layers at Mach 5.8," NASA TN D-2350, July 1964.
- C-2 Charwat, A. F., Dewey, C. F. Jr., Roos, J. N., and Hitz, J. A., "An Investigation of Separated Flows - Part II: Flow in the Cavity and Heat Transfer," Journal of the Aerospace Sciences, Vol. 28, No. 7, pp 502-532, July 1961.
- C-3 Stern, I. and Rowe, W. H., Jr., "Effect of Gap Size on Pressure and Heating Over the Flap of a Blunt Delta Wing in Hypersonic Flow, Journal of Spacecraft and Rockets," Vol. 4, No. 1, pp 109-114, January 1967.
- C-4 Dearing, J. D. and Hamilton, H. H., "Heat Transfer and Pressure Distributions Inside the Hinge-Line Gap of a Wedge Flap Combination at Mach Number 10.4," NASA TN D-4911, November 1968.
- C-5 Jaeck, C. L., "Analysis of Pressure and Heat Transfer on Surface Roughness Elements with Laminar and Turbulent Boundary Layers," NASA CR-537, August 1966.
- C-6 Kaufman, L. G. II, Leng, J., Hill, W. G. Jr, and Konopka, W. L., "Hypersonic Heating Distributions Caused by a Circular Cavity on a Flatplate Surface," Grumman Research Dept. Memo RM-497, March 1971.
- C-7 Röhsehow, W. M. and Choi, H. Y., "Heat, Mass, and Momentum Transfer," Prentice-Hall, Inc., 1961, p. 39.
- C-8 Brevig, O. and Wentink, R. S., "Space Shuttle Attitude Control System (ACS) Thruster Penetration Heating," Monthly Letter Report for August 1972, General Dynamics Convair Division.

APPENDIX D

ALTERNATE PRESSURIZATION CONCEPTS

In depth studies were conducted to evaluate the weight savings potential offered by advanced pressurization concepts. Pump fed, volatile liquid, and hydrazine decomposition (monopropellant systems only) pressurization systems were compared to the reference regulated helium system from the viewpoints of weight and complexity. The alternate systems are shown conceptually in Figure D-1.

A comparison of the primary considerations for the four concepts is presented in Figure D-2. The weight comparisons are based on the systems weight sensitivities to chamber pressure presented in Figures D-3, D-4, and D-5. The significant conclusions drawn from these comparisons are:

1. For monopropellant systems, hydrazine decomposition pressurization does show a weight savings over a regulated helium system but at the expense of increased complexity.
2. A pump fed system is lighter than its regulated helium counterpart, again with increased system complexity. Additionally, this system requires liquid pressure regulators, when used in bipropellant systems, to avoid large mixture ratio excursions.
3. Volatile liquid pressurization, although attractive from a reusable-refillable module aspect, is not weight competitive with any of the other systems.

Figure D-6 summarizes the procedures used in the analysis of the various concepts. These concepts are discussed in detail in the sections that follow.

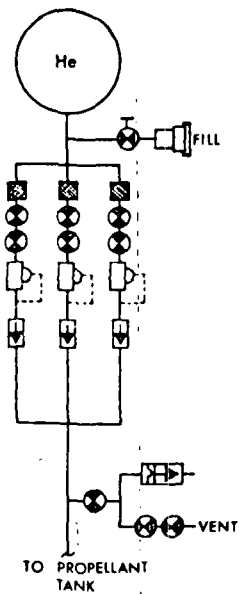
D1 Regulated Helium - A regulated ambient temperature storage helium pressurization system served as the reference for this study. This system, shown in Schematic 1 of Figure D-1, employs gaseous helium stored at 4500 lbf/in.<sup>2</sup> in titanium pressure bottles. For bipropellant systems, the fuel and oxidizer have separate pressurization systems. Propellant tank operating pressure is maintained by the use of pressure regulators, and fail operational/fail safe redundancy is provided with three parallel regulator branches. The advantages of extensive previous usage and minimal development costs overshadow the weight gains afforded by some of the more complex systems.

D2 Hydrazine Decomposition - The use of hydrazine decomposition warm gas pressurization was limited to the monopropellant systems because of compatibil-

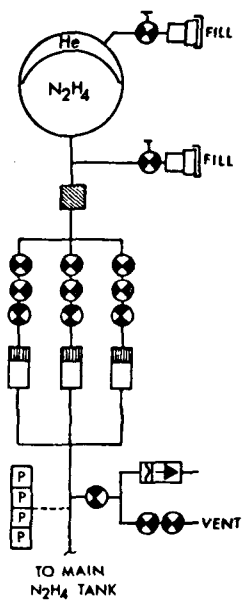
E243-53

ALTERNATE PRESSURIZATION CONCEPTS

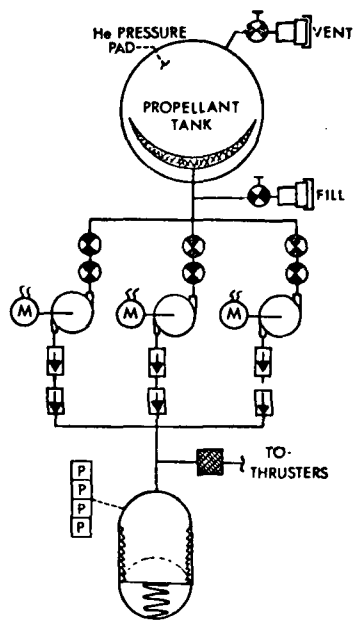
HELIUM



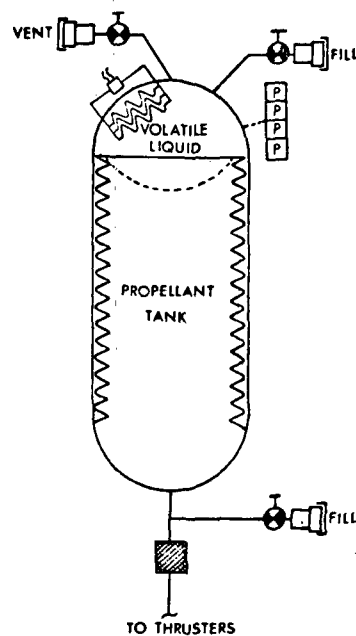
HYDRAZINE  
DECOMPOSITION



PUMP FEED



VOLATILE LIQUID



D-2

Figure D-1

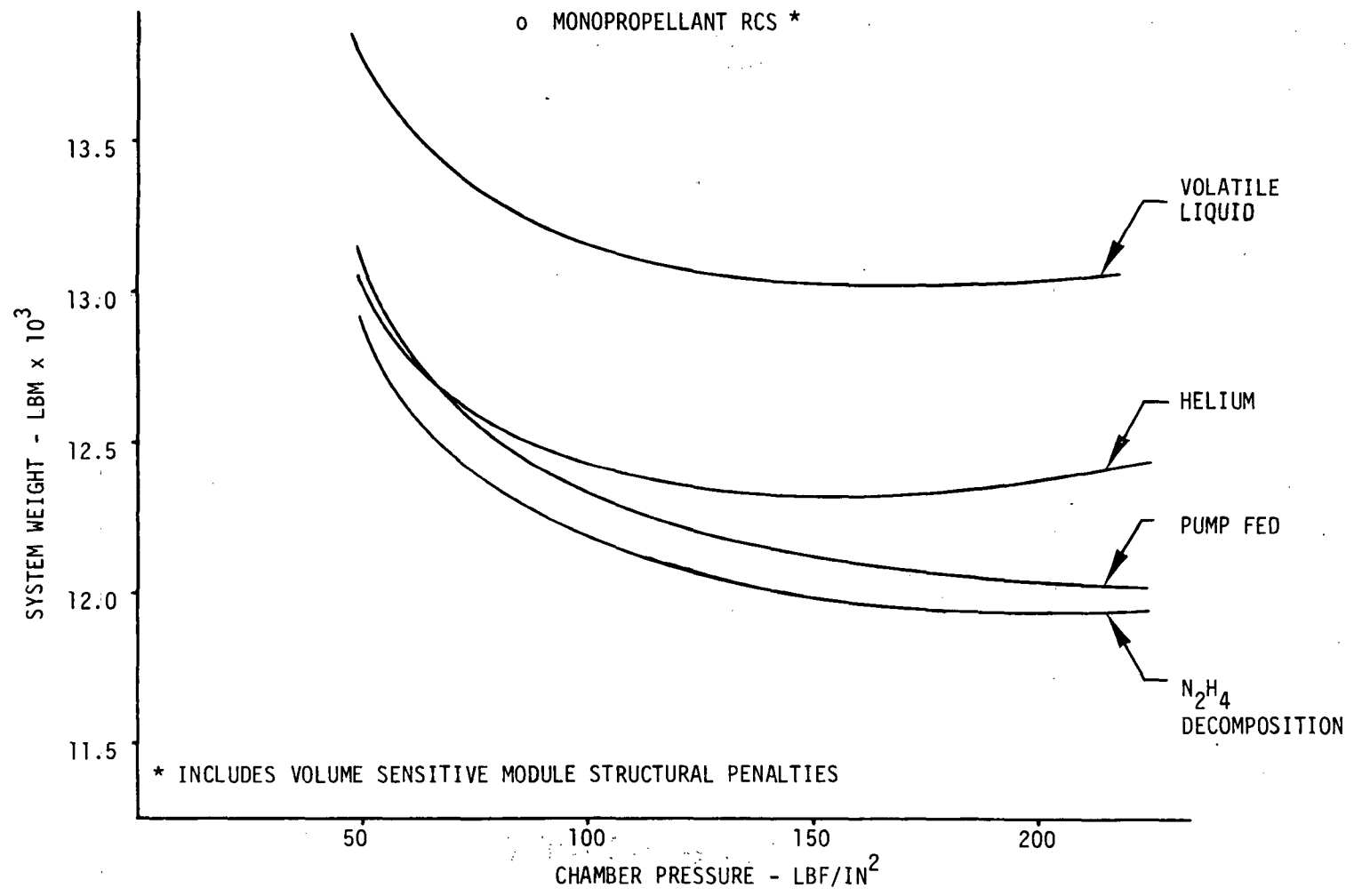
## COMPARISON OF CANDIDATE PRESSURIZATION CONCEPTS

	REGULATED HELIUM	N <sub>2</sub> H <sub>4</sub> DECOMPOSITION	PUMP FEED	VOLATILE LIQUID
RELATIVE WEIGHT				
- APU	+ 137	+ 20	REF	+ 43
- MONOPROPELLANT RCS	+ 375	REF	+100	+ 1075
- BIPROPELLANT RCS (OMS)	+ 700	-	REF	+ 4400
RELATIVE VOLUME	5.0	1.0	2.0	2.2
PRESSURE BAND	+ 2.5%	+ 2.7%	+ 100* - 0%	+ 85* - 0%
DESIGN OPERATING TEMPERATURE	AMBIENT	200°F	AMBIENT	125 - 165°F
SENSITIVITY TO MISSION DUTY CYCLE	FAIRLY INSENSITIVE	FAIRLY INSENSITIVE	ACCUMULATOR SIZE LIMITS RCS ΔV	HEATER POWER LEVEL LIMITS TOTAL RCS THRUST
PROPELLANT UTILIZATION/ UNBALANCE ERROR CONTROL BUDGET	SMALL	SMALL	LARGE O/F ERROR FOR ACCUMULATORS OUT-OF-PHASE	LARGE ERRORS DUE TO MODULE TEMPERATURE DIFFERENCES
MAJOR ADVANTAGES	WIDE APPLICATION; MINIMAL DEVELOPMENT	LIGHTWEIGHT; REDUCES THERMAL CONTROL	LIGHTWEIGHT; PRESSURANT LEAKAGE NOT CRITICAL	RELIABLE-NO-MOVING PARTS, NO FILL/VENT REQUIREMENT FOR RECYCLE
MAJOR DISADVANTAGES	HEAVY; HIGH REGULATOR FAILURE RATE	COMPLEX; TIGHT PRESSURE DEADBAND NECESSITATES MANY PUMP CYCLES; REQUIRES HEAT EXCHANGER	WIDE VARIATION IN THRUSTER INLET PRESSURE OR HIGH PUMP POWER;	HEAVY; WIDE PRESSURE BAND; HIGH POWER REQUIREMENT

\*WITHOUT LIQUID PRESSURE REGULATION

11-278A

# SYSTEM WEIGHT OPTIMIZATION PRESSURIZATION ASSEMBLY CONCEPTS

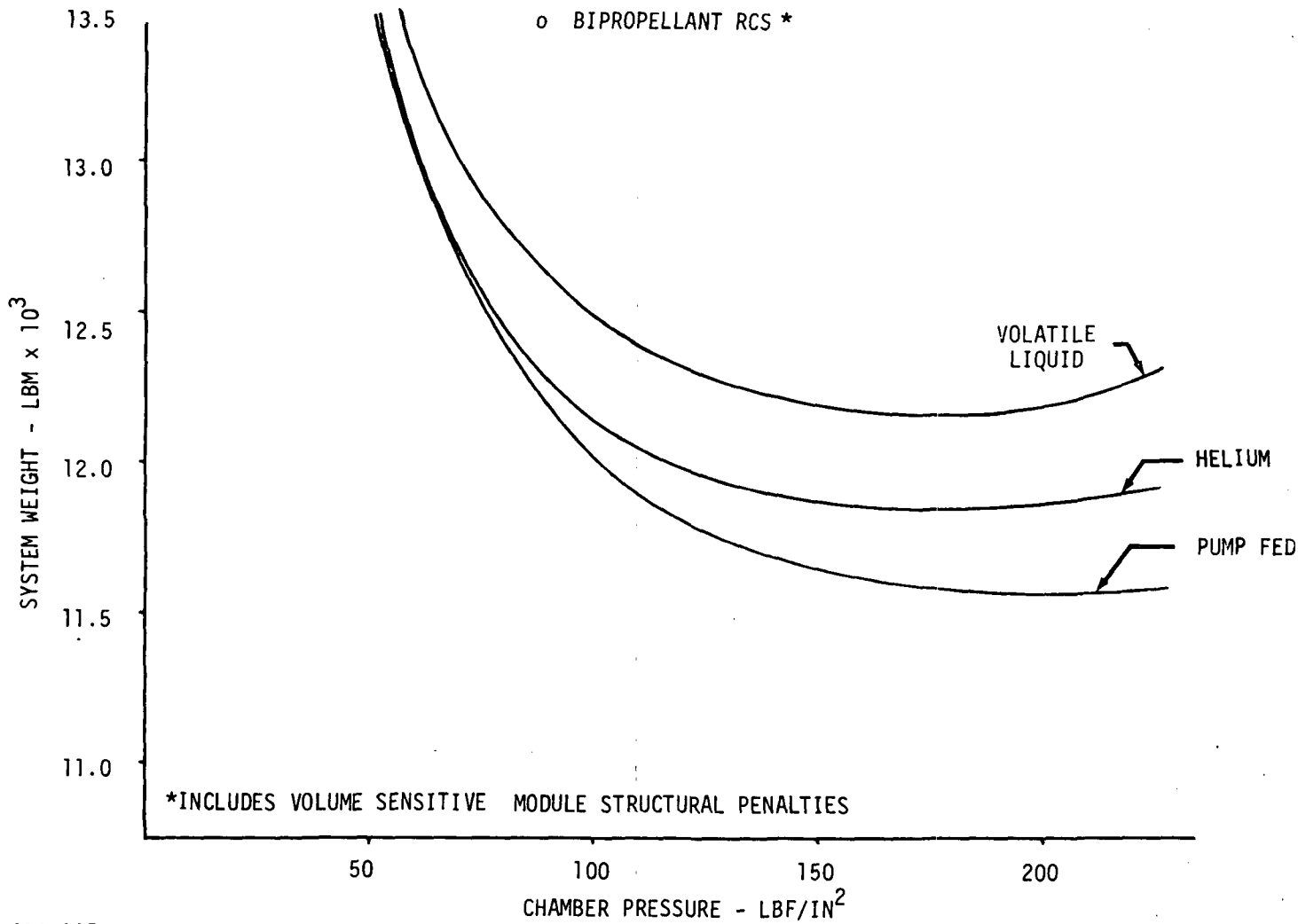


D-4

Figure D-3

APS-391

# SYSTEM WEIGHT OPTIMIZATION PRESSURIZATION ASSEMBLY CONCEPTS



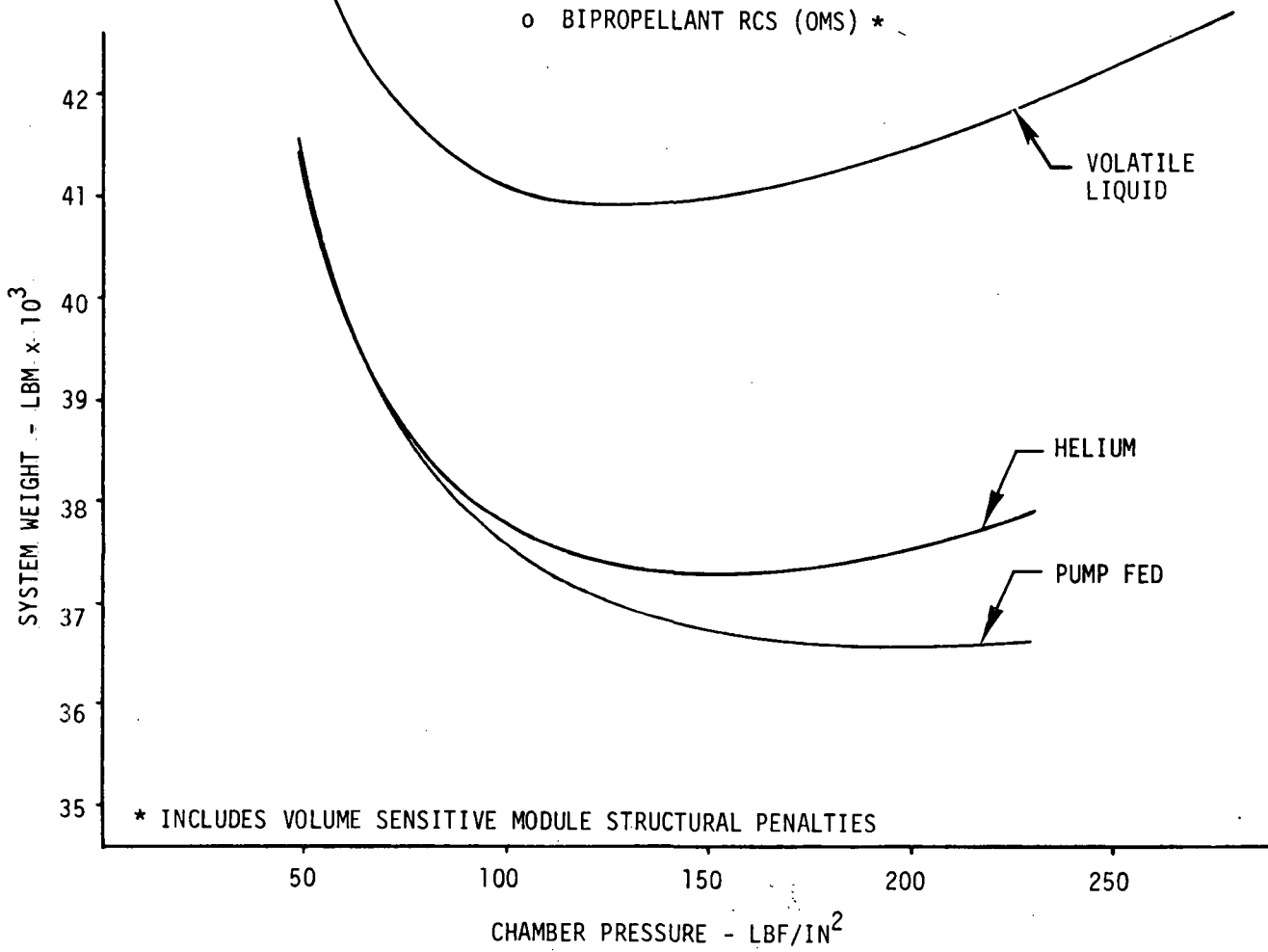
APS-327

D-5

Figure D-4



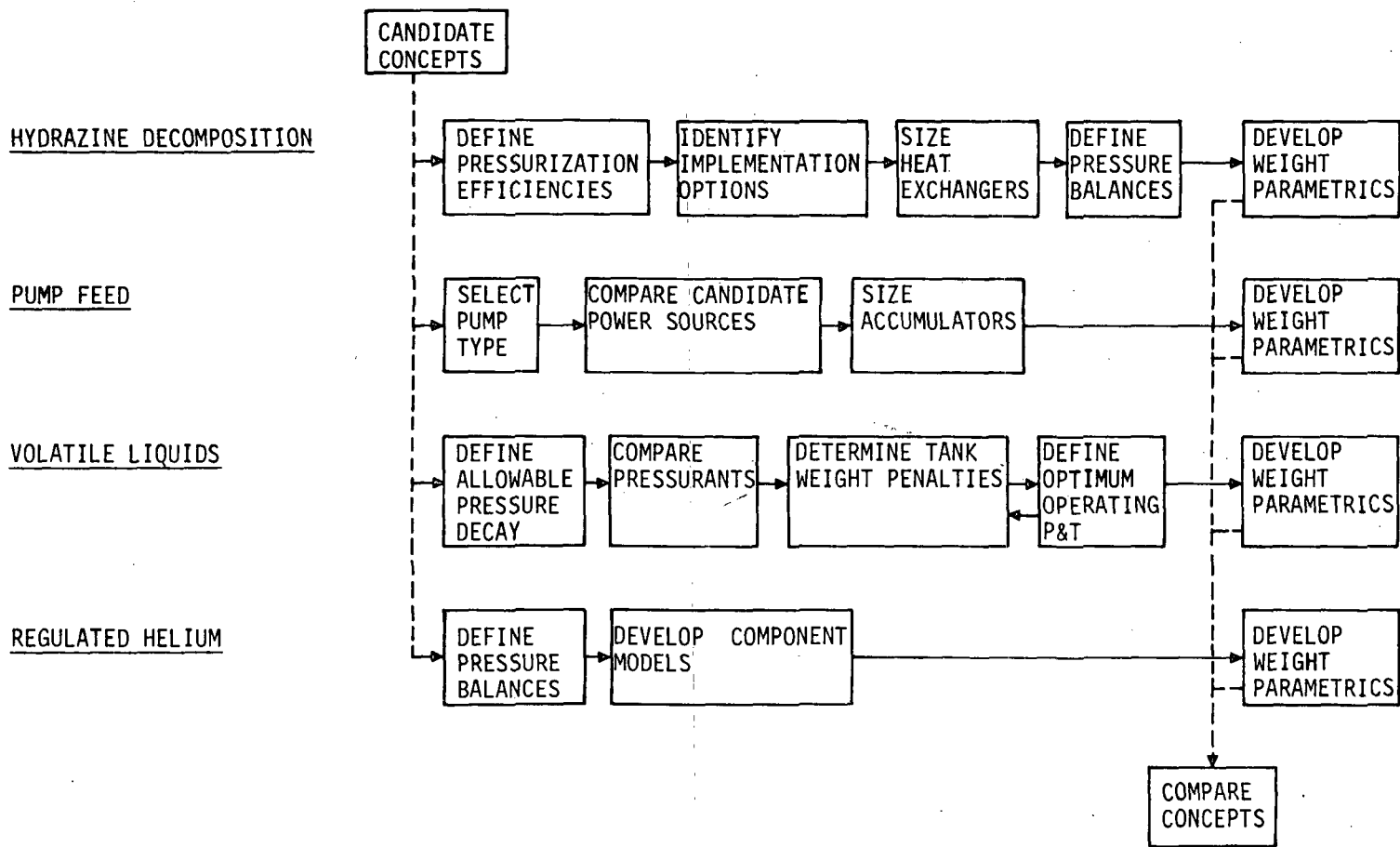
# SYSTEM WEIGHT OPTIMIZATION PRESSURIZATION ASSEMBLY CONCEPTS



D-6

Figure D-5

# ADVANCED PRESSURIZATION CONCEPT STUDIES



D-7

Figure D-6

APS-235

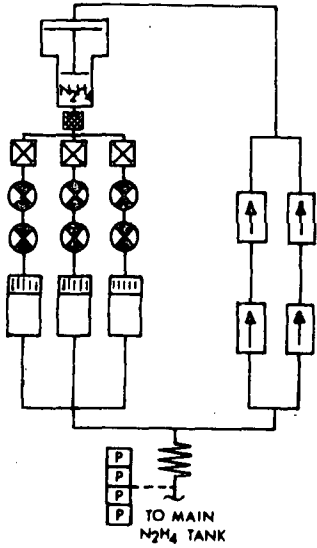
ity problems between the hydrazine reaction products and the oxidizer of a bipropellant system. Various methods of implementing this concept were evaluated and are shown schematically in Figure D-7. Schematic 1 is a single stage gas generator fed by a differential area bootstrap tank. In Schematic 2, a second stage, comprised of a spherical propellant tank and catalytic reactor, has been added. Pressurization of the second stage tank is achieved by the first stage differential area bootstrap tank and gas generator. In Schematic 3, the pressurant tank is operated in a blowdown mode using a helium pressure pad. A pump fed system is considered in Schematic 4. Here, fuel is drawn directly from the main propellant tank to feed the gas generator. Pump head rise is defined by gas generator and propellant tank pressure drops at maximum flow. A gear pump with D.C. motor drive was selected for this approach due to the low flowrates involved.

For all concepts, a heat exchanger is employed downstream of the reactor to control the inlet gas temperature to the main propellant tank to 200°F. The heat exchanger consists of a single stainless steel tube wrapped around the RCS propellant tank. A heat exchanger bypass is used to preclude excessive pressurant energy loss during periods of low demand. The total heat input to the RCS propellant tank is 5.3 KW-HR, or 44 percent of the 11.9 KW-HR heater requirement for the monopropellant RCS thermal control. The resultant savings in fuel cell weight is 31 lbm.

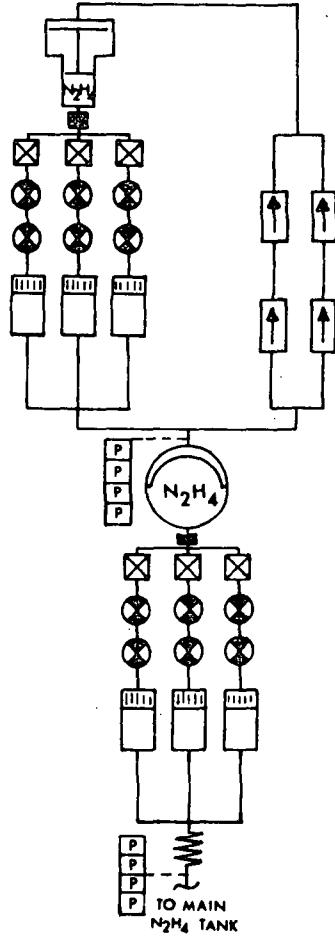
A weight comparison of these hydrazine decomposition pressurization methods is shown in Figures D-8 and D-9 for a wide range of propellant tank volumes and pressures. In Figure D-8, the total pressurization assembly weights are compared to each other and to the reference helium system. This figure indicates that the hydrazine decomposition concept is lighter than the reference system for all implementation methods considered. The mass fractions (pressurant weight/total pressurization assembly weight) are presented in Figure D-9. These results show that the single stage differential area bootstrap system (Schematic 1) is least attractive of the candidate concepts, except at very small pressurant requirements. A detailed weight breakdown at the RCS modular design point is given in Figure D-10 for each concept. Although these concepts show a potential weight savings over a stored gas helium system, they are more complex, requiring relatively sophisticated controls to maintain a tight pressure deadband and a heat exchanger to prevent the possibility of propellant decomposition at the elevated temperatures of the reactor exhaust.

# HYDRAZINE DECOMPOSITION PRESSURIZATION METHODS

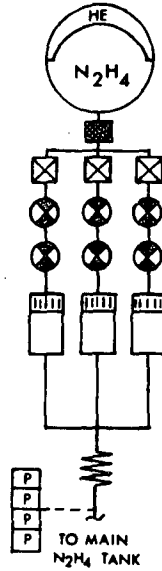
**SCHEMATIC 1**  
SINGLE STAGE GAS GENERATOR,  
DIFFERENTIAL AREA BOOTSTRAP



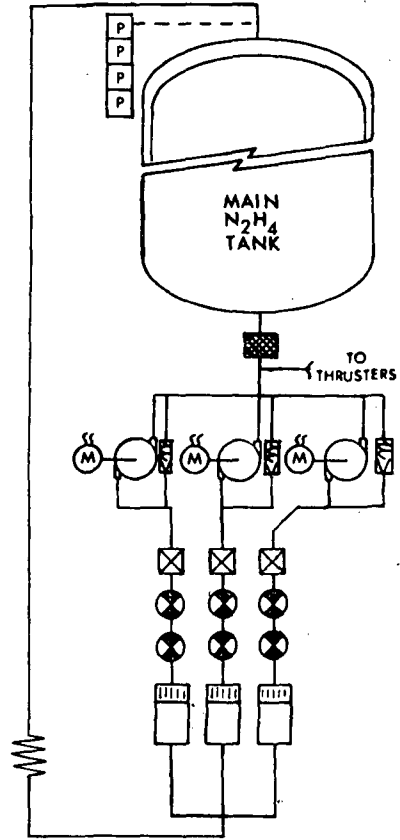
**SCHEMATIC 2**  
TWO STAGE GAS GENERATOR,  
DIFFERENTIAL AREA BOOTSTRAP




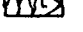
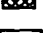
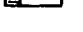
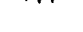


**SCHEMATIC 3**  
HELIUM BLOWDOWN



**SCHEMATIC 4**  
PUMP-FED BOOTSTRAP



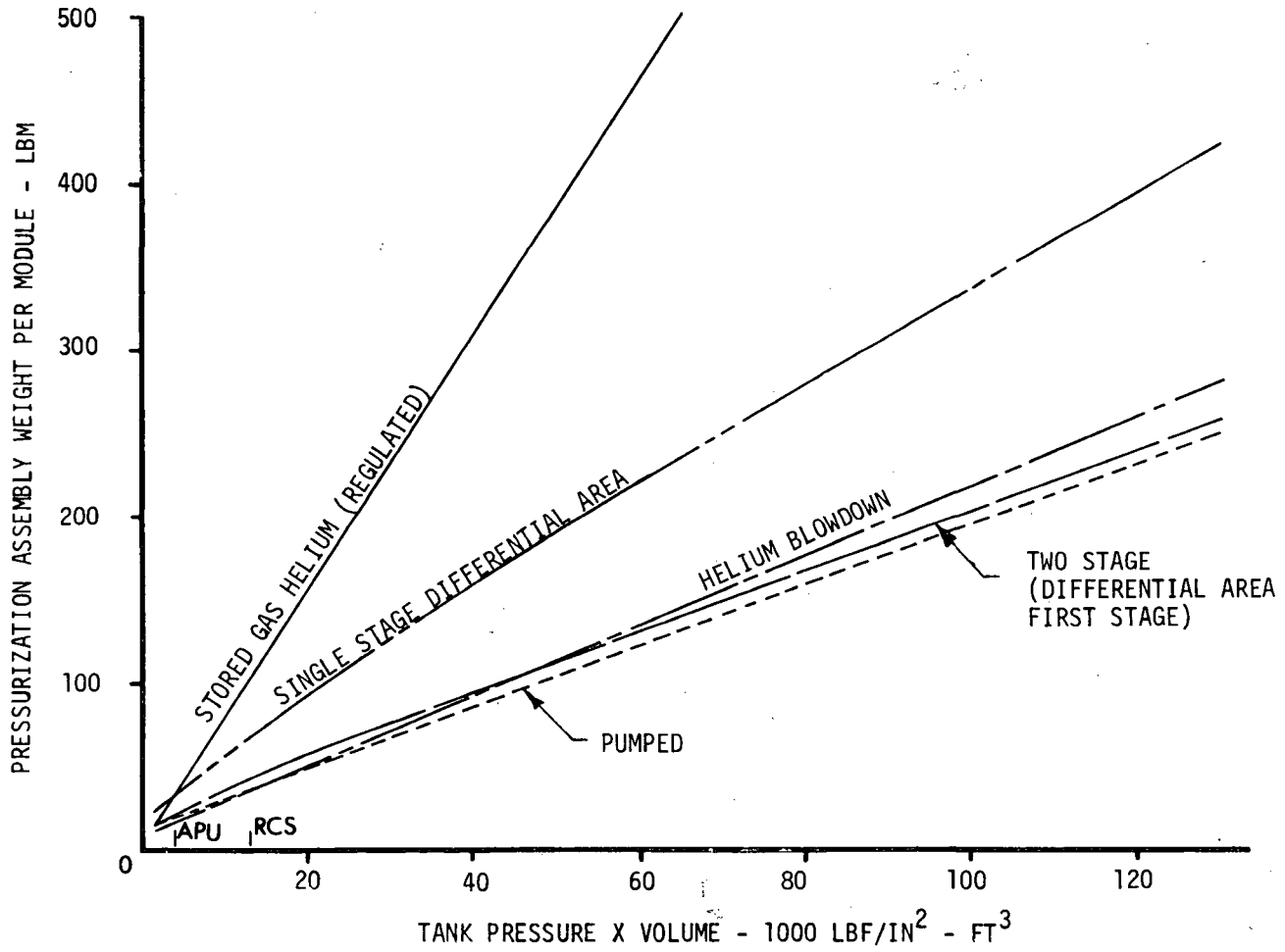
-  CONTROL VALVE
-  ISOLATION VALVE
-  CHECK VALVE
-  BYPASS VALVE
-  FILTER
-  GAS GENERATOR
-  HEAT EXCHANGER

APS-297

D-9

Figure D-7

# HYDRAZINE PRESSURIZATION WEIGHT COMPARISON o MONOPROPELLANT



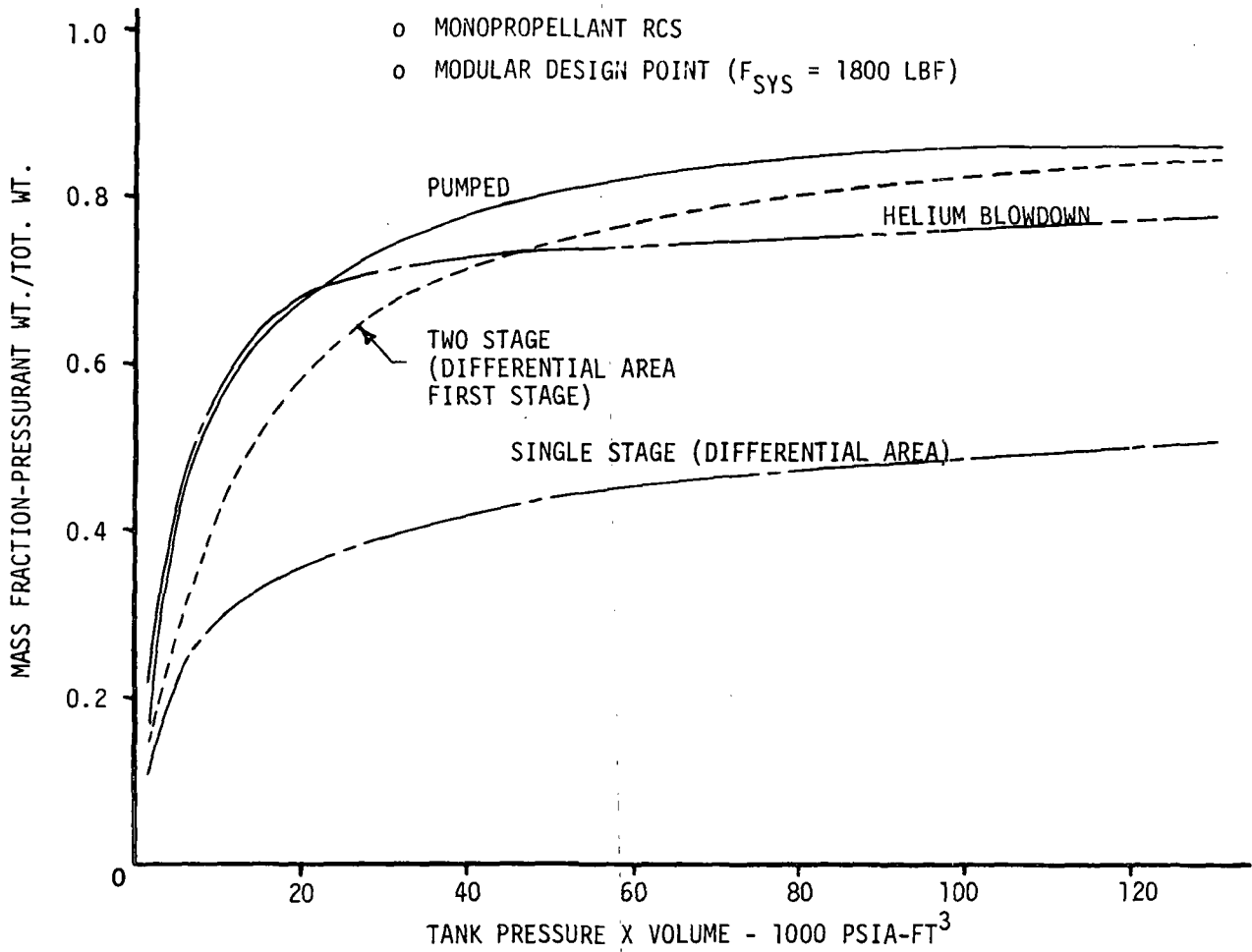
D-10

MCDONNELL DOUGLAS AERONAUTICS COMPANY - EAST

Figure D-8

APS-290

# HYDRAZINE PRESSURIZATION MASS FRACTION



HYDRAZINE DECOMPOSITION PRESSURIZATION COMPONENT WTS.

- o MONOPROPELLANT
- o RCS MODULAR DESIGN POINT

COMPONENT	METHOD			
	1. SINGLE STAGE G.G., DIFF AREA	2. TWO STAGE G.G., DIFF AREA	3. HELIUM BLOWDOWN	4. PUMP FED
DIFFERENTIAL AREA, S.S. GAS GENERATOR	100.50	10.16	-----	-----
PRESSURANT TANK, INC. BLADDER	-----	10.94	17.66	-----
GAS GENERATORS (3)	-----	7.50	7.50	7.50
HEAT EXCHANGER	5.88	5.88	5.88	5.88
PUMP/MOTOR/BATTERIES	-----	-----	-----	21.66
VALVES, CHECK	6.99	8.88	2.98	3.00
ISOLATION	12.46	8.75	3.76	3.76
CONTROL	3.00	6.70	2.56	2.78
LINES	6.16	9.02	3.86	5.48
Δ MAIN TANK WEIGHT, INC. BLADDER	-----	-----	-----	2.22
PRESSURANT	59.02	59.74	59.24	59.48
TOTAL,* LBM	194.01	127.57	103.44	111.76

\* REFERENCE REGULATED HELIUM PRESSURIZATION SYSTEM WEIGHT = 285 LBM

MCDONNELL DOUGLAS ASTRONAUTICS COMPANY - EAST

D-12

Figure D-10

APS-299

D3 Pump Fed - The pump fed system configuration is shown schematically in Figure D-11 for both monopropellant and bipropellants. As shown, propellants are drawn directly from the main propellant tanks; pumped to high pressure by motor-driven pumps; and stored in liquid accumulators from which they are supplied to the thrusters.

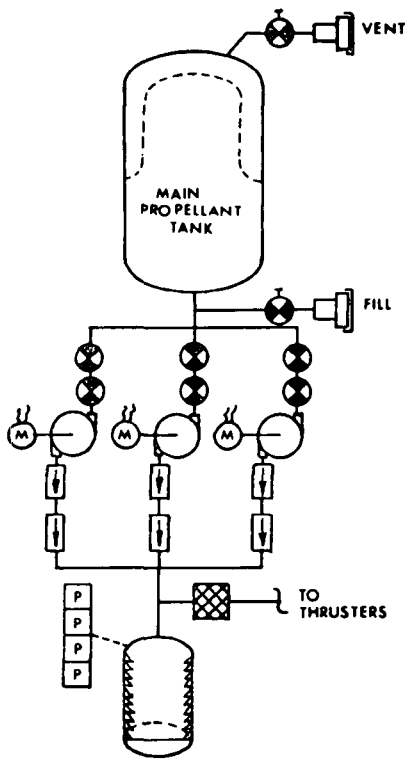
Pump and power source evaluation was based on the previous liquid oxygen hydrogen studies reported in Reference J. For the RCS, piston pumps (5 GPM per propellant) driven by D.C. motors were selected for use. Motor driven vane pumps were selected for use in the RCS(OMS) where propellant flowrates are 25 GPM. Also considered for usage was a motor driven gear pump but, as shown in Figure D-12, it was not weight competitive with the other two pump types considered. Also shown in this figure, is the weight of helium and increased propellant tank pressure shell weight required to supply the needed net positive suction pressure to the pumps. An optimum is obtained at an NPSP of 8 lbf/in.<sup>2</sup> for the piston-pumps and 19 lbf/in.<sup>2</sup> for the vane pumps. Pump power requirements were supplied by fuel cells and rechargeable batteries using the weight penalty model described in Figure D-13. For the RCS, the accumulators provide propellant for a 20 FPS burn in conjunction with two pumps running; pump flow capacities were established by minimum thrust requirements ( $F = 160$  lbf per pod) as dictated by accumulator recharge time during reentry. For the RCS(OMS), the pumps must meet system steady-state flow demands during a translation maneuver ( $F = 2400$  lbf per pod) with the accumulators providing flow during pump start-up (2 sec). The tradeoffs involved in this accumulator sizing optimization are shown in Figure D-14 where pump power requirements (i.e. fuel cell weight) is balanced against accumulator weight.

A weight comparison of the pump fed and the regulated-helium pressurization assemblies is shown in Figure D-15 for the monopropellant and in Figure D-16 for the bipropellant systems. As indicated in these figures, the pump fed assembly provides a significant weight advantage over regulated helium for large products of pressure and volume but at the RCS and RCS(OMS) design points, regulated helium is weight competitive. Detailed weight breakdowns for pump fed systems are tabulated in Figure D-17 for the RCS and RCS(OMS) design points. It should be noted that in this analysis, helium pressurization was assumed for the forward system pods since the high fixed weight of pumps/accumulators makes their use impractical for small tank volumes. This system, even at the larger tank volumes where it is lighter than the regulated helium system, has the disadvantages of supplying the

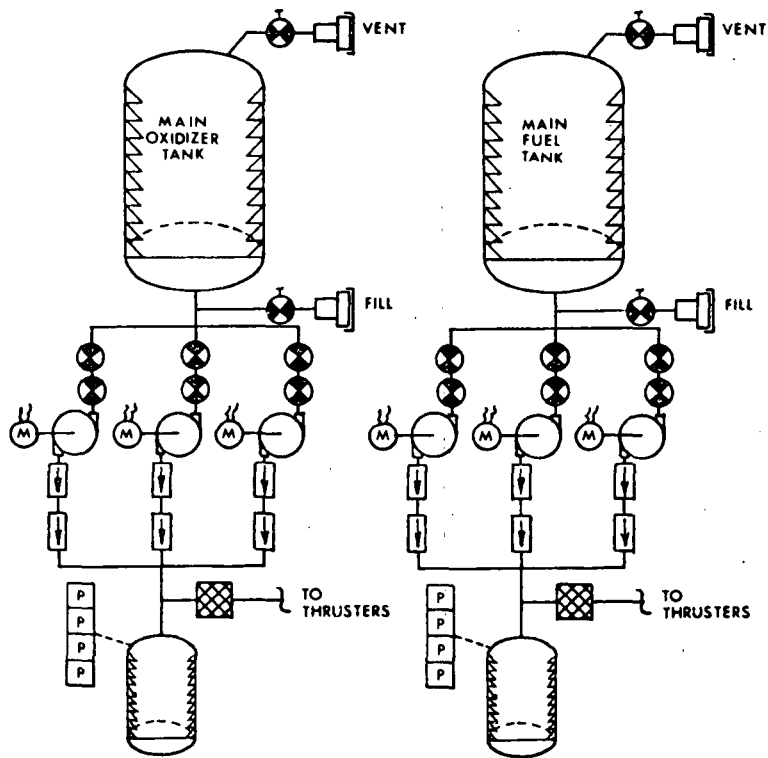


# PUMP FED SYSTEM SCHEMATICS

◦ MONOPROPELLANT

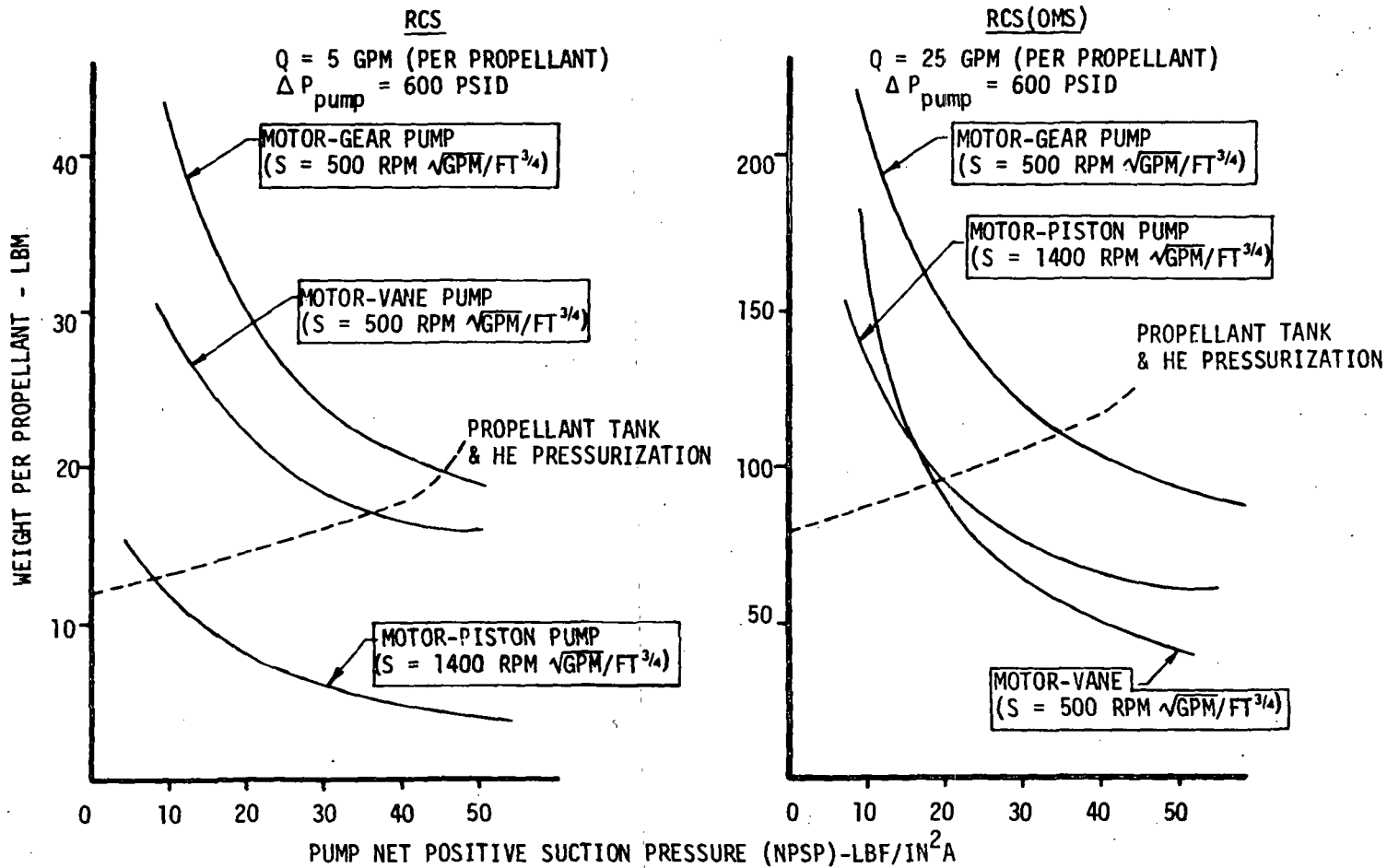


◦ BI-PROPELLANT



NOTE: RCS(OMS) EMPLOYS MAIN TANK SURFACE TENSION DEVICES AS OPPOSED TO BELLOWS AS SHOWN FOR BI-PROPELLANT RCS.

### PUMP TYPE SELECTION



D-15

Figure D-12

APS-788A

## BASIS OF ELECTRICAL POWER PENALTY

### FUEL CELLS

$$W_{F.C.} = (12.5 \text{ LBM/KW}) \times (4/2) + 2 \text{ LBM/KW-HR}$$

↖ FOUR FUEL CELLS; TWO ACTIVE  
 TWO INACTIVE

### RECHARGEABLE BATTERIES

$$W_{BATT.} = (83.5 \text{ LBM/KW-HR}) \times (1/0.5) \times (4/2) \text{ SUPPLYING } 0.03 \text{ KW/LBM}$$

↖ LIMIT DEPTH OF DISCHARGE  
 TO 50%

↖ REDUNDANCY

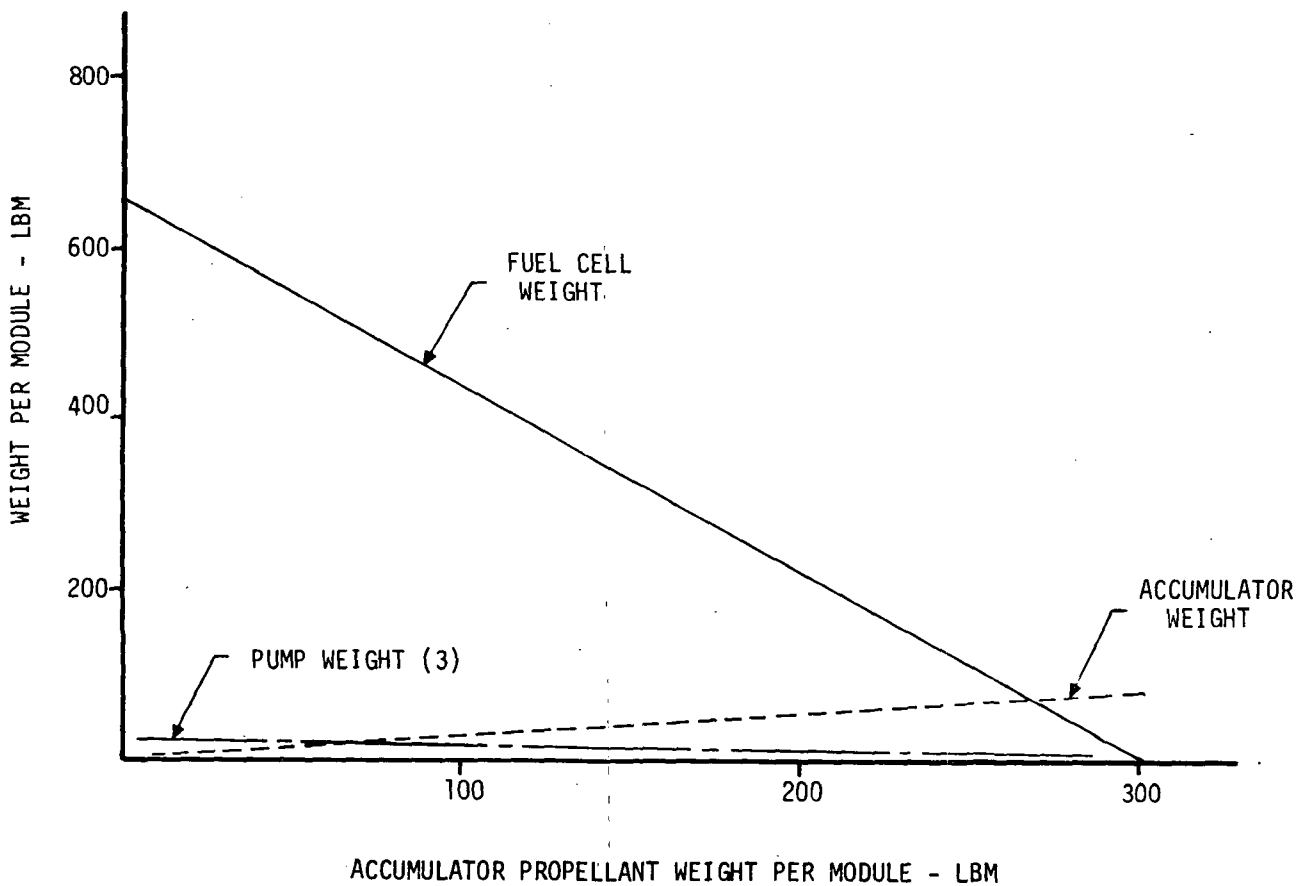
### FUEL CELLS USED WITH BATTERIES

BATTERIES SUPPLY POWER REQUIRED WITH FUEL CELLS SUPPLYING DIFFERENCE BETWEEN ENERGY REQUIRED AND ENERGY SUPPLIED BY BATTERIES.

APS-288

### ACCUMULATOR/PUMP OPTIMIZATION

o MONOPROPELLANT RCS MODULAR DESIGN POINT ( $F_{MOD} = 1800$  LBF)



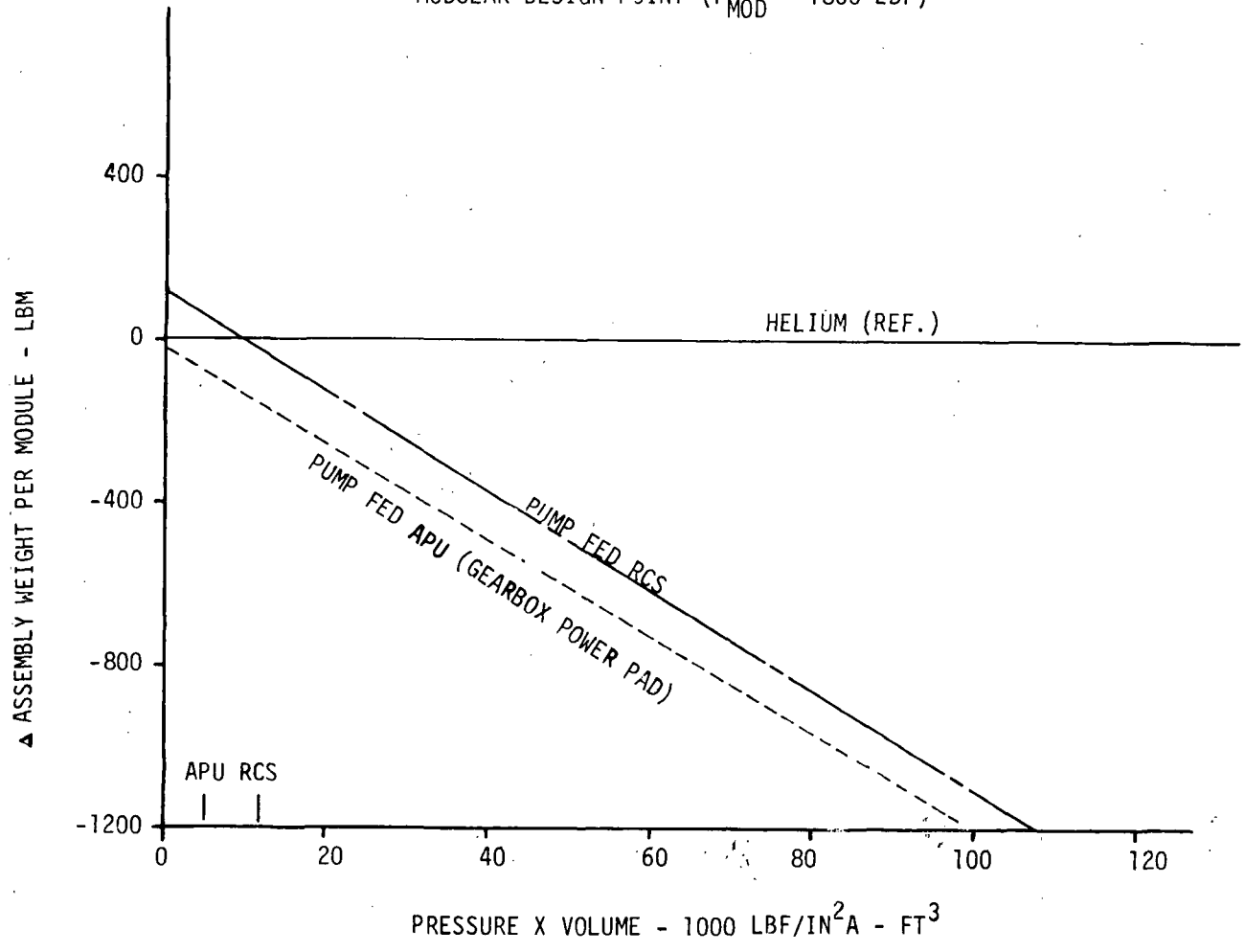
APS-300

D-17

Figure D-14

### PUMP FED SYSTEM WEIGHT COMPARISON

- MONOPROPELLANT
- MODULAR DESIGN POINT ( $F_{MOD} = 1800$  LBF)



MCDONNELL DOUGLAS ASTRONAUTICS COMPANY - EAST

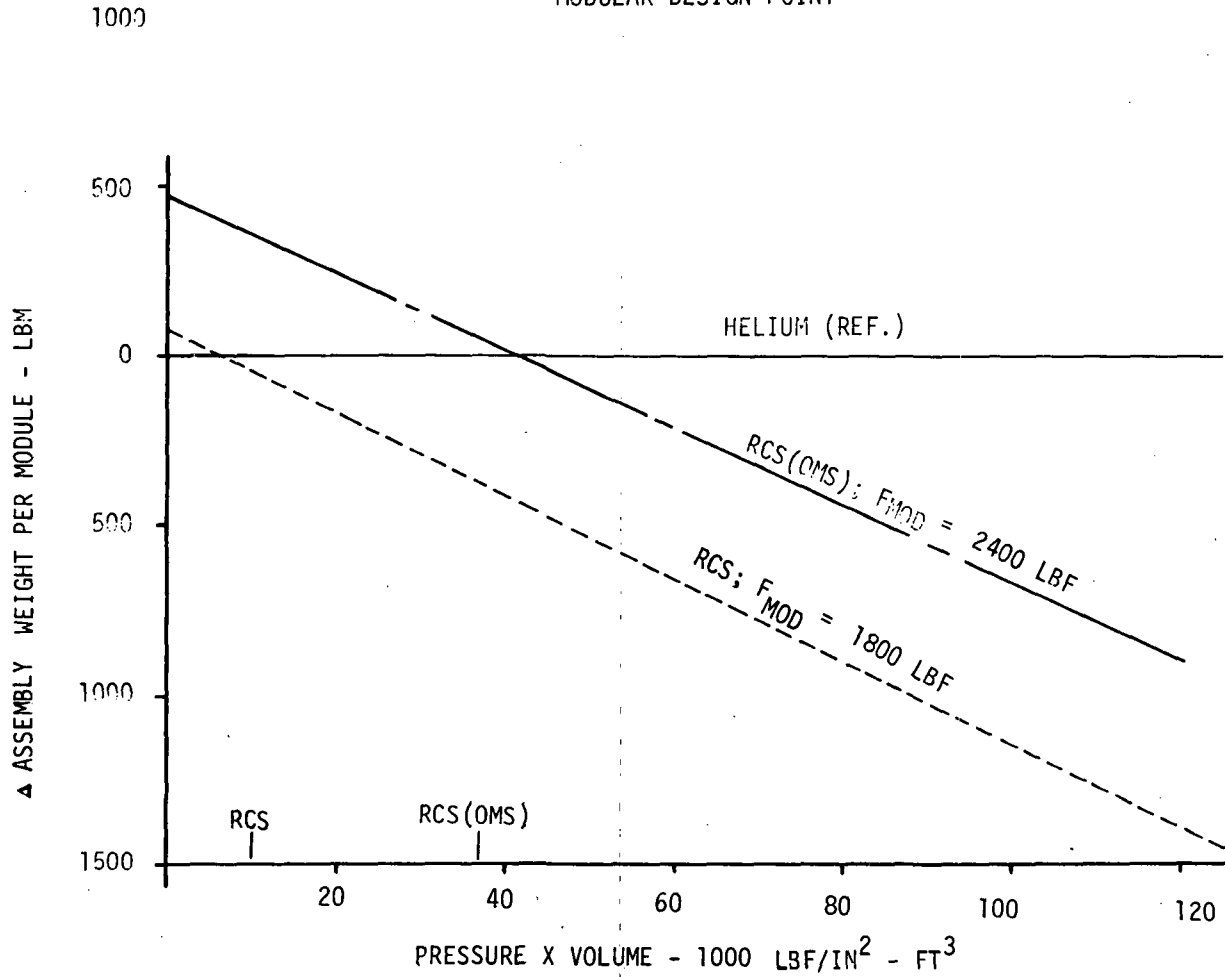
D-18

Figure D-15

APS-301

### PUMP FED SYSTEM WEIGHT COMPARISON

- BI-PROPELLANT
- MODULAR DESIGN POINT



APS-289

D-19

Figure D-16

## PUMP FED SYSTEM COMPONENT WEIGHTS

- MODULAR DESIGN POINT
- REFERENCE DESIGN CONFIGURATION

COMPONENT	CASE			
	APU-MONO.	RCS-MONO.	RCS-BIPROP.	RCS(OMS)-BIPROP
FORWARD POD HELIUM PRESS. WEIGHT	--	77	66	55
ACCUMULATORS	--	153	128	8
HELIUM	6	3	2	1
PUMPS	25	15	20	120
VALVES, CHECK	6	15	16	19
VALVES, ISOLATION	16	24	36	60
LINES	6	11	13	16
Δ TANK WEIGHT	-45	-143	-187	-326
ADDITIONAL FUEL CELL WEIGHT	--	119	90	778
TOTAL	14	274	184	731
REFERENCE HELIUM PRESSURIZATION SYSTEM	151	285	243	715

APS-287

D-20

Figure D-17

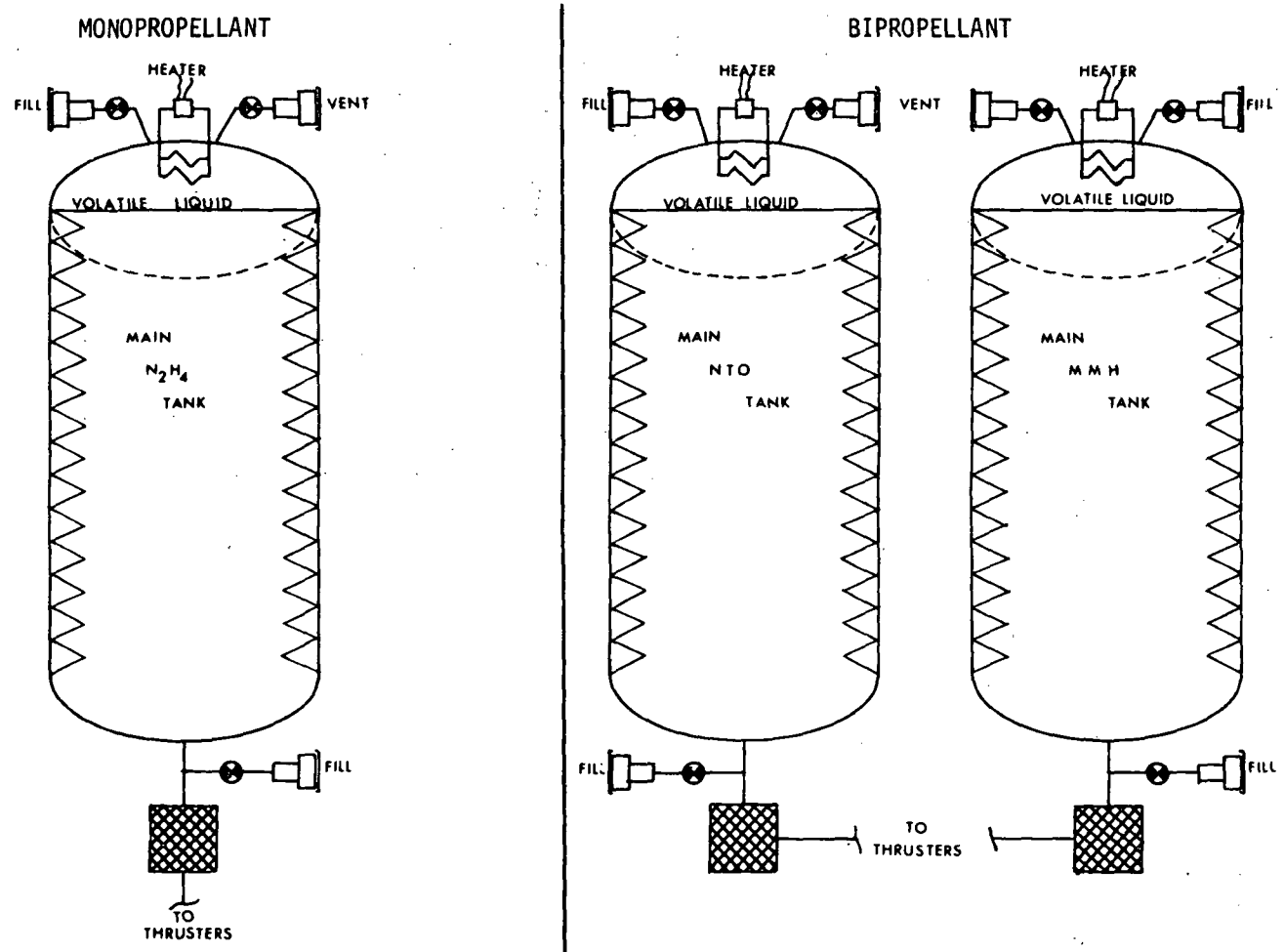
propellants to the thrusters at varying pressures and thus altering system performance accordingly. For bipropellant systems, random pressure fluctuations between fuel and oxidizer can result in unacceptable mixture ratio excursions, and liquid pressure regulators are therefore required.

D4 Volatile Liquids - A detailed analysis and system optimization was performed on a volatile liquid pressurization concept. Schematics for both the monopropellant and bipropellant volatile liquid pressurization assemblies are shown in Figure D-18. Propellant expulsion is accomplished by phase change of a pressurizing volatile liquid. With this concept, the system can be designed to operate in either a blowdown mode, wherein recovery to nominal tank pressure is effected by heat addition between burns, or in a controlled mode wherein high-power heaters maintain a constant pressurant temperature during the expulsion cycle. In this later mode, the input heating rates must satisfy the instantaneous energy requirements for pressurant vaporization and flow work. Inherent advantages of volatile liquids over cold gas are: reduced volume, increased reliability and simplified recycling; that is, there is no need to vent and recharge the pressurant during propellant refill. Propellants are simply loaded at a pressure in excess of the pressurant vapor pressure causing the pressurant to return to its liquid phase. The selection of a suitable volatile liquid is based on its having a saturation vapor pressure equal to tank operating pressure in the temperature range of interest. It must also be compatible with the propellant and should possess a low molecular weight. The procedure employed in the optimization of the volatile liquid system is outlined in Figure D-19. Candidate pressurant characteristics were used in conjunction with tankage and power weight penalties to determine the optimum operating temperature as a function of chamber pressure. RCS weight sensitivities to chamber pressure were then evaluated using this relationship. This resulted in the definition of the most attractive pressurant and its respective optimum chamber pressure and operating temperature for each system.

Figure D-20 shows the saturation temperature versus vapor pressure characteristics for the eight volatile liquids considered in this study. This figure illustrates another quality of the volatile liquid which is important in system weight considerations. The vapor pressure of the pressurant at the upper limit of the operating temperature range determines the maximum pressure for which the propellant tank must be designed. The resulting increase in



# VOLATILE LIQUID SYSTEM SCHEMATICS

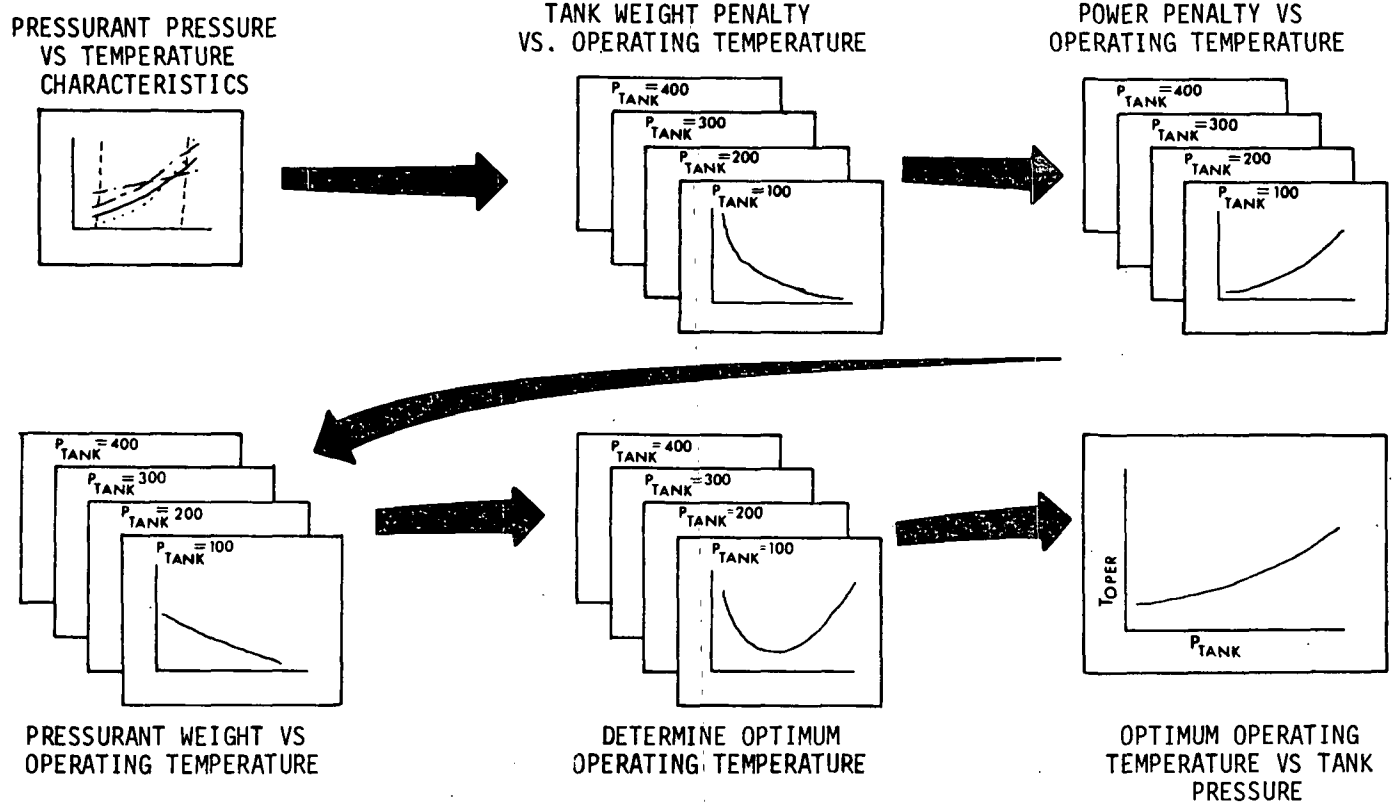


APS-302

D-22

Figure D-18

# VOLATILE LIQUID OPTIMIZATION FLOW CHART

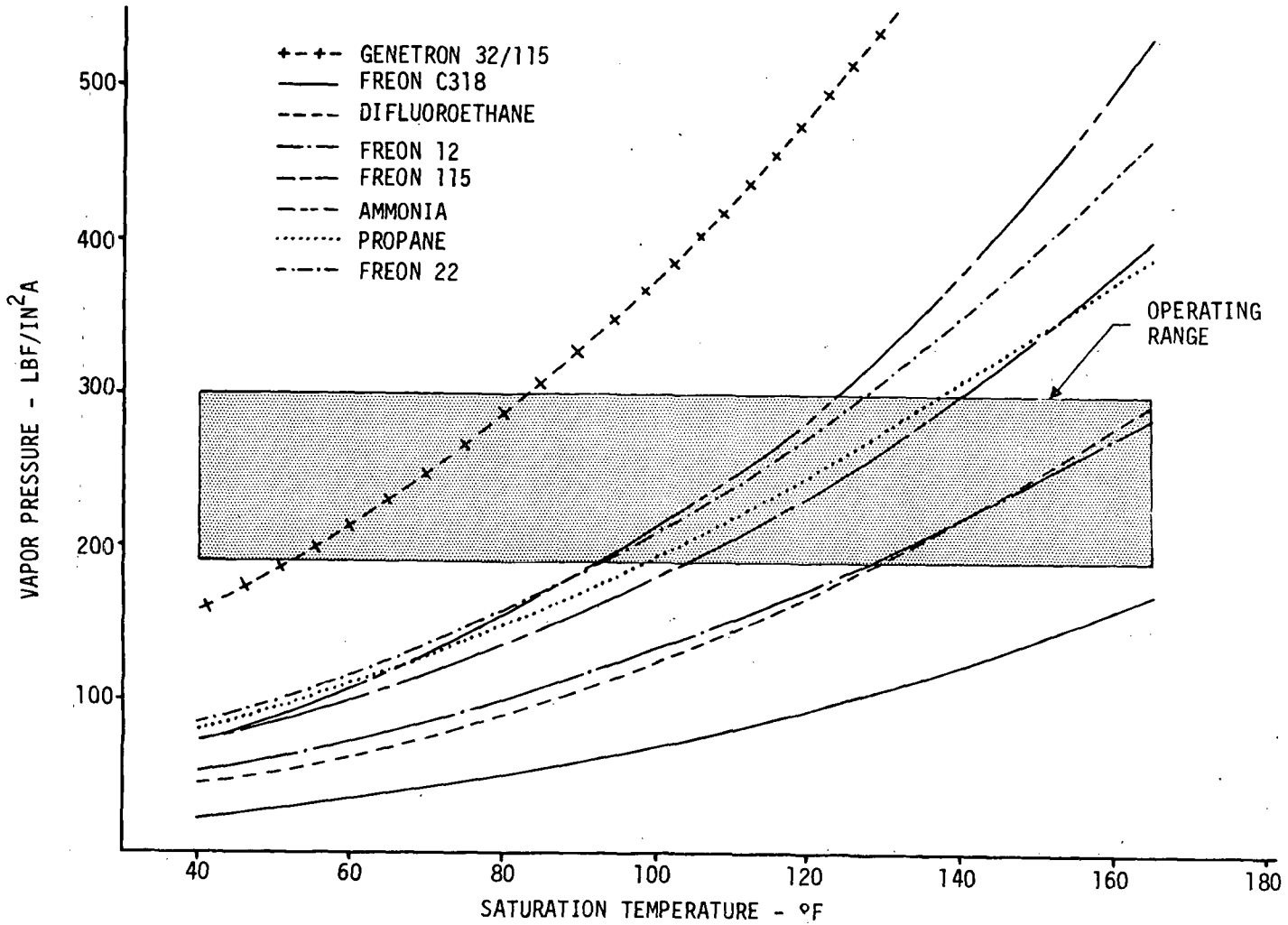


D-23

APS-315

Figure D-19

SATURATION TEMPERATURE/VAPOR PRESSURE  
CHARACTERISTICS FOR CANDIDATE LIQUIDS



D-24

Figure D-20

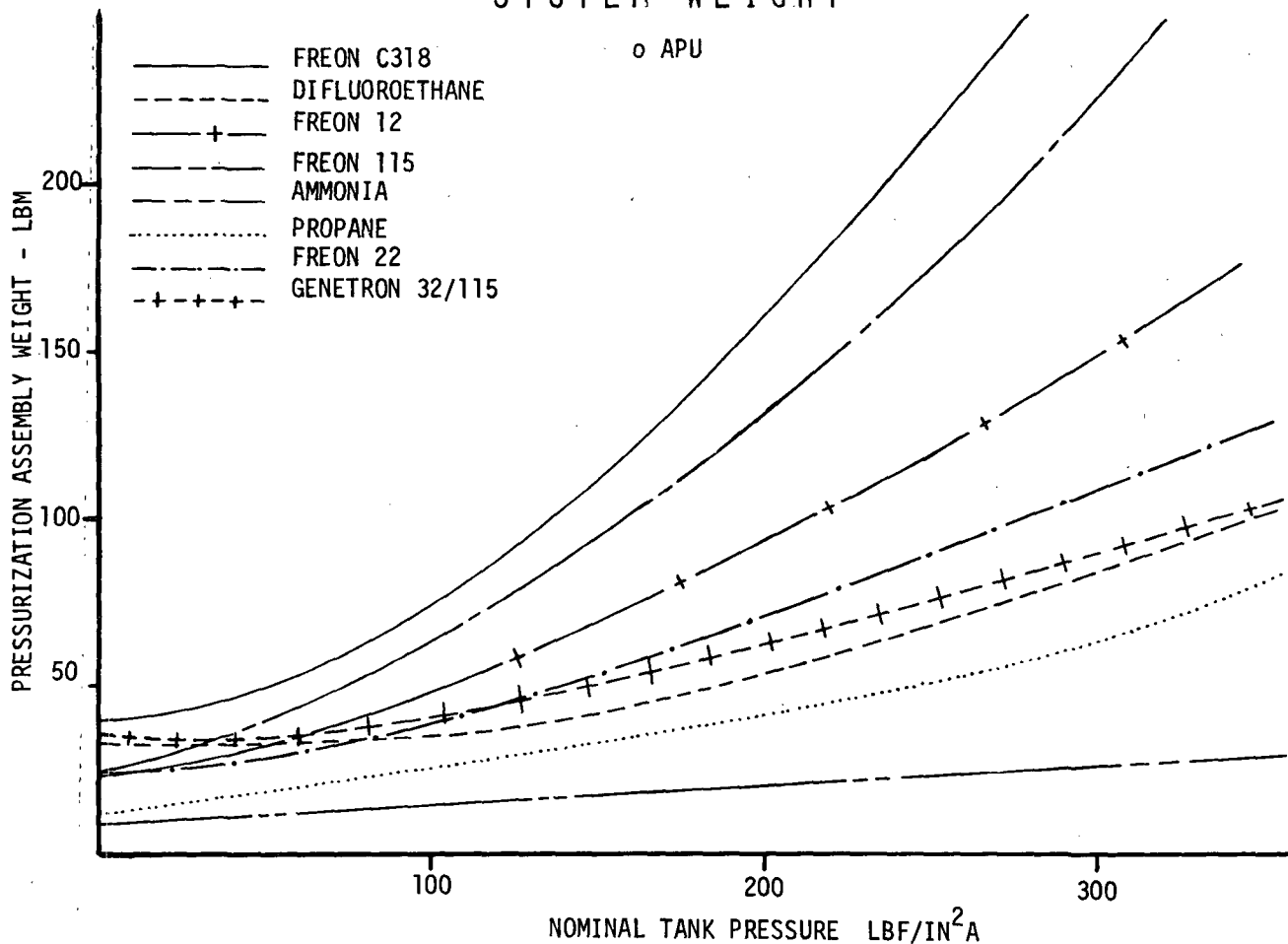
APS-325

tank weight over a tank sized at nominal pressure can be significant. In some cases, this penalty is high enough to overshadow any advantage a particular volatile liquid may have due to low molecular weight and low heat of vaporization.

Figures D-21, D-22, D-23, and D-24 show pressurization assembly weights for a range of tank operating pressures for the modular APU, monopropellant and bipropellant RCS, and RCS (OMS) respectively. These figures show that different volatile liquids give the optimum system weight depending on the operating pressure of the system. Ammonia gives the lightest weight system at the APU, and monopropellant and bipropellant RCS design points and difluoroethane is the optimum volatile liquid for the RCS (OMS) design point. A detailed design point weight breakdown for the four systems is presented in Figure D-25.

These weight estimates were based on an allowable RCS tank pressure decay of 25 psi during a 20 ft/sec RCS maneuver. Fuel cells supply the necessary heater power. For the RCS (OMS), the heaters were sized to provide a constant tank pressure for the longest single burn which is a retrograde from a 500 nmi orbit ( $\Delta V = 900$  ft/sec) during a mission abort. Rechargeable nickel-cadmium batteries were found to be the best power source for the high peak power demands. Figure D-25 also shows that the exorbitant weight penalty associated with these volatile liquid systems far overshadows any operational advantages that could be realized by their use.

### EFFECT OF TANK PRESSURE ON PRESSURIZATION SYSTEM WEIGHT

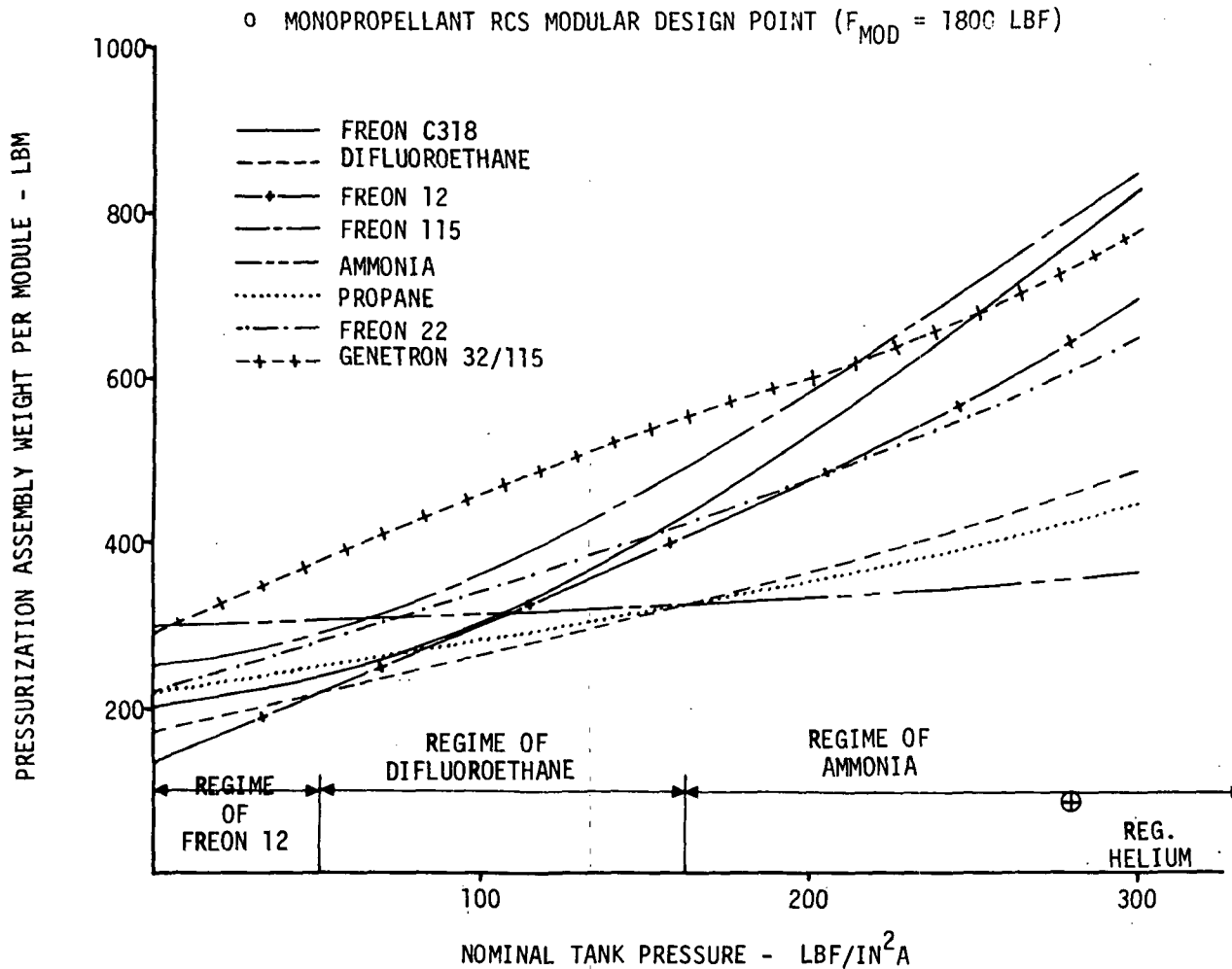


APS-309

D-26

Figure D-21

# EFFECT OF TANK PRESSURE ON PRESSURIZATION SYSTEM WEIGHT

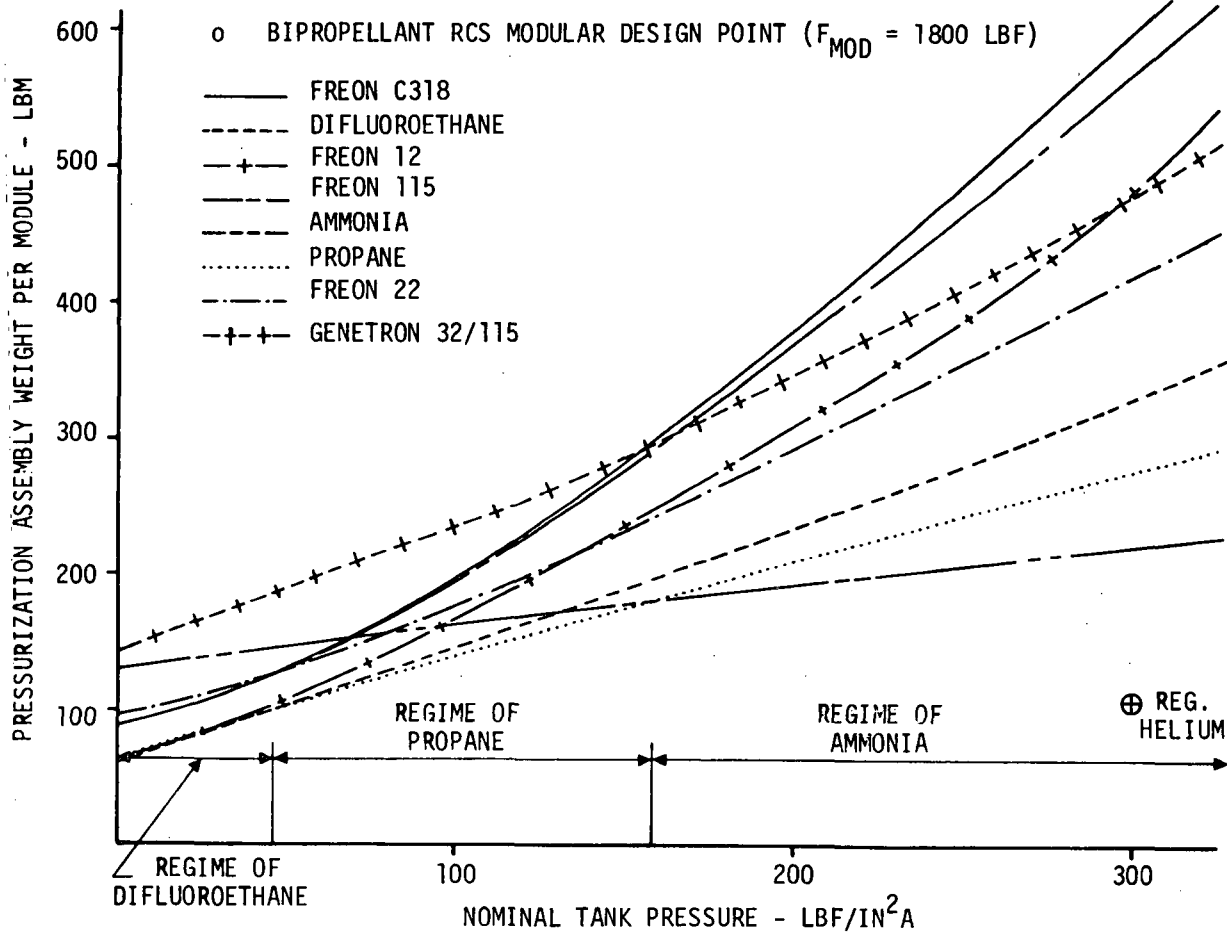


APS-316 A

D-27

Figure D-22

### EFFECT OF TANK PRESSURE ON PRESSURIZATION SYSTEM WEIGHT

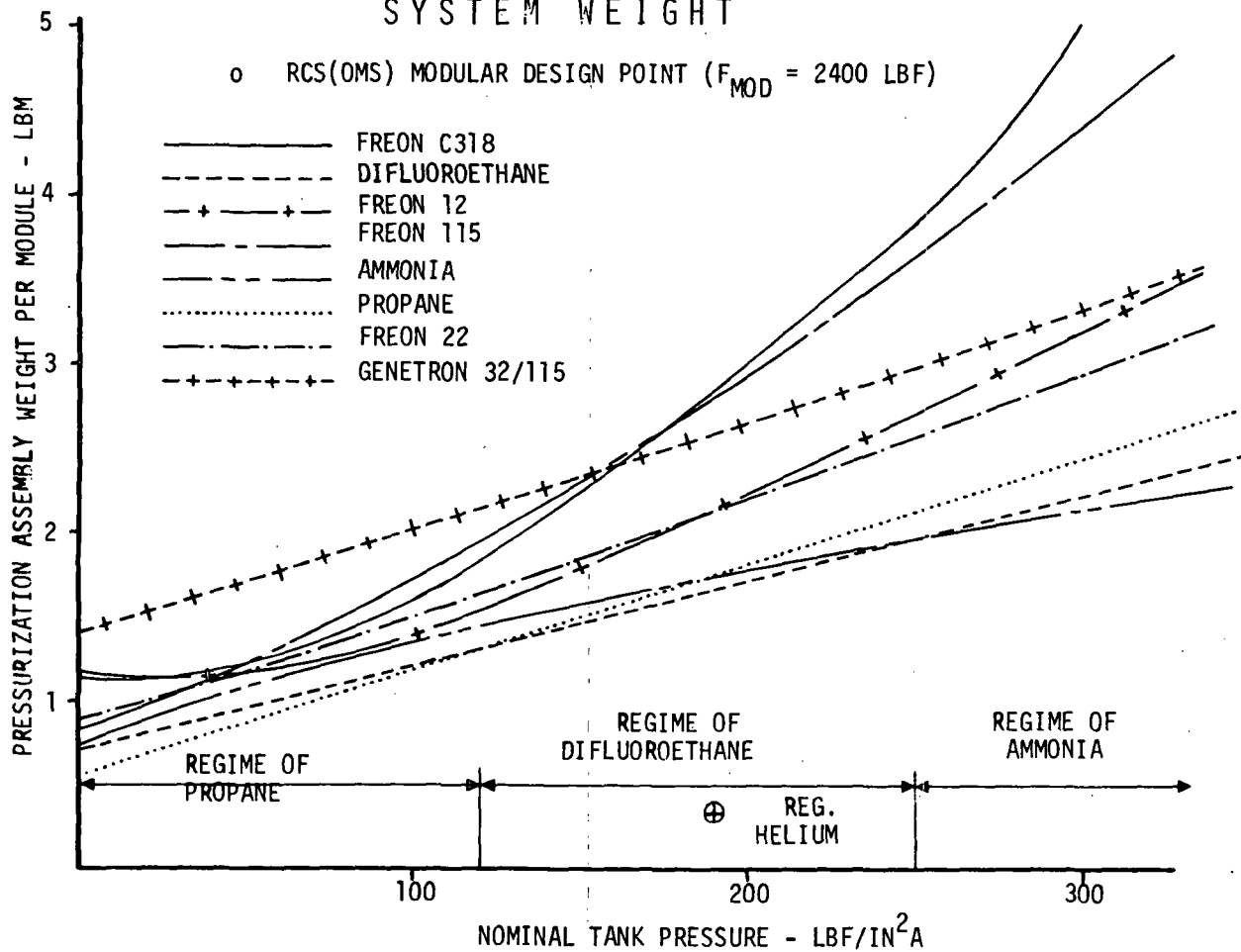


D-28

Figure D-23

APS-326

### EFFECT OF TANK PRESSURE ON PRESSURIZATION SYSTEM WEIGHT



MCDONNELL DOUGLAS AERONAUTICS COMPANY - EAST

D-29

Figure D-24

APS-317



## VOLATILE LIQUID SYSTEM COMPONENT WEIGHTS

- o MODULAR DESIGN POINT
- o REFERENCE DESIGN CONFIGURATION

COMPONENT	CASE			
	APU	RCS-MONO.	RCS-BIPROP	RCS(OMS)
PRESSURANT	36	188	137	843
MAIN TANK INCREASE	--	645*	206	784
HEATERS	16	30	17	78
INSULATION	5	57	34	154
ELECTRICAL POWER PENALTY	--	129	219	2342
<b>TOTAL</b>	<b>57</b>	<b>1049</b>	<b>613</b>	<b>4201</b>
REFERENCE HELIUM PRESSURIZATION	151	285.0	243.0	715.0

\* LARGE Δ TANK WEIGHT DUE TO CHANGE  
IN EXPULSION DEVICE

APS-789

D-30

Figure D-25

APPENDIX E  
TANKAGE AND PROPELLANT ACQUISITION

One of the primary propulsion technology concerns is the successful development of propellant tankage capable of satisfying shuttle life requirements. Effort has been focused on tankage materials, positive propellant expulsion devices, and methods of implementing expulsion redundancy.

Reliability requirements are not normally extended to include propellant expulsion devices. However, redundant acquisition is an attractive option, and therefore methods of incorporating redundancy were extensively investigated. As shown in Figure E-1, the incorporation of multiple tanks to achieve redundancy sufficient for a safe entry results in high weight penalties. One alternative is a back-up start tank concept (Figure E-2). In this concept, propellant contained in a secondary tank could be used to generate settling forces of sufficient magnitude to position the main tank propellants for expulsion. Main tank propellants would then be used for deorbit maneuvers. Another approach is to improve expulsion reliability by incorporating a redundant expulsion device. The weight penalties associated with the implementation of various redundant expulsion devices are summarized in Figure E-3. This concept has been investigated in detail, and is discussed in the sections that follow.

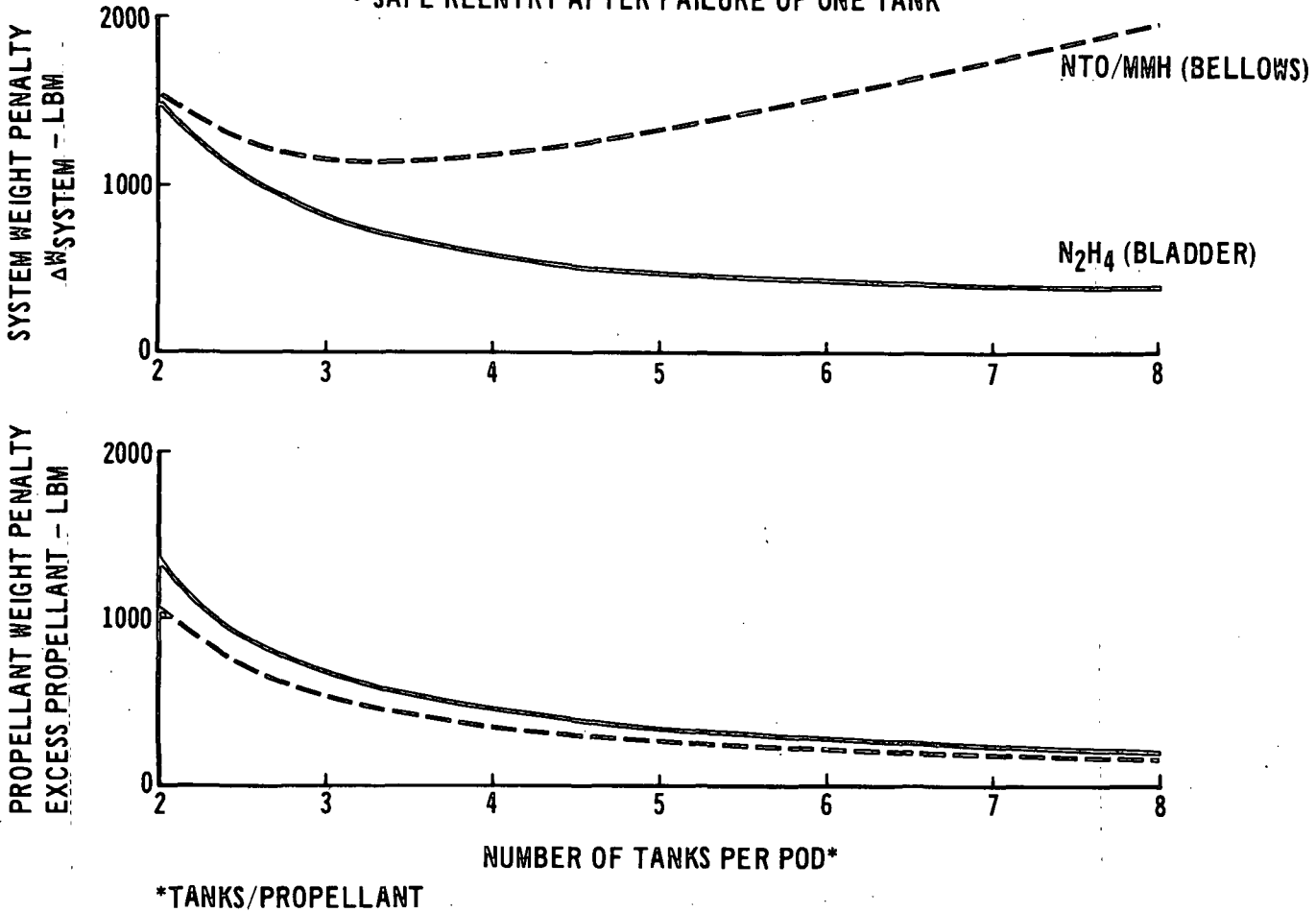
A review of positive expulsion technology has identified the following concepts:

- o Nonmetallic bladders/diaphragms
- o Reinforced metal diaphragms
- o Rolling metal diaphragms
- o Bellows
- o Pistons
- o Capillary devices
- o Surface tension devices
- o Collapsible metal containers

However, shuttle reusability requirements have limited consideration of propellant acquisition concepts to nonmetallic bladders/diaphragms, metallic bellows, pistons and surface tension positive expulsion devices. Figure E-4 summarizes the relative merits of these concepts. Based on the tankage evaluation reported herein, a nonredundant surface tension tank constructed of 6Al-4V

# WEIGHT PENALTY FOR PROPELLANT REDUNDANCY MULTIPLE TANKS

- MODULAR RCS
- SAFE REENTRY AFTER FAILURE OF ONE TANK



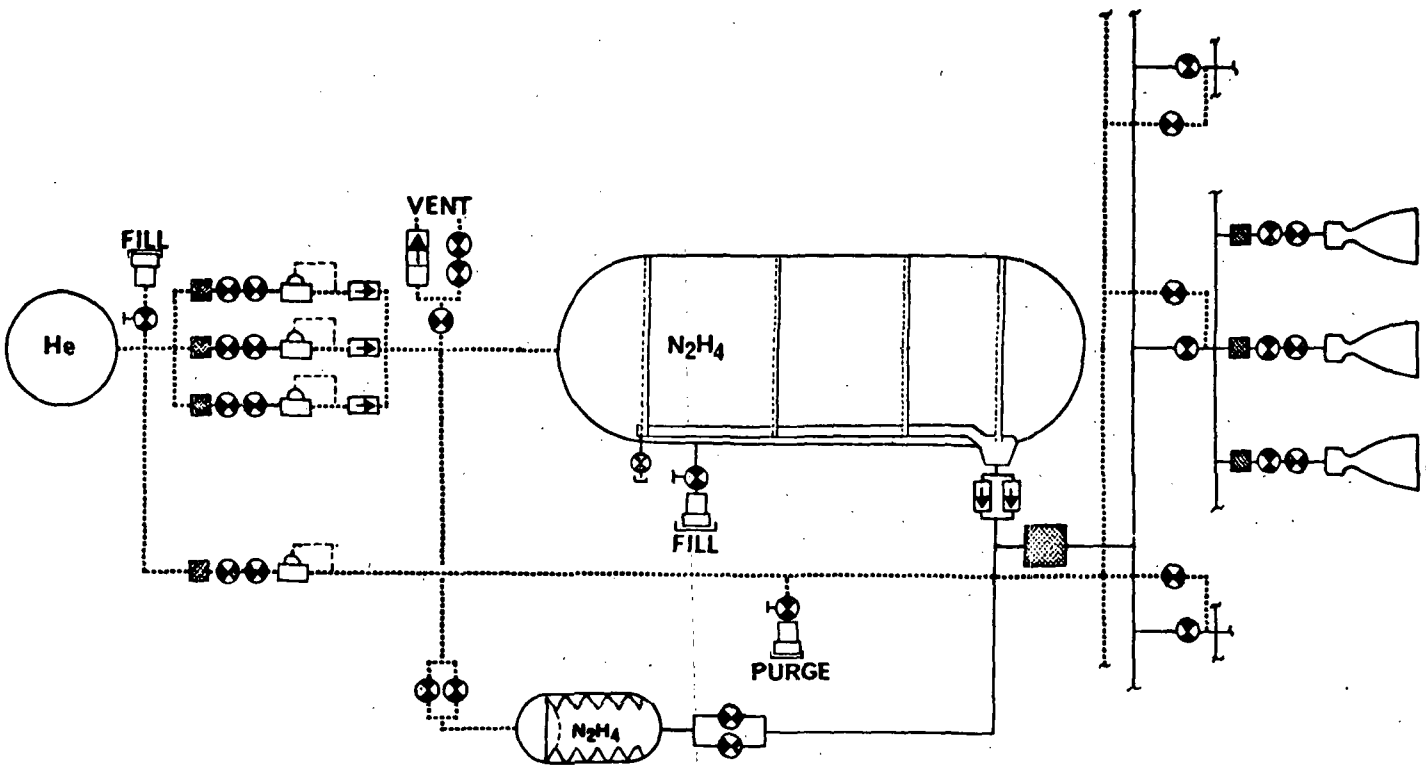
MCDONNELL DOUGLAS AERONAUTICS COMPANY - EAST

E-2

Figure E-1

11-229

# BACK-UP START TANK SYSTEM SCHEMATIC MODULAR RCS - N<sub>2</sub>H<sub>4</sub>



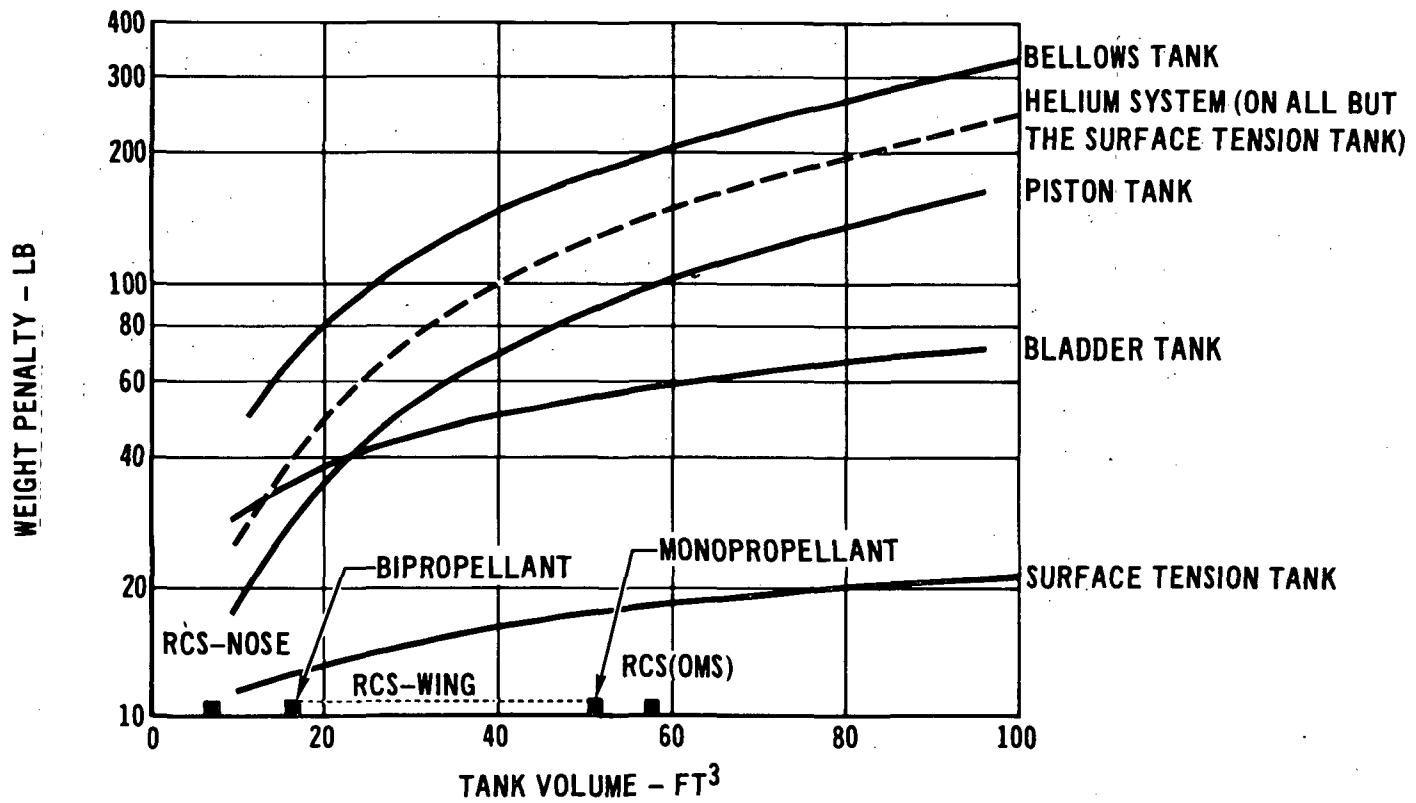
APS-145

Figure E-2

E-3

## WEIGHT PENALTY FOR REDUNDANT PROPELLANT EXPULSION DEVICES

$P_T = 300 \text{ PSIA}, L/D = 3.5$



E-4

Figure E-3

11-233A

Titanium was chosen as the baseline for this study. Titanium was selected due to its weight competitiveness, compatibility properties, and the depth of experience in its use. However, 301 cryoformed stainless steel does offer several attractive properties, and further consideration is warranted prior to final material selection.

E1 Bladders - Figure E-5 summarizes the status of nonmetallic bladder/diaphragm expulsion devices. The recent development of improved elastomeric bladder materials, i.e., AFE 332-7, an EPT rubber, greatly increases the likelihood that a bladder for hydrazine service can be made to meet the full cycle life requirement imposed by Space Shuttle. However, notwithstanding a renewed effort on carboxy nitroso rubber (CNR) bladders, the prospect of developing a compatible high cycle life bladder for nitrogen tetroxide service is much less favorable. Teflon bladders are limited to 6-10 missions, and hence they are unattractive for Shuttle application. The primary problem areas with bladders in general and teflon bladders in particular, are pinhole leaks (bladder bifolds), tears (propellant slosh), and flange leakage.

Past efforts to incorporate redundancy concentrated on the use of multiply bladders. However, multi-ply bladders fail to provide the desired redundancy because the presence of additional plies increases fold strain, promotes abrasive wear between plies, and contributes to interply inflation by the pressurizing gas (thereby preventing adequate filling and expulsion). The preferred approach to redundancy is one in which a redundant bladder/diaphragm is maintained in an inactive status until required for backup operation. Such a concept is shown in Figure E-6. Here, two elastomeric diaphragms are clamped to opposite sides of a propellant manifold ring and the entire assembly is bolted to a flange on the inside of the tank. The tank is welded shut following diaphragm installation. During operation, the pressurizing gas is admitted to one side of the tank, activating that diaphragm for propellant expulsion; the other diaphragm is kept tight against the tank wall by the resulting hydrostatic pressure. Communication between the bulk propellant and outlet manifold ring is facilitated by integrally molded ribs on the inside of the diaphragm. Diaphragm failure is sensed by a gas detector in the propellant outlet line and/or propellant sensors on the pressurant side of the diaphragm. Upon sensing a failure, it is necessary to vent the pressurizing gas to avoid a continual worsening of propellant quality via increased gas entrainment.

## SUMMARY OF CANDIDATE EXPULSION DEVICES

	BLADDER/DIAPHRAGM	METALLIC BELLOWS	PISTON	SURFACE TENSION
CYCLE LIFE	150 (ELASTOMER) 15-30 (TEFLON)	500	> 1000	UNLIMITED
RELATIVE WEIGHT	1.0	3.0	2.7	1.3
PERMEATION/LEAKAGE	HIGH PERMEATION	NEGLECTIBLE	LIQUID FILM ON WALL FOLLOWING EXPULSION	SATURATED PROPELLANTS
SENSITIVITY TO DYNAMIC ENVIRONMENT	SUSCEPTIBLE TO TEARS AND CLAMP-UP FAILURES DURING SLOSH	PRONE TO CONVOLUTION WEAR AND IMPACT DAMAGE	PISTON COCKING	CHANGE IN EFFECTIVE PORE SIZE
DEVELOPMENT STATUS	GOOD	GOOD	FAIR	GOOD → FAIR; SMALL TANKS OR SUMPS FAIR → POOR; LARGE TANKS
DEVELOPMENT RISK	LOWEST RISK AND COST	MODERATE: QUESTIONABLE AVAILABILITY OF LARGE DIAMETER, SEAMLESS TUBING	MODERATE: MAJOR DEVELOPMENT EFFORT ASSOCIATED WITH BACK- UP ROLLING DIAPHRAGM	MODERATE TO HIGH: UNABLE TO GROUND TEST LARGE TANKS
MAJOR ADVANTAGES	SIMPLE, LIGHTWEIGHT DEVICE	POSITIVE SEPARATION OF PROPELLANT AND PRES- SURANT; CONTROL OF FAILURE MODE BY SELEC- TION OF CORE SPRING CONSTANT; GOOD PROPEL- LANT STORABILITY	SIMPLE DEVICE WITH GOOD CYCLE LIFE	PASSIVE DEVICE WITH POTENTIAL FOR UNLIMITED LIFE
MAJOR DISADVANTAGES	POOR CYCLE LIFE; PERMEABLE MATERIALS; BLADDER ADSORBS PROPELLANT	HEAVY AND DIFFICULT TO CLEAN (CORROSION)	RESIDUAL LIQUID FILM; EXPOSURE OF DYNAMIC SEALS TO PROPELLANTS	DIFFICULT TO TEST AND TO VERIFY INTEGRITY; DUTY CYCLE SENSITIVE

11-234

E-6

Figure E-4

# NON-METALLIC BLADDERS/DIAPHRAGMS

## STATE-OF-THE-ART

Cycle Life: 15-30 (Teflon)  
                   ~ 150 (Elastomer)  
 Propellant Storage Life: 1 year  
 Maximum Diameter: 30 in.  
 Maximum L/D: 6  
 Expulsion Efficiency: 99.5%  
 Pressure Drop: 2-5 PSID  
 Duty Cycle Limitations: none

## PROBLEM AREAS

- (a) Propellant - Bladder incompatibility
- (b) Bladder/diaphragm failure under slosh, vibr & acceleration loads (off-loaded condition)
- (c) Pinhole leaks (caused by double folds)
- (d) Gas permeation
- (e) Bladder ply inflation
- (f) Teflon cold flow at clamped fitting (leakage)
- (g) Excessive bladder-wall friction during fill operation

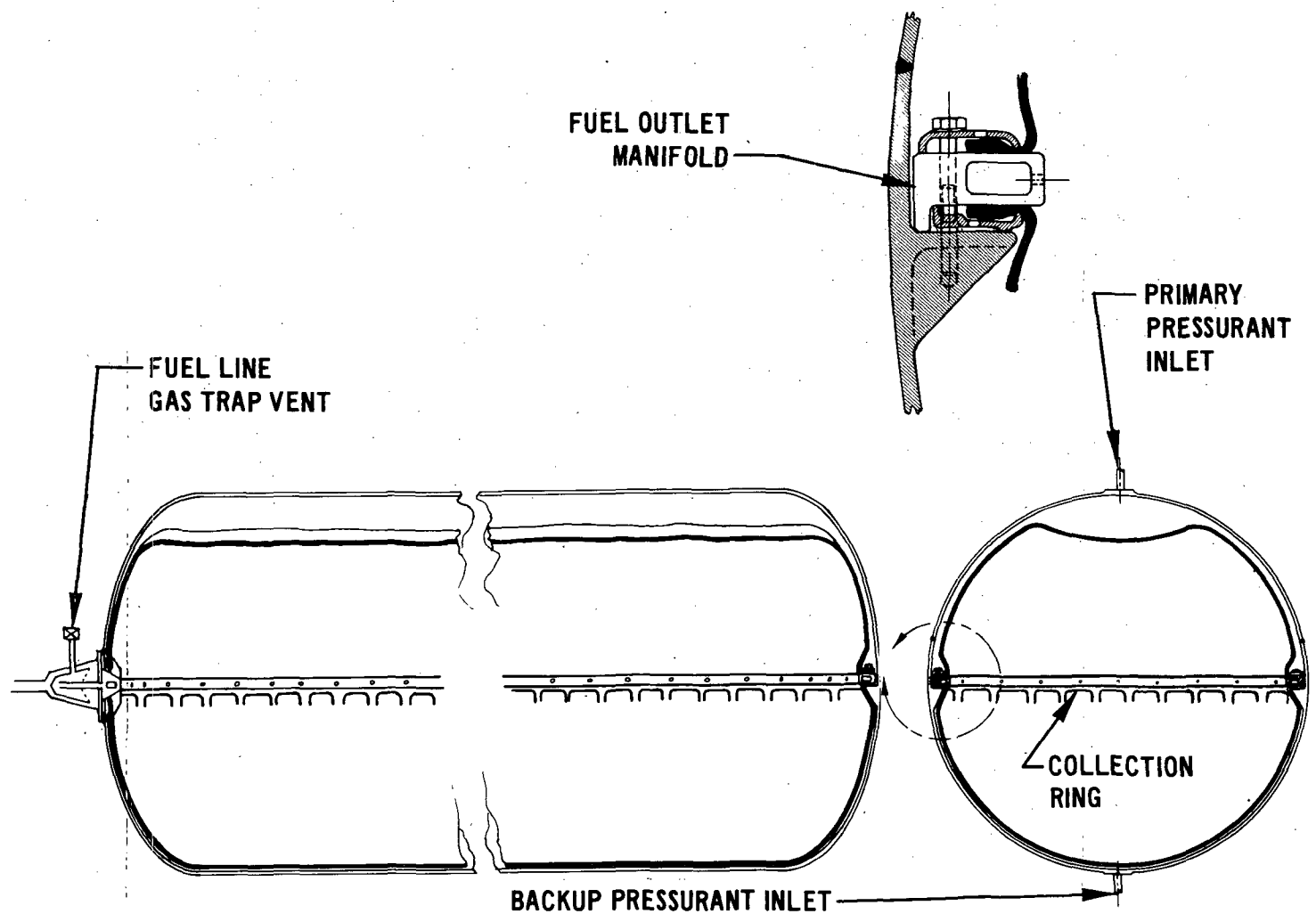
## RECOMMENDED APPROACH

- (a) For Hydrazine: avoid carbon black fillers; use compression - molded EPT-10 or AFE 332-7  
For NTO, MMH: use codispersion TFE-FEP teflon
- (b) Oversize bladder/diaph. to avoid stretching; use high L/D tanks (>3.5) to reduce dynamic loads; support bladder ends
- (c) Provide uniform folding pattern via:
  - high L/D tanks
  - supported bladder ends
  - preformed creases or integral ribs
 Improve flex life (teflon) by increasing sintering time and quenching rapidly during fab. to reduce crystallinity.
- (d) Employ pressurant gas arrestor (trap) at tank outlet
- (e) Use single ply bladders
- (f) Bond bladders to standpipe and weld closure to tank
- (g) Place tanks in horizontal position during fill operations; avoid use of gas to re-expand bladders

APS-348



# REDUNDANT EXPULSION BLADDER DESIGN



11-231

E-8

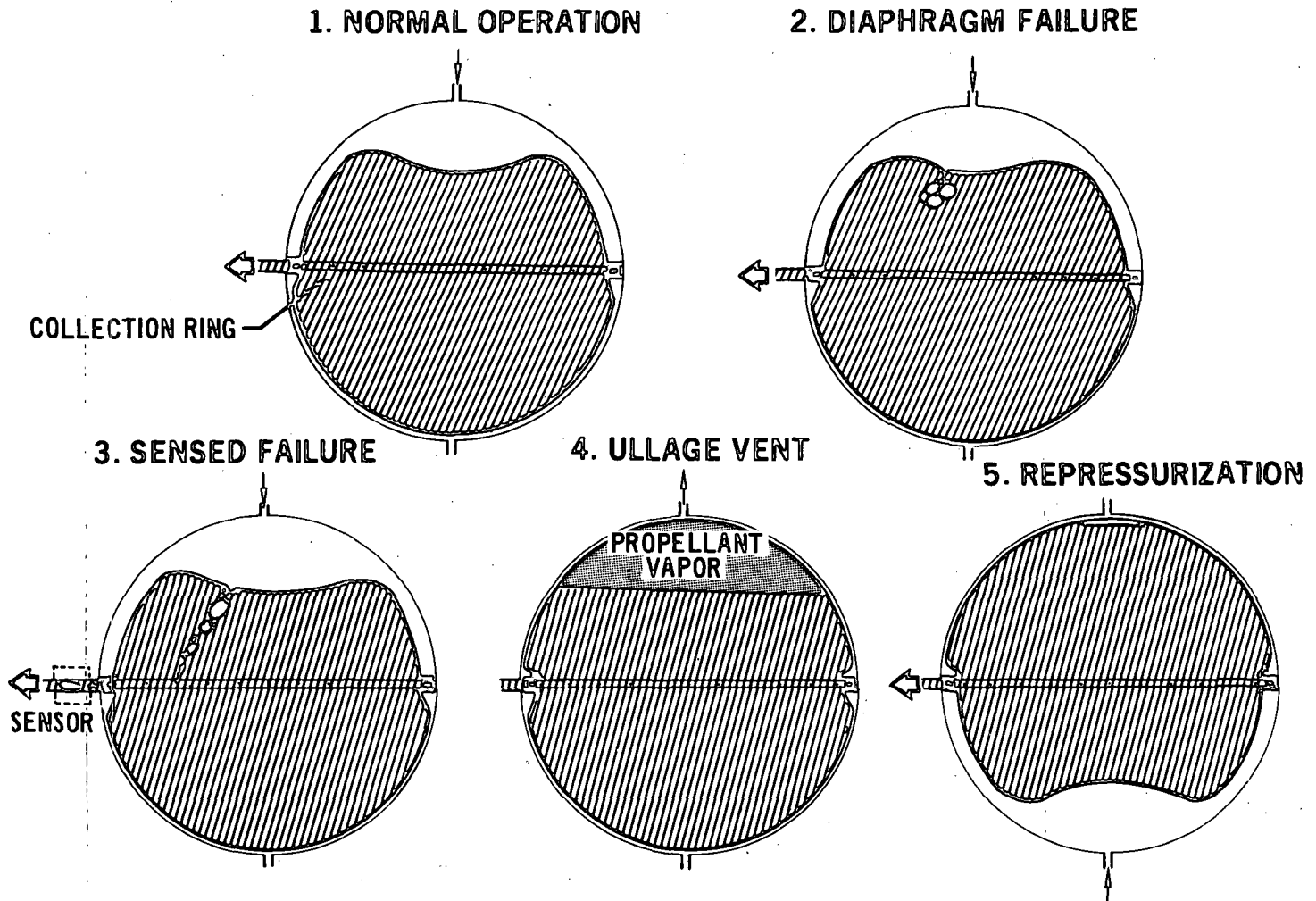
Figure E-6

The sequential operations involved in activating the backup diaphragm following a failure are depicted in Figure E-7. As shown, depressurization of the tank causes the failed diaphragm to be forced against the tank wall by propellant vapor pressure. The change in volume on the liquid side of the diaphragm is occupied by a vapor bubble formed by the boiling propellant. The vent valve is then closed and pressurant gas is admitted to the opposite end of the tank, pressing the backup diaphragm into service. Re-pressurization of the tank collapses the propellant vapor bubble and readies the system for continued operation. (A small amount of pressurant gas may remain trapped within the diaphragms.)

The redundant bladder tankage weight model developed in this study is shown in Figure E-8. The increase in tank weight due to redundancy is minimal; however, pressurant (and therefore pressurant tank) weights must be approximately doubled to accomplish tank venting and repressurization in the event of an expulsion device failure near mission completion.

E2 Bellows - Metallic bellows offer the highest confidence level in providing reliable, multimission operation although they are considerably heavier than the other candidate expulsion devices. Problems associated with the implementation of bellows expulsion devices can be eliminated by effective design, as discussed in Figure E-9. A high cycle life is obtained by designing the bellows elements for a low operating pitch-to-span ratio. The dynamic environments present the greatest threat to bellows integrity and, in this regard, past development problems can generally be traced to excessive clearances between the bellows core and tank shell. A large clearance contributes to high impact loads on individual bellows elements and cocking of the movable bellows head when subjected to shock, acceleration and/or vibration. Dimensional control is particularly difficult for the large tank diameters of the shuttle since diametrical deflection of the tank shell under internal pressure loads is relatively large, i.e.,  $\sim 0.25$  in. In an attempt to overcome this problem, the conceptual design illustrated in Figure E-10, utilizes a thin, pressure-balanced inner wall. External manifolding and valving assure a proper pressure balance across the wall under both normal and failed bellows operating modes. Figure E-11 shows the bellows tankage weight model. In the model, a skirted piston provides the necessary expulsion capability in the event of a bellows failure. The procedure used in switching to the backup mode is similar to that discussed for the bladders/

# SEQUENCE FOR ACTIVATION OF REDUNDANT DIAPHRAGM

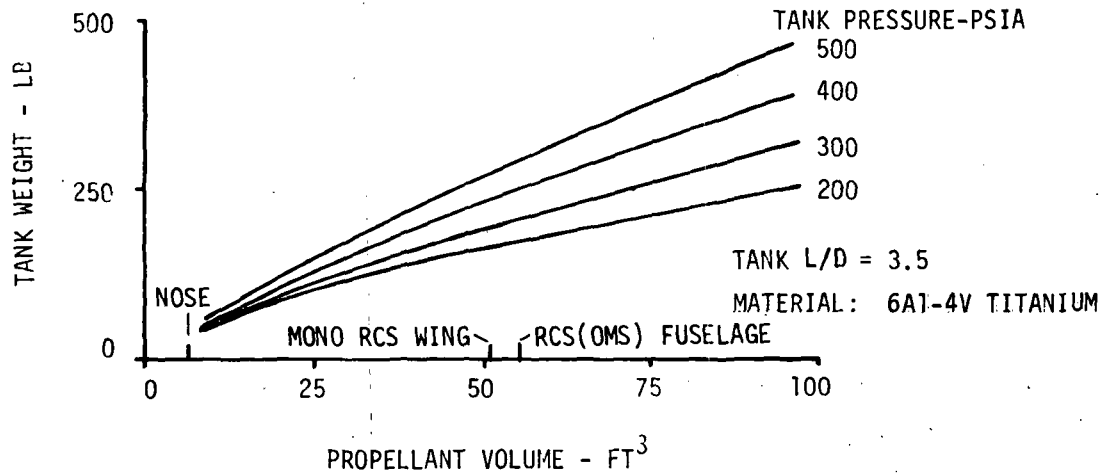
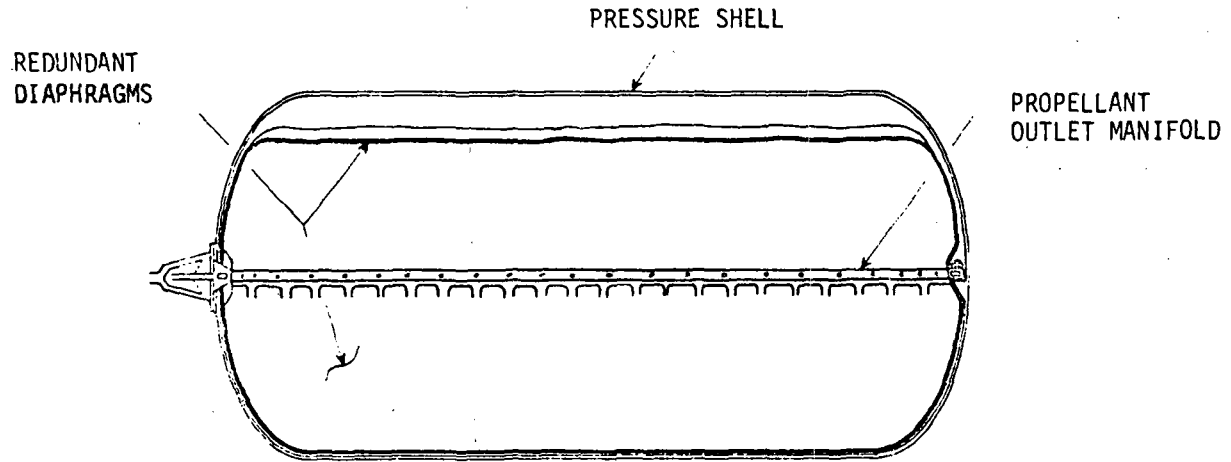


E-10

Figure E-7

11-323

# REDUNDANT DIAPHRAGM TANKAGE WEIGHT MODEL



MCDONNELL DOUGLAS ASTRONAUTICS COMPANY - EAST

E-11

Figure E-8

APS-349

## METALLIC BELLOWS

### STATE-OF-THE-ART

Cycle Life: 500  
 Propellant Storage Life: 5 yrs  
 Maximum Diameter: 24 in.  
 Maximum L/D: 6  
 Expulsion Efficiency: 98%  
 Volumetric Efficiency: 87%  
 Pressure Drop: 3-5 PSID  
 Duty Cycle Limitations: none

### PROBLEM AREAS

- (a) Corrosion
- (b)  $\Delta P$ -induced buckling
- (c) Fatigue failures
- (d) Convolution wear and impact failures
- (e) Unsymmetrical buckling (dynamic loading)

### RECOMMENDED APPROACH

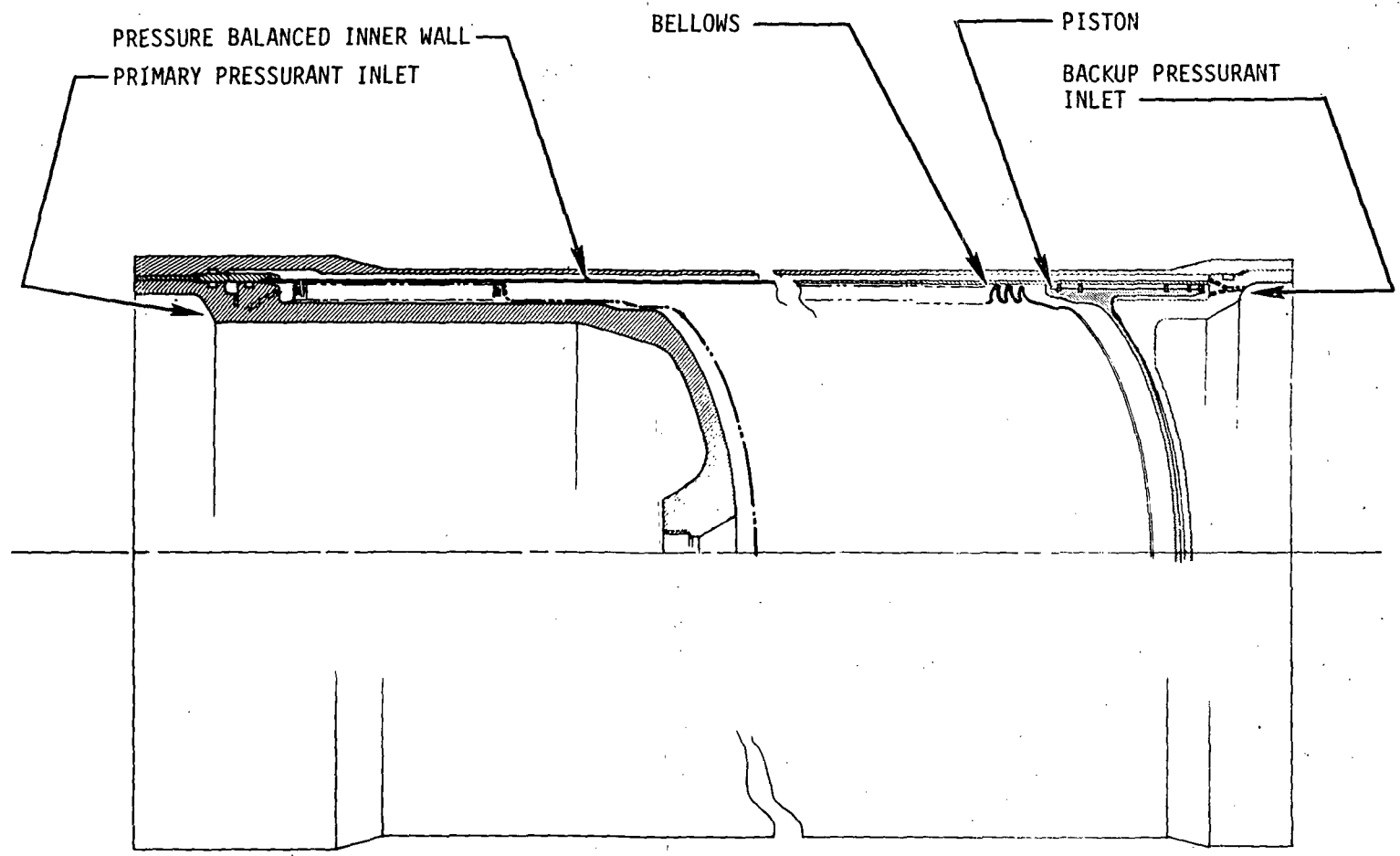
- (a) Select compatible mat'l, i.e., 347 or 304L SS; minimize welds and contamination sites, use:
  - formed seamless tubing
  - Large root and crest bend radius to facilitate cleaning
- (b) Use low fill pressures; contain propellant inside bellows (bellows takes max  $\Delta P$  in nested configuration)
- (c) Provide mechanical stops in nested position; small convolution pitch-to-span ratio ( $<0.5$ ); large root and crest bend radius; nested ripple elements)
- (d) Maintain close tolerance on element-to-element O.D.; smooth surface on shell I.D.; minimize clearance between core O.D. and shell (may require pressure-balanced inner wall for larger tank diameters)
- (e) Minimize head and bellows mismatch during welding; provide ample margin between working and max. pitch; design bellows natural frequency outside vibration environment

E-12

Figure E-9

APS-350

# BELLOWS TANK ASSEMBLY

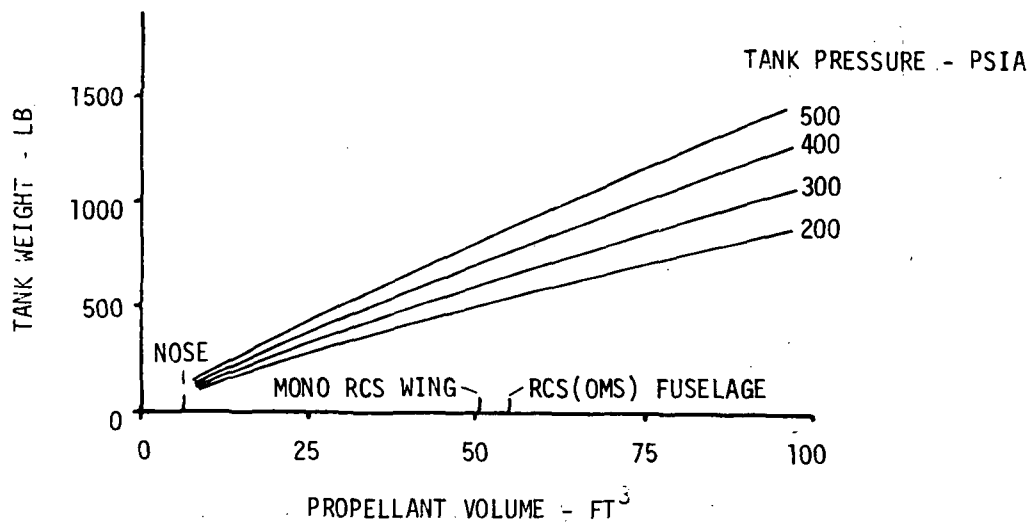
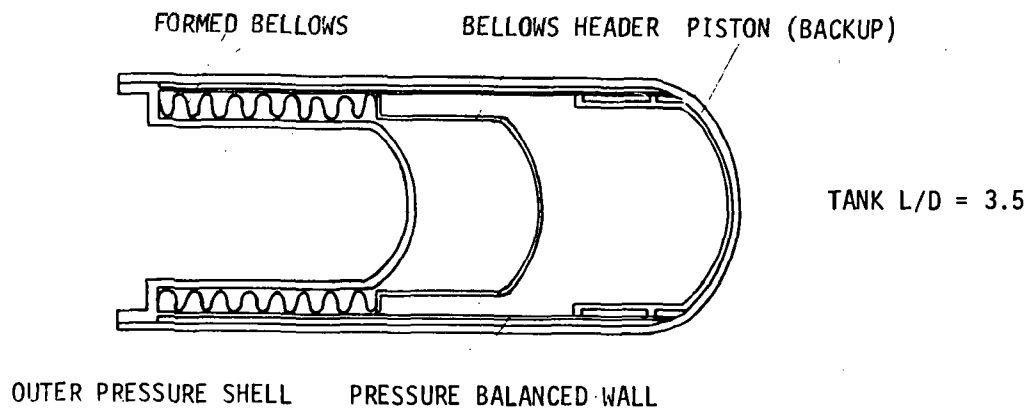


E-13

APS-229

Figure E-10

### BELLOWS TANKAGE WEIGHT MODEL



diaphragms, that is, the bellows are fully extended by propellant vapor pressure before a pressure drop is established across the piston and piston travel is initiated.

E3 Pistons - The inherent cycle life capability of piston propellant expulsion devices is practically unlimited, but the number of qualified piston tanks is relatively small. For small diameter tanks, lighter expulsion devices are readily available while for large diameter tanks, serious development problems have been encountered in establishing and maintaining piston seal integrity. Notable in this latter category are the 22 in. fuel and oxidizer tanks for the Lance missile.

As discussed in Figure E-12, the major problem areas in maintaining seal integrity are piston walking/cocking, low seal dump pressures and piston breakup at the completion of the expulsion cycle. Piston cocking results from unequal propellant pressure distribution on the face of the piston under dynamic loading conditions. To preclude these unwanted moments it is necessary to contour the piston face and control piston mass distribution such that dynamic loads always pass through or near the piston cg. It is also desirable to provide a piston skirt which is a minimum of one tank radius in length.

Low seal dump pressures result from inadequate seal "squeeze" over the full piston stroke. Tank wall deflection and/or out-of-roundness are the primary causes. As with the bellows tank concept, such deficiencies can be avoided by incorporating a thin, pressure-balanced inner wall which will be forced into roundness by the stroking piston.

At the conclusion of the stroke, the piston must be capable of withstanding dynamic settling loads in addition to the full system pressure differential or piston breakup will occur. This problem is alleviated by designing the inside radius of the aft tank closure to a value slightly less than the piston radius. Initial piston contact with the closure is then made at the outer diameter and the thin-wall piston face is allowed to deflect/ yield to the shape of the aft closure.

All of these design concepts were successfully used in the 16 inch diameter hydrogen peroxide tank for the MDAC Ballistic Glide Reentry Vehicle (BGRV) missile. The tank, shown in Figure E-13, was constructed from 301 cryoformed stainless steel, and featured an integral pressurant tank.



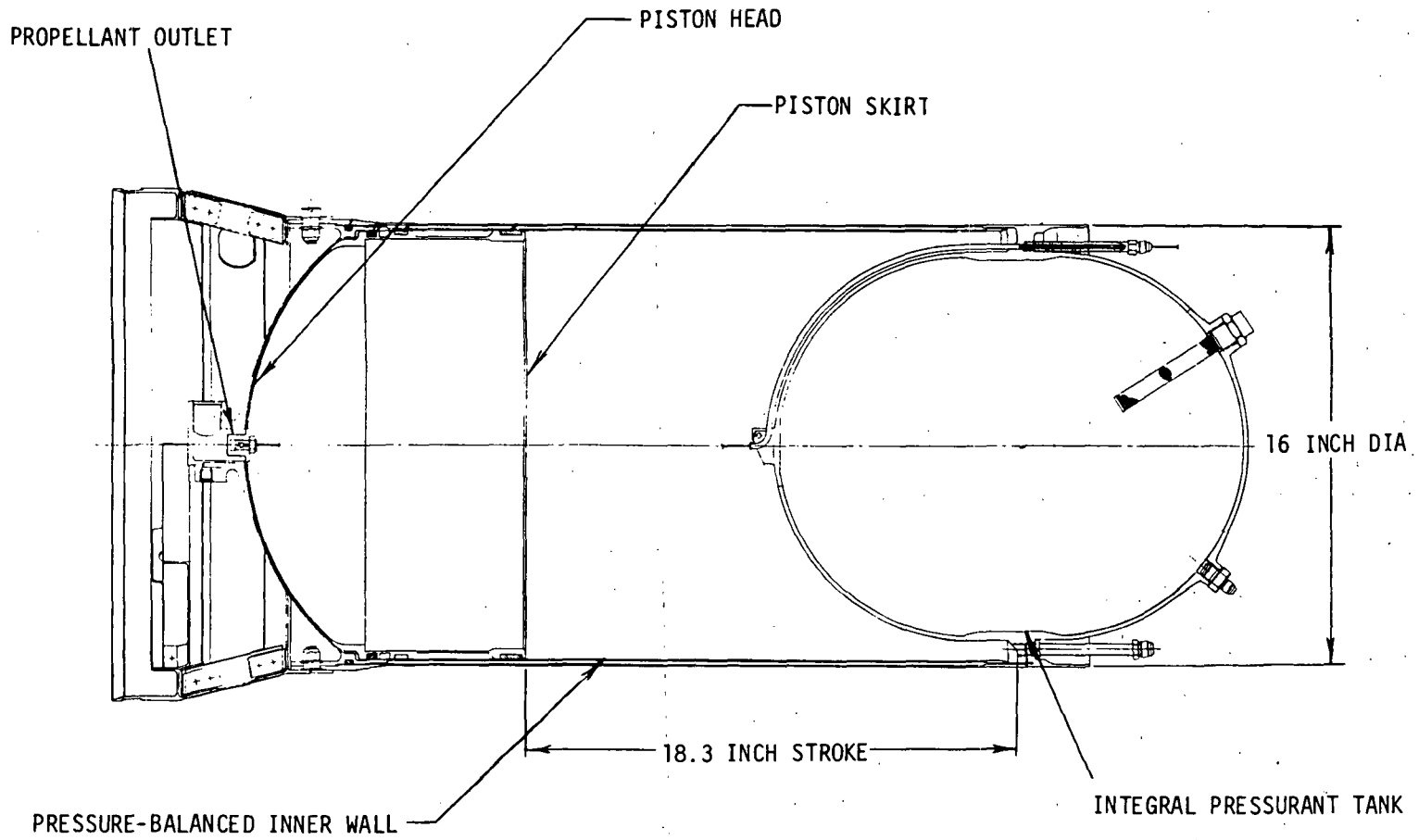
## PISTON TANKS

<u>STATE-OF-THE-ART</u>	<u>PROBLEM AREAS</u>	<u>RECOMMENDED APPROACH</u>
<p>Cycle Life: &gt;1000            Prop. Storage Life (No shear seal): 1 yr            Maximum Diameter: 22 in.            Maximum L/D: 6-7            Expulsion Efficiency: 99.5%            Volumetric Efficiency: 80%            Pressure Drop: 10-50 PSID            Duty Cycle Limitations: none</p>	<p>(a) Propellant-Seal compatibility</p> <p>(b) Seal leakage</p> <p>(c) Piston walking, cocking</p> <p>(d) Piston breakup on bottoming</p>	<p>(a) Select compatible seal mat'l, i.e., teflon or polyethylene; avoid presence of third agent (H<sub>2</sub>O, CO<sub>2</sub>, etc) by pressurizing piston downstream volume with dry nitrogen to 30 PSIG (prelaunch)</p> <p>(b) Use "omniseal" or G-T type seal configuration; incorporate pressure-balanced inner wall to avoid wall deflection under pressure loads; minimize seal wear with &lt;math&gt;\leq 16&lt;/math&gt; RMS surface finish on inner wall</p> <p>(c) Avoid rod-guided pistons; use skirted piston with L/R &gt;1; maintain piston c.g. significantly forward of aft skirt runner; shape piston head so that fluid pressure and dynamic forces pass through piston c.g.</p> <p>(d) Design piston to make initial contact with tank bulkhead at outer diameter; incorporate thin wall piston face that will deform to bulkhead contour</p>

APS-352

# BGRV HYDROGEN PEROXIDE TANK ASSEMBLY

TANK MATERIAL: 301 CRYOFORM STAINLESS STEEL



E-17

APS-268

Figure E-13

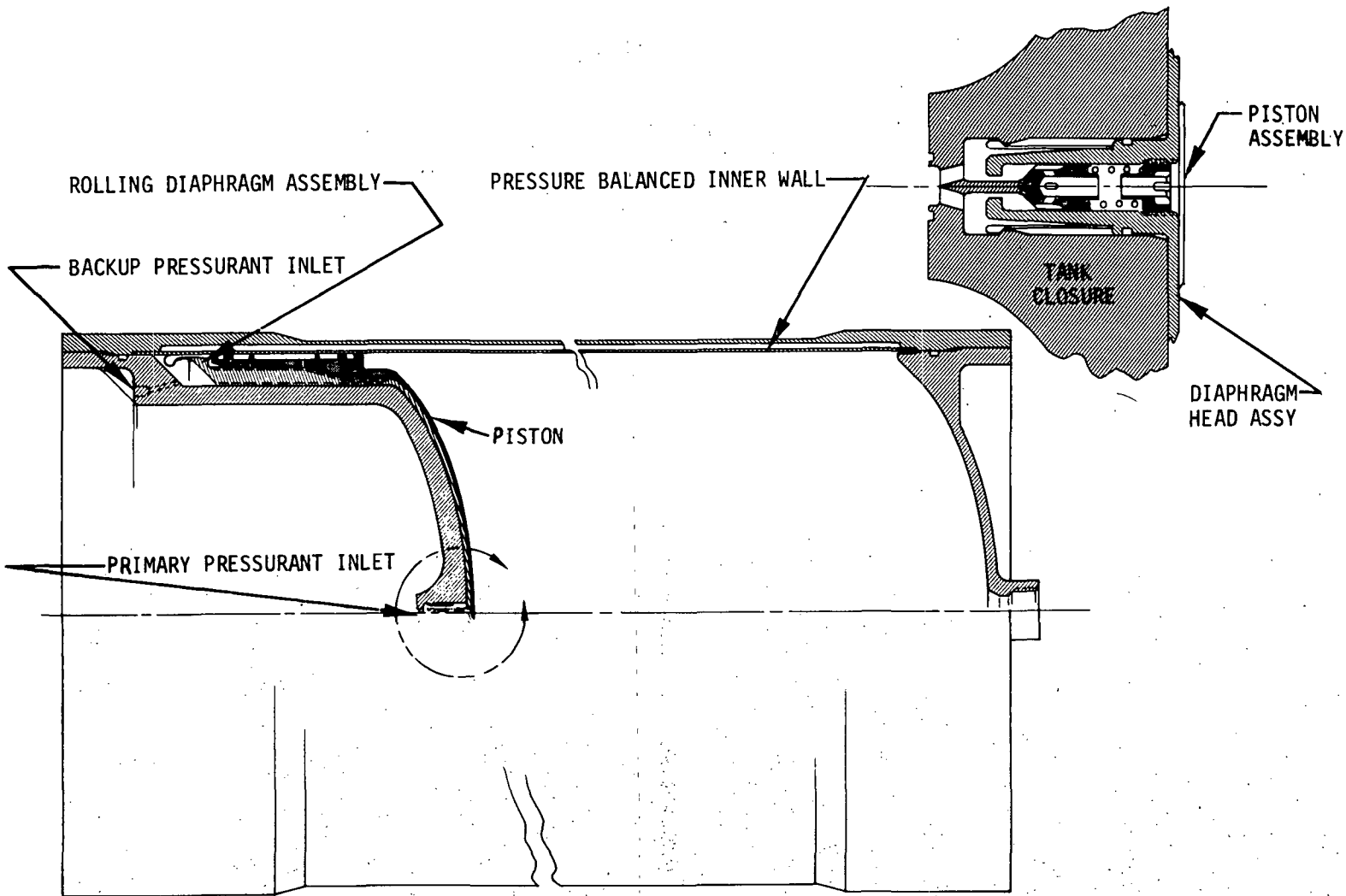
These design concepts have also been incorporated in the redundant expulsion device tank developed in this study. In this design (Figure E-14), the redundant expulsion feature is provided by a rolling metallic diaphragm attached to the piston head. During normal operation, pressurant flow to the primary piston passes through a spring-loaded poppet in the head of the rolling diaphragm assembly (see drawing detail in Figure E-14). A mechanical standoff on the tank bulkhead and a spring retainer clip on the poppet assembly keep the poppet unseated to assure free pressurant flow until the backup expulsion assembly is activated. Once activated, pressurant is admitted to the backside of the diaphragm head and the resulting pressure drop across the head overcomes the clip retention force and moves the head off the standoff. The poppet then seals to provide a leak-tight assembly for backup expulsion.

Figure E-15 presents the redundant piston tank weight model. As with the redundant bladder and bellows tanks, additional pressurant is also required to account for losses incurred during the transfer to the backup expulsion device.

E4 Surface Tension - Nonredundant surface tension devices were chosen as the baseline propellant acquisition method for the study. Since these devices are passive in nature, they are normally regarded as requiring no redundancy. However, in actuality, effective screen pore size can change under imposed slosh, acceleration and vibration loads, as discussed in Figure E-16. Furthermore, flight experience on such devices is limited, and pre-flight verification of integrity is difficult. Therefore, redundancy of the surface tension device was considered to be a desirable objective, and was evaluated in this study.

Because satisfactory performance is contingent upon the maintenance of a stable liquid-gas interface at the screen surface, the dynamic environments and degree of required propellant retention (total or partial) must be thoroughly understood. A screen mesh size must then be selected to withstand the total  $\Delta P$  throughout the device due to hydrostatic, viscous and dynamic effects. Practical limitations are  $192 \text{ lb/ft}^2$  (hydrazine);  $98 \text{ lb/ft}^2$  (monomethylhydrazine), and  $75 \text{ lb/ft}^2$  (nitrogen tetroxide). During entry, the acceleration forces are of sufficient magnitude to exceed the surface tension capabilities, necessitating location of the sump below the settled propellants during this phase of the mission. The candidate tank concept used in Figure E-17 is

# PISTON TANK ASSEMBLY

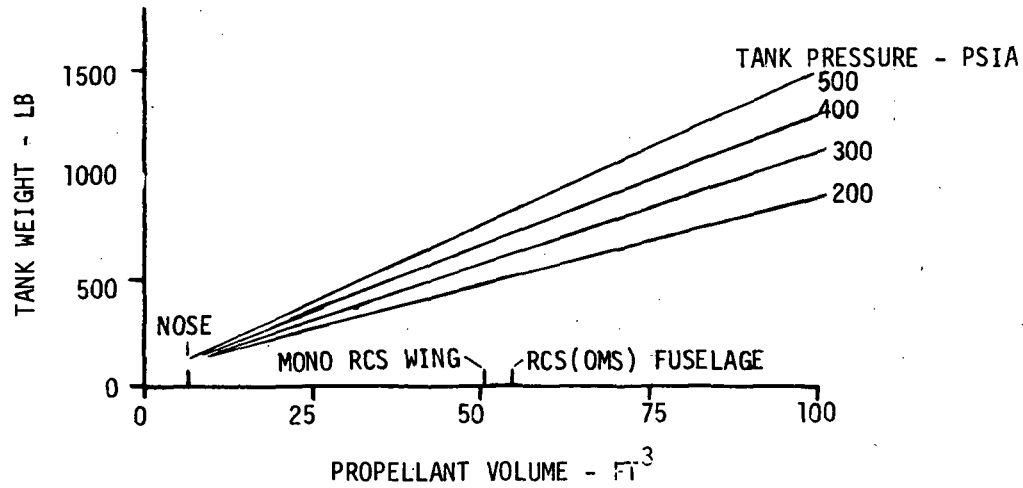
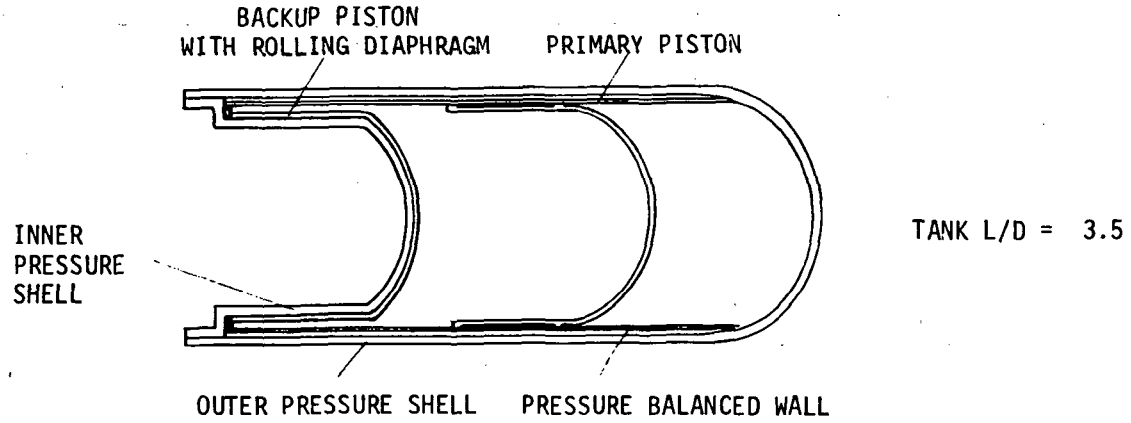


APS-271

E-19

Figure E-14

### PISTON TANKAGE WEIGHT MODEL



## SURFACE TENSION DEVICES

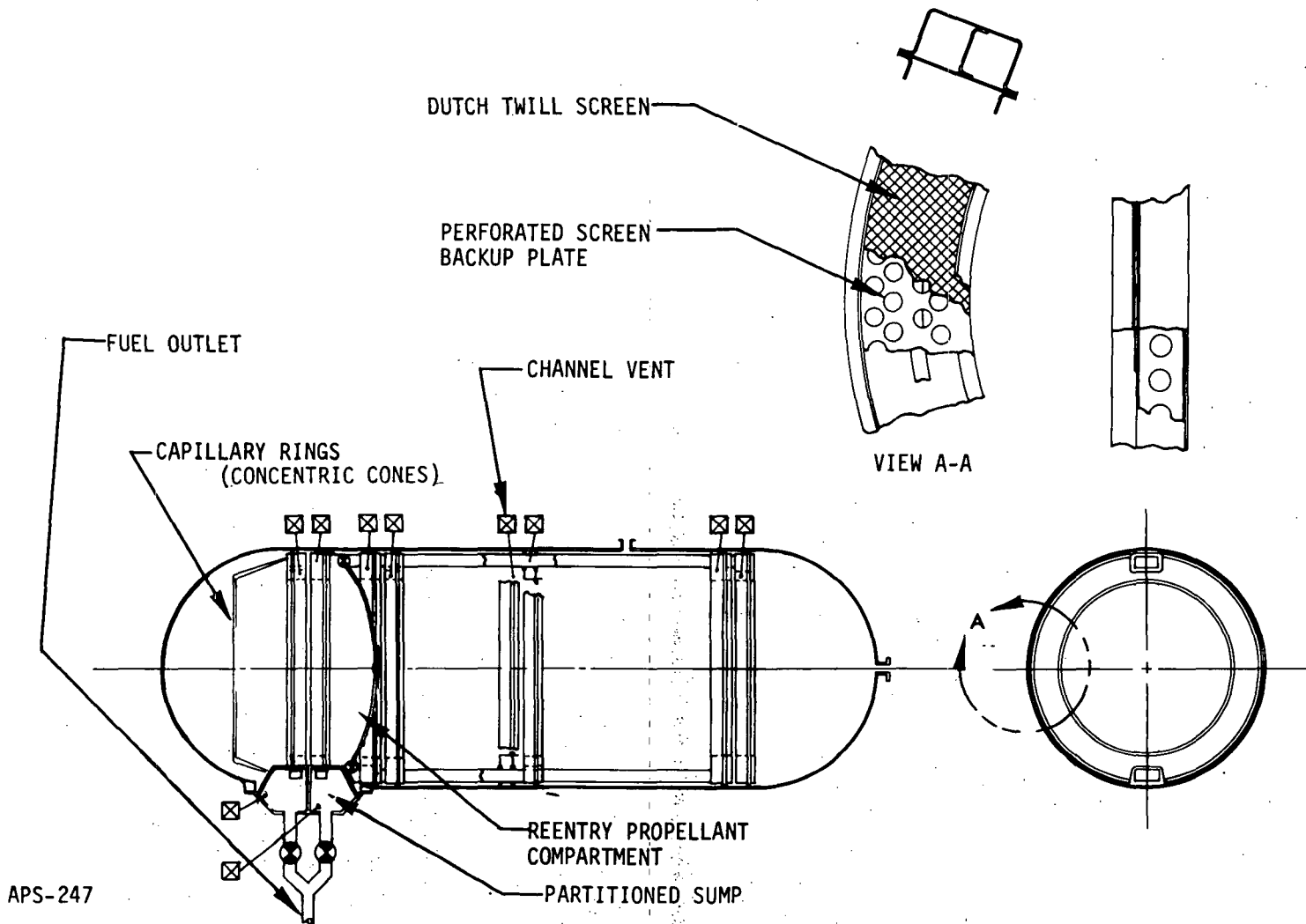
<u>STATE-OF-THE-ART</u>	<u>PROBLEM AREAS</u>	<u>RECOMMENDED APPROACH</u>
<p>Cycle Life: Unlimited                      Propellant Storage Life: 4 yr                      Maximum Diameter: 60 inches                      Maximum Hydrostatic Head (on-orbit):                          <math>N_2H_4</math> MMH - 20-30 ft                          <math>N_2O_4</math> - 8 ft                      Expulsion Efficiency: 99%                      Pressure Drop: 10 PSF                      Duty Cycle Limitations: Limited                          by design propellant extrac-                          tion rate and acceleration                          levels</p>	<p>(a) Corrosion/clogging</p> <p>(b) Change in effective screen pore size (due to dynamic loading, i.e., slosh, vibr., etc)</p> <p>(c) Breakdown in propellant retention</p> <p>(d) Screen drying</p>	<p>(a) Use compatible 347 or 304 dutch twill screen; employ stringent cleaning &amp; drying procedures; filter propellants</p> <p>(b) Provide adequate screen support; avoid propellant backfill during servicing; incorporate bubble point test capability</p> <p>(c) <u>Boost</u>: Assure acquisition device is covered by propellant  <u>On-Orbit</u>: Design for retention under maximum <math>\Delta P</math> (hydrostatic, viscous, dynamic); design propellant pickup natural frequency outside vibration environment; assure adequate communication between bulk propellant &amp; tank outlet  <u>Reentry</u>: Locate tank outlet so it will be covered by propellant during reentry accel; size sump for total reentry propellant requirements</p> <p>(d) Avoid high pressurant ullage temperatures; incorporate thermal resistance between acquisition device and propellant lines/tank wall; provide self-healing capability, i.e., - screen wicking                      - special capillary devices                      - capillary retention between acquisition device &amp; tank wall</p>

APS-353

similar to the screen/channel designs developed under the earlier NASA-MDAC APS studies and improved upon under Contract NAS 8-27685. As shown, two separate and independent sets of acquisition and collector channels are used for redundancy, and a false bottom is incorporated in the tank to isolate sufficient propellant in the lower compartment for entry maneuvers. A valve at the base of each collector channel is closed after retrograde or in the event of a sensed malfunction. Valves are also located at the tank outlets to allow preferential withdrawal of gas-free propellants from the tank sump. The weight models for both redundant and nonredundant surface tension tanks are presented in Figure E-18. With this concept, it is not necessary to vent and repressurize the tank following an expulsion device failure, and therefore a pressurant system weight penalty is not associated with redundancy.

E5 Failure Detection - The inclusion of redundancy implies the capability of failure detection. Gas leakage into the propellant, rather than the reverse situation, is the more likely mode of failure due to the pressure differentials that would exist across the candidate expulsion devices at failure onset. (The bellows tank is the possible exception; the direction of leakage flow would depend on the design bellows spring rate.) Because a gas bubble in the propellant can assume a random orientation in a zero g environment it would be difficult to detect within the propellant tank without an inordinate number of sensors. It is more desirable to draw the bubble into the tank sump or screen trap where it can be detected and vented to vacuum. To accomplish this, it is proposed that the tank heaters be installed near the propellant outlet. This would create a propellant temperature gradient that would cause the bubble to migrate toward the outlet (minimum bubble surface energy) where it would be swept into the gas trap during propellant outflow. The presence of gas within the trap could then be detected by one of the candidate sensors described in Figure E-19. Each of these devices relies on the alteration of a specific property of the fluid, such as density, dielectric coefficient or index of refraction, as a means of detecting a change in fluid quality. All offer continuous monitoring capability and can be incorporated in such a way as to minimize effects on fluid flow. The capacitance probe and refractometer are considered to be the simplest of the candidate detection devices and typical installations for these are depicted in Figure E-20. The remaining sensors represent increasing levels of complexity, with the microwave cavity requiring the most elaborate installation.

# REDUNDANT ACQUISITION SCREEN CHANNEL DESIGN



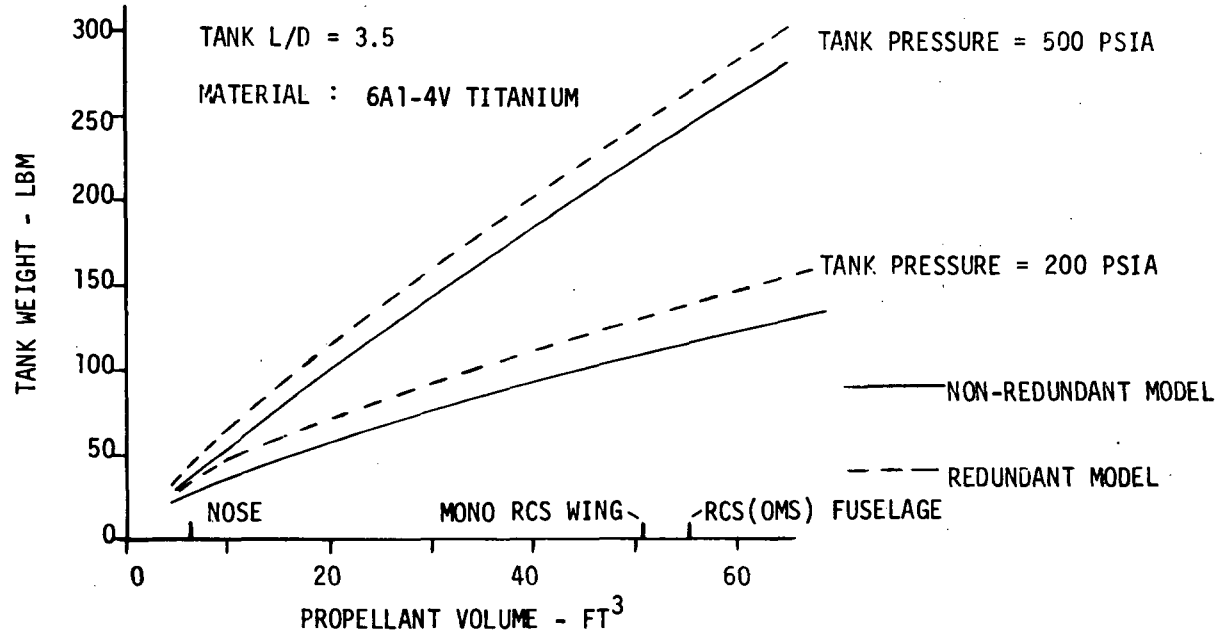
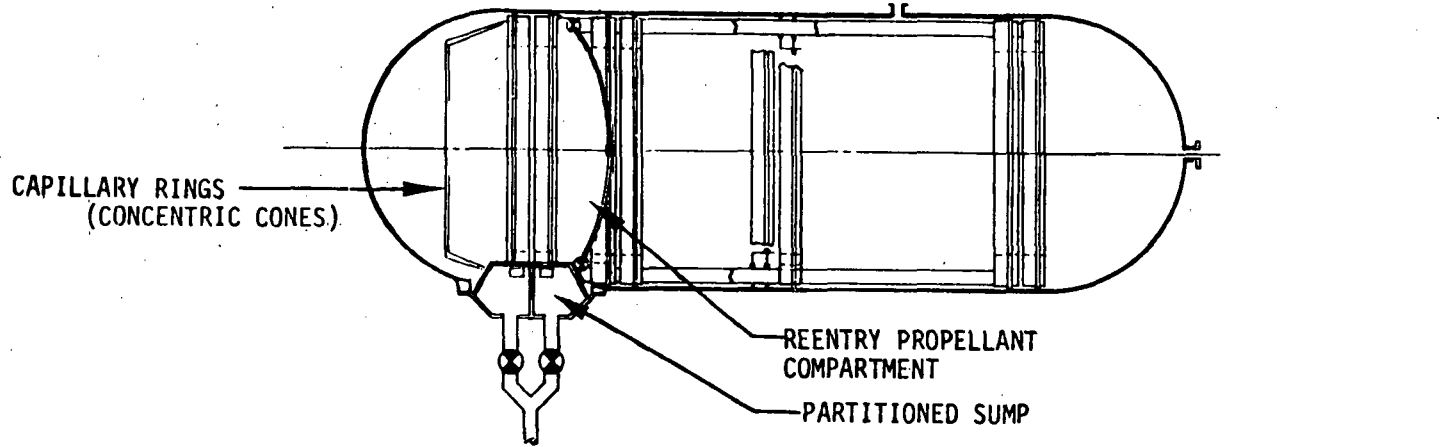
APS-247

E-23

Figure E-17



SURFACE TENSION TANKAGE WEIGHT MODEL



APS-354A

E-24

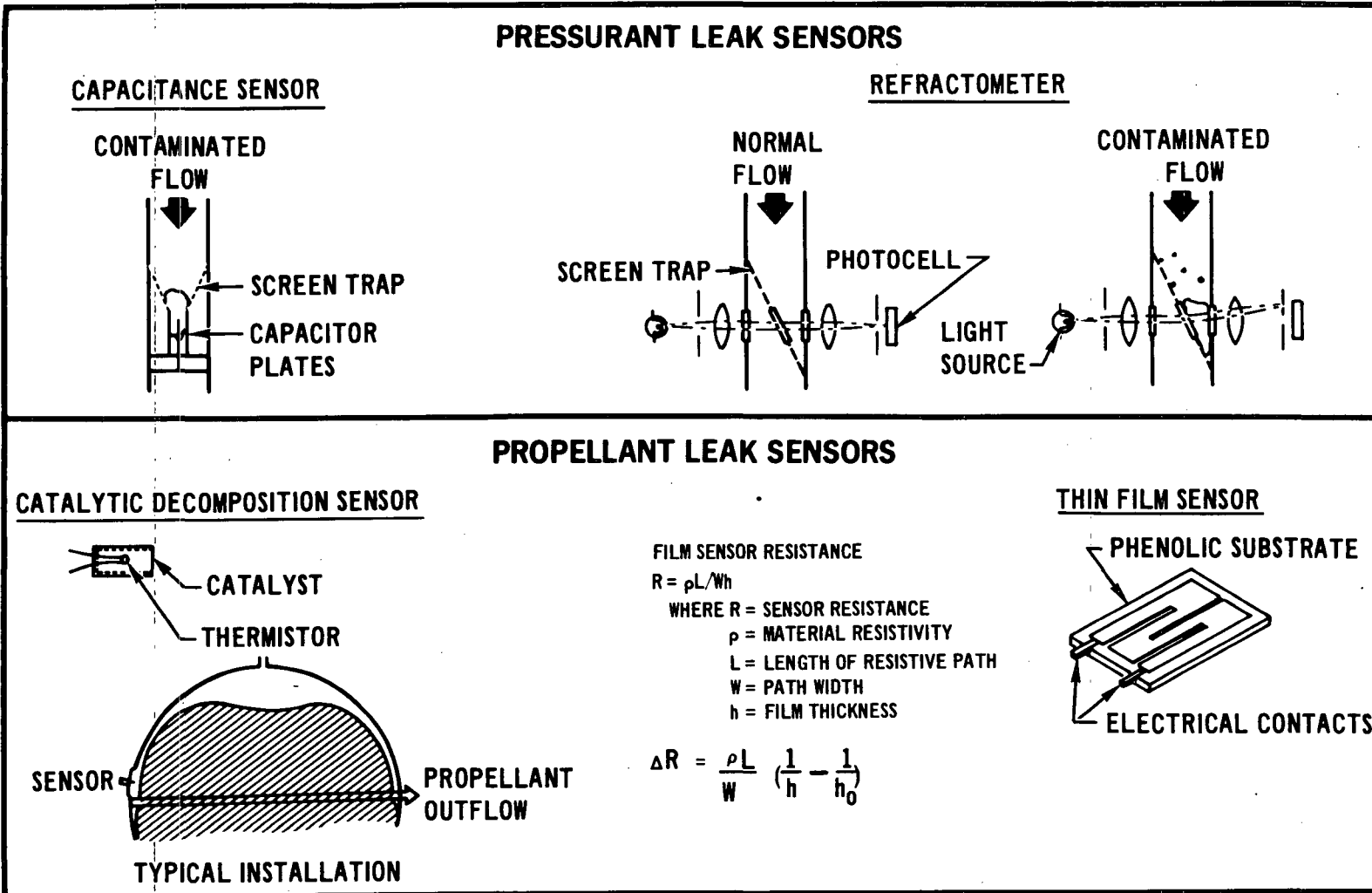
Figure E-18

## PRESSURANT DETECTION INSTRUMENTATION

CONCEPT	PRINCIPAL OF OPERATION	REMARKS	SPACE SHUTTLE POTENTIAL
CAPACITANCE	THE FLUID FLOWS THROUGH A PASSAGE SUCH THAT IT ACTS AS THE DIELECTRIC OF A CAPACITOR. THE PASSAGE OF PRESSURANT GAS RESULTS IN A CHANGE IN THE DIELECTRIC COEFFICIENT OF THE FLUID, THEREBY ALTERING THE ELECTRICAL POTENTIAL OF THE CAPACITOR.	LIGHTWEIGHT AND PASSIVE	GOOD
REFRACTOMETRY	LIGHT RAYS PASSING OBLIQUELY THROUGH THE FLUID ARE REFRACTED. THE ADDITION OF PRESSURANT GAS TO THE FLUID RESULTS IN A CHANGE IN THE ANGLE OF REFRACTION, AND THIS CHANGE IS SENSED BY A PHOTOELECTRIC TRANSDUCER.	ACCURATE METHOD WITH EXTENSIVE COMMERCIAL APPLICATION	GOOD
SONAR	A VARIATION IN THE SPEED OF SOUND AS MEASURED IN THE FLUID MEDIUM INDICATES THE PRESENCE OF PRESSURANT.	INCREASINGLY COMPLEX, SIDE REFLECTIONS	FAIR
MICROWAVE CAVITY	FLUID FLOWS THROUGH AN OPEN-ENDED CAVITY WHICH IS EXCITED AT ITS RESONANT FREQUENCY BY MICROWAVE ENERGY. CHANGES IN THE FLUID'S DIELECTRIC CONSTANT (CAUSED BY THE ADDITION OF PRESSURANT) RESULT IN AN ALTERATION OF THE CAVITY'S RESONANT FREQUENCY. FEEDBACK CIRCUITRY CONSTRAINS THE MICROWAVE INPUT FREQUENCY TO TRACK THE CAVITY'S RESONANT FREQUENCY.	SOPHISTICATED ELECTRONICS; FALSE READINGS POSSIBLE FOR CERTAIN BUBBLE SHAPES & ORIENTATIONS	UNKNOWN
DENSITOMETER	A MAGNETICALLY-DRIVEN REED IN PROPELLANT FLOW PASSAGE VIBRATES AT A KNOWN FREQUENCY. A CHANGE IN FLUID DENSITY (CAUSED BY ADDITION OF PRESSURANT) ALTERS REED SPRING-MASS CHARACTERISTICS AND HENCE, REED FREQUENCY.	SIMPLE; USED IN PETRO-CHEMICAL INDUSTRY FOR MONITORING FLOW OF NATURAL GAS	FAIR

APS-356

# PROPELLANT EXPULSION FAILURE DETECTION



11-232

E-26

Figure E-20

MCDONNELL DOUGLAS ASTRONAUTICS COMPANY - EAST

The detection of contaminants, i.e., propellant, in a gas is a fairly common measurement having widespread industrial application. Several viable concepts were defined and these are summarized in Figure E-21. The first three concepts shown operate by inciting a small chemical reaction between the propellant and sensor. Of these, the catalytic and thin film sensors are simple devices requiring a minimum of peripheral equipment. The kryptonate sensor is also attractive but requires a radiation counter. The difficulty with all three is that their sensitivity is degraded by aging or poisoning, thus necessitating sensor ports in the tank wall to facilitate their periodic removal and replacement. Figure E-20 shows a typical installation for the catalytic and thin film sensors. The sensors would be located in internal tank crevices to take advantage of capillarity in drawing liquid propellant to them. Each of the remaining devices discussed in Figure E-21 require more complex installations, a factor which tends to exclude them from additional consideration.

E6 Composite Tank Materials - To reduce the high inert weights associated with propellant and pressurant tankage, advanced materials, such as those shown in Figure E-22 may be used. For propellant or pressure vessels, fabrication from composite materials is normally accomplished by winding high strength fibers about a mandrel in the presence of a matrix material. The most widely used and fully-developed composite is S-glass in an epoxy matrix. A newer material, Dupont PRD-49, an organic polymer, was designed as a direct substitute for fiberglass, thus taking advantage of existing fabrication tooling. Its advantage lies in its low density. Although relatively new, this material appears most promising. Boron and graphite fibers are also attractive. Their most important advantage is their high modulus. When used with an aluminum matrix, boron is sometimes covered with silicon carbide (Tradename Borsic) to prevent the boron fibers from combining with the aluminum matrix during fabrication. This also improves the materials chemical inertness. Silicon carbide in an epoxy matrix is a new material and only a limited amount of development effort has been expended on it. It combines the advantages of chemical inertness, high modulus and high strength at elevated temperature. Figure E-23 shows the potential weight savings obtainable with composite pressurant vessels when compared to titanium. For

## PROPELLANT DETECTION INSTRUMENTATION

CONCEPT	PRINCIPAL OF OPERATION	REMARKS	SPACE SHUTTLE POTENTIAL
CATALYTIC COMBUSTION	EXOTHERMIC REACTION OF THE PROPELLANT VAPORS BY A CATALYST RESULTS IN A SMALL BUT MEASURABLE TEMPERATURE RISE.	LIGHTWEIGHT AND PASSIVE	GOOD
THIN FILM CORROSION	CORROSION OF A THIN METALLIC FILM BY PROPELLANT VAPORS RESULTS IN THE ALTERATION OF THE FILM'S ELECTRICAL RESISTANCE.	ATTRACTIVE INSTALLATION CAPABILITIES, BUT DEVELOPMENT REQUIRED TO IMPROVE REPRODUCIBILITY	GOOD
KRYPTONATE	THE CHEMICAL ATTACK OF A SOLID RADIOACTIVE SOURCE (KRYPTONATE) BY PROPELLANT VAPORS CAUSES THE RELEASE OF RADIOISOTOPES WHICH ARE DETECTABLE BY A RADIATION COUNTER.	SOMEWHAT MORE COMPLEX ELECTRONICS THAN ABOVE METHODS	GOOD
INFARED ABSORPTION	ENERGY ABSORPTION OVER A NARROW WAVELENGTH BAND BY THE PROPELLANT VAPORS RESULTS IN A REDUCTION IN THE INFARED RADIATION ENERGY REACHING THE SENSOR.	FASTEST RESPONSE, BUT INCREASINGLY MORE COMPLEX	FAIR
MASS SPECTROMETER	THE GAS TO BE ANALYZED IS IONIZED AND PASSED THROUGH A MAGNETIC FIELD, THEREBY CAUSING THE GAS CONSTITUENTS TO TRAVERSE UNIQUE CURVILINEAR PATHS BASED ON THEIR MASS. THE SEPARATED CONSTITUENTS ARE THEN COLLECTED AND QUANTIFIED BY ION CURRENT MEASUREMENTS.	MORE SOPHISTICATED THAN WARRANTED	POOR

MCDONNELL DOUGLAS ASTRONAUTICS COMPANY - EAST

E-28

Figure E-21

APS-358

COMPOSITE TANK MATERIALS

FIBER/MATRIX	ALIGNED FILAMENTS TENSILE PARAMETERS (PSI)		STATUS	FABRICATION
	ULTIMATE STRESS	YOUNG'S MODULUS		
S-901 GLASS/EPOXY DENSITY = 0.072 LB <sub>M</sub> /IN <sup>3</sup> 67% FILAMENT VOL.	220,000	8.3X10 <sup>6</sup>	IN USE FOR SEVERAL YEARS	USUALLY WOUND IN FILAMENT FORM AS EPOXY RESIN IS ADDED. RESIN IS THEN HEAT CURED.
PRD-49-III/EPOXY DENSITY = 0.049 LB <sub>M</sub> /IN <sup>3</sup> 65% FILAMENT VOL.	230,000	12.2X10 <sup>6</sup>	NEW FIBER FROM DUPONT. UNDER- GOING DEVELOPMENT TESTS.	THE SAME AS GLASS.
BORON/EPOXY DENSITY = 0.072 LB <sub>M</sub> /IN <sup>3</sup> 55% FILAMENT VOL.	200,000	32.0X10 <sup>6</sup>	UNDERGOING DEV. TESTS	WOUND IN PRE-IMPREGNATED TAPE FORM AND HEAT CURED. CAN BE FILAMENT WOUND.
HTS GRAPHITE/EPOXY DENSITY = 0.054 LB <sub>M</sub> /IN <sup>3</sup> 60% FILAMENT VOL.	180,000	21.0X10 <sup>6</sup>	UNDERGOING DEV. TESTS	THE SAME AS BORON.
BORSIC/AL6061 (ANNEALED) DENSITY = 0.096 LB <sub>M</sub> /IN <sup>3</sup> 54% FILAMENT VOL.	139,000	32.0X10 <sup>6</sup>	DEVELOPMENT TESTING	BORSIC-ALUMINUM TAPE UNDER A PRESSURE OF ABOUT 500 PSI AT 1000°F FOR 15 MINUTES, AND 15 MINUTES AT 1090° TO 1100°F.
BERYLLIUM/AL1100-0 DENSITY = 0.074 LB <sub>M</sub> /IN <sup>3</sup> 75% FILAMENT VOL.	98,000	34.0X10 <sup>6</sup>	DEVELOPMENT TESTING	BERYLLIUM WIRE COATED IN ALUMINUM IS STACKED OR WOUND. IT IS PRESSED AT 10,000 PSI AND 1000°F.
SiC/EPOXY DENSITY = 0.090 LB <sub>M</sub> /IN <sup>3</sup> 62% FILAMENT VOL.	149,000	32.6X10 <sup>6</sup>	EARLY DEVELOP- MENT TESTING	WOUND IN FILAMENT (OR POSSIBLY TAPE) FORM AND HEAT CURED.

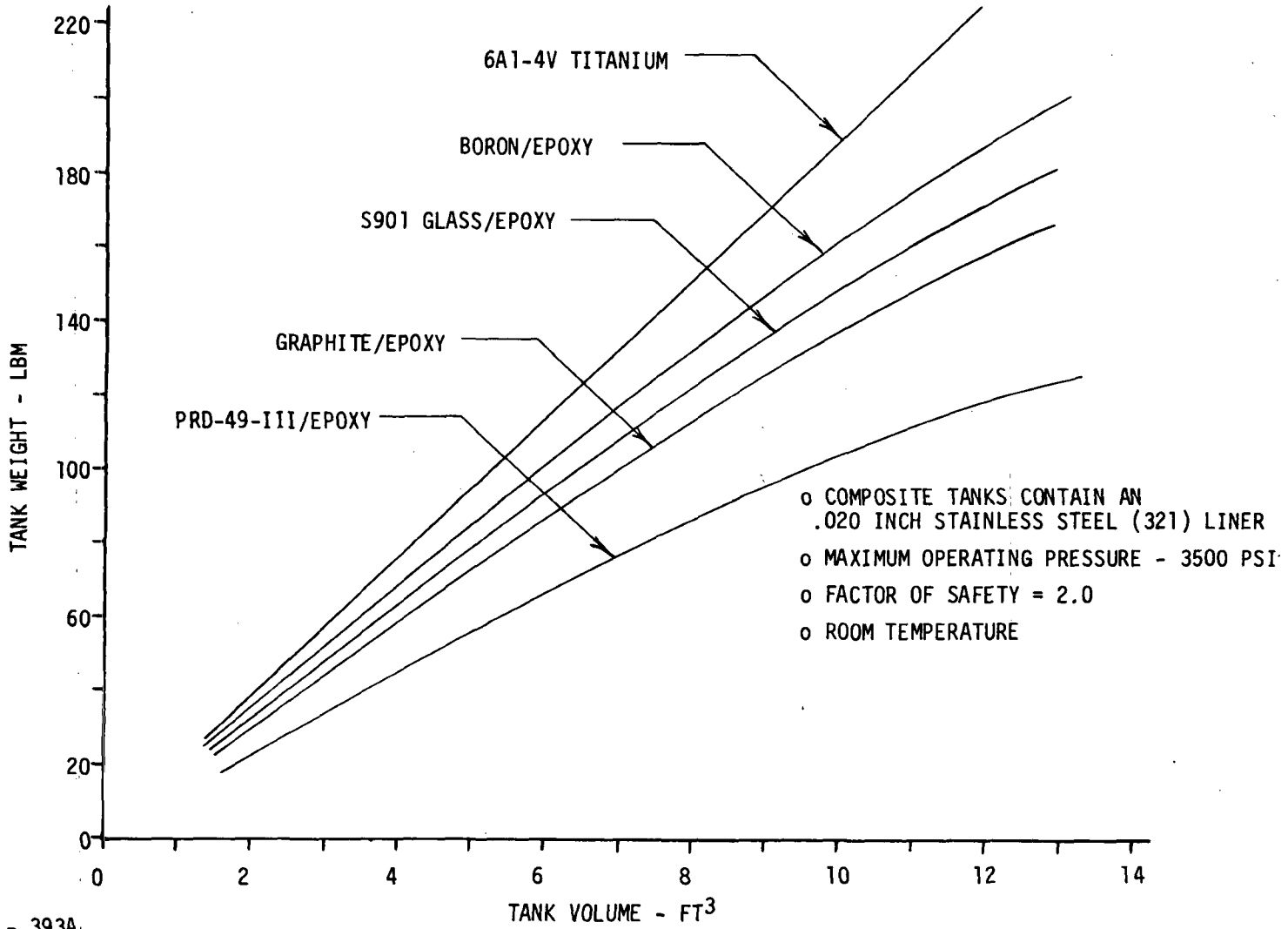
MCDONNELL DOUGLAS ASTRONAUTICS COMPANY - EAST

E-29

Figure E-22

APS-394

### COMPOSITE SPHERICAL PRESSURANT TANK WEIGHTS



APS - 393A

E-30

Figure E-23

those types using a porous matrix, i.e., epoxy, a thin metal liner is used. Liners which have been used successfully include several aluminum alloys, 6Al4V Titanium, Inconel and Stainless Steel.

E7 Compatibility - In the design of propellant tankage for storable propellants, compatibility of materials with the propellants must receive detailed consideration. Accordingly, a literature search has been conducted to accumulate data on materials compatibility, with primary emphasis on the particular requirements of Space Shuttle, namely, reusability and ease of maintenance.

Two classes of test programs have been performed in this field: coupon tests and, to a much lesser degree, representative tankage tests. The coupon tests are quite useful in identifying those materials which are grossly incompatible, but they do not represent conclusive proof of a metal's suitability. It is only at the level of representative tankage testing that all of the factors can be brought into play. In this type of program, the effects of surface condition, weld joint design and fabrication, stress corrosion, and environment can all be realistically duplicated.

Of the several programs of this nature that have been conducted, the "Packaged Systems Storability" program, which has been continuing for the past four years at the Air Force Rocket Propulsion Laboratory, is of special interest. In this program, representative tankage articles, designed and fabricated by various vendors, have been subjected to 85°F and 85 percent relative humidity in the case of oxidizers, and 65°F to 165°F and uncontrolled humidity in the case of fuel. Figure E-24 describes the causes of the failures occurring throughout the course of the program, and Figure E-25 summarizes the performance of the various metals which have been evaluated. It is apparent from these preliminary results that the design and quality control of weld areas is of utmost importance. Double heat welds which occur at start/stop points and at weld intersections or at weld repairs lead to a high incidence of cracks. This condition is especially prevalent in manual repair welds because of poor control of heat input.

Figure E-26 presents the results of the screening of candidate metals. These metals have been evaluated, based on propellant compatibility, weldability, ultimate strength to weight ratio, and fracture-toughness. In the evaluation of propellant compatibility, over thirty sources were reviewed, with more attention given to representative tankage test results. Compatibility



SUMMARY OF RPL "PACKAGED SYSTEMS STORABILITY"  
PROGRAM TANK FAILURES (N<sub>2</sub>O<sub>4</sub> OR N<sub>2</sub>H<sub>4</sub> RELATED)

PROPELLANT	TANK TYPE	TANK MATL	DAYS IN TEST	CONCLUSIONS OF FAILURE ANALYSIS
N <sub>2</sub> O <sub>4</sub>	3" x 6"	2014-T6	5	FAILURE WAS THE RESULT OF POOR CONTAINER END-PLATE JOINT DESIGN WHICH RESULTED IN LACK OF WELD PENETRATION IN THE FLAT 1/4" PLATE TO THE .064" CYLINDRICAL SECTION.
N <sub>2</sub> O <sub>4</sub>	3" x 6"	2014-T6	5	SAME AS ABOVE
N <sub>2</sub> O <sub>4</sub>	3" x 6"	2014-T6	5	SAME AS ABOVE
N <sub>2</sub> O <sub>4</sub>	3" x 6"	2014-T6	5	SAME AS ABOVE
N <sub>2</sub> O <sub>4</sub>	3" x 6"	2014-T6	2	FAILURE DUE TO NITRIC ACID ATTACK ON THE EXTERIOR SURFACE WHICH LED EVENTUALLY TO STRESS CORROSION CRACKING AND VESSEL FAILURE. IT IS NOT APPARENT WHETHER NITRIC ACID RESULTED FROM N <sub>2</sub> O <sub>4</sub> VAPOR LEAK IN THIS VESSEL OR FROM N <sub>2</sub> O <sub>4</sub> LEAKING FROM ANOTHER VESSEL AND CONDENSING ON THE VESSEL IN QUESTION.
N <sub>2</sub> O <sub>4</sub> *	GD/C	5A1-2.5S <sub>n</sub>	14	FAILURE DUE TO STRESS CORROSION CRACKING IN WELD AREAS CAUSED BY INTERNAL ATTACK BY THE UNINHIBITED N <sub>2</sub> O <sub>4</sub> . STRESS LEVELS AND TEMPERATURES WERE CONSIDERED TO BE BELOW STRESS CORROSION THRESHOLD; HOWEVER, WELD AREAS AND HEAT-AFFECTED ZONES PROBABLY EXPERIENCED HIGHER LEVELS THAN ANTICIPATED.
N <sub>2</sub> O <sub>4</sub> *	GD/C	5A1-2.5S <sub>n</sub>	16	SAME AS ABOVE (LEAK - $8.4 \times 10^{-6}$ ATM-CC/SEC)
N <sub>2</sub> O <sub>4</sub> *	MARTIN	6A1-4V	10	SAME AS ABOVE
N <sub>2</sub> O <sub>4</sub> *	MARTIN	6A1-4V	34	SAME AS ABOVE (LEAK - $2 \times 10^{-5}$ ATM-CC/SEC)
N <sub>2</sub> O <sub>4</sub> *	MARTIN	6A1-4V	35	SAME AS ABOVE (LEAK - $1.6 \times 10^{-6}$ ATM-CC/SEC)
APS-709				

SUMMARY OF RPL "PACKAGED SYSTEMS STORABILITY"  
PROGRAM TANK FAILURES (N<sub>2</sub>O<sub>4</sub> OR N<sub>2</sub>H<sub>4</sub> RELATED) (CONTINUED)

PROPELLANT	TANK TYPE	TANK MATL	DAYS IN TEST	CONCLUSIONS OF FAILURE ANALYSIS
N <sub>2</sub> O <sub>4</sub>	GD/C	AM 350	294	CAUSE OF FAILURE WAS A HOT SHORT CRACK OCCURRING IN A REPAIR WELD. AM350 IS CONSIDERED TO HAVE EXCELLENT WELDABILITY; HOWEVER, CRACKING DUE TO MATERIAL CONTRACTION AFTER WELD IS ALWAYS A POSSIBILITY, AND THE WELDING PARAMETERS MUST THEREFORE BE CAREFULLY CONTROLLED. (LEAK-PROFUSE)
N <sub>2</sub> O <sub>4</sub>	MARTIN	7039-T6	555	LEAKAGE OCCURRED AS A RESULT OF STRESS CORROSION CRACKING FROM EXTERNAL TO INTERNAL SURFACES ALONG SHORT TRANSVERSE GRAIN BOUNDARIES. ALLOYS WHICH ARE QUITE SUSCEPTIBLE TO STRESS CORROSION IN SHORT TRANSVERSE GRAIN DIRECTION SHOULD NOT BE HIGHLY STRESSED IN THAT DIRECTION. (LEAK - $1.2 \times 10^{-5}$ ATM-CC/SEC)
N <sub>2</sub> O <sub>4</sub>	MARTIN	17-7PH	295	FAILURE WAS DUE TO CORROSION BY NITRIC ACID FROM THE EXTERIOR SURFACE OF THE TANK. NITRIC ACID WAS APPARENTLY FORMED ON THE FAILED TANK BY CONDENSATION OF WATER AND N <sub>2</sub> O <sub>4</sub> FROM A NEARBY LEAKING VESSEL. HOWEVER, LEAKAGE MAY ALSO HAVE OCCURRED THROUGH A HOT SHORT CRACK IN A WELD AREA. (LEAK - $1.6 \times 10^{-5}$ ATM-CC/SEC)
N <sub>2</sub> O <sub>4</sub>	MARTIN	2014-T6	5-9	ORIGIN OF FAILURE WAS PITTING AND STRESS CORROSION CRACKING IN A WELD FUSION ZONE, CAUSED BY NITRIC ACID WHICH FORMED ON THE TANK AS A RESULT OF N <sub>2</sub> O <sub>4</sub> LEAKAGE FROM ANOTHER VESSEL. TESTS INDICATED THAT MATERIAL WAS IN-T4 CONDITION. THE MATERIAL SHOULD BE IN THE FULLY AGED (-T6) CONDITION FOR BEST CORROSION RESISTANCE. (LEAK - $2.2 \times 10^{-5}$ ATM-CC/SEC)
ClF <sub>5</sub>	GD/C	AM350	294	FAILURE DUE TO CORROSION THROUGH FROM THE EXTERIOR SURFACE CAUSED BY CONDENSATION OF WATER AND N <sub>2</sub> O <sub>4</sub> FROM A NEARBY LEAKING VESSEL. (LEAK-PROFUSE)
ClF <sub>5</sub>	GD/C	AM350	295	SAME AS ABOVE (LEAK-PROFUSE)

\* NTO was Grade MIL-P-26539B (BROWN) and therefore tests do not represent a fair assessment of 6Al-4V compatibility.  
APS-710

E-33

Figure E-24 (Continued)

SUMMARY OF RPL "PACKAGED SYSTEMS STORABILITY"  
PROGRAM MATERIAL EXPERIENCE

PROPELLANT	MATERIAL	NO. OF TEST ARTICLES	NO. OF FAILED TANKS	REMARKS
N <sub>2</sub> O <sub>4</sub>	2014-T6	41	6	4 FAILURES WERE CAUSED BY UNSATISFACTORY WELD DESIGN. 2 FAILURES WERE CAUSED BY NITRIC ACID-INDUCED STRESS CORROSION ON THE TANK EXTERIORS.
N <sub>2</sub> O <sub>4</sub>	2021-T6	9	0	
N <sub>2</sub> O <sub>4</sub>	2219-T6	2	0	
N <sub>2</sub> O <sub>4</sub>	2219-T81	2	0	
N <sub>2</sub> O <sub>4</sub>	5456-T6	2	0	
N <sub>2</sub> O <sub>4</sub>	6061-T6	5	0	
N <sub>2</sub> O <sub>4</sub>	7007-T6	1	0	
N <sub>2</sub> O <sub>4</sub>	7039-T6	2	1	FAILURE CAUSED BY EXCESSIVE STRESS IN SHORT TRANSVERSE GRAIN DIRECTION LEADING TO STRESS CORROSION CRACKING.
N <sub>2</sub> O <sub>4</sub> *	5A1-2.5S <sub>n</sub>	2	2	FAILURE DUE TO STRESS CORROSION CRACKING IN WELD AREAS CAUSED BY INTERNAL ATTACK BY THE UNINHIBITED N <sub>2</sub> O <sub>4</sub> .
N <sub>2</sub> O <sub>4</sub> *	6A1-4V	3	3	FAILURE DUE TO STRESS CORROSION CRACKING IN WELD AREAS CAUSED BY INTERNAL ATTACK BY THE UNINHIBITED N <sub>2</sub> O <sub>4</sub> .
N <sub>2</sub> O <sub>4</sub> **	6A1-4V	3	0	
N <sub>2</sub> O <sub>4</sub>	301 CRYO	10	0	5 TANKS 301 CRYO(AGED) - 5 TANKS 301 CRYO (UNAGED)
N <sub>2</sub> O <sub>4</sub>	AM350	1	1	FAILURE CAUSED BY HOT SHORT CRACK OCCURRING IN A REPAIR WELD
APS-711				

E-34

Figure E-25

SUMMARY OF RPL "PACKAGED SYSTEMS STORABILITY"  
PROGRAM MATERIAL EXPERIENCE (CONTINUED)

PROPELLANT	MATERIAL	NO. OF TEST ARTICLES	NO. OF FAILED TANKS	REMARKS
ClF <sub>5</sub>	AM350	2	2	FAILURE DUE TO EXTERIOR CORROSION CAUSED BY CONDENSATION OF WATER AND N <sub>2</sub> O <sub>4</sub> FROM A NEARBY LEAKING VESSEL.
N <sub>2</sub> O <sub>4</sub>	17-7PH	1	1	FAILURE DUE TO EXTERIOR CORROSION CAUSED BY CONDENSATION OF WATER AND N <sub>2</sub> O <sub>4</sub> FROM A NEARBY LEAKING VESSEL
N <sub>2</sub> H <sub>4</sub>	2014-T6	5	0	
N <sub>2</sub> H <sub>4</sub>	2021-T6	8	0	
N <sub>2</sub> H <sub>4</sub>	2219-T87	5	0	
N <sub>2</sub> H <sub>4</sub>	6A1-4V	8	0	
N <sub>2</sub> H <sub>4</sub>	A286	5	0	
N <sub>2</sub> H <sub>4</sub>	301 CRYO	29	0	15 TANKS 301 CRYO (AGED) - 14 TANKS 301 CRYO (UNAGED)
N <sub>2</sub> H <sub>4</sub>	AM350	5	0	SOME PRESSURE RISE
N <sub>2</sub> H <sub>4</sub>	17-7PH	5	0	SOME PRESSURE RISE

\* NTO WAS GRADE MIL-P-26539B (BROWN) AND THEREFORE TESTS DO NOT REPRESENT A FAIR ASSESSMENT OF 6A1-4V COMPATIBILITY.

\*\* NTO WAS GRADE MSC-PPC-2A (GREEN).

APS-712

E-35

Figure E-25 (Continued)

with wet nitrogen tetroxide has been included since tests have shown that under conditions in excess of 30 percent relative humidity, NTO vapor leaks will not dissipate into the atmosphere, but rather combine with the water vapor to form dilute nitric acid condensate on the tank exterior. The corrosive nature of the nitric acid can then (depending on the material) enlarge the original leak to the extent that liquid leaks occur.

Space Shuttle ease of operation requirements dictate a choice of materials that are relatively insensitive to humid environment and occasional propellant spills. Although several aluminum alloys are well suited for use in the storage of concentrated (>82%) nitric acid, their resistance decreases rapidly with decreasing concentrations, and are therefore poorly suited to the storage of oxidizers on Space Shuttle.

Conclusions as to the compatibility of metals and hydrazine found in the literature have been modified somewhat to the extent that concern over propellant decomposition has been tempered. Many of the documented test programs have been performed specifically for the evaluation of compatibility for multi-year missions. For that type of application, propellant decomposition and the resulting pressure buildup is a significant concern. For the Space Shuttle application, however, where the maximum mission duration is on the order of 30 days, negative conclusions based on long-term propellant decomposition are not necessarily applicable. In general, metals which are satisfactory with hydrazine are also acceptable for use with MMH, since it is no more corrosive, and not as susceptible to catalytic decomposition. Based on these findings, two materials, 6Al-4V Titanium and 301 Cryoformed Stainless Steel were chosen for further evaluation.

E8 Fracture Mechanics - Pressure vessels often contain small flaws or defects that are either inherent in the material, or introduced during fabrication. Even though considerable emphasis is being placed upon improving non-destructive inspection techniques, the fact remains that all defects can not presently be detected. These defects can cause severe reductions in the static load capability and the operational life of the pressure vessel. Fracture Mechanics is considered the most quantitative approach for evaluating the impact of these undetected flaws on pressure vessel design and reuse characteristics.

# MATERIALS OF CONSTRUCTION PROPELLANT COMPATIBILITY

MATERIAL	PROPELLANT COMPATIBILITY				WELDABILITY	ULTIMATE STRENGTH/WT (10 <sup>6</sup> $\frac{\text{LBF-IN}}{\text{LBM}}$ )	FRACTURE-TOUGHNESS (KSI $\sqrt{\text{IN}}$ )
	N <sub>2</sub> H <sub>4</sub>	MMH	N <sub>2</sub> O <sub>4</sub>	WET N <sub>2</sub> O <sub>4</sub>			
1100-0	A	A	A	C <sup>(2)</sup>	A	.13	
2014-T6	B <sup>(1)</sup>	A	A	C <sup>(2)</sup>	C	.70	21
2017	A	I	I	C <sup>(2)</sup>	C	.62	
2024-T3	C <sup>(1)</sup>	A	B <sup>(1)</sup>	C <sup>(2)</sup>	C	.64	
2219-T87	A	A	A	C <sup>(2)</sup>	A	.69	32
3003	A	I	A	C <sup>(2)</sup>	A	.29	
5052	A	I	A	C <sup>(2)</sup>	A	.42	13
5456	C <sup>(1)</sup>	I	I	C <sup>(2)</sup>	A	.56	16
6061-T6	A	A	A	C <sup>(2)</sup>	A	.45	
6066	I	I	I	C <sup>(2)</sup>	A	.57	
7039	I	I	I	C <sup>(2)</sup>	A	.60	19
7075	C <sup>(3)</sup>	I	C <sup>(1)</sup>	C <sup>(2)</sup>	C	.83	27

- A - SATISFACTORY
- B - ACCEPTABLE
- C - UNSATISFACTORY
- I - INSUFFICIENT DATA
- (1) - ADDUCT FORMATION
- (2) - CORROSION
- (3) - PROPELLANT DECOMPOSITION

APS-360

MATERIALS OF CONSTRUCTION PROPELLANT COMPATIBILITY  
(CONTINUED)

MATERIAL	PROPELLANT COMPATIBILITY				WELDABILITY	ULTIMATE STRENGTH/ $\bar{W}T$ ( $10^6 \frac{LBF-IN}{LBM}$ )	FRACTURE-TOUGHNESS ( $KSI\sqrt{IN}$ )
	$N_2H_4$	MMH	$N_2O_4$	WET $N_2O_4$			
356	A	A	I	C <sup>(2)</sup>	A	.38	
5A1-2.5Sn	A	A	A	I	A	.75	46
6A1-4V	A	A	A	A	B	1.00	46
301 CRYO(UNAGED)	A	A	A	A	B	.90	102
302 SS	B <sup>(3)</sup>	I	I	A	A	.26	
304 SS	A	A	B <sup>(1)</sup>	A	A	.27	59
316 SS	C <sup>(3)</sup>	C <sup>(3)</sup>	B <sup>(1)</sup>	A	A	.29	
317 SS	C <sup>(3)</sup>	I	I	A	A	.31	
321 SS	A <sup>(3)</sup>	B <sup>(3)</sup>	B <sup>(1)</sup>	A	A	.31	
347	B <sup>(3)</sup>	B <sup>(3)</sup>	B <sup>(1)</sup>	A	A	.31	
410 SS	C <sup>(3)</sup>	C <sup>(3)</sup>	C <sup>(1)</sup>	C <sup>(2)</sup>	B	.25	
416 SS	C <sup>(1)</sup>	C <sup>(1)</sup>	B <sup>(1)</sup>	C <sup>(2)</sup>	C	.26	
430 SS	C <sup>(3)</sup>	C <sup>(3)</sup>	B <sup>(1)</sup>	B <sup>(2)</sup>	B	.2'	
AM350	A	A	C <sup>(1)</sup>	I	B	.52	
17-4PH	C <sup>(3)</sup>	B <sup>(3)</sup>	C <sup>(1)</sup>	B <sup>(2)</sup>	B	.56	36
17-7PH	C <sup>(3)</sup>	B <sup>(3)</sup>	C <sup>(1)</sup>	B <sup>(2)</sup>	B	.65	65

APS-361

E-38

Figure E-26 (Continued)

The theory of Fracture Mechanics can be used to predict the minimum service life of pressure vessels by assuming that failure will be caused by existing flaws. Failure results when the stress intensity (a parameter which reflects the redistribution of stress in an elastic body due to the presence of a flaw) at the flaw tip reaches a critical value, defined as fracture toughness. Stress intensity increases with increasing flaw size and/or applied stress level. Under imposed cyclic or sustained stresses, such increases can result in critical stress intensity. For any specified environment, a threshold stress intensity level exists, below which sustained flaw growth does not occur. For stress intensities below the threshold value, the cyclic life is limited by the number of cycles required to increase the stress intensity to the threshold level. Above the threshold level, continuous flaw growth occurs, and failure could occur in one additional cycle if the hold time were sufficiently long. This threshold limit is a function of the material's environment. The growth of a flaw in a thick walled vessel produces a catastrophic failure when the stress intensity reaches the critical value. However, if the material fracture toughness and the applied stress are such (high fracture toughness - low applied stress) that the critical flaw size exceeds the vessel wall thickness, flaw growth proceeds through the wall thickness and the failure mode is one of leakage rather than fracture.

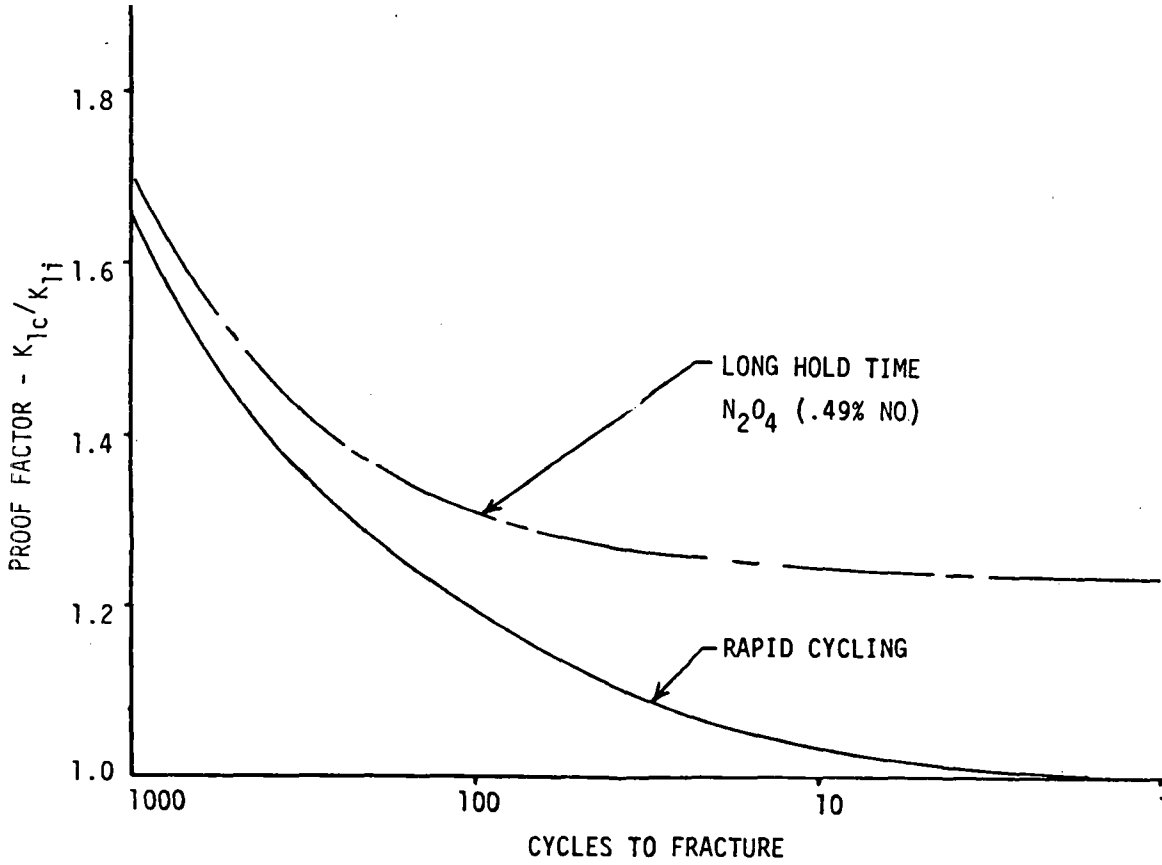
The best known method of verifying pressure vessel life is the proof test. The proof factor necessary to verify a given cycle life is equal to the critical-to-initial-stress intensity ratio corresponding to this life. Figure E-27 presents the proof factors required for 6Al-4V Titanium in a noncorrosive (neutral) environment. For example, to demonstrate a life of 500 cycles, a proof test at 1.45 times the operating pressure is required. If an initial flaw were large enough to cause a failure under operating stresses in less than 500 cycles, then failure would occur at the proof stress during the first cycle.

Successful completion of the proof test implies the absence of flaws above a certain size (the higher the proof pressure, the smaller the possible flaw). In general, larger initial flaw depths are permissible with titanium than with 301 Cryoform for any given design and cycle life requirement.



# PROOF FACTOR

- 6 Al - 4V TITANIUM
- THICK WALLED VESSEL



APS-790

E-40

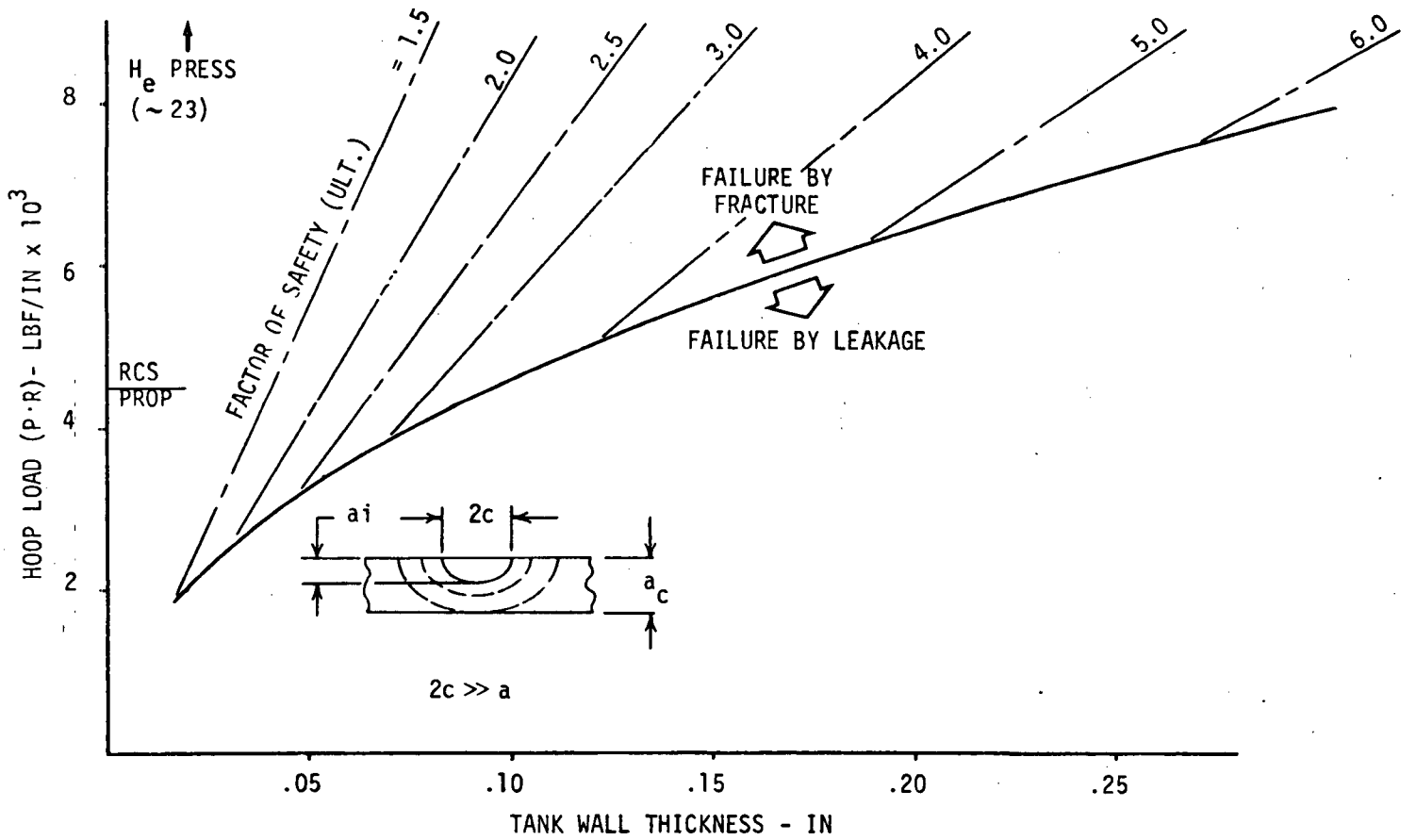
Figure E-27

Titanium, therefore, shows an advantage in this respect by offering a better probability of flaw detection prior to tank fabrication by nondestructive inspection techniques. Radiographic techniques are capable of detecting flaw sizes on the order 0.020 in. Since the allowable initial flaw size necessary to ensure a life of 1000 cycles for the RCS tanks will be on the same order of magnitude, the engineer must rely heavily on proof testing to demonstrate integrity of vessels fabricated from this material. (Several aluminum alloys, notably 2219 T87, are attractive from Fracture Mechanics considerations in that they offer significantly larger allowable flaw sizes. Additionally, since lower factors of safety, consistent with the 1000 cycle life requirement, can be used with aluminum than with steel, weight penalties can be minimized. However, as discussed in Section E7, aluminum is not compatible with NTO in a humid environment. For this reason, its use as a material of construction was not specifically evaluated.)

A desirable feature in pressure vessel design is to have failure occur in the leakage mode rather than the fracture mode. This assures greater safety to vehicle and crew during mission operation, and often prevents catastrophic loss of a component during proof testing. Figures E-28 and E-29 define the conditions necessary to assure failure by leakage rather than by fracture for 6Al-4V Titanium and 301 Cryoform, respectively. For a typical titanium RCS wing pod propellant tank design with a hoop load of approximately 4500 lbf/in (tank pressure =  $300 \text{ lbf/in}^2$ , tank radius = 15 in.), a factor of safety of 3.5 on ultimate stress would be required to preclude failure by fracture. Since the conventional factor of safety based on static considerations is 2.0, designs to provide failure by leakage in a titanium tank would result in 78% increase in tank shell weight, as shown in Figure E-30. However, the same tank made from 301 Cryoform at a factor of safety of 2.0 would provide reasonable assurance that the predominant failure mode was leakage (Figure E-31). This contrast is due to the fact that the fracture toughness of 301 is more than twice the fracture toughness of titanium, resulting in a factor of approximately four between the two sizing boundaries for failure by leakage. For a pressurant vessel, the hoop load is sufficiently high that a design based on failure by leakage is impractical. One approach would be to reduce the hoop load by using multiple tanks of smaller radii. Nevertheless, the weight penalty is high. For example, the weight of four 301 Cryoform pressurant bottles per RCS module,

### TANK SIZING REQUIREMENTS

- 6A1 - 4V TITANIUM  
( $F_{TU} = 168 \text{ KSI}$ ,  $K_{Ic} = 45.6 \text{ KSI}\sqrt{\text{IN}}$ )
- NEUTRAL ENVIRONMENT



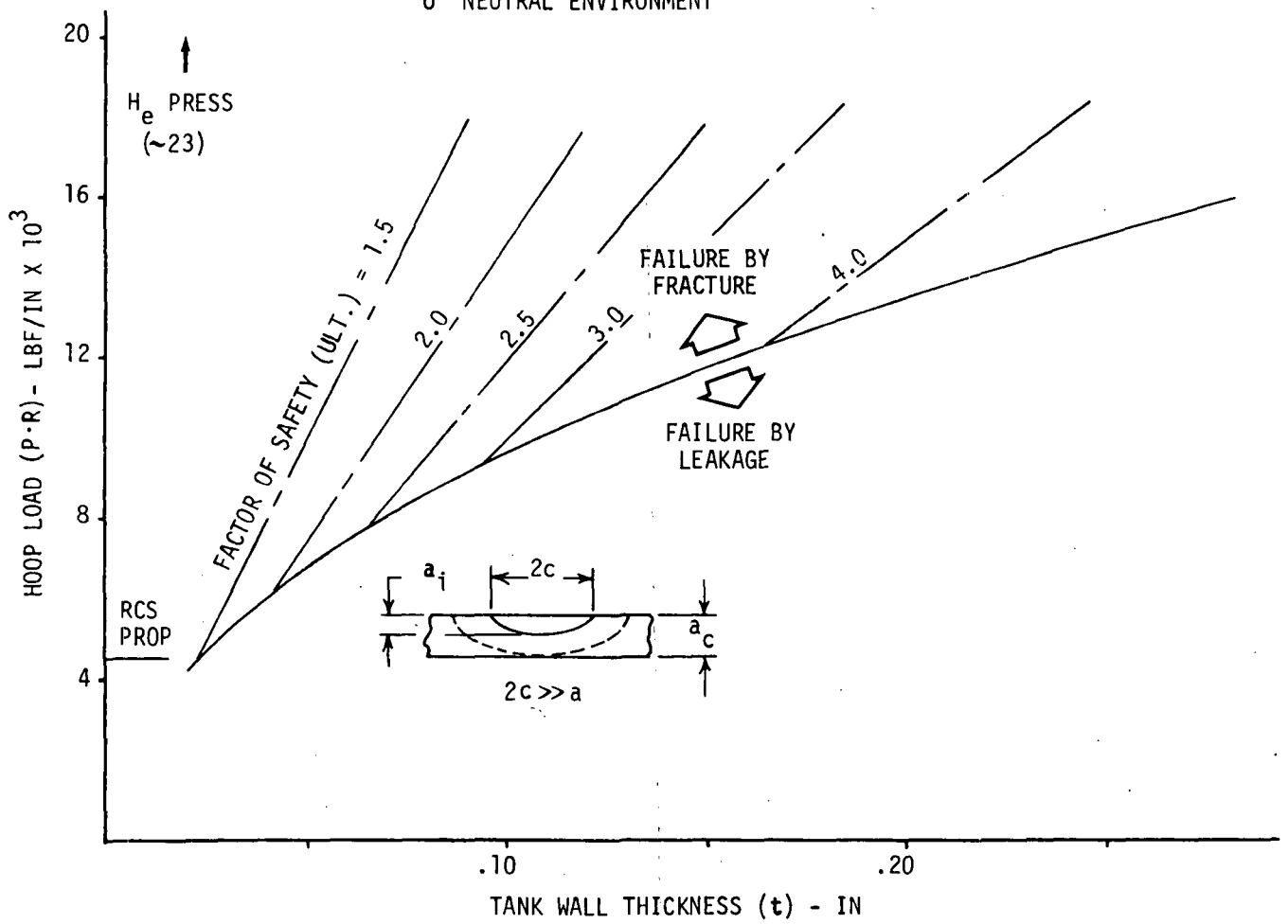
APS-791

E-42

Figure E-28

# TANK SIZING REQUIREMENTS

- o 301 CRYOFORMED STAINLESS STEEL (78% COLD REDUCED)  
( $F_{TU} = 300 \text{ KSI}$ ,  $K_{1c} = 95 \text{ KSI}\sqrt{\text{IN}}$ )
- o NEUTRAL ENVIRONMENT



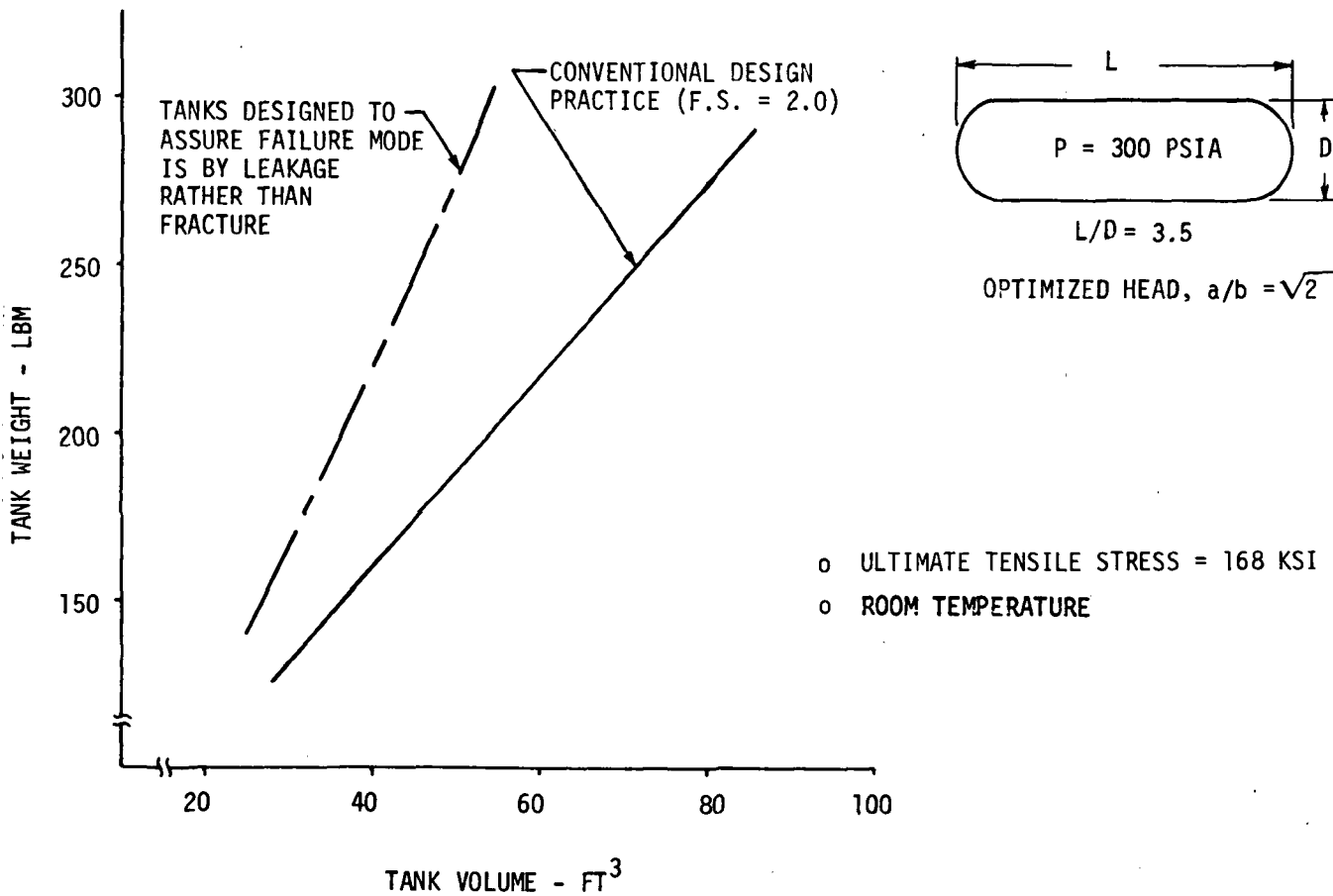
APS-368

E-43

Figure E-29

# EFFECT OF DESIGN CRITERIA ON TANK WEIGHT

DIAPHRAGM TANK  
TITANIUM



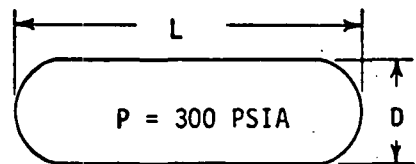
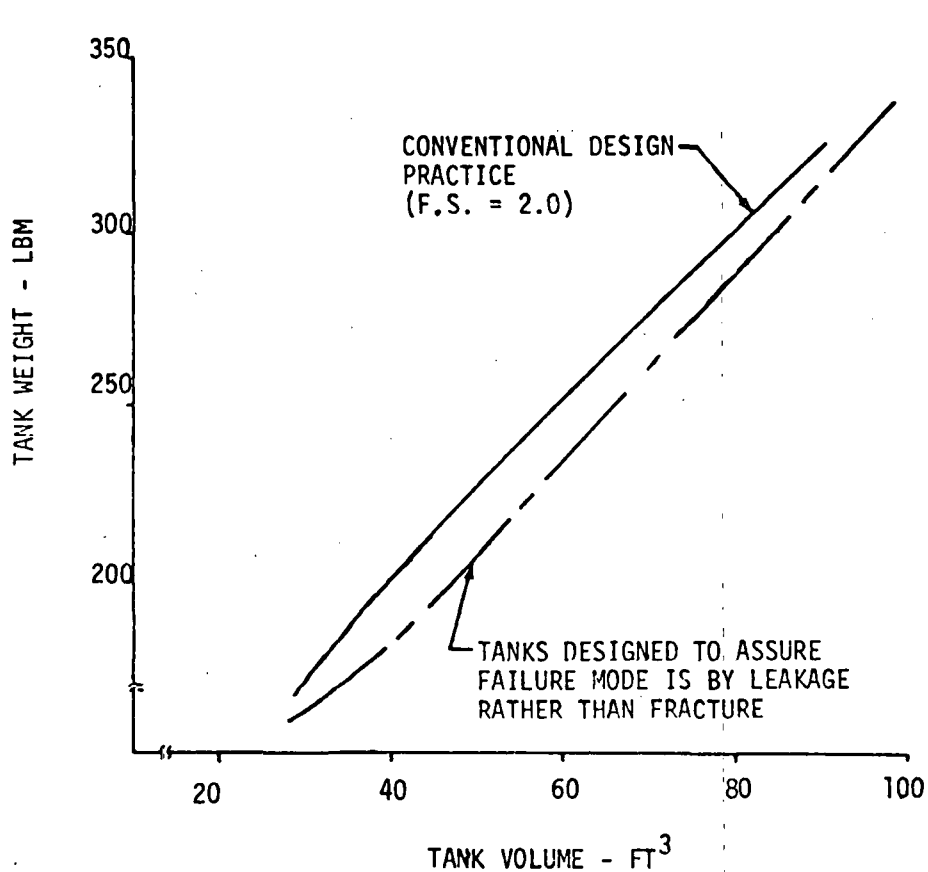
E-44

Figure E-30

APS-396

# EFFECT OF DESIGN CRITERIA ON TANK WEIGHT

DIAPHRAGM TANK  
301 STAINLESS STEEL



$L/D = 3.5$

OPTIMIZED HEAD,  $a/b = \sqrt{2}$

- o ULTIMATE TENSILE STRESS = 270 KSI
- o ROOM TEMPERATURE

APS-792

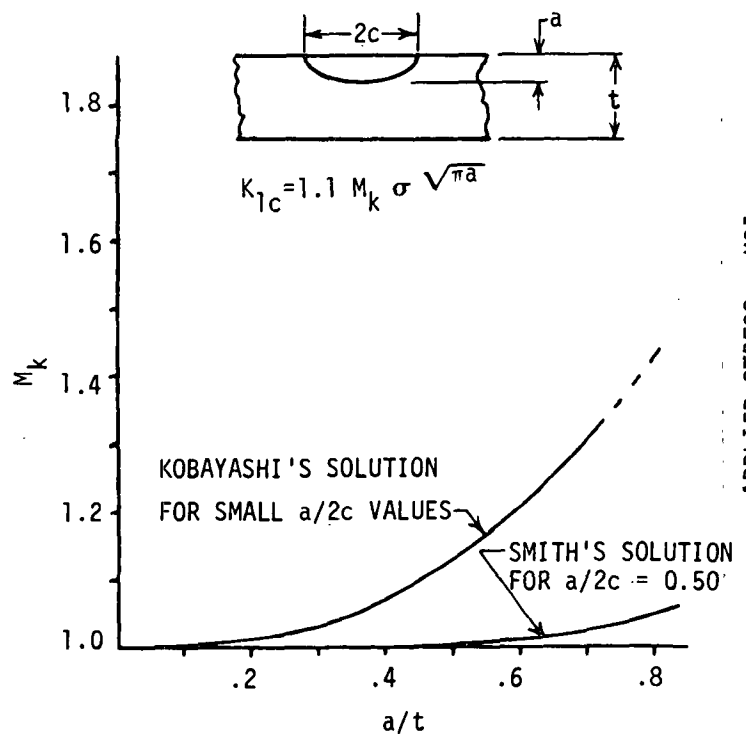
designed for leakage failure, would be 2.4 times the weight of a single bottle designed with a factor of safety of 2.0 to fail by fracture. A more attractive alternative would be to fabricate the pressurant tanks from composite materials, which generally provide leakage as the failure mode.

Thin walled pressure vessels with surface cracks can be analyzed under conditions of plane strain. When flaw depths become deep in relation to the wall thickness, a magnification factor is utilized in the solution of the stress intensity equation. Kobayashi's solution of magnification factors ( $M_K$ ) for deep surface flaws, and an example comparison of critical flaw sizes for thin and thick walled vessels are presented in Figure E-32. For initial flaw depths which are small in relation to the wall thickness, thin walled vessels are, in effect, thick walled vessels, as shown in Figure E-32. However, as flaw size increases, the effects of the magnification factor become progressively more pronounced. As demonstrated in Figure E-33, flaw growth rate accelerates with increasing stress intensity. Since for a given flaw depth and applied stress the stress intensity in a thin walled vessel is greater than that in a thick walled vessel (due to  $M_K$ ), the flaw growth rate can be expected to be greater, and therefore pressure vessel life as predicted by Figure E-27 would be somewhat optimistic. To accurately predict thin walled vessel life the flaw growth rate curve must be integrated for the given vessel design, as described in Reference E-1, using  $M_K$  to account for the increase in stress intensity (and thus increase in growth rate) as the flaw enlarges. Figure E-34 compares the life capability of a typical RCS propellant vessel as predicted by thin and thick walled theory.

Pressure vessels designed for multi-cycle operation require large proof factors to demonstrate life capability. For the case of a typical shuttle RCS propellant tank having a 1000 cycle life requirement, proof factors approaching 2.0 are necessary to verify full life capability. This constraint dictates either high safety factors (and heavier tanks) in order to maintain proof stresses below yield, or a series of proof tests performed throughout the vessel life, each verifying a portion of the total life. An alternative to these two approaches is to take advantage of the change in material properties that takes place at cryogenic temperatures to enhance the efficiency of proof testing. As shown in Figures E-35 and E-36, cryogenic temperatures result in elevated ultimate strengths and, in the case of 301 Cryoform, decreased fracture toughness. Figure E-37 presents a comparison of cryogenic and room temperature proof tests for a typical

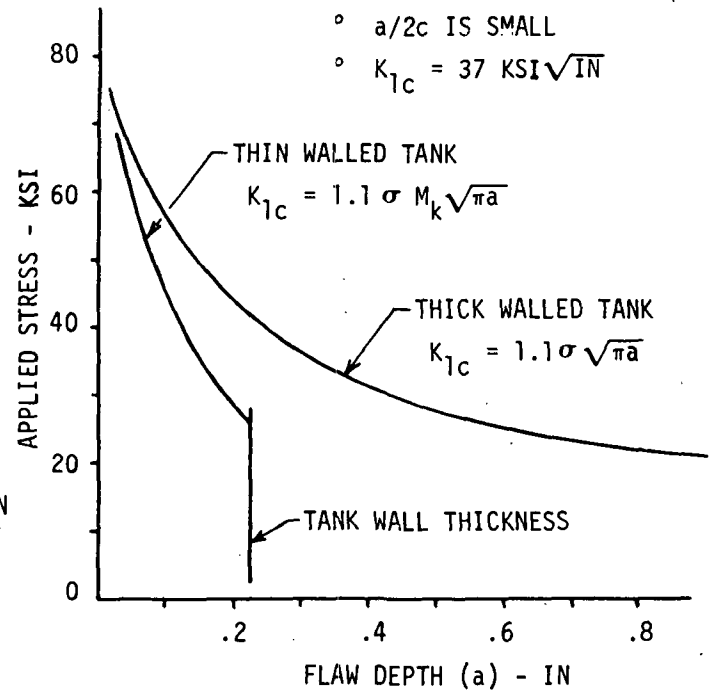
FRACTURE MECHANICS THEORY

STRESS INTENSITY MAGNIFICATION  
FACTORS FOR DEEP SURFACE FLAWS



CRITICAL FLAW SIZE

- 2219-T87 A1 AT -320°F
- $a/2c$  IS SMALL
- $K_{Ic} = 37 \text{ KSI}\sqrt{\text{IN}}$



APS-707

E-47

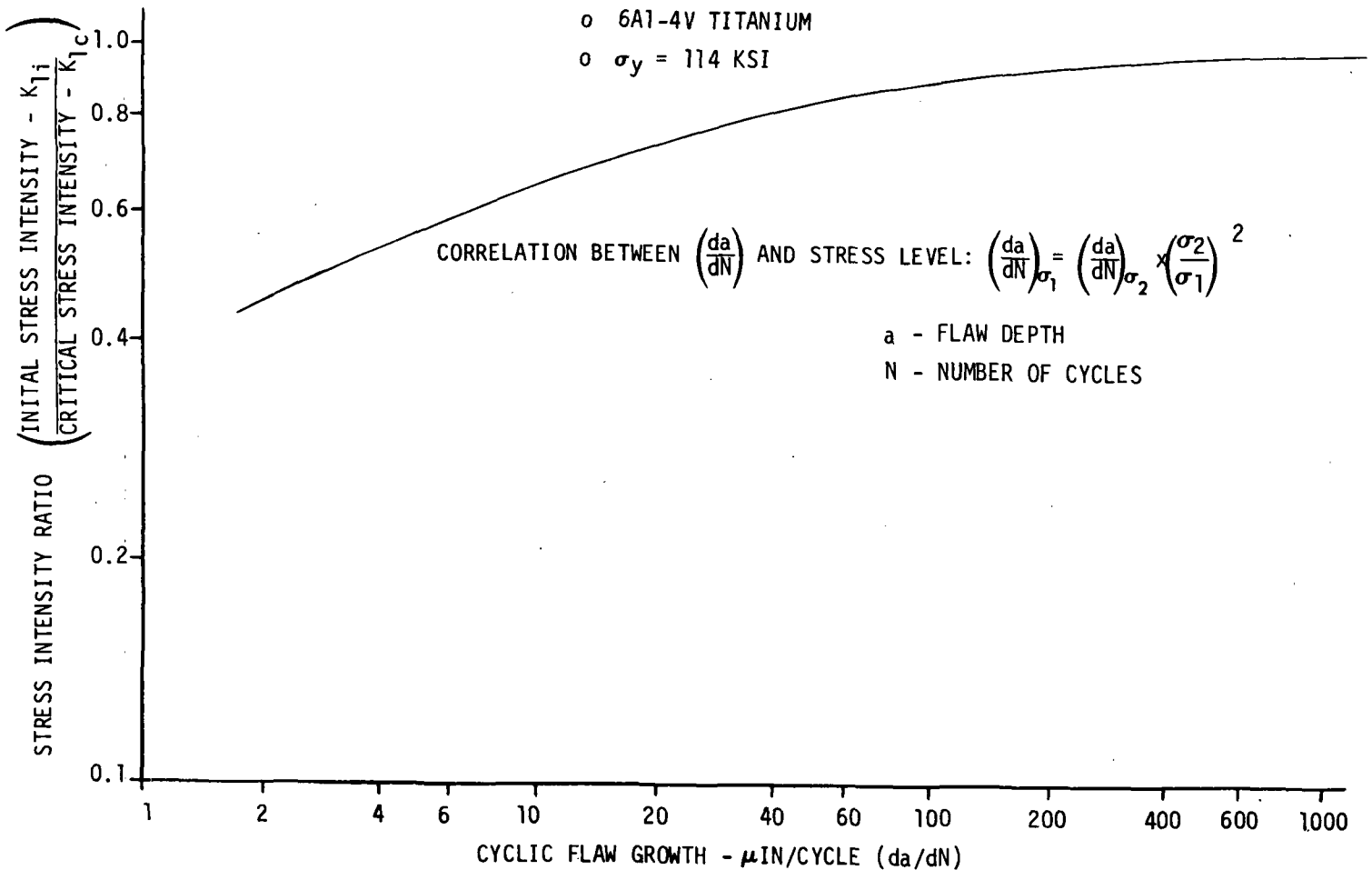
Figure E-32

MCDONNELL DOUGLAS AERONAUTICS COMPANY - EAST



CYCLIC FLAW GROWTH

- o 6A1-4V TITANIUM
- o  $\sigma_y = 114$  KSI



APS-857

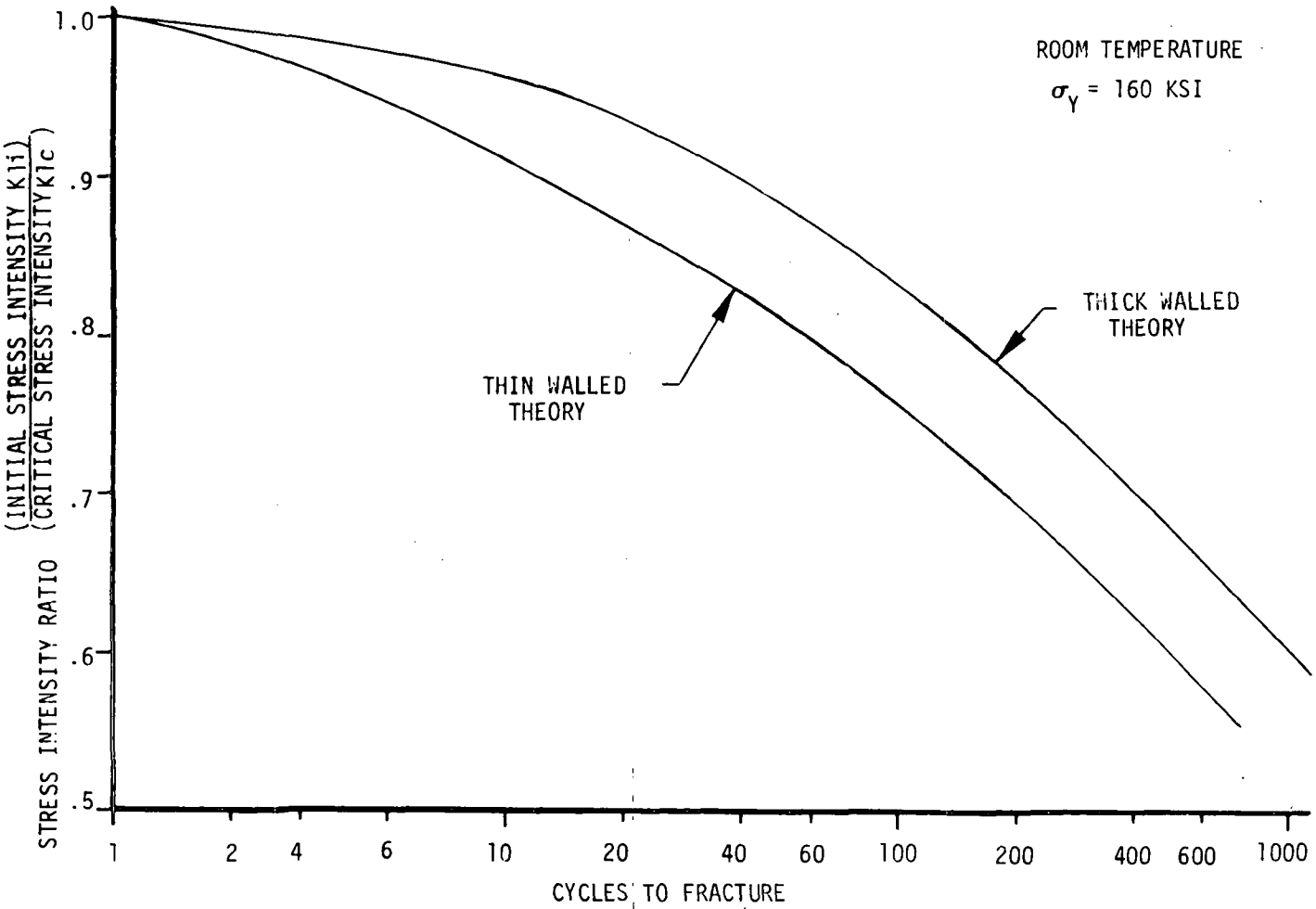
E-48

Figure E-33

# CYCLIC FLAW GROWTH

o 6A1-4V TITANIUM

ROOM TEMPERATURE  
 $\sigma_Y = 160$  KSI



APS-800

E-49

Figure E-34

(thin walled) RCS propellant tank. As shown, limiting room temperature proof stress to 140 KSI ( $0.875\sigma_y$ ) results in the verification of only 600 cycles. By contrast, 1000 cycles can be verified cryogenically at a proof stress of only  $0.7\sigma_y$ . In the case of 301 Cryoform (Figure E-38), the resulting margin at cryogenic temperatures is even greater. By adjusting the factor of safety downward, thereby letting the proof stress more nearly approach  $\sigma_y$ , a lighter weight design could be achieved, consistent with a life of 1000 cycles.

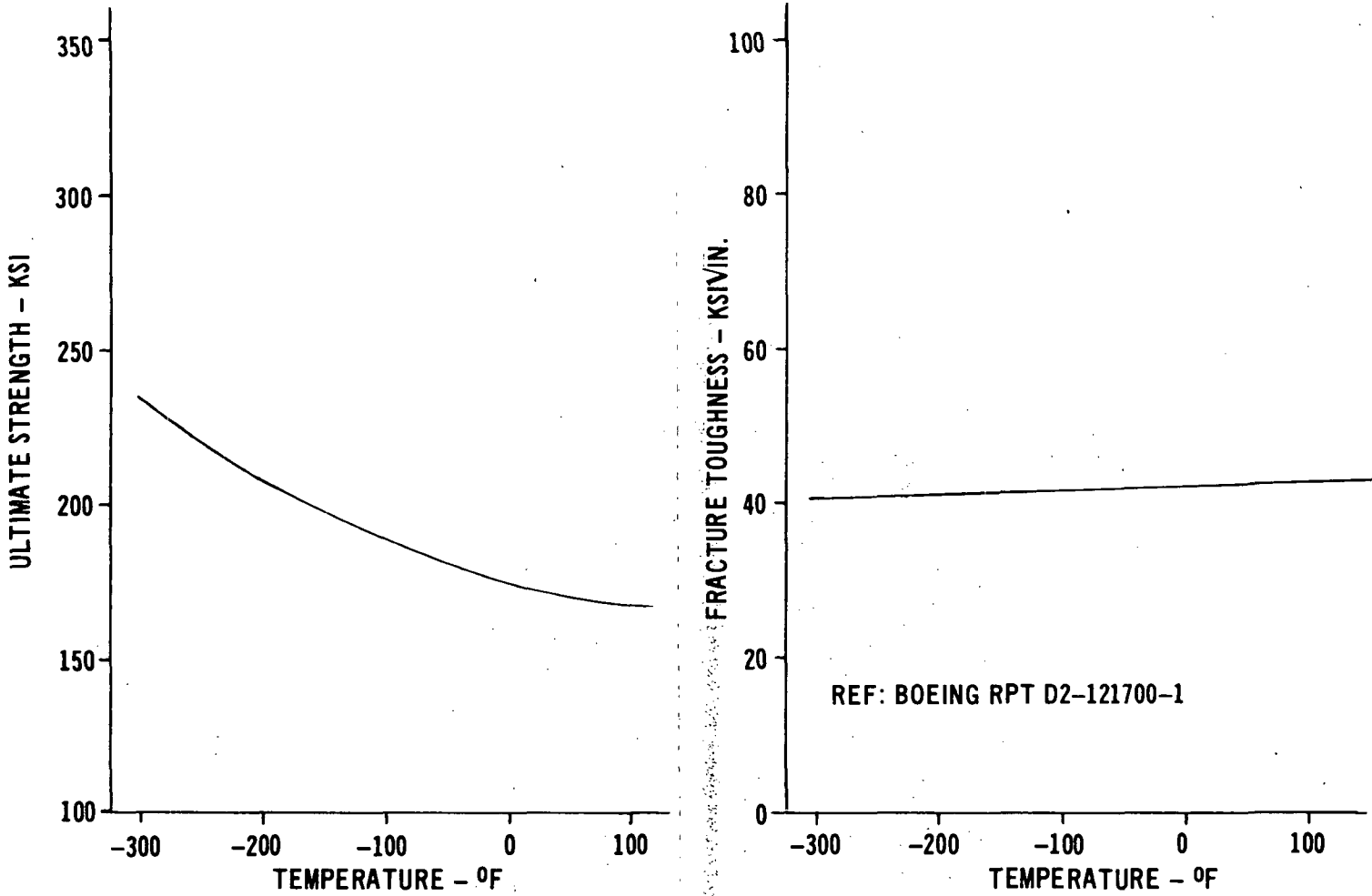
Both titanium and 301 Cryoform appear to be viable materials for the RCS tankage. Titanium was chosen as the baseline for this study based on its weight competitiveness, compatibility properties, and the depth of experience in its use. However, it must be noted that 301 Cryoform does offer attractive failure mode properties. Additionally, 301 Cryoform offers a cost advantage in relation to titanium due to its relative ease of fabrication, and further consideration of this topic is warranted prior to final selection.

The environmental factors affecting Fracture Mechanics material properties are temperature and the prevailing corrosive medium. The expected temperature range of the RCS tankage is 40°F to 165°F. Within this range, changes in fracture toughness and flaw growth rate are relatively small for the materials under consideration. In general, fracture toughness increases and flaw growth rate decreases with increasing temperature.

Sustained loading in the presence of corrosive mediums tends to reduce life. Figure E-39 shows as a function of the initial-to-critical-stress intensity ratio, how subcritical flaw growth affects cycle life for 6Al-4V Titanium. Also shown is the effect of  $N_2O_4$  on life under sustained loading conditions. Flaw growth due to cyclic loading proceeds until the threshold level in  $N_2O_4$  ( $K_{I_i}/K_{I_c} = 0.81$ ) is reached, at which time sustained growth, leading to failure, occurs. For this same intensity ratio, a vessel in a neutral environment would be capable of sustaining an additional 140 cycles (see Figure E-39). Thus, the presence of  $N_2O_4$  results in the loss of 140 cycles. Propellant tank design life is, therefore, the sum of the operating cycle requirement and the cycles lost due to the corrosive environment. Figure E-40 presents a comparison of the threshold levels and cycles lost for 6Al-4V Titanium and 301 Cryoform in various propellant and solvent environments. (It should be noted that considerably more data is available

# EFFECTS OF TEMPERATURE ON MECHANICAL PROPERTIES

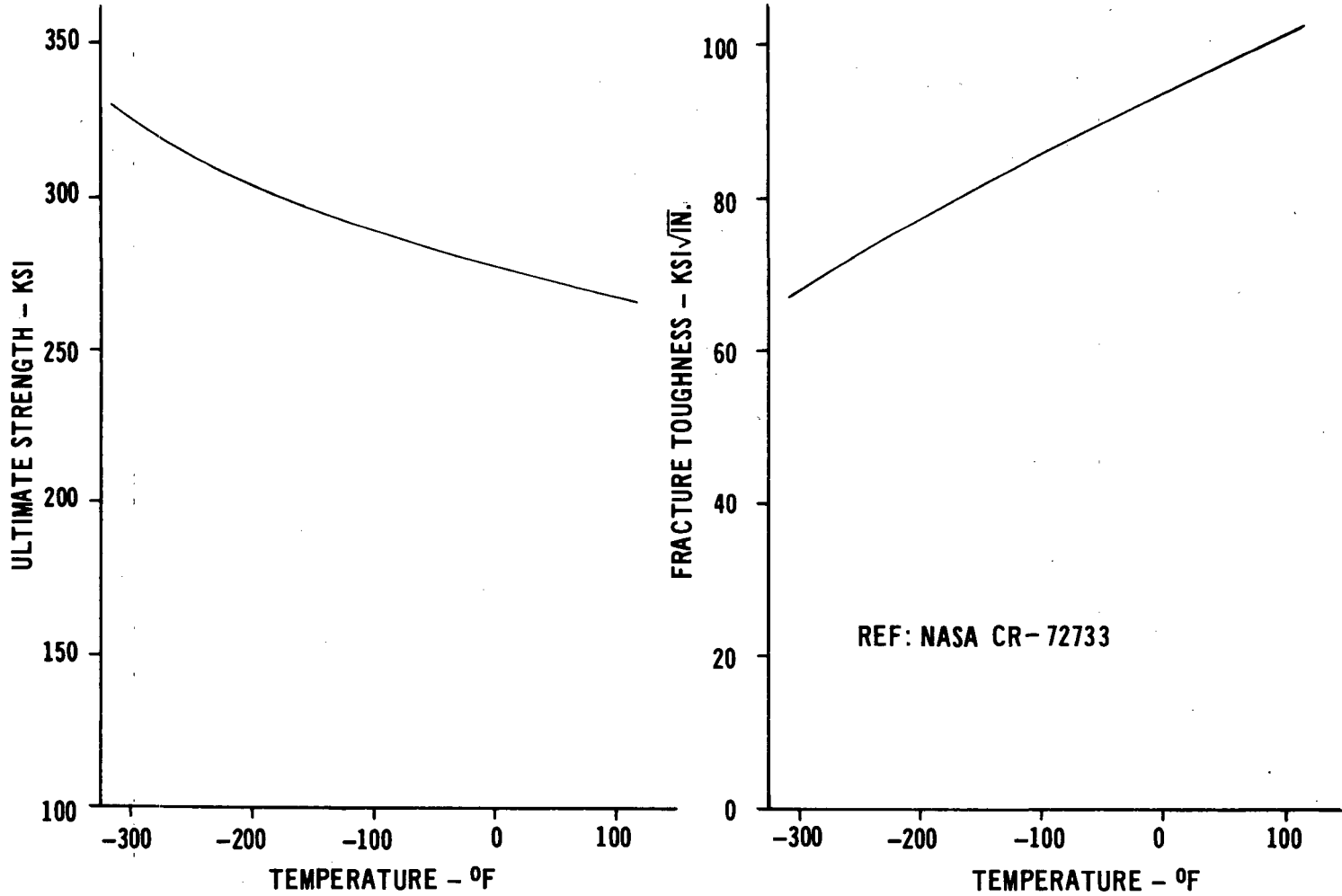
o 6Al-4V TITANIUM



APS-140

# EFFECTS OF TEMPERATURE ON MECHANICAL PROPERTIES

301 CRYOFORM

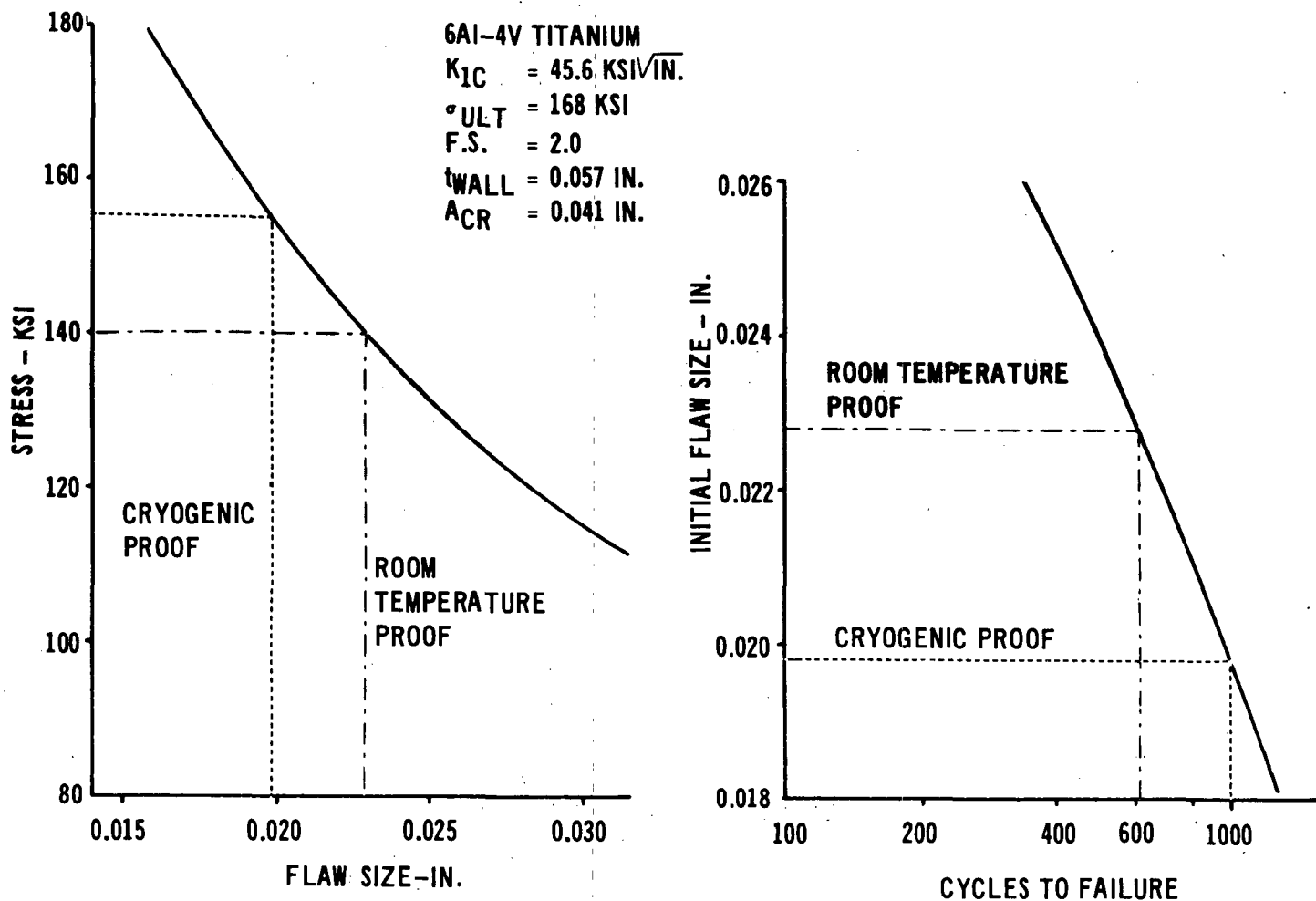


APS-152

E-52

Figure E-36

### AVAILABLE LIFE



MCDONNELL DOUGLAS AERONAUTICS COMPANY - EAST

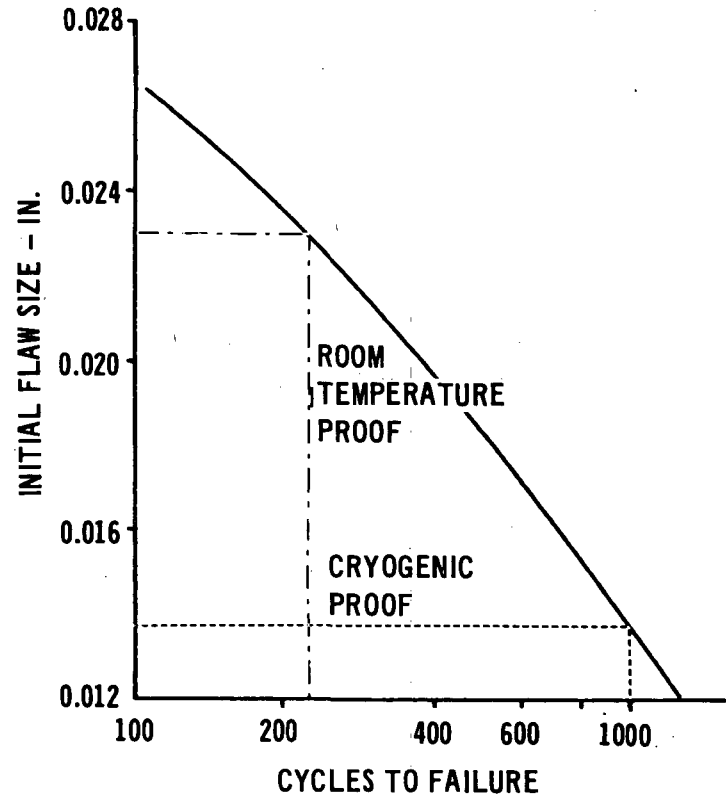
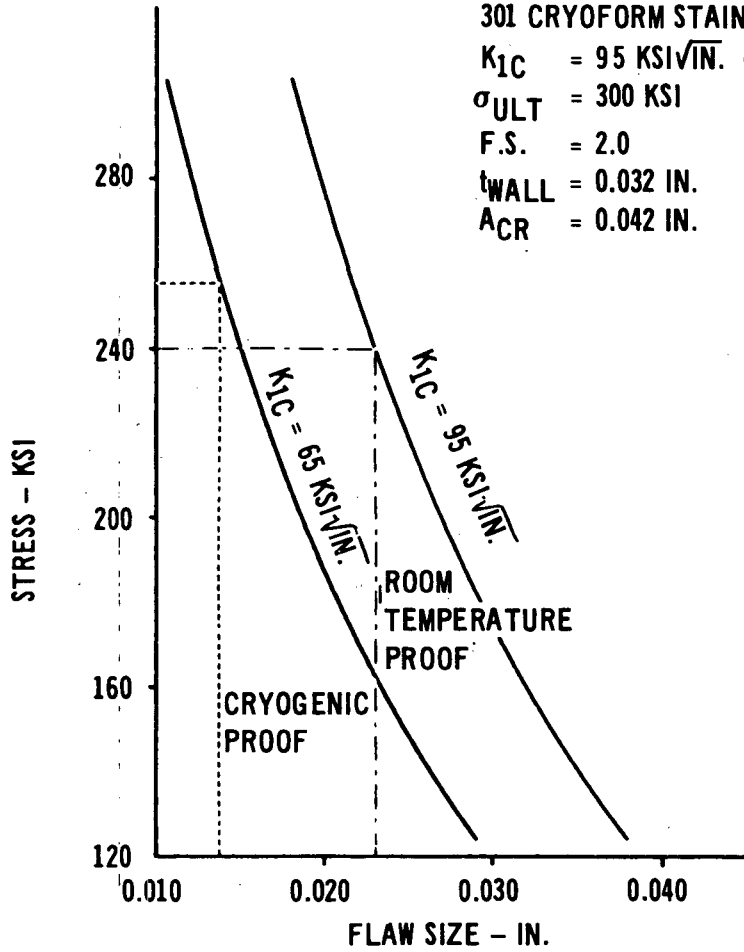
E-53

Figure E-37

APS-119

# AVAILABLE LIFE

301 CRYOFORM STAINLESS STEEL  
 $K_{IC} = 95 \text{ KSI}\sqrt{\text{IN.}}$  (65  $\text{KSI}\sqrt{\text{IN.}}$  AT  $-320^{\circ}\text{F}$ )  
 $\sigma_{ULT} = 300 \text{ KSI}$   
 F.S. = 2.0  
 $t_{WALL} = 0.032 \text{ IN.}$   
 $A_{CR} = 0.042 \text{ IN.}$



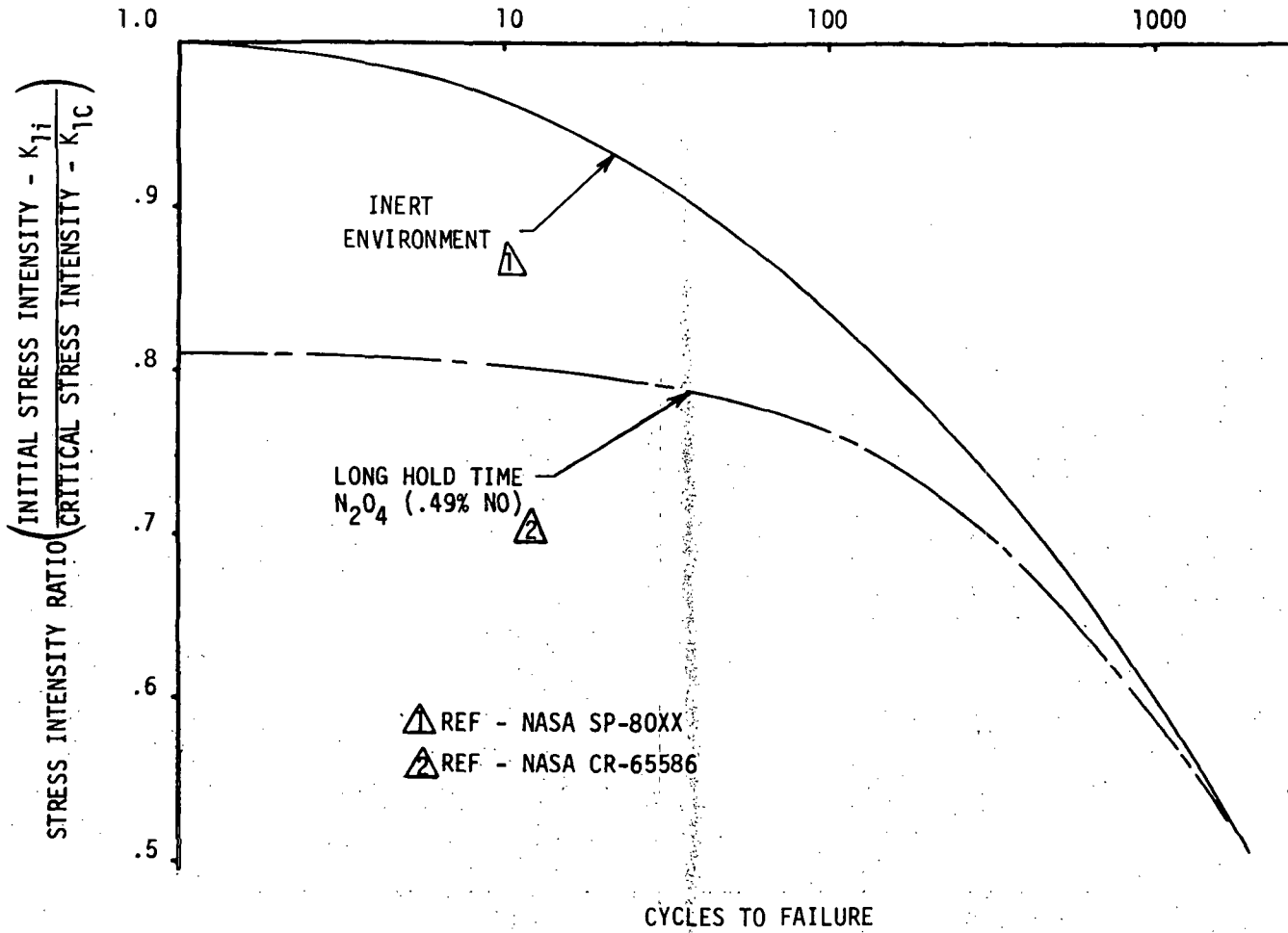
APS-120

E-54

Figure E-38

### CYCLIC FLAW-GROWTH DATA

° 6Al - 4V TITANIUM



APS-364

E-55

Figure E-39



THRESHOLD STRESS-INTENSITY DATA FOR VARIOUS  
FLUID ENVIRONMENTS

FLUID ENVIRONMENT	TEMPERATURE °F	MATERIAL					
		6A1-4V TITANIUM		301 CRYOFORM STAINLESS STEEL (UNAGED)		301 CRYOFORM STAINLESS STEEL (AGED)	
		$K_{TH}/K_{IC}$	CYCLES LOST	$K_{TH}/K_{IC}$	CYCLES LOST	$K_{TH}/K_{IC}$	CYCLES LOST
N <sub>2</sub> O <sub>4</sub> (.30% NO)	RT	.74	300				
N <sub>2</sub> O <sub>4</sub> (.49% NO)	RT	.81	140			.78	340
N <sub>2</sub> O <sub>4</sub> (.60% NO)	RT	.83	108				
N <sub>2</sub> O <sub>4</sub> (.49% NO)	105	.70					
MMH	105	.75					
HYDRAZINE						.73	460
AEROZINE 50	RT	.82	120				
AEROZINE 50	110	.75					
METHANOL	RT	.24	>5000				
ISOPROPANOL		.60					
FREON MF	RT	.58	1200				
FREON TF	RT	.60					
DISTILLED WATER	RT	.86	72	.84	220	.76	390
H <sub>2</sub> O + NaCl	RT					.79	320
SEA WATER	RT					.63	800
H <sub>2</sub> O + Na <sub>2</sub> CrO <sub>4</sub>	RT	.82	120				
AIR	RT	.90	40				
HELIUM	RT	.90	40				
OXYGEN	RT	.90	40	.86	185		
NITROGEN	RT	.90	40			.82	260

APS-370

for titanium, and this disparity would inevitably lead to higher development costs for 301 Cryoform.)

Current thinking on shuttle propulsion system maintenance procedures indicates that best system operation will be achieved by keeping the system wet with propellants and by minimizing flushing operations. However, a variety of failure modes still exist which will require complete or partial system flushing. Solvents will be required for system cleansing and inerting during these maintenance procedures. Additionally, test phase operations will require frequent inerting, and it is important that compatible solvents be used. During previous test programs, referee fluids have been used for pressure testing in place of storable propellants for reasons of personnel safety and test expediency. As shown in Figure E-40, while the propellants of interest exhibit reasonably high threshold levels, some of the candidate cleaning solvents and/or referee fluids represent a serious threat to tank integrity. The use of methanol in particular, results in an extremely low threshold stress intensity level for titanium. Its use as a referee fluid during pressure cycling tests on Apollo SPS fuel tanks resulted in the failure of at least two tanks (Reference E-2). Although Freon MF has been used with Apollo nitrogen tetroxide systems, it also exhibits a low threshold with titanium when compared to  $N_2O_4$ . If purging operations cannot completely remove all traces of solvents such as these, then tank design criteria will have to be altered to compensate for them.

Water would be an effective cleanser, but due to the many inherent traps in the propulsion system and the high boiling point of water, it would be difficult to completely dry the system, and potential acid formation when combined with the propellant could result in corrosion.

In addition to being effective cleansing agents and compatible with materials of construction, cleaning solvents must not react with the propellants. Cleaning techniques usually include system drying with inert gas after solvent removal, but residual solvent can conceivably remain in bellows convolutions, bladder folds, etc. The reaction of residual Freon TF solvent vapor and hydrazine to form  $N_2H_4HCl$  which, in turn, caused corrosion of 6Al-4V Titanium has been observed by the Stanford Research Institute (Reference E-3). Hydrazine containing  $N_2H_4HCl$  would also be corrosive to aluminums and stainless steels. For this reason, chlorinated solvents should not be used in hydrazine systems unless all traces can reliably be removed prior to use.

There is, at present, no single solvent which is satisfactory for use with both fuels and oxidizers. Isopropanol is the proper choice for fuels, replacing methanol on the basis of fracture mechanics considerations. However it cannot be considered for use with oxidizers due to the hypergolic nature of the combination. Either Freon MF or Freon TF appear to be satisfactory for use with oxidizer, with Freon TF being the preferred choice for two reasons. First, it exhibits a slightly higher threshold stress intensity than Freon MF. Second, prospects for reclamation of Freon TF are quite promising due to the separation ( 47°F) in boiling points between TF and NTO, whereas Freon MF and NTO have essentially the same boiling point.

REFERENCES

- E-1 Tiffany, C. F., Masters, J. N., and Pall, F. A., "Some Fracture Considerations in the Design and Analysis of Spacecraft Pressure Vessels", Boeing Co. (S.D.) Paper 66K03, October 1966.
- E-2 Tiffany, C. F., and Masters, J. N., "Investigation of the Flaw Growth Characteristics of 6Al-4V Titanium used in Apollo Spacecraft Pressure Vessels", Boeing Co. Report D2-113530-1, March 1967.
- E-3 Tolberg, W. E., et al., "Chemical and Metallurgical Analysis of 6Al-4V Titanium Test Specimens Exposed to Hydrazine ( $N_2H_4$ ) Liquid Propellant", Stanford Research Institute (SRI) 951581-11, April 1971.

APPENDIX F  
THERMAL CONTROL

Analysis was performed to evaluate the technical complexity and to define the weight implications associated with the thermal control of the alternate RCS configurations. Specifically this effort has focused on the thermal control requirements of wing tip and fuselage modules, and the APU. Module thermal control is required primarily to protect the system from the extreme environments evidenced naturally in space, as well as those induced during entry. Additionally, monopropellant thruster injectors require cooling to preclude explosive decomposition of the propellant under certain malfunction conditions. Thermal control of the APU is necessary to maintain the hydraulic fluid temperature within acceptable operating limits. This appendix discusses the analyses and design considerations involved in the selection of the RCS thermal control system.

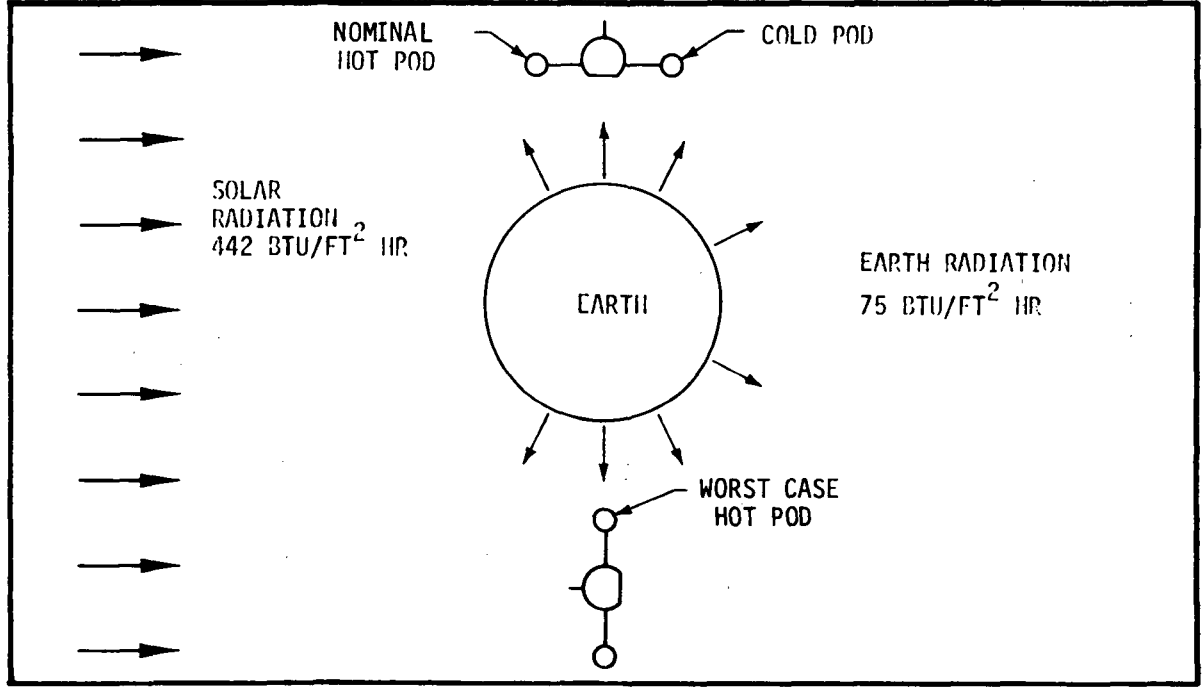
F1 Environments - The environments affecting system operation may be roughly classified as natural and induced. The natural environments include those conditions which represent point values in space, independent of spacecraft mission or design. In the present study only radiative environments have been considered. Values for solar and earth radiative levels are shown below.

NATURAL ENVIRONMENTS

Solar Constant	442 Btu/Ft <sup>2</sup> -hr
Albedo, Average	0.34
Earth Radiation	75 Btu/Ft <sup>2</sup> -hr

A "worst case" philosophy was used to evaluate the vehicle-environment interactions. The module orientation shown in Figure F-1 was selected to provide nominally "hot" and "cold" cases to establish design limits inside the module. The spacecraft was assumed to maintain a "belly down" attitude with one side always receiving direct sun and the other always remaining in the shadow of the spacecraft fuselage. A slightly more severe hot case occurs for a near polar orbit where the upper side of the pod, which has the thinnest TPS, is continuously subjected to direct sunlight. This hot case was used in the definition of the maximum potential wing tip pod temperature extremes.

# RADIATION THERMAL ENVIRONMENT NOMINAL AND WORST CASE ORIENTATIONS



F-2

APS-768

Figure F-1

The principal induced environment is associated with reentry heating. Complementary studies conducted during the Space Shuttle MDAC-E Phase B vehicle design effort were used to size the module thermal protection system. The nominal reference heating rate to a one foot radius sphere is shown in Figure F-2. For this reference rate, the integrated total heat pulse is 66,100 Btu/ft<sup>2</sup>. Peak heating rates and heat pulses for other vehicle locations were scaled using available wind tunnel data and engineering judgement. Nominal entry temperatures for the vehicle were shown previously in Figure C-2. Heating rate ratios and peak temperatures for wing tip and fuselage modules are shown in Figure F-3.

A secondary induced environment is associated with the thermal boundary condition presented to the RCS modules by the main vehicle. For wing tip pod modeling, this interface was evaluated by including enough of the wing structure so that the module and included structure has an adiabatic interface with the remainder of the shuttle wing. For fuselage mounted modules, the spacecraft interface temperature was assumed to be 40°F.

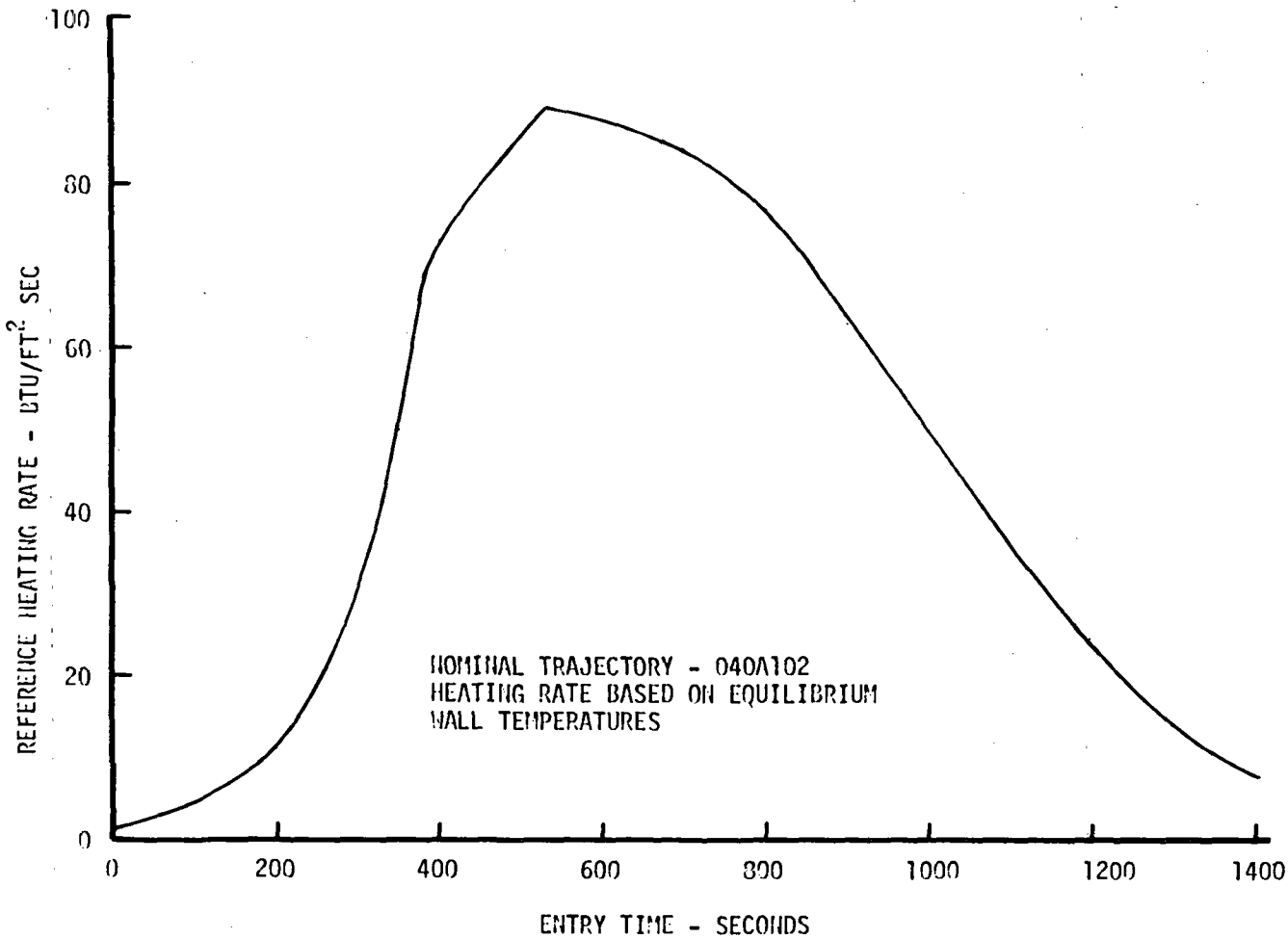
F2 Thermal Requirements - The primary thermal constraints are associated with the propellants and the thrusters. Allowable propellant temperature ranges have been established as follows.

PROPELLANT TEMPERATURE CONSTRAINTS

NTO/MMH	40°F to 125°F
N <sub>2</sub> H <sub>4</sub>	50°F to 125°F

Thruster thermal requirements have been defined in order to provide adequate thruster life and reliability. Figure F-4 summarizes the thermal limitations associated with monopropellant thruster start up, operation, heat soak back, and nonoperation. The valve seat and injector temperatures rise as a result of heat soak back after thruster operation. Valve temperature is limited to a maximum of 200°F to prevent damage to the seals. The counteracting constraints on minimum catalyst bed temperature and maximum injector soak back temperature (500°F) are of primary significance. The restriction on minimum catalyst temperature arises from the poor structural properties of the spontaneous catalyst (Shell 405) and its tendency to generate "fines" under repeated cold thruster starts. Test data (Figure F-4) show that catalyst loss per start increases rapidly with decreasing bed temperature for initial bed temperatures less than 150°F. The restriction on injector temperature is

REFERENCE HEATING RATE, 1100 NM CROSS RANGE

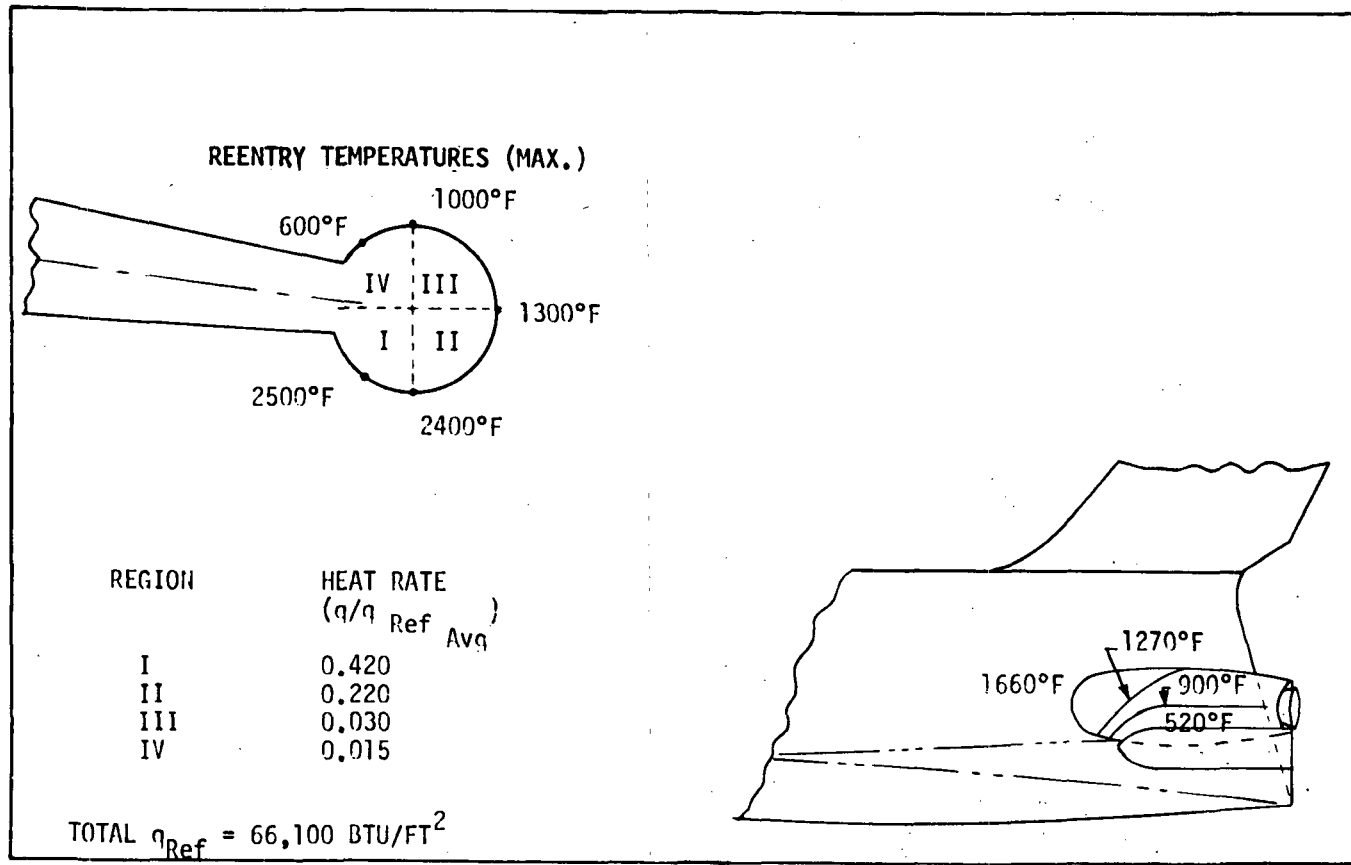


F-4

APS-769



MODULE PEAK TEMPERATURES AND HEATING PULSE RATIOS



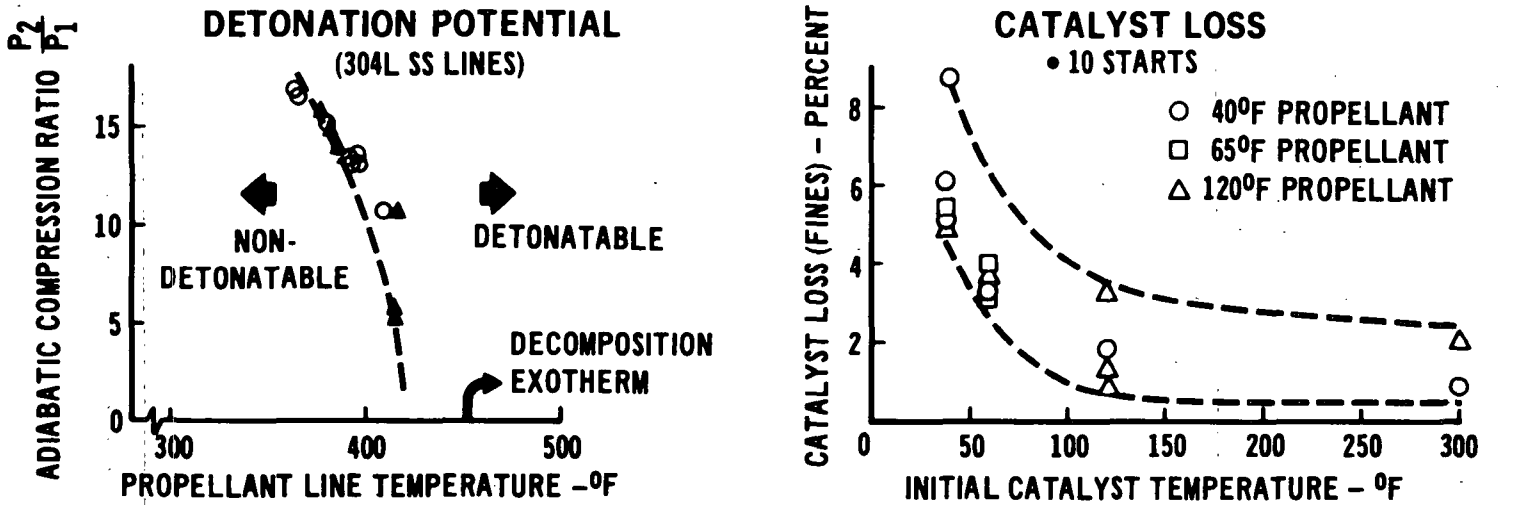
F-5

MCDONNELL DOUGLAS AERONAUTICS COMPANY - EAST

Figure F-3

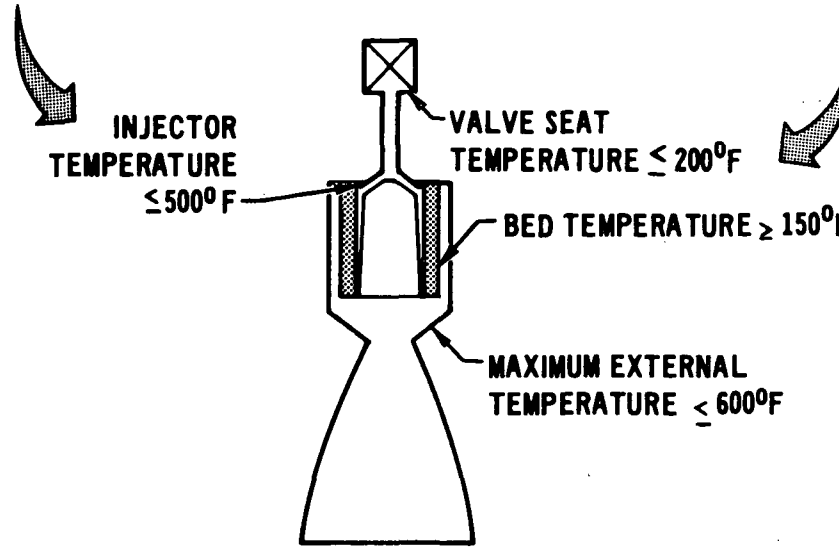
APS-770

# MONOPROPELLANT THRUSTER THERMAL CONSTRAINTS



REF: AFRPL TR 71-41

REF: AFRPL TR 71-103



11-236

based on propellant thermal stability considerations, i.e., the maximum injector temperature is kept sufficiently low so as to preclude explosive detonation of the propellant under conditions of low flow corresponding to valve leakage. Explosive decomposition is known to have occurred at injector temperatures of 600°F. The maximum external temperature of 600°F was imposed to minimize the thermal interaction of the thruster with the surrounding structure and other components.

Thermal control of bipropellant thrusters is not as restrictive. Again, valve temperature is limited to 200°F. The primary concern for bipropellant thrusters is with vacuum-ignition pressure spiking. During pulsing operation, energy-rich detonatable chemical residues (mostly monomethylhydrazine nitrate) can accumulate and, in sufficient quantity, can produce high-magnitude ignition overpressures. To alleviate this problem on the Apollo CSM/LM RCS, the thruster injectors were maintained in excess of 70°F to promote rapid vaporization of the fuel. Meeting this same criteria with 600 lbf thrusters will require a maximum power input of 5.4 watts/thruster.

F3 Wing Tip Module Thermal Control - The steady state and transient thermal response of the wing tip RCS modules have been examined using a two-dimensional thermal model. These calculations indicate that the maximum steady state uncontrolled temperature range is -110 to +165°F. Minimum temperatures, which occur with continuously shaded pods, require heaters to prevent propellant freezing. Heaters are sized to provide a maximum power of 303 watts for the monopropellant system (including 10 watts per thruster to maintain 150°F catalyst temperature), and 161 watts for a bipropellant system. Corresponding maximum energy requirements are 36.8 kwh (monopropellant system) and 17.3 kwh (bipropellant system). The maximum temperature of 165°F is somewhat above the desired maximum temperature, and thermal control is required to prevent propellant overheating. In the sections that follow, the procedures used for sizing the reentry thermal protection system are presented, and orbital analysis, including detailed results for module transient response, described.

F3.1 Reentry TPS - TPS sizing has been accomplished using procedures developed during the MDAC-E Space Shuttle Phase B study. Material selection has been based on the peak entry temperature with unit weight determined by the total heat pulse. Material selection guidelines are shown below.

RANGE OF PEAK TEMPERATURE	MATERIAL
750°F	Low Density Ablator or Reusable Surface Insulation (RSI) -choice depending on Integration with Adjacent Areas
750-2500°F	Reusable Surface Insulation
Local Regions 2500°F	Low Density Ablator
Leading Edge and Nose Regions	High Density Ablator

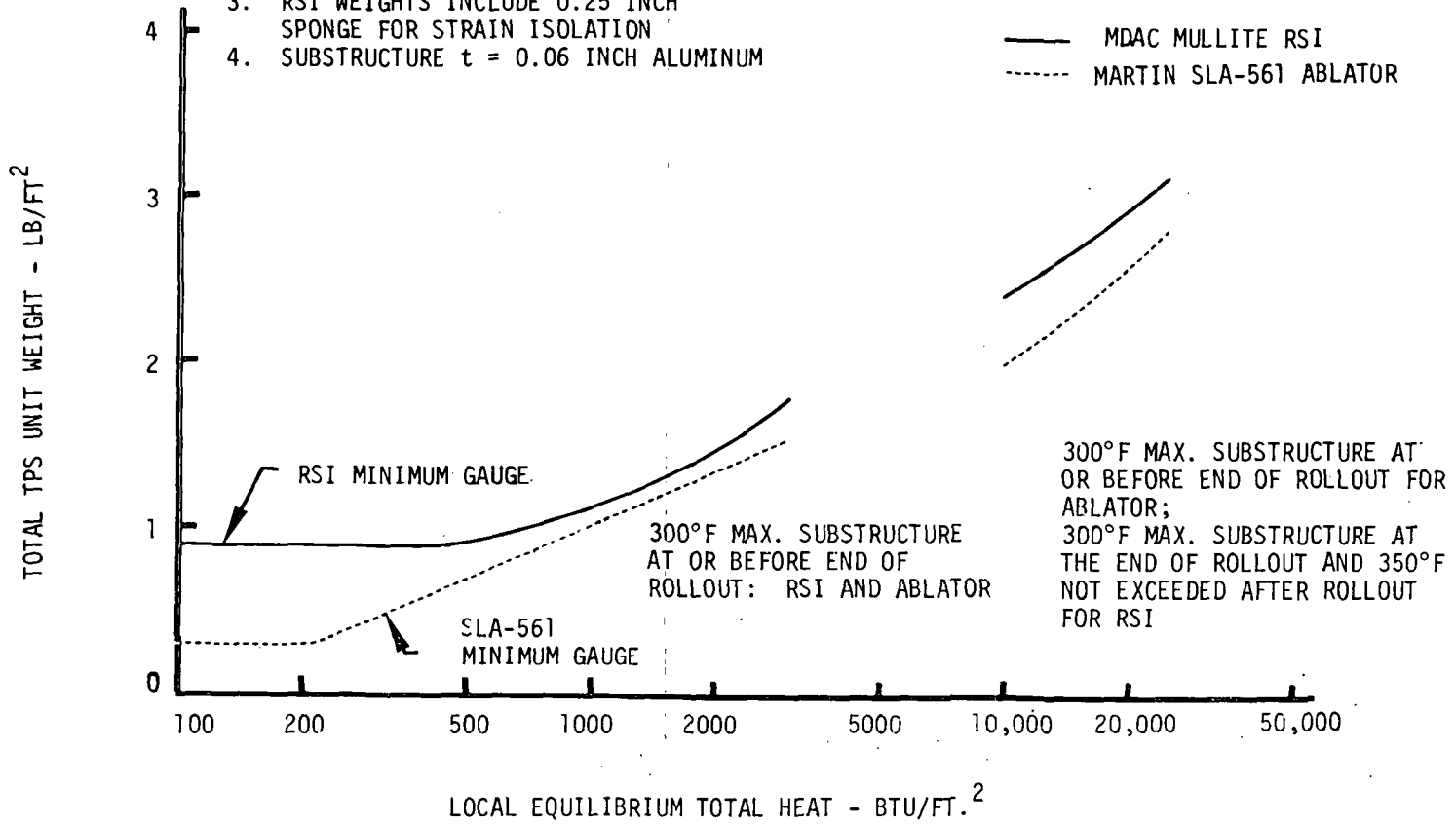
Wing tip module maximum temperatures dictate the use of low density ablator on the module nose, and reusable surface insulation (RSI) on the remainder of the module surface. The unit weight design curves used to size the low density ablator (designated SLA-561) and RSI are shown in Figure F-5. Using this data and the environmental constraints of Figure F-3, the nominal TPS weights shown in Figure F-6 were derived.

Module on orbit thermal control is affected significantly by the ratio of solar absorptivity to surface emissivity ( $\alpha/\epsilon$ ). Through the use of selected coatings, significant thermal control has been achieved on previously flown spacecraft. In particular, the adiabatic surface temperature for an orbiter exposed to direct sunlight can be decreased from 250°F for an  $\alpha/\epsilon = 1$  to 140°F for an  $\alpha/\epsilon = 0.5$ . Such coatings would be useful for the orbiter. However, studies conducted under recent MDAC-CRAD and MDAC-IRAD programs to develop reusable surface insulations indicated that the RSI surface properties cannot be adequately controlled, especially for a reusable application. For these reasons, surface properties approximating uncontrolled surface conditions, namely  $\epsilon = 0.80$  and  $\alpha = 0.75$ , were assumed for all TPS outer surfaces.

# RSI AND ABLATOR DESIGN CURVES

NOTES:

1. 1100 NM NOMINAL REENTRY - 040A102
2. UNIT WEIGHTS INCLUDE WATERPROOF COATING AND ATTACHMENT
3. RSI WEIGHTS INCLUDE 0.25 INCH SPONGE FOR STRAIN ISOLATION
4. SUBSTRUCTURE  $t = 0.06$  INCH ALUMINUM

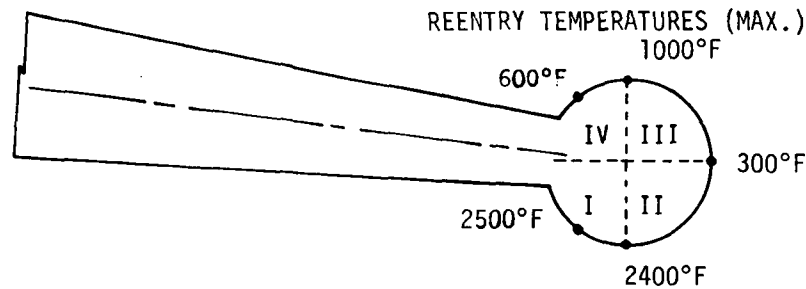


APS-773

F-9

WING TIP MODULE THERMAL PROTECTION SYSTEM (TPS)

E243-137 A



QUADRANT	TPS MATERIAL	TPS UNIT WEIGHT	WEIGHT LBM/MODULE
I	MDAC-RSI	3.25	70.5
II	MDAC-RSI	2.7	81.5
III	MDAC-RSI	2.0	60.5
IV	MDAC-RSI	1.1	23.8
NOSE	SLA-561	2.9	35.8
TOTAL			272.1

CRITERIA: MAXIMUM SUBSURFACE TEMPERATURE DURING REENTRY - 300°F

AVERAGE UNIT WT - 2.34 LBM/FT<sup>2</sup>

MAXIMUM TEMPERATURE AFTER LANDING - 350°F

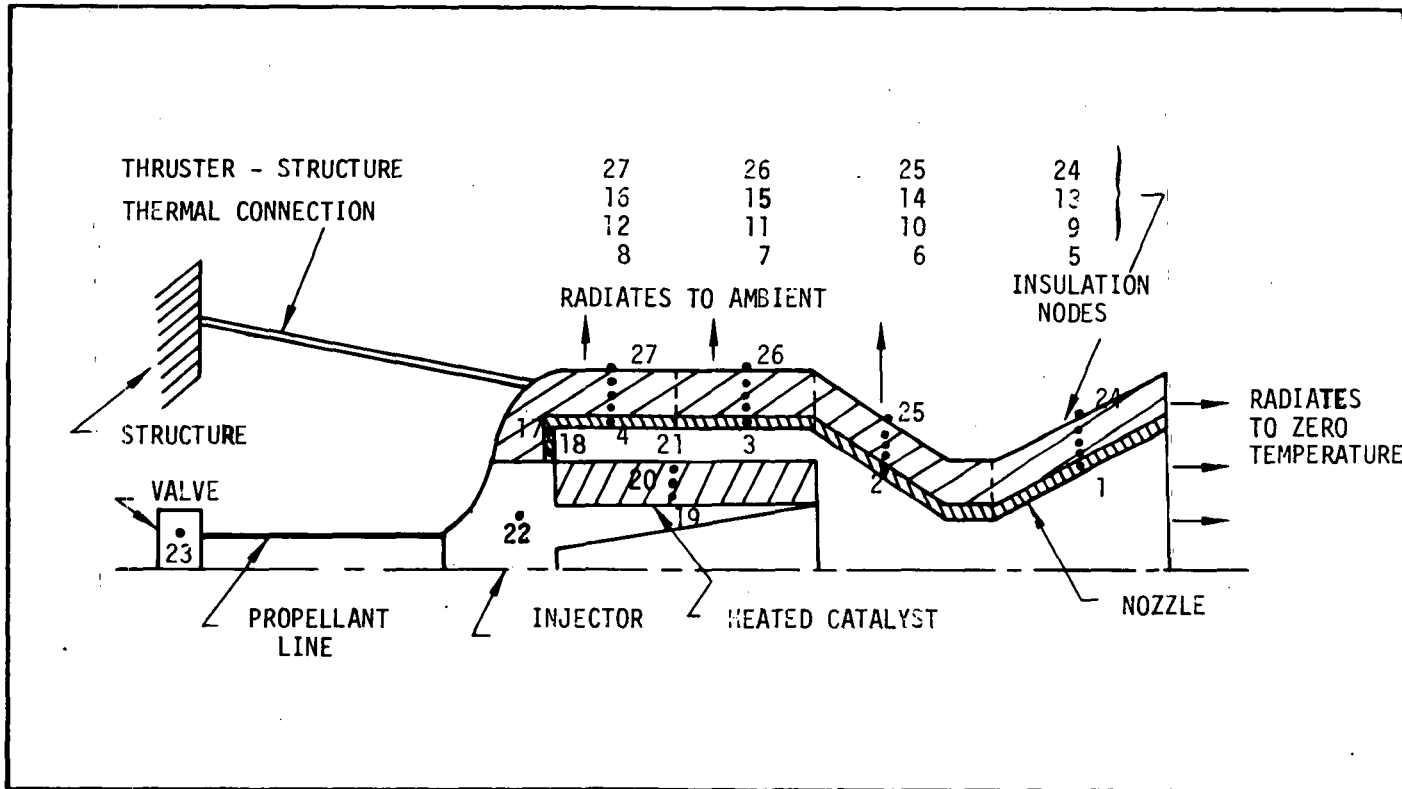
F-10

F3.2 Thruster Thermal Control - The basic aspect of monopropellant thruster thermal control is the thermal connection between the thruster and the surrounding structure. To minimize the injector and valve seat temperature, it would be desirable to attach the injector and valve to massive structure with a high heat capacity. However, such a connection would provide a substantial heat short during periods of nonoperation, and would thus conflict with the goal of minimizing the heater power required to maintain minimum catalyst temperature. The soakback thermal model shown in Figure F-7 was constructed to permit analysis of alternate thruster thermal control techniques. For each technique considered, a soakback calculation and a heater requirement calculation were performed. Detailed thermal property values associated with each node and initial temperature for the soakback calculations are tabulated in Figure F-8.

High temperatures are the worst case for those components heated during soakback. The structure heat sink and the thruster surroundings were thus assumed to be at 150°F, a nominal envelope maximum. However, for modeling heater requirements, the heater power will increase as the ambient temperature falls. Heater sizing requirements were accordingly based on heat sink and surrounding temperatures of 40°F, a nominal minimum temperature for the propellant. The sensitivities of the heater power and maximum injector temperature to thruster-structure thermal resistance are shown in Figure F-9. As the thermal resistance between thruster and structure increases, the heater power decreases to the limit associated with the radiative heat leak from the nozzle to deep space, but with the penalty of increasing maximum injector temperature.

Four thermal connection concepts have been examined. These include a conductive thermal short, a thermal contact switch, a controllable heat pipe, and the use of phase change material as a heat sink. Nominal temperature ranges and power requirements for the first three are shown in Figure F-10. The temperature-time history of Figure F-11 provides a measure of the characteristic times associated with all of the control methods. Injector temperatures peak at approximately 500 seconds following shutdown and continue to cool for times on the order of an hour.

# THRUSTER THERMAL MODEL



F-12

APS-772



# ANNULAR CATALYST THERMAL MODEL DATA

NODE	MATERIAL (1)	WEIGHT (LBM)	NODE C (BTU/°R <sup>P</sup> )	THERMAL RESISTANCE TO NODE (°R/(BTU/HR) EXCEPT VALUES WITH *)			
				NODE	VALUE	NODE	VALUE
1	S.S.	2.50	0.25	5	1.542	2	1.75
1				R2*	0.08*	SR*	0.225*
2		2.50	0.25	6	3.03	1/3	1.75/3.86
2				R1*	0.08*	SR*	0.07*
3		1.22	0.122	7	3.03	2	3.86
3				4	2.125	R21*	0.132*
4		0.0914	0.0914	8	3.145	3	2.125
4				17	1.32	R21*	0.132*
5	INS.	0.0376	0.00902	1	1.542	9	3.08
6		0.0191	0.0046	2	3.03	10	6.06
7		0.0191	0.0046	3	3.03	11	6.06
8		0.0182	0.0044	4	3.145	12	6.29
9		0.0376	0.00902	5	3.08	13	3.08
10		0.0191	0.0046	6	6.06	14	6.06
11		0.0191	0.0046	7	6.06	15	6.06
12		0.0182	0.0044	8	6.29	16	6.29
13		0.0376	0.00902	9	3.08	24	1.54
14		0.0191	0.0046	10	6.06	25	3.03
15		0.0191	0.0046	11	6.06	26	3.03
16		0.0182	0.0044	12	6.29	27	3.15
17	S.S.	0.215	0.02	4	1.32	18	0.619
18	S.S.	0.1209	0.012	17	0.619	22	0.361
19	HAST./CATL.	0.47/0.60	0.132	22	0.14	20	0.3
20	CATL.	1.2	0.180	19	0.3	21	0.35
21	HAST./CATL.	0.50/1.20	0.22	20	0.35	R3*/R4*	0.132*/0.132*
22	S.S.	3.0	0.3	19	0.14	18/23	0.361/29.75
23	S.S.	2.0	0.2	22	29.75	-	-
24				AR*	0.45*	13	1.54
25				AR*	0.229*	14	3.03
26				AR*	0.229*	15	3.03
27				AR*	0.219*	16	3.15

(1) S.S. = STAINLESS STEEL  
 INS. = INSULATION  
 HAST. = HASTELLOY  
 CATL. = CATALYST

\* AR : RADIATION TO AMBIENT  
 Rj : RADIATION TO NODE J  
 SR : RADIATION TO DEEP SPACE

FA → FT<sup>2</sup>

MCDONNELL DOUGLAS ASTRONAUTICS COMPANY - EAST

F-13

Figure F-8

APS-777

APS STUDY  
Phase C and E Report

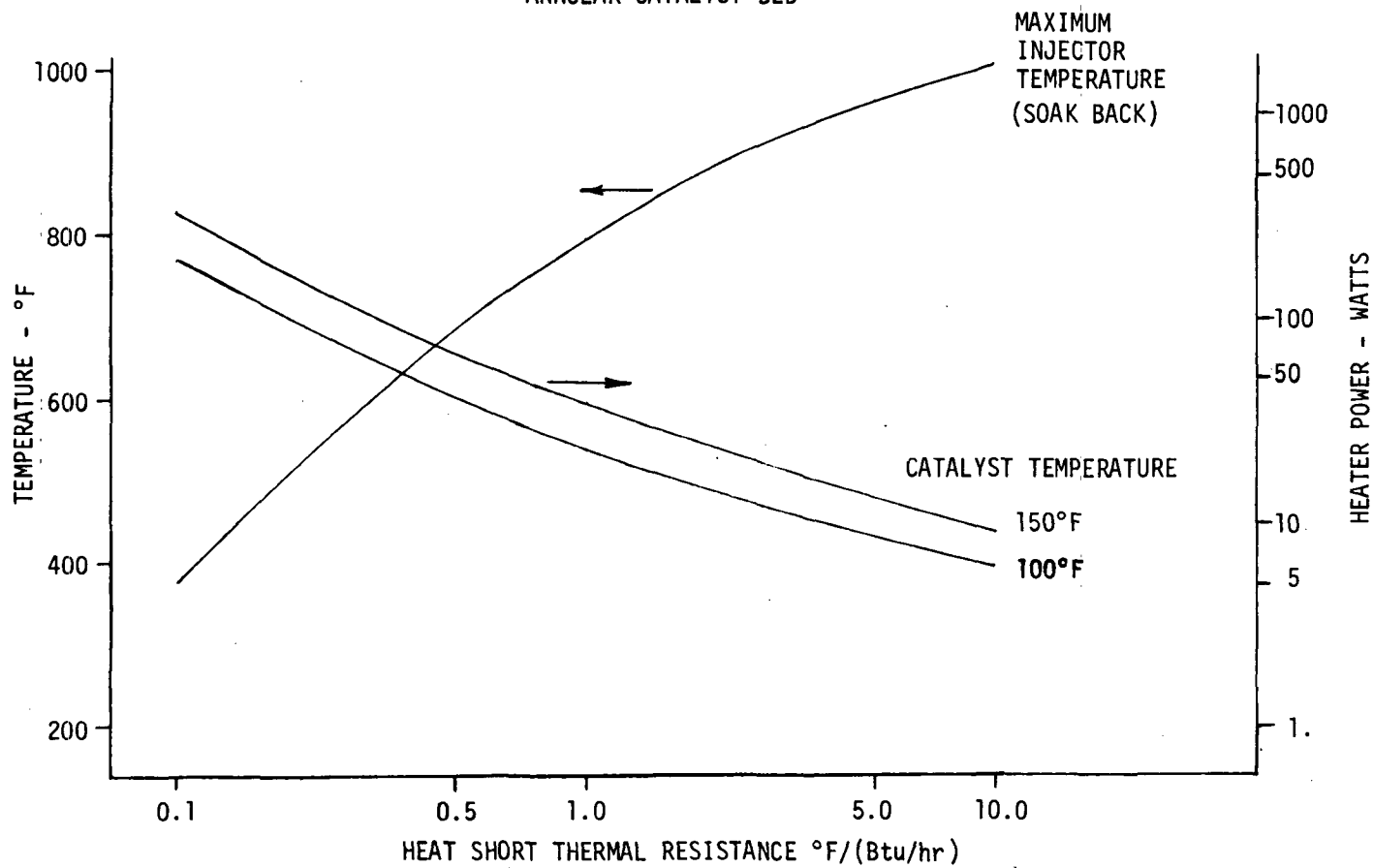
MDC E0708  
29 December 1972

E243-157

### THRUSTER THERMAL RESPONSE

EFFECT OF HEAT SHORTS ON INJECTOR  
TEMPERATURE AND HEATER POWER

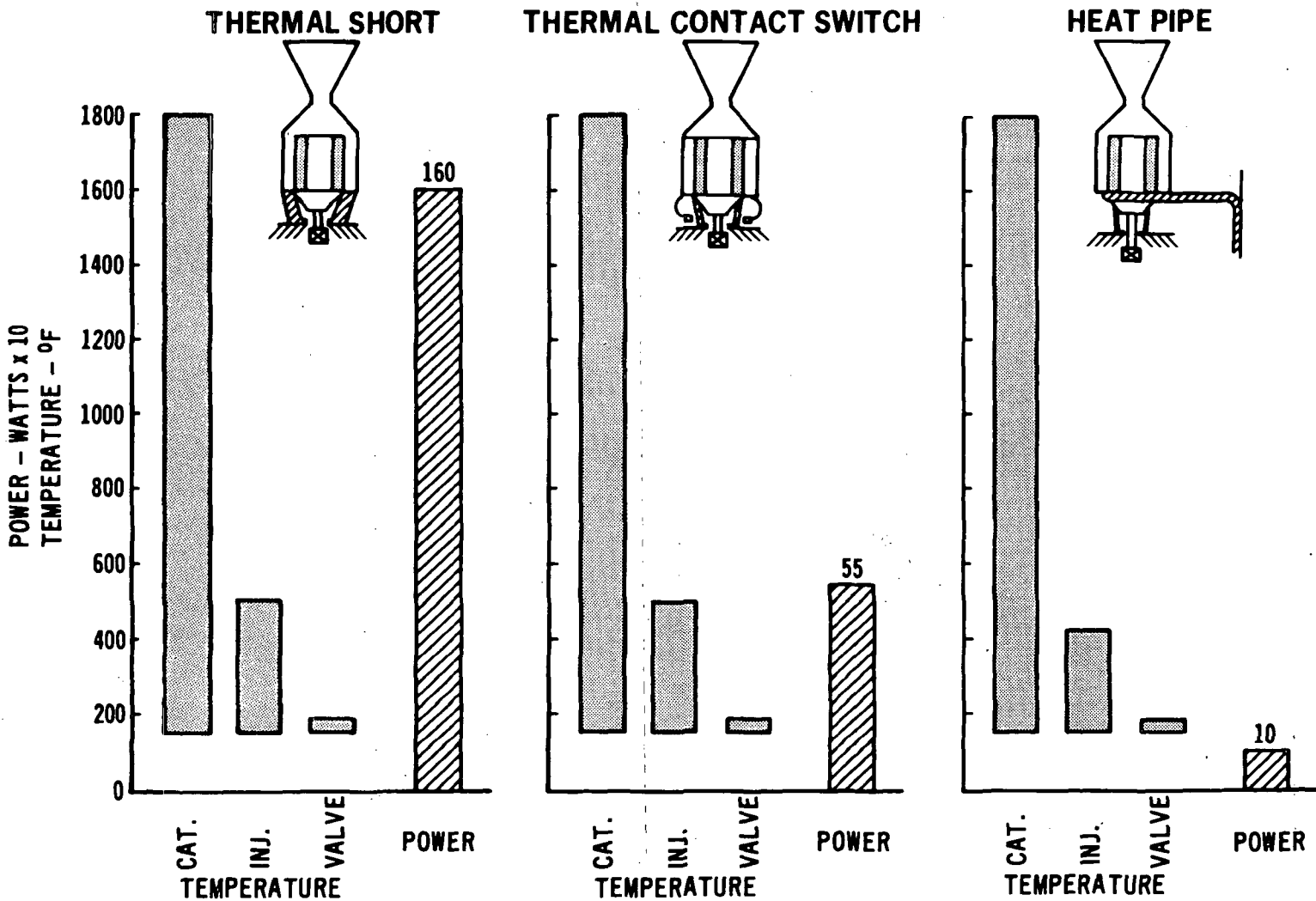
° ANNULAR CATALYST BED



F-14

Figure F-9

# ALTERNATE THERMAL CONTROL CONCEPTS



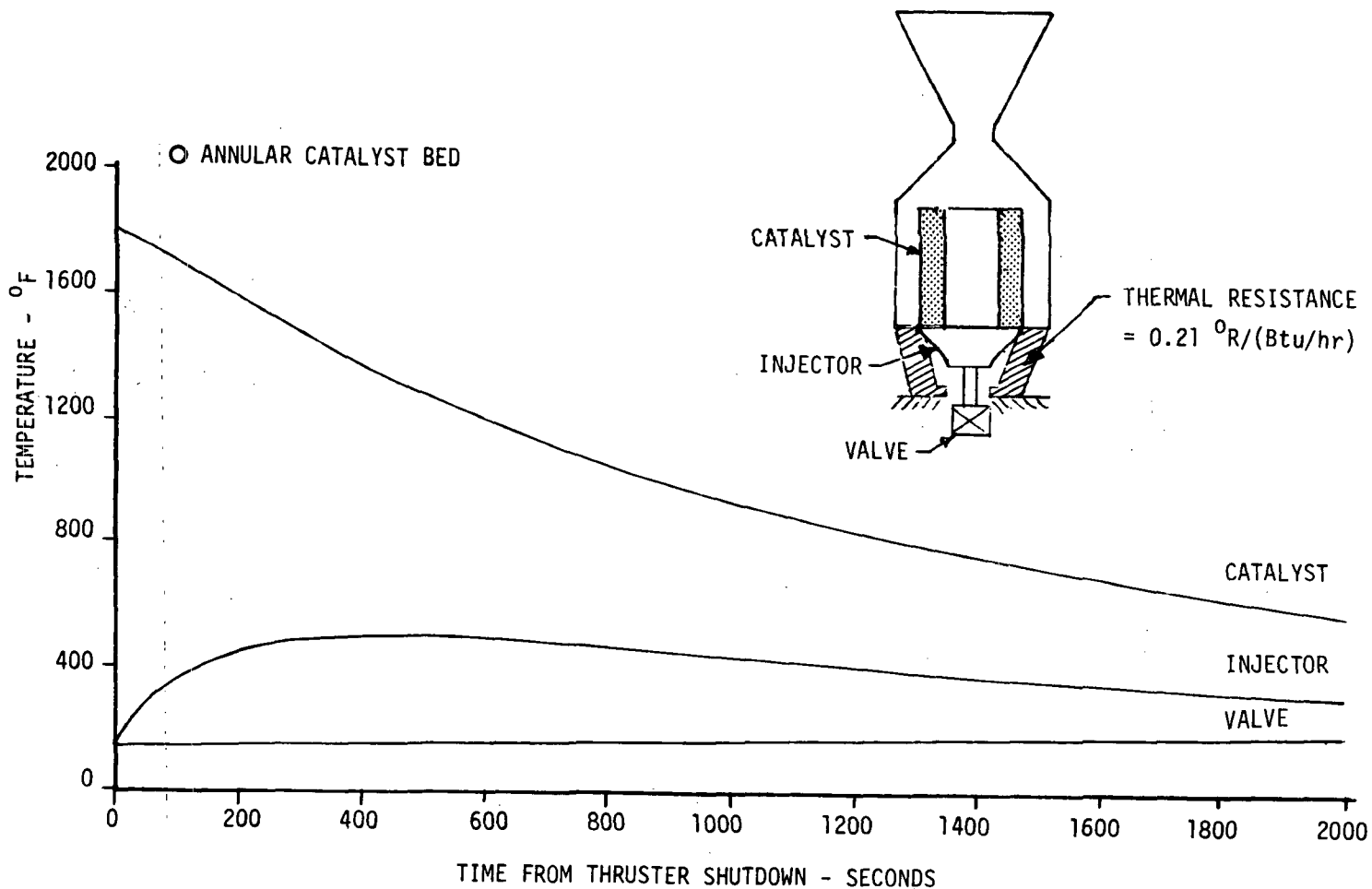
11-254

F-15

Figure F-10

E243-172

# THERMAL SHORT LIMITED INJECTOR TEMPERATURE



F-16

Figure F-11

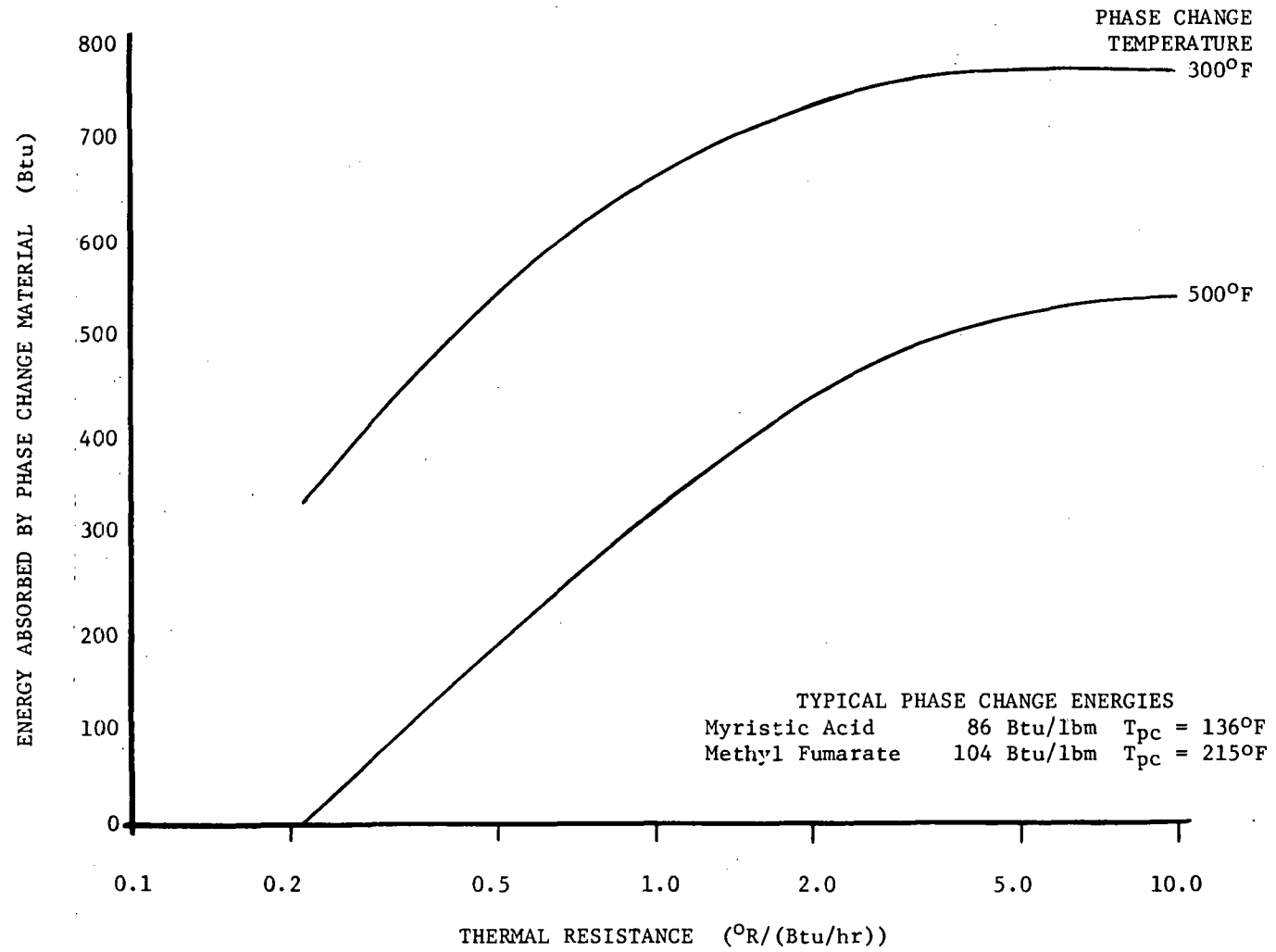
The thermal short case of Figure 9 was defined directly from the data of Figure F-7 and represents attainable conductances using aluminum or copper attachment sections. For the thermal contact switch, conductance of the closed switch was evaluated using References F-1 and F-2. From these calculations, a control surface area requirement of 4 in.<sup>2</sup> was indicated, a value high enough to present installation difficulties. In addition, based on Reference F-1, the reliability of the contact switches is in question.

In the phase change material model, the injector temperature was permitted to rise to an arbitrary temperature after which all incoming heat was assumed to be absorbed by the phase change material. Parametric requirements are shown in Figure F-12. The analysis showed that almost five lb of phase change material would be required to limit injector temperatures to 500°F. In addition, there would be weight penalties associated with conducting the heat into the phase change material and containing the phase change material.

The controllable heat pipe was modeled using a step function change in thermal resistance at an injector temperature of 392°F. Below that temperature the thermal resistance was 10°R/(Btu/hr), while above 392°F a resistance of 0.016°R/(Btu/hr) was used. This performance could be achieved using a 1/2 in. water copper heat pipe with an evaporator length of 9 in. and a one ft movement of the interface between the active and noncondensable fluids. The corresponding power requirement to maintain the 150°F minimum catalyst temperature is approximately 10 watts per thruster. As shown in Figure F-10, this power requirement is substantially less than those offered by alternate thruster cooling concepts, and heat pipes are therefore the preferred approach. Discussion of alternate designs utilizing heat pipes for the transfer of heat between the thrusters, propellant tanks, and ECLS is discussed in Section F3.4.

F3.3 Thermal Response - Thermal analysis has been performed using the two-dimensional nodal model shown in Figure F-13. The length of the wing section included in the model is equal to the pod circumference. This length is sufficient to model conduction from the wing into the pod. The model includes conduction between connected nodes, radiation between node surfaces, and storage. Emissivities of all external surfaces were 0.8, corresponding to a multi-mission vehicle. A coating with a low effective interface emissivity of 0.05 was assumed for the surfaces of the propellant tank and structural shell. This acts primarily to slow the transient thermal response. The struc-

# EFFECTIVENESS OF PHASE CHANGE MATERIAL



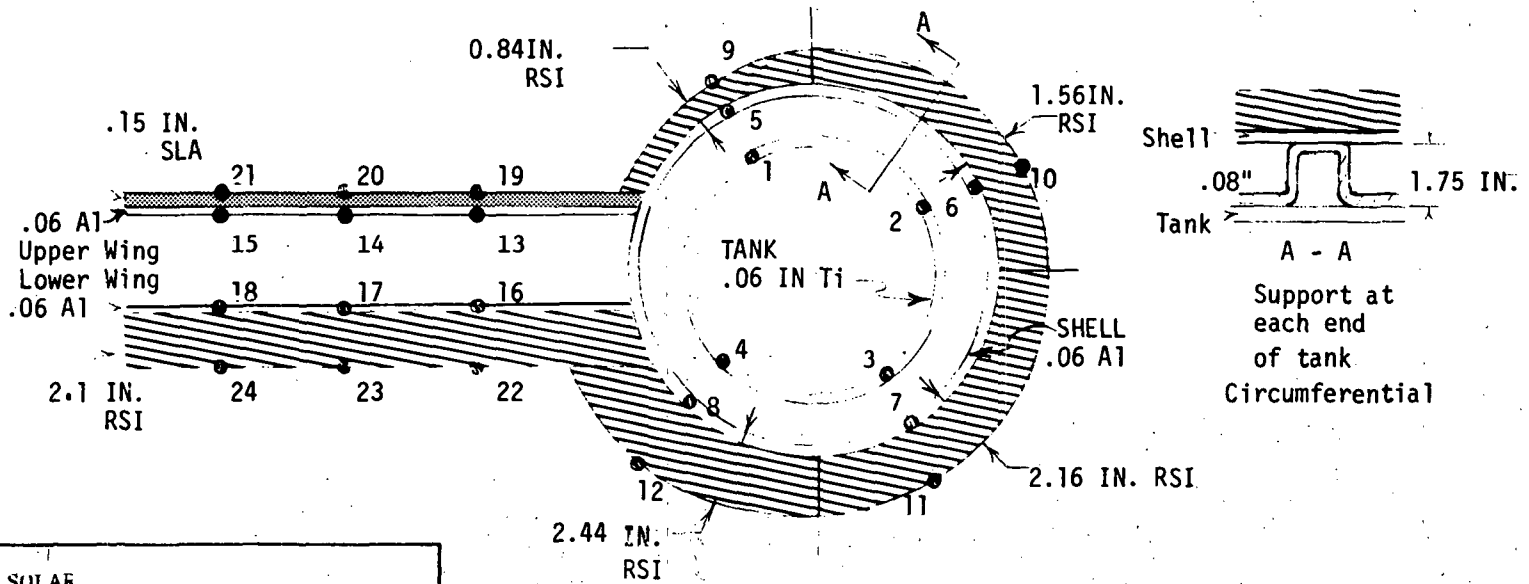
APS-771

F-18

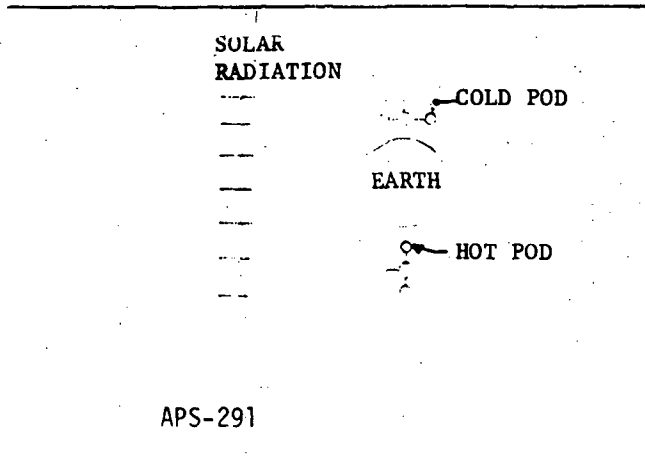
MCDONNELL DOUGLAS AERONAUTICS COMPANY - EAST

Figure F-12

WINGTIP POD THERMAL MODEL



F-19



APS-291

EMISSIVITY ALL SURFACES = .8 (EXCEPT INTERNAL TANK TO SHELL = 0.05)

SOLAR ABSORPTIVITY ALL SURFACES = .75

CONDUCTANCE BETWEEN TANK AND SHELL

1. Conductance of end support corresponds to section of tank near ends.
2. Conductance equals 1/60 of end support conductance; corresponds to midpoint section of tank.

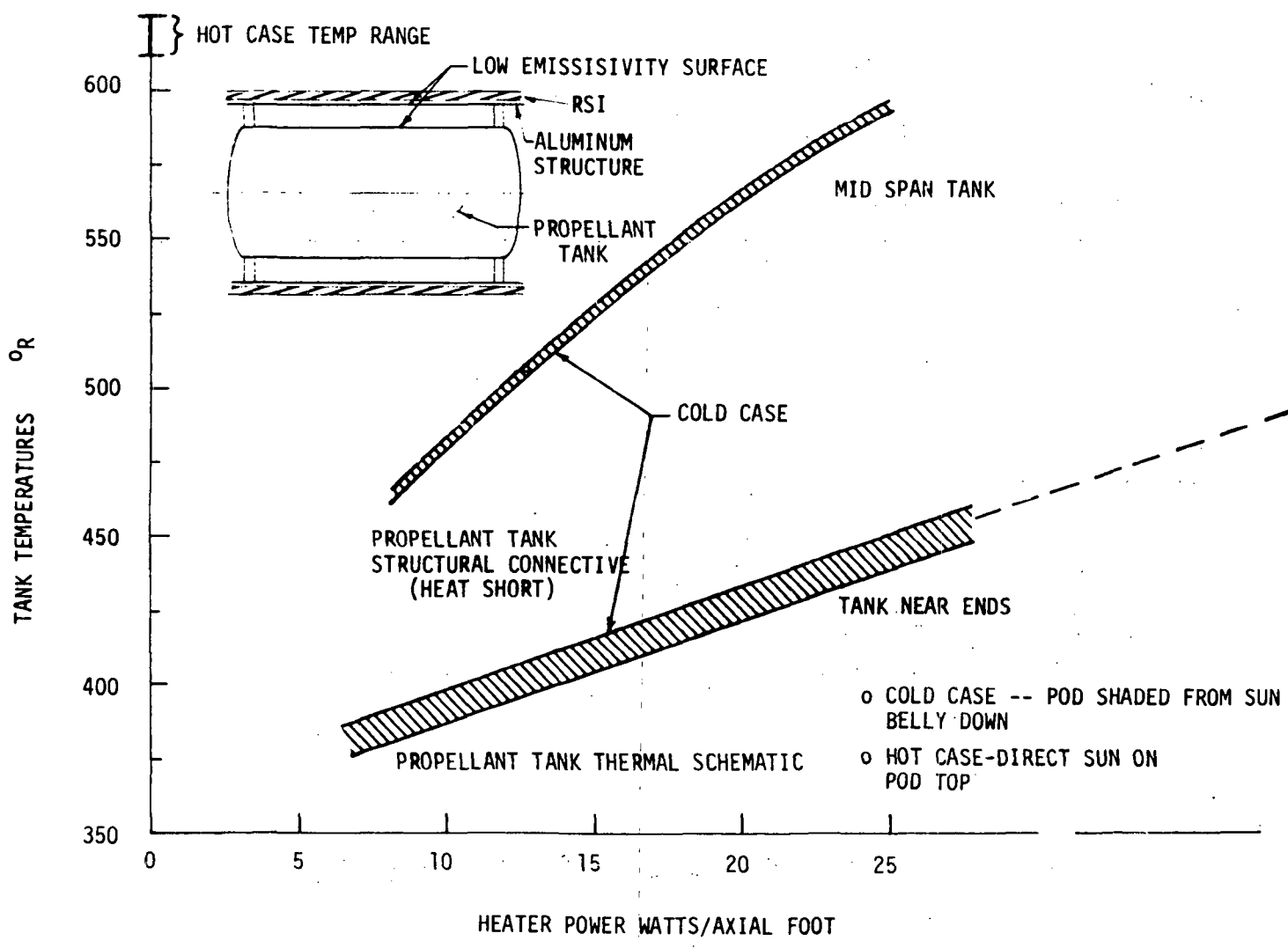
tural connections provide the principal heat leaks between the outer structure and the tank.

Steady state tank temperatures are shown in Figure F-14. For the hot case the tank temperature is 150° to 165°F, somewhat higher than the desired maximum propellant temperature of 125°F. For the cold case, typical temperatures have been obtained for both the tank midpoint and ends. The differences in the heater power required for the tank ends and middle are the direct result of the annular support structure thermal short. Nominal power requirements have been estimated by assuming that the mid-tank properties extend over approximately the central 70 percent of the tank, with end-tank properties prevailing for the remaining 30 percent. Thus, about 153 watts would be required to maintain a 50°F propellant temperature. While the tankage configuration would be somewhat different for a bipropellant system, the hydrazine calculations provide a good estimate of the heater power requirement. The lower freezing points of  $N_2O_4$  and MMH would permit design operation at 40°F providing an accompanying reduction in heater power to 131 watts.

The heat capacity of the propellant itself is a significant factor in determining the total energy requirement. To provide an estimate of this effect, transient calculations for both hot and cold extremes have been performed assuming a propellant temperature at orbit insertion of 100°F for both the tank region and the regions near the thruster enclosure. This thermal response is shown in Figure F-15. In the thruster enclosures, the thruster valves and support structure were lumped together assuming a high emissivity ( $\epsilon = 0.8$ ) for both components and surroundings. As the figure shows, the thruster enclosure temperature approaches steady state conditions for the hot case in about ten hours. The cold case temperature falls to 50°F in about 3-1/2 hours and would require heating thereafter. Nominal total heating levels for thruster enclosures may be estimated from the mid tank curve in Figure F-14. Both the heater power required to maintain catalyst temperatures (10 watts per thruster, or about 14 watts per axial foot) and the chemical energy dissipated in internal thruster losses (on the average of about 7 watts per axial foot) will tend to reduce the level of power required to maintain desired conditions. Since most of the thruster losses occur during stationkeeping burns, the dissipation losses were assumed to be uniformly distributed in time. For purposes of total power estimation, it has been assumed that one-half the power required to maintain



# STEADY STATE WINGTIP POD TANK TEMPERATURE



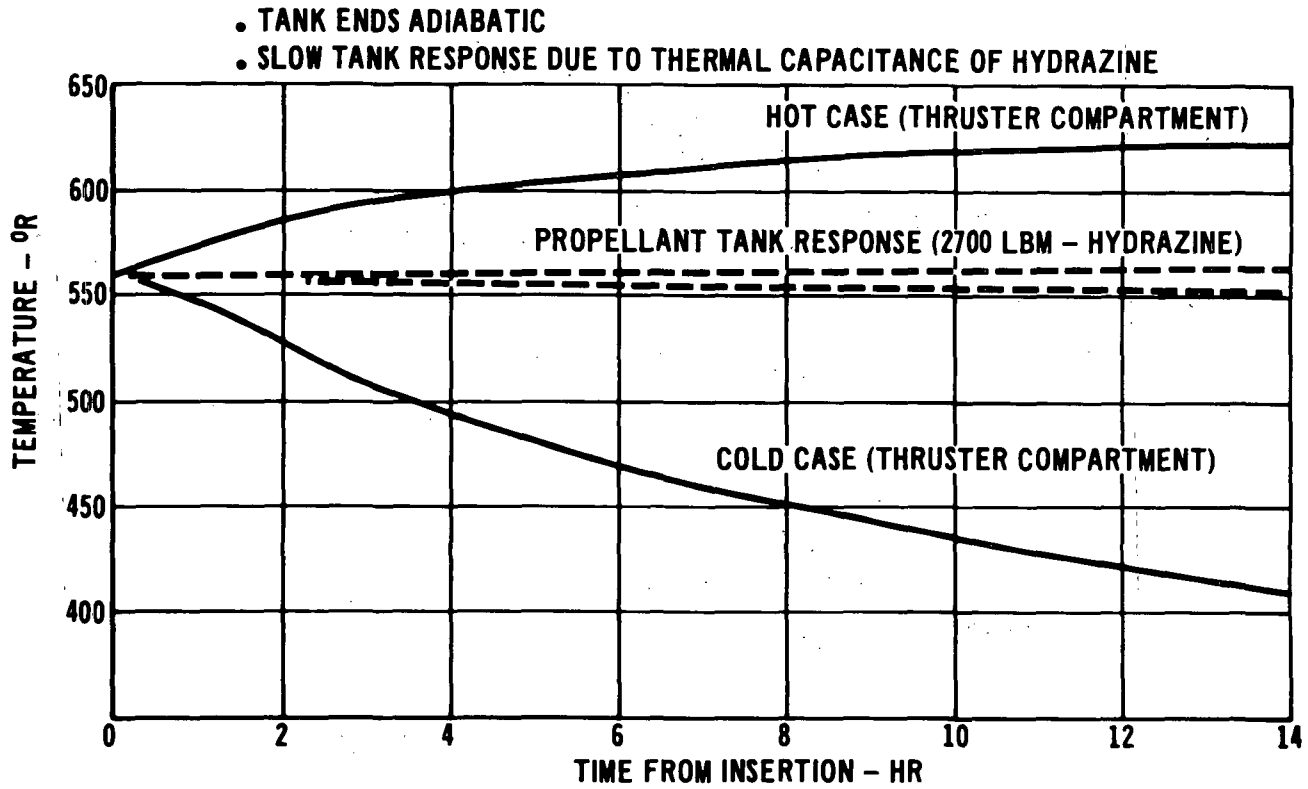
F-21

MCDONNELL DOUGLAS AERONAUTICS COMPANY - EAST

Figure F-14

APS-293

# WING TIP POD THERMAL ENVIRONMENT TRANSIENT RESPONSE



F-22

MCDONNELL DOUGLAS ASTRONAUTICS COMPANY - EAST

Figure F-15

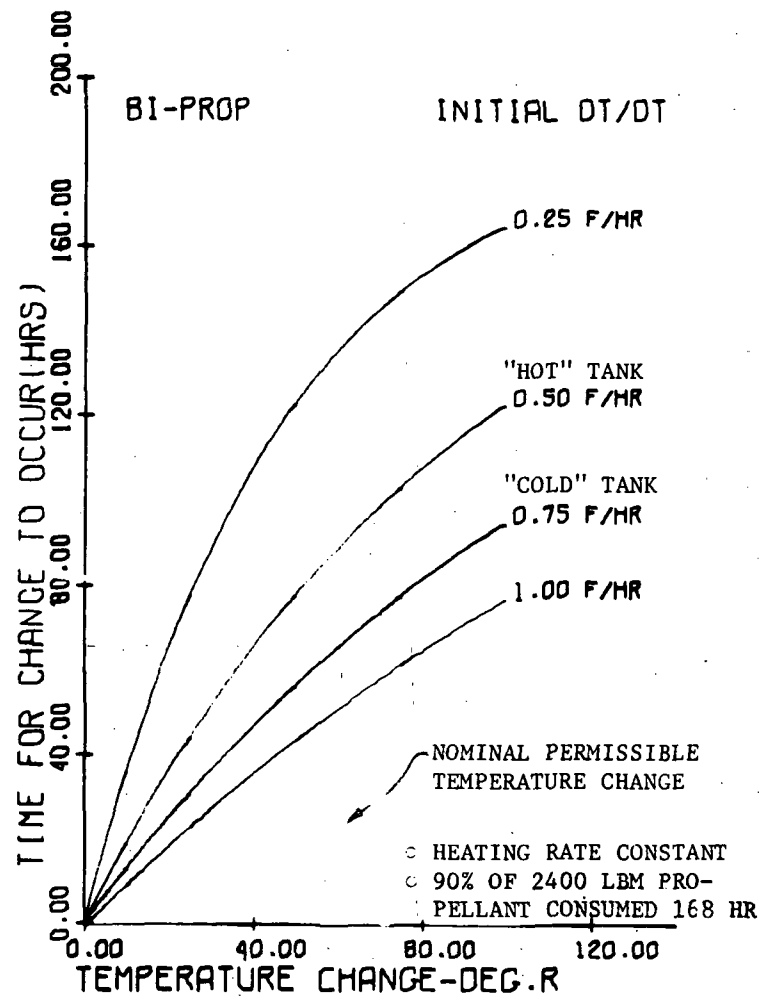
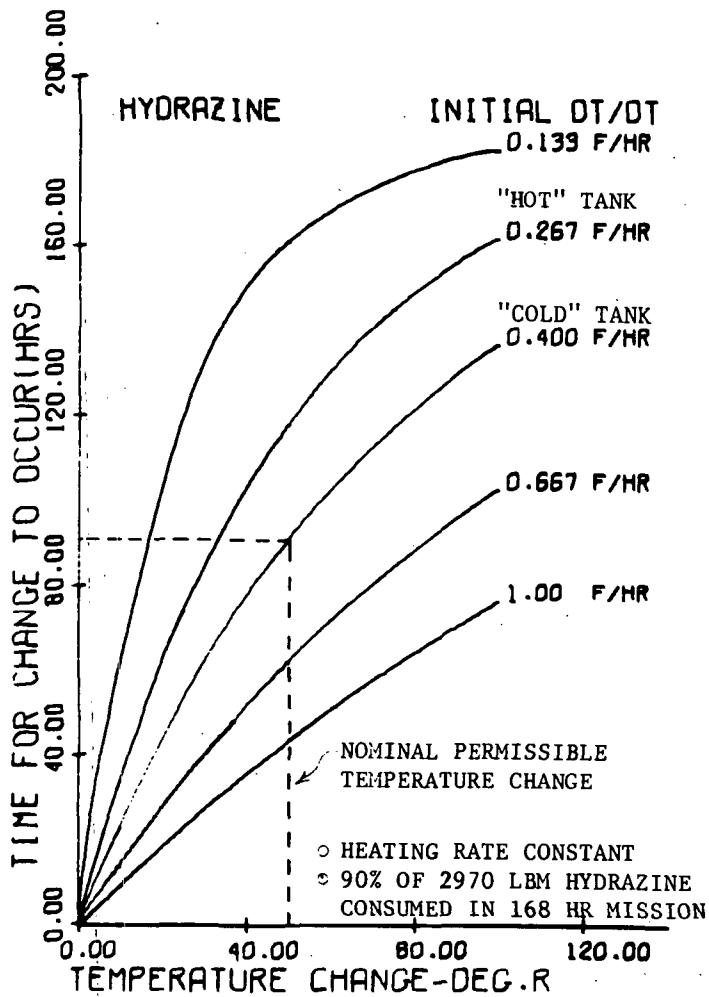
catalyst temperatures, or 5 watts per thruster, would be rejected directly to space. The catalyst heater power not lost directly to space and to the thruster inefficiencies yields a net internal power dissipation of about 14 watts per axial foot in the thruster compartment. Figure F-14 (using the mid-tank curve) shows that the enclosure temperature would be maintained at about 50°F.

For the bipropellant system, thruster inefficiency losses would be of the same order. While catalyst heaters would not be required, 5.4 watt injector heaters will be required to maintain the 70°F temperature necessary to prevent ignition spiking. The combined valve heater and thruster inefficiency heating would provide a thruster compartment power level of about 12 watts per axial foot, which would maintain a steady state temperature of about 40°F, a value consistent with the 11.8°F freezing point of the  $N_2O_4$  and minimum desired propellant temperatures.

The propellant tank temperature changes slowly because of the large heat capacity of the propellant. For propellant nominally at 100°F at orbit insertion, this means that no heating is required for substantial lengths of time. The transient calculation of Figure F-15 has been used to estimate a nominal initial heating rate based on the response during the first 15 hours following insertion. Conservative estimates of the time in which temperature changes occur have then been obtained by assuming that the initial heating rate remains constant throughout the mission. The actual heating rate would, of course, decrease as steady state conditions are approached. The total propellant heat capacity decreases as the propellant is expended and was assumed to decrease linearly throughout the 168 hour mission to 10% of the initial value.

The tank response obtained for both monopropellant and bipropellant systems is shown in Figure F-16, with heating rates expressed as initial temperature change rates. For this calculation, temperature changes may be either positive, as for heating, or negative for cooling. The curve labeled "cold tank" reflects the calculated response noted in Figure F-14. Dotted lines show the permissible temperature drop which can be experienced by the propellant before tank heaters are turned on. An initial temperature of 100°F and minimum temperatures of 50°F and 40°F for the hydrazine and bipropellant systems was assumed. From the curve, it will be noted that this corresponds to a 92-hour delay for a monopropellant system and a 74-hour delay for the bipropellant system before heating is required. The shorter delay for the bipropellant system occurs in spite of

# WINGTIP TANK TRANSIENT THERMAL RESPONSE



the lower permissible operating temperature because the heat capacity of the bipropellants is significantly lower than the capacity of the hydrazine. The total energy requirements for the 168-hour mission are shown in Figure F-17. The values shown are for a single cold pod. The power and energy requirements should not be doubled to account for two pods, however, because no case is anticipated which could cause two pods to be cold simultaneously. It is more likely that one pod would be experiencing a hot case at the same time that the other pod is experiencing a cold case.

The large variation in power requirements, shown in Figure F-14 between the tank midspan and ends, show the extreme importance, from a thermal standpoint, of the structural support of the pod. Similarly, the use of low emissivity coatings inside the structural shell provides a means of reducing heater power requirements without adding the weight associated with insulation. However, should such insulation be required to provide additional entry heating thermal protection, it would also materially reduce the heat transport from the surrounding surfaces to the tank and could eliminate the need for the low emissivity coatings on the shell and surroundings.

F3.4 Combined Thruster - Module Thermal Control - The high propellant temperature possible for a wing tip module indicates a need for heaters to maintain minimum propellant temperatures as well as some thermal control system to prevent overheating of the propellant. One approach to such temperature control would be to run the environmental control and life support (ECLS) fluid lines to the end of the wings into a heat exchanger there. This heat exchanger would then provide a sink for the thrusters and tankage located in the wing tip module and provide a positive means of controlling the temperature. It would thus be used to maintain minimum temperatures and prevent overheating as well. The operation of such a thermal control system is examined in this section.

F3.4.1 Thermal Control Alternatives - A number of techniques were considered to connect equipment in the module to an ECLS cold plate. These included the use of thermal conduction through aluminum or copper bars, a separate active cooling system in the module, and the use of heat pipes to deliver the heat from equipment in the module to the cold plate interface. The use of solid material for conduction presents significant weight problems. To achieve the required heat transfer levels, the conductive area must be so large that it presents weight problems and, in fact, acts as a heat sink or

## WING POD THERMAL CONTROL REQUIREMENTS

	MONOPROPELLANT HYDRAZINE		BIPROPELLANT NTO/MMH	
	POWER LEVEL (WATTS)	ENERGY (KWH)	POWER LEVEL (WATTS)	ENERGY (KWH)
THRUSTER HEATERS	150	25.2	81	13.6
TANK HEATERS	153	11.6	140	14.3
TOTAL	303	36.8	221	27.9
ASSOCIATED FUEL CELL WEIGHT				
POWER AT 286 LBM/KW	87 LBM	-	63 LBM	-
ENERGY AT 1.98 LBM/KWH	-	73 LBM	-	55 LBM
TOTAL WEIGHT PENALTY FOR HEATER POWER/ENERGY REQUIREMENTS	160 LBM		118 LBM	

F-26

MCDONNELL DOUGLAS ASTRONAUTICS COMPANY - EAST

Figure F-17

thermal capacitor rather than a conductor. An active system using pumps and appropriate valves and connectors also adds considerable complexity. A simple system which provides the greatest heat transfer capability with the lightest weight and greatest reliability is provided through the use of heat pipes.

Various possibilities are feasible for the implementation of a heat pipe system. Four of these are shown in Figure F-18. These include: (1) a heat pipe system in which the cold heat pipe condenser and evaporator sections are attached to detachable plates thereby permitting removal of the heat pipe system, (2) a system in which the heat pipe is directly attached to the mounting plate, (3) an indirect dual control system where thermal communication is maintained between the thruster support plate and the propellant tank, and a separate heat pipe is used to communicate energy from the propellant tank to the cold plate, and (4) an indirect dual heat pipe system which utilizes detachable rings on both heat pipes to facilitate their removal and replacement.

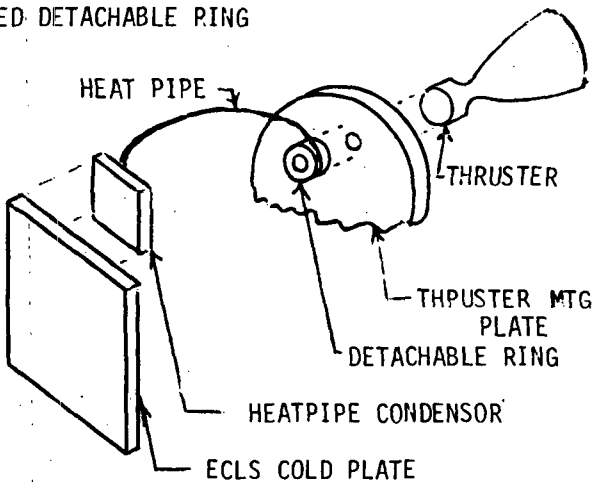
F3.4.2 Analysis - In order to determine the operational considerations of using such a system, a thermal model of the module, including thruster, mounting plate, module structure, and cold plate connection, has been constructed to determine steady state requirements for heaters necessary to maintain thruster minimum temperatures and to determine the heat delivered to the ECLS during thruster soakback and the system transient response.

A typical thruster heat pipe installation for such a system is shown in Figure F-19. In this installation, the heat pipes are attached directly to the thruster mounting plate. The mounting plate provides heat capacity and surface area required for heat pipe attachment. The propellant valves, which also have a temperature requirement during soakback, are mounted to a separate plate to minimize direct heating from the thruster or thruster mounting plate.

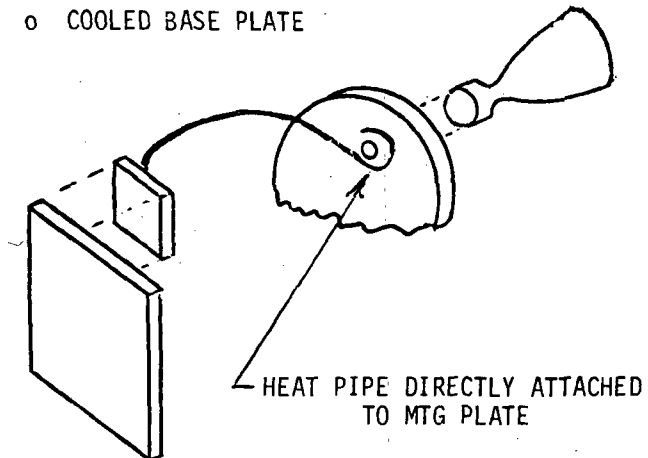
For a heat pipe system, the principle thermal resistances are associated not with the heat pipe itself, but with the interfaces between the heat pipe and the other components to which it is connected. The nominal levels of these thermal resistances are shown in Figure F-20. As shown in this diagram, typical thermal resistances are about  $0.1^{\circ}\text{R}/(\text{Btu}/\text{hr})$  when interstitial grease is used between the heat pipe and cold plate. The curve of Figure F-20 illustrates the dependence of the heat pipe input power on injector temperature. The power which can be delivered through the heat pipe increases approximately linearly with the injector temperature. This linear dependence occurs primarily because of the interface thermal resistances.

# ALTERNATE IMPLEMENTATION TECHNIQUES

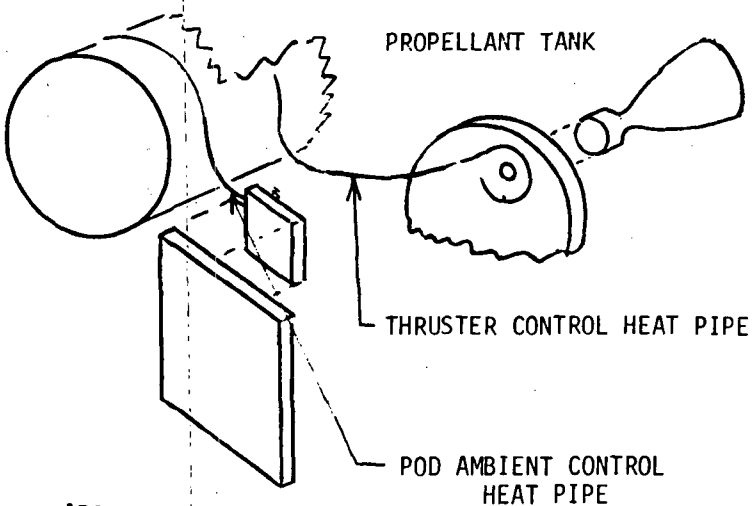
o COOLED DETACHABLE RING



o COOLED BASE PLATE

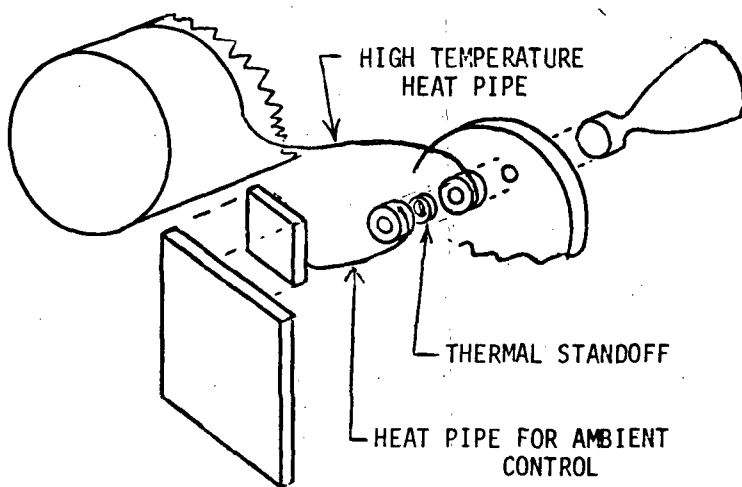


o INDIRECT CONTROL, DUAL HEAT PIPE



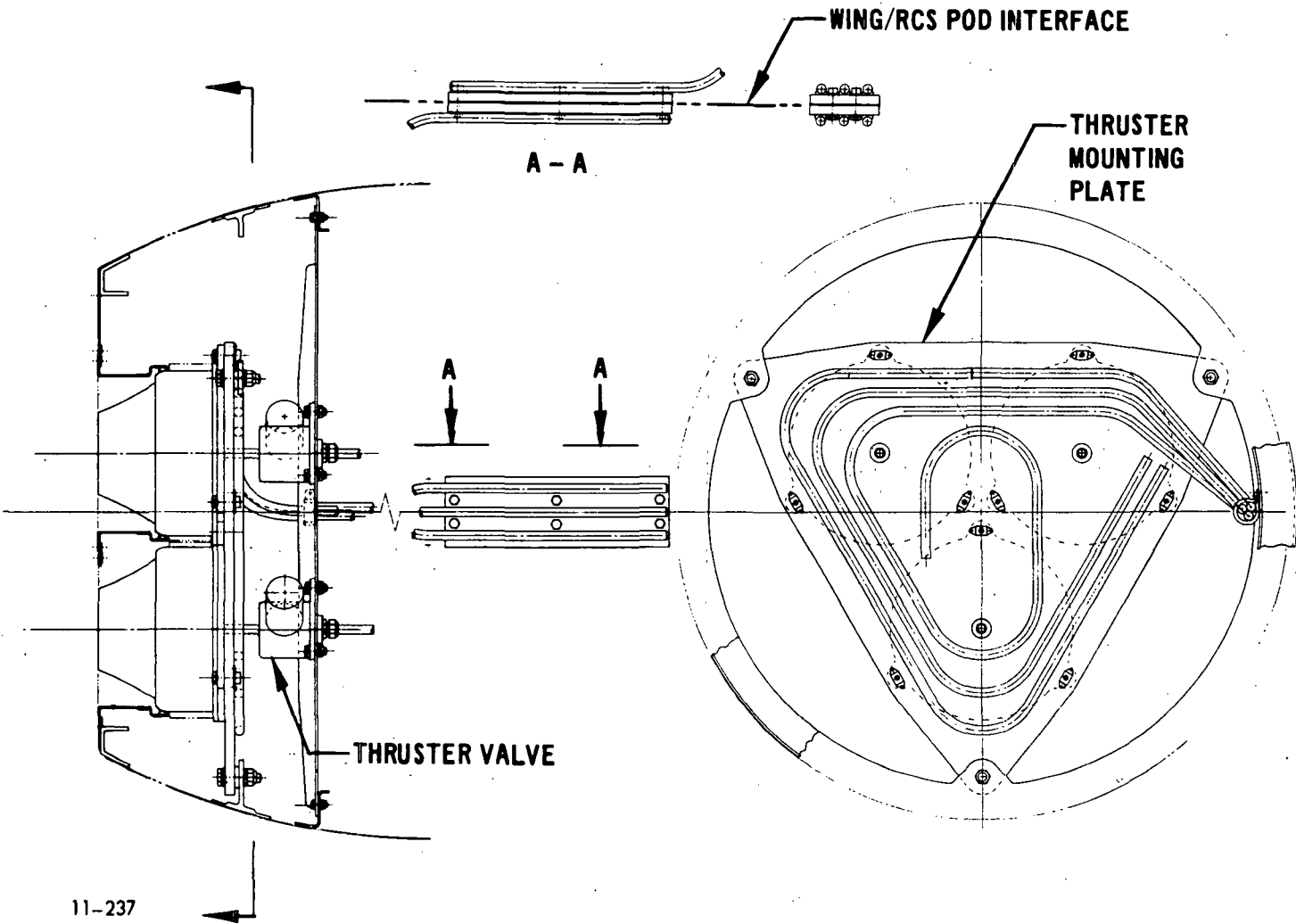
APS-388

o DUAL HEAT PIPE WITH DETACHABLE RINGS





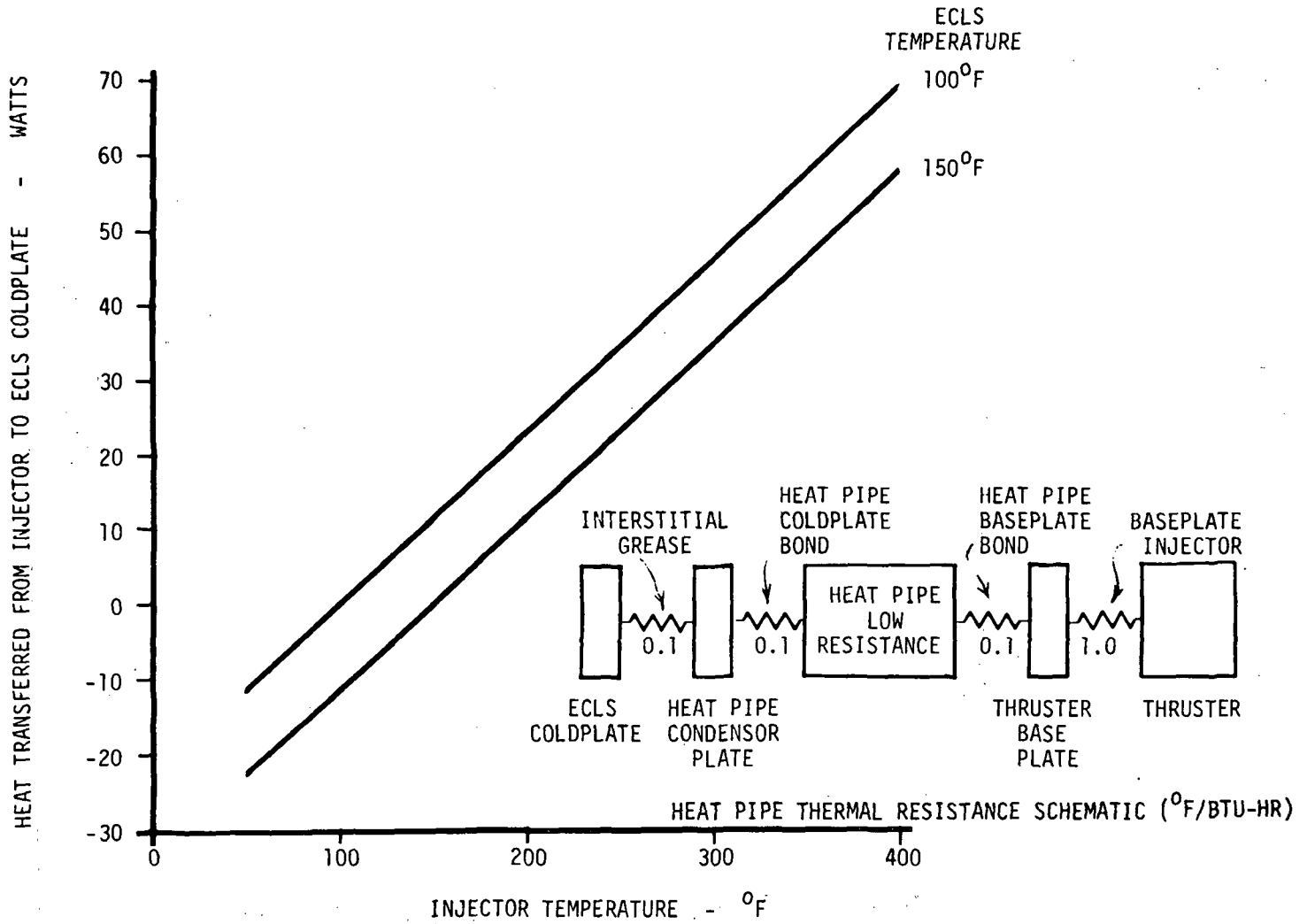
# THRUSTER HEAT PIPE INSTALLATION



F-29

Figure F-19

# HEAT PIPE DEPENDENCE ON OPERATING TEMPERATURE



HEAT TRANSFERRED FROM INJECTOR TO ECLS COLDPLATE - WATTS

70  
60  
50  
40  
30  
20  
10  
0  
-10  
-20  
-30

INJECTOR TEMPERATURE - °F

ECLS TEMPERATURE  
100°F  
150°F

0 100 200 300 400

F-30

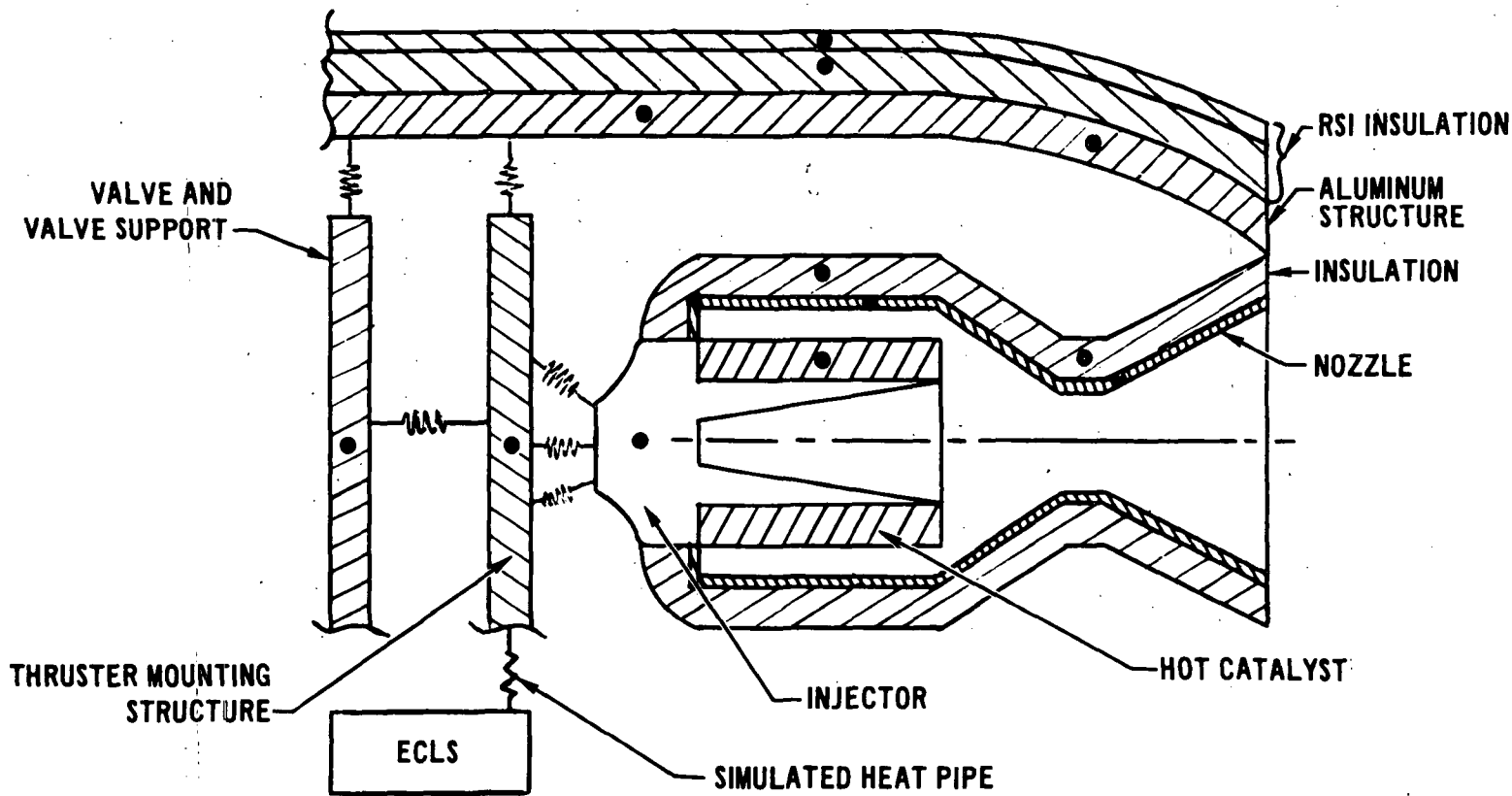
APS-381

The thermal model utilized to evaluate the thermal response of the thruster module heat pipe ECLS is shown in Figure F-21. The model includes radiation from the thruster to deep space via the nozzle and to the surrounding module structure, and soakback from the thruster to the thruster mounting support. The heat pipe was simulated by assuming a constant thermal resistance from the thruster mounting structure to the ECLS. Hot and cold nominal cases correspond to the possible combinations of the ECLS extremes and module surrounding temperature extremes.

Steady state power requirements per thruster are shown in Figure F-22 for hot and cold ECLS and surrounding temperatures. The ECLS temperature range was assumed to be 100°F to 150°F. Ambient conditions, based on module thermal response calculations were allowed to vary from 40°F, the minimum propellant temperature, to a maximum of 165°F, associated with operation in the direct sun. The results show that a nominal heater power of 10 watts per thruster is still required; however, for the case in which both the ECLS and the surroundings are at a minimum condition, 25 watts would be required. A catalyst temperature of 150°F was assumed for all calculations. Power delivered to the ECLS varies from 10 watts when the ambient conditions are hot and the ECLS is hot to -10 watts when the surroundings are cold but the ECLS is at a maximum. For that case, the module would actually provide a heat sink for the ECLS.

The results presented in Section F3.2 established a need for special thermal control techniques to minimize thruster soakback heating. The thruster-ECLS model was applied to a soakback situation to examine the response of the thruster, the mounting plate, and the module. Results of the soakback response calculation for both a hot and cold system are shown in Figure F-23. The cold case presents no problem. However, for the hot case, the injector temperature without the heat pipe rises to 500°F. With the heat pipe, the injector does not rise as far and is cooled more rapidly. The single soakback response of course is not expected to present a significant problem. Problems will arise, however, when multiple firings occur. Calculations were performed for simulated multiple firing case with the results shown in Figure F-24. For this case, soakback was allowed to continue for 2,000 seconds. At that time, it was assumed that a second pluse occurred in which the thruster and catalyst temperatures were elevated to the steady state hot conditions before firing termination. The mounting plate temperature, however, was not allowed to change during

# THRUSTER/MODULE THERMAL ANALYSIS MODEL

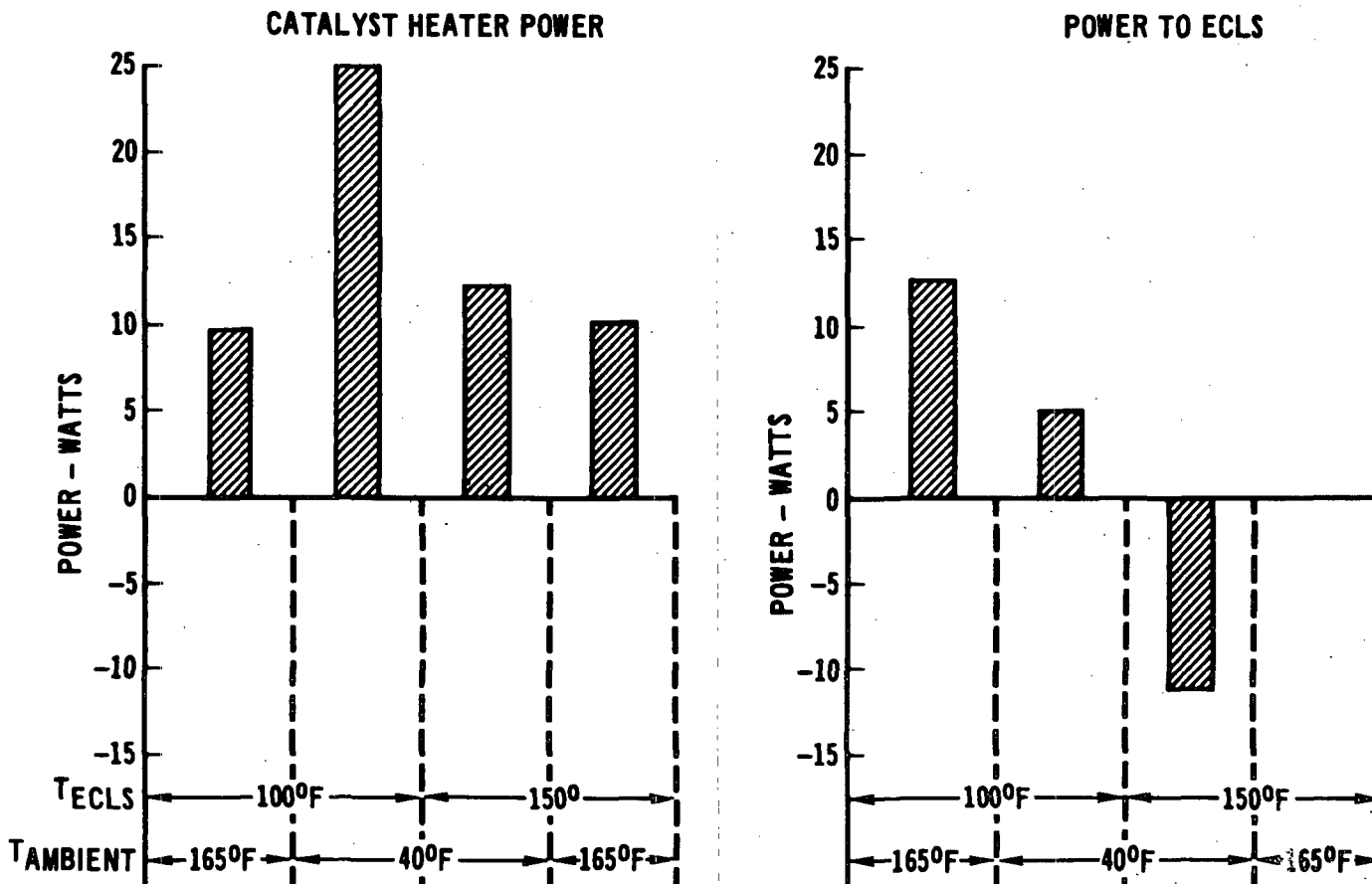


F-32

11-255

# STEADY STATE POWER REQUIREMENTS PER THRUSTER

$T_{\text{CATALYST MIN.}} = 150^{\circ}\text{F}$



11-256

F-33

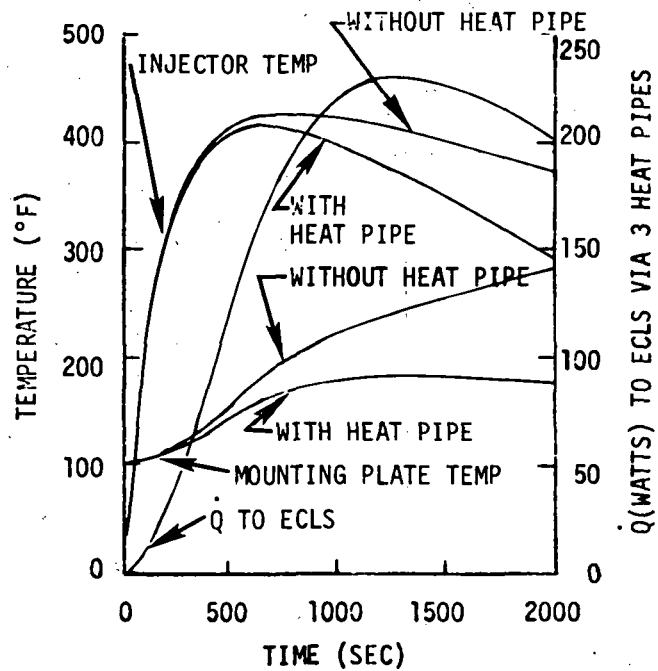
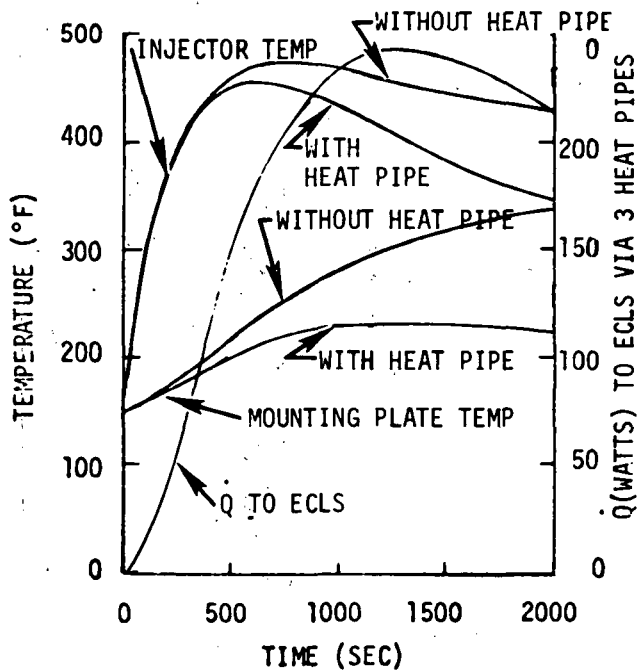
Figure F-22

## MODULE THERMAL SOAKBACK RESPONSE

- 1/3 OF STRUCTURAL THERMAL CAPACITY ALLOCATED TO EACH THRUSTER CONTROL SYSTEM
- ALL HEAT CAPACITY OF 9.1bm MOUNTING PLATE USED.

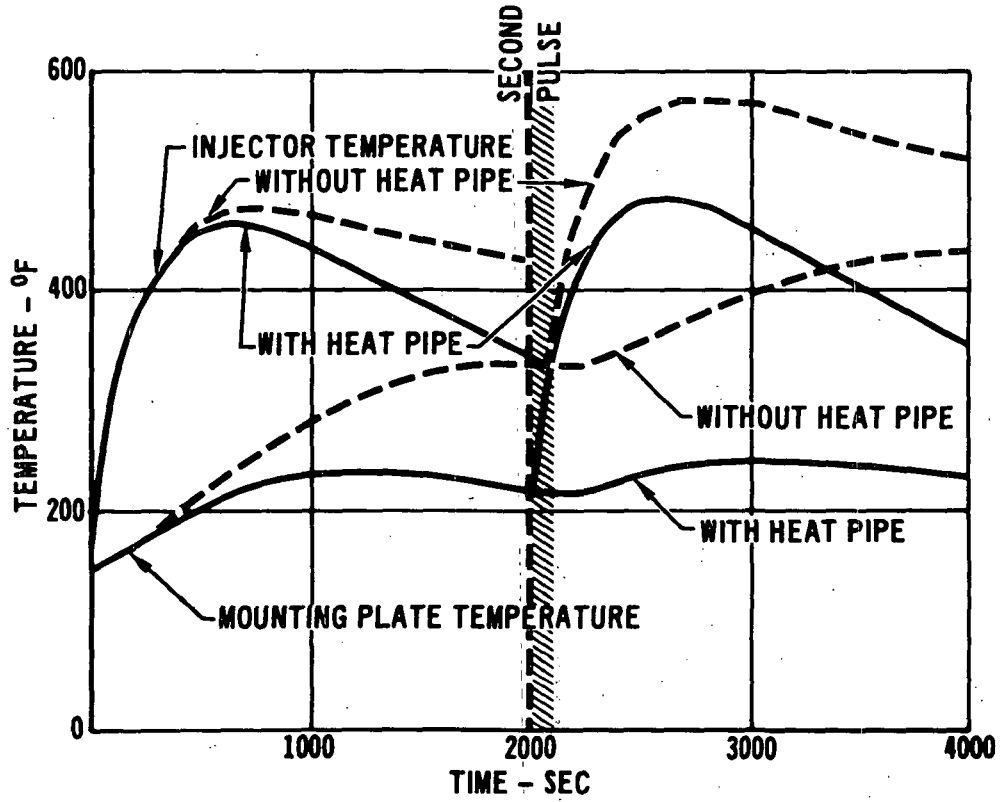
o  $T_{\text{AMBIENT}} = 165^{\circ}\text{F}$   
o  $T_{\text{ECLS}} = 150^{\circ}\text{F}$

o  $T_{\text{AMBIENT}} = 40^{\circ}\text{F}$   
o  $T_{\text{ECLS}} = 100^{\circ}\text{F}$



F-34

# EFFECT OF PULSE OPERATION ON THRUSTER TEMPERATURE TRANSIENTS



F-35

MCDONNELL DOUGLAS ASTRONAUTICS COMPANY - EAST

Figure F-24

11-238

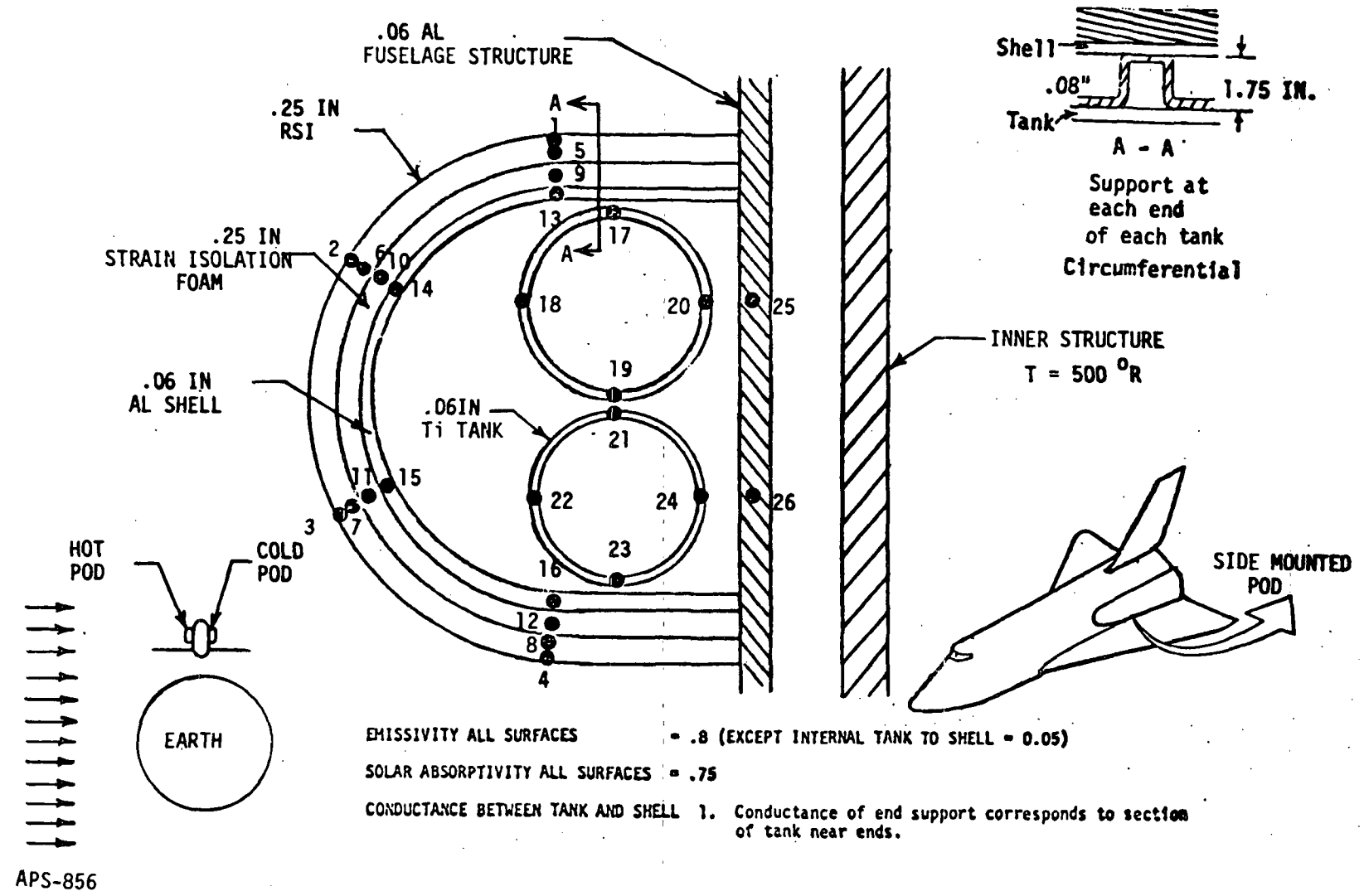
the simulated firing. Because the mounting plate temperature was higher following the second firing, heat transfer to the mounting plate is reduced and the injector temperature rises significantly. With a heat pipe system, the injector temperature does not exceed the 500°F maximum injector temperature. For the uncontrolled system using only the capacitance of the module and the thruster mounting plate, however, the injector temperature rises to about 560°F, well above the maximum limit. These thruster-module-ECLS calculations indicate that satisfactory operation can be achieved linking the module to the ECLS. The heat pipe provides a simple lightweight reliable system without the complexity of additional pumps, valves or controls.

F4 Fuselage Mounted RCS (OMS) Module Thermal Response - Steady state and transient thermal responses have been examined for the fuselage mounted module. Maximum uncontrolled propellant temperatures (115°F) were somewhat less than for the wing tip pod because of additional communication with the vehicle itself. However, heater power levels required to maintain minimum temperatures were substantially higher, due to the increased tank size and reduced thermal communication with earth. Tank structure and support transients have been examined to evaluate techniques for reducing the principal leaks. The results show that to maintain 40°F conditions for the four tanks in a module subjected to a cold environment requires an input of 330 watts.

A cross-section of the 3-dimensional thermal model used for the fuselage mounted pod is shown in Figure F-25. Calculations were performed for the nominal hot and cold cases indicated in the inset. The fuselage mounted pod differs thermally in two principal ways from the wing tip pod. The wing length, which tends to isolate the wing tip pod from the influence of the fuselage both by direct conduction and by radiation from exposed surfaces, merely serves as a radiation shield between the fuselage mounted pod and the earth. Secondly, the orbiter fuselage structure is directly exposed to the tanks and thus exerts a direct influence on the tank thermal behavior. The influence of the inner fuselage structure has been modeled by assuming an inner fuselage surface temperature of 500°F and radiative connection from nodes 25 and 26 to this source/sink. No direct sunlight is received by the wing upper surfaces for either the hot or cold cases, and the nominal temperature is approximately 370°R for both cases. This temperature is also applicable for the cold-side fuselage structure. However, the hot-side space exposed fuselage is affected by direct sunlight, and therefore reaches 692°R.



# FUSELAGE MOUNTED POD THERMAL MODEL



F-37

MCDONNELL DOUGLAS AERONAUTICS COMPANY - EAST

Figure F-25

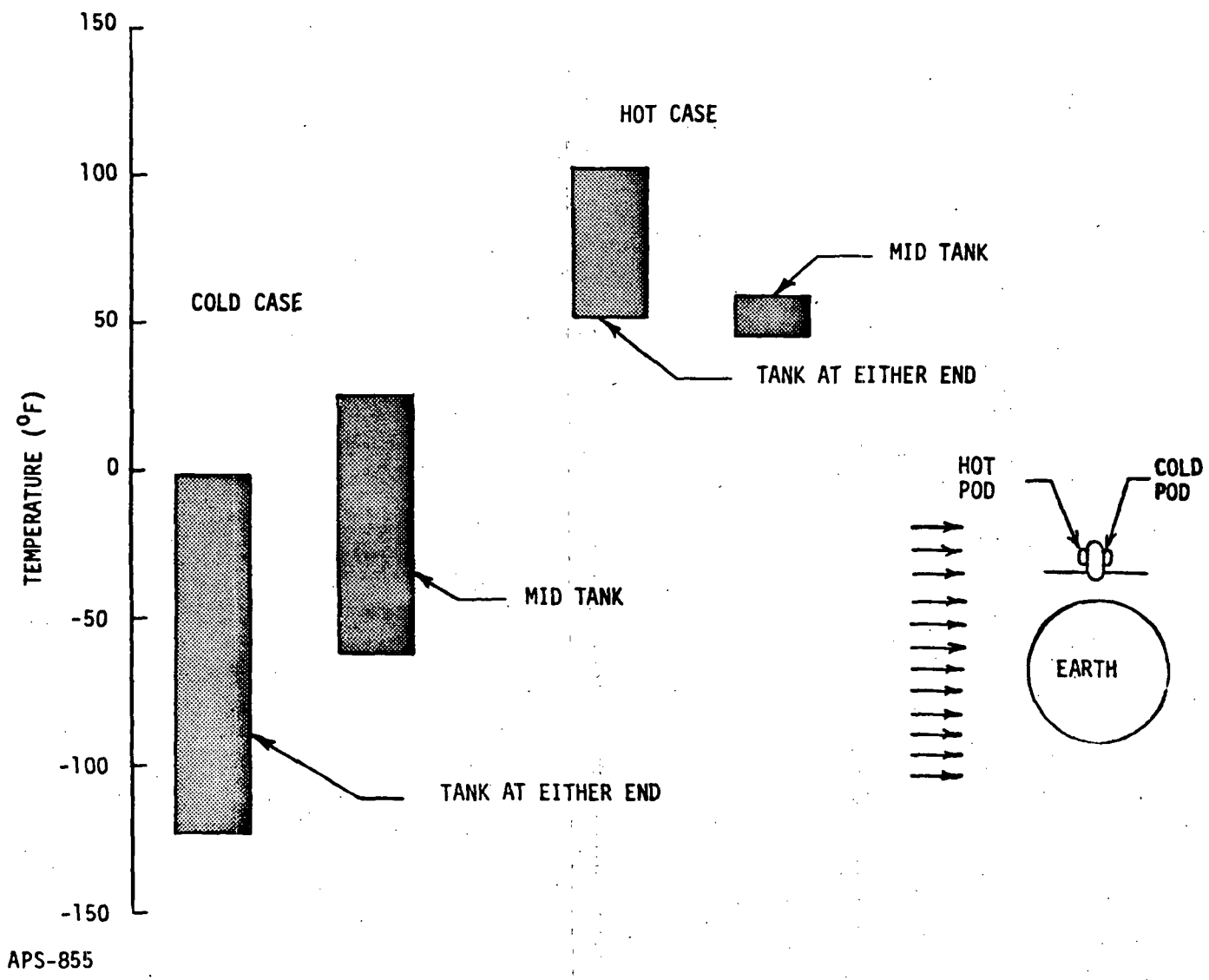
APS-856

TPS requirements for the fuselage modules were less stringent than for the wing modules. Accordingly, an average unit weight of  $2.0 \text{ lbm/ft}^2$  of RSI was assumed for weight calculations.

The initial tank support model investigated was analogous to the wing tip module tank support. Aluminum circumferential channels were located at each end, and connected directly to the vehicle structure, as shown in Figure F-25. For transient calculations, propellant loads of 2600 lbm MMH and 4350 lbm  $\text{N}_2\text{O}_4$  were assumed to be distributed uniformly in proportion to the tank surface area over the tank thermal model nodes. Steady state temperatures were obtained using the transient model by setting material densities to the minimal values.

The fuselage module transient response is similar to the response for the wing tip mounted modules. The propellant thermal capacity again is so large that although the temperature of the enclosure itself changes rapidly, response times associated with the propellant are very long. The tank temperature distribution for aluminum circumferential-channel supported tanks is shown in Figure F-26. The maximum propellant tank temperature is  $115^\circ\text{F}$ , and therefore, no propellant cooling will be required for fuselage module configurations. However, propellant heating is still required; these calculations indicate that a power input of 1610 watts would be required by tanks supported by circumferential aluminum channels. This represents an excessive power requirement, and two alternate structural connections have been evaluated to determine ways of reducing the heater power. In the first, the aluminum structural ring was replaced by a titanium ring of identical dimensions. The low thermal conductivity of the titanium compared to aluminum reduces substantially the heat transferred via the support channel and smaller heating power requirements are required to maintain tanks at specified temperature levels. In the second alternative, tank support was provided by aluminum structure cantilevered from the fuselage side. In this side-only support case, there is no conduction heat transfer from the tank to the thruster enclosure, and the thruster enclosure serves as a radiation shield between tanks and space. A comparison of the alternate tank support models is shown in Figure F-27. The use of circumferential titanium supports does reduce the power requirements to 770 watts. However, support from the fuselage side only results in a power requirement of only 330 watts, and is therefore the preferred approach. This heating requirement could be further reduced through the use of low-density insulation between the tanks and the outer enclosure.

### TANK TEMPERATURE RANGE DISTRIBUTION



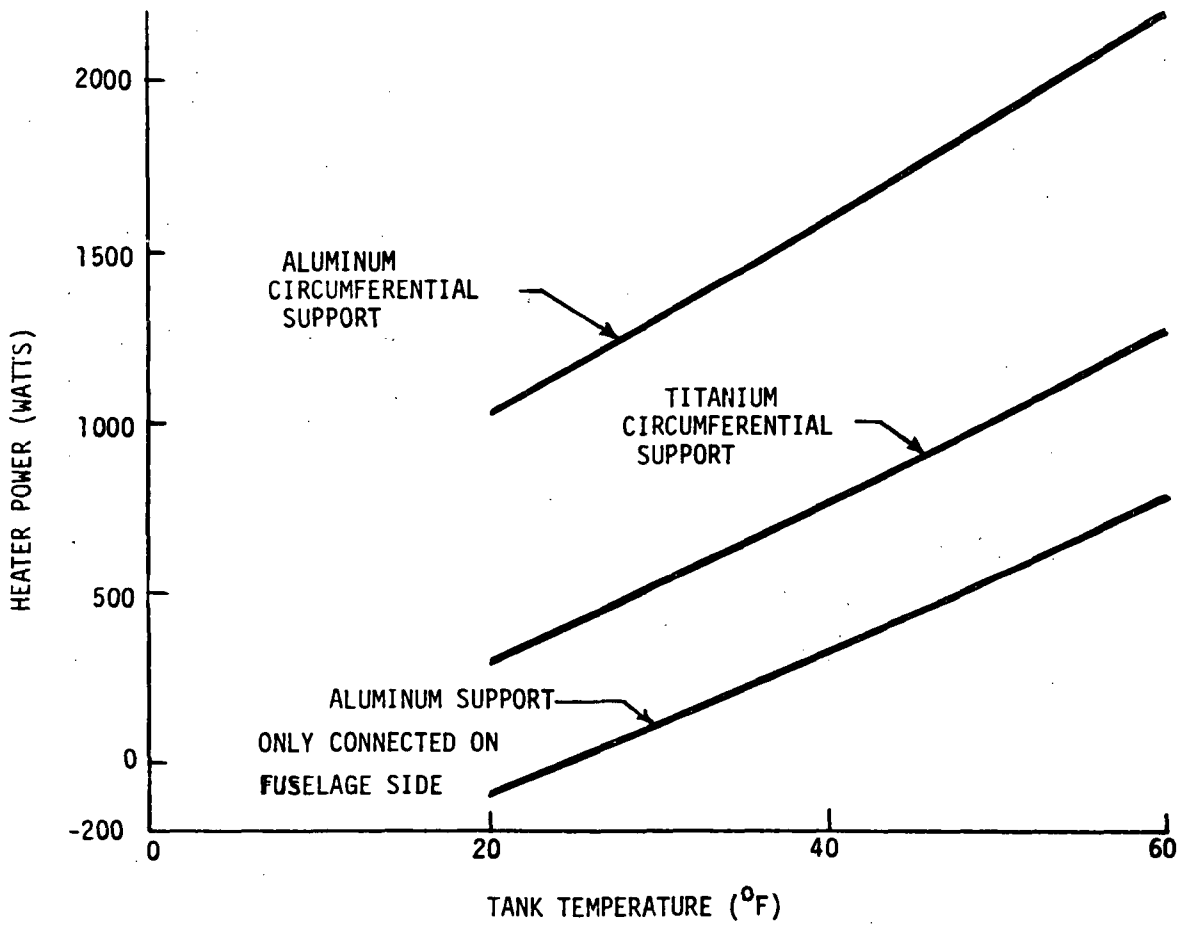
F-39

MCDONNELL DOUGLAS AERONAUTICS COMPANY - EAST

Figure F-26

APS-855

# ALTERNATE TANK SUPPORT HEATER REQUIREMENTS



APS-854

F-40

F5 APU Thermal Control - The APU implementation trade study has been discussed in Appendix B6. In this appendix the thermal environment, heat load to the hydraulic fluid and heat exchanger analysis will be discussed.

F5.1 Environments and Heat Loads - The APU operation is affected by ascent and entry environments. For ascent, natural convection decreases with altitude, minimizing APU interaction with its surroundings. During reentry, however, the importance of convection increases as touchdown approaches and cannot be neglected. TPS guidelines limit the maximum structure temperature to 300°F. The APU surroundings were therefore assumed to increase linearly during entry from 100°F to 300°F.

The dominant requirement on the APU coolant is the power dissipated in the hydraulic fluid by the APU driven equipment. Nominal ascent and reentry heating rates for this equipment are shown in Figure F-28. Because of increased power levels, these heating rates are somewhat higher than those used during the preliminary systems analysis discussed in Appendix B6. To derive these power levels the entire power consumed by the hydraulic pump was assumed to be dissipated in the hydraulic fluid. In addition, losses associated with gear box operation have been included. Alternator losses included in the preliminary systems study were not included since the alternator in the current design is cooled conductively.

F5.2 Thermal Model - The thermal conditioning requirements for the APU are concerned primarily with the hydraulic fluid temperature control. Thermal analysis has been performed for both the water and hydrogen cooling concepts discussed in Appendix B using a program which performs a transient thermal accounting of the hydraulic fluid energy balance.

The heat capacity of structure which can be associated with the fluid is included by using a bulk specific heat for fluid and structure.

$$C_p = 0.144 *(\text{Structural wt}) + 0.5 *(\text{Fluid wt}) \left[ \frac{\text{Btu}}{\text{°F}} \right]$$

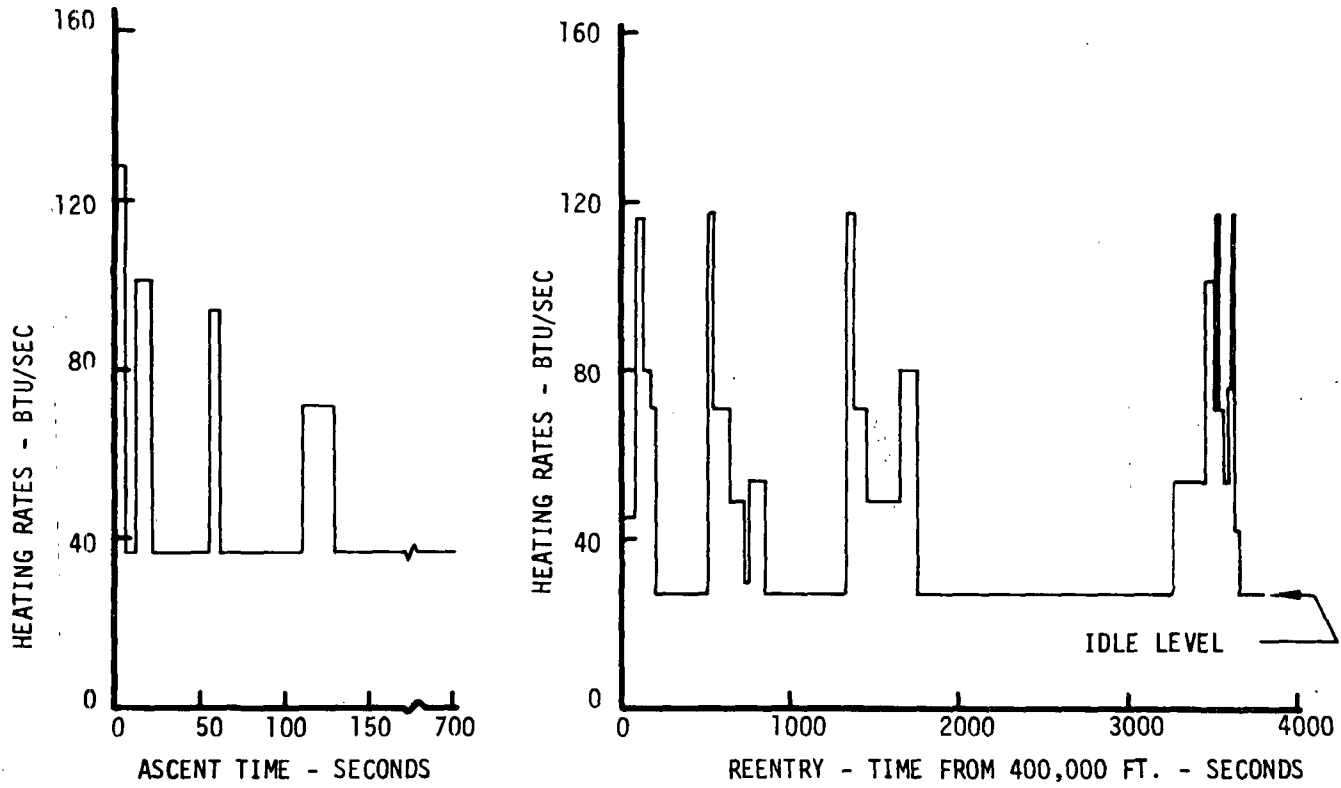
For the sizing calculation summarized in Figure B-41, structural and fluid weights of 818 and 155 lbm were used.

The total heat load is composed of an APU power term and a convective heating term

$$\dot{q}_{\text{tot}} = \dot{q}_{\text{power}} + h_c (T_{\text{ambient}} - T_{\text{hyd}}) A_{\text{eff}}$$

Where  $A_{\text{eff}}$  is the effective surface area. The convective coefficient,  $h_c$ , increases linearly with time from 0 at the start of reentry to 2.0 Btu/hr-ft<sup>2</sup>-°F at the end of entry.

# APU ASCENT AND REENTRY HEATING LOADS (EXCLUSIVE OF ENVIRONMENTAL HEATING)



F-42

MCDONNELL DOUGLAS AERONAUTICS COMPANY - EAST

Figure F-28

APS-774

Heat exchanger modeling has been performed around baseline heat exchanger performance parameters derived from References F-3, F-4, F-5, and MDAC Space Shuttle Phase B vehicle design efforts. The water flash evaporator heat exchanger model assumed a constant exit vapor temperature (250°F), a constant heat of vaporization (1092 Btu/lbm), and an evaporator efficiency of 93%. The baseline model of the cryogenic hydrogen-hydraulic fluid heat exchanger, shown previously in Figure B-37, was obtained from Reference F-5.

For the design conditions, the thermal conductances of hydrogen-wall, wall-thickness, and wall-hydraulic fluid were calculated to be nominally in the ratio of 200: 0.7: 2.0. An off design overall heat transfer coefficient was thus estimated:

$$h = h_{\text{design}} \frac{(200 + 0.7 + 2.0)}{\left[ 200 \cdot \left( \frac{\dot{w}_{\text{LH}_2\text{-DES}}}{\dot{w}_{\text{LH}_2}} \right)^{0.8} + 0.7 + 2.0 \left( \frac{\dot{w}_{\text{HYD-DES}}}{\dot{w}_{\text{HYD}}} \right)^{0.8} \right]}$$

Coolant mass flows were set arbitrarily according to the implementation option being examined. These included being on continuously after some preset temperature had been reached, ON-OFF operation at a constant flow rate with ON-OFF changes dictated by temperature variations, and a modulated option in which coolant flow rate was proportional to APU power. The hydraulic fluid transient temperature history for these options has been previously presented in Appendix B6.

REFERENCES

- F-1 Vickers and Garipay, "Thermal Design Evaluation and Performance of the Surveyor Spacecraft," AIAA Paper 68-1029.
- F-2 Fletcher, L. S. and D. A. Gyrog, "Prediction of Thermal Contact Conductance Between Similar Metal Surfaces," AIAA Paper 70-852. (Also Progress in Astronautics and Aeronautics, Vol. 24).
- F-3 Gaddis, J. L., "Development of a Laboratory Prototype Spraying Flash Evaporator," ASME Paper 72-ENAv-28, August 1972.
- F-4 Gaddis, J. L., "Feasibility Demonstration of a Spraying Flash Evaporator," NASA CR114913, Final Report, Contract NAS9-11254, May 7, 1971.
- F-5 Agustee, Ron, Hamilton Standard, Windsor Locks, Conn. Personal Communication.



APPENDIX G

PROPELLANT UTILIZATION

The preliminary system design points and system sizing data for the selected RCS/OMS/APU concepts were refined to include the necessary propellant margins. This appendix identifies the analyses performed to predict propellant utilization and unbalance uncertainties under both normal operating and failure mode conditions. Uncertainties in propellant flow rates and mixture ratios were evaluated using historical tolerance data for valve and regulator accuracies together with expected off-nominal mixture ratio characteristics for the thrusters. Additional factors affecting propellant margins include cg envelope and variations in pod thrust levels, inertial measuring unit (IMU) tolerance, engine or thruster specific impulse, and propellant loading accuracy. These factors are discussed herein and were used to define the required propellant loading margins for the selected concepts. A summary of the propellant loading margin criteria for the baseline and fuselage module concepts is presented in Figures G-1 and G-2. These charts delineate, for the various propellant, tankage, engine or thruster, and control options, the margins required to balance the tolerance effects of C.G., pod thrust, engine specific impulse, and mixture ratio.

G1 Vehicle Center of Gravity - The variation in the vehicle center of gravity (C.G.) was obtained from the orbiter mass properties for the easterly launch mission. These variations are primarily the result of uncertainties in the payload configuration and are applicable during the mission phases of injection, on-orbit, and pre-retro. The CG envelope is as follows:

x C.G.	+40 in.
y C.G.	+2.7 in.
z C.G.	+10 in.

For those configurations employing dedicated OMS engines, the C.G. and thrust malalignment tolerances have no effect on propellant loading since the OMS engines are gimballed and any disturbance torques can be nulled out. However, for the RCS(OMS), excess propellant is required to offset potential unbalances since the RCS thrusters are fixed. Also, in addition to the torque resulting from the thrust axis not passing through the C.G., the yaw torque that is produced by the RCS(OMS) thrust malalignment during -X axial translation must also be included with the C.G. offset when computing propellant

## SUMMARY OF PROPELLANT LOADING MARGIN CRITERIA BASELINE CONCEPTS

11-450

SYSTEM DESIGN CHARACTERISTICS			PROPELLANT MARGIN CRITERIA TO OFFSET TOLERANCES			
SYSTEM	VEHICLE CONTROL DURING OMS BURN	OMS FIRING LOGIC	CG TOLERANCE	POD THRUST TOLERANCE	ENGINE $I_{sp}$ TOLERANCE	MIXTURE RATIO TOLERANCE
MODULAR MONOPROPELLANT RCS	-	-	NO EFFECT	NO EFFECT	DESIGN $I_{sp}$ BASED ON STATISTICAL MINIMUM USING UNIT TO UNIT PERFORMANCE VARIATIONS	FUEL AND OXIDIZER MARGINS BASED ON STATISTICAL SUMMATION OF COMPONENT TOLERANCES AND ENVIRONMENTAL EFFECTS
MODULAR BIPROPELLANT RCS	-	-	NO EFFECT	NO EFFECT		
MODULAR BIPROPELLANT RCS (OMS)	OFF LOGIC	PARALLEL	EXCESS PROPELLANT IN EACH POD TO OFFSET UNBALANCE OF ONE ENGINE IN MAXIMUM OR MINIMUM YAW DUTY CYCLE	INU TOLERANCE EFFECT ONLY	DESIGN $I_{sp}$ BASED ON STATISTICAL MINIMUM ASSUMING BATCH SCREENING AND RUN-TO-RUN VARIATIONS	
	RCS	PARALLEL	EXCESS RCS NOSE POD IMPULSE EQUIVALENT TO OMS TORQUE IMPULSE AT MAXIMUM CG DISPLACEMENT	EXCESS PROPELLANT IN EACH POD EQUAL TO POSITIVE FLOW TOLERANCE OF COMPLETE OMS & INU		
INTEGRATED BIPROPELLANT RCS/OMS	GIMBAL	SERIES	NO EFFECT	INU TOLERANCE EFFECT ONLY	DESIGN $I_{sp}$ BASED ON STATISTICAL MINIMUM USING UNIT TO UNIT PERFORMANCE VARIATIONS	
		PARALLEL	NO EFFECT	INU TOLERANCE EFFECT ONLY		
INTEGRATED MONOPROPELLANT RCS/APU	-	-	NO EFFECT	NO EFFECT		
MODULAR MONOPROPELLANT APU	-	-	NO EFFECT	NO EFFECT	DESIGN $I_{sp}$ BASED ON STATISTICAL MINIMUM USING UNIT TO UNIT PERFORMANCE VARIATIONS	
BOGEY BIPROPELLANT OMS	GIMBAL	SERIES	NO EFFECT	NO EFFECT	DESIGN $I_{sp}$ BASED ON STATISTICAL MINIMUM USING UNIT TO UNIT PERFORMANCE VARIATIONS	
		PARALLEL	NO EFFECT	EXCESS PROPELLANT IN EACH POD EQUAL TO POSITIVE FLOW TOLERANCE OF COMPLETE OMS		

G-2

MCDONNELL DOUGLAS AERONAUTICS COMPANY - EAST

Figure G-1

# SUMMARY OF PROPELLANT LOADING MARGIN CRITERIA FOR RCS/OMS ALTERNATE CONCEPTS

POD DESIGN CHARACTERISTICS					PROPELLANT MARGIN CRITERIA TO OFFSET TOLERANCES					
RCS/OMS TANKAGE	PROPELLANTS		RCS/OMS ENGINES	VEHICLE CONTROL DURING OMS BURNS	OMS FIRING LOGIC	CG TOLERANCE	POD THRUST TOLERANCE	ENGINE I <sub>sp</sub> TOLERANCE	MIXTURE RATIO TOLERANCE	
	RCS	OMS								
COMMON	H <sub>2</sub> O <sub>4</sub>	H <sub>2</sub> O <sub>4</sub>	DEDICATED	GIMBAL	SERIES	NO EFFECT	MINU TOLERANCE EFFECT ONLY	DESIGN I <sub>sp</sub> BASED ON STATISTICAL MINIMUM USING UNIT TO UNIT PERFORMANCE VARIATION OF OME'S	FUEL AND OXIDIZER MARGINS BASED ON STATISTICAL SUMMATION OF COMPONENT TOLERANCES AND ENVIRONMENTAL EFFECTS	
COMMON	H <sub>2</sub> O <sub>4</sub>	H <sub>2</sub> O <sub>4</sub>	DEDICATED	GIMBAL	PARALLEL	NO EFFECT	EXCESS PROPELLANT IN EACH POD EQUAL TO POSITIVE FLOW TOLERANCE OF COMPLETE OMS # MINU	DESIGN I <sub>sp</sub> BASED ON STATISTICAL MINIMUM USING UNIT TO UNIT PERFORMANCE VARIATION OF OME'S		
COMMON	H <sub>2</sub> O <sub>4</sub>	H <sub>2</sub> O <sub>4</sub>	COMMON	OFF LOGIC	PARALLEL	EXCESS PROPELLANT IN EACH POD TO OFFSET UNBALANCE OF ONE ENGINE IN MAXIMUM OR MINIMUM YAW DUTY CYCLE	MINU TOLERANCE EFFECT ONLY	DESIGN I <sub>sp</sub> BASED ON STATISTICAL MINIMUM ASSUMING BATCH SCREENING AND RUN-TO-RUN VARIATIONS		
COMMON	H <sub>2</sub> O <sub>4</sub>	H <sub>2</sub> O <sub>4</sub>	COMMON	RCS	PARALLEL	EXCESS RCS NOSE POD IMPULSE EQUIVALENT TO OMS TORQUE IMPULSE AT MAXIMUM CG DISPLACEMENT	EXCESS PROPELLANT IN EACH POD EQUAL TO POSITIVE FLOW TOLERANCE OF COMPLETE OMS # MINU	DESIGN I <sub>sp</sub> BASED ON STATISTICAL MINIMUM ASSUMING BATCH SCREENING AND RUN-TO-RUN VARIATIONS		
DEDICATED	H <sub>2</sub> O <sub>4</sub>	H <sub>2</sub> O <sub>4</sub>	DEDICATED	GIMBAL	SERIES	NO EFFECT	NO EFFECT	DESIGN I <sub>sp</sub> BASED ON STATISTICAL MINIMUM USING UNIT TO UNIT PERFORMANCE VARIATION OF OME'S		
DEDICATED	H <sub>2</sub> O <sub>4</sub>	H <sub>2</sub> O <sub>4</sub>	DEDICATED	GIMBAL	PARALLEL	NO EFFECT	EXCESS PROPELLANT IN EACH POD EQUAL TO POSITIVE FLOW TOLERANCE OF COMPLETE OMS	DESIGN I <sub>sp</sub> BASED ON STATISTICAL MINIMUM USING UNIT TO UNIT PERFORMANCE VARIATION OF OME'S		
DEDICATED	H <sub>2</sub> O <sub>4</sub>	H <sub>2</sub> O <sub>4</sub>	COMMON	OFF LOGIC	PARALLEL	EXCESS PROPELLANT IN EACH POD TO OFFSET UNBALANCE OF ONE ENGINE IN MAXIMUM OR MINIMUM YAW DUTY CYCLE	NO EFFECT	DESIGN I <sub>sp</sub> BASED ON STATISTICAL MINIMUM ASSUMING BATCH SCREENING AND RUN-TO-RUN VARIATIONS		
DEDICATED	H <sub>2</sub> O <sub>4</sub>	H <sub>2</sub> O <sub>4</sub>	COMMON	RCS	PARALLEL	EXCESS RCS NOSE POD IMPULSE EQUIVALENT TO OMS TORQUE IMPULSE AT MAXIMUM CG DISPLACEMENT	EXCESS PROPELLANT IN EACH POD EQUAL TO POSITIVE FLOW TOLERANCE OF COMPLETE OMS	DESIGN I <sub>sp</sub> BASED ON STATISTICAL MINIMUM ASSUMING BATCH SCREENING AND RUN-TO-RUN VARIATIONS		
DEDICATED	H <sub>2</sub> N <sub>4</sub>	H <sub>2</sub> O <sub>4</sub>	DEDICATED	GIMBAL	SERIES	NO EFFECT	NO EFFECT	DESIGN I <sub>sp</sub> BASED ON STATISTICAL MINIMUM USING UNIT TO UNIT PERFORMANCE VARIATION OF OME'S		
DEDICATED	H <sub>2</sub> N <sub>4</sub>	H <sub>2</sub> O <sub>4</sub>	DEDICATED	GIMBAL	PARALLEL	NO EFFECT	EXCESS PROPELLANT IN EACH POD EQUAL TO POSITIVE FLOW TOLERANCE OF COMPLETE OMS	DESIGN I <sub>sp</sub> BASED ON STATISTICAL MINIMUM USING UNIT TO UNIT PERFORMANCE VARIATION OF OME'S		

MCDONNELL DOUGLAS AERONAUTICS COMPANY - EAST

G-3

Figure G-2

11-338 A

requirements. Factors contributing to malalignment include mechanical and operational thrust vector variations, thruster/pod and pod/vehicle alignment errors, and structural deflection. The individual values of these errors are tabulated in Figure G-3 as well as the total yaw disturbance torque.

Two methods of compensating for these disturbances in the RCS(OMS) were evaluated: Control with the RCS, and off-logic with the -X translational thrusters. Control with the RCS is accomplished by the application of pure pitch and yaw couples as required to null the disturbance torques, and therefore additional propellant must be included in each module. Control by off-logic consists of intermittently shutting down -X translational thrusters as required to null the disturbance torques. Since the -X translational thrusters are canted such that the upper and lower thrusters produce  $\pm$  pitch torques when fired separately, pitch disturbances are readily compensated for by simultaneously pulsing "mirror-image" thrusters from both pods. This method maintains equal thrust and propellant expenditure between pods, and therefore no propellant penalty for pitch disturbance control is incurred. No analogy exists for yaw disturbance control; thrusters from either the left or right pod must be shut down to achieve the required control. This results in a propellant unbalance since the pods no longer share equally in the  $\Delta V$  allotment, and therefore propellant margins for yaw disturbance control must be added to both fuselage pods. This weight penalty can be minimized by canting the outboard X translational thrusters, as shown in Figure G-4. As the angle  $\alpha$  is increased, the effectiveness of the off-logic control improves. The optimum occurs when the resulting -X cosine losses balance the off-logic gains.

The effect of C.G. offset, including thrust malalignment on propellant requirements, is illustrated in Figure G-5 for the RCS and off-logic control concepts. At the C.G. envelope limits, the RCS control requires about 200 lbm propellant for yaw and about 1100 lbm for pitch control, while the off-logic control requires approximately 600 lbm propellant for yaw and has no pitch penalty. Analysis of these results suggests that a hybrid system, consisting of off-logic for pitch control and RCS yaw control is the most attractive approach. The resulting hybrid control logic propellant requirements are only 200 lbm (total vehicle) compared to total requirements of 1300 and 600 lbm respectively for pure RCS and off-logic control.

RCS(OMS) THRUST MALALIGNMENT - AXIAL TRANSLATION  
· ECCENTRICITY MEASURED ABOUT YAW AXIS

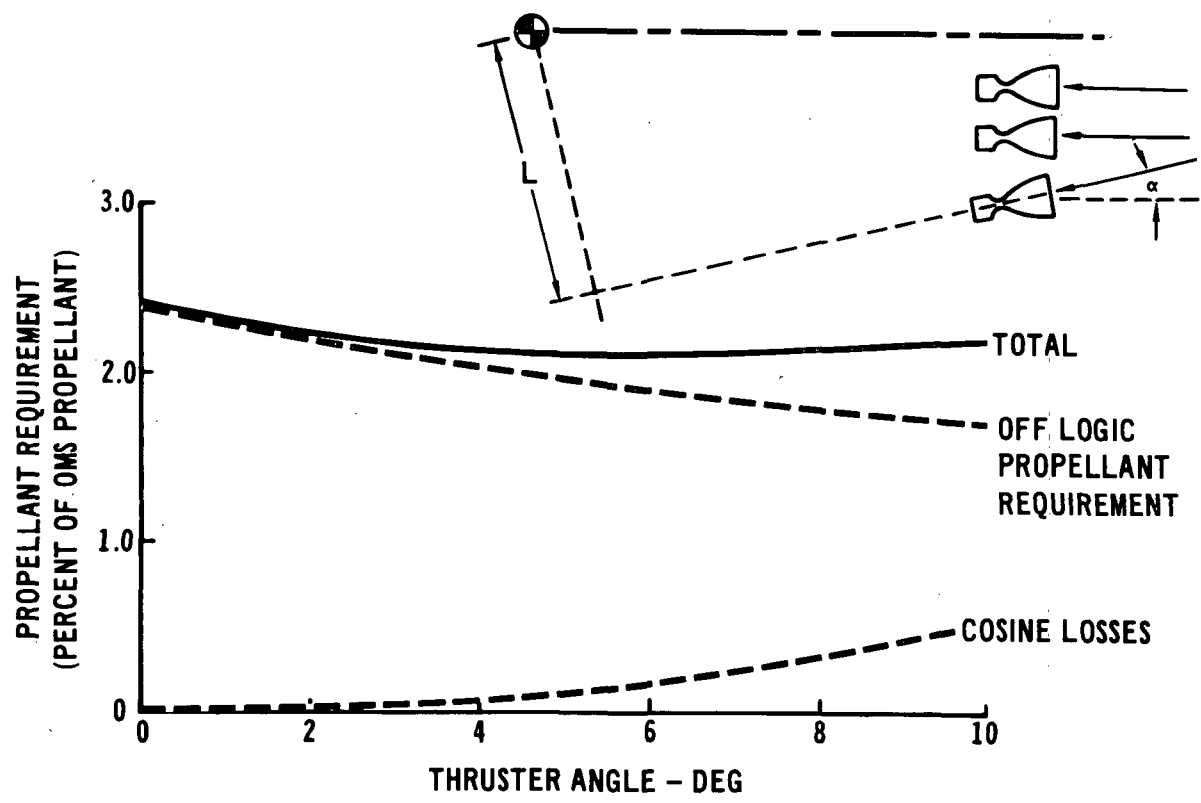
<u>ALIGNMENT ERROR</u>	<u>+ VALUE, in.</u>	<u>(+ VALUE)<sup>2</sup></u>
1. LATERAL C.G. UNCERTAINTY	2.70	7.29
2. THRUST VECTOR*		
- between mechanical and 'true' - 0°6'	0.27	0.07
- variation during burn - 0°10'	0.45	0.20
3. ALIGNMENT*		
- thruster/pod - 0°15'	0.68	0.46
- pod/vehicle - 0°20'	0.90	0.81
4. STRUCTURAL DEFLECTION	<u>0.51</u>	<u>0.26</u>
		$\Sigma(+ \text{VALUE})^2 = 9.09$
		TOTAL ROOT SUM
		SQUARE $\sqrt{\Sigma(\text{VALUE})^2} = 3.02 \text{ in.}$

YAW DISTURBANCE TORQUE (n·F·e) = 18,000 in-lb

\* THRUST ECCENTRICITIES ARE AVERAGE FOR EIGHT THRUSTERS.

APS-345

# DETERMINATION OF OPTIMUM THRUSTER ANGLE FOR OFF LOGIC CONTROL IN YAW

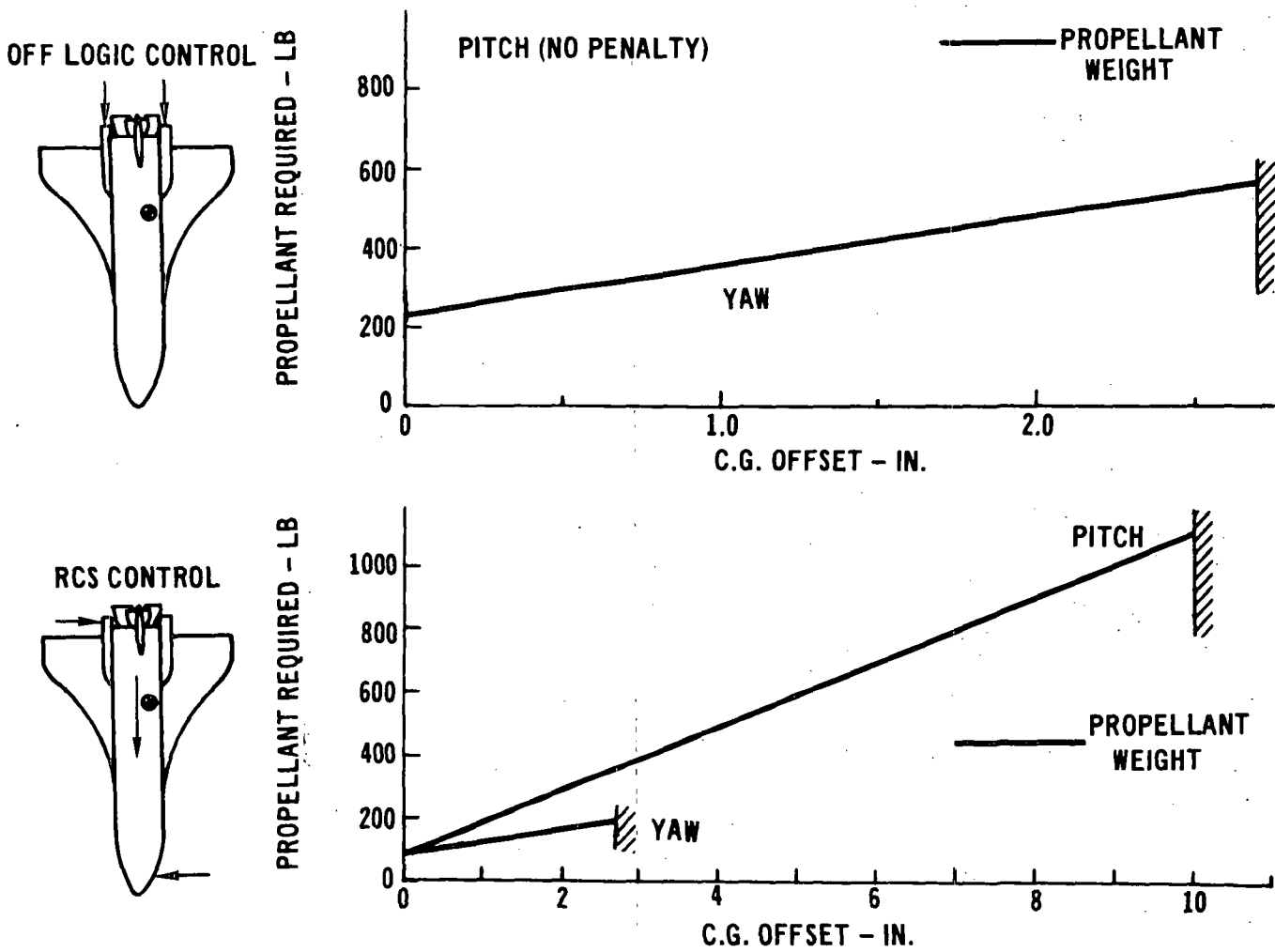


G-6

Figure G-4

11-328

# EFFECT OF C.G. OFFSET ON PROPELLANT REQUIREMENTS



G-7

Figure G-5

11-326

G2 Pod Thrust Tolerance and IMU - Pod thrust tolerance is a function of the system flow characteristics, which vary as the result of component tolerances and propellant temperature differentials. The ramifications of these deviations are unequal propellant expenditure rates between pods, due to flow-rate tolerances, and control disturbances resulting from unequal thrust between pods. Depending on the system configuration, propellant margins are required to compensate for either one or both of these effects.

The component tolerances, and propellant temperature ranges, and differentials pertinent to this study are summarized in Figure G-6. The effects of these tolerances were assessed by root-sum-squaring (RSS) their resulting flowrate variances. Variations in OMS engine and RCS thruster flowrates are functions of the valve and injector mechanical tolerances. The thruster and engine flow tolerances were based on the Marquardt R4D bipropellant thruster used on the Apollo LM and Service Module, and the Aerojet SPS engine, also used on the Apollo Service Module. The remaining component tolerances were compiled from existing component operating data obtained during the Phase B oxygen-hydrogen study, and are discussed in Reference H.

For those systems employing dedicated OMS engines, flowrate unbalance is of concern only in the case of parallel OMS firing since simultaneous burnout is required; if the OMS engines burn in series, no margins are required for flowrate unbalance. The effect of flowrate unbalance for the parallel burn case is depicted graphically in Figure G-7. In this figure, a comparison is made between both pods operating at nominal thrust and flow versus one pod at nominal and one pod at low thrust and flow conditions. The result of low flow in one pod is that burn time must be increased in both pods, and therefore excess propellant must be added to each pod, equal to 50 percent of the positive flow tolerance of the OMS. No margins result from thrust unbalance, since disturbance torques can be nulled out by engine gimbaling.

For systems utilizing an RCS(OMS), the pod thrust margins requirements vary, depending on the method used to compensate for disturbance torques. If pure RCS control is employed, additional propellant is required in the fuselage pods to account for the flow tolerances, and also, propellant must be added to the nose and fuselage pods to compensate for the disturbance torques. If pure off-logic is utilized, no margins are required for either thrust tolerances or flow tolerances, since the same off-logic control used to null the disturbance torques tends to equalize the pod flow rates. When hybrid control is



## COMPONENT TOLERANCES FOR MR EXCURSIONS

RCS/OMS TANKAGE	PROPELLANT		RCS/OMS ENGINES	PRESSURE EQUALIZER	PROPELLANT TEMPERATURE ( $T_F - T_0$ ) DEG	SHUTOFF VALVES ( $\Delta A$ ) (PERCENT)	TRIM ORIFICE ( $\Delta A$ ) (PERCENT)	ENGINE TO ENGINE MR (PERCENT)
	RCS	OMS						
COMMON	$N_2O_4/MMH$	$N_2O_4/MMH$	DEDICATED	$\pm 0.6$	20	$\pm 1$	$\pm 1$	$\pm 2.64/1.25^{(1)}$
↓	↓	↓	COMMON	$\pm 0.6$	↓	↓	↓	$\pm 2.64$
DEDICATED	↓	↓	DEDICATED	$\pm 0.6/0^{(1)}$	↓	↓	↓	$\pm 2.64/1.25^{(1)}$
↓	↓	↓	COMMON	$\pm 0.6/0^{(1)}$	↓	↓	↓	$\pm 2.64$
↓	$N_2H_4$	$N_2O_4/MMH$	DEDICATED	$0/0^{(1)}$	0	↓	↓	$0/1.25^{(1)}$

(1) RCS/OMS

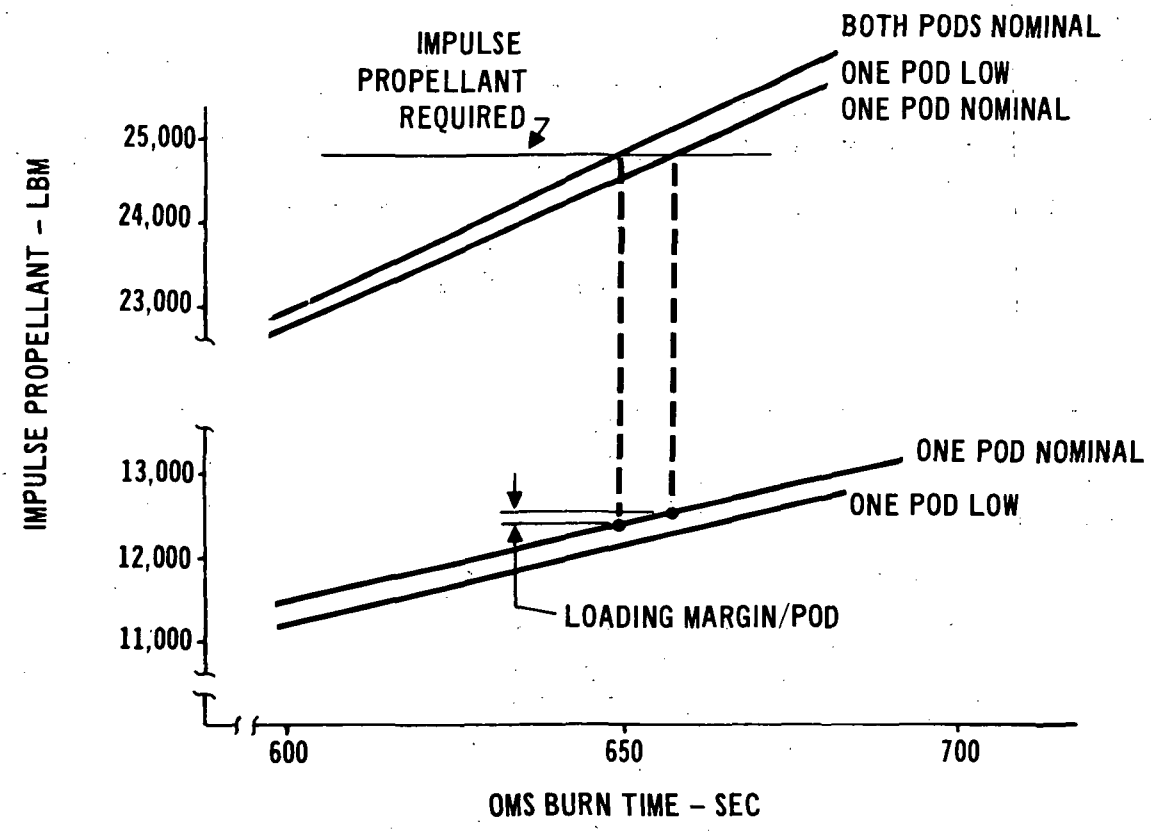
## FOR FLOW EXCURSIONS

RCS/OMS TANKAGE	PROPELLANT		RCS/OMS ENGINES	TRIM ORIFICE ( $\Delta A$ ) (PERCENT)	REGULATOR (PERCENT)	PROPELLANT TEMPERATURE ( $T_{MAX} - T_{MIN}$ )	SHUTOFF VALVES (PERCENT)	THRUSTER FLOW (PERCENT)
	RCS	OMS						
COMMON	$N_2O_4/MMH$	$N_2O_4/MMH$	DEDICATED	$\pm 1$	$\pm 2.45$	50	$\pm 1$	$\pm 1.86/1.0^{(1)}$
↓	↓	↓	COMMON	↓	↓	↓	↓	$\pm 1.86$
DEDICATED	↓	↓	DEDICATED	↓	↓	↓	↓	$\pm 1.86/1.0$
↓	↓	↓	COMMON	↓	↓	↓	↓	$\pm 1.86$
↓	$N_2H_4$	$N_2O_4/MMH$	DEDICATED	↓	↓	↓	↓	$\pm 1.86/1.0$

(1) RCS/OMS

# EFFECT OF POD FLOW TOLERANCE

COMMON TANKAGE  
DEDICATED ENGINES - PARALLEL BURN



G-10

Figure G-7

11-327 A

employed (off-logic for pitch, RCS control for yaw), the margin requirements are equivalent to the pure RCS control margins, since the off-logic pitch control pulses equivalent thrusters from both pods, and therefore pod flow unbalance continues.

One additional margin has been included under pod thrust tolerance. Errors of the Inertia Measuring Unit (IMU) in measuring velocity increments ( $\Delta V$ ) can result in the expenditure of excessive propellant during the high impulse translations. In those systems utilizing common RCS and OMS tankage this expenditure of excessive propellant could result in a shortage of propellant during RCS entry maneuvers. The IMU tolerance was set at  $\pm 0.25$  percent, based on previous space program experience.

G3 Specific Impulse Tolerance - Specific impulse is dependent on vaporization and mixing efficiencies which are a function of injector tolerances. Specific impulse tolerance values of  $\pm 2.145$  percent ( $3\sigma$ ) about the nominal were used for both monopropellant and bipropellant RCS thrusters. This data was based on the Marquardt R4D bipropellant Apollo thruster data. For all maneuver RCS systems, the variation in -X translational thruster performance has been minimized through the selective screening procedures discussed in Section 4.5. The  $3\sigma$  tolerance on these thrusters was computed to be less than the run to run tolerance, and therefore, the run to run tolerance of  $\pm 1.1$  percent was used.

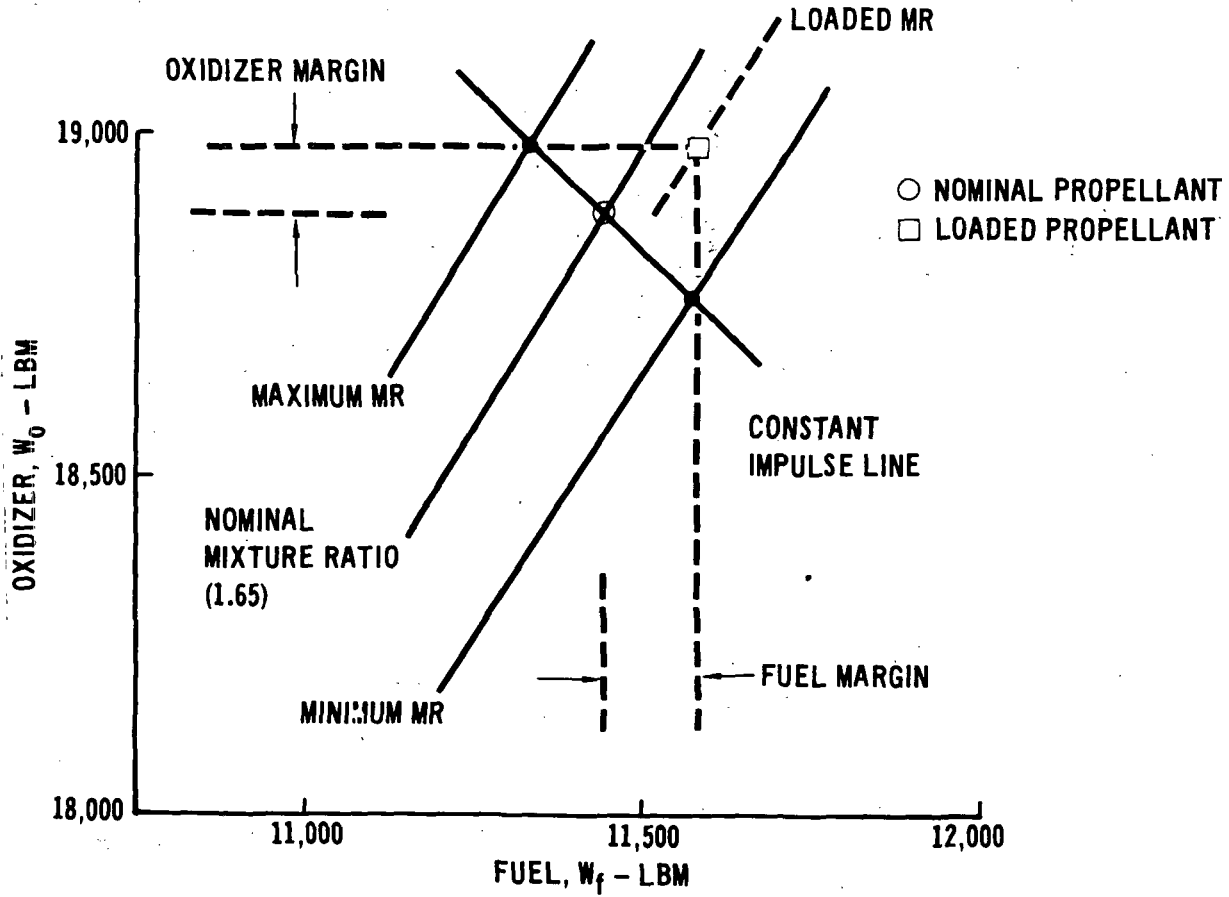
The OMS engine  $3\sigma$  unit to unit specific impulse tolerance was assumed to be  $\pm 1.0$  percent based on Aerojet SPS engine firing data. Run to run firing data obtained on one sample at AEDC-Tullahoma indicated a  $\pm 1.59$  sec variation about the nominal value of 313 sec or about a  $\pm 0.506$  percent  $3\sigma$  variation. This value was increased due to the limited firing data available.

G4 Mixture Ratio Tolerance - Variations in mixture ratio result in unequal expenditure of fuel and oxidizer from the same pod, and all bipropellant systems require margins to compensate for the discrepancy. The effect of propellant mixture ratio tolerances on loaded mixture ratio is depicted graphically in Figure G-8. The nominal mixture ratio of 1.65 is based on equal volume tanks, and is shown along with the calculated minimum and maximum operating mixture ratios. The required total impulse line dictates the fuel and oxidizer margins, and permits calculation of the loaded mixture ratio.

The tolerances which contribute to mixture ratio variations are summarized in Figure G-6. Fuel and oxidizer margins were based on the statistical summa-

# EFFECT OF PROPELLANT MARGINS ON LOADED MIXTURE RATIO

## RCS & OMS



G-12

Figure G-8

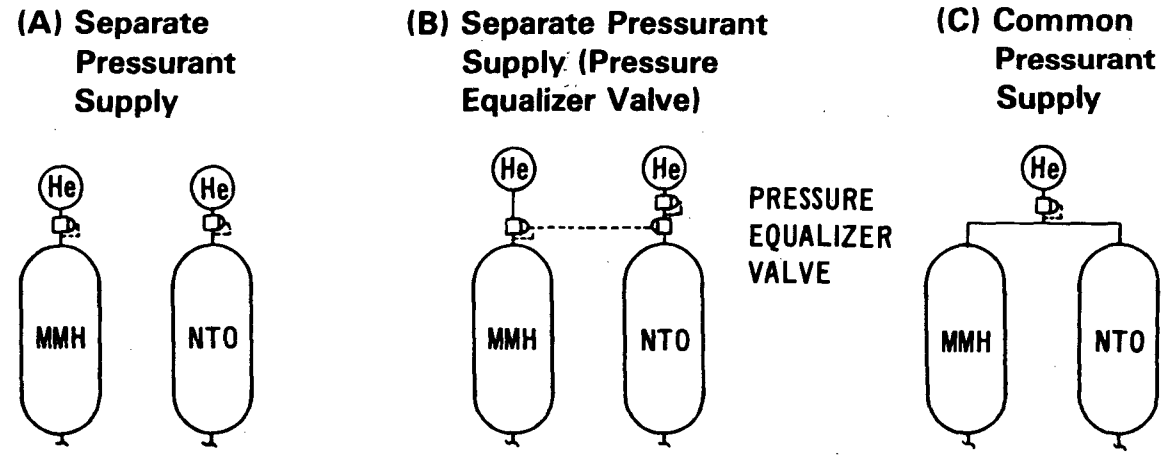
11-329 A

tion of the component tolerances and environmental effects. Various approaches to bipropellant pressurization subsystem implementation were evaluated and a preferred approach selected based on propellant utilization considerations. The candidate concepts included a common pressurant supply, separate supplies for the fuel and oxidizer tanks, and separate supplies with a pressure equalizing valve. These schematics are presented in Figure G-9. The separate helium supply, approach A, removes the potential for propellant vapor mixing and reaction within the pressurization subsystem. Conversely, the common pressurant supply, approach C, is undesirable for the above reason. In approach B, a pressure equalizing valve is installed downstream of the oxidizer helium regulator. The valve basically functions as a dome-loaded regulator with regulator dome pressure being provided by the fuel tank pressurizing gas. Oxidizer tank pressure is adjusted accordingly and a valve diaphragm precludes vapor mixing between the fuel and oxidizer. The propellant utilization losses are tabulated in Figure G-9 for each pressurization approach for an RCS(OMS) system. The propellant losses associated with separate pressurant supplies are excessive, while the concept employing the pressure equalizing valve is competitive with a common pressurant supply. The pressure equalizing valve concept was therefore adopted as baseline since the common pressurant supply is unacceptable for an RCS based on potential propellant mixing and reaction within the pressurization subsystem.

G5 Loading Accuracy - A tankage loading tolerance or measuring accuracy of 0.5% of usable propellant weight was used based on previous space program experience including Gemini and is an attainable value for current Ground Support Equipment (GSE).

G6 Failure Mode Conditions - The propellant unbalances produced by a failed thruster or a partially clogged filter were evaluated for both a monopropellant and bipropellant RCS and a bipropellant RCS(OMS). The failure mode results are shown in Figure G-10 and are compared to normal operation unbalances. The failed-thruster unbalance contribution is based only on the entry mission phase since it is assumed that an on-orbit thruster failure could be detected and corrective action taken to reestablish balanced thruster operation. These results indicate that propellant interconnects between RCS pods and RCS(OMS) pods are unnecessary.

## INFLUENCE OF PRESSURIZATION CONCEPT ON RCS (OMS) PROPELLANT UTILIZATION



	(A) Separate Pressurant Supply	(B) Separate Pressurant Supply (Pressure Equalizer Valve)	(C) Common Pressurant Supply
REQUIRED FUEL MARGINS (-MR TOLERANCE)	226	149	139
REQUIRED OXIDIZER MARGINS (+ MR TOLERANCE)	202	106	93
TOTAL REQUIRED MARGINS	428	255	232

G-14

Figure G-9

PROPELLANT UNBALANCE BETWEEN MODULES

CONDITION	+ 3σ PROPELLANT UNBALANCE (LBM)		
	N <sub>2</sub> H <sub>4</sub> RCS	N <sub>2</sub> O <sub>4</sub> /MMH RCS	N <sub>2</sub> O <sub>4</sub> /MMH RCS (OMS)
NORMAL OPERATION			
- COMPONENT TOLERANCES	82	80	372
- BIASED DISTURBANCE TORQUE	-	-	206
TOTAL (RSS)/POD	82	80	425
FAILURE MODES			
- THRUSTER FAILURE (PITCH)	9	7	6
- FILTER BLOCKAGE (20%)	5	2	18

APS-346

G-15

Figure G-10

G7 Propellant Loading Margins - Propellant loading margins were determined for the baseline concepts of Section 4.4 and the fuselage module concepts of Section 4.5 using the component tolerance effects discussed in the previous sections. The combined RCS and OMS propellant margins during normal operation are tabulated in Figures G-11 and G-12 respectively for the baseline and alternate systems. Margins are listed for each effect as well as the combined RSS value. Two conclusions based on these results are:

1. For an RCS(OMS), hybrid control (off-logic pitch control, RCS yaw control) is the preferred approach since it minimizes overall margins.
2. For systems employing dedicated OMS, series firing logic minimize propellant margins, and was therefore used in subsequent studies. However, the  $\Delta V$  losses associated with only one 6000 lbf engine operating essentially negate the advantage, and guidance and control considerations will likely decide this issue.



## SUMMARY OF PROPELLANT LOADING MARGINS BASELINE CONCEPTS

SYSTEM DESIGN CHARACTERISTICS			COMBINED RCS AND OMS MARGINS - LB PER NOSE POD/LB PER AFT POD					
SYSTEM	VEHICLE CONTROL DURING OMS BURNS	OMS FIRING LOGIC	CG MARGIN	POD THRUST AND IMU MARGIN	ENGINE I <sub>SP</sub> MARGIN	MIXTURE RATIO MARGIN	PROPELLANT LOADING MARGIN	RSS OF MARGINS
MODULAR MONOPROPELLANT RCS	-	-	0	0	15/27	0	11/15	81
MODULAR BIPROPELLANT RCS	-	-	0	0	12/21	15/21	9/12	85
MODULAR BIPROPELLANT RCS (OMS)	OFF LOGIC	PARALLEL	0/281	0/33 (IMU)	6/63	15/118	8/77	660
	HYBRID OFF LOGIC - PITCH RCS CONTROL - YAW	PARALLEL	66/66	0/33 (IMU) 44/185	6/63	15/118	8/77	587
	RCS	PARALLEL	433/433	0/33 (IMU) 44/185	6/63	15/118	8/77	1426
INTEGRATED BIPROPELLANT RCS/OMS	GIMBAL	SERIES	0	33 (IMU)	121	156	157	320
		PARALLEL	0	33 (IMU)	121	156	157	320
INTEGRATED MONOPROPELLANT RCS/APU	-	-	0	0	92	0	48	114
MODULAR MONOPROPELLANT APU	-	-	0	0	49	0	6	49
BOGEY BIPROPELLANT OMS	GIMBAL	SERIES	0	0	0/86	0/99	0/63	292
		PARALLEL	0	0/136	0/86	0/99	0/63	396

MCDONNELL DOUGLAS ASTRONAUTICS COMPANY - EAST

G-17

Figure G-11

## SUMMARY OF PROPELLANT LOADING MARGINS ALTERNATE CONCEPTS

RMS OMS TANKAGE	POD DESIGN CHARACTERISTICS					COMBINED RCS & OMS MARGINS - LB PER NOSE POD 'LB PER AFT POD						
	PROPEL- LANTS		RCS OMS ENGINES	VEHICLE CONTROL DURING OMS BURNS	OMS FIRING LOGIC	CG MARGIN	POD THRUST & IMU MARGIN	ENGINE ISP MARGIN	MIXTURE RATIO MARGIN	PROPELLANT LOADING MARGIN	RSS OF MARGINS	
	RCS	OMS									RCS	OMS
COMMON ↓ ↓ ↓ ↓ ↓ ↓ ↓ ↓ ↓ ↓	N <sub>2</sub> O <sub>4</sub> MMH	N <sub>2</sub> O <sub>4</sub> MMH	DEDICATED	GIMBAL	SERIES	0	0.31 (IMU)	6.99	15.108	8.75	365	
			↓	↓	PARALLEL	0	0.31 (IMU) 0.136	6.99	15.108	8.75	451	
	↓	↓	COMMON	OFF LOGIC	↓	0.281	0.33 (IMU)	6.63	15.118	8.77	660	
	↓	↓	↓	HYBRID OFF LOGIC-PITCH RCS CONTROL-YAW	↓	66.66	0.33 44.185	6.63	15.118	8.77	587	
	↓	↓	↓	RCS	↓	433/433	0.33 (IMU) 44.185	6.63	15.118	8.77	1426	
	↓	↓	DEDICATED	GIMBAL	SERIES	0	0	6.99	15.123	8.77	78   292 (370)	
	↓	↓	↓	↓	PARALLEL	0	0.136	6.99	15.123	8.77	78   396 (474)	
	↓	↓	COMMON	OFF LOGIC	↓	0.281	0	6.63	15.110	8.73	66   612 (678)	
	↓	↓	↓	HYBRID OFF LOGIC-PITCH RCS CONTROL-YAW	↓	66.66	0.33 44.185	6.63	15.110	8.73	247   380 (627)	
	↓	↓	↓	RCS	↓	433/433	44.185	6.63	15.110	8.73	1305   376 (1681)	
↓	N <sub>2</sub> H <sub>4</sub>	↓	DEDICATED	GIMBAL	SERIES	0	0	6.99	0.99	10.80	53   292 (345)	
↓	↓	↓	↓	↓	PARALLEL	0	0.136	6.99	0.99	10.30	53   396 (449)	

MCDONNELL DOUGLAS AERONAUTICS COMPANY - EAST

G-18

Figure G-12

11-331 A

## APPENDIX H

### REUSE

A vehicle designed for multiple and extended usage such as the Space Shuttle requires emphasis on reusable systems. For this type of application, the cost of repair and replacement of components which fail during the flight program becomes an important factor in overall cost. System designs which minimize maintenance by ensuring adequate component and subsystem life, coupled with ease of replacement, provide the most cost effective vehicle.

Data from prior related propulsion systems has been analyzed for the purpose of identifying those components which adversely affect reusability. Additionally, the status of rheopexy has been reviewed to evaluate its potential impact on propulsion system operation and maintenance.

H.1 Related Systems Experience - A great quantity of data has been accumulated during the development and operation of propulsion systems on related programs which can be useful in directing the design of a reusable propulsion system toward the use of those components and subsystems which are low maintenance items, and away from those which frequently malfunction. Also, these data show the types of failure which are most prevalent and thus permit the designer to avoid designs which are susceptible to such failures.

To take advantage of the experience gained on existing and prior related programs, failure data from the X-15, Gemini, and several Apollo propulsion systems have been tabulated, reviewed, and analyzed in various ways to provide information which will help the designer in achieving a low maintenance system. The data used, the methods of utilization, the results obtained, and the conclusions generated are discussed below.

Data from seven propulsion systems were analyzed. These are the X-15 main engine, the Gemini orbital attitude maneuvering system, the Gemini reaction control system, the Apollo lunar module descent and ascent engines (combined), the Apollo lunar module reaction control system, the Apollo service module propulsion engine, and the Apollo command and service module reaction control system.

In each program investigated, the data available were recorded differently. The X-15 data consisted of a tabulation of flight and aborted flight failures by mode of failure and the subsystem which failed. This data included only 29 failures, and, since no causes were given, were of little use. The Gemini data, listed by

component or subsystem with a paragraph describing each failure, failure analysis, and corrective action, were more useful. Apollo data was even more valuable. Here, data were presented in three ways: a single line summary of each failure by component, including mode and cause of failure; a single page report which described each failure, failure analysis, and corrective action (similar to the Gemini data); and a closeout package which consisted of all the records pertinent to that failure. There were about 900 Gemini and 7200 Apollo failures, providing a comprehensive picture of the most prevalent failure types and modes, and of the most failure susceptible components.

The failure modes and causes are tabulated in Figures H-1 to H-7, and are consolidated by percentages in Figures H-8 and H-9. The primary failure modes were as follows:

1. Leakage
2. Out-of-specification operation
3. Improper operation
4. Contaminated

Of these, the largest was leakage which accounted for 35 percent of all Apollo and Gemini failures. The major causes of failure were the following:

1. Contamination
2. Manufacturing
3. Design
4. Written procedure
5. Not determined

Contamination was the most prevalent cause of failure accounting for more than 21 percent.

Since this analysis is directed toward vehicle reusability, the failures due to manufacturing, design, and written procedure errors were not considered further because they would normally be detected, isolated, and corrected prior to any vehicle flight and, therefore, would not affect vehicle reuse. Those listed as "not determined" were discarded because they defy analysis as far as the scope of this effort is concerned. However, the contamination failures can be a continuing source of problems throughout the life of a program. For this reason, and because it was responsible for more failures than any other cause, contamination failures were selected for a more detailed analysis.

## APOLLO LM DESCENT AND ASCENT ENGINE SYSTEM FAILURES

MODE CAUSE	MODE																				TOTAL			
	CRACKED OR DEFECTIVE	DAMAGED	LEAKING	LEAK-LOSS OF PRESSURE	CONTAMINATED	OPERATION IMPROPER	OUT OF SPEC	PART OR MATERIAL DAMAGED	SEAL DAMAGED/ DEFECTIVE	STUCK/SEIZED/ BINDING/FROZEN	NO FAILURE*	PART OR MATERIAL FAULTY	BROKEN	ASSEMBLY IMPROPER	FAILED TO OPERATE	WELDING	OSCILLATIONS	EXCESSIVE PRESSURE	TORQUE INCORRECT	GOUGED		SHORTED	MISCELLANEOUS	
1. PART			43		2	9	7		8	8		12			2		1						14	106
2. TEST EQUIPMENT	1	4	17		1	9	21			2	7		2		2		7	2	1				17	93
3. ASSEMBLY IMPROPER	5	6	18		1	2	10	2	4	1		1		6		2	1		2		1	12	74	
*4. NO FAILURE			56			10	31	1		2	15		1		2		2					12	132	
5. WRITTEN PROCEDURE	3	5	45			3	31		1		2			1	1			1	2				8	103
6. CONTAMINATION			288	5	84	15	32	7	19	3	1				1				1	6		23	485	
7. MANUFACTURING	13	7	85	2	1	13	45	5	5			2	4	5	6	24			4	4	9	58	292	
8. MISHANDLING	5	11	12		2	2	3	4		2		1		1	4						5	9	61	
9. TESTING ERROR	2	7	12		4	12	19	2	2	1	4	1			1			3			1	39	111	
10. WORKMANSHIP	2	8	21		5	1			1	4		1	2	6	1	3			1			11	67	
11. DESIGN INADEQUACY	13	5	39	3	5	17	14	7	3	2		5	8	3	3		2	2	1	4	6	72	214	
12. NOT DETERMINED	1		21	1		6	33								1			1				9	73	
13. DEFECTIVE MATERIAL	2		2	2		1	2					2						2	2			7	22	
14. TESTED BEYOND LIMITS	5		13			2	4			1			5		2		1			2	1	13	49	
15. ENGINEERING	4		16		1		5	3				2					8					3	42	
16. ENVIRONMENTAL PROBLEM	1	1	6				6	1					1		2			1			1	5	25	
17. WEAROUT	1		17	1	1	1			2	2					1							7	33	
18. OPERATOR ERROR			6		2	1	10	3		1	1	1						6				13	44	
19. ADJUSTMENT IMPROPER			5		1	4	4								2				2			8	26	
20. MISCELLANEOUS	2	2	20	1	5	4	10	2	3	-	1	1	1	-	5	-	2	-	-	1	1	102	163	
TOTAL	60	56	742	15	115	112	287	37	48	29	31	29	24	22	36	29	24	18	16	17	25	442	2214	

\*INVALID REPORTS

APS-750

MCDONNELL DOUGLAS ASTRONAUTICS COMPANY - EAST

H-3

Figure H-1

## APOLLO SERVICE MODULE PROPULSION SYSTEM ENGINE FAILURES

MODE CAUSE	CRACKED OR	DAMAGED	LEANING	LEAN-LOSS	CONTAMINATED	OPERATION	OUT OF	PART OR MATERIAL	SEAL DAMAGED/	STUCK/SEIZED/	NO FAILURE*	PART OR MATERIAL	BROKEN	ASSEMBLY IMPROPER	FAILED TO	WELDING	OSCILLATIONS	EXCESSIVE	TORQUE	COUGED	SHORTED	MISCELLANEOUS	TOTAL	
	DEFECTIVE			OF PRESSURE		IMPROPER	SPEC	DAMAGED	DEFECTIVE	BINDING/FROZEN		FAULTY			OPERATE			PRESSURE	INCORRECT					
1. PART																								
2. TEST EQUIPMENT																								
3. ASSEMBLY IMPROPER	1	1		22	1	1	3							5								4	38	
*4. NO FAILURE						3	2															5	10	
5. WRITTEN PROCEDURE	8	1		56	6	109	9						3		6							7	205	
6. CONTAMINATION	5	3		135	28	24	2								1							6	204	
7. MANUFACTURING	7	1		13	2	6	1							1	1								32	
8. MISHANDLING	6	6		15	1	11				2					2							1	44	
9. TESTING ERROR	3	3		22	3	82	3						3		1							10	130	
10. WORKMANSHIP	8	6		63	2	44	8						5	2	7	5						14	164	
11. DESIGN INADEQUACY	66	18		85	18	145	11			1					12	15						19	390	
12. NOT DETERMINED	26	11		139	14	181	11			1			6		24							17	430	
13. DEFECTIVE MATERIAL	2	3		12		1																2	20	
14. TESTED BEYOND LIMITS	12	5		9	2	7							3									5	41	
15. ENGINEERING																								
16. ENVIRONMENTAL PROBLEM				6	2	11	1								2								22	
17. WEAROUT	1	3		5									1										10	
18. OPERATOR ERROR		6		13		14	1															1	35	
19. ADJUSTMENT IMPROPER				3	4	27								12	1							1	40	
20. MISCELLANEOUS	5	3		30	4	21	9						2		1	2						2	79	
TOTAL	150	68	-	628	87	687	61	-	-	4	-	-	23	20	58	22	-	-	-	-	-	94	1902	

\*INVALID REPORTS

APS-751

H-4

Figure H-2

LUNAR MODULE REACTION CONTROL SYSTEM FAILURE

MODE CAUSE																		TOTAL					
	CRACKED OR DEFECTIVE DAMAGED	LEAKING	LEAK-LOSS OF PRESSURE	CONTAMINATED	OPERATION IMPROPER	OUT OF SPEC	PART OR MATERIAL DAMAGED	SEAL DAMAGED/DEFECTIVE	STUCK/SEIZED/BINDING/FROZEN	NO FAILURE*	PART OR MATERIAL FAULTY	BROKEN	ASSEMBLY IMPROPER	FAILED TO OPERATE	WELDING	OSCILLATIONS	EXCESSIVE PRESSURE		TORQUE INCORRECT	GOUGED	SHORTED	MISCELLANEOUS	
1. PART	1		4			7			1														14
2. TEST EQUIPMENT					4	2	7			10	3			2								12	40
3. ASSEMBLY IMPROPER			1			2			2				4		1	1			1			2	14
*4. NO FAILURE			8	1		4	23			3	34											7	80
5. WRITTEN PROCEDURE			4			4	2															6	16
6. CONTAMINATION		3	148	8	99	6	59	9	26	1		2		5								14	380
7. MANUFACTURING	4		12	6	45	10	33	2	11			7	3	12	3						5	46	199
8. MISHANDLING		3	12	1	8	6	1	4	4	1											3	20	63
9. TESTING ERROR	2		4		3	15	2	1			9		1	1		1	4				2	54	99
10. WORKMANSHIP	1	7	11	1	5		3	2	2	1			2	1								24	60
11. DESIGN INADEQUACY			4	5	2	8	4	1				4	4		2							25	59
12. NOT DETERMINED														1								4	5
13. DEFECTIVE MATERIAL	2				8		3							1								14	28
14. TESTED BEYOND LIMITS			3			9	1						1				1					0	15
15. ENGINEERING				2										1								6	9
16. ENVIRONMENTAL PROBLEM			3				5															0	8
17. WEAROUT						2																0	2
18. OPERATOR ERROR			3		2	1	4	1			1		1					8			1	13	35
19. ADJUSTMENT IMPROPER													1									3	4
20. MISCELLANEOUS	0	0	2	5	4	4	3	8	0	0	1	1	0	1	1	0	2	0			1		33
TOTAL	10	13	219	29	180	80	150	28	46	6	55	17	2	16	25	6	4	13	1		122	51	1163

\*INVALID REPORTS

APS-752

COMMAND AND SERVICE MODULE REACTION  
CONTROL SYSTEM FAILURES

CAUSE \ CODE	CODE																							
	CRACKED OR DEFECTIVE	DAMAGED	LEAKING	LEAK-LOSS OF PRESSURE	CONTAMINATED	OPERATION IMPROPER	OUT OF SPEC	PART OR MATERIAL DAMAGED	SEAL DAMAGED/ DEFECTIVE	STUCK/SEIZED/ BINDING/FROZEN	NO FAILURE*	PART OR MATERIAL FAULTY	BROKEN	ASSEMBLY IMPROPER	FAILED TO OPERATE	WELDING	OSCILLATIONS	EXCESSIVE PRESSURE	TORQUE INCORRECT	COULDED	SHORTED	MISCELLANEOUS	TOTAL	
1. PART																								
2. TEST EQUIPMENT																								
3. ASSEMBLY IMPROPER				11		8		1						2							1	13	36	
*4. NO FAILURE				2		2																3	7	
5. WRITTEN PROCEDURE				53	1	45		1							1						3	35	140	
6. CONTAMINATION				219	55	63		11						2	8							38	396	
7. MANUFACTURING														1			1					6	8	
8. MISHANDLING	1			44	4	9		12						1								12	83	
9. TESTING ERROR	2			34	1	43		2							2						1	51	136	
10. WORKMANSHIP	1			38	10	47		10						2	1	3	1				1	33	147	
11. DESIGN INADEQUACY	14			63	3	25		17						8	1	4	1					51	187	
12. NOT DETERMINED	2			102	30	136		5		2				1	1	5					1	66	351	
13. DEFECTIVE MATERIAL				37		10																1	10	56
14. TESTED BEYOND LIMITS	1			3		3		1						3								1	7	19
15. ENGINEERING				2	2										1								2	7
16. ENVIRONMENTAL PROBLEM				5	2	3		1						1									4	16
17. WEAROUT						1		2		1					1									5
18. OPERATOR ERROR				12	1	6		4						1	1							12	37	
19. ADJUSTMENT IMPROPER				2		6																	7	15
20. MISCELLANEOUS	7			103	9	109		4		1				1	1	1	1					39	276	
TOTAL	28	-	-	730	118	516	-	71	-	4	-	-	10	10	26	-	4	-	-	-	9	390	1924	

\*INVALID REPORTS

APS-753



GEMINI  
REACTION CONTROL SYSTEM FAILURES

MODE CAUSE																					TOTAL		
	CRACKED OR DEFECTIVE	DAMAGED	LEAKING	LEAK-LOSS OF PRESSURE	CONTAMINATED	OPERATION IMPROPER	OUT OF SPEC	PART OR MATERIAL DAMAGED	SEAL DAMAGED/ DEFECTIVE	STUCK/SEIZED/ BINDING/FROZEN	NO FAILURE*	PART OR MATERIAL FAULTY	BROKEN	ASSEMBLY IMPROPER	FAILED TO OPERATE	WELDING	OSCILLATIONS	EXCESSIVE PRESSURE	TORQUE INCORRECT	COJUGED		SHORTED	MISCELLANEOUS
1. PART			2																				2
2. TEST EQUIPMENT	2					5	13			1					1							1	23
3. ASSEMBLY IMPROPER			22			1				2													25
*4. NO FAILURE			37				8				1				1								47
5. WRITTEN PROCEDURE	4	2	2			1	17																26
6. CONTAMINATION	1		121		3	9	29			11					14								188
7. MANUFACTURING		1	33			3	6						1	1	1							1	47
8. MISHANDLING			18			1	1	1		1			3										25
9. TESTING ERROR	2	5	4				4						3	1									19
10. WORKMANSHIP			7				5						2										14
11. DESIGN INADEQUACY	7		18			13	12			1		2	4	3				1					61
12. NOT DETERMINED	4	2	15			6	13						4	4									48
13. DEFECTIVE MATERIAL			10																				10
14. TESTED BEYOND LIMITS	1		1																				2
15. ENGINEERING																							0
16. ENVIRONMENTAL PROBLEM																							0
17. WEAROUT						1	2																3
18. OPERATOR ERROR																							0
19. ADJUSTMENT IMPROPER			1																				1
20. MISCELLANEOUS			7										1										8
TOTAL	21	10	298	0	3	40	110	1	0	16	1	0	16	0	26	0	4	0	1	0	2	0	549

\*INVALID REPORTS

APS-754

## GEMINI ORBITAL MANEUVERING SYSTEM FAILURES

CAUSE \ CODE	CODE																			TOTAL				
	CRACKED OR DEFECTIVE	DAMAGED	LEAKING	LEAK-LOSS OF PRESSURE	CORRUPTED	OPERATION IC/PROPER	OUT OF SPEC	PART OR MATERIAL DAMAGED	SEAL DAMAGED/ DEFECTIVE	STUCK/SEIZED/ BINDING/FROZEN	NO FAILURE*	PART OR MATERIAL FAULTY	BROKEN	ASSEMBLY IC/PROPER	FAILED TO OPERATE	WELDING	OSCILLATIONS	EXCESSIVE PRESSURE	TORQUE INCORRECT		GOUGED	SHORTED	MISCELLANEOUS	
1. PART	1																							1
2. TEST EQUIPMENT			6				8								3									17
3. ASSEMBLY IC/PROPER			12			2	9																	23
*4. NO FAILURE	2	5	16			2	3																	28
5. WRITTEN PROCEDURE			21				3			1														25
6. CONTAMINATION	3	2	38			8	19			1					13									84
7. MANUFACTURING			33			6	12			2					7									61
8. MISHANDLING			4																					4
9. TESTING ERROR			4			2	5																	11
10. WORKMANSHIP																								0
11. DESIGN INADEQUACY	6	3	21			9	8						3		2									52
12. NOT DETERMINED			16				5																	21
13. DEFECTIVE MATERIAL			1																					1
14. TESTED BEYOND LIMITS																								0
15. ENGINEERING																								0
16. ENVIRONMENTAL PROBLEMS																								0
17. WEAROUT																								0
18. OPERATOR ERROR																								0
19. ADJUSTMENT IC/PROPER																								0
20. MISCELLANEOUS			13				7																	20
TOTAL	12	10	185	0	0	29	79	0	0	4	0	0	4	0	25	0	0	0	0	0	0	0	0	348

\*INVALID REPORTS

APS-755

X-15  
ENGINE SYSTEM FAILURES

MODE CAUSE	CRACKED OR DEFECTIVE	DAMAGED	LEAKING	LEAK-LOSS OF PRESSURE	CONTAMINATED	OPERATION IMPROPER	OUT OF SPEC	PART OR MATERIAL DAMAGED	SEAL DAMAGED/ DEFECTIVE	STUCK/SEIZED/ BINDING/FROZEN	NO FAILURE*	PART OR MATERIAL FAULTY	BROKEN	ASSEMBLY IMPROPER	FAILED TO OPERATE	WELDING	OSCILLATIONS	EXCESSIVE PRESSURE	TORQUE INCORRECT	GOUGED	SHORTED	MISCELLANEOUS	TOTAL	
	1. PART																							
2. TEST EQUIPMENT																								
3. ASSEMBLY IMPROPER																								
*4. NO FAILURE																								
5. WRITTEN PROCEDURE																								
6. CONTAMINATION																								
7. MANUFACTURING													1											1
8. MISHANDLING																								
9. TESTING ERROR																								
10. WORKMANSHIP																								
11. DESIGN INADEQUACY		2												1	1									4
12. NOT DETERMINED																								
13. DEFECTIVE MATERIAL																								
14. TESTED BEYOND LIMITS																		1						1
15. ENGINEERING																								
16. ENVIRONMENTAL PROBLEM																								
17. WEAROUT																								
18. OPERATOR ERROR																								
19. ADJUSTMENT IMPROPER																								
20. MISCELLANEOUS			2			11				1					7							2	23	
TOTAL		2	2			11				1			2		8			1				2	29	

\*INVALID REPORTS

APS-766

PRIMARY MODES OF FAILURES

MODE	PERCENTAGE OF FAILURES						
	APOLLO LEMA & LMDE	APOLLO SPS	GEMINI OAMS	GEMINI RCS	X-15	APOLLO RCS	APOLLO LM RCS
1. LEAKING	34.2	31.6	53.2	54.3	6.9	38.0	21.3
2. DEFECTIVE (PHYSICAL DAMAGE)	17.4	16.6	7.2	9.2	17.2	6.1	10.0
3. IMPROPER OPERATION (OUT OF SPEC.)	18.1	37.2	31.0	27.3	38.0	27.0	20.1
4. FAILED TO OPERATE	1.6	3.1	7.2	4.7	31.0	2.0	3.7
5. OTHER	28.7	11.5	1.4	4.5	6.9	26.9	44.9

H-10

Figure H-8

APS-757

PRIMARY CAUSES OF FAILURES

CAUSE	PERCENTAGE OF FAILURES						
	APOLLO LEMA & LMDE	APOLLO SPS	GEMINI OAMS	GEMINI RCS	X-15	APOLLO RCS	APOLLO LM RCS
1. DESIGN INADEQUACY	9.7	20.2	14.9	11.3	13.8	9.7	5.1
2. CONTAMINATION	21.9	10.4	6.9	20.0	-	20.6	32.6
3. MANUFACTURING	19.5	14.7	24.1	15.7	3.4	9.9	23.5
4. TESTING	11.2	9.2	8.4	8.1	3.4	8.1	9.8
5. WRITTEN PROCEDURE	4.6	10.6	7.2	4.7	-	7.3	1.4
6. PERSONNEL	6.0	6.6	1.2	4.8	-	7.0	8.8
7. UNKNOWN	3.3	23.3	21.8	22.6	-	18.2	0.4
8. OTHER	22.8	5.0	15.5	12.8	79.4	19.2	18.4

MCDONNELL DOUGLAS ASTRONAUTICS COMPANY - EAST

H-11

Figure H-9

APS-756

Although contamination is listed as a cause of failure, it is really the result of another condition which produced the contamination. It is this other condition to which corrective action should be directed. With this in mind, the contamination failures were reviewed in detail to attempt to isolate the contamination source.

The results of this review are presented in Figures H-10 to H-15. The figures are tabulations which show the modes of failure versus the type of contamination involved and the source. Included under "modes" are "defective", which is defined as an inoperative part or component, and "contamination", which means a visually observed abnormal condition not producing a failure. Under "types" the following definitions apply. "Particles" includes non-metallic or a combination of metallic and nonmetallic particles. "Vapor" means moisture or other vapor exclusive of the propellants. "Seal" means that the seal material was the contaminant. "Propellant" is used when both propellants are involved or when the specific propellant is not given in the description. The remaining items in the figures are self-explanatory.

The figures show that the overwhelming result of contamination is leakage: an average of 75% of the total. The primary types of failure are "particles", "metal chips", and "undetermined". Since most of the undetermined failures are attributed to transient particles which were flushed away prior to examination, these can be combined with the "particle" and "metal chip" categories to show that approximately 83 percent of the contamination was metallic or nonmetallic particles. The total contribution of the fuel and/or oxidizer to contamination failures was less than nine percent. The sources are fairly well distributed: More than 40 percent are unknown, over one quarter originated during manufacture, and about 15 percent were caused by the testing operations exclusive of vendor type tests, such as component acceptance, which are included under "manufacturing". This analysis was based on a total of 1737 Gemini and Apollo contamination problems.

A further step in this analysis was to show which components or assemblies were most susceptible to contamination, and also how many failures were detected prior to vehicle assembly and how many were found at the system level. The former would not be applicable to reusability but the latter would, because system disassembly and repair or replacement would be involved. This analysis was performed on the four Apollo propulsion systems previously mentioned. The compilation is shown in Figures H-16 to H-21 which separate components into

CONTAMINATION FAILURES  
LMDE AND LMA

MODE	TYPE									SOURCE						
	UNDETERMINED	PARTICLES	METAL CHIPS	VAPOR	LUBRICANT	SEAL	OX RESIDUE	FUEL RESIDUE	PROPELLANT	MFG	HANDLING	TEST	DESIGN	UNKNOWN	TOTAL	PERCENT
LEAKAGE	218	80	47	9	8	5	8	3	7	151	25	24	22	163	385	79.4
OUT OF SPEC	31	8	3	12	3	-	2	6	-	15	-	15	8	27	65	13.4
DEFECTIVE	1	9	-	3	-	1	1	1	-	8	1	-	3	4	16	3.3
CONTAMINATION	-	10	-	4	1	1	2	-	1	12	1	-	1	5	19	3.9
TOTAL	250	107	50	28	12	7	13	10	8	186	27	39	34	199	485	-
PERCENT	51.6	22.0	10.3	5.8	2.5	1.4	2.7	2.1	1.6	38.4	5.6	8.0	7.0	41.0	-	100

H-13

Figure H-10

APS-758

CONTAMINATION FAILURES  
APOLLO SPS

MODE	TYPE									SOURCE						
	UNDETERMINED	PARTICLES	METAL CHIPS	VAPOR	LUBRICANT	SEAL	OX RESIDUE	FUEL RESIDUE	PROPELLANT	MFG	HANDLING	TEST	DESIGN	UNKNOWN	TOTAL	PERCENT
LEAKAGE	54	47	25	-	5	3	21	-	3	63	1	44	11	39	158	76.1
OUT OF SPEC	1	1	1	2	2	1	-	-	8	5	-	11	-	-	16	8.3
DEFECTIVE	1	-	1	5	1	3	-	-	5	5	-	11	-	-	16	8.3
CONTAMINATION	4	3	2	3	2	-	-	-	-	7	-	6	-	1	14	7.3
TOTAL	60	51	29	10	10	7	21	-	16	80	1	72	11	40	204	-
PERCENT	29.4	25.0	14.2	4.9	4.9	3.4	10.3	-	7.9	39.3	0.5	35.3	5.4	19.6	-	100

H-14

MCDONNELL DOUGLAS AERONAUTICS COMPANY - EAST

Figure H-11

APS-759



# CONTAMINATION FAILURES

LM RCS

MODE	TYPE									SOURCE						
	UNDETERMINED	PARTICLES	METAL CHIPS	VAPOR	LUBRICANT	SEAL	OX RESIDUE	FUEL RESIDUE	PROPELLANT	MFG	HANDLING	TEST	DESIGN	UNKNOWN	TOTAL	PERCENT
LEAKAGE	151	112	26	-	1	-	-	-	-	30	54	17	-	189	290	75.8
OUT OF SPEC	55	3	6	1	1	-	-	-	1	9	1	1	-	56	67	18.0
DEFECTIVE	12	1	-	-	-	-	-	2	1	1	-	4	-	11	16	4.3
CONTAMINATION	6	1	-	-	-	-	-	-	-	3	1	-	-	3	7	1.9
TOTAL	224	117	32	1	2	-	-	2	2	43	56	22	-	259	380	-
PERCENT	59.0	30.8	8.4	0.3	0.5	-	-	0.5	0.5	11.3	14.7	5.8	-	68.2	-	100

APS-760

H-15

Figure H-12

# CONTAMINATION FAILURES

o APOLLO COMMAND SERVICE MODULE RCS

MODE	TYPE									SOURCE					TOTAL	PERCENT
	UNDETERMINED	PARTICLES	METAL CHIPS	VAPOR	LUBRICANT	SEAL	OX RESIDUE	FUEL RESIDUE	PROPELLANT	MFG	HANDLING	TEST	DESIGN	UNKNOWN		
LEAKAGE	113	77	54	9	-	15	1	-	-	69	8	58	18	116	269	68.4
OUT OF SPEC	25	12	26	7	4	-	1	1	1	25	1	11	16	24	77	19.2
DEFECTIVE	11	3	4	4	2	-	4	-	5	8	2	3	12	8	33	8.2
CONTAMINATION*	6	5	3	3	-	-	-	-	-	3	-	5	-	9	17	4.2
TOTAL	155	97	87	23	6	15	6	1	6	105	11	77	46	157	396	-
PERCENT	39.2	24.5	22.0	5.8	1.5	3.8	1.5	0.2	1.5	26.5	2.8	19.5	11.6	39.6	-	100

\*CONTAMINATION EVIDENT IN VISUAL INSPECTION

APS-399

MCDONNELL DOUGLAS ASTRONAUTICS COMPANY - EAST

H-16

Figure H-13

# CONTAMINATION FAILURES

GEMINI OAMS

MODE	TYPE									SOURCE						
	UNDETERMINED	PARTICLES	METAL CHIPS	VAPOR	LUBRICANT	SEAL	OX RESIDUE	FUEL RESIDUE	PROPELLANT	MFG	HANDLING	TEST	DESIGN	UNKNOWN	TOTAL	PERCENT
LEAKAGE	3	12	9	1	-	-	12	1	-	15	2	4	11	6	38	45.3
OUT OF SPEC	6	7	3	1	-	-	2	-	-	10	-	3	1	5	19	22.6
DEFECTIVE	8	5	4	1	1	-	6	1	1	7	1	6	4	8	26	30.9
CONTAMINATION	1	-	-	-	-	-	-	-	-	1	-	-	-	-	1	1.2
TOTAL	17	24	16	3	1	-	20	2	1	33	3	13	16	19	84	-
PERCENT	20.2	28.6	19.0	3.6	1.2	-	23.8	2.4	1.2	39.3	3.6	15.5	19.0	22.6	-	100

APS-761

H-17

Figure H-14

CONTAMINATION FAILURES  
GEMINI RCS

MODE	TYPE									SOURCE						
	UNDETERMINED	PARTICLES	METAL CHIPS	VAPOR	LUBRICANT	SEAL	OX RESIDUE	FUEL RESIDUE	PROPELLANT	MFG	HANDLING	TEST	DESIGN	UNKNOWN	TOTAL	PERCENT
LEAKAGE	35	46	8	1	1	2	22	6	-	38	6	20	19	38	121	64.4
OUT OF SPEC	8	8	5	5	1	-	2	-	-	11	-	4	4	10	29	15.4
DEFECTIVE	8	7	7	2	2	-	8	1	-	13	-	6	11	5	35	18.6
CONTAMINATION	1	1	-	1	-	-	-	-	-	2	-	1	-	-	3	1.6
TOTAL	52	62	20	9	4	2	32	7	-	64	6	31	34	53	188	-
PERCENT	27.7	33.0	10.6	4.8	2.1	1.1	17.0	3.7	-	34.0	3.2	16.5	18.1	28.2	-	100

H-18

Figure H-15

APS-762

## COMPONENT FAILURE SUMMARY LMDE & LMA

COMPONENT		COMPONENT LEVEL		SYSTEM LEVEL		TOTAL
		LMDE	LMA	LMDE	LMA	
PRESSURANT	QUAD CHECK	53		75		128
	LATCHING SOL.	10		6		16
	REGULATOR	17	16	6	3	42
	RELIEF	14	20	1	1	36
	COUPLING	10	-	34	-	44
	QUICK DISCONNECT	10	-	3	-	13
	BURST DISC	6	-	-	-	6
PROPELLANT	COUPLING	2	-	9	-	11
	QUANTITY GAUGE	3	-	8	-	11
	PREVALVE	14	-	-	-	14
	SHUTOFF VALVE	78	26	5	4	113
	ACTUATOR ASS'Y	5	-	1	-	6
	FLOW CONTROL	5	-	-	-	5
	ENGINE	2	16	-	2	20
	MISC.	16	3	3	1	23
SUBTOTAL		182	81	70	11	
TOTAL		326		162		488

APS-767

H-19

Figure H-16

COMPONENT FAILURE SUMMARY  
APOLLO SPS

COMPONENT		TEST LEVEL		TOTAL
		COMPONENT	SYSTEM	
PRESS.	SOLENOID VALVE	13	3	16
	CHECK VALVE	19	13	32
	REGULATOR	2	-	2
PROPELLANT	TANK ASS'Y	3	2	5
	PROP VALVE	30	11	41
	ACTUATOR	12	-	12
	TWO-WAY SOL.	12	1	13
	THREE-WAY SOL.	15	-	15
	N <sub>2</sub> REGULATOR	15	-	15
	ENGINE	5	4	9
	FUEL PROBE	11	1	12
	MISC.	7	4	11
TOTAL		144	39	183

APS-763

H-20

Figure H-17

COMPONENT FAILURE SUMMARY  
LMRCS

COMPONENT		TEST LEVEL		TOTAL
		COMPONENT	SYSTEM	
PRESS.	QUAD CHECK	19	10	29
	RELIEF/CHECK	3	9	12
	H <sub>e</sub> F/V COUPLING	24	11	35
PROPELLANT	PROP. F/V COUPLING	1	7	8
	PROP SOL. VALVE	136	103	239
	ENGINE	4	4	8
	PRESSURE SWITCH	3	13	16
	MISCELLANEOUS	11	11	22
	TOTAL	201	168	369

APS-706

H-21

Figure H-18

# CONTAMINATION COMPONENT FAILURE SUMMARY

o APOLLO COMMAND SERVICE MODULE RCS

COMPONENT		TEST LEVEL		TOTAL
		COMPONENT	SYSTEM	
PRESS.	QUAD CHECK	38	9	47
	RELIEF	14	2	16
	COUPLING	39	9	48
	REGULATOR	26	2	28
PROP.	PROP VALVE	131	18	149
	ENGINE	60	29	89
	MISC.	11	9	20
	TOTAL	319	78	397

APS-398

H-22

Figure H-19



COMPONENT FAILURE SUMMARY  
GEMINI OAMS

COMPONENT		TEST LEVEL		TOTAL
		COMPONENT	SYSTEM	
PRESSURANT	PRESSURANT TANK	1	-	1
	EXPL, MAN. VLV., COUPLINGS COMPONENT PACKAGE A	1	-	1
	EXPL., MAN. VALVES, PR.SW., SOL., FILTER COMPONENT PACKAGE E	18	1	19
	REL., MAN. VALVES, BURST DIAPH., C.V., COUP., FILT. COMPONENT PACKAGE B	3	1	4
PROPELLANT	OX TANK	31	1	32
	FUEL TANK	17	2	19
	EXPL., MAN. VALVES, COUPLINGS, FILTER COMPONENT PACKAGE C (OXIDIZER)	4	-	4
	EXPL., MAN. VALVES, COUPLINGS, FILTER COMPONENT PACKAGE D (FUEL)	5	-	5
	TCA: 25LB	131	26	157
	TCA: 85LB	34	7	41
	TCA: 100LB	50	13	63
	MISC.	5	-	5
TOTAL		300	51	351

APS-764

H-23

Figure H-20

COMPONENT FAILURE SUMMARY  
GEMINI RCS

COMPONENT		TEST LEVEL		TOTAL
		COMPONENT	SYSTEM	
PRESSURANT	PRESSURANT TANK	4	-	4
	PRESSURE XDUCER	12	1	13
	XPL., MAN. VALVES, COUPLINGS, PR XDCC COMPONENT PCAKAGE A	19	1	20
	REGULATOR	8	7	15
	REL., MAN. VALVES, B.D., C.V., COUPL., FILT. COMPONENT PACKAGE B	104	7	111
PROPELLANT	OX TANK ASS'Y	9	-	9
	FUEL TANK ASS'Y	22	2	24
	XPL, MAN VALVES, COUPLINGS, FILTER COMPONENT PACKAGE C (OXIDIZER)	14	2	16
	COMPONENT PACKAGE D (FUEL)	3	2	5
	ENGINE	198	30	228
MISC	CARTRIDGES	24	-	24
	(HEATER ASS'Y)	(45)	(7)	(52)
	MISC	50	10	60
TOTAL		467	62	529

MCDONNELL DOUGLAS ASTRONAUTICS COMPANY - EAST

H-24

Figure H-21

APS-765

the pressurant subassembly and the propellant subassembly. Approximately two-thirds were detected at the component or subassembly level and do not pertain to reusability. The remaining third, or 447 failures, are the items pertinent to this study. The most susceptible components in the propellant subsystem were the propellant shutoff valves, and the most failure-prone components in the pressurant system were the quad check valves. Together they account for over half of the contamination failures.

For comparison, a tabulation of failure percentages due to all causes by propulsion system and by component is included in Figure H-22. This indicates that propellant valve failures are high in every system investigated. Engine problems are another major category. Note that check valve failures appear to be much less significant on an overall basis than when only contamination is considered. However, since it is recognized that contamination failures are linked to reusability, the check valve remains as one of the most susceptible components.

In summary, this literature search has established the following:

1. The most prevalent failure mode is leakage.
2. The primary cause of failure is contamination.
3. The major type of contamination is particulate - both metallic and nonmetallic.
4. Propellant induced contamination accounts for only about nine percent of all of the contamination failures.
5. One-third of all of the contamination failures pertain to reuse.
6. The components most susceptible to contamination are the pressurant check valves and the propellant valves.

Several conclusions are derived from this literature search. The first is that particular emphasis must be placed on the cleanliness of parts, facilities, and environment during the manufacturing and testing operations. Facilities, and particularly ground support equipment must be carefully controlled and maintained, and all fluids introduced into the vehicle must be adequately filtered. Handling procedures must be devised which will prevent the generation of contamination. Cleaning and flushing procedures must be instituted which remove contaminants produced during component manufacturing, so that the vehicle is clean when assembled. Test methods must provide for complete removal of all test fluids and provide a clean vehicle when testing is complete.

COMPONENT FAILURES (PERCENT)

COMPONENT	APOLLO				GEMINI	
	LMDE/LMA	SPS	LM RCS	CSM RCS	RCS	OAMS
CHECK VALVE	6.2	4.7	4.3	8.4	8.1	0.3
RELIEF VALVE	5.6	1.6	5.1	5.5	9.1	0.8
REGULATOR	11.5	4.8	3.9	8.9	2.8	-
He COUPLING	5.8	1.7	6.1	7.9	-	-
PROP VALVES	21.2	11.3	39.3	27.2	26.8	41.6
ENGINE	7.7	22.2	7.0	17.7	16.4	32.8
ACTUATORS	2.3	22.8	-	-	-	-
TANKS	1.4	1.5	2.0	2.5	7.0	14.8
INSTRUMENTATION	8.5	6.3	21.2	7.0	5.3	2.3
ELECTRICAL	4.7	4.3	3.8	2.1	9.8	-
HARDWARE	6.2	4.3	1.0	2.2	-	-
CARTRIDGES	-	-	-	-	4.5	-
MISC	18.9	14.5	6.3	10.6	10.2	7.4

MCDONNELL DOUGLAS ASTRONAUTICS COMPANY - EAST

H-26

Figure H-22

APS-402

A second conclusion is that design effort should be directed to a "contamination-proof" valve seat. Since it is impossible to achieve absolute contamination control, and valve seats are known to be susceptible to failure because of contamination, valve seats which are either self-cleaning or insensitive to small particles would ensure reusability in the presence of any particulate material which insinuates itself into the propulsion system in spite of the most thorough precautions.

The third conclusion is that the storable propellants - amine fuels and nitrogen tetroxide oxidizer - are not major contributors to contamination failures. Careful flushing and control of the environment in the presence of the propellants are essential, but if the proper procedures are established and maintained and compatible materials are used, these propellants should not degrade vehicle reusability.

The pressurant check valves require particular emphasis during the system definition and design phase. The primary purpose of these check valves is to prevent mixing of propellant vapors when a single pressurant source is used for both propellants. However, the primary contributor to check valve contamination is the very mixing process it is supposed to prevent. Check valve pressure drops have historically been kept low to minimize system pressure budgets and hence, system weight. Low pressure drops imply low poppet seating forces. During periods of system inactivity, the seating force was often inadequate to seal against the upstream migration of propellant vapors. Resolution of this problem can be effected by either increasing the poppet seating force or by providing separate pressurant sources for each propellant.

H.2 Rheopexy - There has been little progress in determining the causes and preventions of the precipitation of nitrated iron in propellant grade nitrogen tetroxide. The precipitate is  $\text{NOFe}(\text{NO}_3)_4$  and takes the form of a viscous gel. The iron exists as an inherent impurity in  $\text{N}_2\text{O}_4$  due to the stainless steel components employed in  $\text{N}_2\text{O}_4$  processing systems. Additional iron is obtained over a period of time from the storage container walls in which the  $\text{N}_2\text{O}_4$  is shipped. It is theorized that this iron forms a colloidal suspension and that precipitation is caused by a variety of interrelated variables. The use of chemical additives to preclude rheopexy has received much attention. Studies were performed by Rocketdyne in 1966 and 1967 under contract to the Air Force to investigate elimination of the ferric nitrate

species in  $N_2O_4$ . Certain chemical additives or reagents were found which would successfully inhibit  $N_2O_4$  flow decay. However, the effectiveness of these additives was found to decrease with time, and additional effort would be required to achieve an operational status.

Current studies have been directed toward the use of molecular sieves to remove the iron nitrate prior to vehicle loading. Molecular sieves are currently in use for a variety of filtering objectives, e.g., the removal of moisture from gases. Although the purification of NTO is a recent application, preliminary results indicate that in excess of 90% of the suspended iron nitrate can be removed by this process. Based on these results, molecular sieves appear to be a promising solution to the problem of flow decay, and additional development effort is warranted.